

**School of Pharmacy and Biomedical Science  
Curtin Health Innovation Research Institute**

**The Influence of Cholesterol on  $\beta$ -cell Function**

**Gawyn Colleen Ellison**

**This thesis is presented for the Degree of  
Doctor of Philosophy  
of  
Curtin University**


**March 2019**

# Author's Declaration

To the best of my knowledge and belief this thesis contains no material previously published by any other person except where due acknowledgment has been made.

This thesis contains no material which has been accepted for the award of any other degree or diploma in any university.

**Animal Ethics** The research presented and reported in this thesis was conducted in compliance with the National Health and Medical Research Council Australian code for the care and use of animals for scientific purposes 8th edition (2013). The proposed research study received animal ethics approval from the Curtin University Animal Ethics Committee, Approval Number # AEC\_2016\_17

Signature:  .....

Date: ..... 12/03/2019 .....

## Statement of Contributors

All experimental design, laboratory work and data analysis were undertaken by me in consultation with Cyril Mamotte unless stated otherwise. Philip Newsholme and Ross Graham contributed as co-supervisors, and in advising on final drafts. I am indebted to several people for their help with the animal study described in Chapter 5. The study design was undertaken by me in consultation with other team members, particularly Ricky LaRue, Rodrigo Carlessi and Cyril Mamotte. The ethics application was prepared by me, Ricky LaRue and Rodrigo Carlessi, while Cyril Mamotte oversaw the entire study and took ultimate responsibility for it. Animal husbandry and daily handling was undertaken by me, Rodrigo Carlessi, Heloisa Helena de Oliveira Alves, Stephanie Allen and Thiruvarutchelvan Sabapathy, and Ricky LaRue provided training in specific procedures. At the close of the study, Ricky LaRue, Rodrigo Carlessi, Heloisa Helena de Oliveira Alves, Stephanie Allen, Thiruvarutchelvan Sabapathy and Ross Graham helped me with blood collection and organ harvest. Several other projects were facilitated by the collection of relevant tissues from this study, and collaboration was actively solicited to this end to maximise benefit and fulfil ethical considerations. Data for Figure 5.7 was provided by Thiruvarutchelvan Sabapathy, who completed the analysis of hepatic cholesterol content for his project. Islet extraction was done by Rodrigo Carlessi and myself, while I took responsibility for blood analysis and the insulin secretion studies.

# Abstracts and Publications

During this PhD project the following publications, abstracts and orals have been presented.

## **Publications:**

Carlessi R, Rowlands J, **Ellison G**, Alves HHdO, Newsholme P, Mamotte C. Glutamine deprivation induces metabolic adaptations associated with beta cell dysfunction and exacerbate lipotoxicity. *Molecular and Cellular Endocrinology*. 2019. (1)

Bridgeman S, Northrop W, **Ellison G**, Sabapathy T, Melton P, Newsholme P, Mamotte, C. Statins do not directly inhibit the activity of major epigenetic modifying enzymes. *Cancer*. 2019. (2)

**Ellison G**, Mamotte C, Cruzat VF, Newsholme P. Importance of glutamine to insulin secretion, insulin action and glycemic control. In: Meynial-Denis D, editor. *Glutamine: Biochemistry, Physiology, and Clinical Applications* CRC Press, Taylor & Francis Group; 2017. (3)

## **Abstracts and oral presentations:**

- Mechanisms of the diabetogenic effect of statins: focus on insulin secretion and mitochondrial function. Poster presented at Science on the Swan, 2018.
- Influence of Statins on Pancreatic  $\beta$ -cell glycolytic and mitochondrial activity. Poster presented at The Australian Islet Study Group Meeting, 2017.
- Statin-mediated alteration of cellular cholesterol blunts maximal insulin secretion in  $\beta$ -cells. Poster presented at The Australian Diabetes Society (ADS) & ADEA Annual Scientific Meeting, 2017.
- Cholesterol: Friend or fiend in  $\beta$ -cell function? Poster presented at Science on the Swan, 2017.
- Is Cholesterol Content Linked to Insulin Secretion in the  $\beta$ -cell? Poster presented at Science on the Swan, 2016.
- The Effect of Modified  $\beta$ -cell Cholesterol Content on Insulin Secretion. Poster presented at Combined Biological Sciences Meetings, 2015.
- Manipulation of  $\beta$ -cell Cholesterol Content Influences Insulin Secretion. Poster presented at Mark Liveris Student Research Seminar, 2015.
- Unravelling the cholesterol-diabetes connection. Poster presented at Mark Liveris Student Research Seminar, 2014.
- Exploring the Diabetes – Cholesterol Connection. Invited oral presentation at Avondale College Science Seminar Series, NSW, 2014.
- The Influence of Cholesterol on  $\beta$ -cell Function. Oral candidacy presentation at Curtin School of Biomedical Sciences Seminar series, 2013.

# Abstract

Cardiovascular disease (CVD) and Type 2 diabetes (T2D) are leading contributors to the burden of disease in Australia and elsewhere. They can occur concomitantly and are characterised by similar risk factors. For example, insulin resistance, elevated total and LDL cholesterol and low protective HDL cholesterol are common to both conditions. The cholesterol-lowering drugs known as statins are regularly prescribed to treat dyslipidaemia, including in CVD and T2D. However, while statins prevent deaths from CVD, they have been associated with an increase in the incidence and progression of diabetes. High plasma cholesterol levels have also been correlated with insulin insufficiency and  $\beta$ -cell death, possibly due to oxidative stress and exhaustion.

Statins competitively inhibit 3-hydroxy-3-methylglutaryl-coenzyme A (HMG-CoA) reductase, the initial rate-limiting enzyme in cholesterol synthesis. The diabetogenic effect of statins may be a result directly related to this inhibition, leading to reduced total cellular cholesterol concentrations and to reduced availability of compounds such as coenzyme Q10, which are derived from intermediates of the mevalonate pathway. There are also potential downstream effects, such as inhibition of membrane channel proteins, interference in exocytotic processes, impaired mitochondrial function and increased reactive oxygen species. It is also possible that various members of the statin family have differential extrahepatic effects based on varying lipophilicity, and thus cellular penetration and impact. A comprehensive review of the literature has been undertaken to understand these influences on  $\beta$ -cells.

In this project, the effect of cholesterol content on  $\beta$ -cell function was addressed, with particular attention to insulin secretion, mitochondrial function and the evaluation of strategic proteins involved in glucose sensing, exocytosis and cholesterol transport. BRIN-BD11 cells, a glucose-sensitive  $\beta$ -cell model, were exposed to lipophilic and hydrophilic statins and insulin secretion was stimulated using a variety of nutritional and therapeutic secretagogues. To evaluate the contribution of mechanisms related to cellular cholesterol abundance on  $\beta$ -cell health and insulin secreting potential, the cholesterol-sequestering agent methyl  $\beta$ -cyclodextrin (M $\beta$ CD) was used, in both its pre-loaded and empty states to manipulate the cholesterol content. Both an increase and a decrease in cell cholesterol content, using cholesterol loaded M $\beta$ CD and statins, respectively, reduced robustly stimulated insulin secretion, with little effect on basal stimulation. Effect size appeared to be dependent on both the capacity to vary cholesterol from its native abundance and the strength of insulin secretion stimulation. Greater changes in cholesterol blunted the insulin secretion response to more potent secretagogues.

Stimulus-secretion coupling is central to appropriate insulin secretion and ATP generated through mitochondrial respiration is an important coupling agent. For this reason,

mitochondrial function and high oxidative respiration capacity in  $\beta$ -cells is key to whole-body glucose homeostasis. Statins have been found to adversely affect mitochondrial function in muscle, and it is not known whether this could also occur in  $\beta$ -cells. The metabolic effects of several statins were characterised using mitochondrial function studies and a Seahorse extracellular flux analyzer. Statins provoked an increase in glycolysis and adversely affected maximum mitochondrial respiration, although glucose uptake was not altered. ATP production stimulated by 25 mM glucose was reduced by atorvastatin treatment. A panel of antibodies directed against glycolytic enzymes in Western blots indicated that increases in hexokinase I expression and GSK3 $\beta$  phosphorylation at serine 9 attended this change. Further observations regarding other  $\beta$ -cell functions included increased expression of the cholesterol transporter ABCA1 and the mitogenic regulator mTOR, and increased insulin receptor phosphorylation.

Glutamine can improve glycaemic status in T2D patients, contributes carbons to the TCA cycle and is protective of oxidant injury. Therefore, the addition of glutamine in its stable dipeptide form with alanine was investigated as a potential moderator of the effects of statin on mitochondrial function and insulin secretion. However, no beneficial effect was observed on either insulin secretion or mitochondrial function; to the contrary, high concentrations of alanyl-glutamine had adverse effects.

*In vitro* effects may be different from those in the complex *in vivo* environment, and a study using male C57Bl/6J mice fed either a high fat or normal diet in conjunction with pravastatin, atorvastatin (both 10 mg/kg/day) or no statin treatment was therefore undertaken. Diet was found to have a greater effect than statins on glucose tolerance and fasting blood glucose, insulin and glucagon. However, atorvastatin was associated with diet-dependent variations in  $\beta$ -cell secretion, as indicated by HOMA-%B, significantly increasing the latter in the normal diet cohort while mice on the high fat diet were not affected. Additional subtle beneficial and adverse tendencies on insulin resistance (HOMA-IR) in the high fat and normal diet cohorts, respectively, were also observed, and fasting glucagon was elevated in association with atorvastatin and a high fat diet.

This study demonstrates that maintenance of intracellular cholesterol homeostasis is required for optimal  $\beta$ -cell function. Sub- and supra-optimal cholesterol content resulted in the blunting of maximal insulin secretion stimulated by nutrient and therapeutic secretagogues. Further, this effect was relative to both the magnitude of the change in cholesterol concentration and the strength of insulin secretion stimulus. Statin treatment also adversely affected stimulus-secretion coupling in BRIN-BD11  $\beta$ -cells, characterised by decreased respiration and ATP production. The associated increase in glycolysis may be a compensatory response, and there appear to be some comparisons between these results and the characteristics of  $\beta$ -cell

dedifferentiation. In accordance with other studies, pravastatin demonstrated a reduced, though consistently similar influence compared to atorvastatin, possibly due to its hydrophilicity.

The results of this study contribute to the body of research assessing the complex relationship between cholesterol and glucose homeostasis. Insulin secretion is adversely affected by both increased and decreased cellular cholesterol, supporting the conclusion that optimal cellular cholesterol content is required for healthy  $\beta$ -cell function. Lipophilic statins are associated with impaired ATP production, providing a putative mechanism for the decline in stimulated insulin secretion. In mice, the diabetogenic effect of statins appears to be conditional on other factors such as diet-induced insulin resistance, and may implicate anomalies in both glucagon and insulin secretion. This work may be relevant to clinical decisions on the responsible use of statins, and highlights potentially productive areas of future research to further examine cellular responses to cholesterol changes within  $\beta$ -cells and the associated systemic consequences for glucose homeostasis.

# Acknowledgements

I've learned that while that elusive 'perfect PhD' may exist, you possibly learn more from the imperfect one. You make mistakes, and indelible lessons result.

I've learned that at the end of your carefully deliberated work, when you leave the lab and meticulously assemble the story, the 'if only's begin. Prepare for the revelation of a previously un contemplated aspect that, if only you had realised earlier, would have elevated your project to a whole new level, perhaps in a tangential direction.

I have enjoyed the human side of science: the hallway discussions, the quirky humour, good-natured banter, the celebrations when success drops in to visit. The opportunities to meet amazing people. The discovery that she who goes by THIS name inconceivably requires food, water and bathrooms like everyone else. I've learned that the social and communication aspects of science, collaboration and free exchange of ideas, are keys to success.

I've learned that the accumulation of knowledge over time has privileged those of us who follow. Climb to the peak of human knowledge and mix cement for the next paver! Assess the foundations by all means, but deliver your handful of lime before you chip at the earth that supports them. There is probably a very good reason why a published protocol includes that particular step, and it is best to be very familiar with it before your small wisdom grandly seeks to 'improve' it. Think outside the square for sure, but examine your new angles with precision, honesty and a sense of duty to humanity.

I am indebted to those who have walked beside me on this journey. To my supervisor, Associate Professor Cyril Mamotte, who issued my boarding pass and waved me aboard, attended to my academic needs, supplied finances along the way to support my lab work and was there to usher me through to the light at the end of the interminable editing tunnel. A sincere thank you for the opportunity and support. To my associate supervisors, Dr Ross Graham and Professor Philip Newsholme, I have the greatest respect for your knowledge. Many thanks for your helpful suggestions. To my biological and adoptive lab groups, an enormous thank you. Your willingness to share ideas, reagents, banter and occasionally, cake, has made the difference between a journey and an adventure. I love you all. Thiru Sabapathy, thank you for your support, ideas and unending good nature. Rodrigo Carlessi, your optimism, passion for science, and willingness to discuss ideas has been incredibly helpful. To my office roomies, colleagues and staff at Curtin Health Innovation Research Institute (CHIRI), you are all wonderful! I couldn't have been blessed with a nicer group of people, a better facility or more helpful staff. Special mention to Ganga, Julia, Aparna, Hilai, Malini, Revathy, Chee, Adnan, Mo, Younan, Alex, Yeakuty and Naz and my dear church community friends. Your friendship and support have been enormously motivating. My sincere thanks.

To the people of Australia who, through the Australian Postgraduate Awards scheme, partially funded me and to the administrators at Curtin University who saw fit to endow me with a share, I made a silent commitment at the outset to ensure that this would be a good investment. I will do all in my power to keep that promise as I seek to put learning into practice into the future. My thanks also to Diabetes Australia Research Trust and the School of Pharmacy and Biomedical Science, who helped fund this project.

To my family: Phil, Adam, Alexandra, Hayden, Franzi, Kimberley, Michael, and Andrew. You are my inspiration, my support team and both my investment and legacy. I live and breathe for you more than for anything else on earth. Your encouragement and confidence mean the world to me.



# Poetic Précis

As we in Oz our waistlines fatten  
And fill our scripts for daily statin  
Some may find their diabetes  
Appears despite a ban on sweeties

So why this injury to metabolism?  
Is it due to polymorphism?  
Or does our industrious mitochondrion  
Tire from the drug phenomenon?

Does cholesterol deposition  
Affect our glycaemic disposition?  
Do proteins in the membrane  
Displace or fail to maintain  
Stability with altered fluidity?

Can we blame dedifferentiation  
Or maybe cellular inflation?  
Do enzymes rare upregulate  
Glycolysis to accelerate?  
So many things to postulate!

Not wishing to be negligent  
And causing no-one detriment  
We find it now quite pertinent  
To try our best to circumvent  
A problem somewhat prevalent  
To statin use inherent

And cholesterol so oft maligned  
Is with glucose status intertwined.  
So! Despite rampant consumerism  
We must maximise athleticism  
And care for our metabolism.

-Gae Ellison

# Dedication

To two strong women on whose shoulders I stand, who along with their DNA, bestowed in me the resilience, creativity and persistence necessary to accomplish this task.



**Sylvan Dardanelle Marne Pilgrim:**  
*named for a battle, quietly fought  
injustice, economic hardship,  
disadvantage.*



**Enid Mavis Southon:**  
*wise, resourceful, resolute,  
Best-Mum-Ever.*

# Table of Contents

Author's Declaration.....	ii
Statement of Contributors.....	iii
Abstracts and Publications.....	iv
Abstract.....	v
Acknowledgements.....	viii
Poetic Précis.....	ix
Dedication.....	x
Table of Contents.....	xi
List of Figures.....	xvi
List of Tables.....	xvii
List of Abbreviations.....	xviii
Chapter 1 Cholesterol and insulin secretion: What is the link?.....	22
1.1 Diabetes.....	22
1.2 Cholesterol.....	24
1.2.1 Cholesterol synthesis.....	24
1.2.2 Cholesterol function.....	26
1.2.3 Other products of the mevalonate pathway.....	27
1.2.4 Cholesterol transport.....	28
1.2.5 Pathologies of cholesterol storage and trafficking.....	30
1.2.6 Cholesterol regulation.....	31
1.2.6.1 Regulation of synthesis.....	32
1.2.6.2 Regulation of intestinal uptake.....	34
1.2.6.3 Cholesterol disposal.....	34
1.2.7 Therapies for cholesterol dyslipidaemias.....	35
1.3 Statins.....	37
1.3.1 Pharmacology/Dose/Elimination.....	37
1.3.2 Lipid lowering mechanism.....	38
1.3.3 Efficacy.....	39
1.3.4 Pleiotropy.....	40
1.3.4.1 T2D.....	40
1.3.4.2 Myopathy.....	41
1.3.4.3 Pleiotropy related to reactive oxygen species.....	41
1.4 $\beta$ -cells and Insulin secretion.....	43
1.4.1 $\beta$ -cells are metabolically distinct.....	44
1.4.2 Mechanism of insulin secretion.....	46

1.5	The insulin/cholesterol link .....	51
1.5.1	Membrane characteristics and associated proteins .....	51
1.5.1.1	Glucose transporters.....	52
1.5.1.2	Ion channels .....	52
1.5.1.3	Granule fusion, SNARE proteins and exocytosis .....	53
1.5.1.4	ABCA1/ABCG1 cholesterol transport .....	55
1.5.2	Mitochondrial function .....	56
1.5.3	Cholesterol effects on ROS .....	58
1.5.4	Other metabolic pathways .....	59
1.6	Experimental models .....	61
1.6.1	Use of statins <i>in vitro</i> and in mice .....	61
1.6.2	M $\beta$ CD .....	63
1.6.3	BRIN-BD11 cells.....	65
1.7	Summary, Significance.....	66
Chapter 2	Effects of Cholesterol modification on stimulated insulin secretion.....	69
2.1	Methods .....	70
2.1.1	Materials .....	70
2.1.2	Tissue culture.....	70
2.1.3	Preparation of LPDS.....	70
2.1.4	Cholesterol reduction and enhancement using cyclodextrins.....	70
2.1.5	Cholesterol reduction using statins.....	71
2.1.6	Cholesterol measurement.....	71
2.1.7	Stimulated insulin secretion.....	72
2.1.8	Islet extraction .....	73
2.1.9	Insulin ELISA.....	73
2.1.10	Protein quantification.....	73
2.1.11	Statistical methods .....	74
2.2	Results.....	74
2.2.1	Cholesterol absorption using c-M $\beta$ CD, but not desorption using M $\beta$ CD, blunted maximal stimulated insulin secretion. ....	74
2.2.2	Statins reduced cellular cholesterol and adversely influenced insulin secretion.....	76
2.2.3	Effect of statin on stimulated insulin secretion in isolated rat islets.....	82
2.3	Discussion.....	83
2.3.1	M $\beta$ CD-mediated cholesterol manipulation effects on insulin secretion.....	83
2.3.2	Statins reduced cholesterol and blunted maximal insulin secretion .....	86
2.3.3	Lipophilic vs hydrophilic statins .....	88
2.3.4	Atorvastatin does not acutely affect insulin secretion .....	89
2.3.5	Conclusion .....	90
2.3.6	Limitations and future directions.....	90

Chapter 3	Metabolic effects of statins in $\beta$ -cells .....	92
3.1	Background.....	92
3.1.1	$\beta$ -cell metabolism .....	92
3.1.2	Metabolic implications in statin treatment .....	93
3.2	Methods .....	94
3.2.1	Cells and reagents.....	94
3.2.2	Tissue culture and LPDS preparation.....	94
3.2.3	Mitochondrial and Glycolytic stress tests.....	94
3.2.4	Glucose uptake and mitochondrial function by alamar blue assay.....	96
3.2.5	Whole cell ATP/ADP assessment .....	97
3.2.6	Quantification of glycolytic proteins by Western Blotting.....	97
3.2.7	Statistical Analysis.....	98
3.3	Results.....	99
3.3.1	Mitochondrial function .....	99
3.3.2	Oxygen Consumption Rate (OCR).....	99
3.3.3	Extracellular Acidification Rate (ECAR).....	100
3.3.4	Alamar blue mitochondrial function assay .....	101
3.3.5	Quantifying ATP/ADP Production.....	101
3.3.6	Glucose Uptake.....	104
3.3.7	Influence of statins on selected glycolytic enzymes.....	105
3.4	Discussion.....	106
3.4.1	Statins induced a shift to glycolysis and reduced respiration .....	107
3.4.2	Glucose uptake.....	108
3.4.3	ATP production .....	108
3.4.4	Expression of enzymes dictating the fate of glucose.....	108
3.4.5	Putative mechanism of statin-related mitochondrial dysfunction .....	111
3.4.6	Further work and limitations .....	112
3.4.7	Conclusion .....	114
Chapter 4	Effects of cholesterol manipulation on selected proteins central to $\beta$ -cell function.....	115
4.1	Background.....	116
4.2	Methods .....	117
4.2.1	Cell culture.....	117
4.2.2	Cell lysate preparation for Western Blot analysis .....	118
4.2.3	Cell fraction preparation for Western Blot analysis .....	119
4.2.4	Protein quantitation by Western Blot analysis.....	120
4.2.5	Protein quantitation by iTRAQ analysis.....	120
4.2.6	Flow cytometry.....	121
4.3	Results.....	124

4.3.1	Statin-associated changes in proteins involved in oxidative stress and signalling.....	124
4.3.2	Determination of the cellular localisation of specific proteins .....	125
4.3.3	The influence of M $\beta$ CD, c-M $\beta$ CD and atorvastatin on physical characteristics of BRIN-BD11 cells .....	135
4.3.4	Flow cytometric analysis of the effects of c-M $\beta$ CD and M $\beta$ CD on selected proteins .....	138
4.4	Discussion.....	142
4.4.1	The influence of cholesterol manipulation on protein localisation .....	142
4.4.2	Does cholesterol flux have a role in insulin secretion? .....	145
4.4.3	Regulatory modifications resulting in blunting of maximal insulin secretion may be associated with upregulation of mTOR and I-R activation.....	147
4.4.4	Cholesterol manipulation affects cell granularity.....	149
4.4.5	Cell swelling is associated with cholesterol loading and depletion.....	150
4.4.6	Notes regarding the use of flow cytometry in this project.....	150
4.4.7	Summary.....	151
4.5	Future direction.....	152
Chapter 5	The metabolic effects of statins in mice .....	154
5.1	Abstract.....	154
5.2	Background.....	155
5.3	Methods .....	157
5.3.1	Mice and diets.....	157
5.3.2	Treatments .....	157
5.3.3	OGTT.....	157
5.3.4	Organ retrieval .....	158
5.3.5	Calculation of Insulin Sensitivity .....	158
5.3.6	Statistical analysis.....	160
5.4	Results.....	160
5.4.1	Weight & food consumption .....	160
5.4.2	Metabolic parameters.....	164
5.5	Discussion.....	171
5.5.1	The influence of diet and statins on weight .....	172
5.5.2	The influence of diet and statins on glucose homeostasis .....	172
5.5.3	Further influences on Insulin sensitivity.....	174
5.5.4	Other observations .....	176
5.5.5	Limitations and future studies .....	178
5.6	Conclusion .....	180
Chapter 6	Statin-Glutamine Interactions in the $\beta$ -cell.....	181
6.1	Background.....	181
6.2	Methods .....	183

6.3	Results.....	184
6.4	Discussion.....	188
6.4.1	Summary and future directions.....	191
Chapter 7	Conclusion .....	193
7.1	Cellular cholesterol changes intrinsically influence $\beta$ -cell function.....	198
7.2	Differential effects of statins .....	199
7.3	Mitochondrial impairment associated with statins .....	201
7.4	Environmental factors in statin-associated $\beta$ -cell dysfunction .....	204
7.5	Phenotypic $\beta$ -cell adaptations associated with cellular cholesterol modification.....	205
	Bibliography .....	207
Appendix A	Supplementary Material.....	251
A.1	Chapter 2 Supplementary Figure .....	251
A.1.1	Failure to rescue insulin after cholesterol restoration.....	251
A.2	Chapter 3 Supplementary Table .....	253
A.3	Chapter 5 Supplementary Figure .....	255
Appendix B	iTRAQ Results in Full.....	256
Appendix C	Diet Description.....	276

# List of Figures

Figure 1.1. Cholesterol Biosynthetic Pathway.....	25
Figure 1.2. Mechanisms of SREBP-mediated cholesterol regulation.....	33
Figure 1.3. Mitochondrial metabolism and insulin secretion in pancreatic $\beta$ -cells. ....	47
Figure 1.4. The influence of cholesterol on $\beta$ -cell function: A graphic project overview.....	68
Figure 2.1. Effects of M $\beta$ CD or c-M $\beta$ CD on total cellular cholesterol (A, B), and insulin secretion in response to nutrients (C,D) and sulphonylureas (E,F and G,H).....	75
Figure 2.2. Effects of pravastatin on cholesterol and insulin secretion in BRIN-BD11 cells.....	77
Figure 2.3. Effect of atorvastatin on cellular cholesterol and insulin secretion.....	79
Figure 2.4. Effect of simvastatin and fluvastatin on cholesterol and insulin secretion. ....	80
Figure 2.5. Acute effects of statins on insulin secretion. ....	81
Figure 2.6. Effect of statins on islet insulin secretion.....	82
Figure 2.7. Correlation between cholesterol and Insulin. ....	88
Figure 3.1. Stress test kinetics.....	95
Figure 3.2. Mitochondrial stress test kinetics. ....	100
Figure 3.3. Glycolytic function analysis. ....	102
Figure 3.4. Metabolic potential and reserve.....	103
Figure 3.5. Further metabolic assessment of statins in BRIN-BD11 cells. ....	104
Figure 3.6. The effect of statins on cell death as assessed by trypan blue exclusion. ....	105
Figure 3.7. The effect of statins on glycolytic enzyme expression.....	106
Figure 4.1. Overview of techniques and research questions in Chapter 4.....	118
Figure 4.2. Flow diagram of fractionation B protocol for sub-cellular protein location analysis by Western blot.....	119
Figure 4.3. Gating hierarchy for flow cytometry.....	122
Figure 4.4. Western blot assessment of the effect of statins on selected proteins related to oxidative stress (A) and signalling (B). ....	124
Figure 4.5. Cellular localisation of proteins from M $\beta$ CD treated cells. ....	127
Figure 4.6. Cellular localisation of proteins from statin-treated cells.....	128
Figure 4.7. Characterisation of iTRAQ protein samples. ....	129
Figure 4.8. iTRAQ analysis of 'P' fractions from BRIN-BD11 cells treated with M $\beta$ CD or c-M $\beta$ CD.....	133
Figure 4.9. Autofluorescent characteristics of BRIN-BD11 cells aids in differentiating insulin positive and negative cells. ....	136
Figure 4.10. Changes in physical characteristics of BRIN-BD11 cells associated with M $\beta$ CD treatment. ....	137
Figure 4.11. Changes in physical characteristics of BRIN-BD11 cells associated with atorvastatin treatment.....	138
Figure 4.12. Isotype controls for flow cytometry. ....	140



Figure 4.13. Flow cytometric analysis of the effect of M $\beta$ CD on proteins related to lipid homeostasis (A-C, J), glucose homeostasis (D-G, K) and insulin secretion (H, I, L).....	141
Figure 5.1. Effect of diet and statins on weight gain and food consumption. ....	162
Figure 5.2. Effect of diet and statins on energy consumption. ....	163
Figure 5.3. The effect of diet and statins on metabolic parameters. ....	167
Figure 5.4. The effect of diet and statins on glucose tolerance (OGTT). ....	168
Figure 5.5. Heat-map of metabolic parameters.....	169
Figure 5.6. Correlations between insulin or cholesterol and other metabolic parameters.....	170
<b>Figure 5.7. Effect of diet and atorvastatin on hepatic cholesterol. ....</b>	<b>170</b>
Figure 5.8. Measures of Insulin sensitivity compared. ....	171
Figure 6.1. Dose-response of Ala-Gln pretreatment on insulin secretion stimulated by high glucose (16.7 mM) + 10 mM L-alanine. ....	184
Figure 6.2. Effect of alanyl-glutamine (Ala-Gln) on acute and chronic insulin secretion.....	185
Figure 6.3. Metabolic effects of Ala-Gln in combination with atorvastatin. ....	187
Figure 6.4. Effect of Ala-Gln and atorvastatin on energetic state of BRIN-BD11 cells. ....	187
Figure 7.1. Potential hypoinsulinaemic mechanisms of statins in $\beta$ -cells .....	197
Figure SA.1 Cholesterol ‘rescue’ .....	252
Figure SA.2 The effect of diet and statins on metabolic parameters minus the outlier.....	255

## List of Tables

Table 1.1. Statin use and the risk of diabetes.....	42
Table 2.1. Stimulated insulin secretion after 24 h statin treatment.....	78
Table 3.1. Table of equations for mitochondrial and glycolytic parameters .....	96
Table 4.1. Antibodies used in Western Blot and Flow Cytometry experiments.....	123
Table 4.2. Summary of the influence of M $\beta$ CD (M), c-M $\beta$ CD (C), atorvastatin (A) or pravastatin (P) on BRIN-BD11 protein expression as measured by Flow Cytometry and Western Blotting (WB).....	126
Table 4.3. Proteins from ‘P’ fractions after M $\beta$ CD treatment. ....	133
Table 4.4. Proteins from ‘P’ fractions after c-M $\beta$ CD treatment.....	134
Table 5.1. Equations used in insulin sensitivity calculations.....	159
Table 7.1. Pharmacological variations between Pravastatin and Atorvastatin. ....	200
Table SA.1. Table of Enzymes Assessed in Chapter 3.....	253

# List of Abbreviations

2-NBDG, 2-(N-(7-Nitrobenz-2-oxa-1,3-diazol-4-yl)amino)-2-Deoxy-D-glucose, a glucose analogue

2DG, 2-deoxy-glucose, a glucose analogue

A, atorvastatin

ABCG1, ATP-Binding Cassette (ABC) Subfamily G Member 1

ACAT2, acetyl-CoA acetyltransferase 2

ADP, adenosine diphosphate

Ala, alanine, an amino acid

AMP, adenosine monophosphate

A-ND, atorvastatin-treated mice fed a normal diet

AP, ATP production

Apo, apolipoprotein

ARC, Animal Resources Centre

BBB, blood-brain barrier

BCA, bicinchoninic acid assay used to quantify protein

BR, basal respiration

BRIN-BD11, a rat-derived  $\beta$ -cell line

BSA, bovine serum albumin

c-M $\beta$ CD, cholesterol loaded methyl- $\beta$ -cyclodextrin

cAMP, cyclic adenosine monophosphate

Ca<sub>v</sub>1.2, A calcium channel

Ca<sub>v</sub><sup>2+</sup>, voltage gated L-type calcium channels

CE, cholesteryl ester

CE, coupling efficiency

CETP, cholesteryl ester transfer protein

CopII, coat protein II

CoQ10, co-enzyme Q10, also known as ubiquinone

CVD, cardiovascular disease

CYP3A4, an isoenzyme in the cytochrome P450 family

DHCR24, 24-dehydrocholesterol reductase

DHCR7, 7-dehydrocholesterol reductase

DMEM, Dulbecco's Modified Eagle's medium

DMSO, dimethyl sulphoxide

DNA, deoxyribose nucleic acid

ECAR, extracellular acidification rate

ECL, enhanced chemiluminescence

EDTA, ethylenediaminetetraacetic acid, a chelating agent

EGTA, ethylene glycol-bis(2-aminoethylether)-N,N,N',N'-tetraacetic acid, a chelating agent

ELISA, Enzyme Linked Immunosorbent Assays

Epac2A, exchange protein directly activated by cAMP 2

ER, endoplasmic reticulum

ERK, extracellular signal-regulated kinase

ETC, electron transport chain

EtOH, Ethanol

Ex-4, exendin-4, a GLP-1 incretin hormone analogue  
F, fluvastatin  
FAD, flavin adenine dinucleotide  
FBS, foetal bovine serum  
FCCP, carbonyl cyanide-4-(trifluoromethoxy) phenylhydrazone, causes mitochondrial uncoupling  
FDA, Food and Drug Administration  
FF-MAS, follicular fluid meiosis activating sterol  
FH, familial hypercholesterolaemia  
FPP, farnesyl pyrophosphate  
FSC-A, forward scatter - area  
FXR, farnesoid X-receptor  
G3P, glycerol-3-phosphate  
GAPDH, glyceraldehyde 3-phosphate dehydrogenase  
GC, glycolytic capacity  
GDH, glutamate dehydrogenase  
GFAT, glutamine:fructose-6-amidotransferase  
GGPP, geranylgeranyl pyrophosphate  
GLK, glucokinase  
gln/leu, glutamine + leucine  
GLP-1, glucagon-like peptide 1  
GLUT2, glucose transporter 2  
Glyc, glycolysis  
GPDH, glycerol-3-phosphate dehydrogenase  
GPx, glutathione peroxidase  
GTR, glutathione reductase  
GR, glycolytic reserve  
GS, glutamine synthase  
GSH, glutathione  
GSIS, glucose stimulated insulin secretion  
GSK3 $\beta$ , glycogen synthase kinase 3  $\beta$   
GSSG, oxidised glutathione  
GTP, guanine triphosphate  
H<sub>2</sub>O<sub>2</sub>, hydrogen peroxide  
HbA1c, glycated haemoglobin  
HBP, hexosamine biosynthetic pathway  
HBSS, Hank's Balanced Salt Solution  
HDL, high density lipoprotein  
HEPES, an organic buffering agent  
HFD, high fat diet  
HIF, hypoxia inducible factor  
HMG-CoA, 3-hydroxymethyl-3-glutaryl coenzyme A  
HOMA-%B, homeostatic model assessment –  $\beta$ -cell function (%)  
HRP, Horseradish peroxidase  
INSIG, insulin induced gene  
I-R, insulin receptor

IR, insulin resistance  
iTRAQ, isobaric tag for relative and absolute quantitation  
K-R pathway, Kandutsch-Russell pathway of cholesterol synthesis  
 $K^+_{ATP}$ , ATP-sensitive potassium channels  
KRBB, Krebs-Ringer Bicarbonate buffer  
LDH, lactate dehydrogenase  
LDHA, lactate dehydrogenase A  
LDL, low density lipoprotein  
LDLc, low density lipoprotein cholesterol  
LDLr, low density lipoprotein receptor  
LPDS, lipoprotein deficient serum  
LpL, lipoprotein lipase  
MCF, mitochondrial coupling factors  
MCT, monocarboxylate transporters  
MELADL, a hexapeptide amino acid sequence  
MR, Maximal respiration  
mRNA, messenger RNA  
mTOR, mammalian target of rapamycin  
M $\beta$ CD, methyl- $\beta$ -cyclodextrin  
NADH, nicotinamide adenine dinucleotide  
NADPH, the reduced form of NADP<sup>+</sup>  
NAFLD, non-alcoholic fatty liver disease  
NAFPD, non-alcoholic fatty pancreas disease  
ND, normal diet  
NIR, near infra-red  
NK, natural killer cells  
N<sup>+</sup>K<sup>+</sup>ATPase, sodium-potassium adenosine triphosphatase  
NNT, numbers needed to treat  
NMO, non-mitochondrial oxidation  
NMR, non-mitochondrial oxygen consumption  
Nox, NADPH oxidase  
NPC, Niemann-Pick type C  
NPC1, Niemann-Pick type C Intracellular Cholesterol Transporter 1  
NPC1L1, NPC1 Like Intracellular Cholesterol Transporter 1  
NT, no treatment  
OATP, organic anion transporting peptide  
OGTT, oral glucose tolerance test  
OxPhos, oxidative phosphorylation  
P, pravastatin  
PBS, phosphate buffered saline  
PCSK9, proprotein convertase subtilisin/kexin type 9  
PDH, pyruvate dehydrogenase  
PDK, pyruvate dehydrogenase kinase  
PDX-1, pancreatic duodenal homeobox-1  
PFKP, phosphofructokinase – platelet

pI-R, phosphorylated insulin receptor  
PK, pyruvate kinase  
PKA, protein kinase A  
PKM2, pyruvate kinase muscle type 2  
PL, proton leak  
PPAR, peroxisome proliferator-activated nuclear receptor  
PXR, pregnane X receptor  
QUICKI, Quantitative Insulin Sensitivity Check Index  
RAC1, Rac Family Small GTPase 1  
RB, reaction buffer  
RCT, randomised controlled trial  
RIPA, radioimmunoprecipitation assay buffer  
ROS, reactive oxygen species  
RPMI, Roswell Park Memorial Institute medium  
S, simvastatin  
S2P, site-2 protease  
Sar1/Sec 23/24, complex of the COPII vesicle coat that forms before budding  
Scap, SREBP cleavage-activating protein  
SD, standard deviation  
SDHA, succinate dehydrogenase complex subunit A  
SDS-PAGE, polyacrylamide gel electrophoresis using SDS to denature the proteins  
SDS, sodium dodecyl sulphate, a detergent  
SEM, standard error of the mean  
SM, squalene monooxygenase  
SNAP25, synaptosomal associated protein 25  
SNARE, soluble N-ethylmaleimide-sensitive factor activating protein receptor  
SR-B1, scavenger receptor type B class 1  
SRC, spare respiratory capacity  
SREBP, sterol-regulatory element-binding protein  
SSC-A, side scatter - area  
SUR1, sulphonylurea receptor 1  
T-MAS, testes meiosis activating sterol  
T2D, type 2 diabetes mellitus  
TBST, a Tris base buffer containing detergent  
TCA cycle, tricarboxylic acid cycle  
TICE, transintestinal cholesterol excretion  
TMB, 3,3',5,5' Tetramethyl-benzidine  
UCP, uncoupling protein  
V, vehicle  
VAMP2, vesicle-associated membrane protein 2  
VC, vehicle control  
VDAC, voltage dependent anion channel  
VLDL, very low density lipoproteins  
WB, Western blot  
WHO, World Health Organisation

# Chapter 1           Cholesterol and insulin secretion: What is the link?

Type 2 diabetes (T2D) is a significant contributor to disease burden in Australia and globally. Together with cardiovascular disease (CVD), which shares similar risk factors, these two diseases are of considerable concern in terms of cost and suffering. The cholesterol lowering drugs known as statins are often prescribed to protect diabetics from CVD. However, while statins are efficacious in preventing deaths from CVD, they have also recently been associated with an increased risk of new-onset T2D. Given that these drugs regularly feature in the top 10 most prescribed drugs list in Australia and elsewhere, it is important to investigate their influence on insulin secretion and potential diabetic mechanisms. This review provides a background for the studies reported in the following chapters. To keep this review up-to-date in a burgeoning research area, some of the literature included was published after the commencement of this project and includes information that was not available during the planning and data acquisition stages.

## 1.1     Diabetes

Of the so-called ‘diseases of affluence’ of the modern era, type 2 diabetes (T2D) is an epidemic (4-6). Much research effort has been invested in understanding the lifestyle and other risk factors that contribute to its development and progression. Globally the impact of this largely preventable chronic illness was such that the World Health Organisation promoted a ‘Beat Diabetes’ campaign in 2016 (7).

Diabetes was the 12<sup>th</sup> leading cause of death globally in 2000 and 6<sup>th</sup> in 2015, accounting for 1.8 and 2.8% of deaths respectively (8). While most T2D-related deaths are in the > 50 year old age-group, children (<18 years old) do not escape its effects (9), and it is anticipated that by 2025 there will be 91 million obese children globally, of whom 4 million will have T2D unless effective interventions become available (10).

T2D is characterised by increased insulin resistance which, in the initial stages, is managed by increased insulin secretion to maintain normoglycaemia. With the consequent increase in  $\beta$ -cell metabolism and changes in the environmental milieu such as dyslipidaemia, glucagon dysregulation, cytokine release and associated reactive oxygen species (ROS) generation, the condition progresses to  $\beta$ -cell fatigue, dedifferentiation and apoptosis. This further leads to inadequate insulin secretion, hyperglycaemia and, eventually, insulin dependence (11-14).

T2D progression is thought to be driven by insulin resistance resulting from metabolic derangements associated with obesity and dyslipidaemia. Dyslipidaemia associated with T2D is

characterised by elevated triglycerides both in the fasting and post-prandial states, low levels of protective high density lipoproteins (HDL, refer to Section 1.2.4) and increased abundance of small, dense low density lipoproteins (LDL) (15). High levels of circulating free fatty acids (FFA) stimulate  $\beta$ -cell compensatory hyperplasia and hypersecretion of insulin, particularly at pre-stimulatory glucose concentrations in healthy islets (16, 17). It is widely believed that FFA, particularly those that are saturated, such as palmitate, induce lipotoxicity, manifest by peripheral insulin resistance and  $\beta$ -cell dysfunction through mechanisms including endoplasmic reticulum (ER) stress and increased ROS (18). Accumulation of fat in the islets and pancreas (19) is associated with elevated proinflammatory cytokines and may lead to  $\beta$ -cell apoptosis and endocrine dysfunction (20).

Diabetes mellitus is associated with macro and microvascular disease complications including cardiovascular disease (CVD), stroke, nephropathy, retinopathy, neuropathy and sexual dysfunction (reviewed in 21) as well as non-vascular conditions such as depression and dementia (22).

The relationship between T2D and CVD is of particular relevance in this project. CVD is the most likely cause of death among people with T2D (23, 24) and among ~27,000 deaths from ischaemic heart disease in New York over a period of 18 years, young women (< 25 years) were 5 times more likely to have T2D listed as a contributing cause than men or older women (25). In addition, a recent meta-analysis found that T2D independently conferred an ~2-fold risk for CVD and accounted for an estimated 11% of CVD-related deaths over 8.49 million person-years in an adult population, of whom 10% had T2D (26).

The strong link between T2D and CVD (27) results in widespread prescription of lipid lowering drugs, mainly from the statin family, in T2D patients (28). Indeed, clinical guidelines from the American College of Physicians advocate its use in all patients presenting with T2D, regardless of baseline lipid levels (29, 30). Australian guidelines are a little more conservative, suggesting that secondary causes of raised blood lipids be treated prior to beginning drug therapy (31). While proactive risk monitoring and statin medication are changing the prevalence of complications related to dyslipidaemia among diabetics (32), recent evidence that statins are associated with increased new onset and progression of T2D is a cause for concern (reviewed in 33, 34).

There is an accumulating body of evidence to suggest that a link exists between statin medication and glucose tolerance, including new onset diabetes. First widely recognised after the publication of the JUPITER and WOSCOP studies (35, 36), further meta analyses of clinical trials have shown conclusively that a link exists (see Table 1.1). While benefit vs harm considerations lie in favour of the continued use of statins (30), the scale of their global use implies an enormous potential for harm, even given very low harm ratios. Causation has not yet

been established, however, and many studies, including those in this thesis, are investigating this link and possible contributing mechanisms. Section 1.5 reviews the literature to date linking cholesterol and glycaemic health, but first the synthesis and role of cholesterol in the body is reviewed.

## 1.2 Cholesterol

Cholesterol is essential for life and development (37). Most of the ~1.5 g daily adult requirement is biosynthesised (38), mainly during the night and early morning (39), and a variable amount (~5%) is of dietary origin (40). Although the liver has traditionally been considered the major site of cholesterol synthesis, reports vary. In rodents, the liver contributes 10-50% with skin (20%), intestine (10-20%) and other extrahepatic tissue accounting for the remainder (41, 42). In humans, reliable *in vivo* data is unavailable (42).

Movement of cholesterol in the circulation is accomplished by means of lipoprotein particles; these can deliver to and accept cholesterol from cells, for example by low density lipoprotein (LDL) and high density lipoprotein (HDL), respectively. Given that cholesterol is an indispensable component of cellular membranes, it is not surprising that machinery for its production is ubiquitous, and all nucleated cells, including pancreatic  $\beta$ -cells, are capable of synthesising it (43). Hence, in many tissues, both endogenous (biosynthesised) and exogenous (delivered by lipoproteins) cholesterol is available, providing two mechanisms of acquisition. However, some cells, for example those synthesizing steroid hormones, have high cholesterol requirements and these are more dependent on that delivered in the form of LDL.

### 1.2.1 Cholesterol synthesis

Over 20 enzymes are required for cholesterol synthesis, including 3-hydroxy-3-methylglutaryl-CoA reductase (HMGCR), well-known as the target of statins and for catalysing the key rate-limiting step. Recently, squalene monooxygenase (SQM, also called squalene epoxidase) has also been attributed with a rate-limiting function and several additional enzymes in the pathway have been found to contribute further regulatory control over synthesis of cholesterol and several biologically significant intermediates (44) (also reviewed in (45), discussed further below).

Cholesterol is synthesised via the mevalonate pathway which gives rise to two alternative pathways diverging from lanosterol, known as the Bloch<sup>1</sup> and Kandutsch-Russell (K-R) pathways (45, 47-49) (see Figure 1.1). By means of these parallel synthetic pathways, a degree of redundancy exists. Moreover, great flexibility for the provision of additional intermediates

---

<sup>1</sup> Konrad Bloch and Feodore Lynen were awarded the Nobel Prize for Physiology or Medicine in 1964 “for their discoveries concerning the mechanism and regulation of the cholesterol and fatty acid metabolism” (46)



results from tissue-specific flux through either or both pathways (50-52). Indeed, side-chain modification can theoretically occur on any K-R intermediate, allowing ‘bridges’ between the two pathways (53), and a modified pathway utilising combinations of both traditional pathways was recently discovered (50). Relative flux through each pathway may thus vary, and this was demonstrated in several tissues including adipose, liver and brain (~85%, ~65% and ~22% Bloch pathway, respectively).

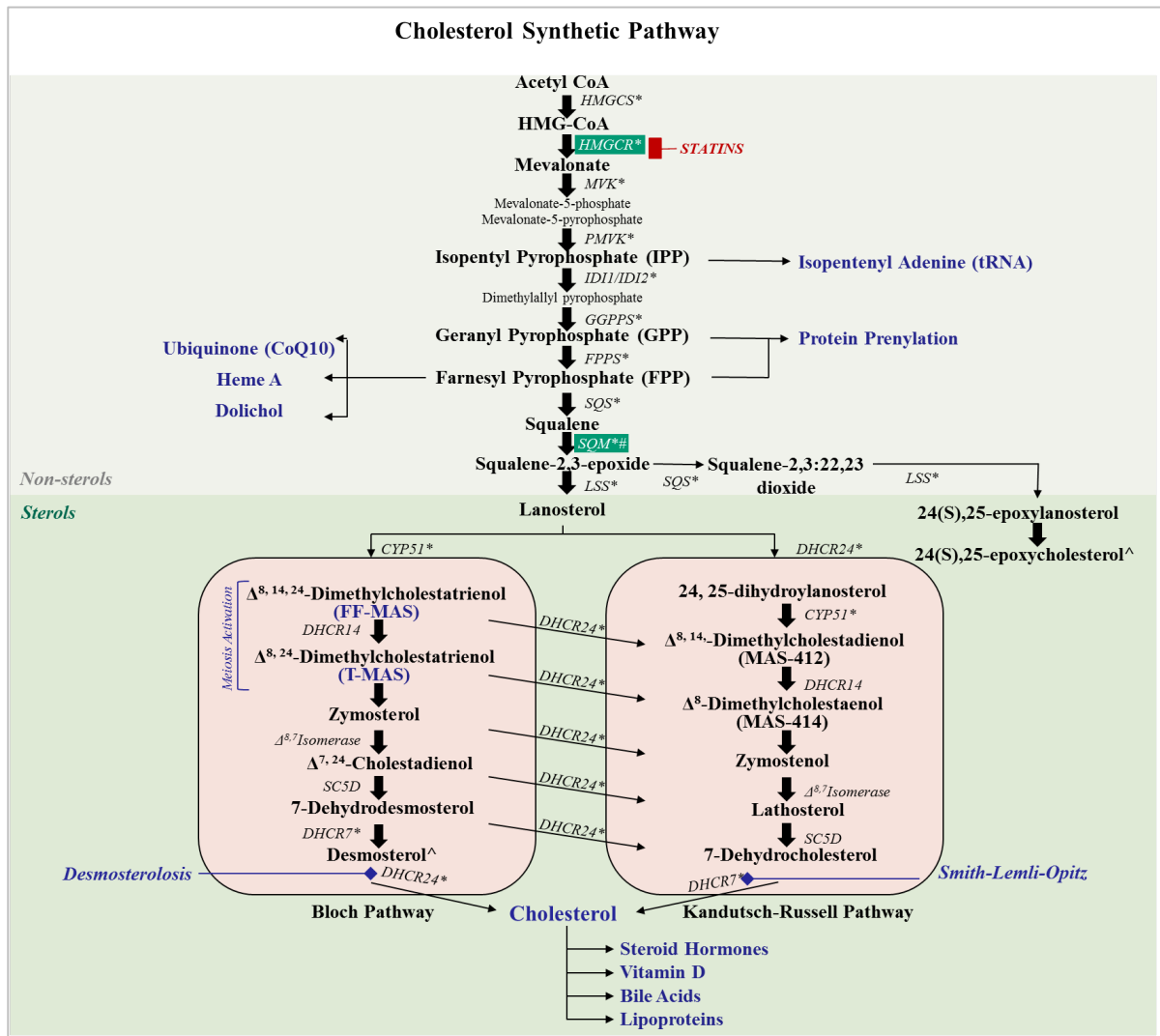


**Figure 1.1. Cholesterol Biosynthetic Pathway.**

The mevalonate pathway diverges into the Bloch and Kandutsch-Russell pathways for further metabolism of lanosterol to cholesterol. Statins inhibit synthesis early in the mevalonate pathway (indicated in red), rate-limiting enzymes are indicated using white text in a green box, and biologically relevant intermediates, products or pathologies are indicated in blue. HMGCS, HMG-CoA synthase; HMGCR, HMG-CoA reductase; MVK, mevalonate kinase; PMVK, Phosphomevalonate kinase; IDI1/IDI2, Isopentenyl-diphosphate  $\Delta$ -isomerase 1/2; GGPPS, geranyl pyrophosphate synthase; FPPS, farnesyl pyrophosphate synthase; SQS, squalene synthase; SQM, squalene monooxygenase (squalene epoxidase); LSS, Lanosterol synthase; CYP51, Sterol 14 $\alpha$ -demethylase cytochrome P450; DHCR24, 24-Dehydrocholesterol reductase; DHCR14, 14-Dehydrocholesterol reductase; SC5D, Sterol-C5-desaturase; DHCR7, 7-Dehydrocholesterol reductase. Items marked \* are known targets of SREBP (49); # indicates direct regulation by cholesterol; ^ indicates involvement in negative regulatory feedback. Adapted from (54).

### 1.2.2 Cholesterol function

In addition to being a vital component of cellular membranes, cholesterol is also a precursor for Vitamin D, bile salts and steroid hormones including testosterone, oestrogen, progesterone and the corticosteroids. In male mice, it is used in the synthesis of pheromones in the preputial glands (50, 55). Twenty percent of total cholesterol content is found in the brain where it is involved in axon myelination and other brain functions (56). Skin and adrenal glands are also cholesterol enriched.

The intracellular compartmentalisation of cholesterol varies, with most contained in the plasma membrane, where it plays critical structural and functional roles as described below.

Intracellular membranes also contain cholesterol and, in at least some cases, its concentration is strictly controlled. Indeed, cholesterol concentration in the endoplasmic reticulum (ER) provides the cue to up- or down-regulate cholesterol synthesis (57).

Each cell is bound by a phospholipid bilayer enriched with cholesterol to maintain a hydrophilic barrier. Lipids constituting the plasma membrane are amphipathic in nature and are oriented in a manner that separates their hydrophobic residues from the aqueous cytosolic and extracellular areas. Translocation from one lipid bilayer to the other requires a 180° turn, often facilitated by a transporter (58). Cholesterol, however, can spontaneously translocate between bilayers (59). While cholesterol has traditionally been thought to be present in higher concentrations in the inner leaflet (60), recent evidence challenges this view, perhaps due to improved imaging tools. Instead, cholesterol was found to be more concentrated in the outer leaflet and the asymmetry maintained between the two leaflets is thought to facilitate signalling activities by means of stimulus-responsive transfer of cholesterol between the inner and outer membrane leaflets (59).

Besides its potential signalling role, the cholesterol content of membranes influences several of its biophysical properties, including viscosity and curvature. It decreases membrane fluidity, producing tighter packing of surrounding phospholipids resulting in a membrane thickening effect (reviewed in 61). Overall, cholesterol constitutes ~10 – 45 mol% of the lipid content of cell membranes (59)<sup>2</sup>, but its distribution is not uniform; for example there are regions of higher concentration in lipid rafts, where it interacts with sphingolipids (61, 62). These lipid rafts, characterised by greater orderliness and increased accumulation of transmembrane proteins (63), are critically important in the maintenance and function of proteins involved in cell signalling and exocytosis (reviewed in 64).

In  $\beta$ -cells, membrane cholesterol affects several lipid raft-associated proteins involved in insulin exocytosis. These include voltage-gated  $\text{Ca}^{2+}$  channels ( $\text{Ca}^{2+}_v$ ) and various granule fusion proteins including synaptosomal associated protein 25 (SNAP25) and vesicle-associated

---

<sup>2</sup>Quantification of membrane cholesterol varies within the literature, and HeLa cells have ~22 mol% in membranes (59).

membrane protein 2 (VAMP2) (65, 66). In addition, other transport and/or signalling proteins including low density lipoprotein receptor (LDLR) and insulin receptor (I-R), but not glucose transporter 2 (GLUT-2) (67), are also raft-associated. ATP-sensitive  $K^+$  channels ( $K^+_{ATP}$ ), crucial in  $\beta$ -cell stimulus-secretion coupling, may be located within lipid rafts, although some discrepancy occurs in the literature (68, 69). Surprisingly, caveolin 1, usually associated with cholesterol-rich caveolae at the plasma membrane, was only found intracellularly in  $\beta$ -cells (69). It is thought to be located within lipid rafts on the granule membrane where it may have a cholesterol-regulating function (70). Further discussion on the roles of these proteins can be found in Sections 1.5.1. and 1.1.

Within the  $\beta$ -cell, and similarly to other secretory cells, insulin secretory granules containing crystalline insulin are enclosed within cholesterol-enriched lipid membranes (71, 72). This facilitates exocytosis in two ways: it enhances  $Ca^{2+}$  sensitivity as a fusion signal, and the spontaneous negative curvature bestowed by cholesterol expedites fusion (73, 74). Sato and Herman (1981, cited in 72) point out that the total surface area of these granules (and thus cholesterol requirements) is significant, given that each  $\beta$ -cell contains 9,000-10,000 granules.

Additional roles exist for cholesterol in all cell types, but those outlined above allow an appreciation of the importance of cholesterol in  $\beta$ -cell function and glucose homeostasis. Furthermore, the long and complex cholesterol synthetic pathway produces many transitional molecules, some of which are of interest in glucose homeostasis.

### 1.2.3 Other products of the mevalonate pathway

There are other products stemming from intermediates of the mevalonate pathway which serve important biological functions. The best-known of these are the isoprenoids, including coenzyme Q10 (CoQ10), also known as ubiquinone, and the prenylation moieties geranylgeranyl pyrophosphate (GGPP) and farnesyl pyrophosphate (FPP).

CoQ10 has a structure similar to Vitamin K and is important in cellular redox processes and as a member of the electron transport chain (75). Each CoQ10 molecule can carry 2 electrons and is involved in electron transfer between complexes 1, 2 and 3 in the electron transport chain (ETC) (76). CoQ10 is functionally important in  $\beta$ -cells, not only for cell respiration but also for insulin secretion because nutrient-generated ATP is a potent stimulus-secretion coupling factor in insulin secretion (77).

GGPP and FPP are likewise involved in redox and secretory processes via activation and recruitment to the membrane of small signalling G-proteins (78). In addition, numerous proteins require enzymatic prenylation for biological function (79-81). Notably, Haem A, essential as a cofactor of cytochrome c oxidase, complex IV of the respiratory chain,

incorporates a farnesyl tail group requisite for precisely locating the haem within the cytochrome complex (82, 83).

Several additional intermediates with novel biological activities have also recently been postulated based on mathematical modelling, flux losses in the post-lanosterol pathway, and the discovery that cytochrome P450 exhibits sterol metabolising enzyme activity, providing a novel mechanism for sterol processing (52, 53). Oxysterol metabolites of various intermediates have likewise been flagged as potentially biologically active in health and disease (84, 85), indicating that the roles of cholesterol, its intermediates and products are still being deciphered and further avenues of influence on metabolic processes may yet be determined.

#### 1.2.4 Cholesterol transport

Systemically, cholesterol is transported in the aqueous plasma environment in millimolar quantities (~4 mmol/L in healthy adults) as a component of lipoparticles of varying size and density. Synthesis and metabolic disposition of these lipoproteins is dependent on a family of proteins known as apolipoproteins (apo) (recently reviewed in 86). The liver is the hub of the transport system and functions as a terminal for processing incoming and outgoing lipoproteins and their cargo including cholesterol, cholesteryl esters and triglycerides.

In humans, dietary cholesterol and fats are assimilated in enterocytes into large, triglyceride-rich lipoproteins known as chylomicrons; these enter the blood stream via the lymphatics and are hydrolysed in tissues such as adipose and muscle by lipoprotein lipase to release fatty acids for incorporation into tissue lipids, for oxidation as fuel or, in adipose tissue, for storage. Very low density lipoproteins (VLDL), originating from the liver, perform a similar task. Circulating high density lipoproteins (HDL) support this process by donating apo C and apo E to nascent chylomicrons and VLDL particles. As chylomicron and VLDL triglycerides are lost through the action of lipoprotein lipase, the particles become progressively more dense and the relative cholesterol and cholesteryl ester concentration increases. Known at this stage as chylomicron remnants (from chylomicrons) and intermediate-density lipoproteins (IDL, arising from VLDL), either can be taken up and metabolised by the liver. Mostly, the IDL are metabolised by hepatic lipase in the liver to form low density lipoproteins (LDL), which deliver cholesterol to extrahepatic tissues (~30% of LDL) or recirculate it to the liver (~70%). HDL arises from the liver and intestine and is involved in reverse cholesterol transport, accepting cholesterol from extrahepatic tissue via the ATP-binding cassette transporter family A member 1 (ABCA1) (87).

LDL binds to its cognate receptor (LDLR) on the cell membrane and together, receptor and LDL are internalised in clathrin-coated pits. Ultimately, the receptor is recycled to the cell surface and the cholesterol is made available for use by the cell after lysosomal degradation of

the lipoprotein particle (57). However, proprotein convertase subtilisin kexin 9 (PCSK9) can prevent the recycling of LDLR and enhance its endosomal degradation (88).

In the context of cardiovascular risk, high levels of plasma LDL cholesterol content is widely recognised as an independent risk factor for CVD (89), while HDL is largely considered protective (90). HDL is also protective of  $\beta$ -cells *in vitro*, even in the presence of various stressors (91).

Apart from cholesterol, both free and in the esterified form, lipoproteins also transport fat-soluble vitamins and CoQ10 (92). The lipoproteome has recently been found to be surprisingly large, with 95 and 22 validated proteins in HDL and LDL, respectively, and knowledge of the functions of many included proteins is expanding (93, 94). Interestingly, disparate HDL proteomes found in heart failure patients are highly predictive of survival (95). This may lead to future biomarkers and greater understanding of the role of HDL proteins in sickness and health. An independent lipoprotein transport system operates in the brain, shuttling cholesterol from astrocytes, where most synthesis occurs, to neurons (reviewed in 96).

A range of specialised proteins is also required for cholesterol transport at the cellular level. These fall into two categories: those that interact with lipoproteins, and those involved in synthesis and intracellular localisation. It is of interest in this project to review cellular cholesterol transporters in the context of  $\beta$ -cells.

Cholesterol efflux via HDL is facilitated by ATP-Binding Cassette (ABC) Subfamily G Member 1 and ABC Subfamily A Member 1 and these cholesterol transporters are expressed in  $\beta$ -cells. ABCG1 is also involved in intracellular cholesterol trafficking, including to insulin granules (97) and both ABCA1 and ABCG1 may facilitate cholesterol signalling by maintaining trans-bilayer asymmetry of the plasma membrane that responds to stimulation by cholesterol translocation (59).

Scavenger receptor class B type 1 (SR-B1) is widely expressed, including in  $\beta$ -cells (91), and is described as a 'lipid trader'. It both specifically hydrolyses cholesteryl ester (CE) from LDL particles, incorporating it into cell membranes, and facilitates cholesterol efflux to HDL particles (92). It is a multiligand receptor for HDL, modified LDL (oxidised and acetylated) and advanced glycation end-products and plays a minor role as a native LDL receptor.

Additional transport and storage facilitator molecules beyond the scope of this review contribute to cholesterol homeostasis, many of which are involved in cholesterol storage and related pathologies (70, 80, 98, 99). Interestingly, continuous cycling of free cholesterol through membrane and storage pools and between the esterified and hydrolysed forms supports cholesterol sensing (100), providing an additional rationale for the presence of a variety of

transporters in cholesterol sensitive tissue such as  $\beta$ -cells. Non-vesicular transfer of cholesterol also occurs rapidly at sites of membrane contact (100). Lipoprotein lipase (LpL), responsible for hydrolysis of triglycerides in VLDL and chylomicrons, and usually found tethered to endothelial cells in capillaries, is also expressed in  $\beta$ -cells in a leptin-dependent manner where its activity is stimulated by glucose, but its specific function in these cells is unknown (101).

### 1.2.5 Pathologies of cholesterol storage and trafficking

Much information regarding cholesterol and its metabolism has been derived through the study of primary hyperlipidaemias, that is, lipidaemias caused by genetic abnormalities. Several illustrative examples are included in this discussion. For instance, decreased LDL clearance in familial hypercholesterolaemia (FH) can be due to either an LDLR defect, defective apo B such that it is a poor ligand for the LDLR or increased catabolism of the LDLR. The LDL receptors, and consequently the role of LDL in CVD, were discovered through the study of FH (102). Genetic clues also facilitated the discovery of PCSK9 and its function in the disruption of LDLR recycling (cited in 103). Gain-of-function (104) and loss-of-function (105) PCSK9 mutations increase and decrease circulating LDL, respectively, due to reduced or increased (respectively) membrane surface LDLR expression. The reduced risk of CVD associated with loss of function mutations provides further evidence of the involvement of LDL in CVD.

The importance of synchronised steps in cholesterol synthesis to avoid intermediate accumulation, on the one hand, and to provide adequate intermediates for other biological processes, on the other hand, is demonstrated by various cholesterol-related pathologies (85). For example, the developmental disorder Smith-Lemli-Opitz syndrome is caused by failure to produce adequate 7-dehydrocholesterol reductase (DHCR7), the final enzyme in the K-R pathway of cholesterol synthesis. Furthermore, desmosterolosis, caused by mutations in the 24-dehydrocholesterol reductase (DHCR24) gene that converts desmosterol to cholesterol in the final step of the Bloch pathway, can also cause lethal abnormalities (106). These pathologies are characterised by both an accumulation of cholesterol intermediates and a deficiency in cholesterol.

In some instances, a tissue-specific requirement for the accumulation of certain intermediates exists. An example is follicular fluid meiosis activating sterol (FF-MAS, or 4,4-dimethyl-5 $\alpha$ -cholest-8,14,24-trien-3 $\beta$ -ol) and its male counterpart in the family of meiosis activating sterols, T-MAS, that stimulate oocyte and sperm maturation, respectively (107). Further research into the link between this cholesterol intermediate and fertility is ongoing (108). Besides highlighting the importance of regulating intermediates, these examples also demonstrate the under-appreciated role of cholesterol synthetic pathways during development.

The role of appropriate sterol trafficking, storage, intestinal uptake and degradation has been revealed by other cholesterol-related pathologies. For example, in Niemann-Pick type C, caused by mutations in the lipid transporters NPC1 or 2, a failure of appropriate cholesterol trafficking for storage results in cholesterol accumulation and progressive loss of brain function. Sitosterolaemia is similarly due to mutations in the cholesterol trafficking protein heterodimer ABCG5/8, causing increased gut cholesterol uptake and phytosterol accumulation (109).

A gene closely related to NPC1 and 2, known as NPC1L1, is also involved in cholesterol uptake in the intestine. This transporter was first described by Davies, Levy & Ioannou in 2000 (110) and later discovered to be the target of ezetimibe (111). Loss-of-function mutations in NPC1L1 reduce dietary cholesterol uptake and provide a 53% reduction in the risk of developing heart disease (112). Cholesteryl ester storage disease, due to lysosomal acid lipase deficiency and subsequent failure to degrade cholesteryl ester, results in accumulation of cholesteryl ester, hepatomegaly and accelerated atherosclerosis (113). Cholesteryl esters also accumulate in many tissues in Tangier Disease due to defective ABCA1 and loss of cholesterol efflux to HDL (114). This can result in large, yellow-orange tonsils, neuropathy, hepato- and splenomegaly, foam cell formation and premature myocardial infarction or stroke.

While primary hyperlipidaemias led to an understanding of how lipids are metabolised, most causes of hyperlipidaemia are secondary to other disease processes including T2D, non-alcoholic fatty liver and pancreas diseases (NAFLD (115) & NAFLD, (116, 117)), thyroid disease, and diet and energy imbalances such as is associated with excessive alcohol intake, obesity and metabolic syndrome. Many of the former have been associated with triglyceride and cholesterol dysregulation. These have thus also contributed to an understanding of factors which influence cholesterol metabolism. In fact, cholesterol became the focus of intense study following the 1910 discovery that atherosclerotic plaques contained 25-fold higher cholesterol than healthy vessels (103). Dysfunctional cholesterol metabolism may also be symptomatic in chronic neurological diseases such as Alzheimer, Huntington and Parkinson diseases, although it is not known whether cholesterol is a cause or consequence of pathophysiology (56, 96).

### 1.2.6 Cholesterol regulation

Cholesterol synthesis is tightly regulated, though variations up to hundreds of fold may occur (57). Its essential nature is emphasised by the many diseases of dysregulation. Beside general physiological influences such as genotype, circadian rhythm and body weight (118, 119), a complex endogenous regulatory network ensures cholesterol homeostasis.

Systemic cholesterol homeostasis is mainly achieved through three avenues: regulation of a) synthesis, b) gut absorption, and c) disposal. Synthesis and absorption have been found to

operate reciprocally such that when dietary absorption increases, synthesis is reduced (118). Additional tissue-specific regulation can be achieved by influx or efflux via lipoproteins.

### 1.2.6.1 Regulation of synthesis

Regulation of cholesterol synthesis was one of the first negative feedback regulatory mechanisms documented and took many years of dedicated research to fully describe. Indeed, the availability of more powerful technologies is facilitating new revelations, demonstrating ‘unforeseen complexity’ in this field (45).

Early research focused on HMGCR and its transcription factor, sterol-regulatory element-binding protein (SREBP-2). HMGCR is the key rate-limiting enzyme in cholesterol biosynthesis (120, 121). It, LDLR<sup>3</sup> and many other enzymes in the cholesterol pathway are subject to regulation by SREBP-2<sup>4</sup> (124), being transcriptionally down-regulated in response to increased cellular cholesterol from both nascent synthesis and LDL-derived sources (125). A delightfully accessible review, written by Brown and Goldstein, the Nobel laureates awarded for elucidating this complex mechanism, is available (57). Briefly, SREBP-2 is bound to the ER membrane, oriented in a hairpin shape, with the transcription factor (N-terminal) and regulatory (C-terminal) domains projecting into the cytosol and the mid-protein hydrophilic loop extending into the ER lumen (Figure 1.2). Proteolytic cleavage of SREBP-2 occurs twice to liberate the transcription factor domain for migration to the nucleus. A complex, sterol-dependent process is involved in its transportation to the Golgi, where this cleavage takes place. Briefly, in the presence of cholesterol, SREBP-2, complexed with SREBP cleavage-activating protein (SCAP), is anchored to the ER membrane by the association of cholesterol with insulin induced gene 1 or 2 (INSIG1 or 2). SCAP contains a domain known as MELADL that is rendered unavailable due to conformational changes when bound to INSIG. When cholesterol represents <5% of total ER lipids the MELADL site becomes available and a G-protein-containing complex known as Sar1/Sec 23/24 binds to MELADL. This event triggers the formation of a CopII vesicle containing the SREBP/SCAP complex and a portion of ER membrane, which is quickly sequestered to the Golgi. SREBP can then be cleaved, initially by site-1 protease (S1P) in the luminal loop, followed by the hydrophobic site-2 protease (S2P) in the first known example of regulated intramembrane proteolysis. This finally releases the transcription factor, which migrates to the nucleus and facilitates transcription of various target genes (126-130). Figure 1.2 illustrates these events.

---

<sup>3</sup> Howe *et al* (122) describes how LDLR and the two major rate-limiting enzymes in cholesterol synthesis (HMGCR and SQLE) can be regulated independently by different concentrations of SREBP-2. Only high concentrations of SREBP-2 influence transcription of the enzymes due to the presence of two sterol regulatory elements in the promoter regions, whereas LDLR has only one sterol regulatory element and lower SREBP2 concentrations are adequate to cause up-regulation.

<sup>4</sup> There are several forms of SREBP. SREBP-2 is mainly involved with cholesterol regulation while SREBP-1 has more influence on genes regulating fatty acid metabolism (123).



Further layers of synthetic regulation have also been described. A feedback loop exists between SREBP and INSIG1; SREBP also acts as a transcription factor for INSIG1. Additionally, rapid ubiquitination and degradation of INSIG1 occurs in the absence of sterols and in HMGCR in the presence of INSIG 1 or 2 and sterols (80, 131). Furthermore, squalene monooxygenase (SM) is thought to regulate flux in a cholesterol-dependent manner, not only by SREBP-related transcription, but also by proteasomal degradation (44).

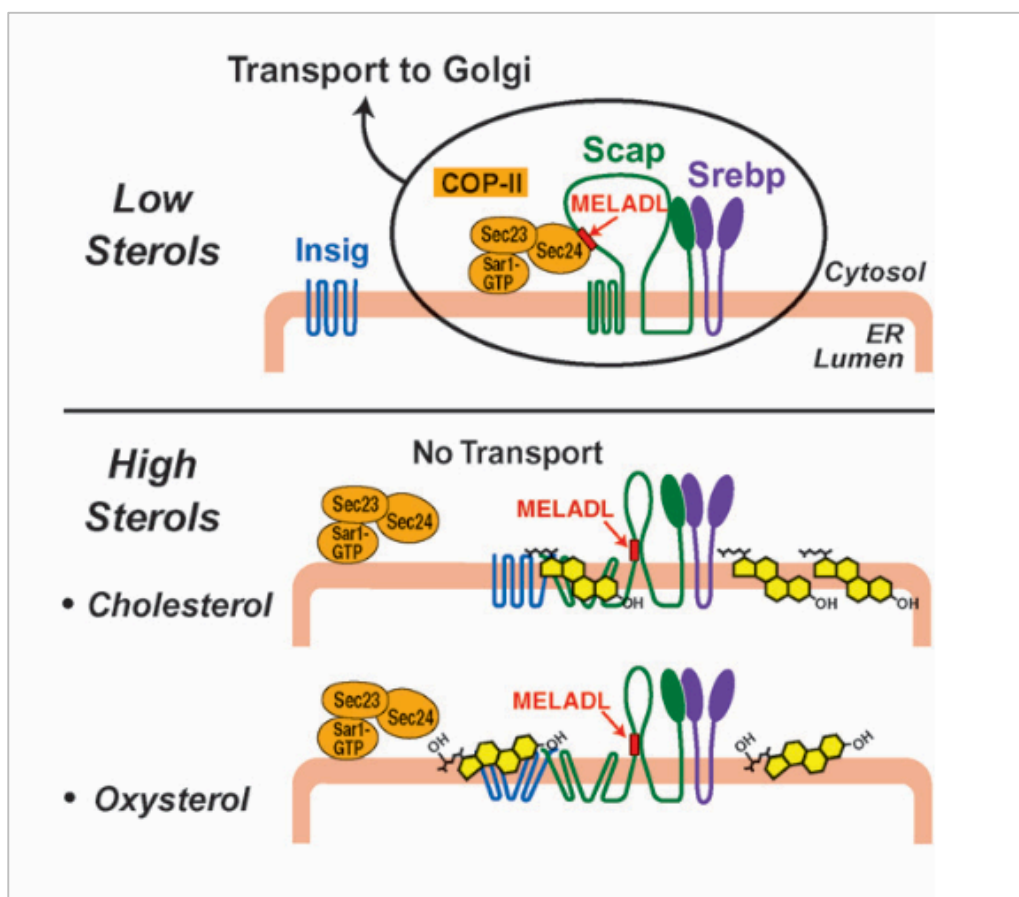


**Figure 1.2. Mechanisms of SREBP-mediated cholesterol regulation.**

In low sterol conditions, Insig is not bound to Scap. This allows access of the COPII coat protein complex Sar1/Sec23/Sec24 to the MELADL binding site and formation of a COPII vesicle containing SREBP, which is transported to the Golgi for processing. In high sterol conditions, oxysterols or cholesterol bind to Insig or Scap, respectively, causing conformational changes inhibiting MELADL site binding of COPII coat proteins. This image was originally published in the *Journal of Lipid Research*. Brown, M. S., and J. L. Goldstein. Cholesterol feedback: from Schoenheimer's bottle to Scap's MELADL. *J. Lipid Res.* 2009; 50: S15–S27. (57).

Other intermediates, for example desmosterol (132), (24S,25)-epoxycholesterol, (133) and DHCR24 (132) and DHCR7<sup>5</sup> (51), the terminal enzymes in the Bloch and K-R pathways, respectively, have also been implicated in negative feedback mechanisms for cholesterol regulation. An interesting proposition from Mitsche *et al*'s (50) work is that the two pathways of cholesterol synthesis could be subject to a degree of independent regulation. They postulated

<sup>5</sup> DHCR7 has also been recognised as a regulatory switch in Vitamin D synthesis, a metabolite of cholesterol (51).

that the K-R pathway could be constitutive, as it exhibited transcriptional regulation that was independent of SREBP. Further, tissue-specific regulation was documented. The Bloch pathway, under SREBP-2 control, was used preferentially in high cholesterol turnover tissue types such as those involved in steroid hormone production, where cholesterol was used as a substrate for further products, and synthesis fluctuated with demand.

Besides feedback by direct cholesterol intermediates, some oxysterol metabolites of intermediates are also thought to regulate cholesterol synthesis (85, 134). Additionally, non-cholesterol related regulation possibly occurs. For example, the membrane-bound ion pump  $\text{Na}^+\text{K}^+\text{ATPase}$  has been associated with cholesterol flux (135), as has the ratio between the abundant membrane phospholipid, phosphatidylcholine, and cholesterol (reviewed in 100). Ubiquitylation and proteasomal degradation is also important in the post-translational regulation of proteins involved in cholesterol synthesis, uptake and efflux (136).

#### 1.2.6.2 Regulation of intestinal uptake.

Synthesis of cholesterol is inversely linked with intestinal absorption to maintain an appropriate cholesterol balance (137). Cholesterol entering the gut is from two sources; dietary intake and cholesterol excreted from the liver via bile, which usually accounts for ~75% of lumen cholesterol content (70). Both biliary and dietary cholesterol are internalised by NPC1L1 in concert with clathrin and adaptor protein 2. The ABC transporter G5/G8 dimer facilitates cholesterol efflux from the enterocytes back into the lumen (reviewed in 70). While reciprocal changes clearly take place in cholesterol absorption in response to changes in synthesis and vice versa (118), the mechanisms of this regulation are not clearly understood. From mouse knockout studies, acetyl-CoA acetyltransferase 2 (ACAT2) (138), farnesoid X-receptor (FXR) (139) and mucin 1 (140) have all been implicated. Caveolin1 has also recently been found to play a role in lipid uptake in intestinal epithelial cells (141). Interestingly, caveolin 1 in intestinal epithelial cells also appears to be involved in LDL cholesterol regulation, although dietary cholesterol absorption is not interrupted by its absence.

#### 1.2.6.3 Cholesterol disposal

Apart from a small amount of cholesterol lost through sloughing of skin cells and in various secretions, most undergoes specific removal, as it is well-known that limited catabolism of cholesterol occurs *in vivo* (99). Post-lanosterol sterols (refer to Figure 1.1) can be lost to the systemic pool by i) formation of oxysterols for alternative biological functions, ii) hepatic conversion of cholesterol to bile acids and subsequent excretion and, more recently described, iii) transintestinal cholesterol excretion (TICE).

**Oxysterol formation.** In addition to tissue-specific synthesis of cholesterol metabolites such as Vitamin D and steroid hormones, metabolism of cholesterol and its post-lanosterol

intermediates is also hypothesised to be partly via formation of oxysterols and subsequent efflux for alternative biological processes (84, 142). For example, in mouse liver and cultured human hepatocytes, 5-10% of sterols produced were converted to dihydrolanosterol and exited the cholesterol biosynthetic pathway (50). However, many diseases are associated with oxysterol production including T2D (143), and much research is being undertaken in this emerging field (84), including the mechanisms of eventual elimination. Oxysterols efflux from the cell independently of HDL, i.e., without the rate limitation imposed by transporters, and may be particularly important as a cholesterol efflux alternative in low HDL environments such as in tendons. Oxysterol efflux is critical to cholesterol homeostasis in the rodent brain where the blood-brain barrier prevents the entry of lipoprotein particles (144, 145).

**Bile acids.** Cholesterol in the liver is metabolised to bile acids and transported via the gallbladder and bile ducts to the small intestine. These sterols may then be recycled via intestinal uptake or be excreted in the faeces. Regulation of bile acid synthesis occurs partly through bile acid binding to farnesoid X-receptor (FXR) and the subsequent release of an inhibitory fibroblast growth factor. Hepatobiliary excretion has been well described, and was thought to be the only route of exit for cholesterol. However, as pointed out previously (99, 146), a study revealing the faecal excretion of non-dietary neutral sterols in patients suffering total biliary occlusion (147), combined with more recent studies, offer compelling evidence for an alternative, independent pathway of transintestinal cholesterol excretion.

**Transintestinal cholesterol excretion.** Transintestinal cholesterol excretion (TICE) is the net excretion of cholesterol after accounting for bidirectional movement at both apical and basolateral surfaces of the enterocyte (reviewed in 99, 146). It appears to be mediated in part, at least in mice, by NPC1L1 and ABCG5/8 at the intestinal luminal surface where enterocytes take up cholesterol delivered by VLDL and LDL from the blood at the basolateral surface, but further characterisation is necessary. An important human stable isotope study has found that TICE accounts for 35% of neutral sterol excretion under basal conditions (148), and it is readily inducible by diet, physiological factors and pharmacotherapy (see reviews mentioned above). This makes it an interesting therapeutic target for dyslipidaemias, including in the context of CVD and T2D, as evidenced by the volume of very recent literature (99, 146, 148-152).

### 1.2.7 Therapies for cholesterol dyslipidaemias

Therapies for dyslipidaemia can be best understood and evaluated in terms of the regulatory mechanisms they target. The primary clinical goal is usually to lower LDL cholesterol levels. Lowering total cholesterol and triglycerides and increasing HDL cholesterol are secondary goals (153). To achieve this, reducing cholesterol synthesis with statins is typically the initial

pharmacological strategy<sup>6</sup>. Several pharmaceuticals are also available for decreasing intestinal cholesterol and bile acid uptake. More recently, interference with LDL receptor recycling and degradation has become an additional strategy with the development of PCSK9 inhibitors.

These therapeutic approaches are described briefly below.

Ezetimibe is a drug that reduces cholesterol uptake from the intestine and bile. It is a ligand for NPC1L1, a critical cholesterol transport protein in the brush border of the small intestine (154) and the hepatic canalicular membrane (155). Jakulj *et al* (148) demonstrate that in addition to inhibiting uptake, this protein also increases TICE (and thus faecal removal of cholesterol) by ~ 4-fold. Additionally, it has been found to significantly reduce cell membrane expression of ABCA1 (156), which mediates cholesterol efflux to HDL; however, the implications of this pleiotropic action are not known.

The LDL receptor cycles between the plasma membrane surface and endocytic vesicles, and proprotein convertase subtilisin/kexin type 9 (PCSK9) is a protease responsible for the degradation of the LDL receptor, preventing its recycling. Inhibition of this protease increases cell surface LDLR expression, with resulting increased uptake of LDL (reviewed in 157, 158). Two monoclonal antibody-based drugs targeted against PCSK9, evolucumab and alirocumab, have recently been approved by the Food and Drug Administration for selected patients (159), and Phase III clinical trials are ongoing for more general use.

Neither ezetimibe nor PCSK9 inhibitors are listed in ATPIII guidelines for cholesterol management, due partly to their recent arrival on the market. They are recommended in other recent therapeutic guidelines such as those published by the Baker International Diabetes Institute (approved by the NHMRC) (160). Other recommended therapies include bile acid sequestrants, nicotinic acid and fibric acids (153). Bile acid sequestrants such as cholestyramine, colestipol and colesevelam bind to bile acids in the intestine. The insoluble, indigestible complex is then excreted in the faeces, reducing enterohepatic recirculation (154, 161).

Nicotinic acid inhibits the key enzyme in the triglyceride synthesis pathway, diglycerol acyltransferase 2, inhibiting triglyceride and VLDL synthesis (162). Fibrates such as fenofibrate and gemfibrozil reduce triglycerides by activation of peroxisome proliferator-activated nuclear receptor (PPAR)  $\alpha$ , thereby increasing the transcription of genes involved in fatty acid  $\beta$ -oxidation (163). Notably, the latter agents influence plasma triglyceride concentrations, and are sometimes used in conjunction with plasma cholesterol reduction therapies.

---

<sup>6</sup>Three months is recommended to achieve LDL goals by means of lifestyle changes including dietary and exercise modifications usually precede initiation of drug therapy in Australia.

In addition to these oral therapies, bariatric surgery is successful in treating dyslipidemias, and related metabolic disorders such as obesity and accompanying insulin resistance (164). TICE is also regarded as a new potential target to correct lipid profiles. Currently-used drugs including PCSK9 inhibitors and ezetimibe are thought to increase TICE in addition to their main known effect (99). Plant sterols are also known to increase TICE and reduce dietary cholesterol uptake through competition for sterol transporters (99, 132). An interesting study by Santosa *et al* (118) describes a reciprocal relationship between cholesterol uptake and synthesis in association with commonly used cholesterol therapeutics, similar to that originally described in 1933 by Rudolf Schoenheimer with cholesterol measurements of his mice living in bottles (57). Drugs that reduce cholesterol synthesis also increase its uptake from the gut and vice-versa. For this reason, therapies are often combined using, for example, a gut-acting drug such as ezetimibe to compensate the pleiotropically increased cholesterol absorption of a co-administered statin. However, multiple medications can increase the risk of adverse events (165).

## 1.3 Statins

As mentioned above, statins are a class of drugs that competitively inhibit HMGCR, the first enzyme in cholesterol synthesis (see Section 1.2). Originally purified independently from two different moulds, *Aspergillus terreus* and *Monascus ruber*, the first statin, lovastatin, was approved for use by the FDA in 1987 (166). In the thirty years since, the statin class has grown to 6 commonly used drugs, revolutionising treatments for dyslipidaemia and becoming the most prescribed drug globally (167).

The statins are characterised by a molecular structure similar to HMG-CoA, the enzyme's substrate (168, 169). Different binding characteristics accompany variations in structure, with rosuvastatin having the greatest binding affinity (168). Pravastatin and rosuvastatin are hydrophilic, while others such as fluvastatin, simvastatin and atorvastatin are lipophilic. While hydrophilic forms of the drug are considered to be hepato-specific due to dependence on transporter proteins for entry into the cell, lipophilic statins have access to a greater range of tissues and are thus considered to be more prone to pleiotropic effects, both harmful and beneficial (170). Both hydrophilic and lipophilic statins can cross the blood-brain barrier, but, unlike its lipophilic counterpart simvastatin, pravastatin does not influence cholesterol synthesis in the brain (Thelen et al in 56).

### 1.3.1 Pharmacology/Dose/Elimination

The extent of intestinal absorption ranges from 30-98% for statins, depending on several factors including lipophobicity. Subsequently, hepatic selectivity is usually higher in hydrophilic statins (169). However, this may be affected by the availability of specific protein carriers

(171), which may account for the contradictory finding of high hepatic extraction in hepatic cell lines for statins other than pravastatin in one study (172).

Lipophilic statins are metabolised by the cytochrome P450 system, and thus potential interactions with other drugs similarly metabolised (e.g. warfarin) are considered by clinicians (Christians (1998) cited in 172). Grapefruit ingestion was also found to interact with some drugs including statins (173, 174). Indeed, cerivastatin was withdrawn from the market due to adverse drug-drug interactions with the fibrate gemfibrozil (175). Pravastatin, which is water soluble, does not undergo such metabolism.

Peak plasma concentration is achieved within 4 h (169). Plasma concentrations in the nanomolar range (e.g., 2-200 nmol/L for atorvastatin) can be expected from doses of 10-80 mg/day, but the bioavailability of statins is reduced by serum protein binding (176, 177). Metabolites of the lipophilic statins are excreted in the bile, whereas pravastatin is subject to glomerular filtration and renal excretion (172). The elimination half-life is 0.5-3.0 h for most statins (but up to 20 h for atorvastatin (177)), and this, combined with the synthesis of cholesterol on a circadian cycle and mainly at night, means statins are most effective when taken in the evening (169).

### 1.3.2 Lipid lowering mechanism

Statins mainly target the liver and reduce circulating plasma cholesterol through two interconnected mechanisms: reduced synthesis and increased LDL catabolism (169). Reduced synthesis is achieved by the competitive inhibition of HMGCR binding to its substrate, HMG-CoA. The reversible binding of statins to HMGCR is highly efficient, with an affinity in the nanomolar range compared to the micromolar range of the natural substrate, HMG-CoA (79, 178, 179). Due to the obligatory, rate-limiting nature of this enzyme, synthesis is strongly inhibited. Homeostatic responses to the reduction in membrane cholesterol (detailed in Section 1.2.6.1) result in up-regulation of numerous proteins to restore intracellular cholesterol, including HMGCR and the LDL receptor. The latter results in elevations in the net increase in LDL uptake and thus lowering of plasma LDL-cholesterol.

Surprisingly, these mechanisms have been examined *in vitro* but rarely *in vivo*. Furthermore, few studies have addressed the consequences of the expected accumulation of HMG-CoA, HMGCR's substrate, or other upstream components, such as acetyl CoA. Schonewille *et al* (180) recently set out to determine the statin-moderated cholesterol synthetic rate using <sup>13</sup>C-acetate, validated using deuterium oxide, in a statin-treated mouse model. They demonstrated a paradoxical increase in hepatic-specific cholesterol synthesis with statin treatment. They also reported an increase in faecal cholesterol excretion through either the hepatobiliary route (rosuvastatin and lovastatin) or TICE (atorvastatin) and a slight decrease in

plasma cholesterol. Both mRNA and protein levels of HMGCR were greatly increased, and HMG, measured as a proxy for HMG-CoA, was also increased, leading to the conclusion that up-regulation of the enzyme and accumulation of its natural substrate may out-compete statin inhibition. In humans, an 11.8-fold increase in HMGCR activity was demonstrated in microsomes from liver samples taken from 10 patients given pravastatin for 3 weeks before cholecystectomy, the final dose being 12 h prior to surgery (181), which supports this possibility. Not supportive, however, is the accompanying plasma cholesterol reduction of 26% in the pravastatin-treated patients.

The discovery that LDL and its receptor affect CVD arose from studies of familial hypercholesterolemia (FH) (182). FH patients who lack functional LDL receptors also find little or no benefit from statin therapy (183). The hypothesis that statins elevate LDLR expression on the plasma membrane, leading to increased LDL uptake was supported by experiments demonstrating that livers from dogs given a bile acid sequestrant and a statin (mevinolin, later known as lovastatin) showed increased <sup>125</sup>I-LDL binding (184). Similar results were found in rabbits fed cholesterol and treated with pravastatin or simvastatin (185). At the mRNA and protein levels, LDLR was upregulated after statin treatment *in vitro* in several hepatic cell lines (186, 187). Indirect evidence in humans is also available (188). In the first description of its kind in humans (43), the binding of radiolabelled LDL to liver biopsy homogenates taken from 5 patients undergoing cholecystectomy after 3 weeks of statin treatment demonstrated a 1.8-fold increase (181).

Further, it has been established that LDLR mRNA, but not HMGCR mRNA, is increased in circulating mononuclear cells after 4 weeks of atorvastatin treatment in healthy human volunteers (189) and that LDLR and HMGCR gene expression in humans are correlated (190), at least in the absence of statin therapy. Direct evidence of hepatic LDL receptor up-regulation *in vivo*, however, is difficult to find. Furthermore, LDL receptor knockout mice show reduced plasma cholesterol after statin treatment (191, 192) and mice with intact LDL receptors show little (180) or no (193) plasma cholesterol reduction. This could be due to the well-known differences in cholesterol metabolism between species, including the lesser role played by LDL in rodents (194). In hamsters, a more accurate model of human atherosclerotic plaque development, lovastatin did upregulate liver LDLR mRNA (195), however the possibility of a discontinuity between mRNA and protein expression means further studies (such as immunohistochemistry) would be beneficial.

### 1.3.3 Efficacy

While there may be continued discussion about precise mechanisms of action, the efficacy of statins in lowering LDL cholesterol levels in humans is undisputed; however, the extent to which they reduce risk of death from CVD is more controversial, particularly in the low risk

cohort. In a meta-analysis aimed at assessing the number needed to treat, statins did not reduce the risk of death from CVD when used in primary prevention. It prevented 1 in 60 statin users from non-fatal myocardial infarction and 1 in 268 from stroke (196). At the same time, 1 in 50 developed diabetes and 1 in 10 suffered muscle damage, while 98% saw no benefit. In contrast, another meta-analysis found a decreased risk of all-cause and cardiovascular mortality (RR=0.86, 0.69 respectively) in a population at high-risk of CVD but without previous events (197). Additional reviews and meta-analyses on both sides of the debate are available (198, 199), and criticism of methods have been made (for example, re the JUPITER clinical trial (200)), making an unbiased finding difficult. A website maintained by an independent group of physicians, ‘theNNT’ (numbers needed to treat), is designed to give impartial advice using a traffic light system. Statins prescribed for persons at low risk of CVD, for those without prior heart disease, and for acute coronary syndrome have been nominated red (not recommended) while green is given for heart disease prevention in persons with known heart disease ([www.thennt.com](http://www.thennt.com)).

These discrepancies fuel the debate about whether lowering LDL cholesterol is the most appropriate strategy towards protection against CVD. Genetic studies clearly show the relationship between high LDL cholesterol and CVD (103) but the ‘fireman at the fire’ suggestion, that cholesterol may be a responder to inflammatory conditions rather than a cause, persists. DuBroff (201) challenges the hypothesis that low plasma cholesterol prevents heart disease and demonstrates with a table of 44 randomised controlled trials that tested a variety of cholesterol lowering therapies (26 with statins or statin/other drug combinations), 30 of which did not show a reduction in CVD events. Hamuzaki (202) takes it one step further, providing evidence that, particularly in the elderly, high plasma cholesterol is protective.

### 1.3.4 Pleiotropy

The vital functions that cholesterol and its many intermediates play in the body and its exquisitely fine-tuned regulation suggest that pleiotropy can be anticipated with pharmacological interventions, and indeed this is the case for statins. Both beneficial and deleterious pleiotropic effects have been reported but for the purposes of this study the discussion will be limited to a brief mention of two effects of interest and a more complete investigation of T2D below and in Section 1.5, diabetes being of principal interest to this thesis.

#### 1.3.4.1 T2D

There is increasing evidence linking statins with a dose-dependent increased risk of T2D (203), but this is still contentious. Among a large panel of clinician experts, only 54% agreed that the diabetogenic effect is beyond doubt (204). Randomised controlled trials (RCT), observational epidemiological studies, meta-analyses of RCTs and a large Mendelian randomisation study all provide evidence of this effect (205) and these studies are summarised in Table 1.1. In



February 2012, the FDA published a safety update regarding this risk (206). However, as of 2015, no interventional studies existed with the primary goal of assessing the association of statin use with the onset of T2D (33). Recently, Park *et al* (207) have planned a prospective RCT comparing the diabetogenic effect of pitavastatin and atorvastatin, due to be completed in November 2019. A primary endpoint will be glycated haemoglobin (HbA1c) measured at baseline and after 24 months of statin treatment.

Evidence suggests that the benefit of statins outweighs the T2D risk, and practitioners are urged to prescribe statins with the individual needs of patients in mind (30). Moreover, causal aspects of the statin – T2D nexus are not yet fully elucidated. The evidence to date points broadly to several potential mechanisms related to both insulin secretion and resistance (208). Those related to insulin secretion and  $\beta$ -cell function are outlined in Section 1.5.

#### 1.3.4.2 Myopathy

Muscle pain and weakness is the most often reported adverse effect of statin therapy, affecting up to 1 in 10 users (209). It is beyond the scope of this project to explore this in depth but two points should be made. Firstly, reduced activity resulting from statin-related myopathy can contribute to lifestyle factors key to metabolic health and T2D (199). Secondly, there may be common mechanisms in myopathy and the diabetogenic effect of statins. This is explored in further detail below and in Section 1.5.2.

#### 1.3.4.3 Pleiotropy related to reactive oxygen species

Statins reportedly modulate oxidative stress mechanisms, but with apparently contradictory effects on systemic versus tissue oxidative stress. Diminished systemic oxidative stress has been reported as a beneficial pleiotropic effect of statins, providing additional benefits in the protection against CVD (210-213), although clinical observations do not always support this (214). The mechanisms of vascular oxidative benefits from statins are reviewed in Costa *et al* (210). Briefly, prenylation of small signalling molecules, specifically Rac1, is required for membrane localisation and its subsequent participation in the formation of the NADPH oxidase (Nox) 2 activating complex. Insufficient isoprenoids due to inhibition of the mevalonate pathway by statins means Rac1 is unavailable for its role in Nox2 activation. This reduces vascular ROS generation with beneficial consequences on reduced atherosclerotic plaque formation. Additional mechanisms may also play a role (210, 212). However, another perspective challenges this, whereby the suppression of cholesterol intermediates is thought to stimulate heart disease by a combination of factors including vitamin K<sub>2</sub> and selenoprotein deficiency and peroxidative stress (215).

**Table 1.1. Statin use and the risk of diabetes**

Full Study Name	Study	Type of study	Cohort - Dose	Participants Control arm or (Total)	Participants Treatment arm	Statin	Diabetes risk	Reference
The Pravastatin or Atorvastatin Evaluation and Infection Therapy trial	PROVE-IT	RCT	Moderate vs intense dose	1,688	1,707	All statins	(OR 1.01, CI 0.76 - 1.34)	(216)
	A to Z	RCT	Moderate vs intense dose	1,736	1,768	All statins	(HR 1.37, CI 0.94 - 2.01)	(216)
Taiwan National Health Insurance Resarch Database	NHIRD	Retrospective longitudinal study	High risk of CV events	33,648	4,448	All statins	(HR 1.11, CI 0.83 - 1.49)	(217)
Metabolic Syndrome in Men	METSIM	Prospective cohort study	Non-diabetic males, 45 - 73 years	6,607	2,142	All statins	(HR 1.46, CI 1.22 - 1.74)*	(218)
Treating to New Targets	TNT	RCT	80 mg vs 10 mg	3,797	3,798	Atorvastatin	(HR 1.16, CI 1.03 - 1.30)*	(219)
Incremental Decrease in Endpoints Through Aggressive Lipid Lowering	IDEAL	RCT	80 mg vs. Simvastatin 20 mg	3,724	3,737	Atorvastatin	(HR 1.19, CI 0.98 - 1.43)	(220)
Stroke Prevention by Aggressive Reduction in Cholesterol Levels	SPARCL	RCT	80 mg vs. placebo	1,898	1,905	Atorvastatin	(HR 1.37, CI 1.08 - 1.75)*	(220)
Collaborative Atorvastatin in Diabetes Trial	CARDS	RCT-discontinued prematurely	T2D	1,353	1,368	Atorvastatin	(HR 1.18, CI 1.08 - 1.29)*	(221)
Anglo-Scandinavian Cardiac Outcomes Trial-Lipid-Lowering Arm	ASCOT-LLA	RCT	10 mg vs. placebo	3,863	3,910	Atorvastatin	(HR 1.15, CI 0.91 - 1.44)	(220)
Air Force/Texas Coronary Atherosclerosis Prevention Study	AFCAPS/TEXCAPS	RCT	Normal TC and LDL, low HDL	3301	3308	Lovastatin	(OR 0.98, CI 0.70 - 1.38)	(222)
Japan Prevention Trial of Diabetes by Pitavastatin in Patients with Impaired Glucose Tolerance	J-PREDICT	RCT	Impaired glucose tolerance. 1-2 mg + lifestyle modifications vs lifestyle modifications only	(1,269)	Unknown	Pitavastatin	(HR 0.82, CI 0.68 - 0.99)*	(218)
PROspective Study of Pravastatin in the Elderly at Risk.	PROSPER	RCT	40 mg vs. placebo	2,513	2,510	Pravastatin	(HR 1.32, CI 1.03 - 1.69)*	(222)
West of Scotland Coronary Prevention Study	WOSCOPS	RCT	40 mg vs. placebo	2,975	2,999	Pravastatin	(HR 0.70, CI 0.50 - 0.99)	(220)
Long-term Intervention with Pravastatin in Ischemic Disease	LIPID	RCT	40 mg vs. placebo	3,501	3,496	Pravastatin	(HR 0.95, CI 0.77 - 1.16)	(220)
Management of Elevated Cholesterol in the Primary Prevention Group of Adult Japanese	MEGA	RCT	10-20 mg vs. no treatment	3,073	3,013	Pravastatin	(HR 1.07, CI 0.86 - 1.35)	(220)
Antihypertensive and Lipid-Lowering Treatment to Prevent Heart Attack Trial Lipid-Lowering Trial	ALLHAT-LLT	RCT	Hypertensive, hypercholesterolaemia 40 mg vs. no treatment	3,070	3,017	Pravastatin	(HR 1.15, CI 0.95 - 1.41)	(220)
Gruppo Italiano per lo Studiodella Sopravvivenza nell'InfartoMiocardico Prevenzione	GISSI PREV	RCT	20 mg vs. no treatment	1,717	1,743	Pravastatin	(HR 0.89, CI 0.67 - 1.20)	(220)
Justification for the Use of Statins in Prevention: an Intervention Trial Evaluating Rosuvastatin	JUPITER	RCT-discontinued prematurely	Primary prevention, 20 mg vs. placebo	8,901	8,901	Rosuvastatin	(HR 1.25, CI 1.05 - 1.49)*	(223)
Controlled Rosuvastatin Multinational Study in Heart Failure	CORONA	RCT	20 mg vs. placebo	1,763	1,771	Rosuvastatin	(HR 1.13, CI 0.86 - 1.50)	(220)
Gruppo Italiano per lo Studiodella Sopravvivenza nell'InfartoMiocardico-Heart Failure	GISSI HF	RCT	10 mg vs. placebo	1,718	1,660	Rosuvastatin	(HR 1.10, CI 0.89 - 1.35)	(220)
Scandinavian Simvastatin Survival Study	4S	RCT	20-40 mg vs. placebo	2,126	2,116	Simvastatin	(HR 1.03, CI 0.95 - 1.41)	(220)
Heart Protection Study	HPS	RCT	40 mg vs. placebo	7,282	7,291	Simvastatin	(HR 1.14, CI 0.98 - 1.33)	(220)
Study of the Effectiveness of Additional Reductions in Cholesterol and Homocysteine	SEARCH	RCT	Compared low to high dose (20, 80 mg/day)	5,399	5,398	Simvastatin	(OR 1.07, CI 0.95 - 1.21)	(216)
Women's Health Initiative	WHI	Prospective cohort study	Postmenopausal women	(143,006)	10,834	All statins	(HR 1.48, CI 1.38 - 1.59)*	(224)
				(143,006)	2,949	Lovastatin	(HR 1.35, CI 1.19 - 1.55)*	(224)
				(143,006)	3,247	Simvastatin	(HR 1.41, CI 1.25 - 1.61)*	(224)
				(143,006)	1,313	Fluvastatin	(HR 1.61, CI 1.35 - 1.92)*	(224)
				(143,006)	839	Atorvastatin	(HR 1.61, CI 1.26 - 2.06)*	(224)
				(143,006)	2,423	Pravastatin	(HR 1.63, CI 1.43 - 1.87)*	(224)
The Health Improvement Network	THIN trials	Retrospective longitudinal study	50-84 years of age statin vs no treatment	(3,765,906)	37,915	Simvastatin	(HR 1.14, CI 1.09 - 1.20)*	(225)
				(3,765,906)	7,438	Atorvastatin	(HR 1.22, CI 1.12 - 1.32)*	(225)
				(3,765,906)	1,442	Pravastatin	(HR 1.01, CI 0.84 - 1.21)	(225)
				(3,765,906)	1,175	Rosuvastatin	(HR 1.11, CI 0.89 - 1.38)	(225)
				(3,765,906)	282	Fluvastatin	(HR 1.02, CI 0.69 - 1.50)	(225)

RCT: random controlled trial; HR: hazard ratio; OR: odds ratio; CI: 95% confidence interval; \* Indicates significance (P < 0.05).

A differential effect in diverse tissues could help explain apparent inconsistencies between studies. In cardiac muscle, low levels of statin-induced ROS results in stimulation of mitochondrial biosynthesis, whereas in skeletal muscle, high ROS levels resulting from the same statin dose were deleterious to mitochondrial function (226). A later study from the same group further determined that atorvastatin (10 mg/kg/day for 14 days) increased oxidative stress to a greater degree in glycolytic (plantaris) than oxidative (soleus) muscle phenotypes in rats, possibly due to differences in antioxidant potential (227). Besides inter-tissue variations, differences in statin dose may play a role in the outcome of different studies. For example, dose-dependent (1-50 mg/kg/day) ROS-induced liver mitochondrial damage resulted from eight weeks of atorvastatin treatment in mice (228). However, in mitochondria isolated from rat livers, very low doses (1-3  $\mu$ M) of atorvastatin and simvastatin decreased mitochondrial oxidase activity (229). These studies demonstrate the wide range of information available and the difficulty in determining exactly what effect statins may have on oxidative mechanisms.

Such pleiotropy is of interest in this review as it pertains to possible diabetogenicity, and attention is now directed to glucose homeostasis and pancreatic  $\beta$ -cells, the source of insulin, a hormone largely responsible for the regulation of blood glucose.

## 1.4 $\beta$ -cells and Insulin secretion

Insulin is secreted exclusively by pancreatic  $\beta$ -cells in most mammalian species. Both controlled insulin secretion and appropriate insulin binding and signalling, i.e., sensitivity, are central to glycaemic homeostasis. This study focuses on the insulin secretion portion of glucose control; thus, it is important to understand the nature and function of  $\beta$ -cells.

$\beta$ -cells, each containing  $\sim$ 13,000 insulin-filled secretory granules (230, 231) make up the majority of cells in the endocrine pancreas in most species, accounting for approximately 50% or 60-80% of the mass of islets of Langerhans in humans and mice, respectively. However, islets exhibit considerable plasticity, their structure adjusting with development and over the life span as well as with changing metabolic requirements (232, 233). Although  $\beta$ -cells in mammals are usually long-lived, with low replication levels, proliferation rates can be increased in response to increased demand for insulin such as in loss of peripheral insulin sensitivity (234). Interestingly,  $\beta$ -cell function can also be influenced by maternal gestational glucose levels, with prenatal exposure to elevated glucose contributing to reduced peripheral insulin sensitivity and, independently, increased static  $\beta$ -cell response in childhood (235).

Within an islet  $\beta$ -cell population, considerable heterogeneity exists. For example, there is variability between cells in speed of responsiveness to small elevations in glucose, thus preventing over-

secretion of insulin in response to low stimulation (236). This differential glucose sensitivity may be due to distinctive enzyme expression; cells displaying lower sensitivity have been found to have increased expression of glycolytic but not mitochondrial enzymes (237). Proliferative versus mature  $\beta$ -cell populations can also be identified by fluorescence-activated cell sorting (FACS) (238). A recent, very interesting study has reported that 1-10% of  $\beta$ -cells demonstrate reduced insulin secretion but increased mitochondrial ATP generation, and possess pacemaker properties, acting as ‘hubs’ connecting many ‘follower’  $\beta$ -cells. They are responsible for a coordinated, whole-islet, calcium-dependent insulin response (239).

$\beta$ -cells are provided with an ample blood supply, estimated to be ten times more abundant than surrounding exocrine cells (234). Fenestrations in the walls of adjacent capillaries ensure adequate nutrient exchange. Innervation follows vascularisation, both chronologically in development and spatially (240). Autocrine and paracrine activity from intra- and extra-islet hormones and neurotransmitters play an important role in islet control, but human and rodent islets differ in the degree of innervation (241, 242). Further study is required to understand these differences and the exact role that neuronal control plays. It is known, however, that cholesterol-rich Schwann cells similar to those that myelinate the central nervous system surround neurons located in the islet (242) and it would be interesting to investigate what impact cholesterol-lowering drugs might have on these structures.

#### 1.4.1 $\beta$ -cells are metabolically distinct

$\beta$ -cells are exquisitely adapted towards tight control of serum glucose levels via the secretion of insulin in response to glucose stimulation<sup>1</sup>. Distinct metabolic features include specific metabolic pathways, obligatory continuous glucose flux and glucose sensing adaptations as outlined below (243-246).

Tight coupling of glycolytic flux to mitochondrial oxidation is achieved through a combination of  $\beta$ -cell-specific preferred and repressed pathways. Of these, it is perhaps the ‘forbidden’ pathways that are most extraordinary. In  $\beta$ -cells, lactate dehydrogenase (LDH) and monocarboxylate-1 transporter (MCT1) expression is repressed by several layers of inhibition, including epigenetic, pre- and post-translational inhibition (245, 247-249). This supports accurate glucose sensing and prevents the stimulation of inappropriate insulin secretion in response to production of lactate or pyruvate in extra-islet tissues. For example, anaerobic exercise can lead to hypoglycaemia in patients with MCT1-expressing insulinoma and in cases of inherited exercise-induced hyperinsulinism, where MCT1 repression in  $\beta$ -cells fails (250, 251). This adaptation also means that  $\beta$ -cell glycolysis is essentially aerobic (252), being deprived of the otherwise ubiquitous ability to convert pyruvate to lactate.

---

<sup>1</sup> In addition to glucose, the most important and physiologically relevant secretagogue, there are other nutrient, non-nutrient and therapeutic agents that stimulate insulin secretion.

Selective suppression of several additional genes in  $\beta$ -cells has been assessed, with five (including *Pdgfra*, *Igfbp4*, *Cxcl12*, *Oat* and *Cd302*) being verified by two independent microarray studies (245, 249, 253). The metabolic implications of these repressed genes are being investigated (245).

Less exclusively, some forms of hexokinase such as isoforms I and II are repressed in both islets and liver in favour of glucokinase (hexokinase IV), an isoform with a higher  $K_m$  of about 10 mM. This characteristic of glucokinase confers on  $\beta$ -cells the property of a rapid rise in activity proportional to an increase in glucose concentration. Importantly, glucokinase is not inhibited by its product, allowing continuous activity regardless of high glycolytic activity (234).

Similarly, the glucose transporter GLUT-2 is specific to liver and islets in rodents, and has low affinity for glucose. These adaptations protect against hypoglycaemia, allowing detection of changes in glucose within physiological concentrations ( $>4$  mM) but disallowing insulin secretion in response to very low levels of glucose (245, 246, 252). GLUT-3, known to be expressed in the brain, and the ubiquitously expressed glucose transporter 1 (GLUT-1) are the predominant glucose transporters in human islets (67, 254, 255). These two transporters have a higher affinity for glucose than GLUT-2, with  $K_m$  of 3-6.9, 11.2-17 and 1.4 mM for GLUT-1, 2 and 3, respectively (256, 257). It is not clear why low affinity glucose transporters are required for mouse but not human  $\beta$ -cells. The higher plasma glucose concentrations found in mice compared to humans may be one consideration. It may also be compensated for by the high  $K_m$  of glucokinase; however, this remains to be resolved.

Another selectively subdued process in  $\beta$ -cells relates to oxidative stress. Reduced levels of mRNA for microsomal glutathione S-transferase 1 (249) and 3 (253), glutathione peroxidase, catalase and various forms of superoxide dismutase (SOD) (258) have been reported. This exposes the  $\beta$ -cell to significant risk of oxidative damage, particularly considering its highly oxidative phenotype, and many studies have recorded a link between T2D and increased  $\beta$ -cell ROS (259-261). Pullen *et al* (245) have suggested that a signalling role for ROS in insulin secretion compensates the risk associated with this adaptation.

In addition to the specifically repressed pathways mentioned above, metabolic pathways favoured by  $\beta$ -cells also exist. First and foremost, only  $\beta$ -cells express insulin, and like other exocytic cells, they can efficiently up-regulate synthetic pathways to meet demand. Further preferential synthetic activity occurs in the expression of certain enzymes in relatively higher concentrations compared to other tissue, including glycerol-3-phosphate dehydrogenase (GPD1) and pyruvate carboxylase (252). GPD1 is found in two forms, cytosolic and mitochondrial, which must be expressed in equimolar proportions for functional glycerophosphate shuttle activity. The cytosolic form catalyses the reduction of dihydroxyacetone phosphate to glycerol-3-phosphate using a proton donated by nicotinamide adenine dinucleotide (NADH). The mitochondrial form catalyses the reverse oxidation

of glycerol-3-phosphate (G3P), simultaneously transferring two electrons to ubiquinone via flavin adenine dinucleotide (FAD). Thus, the GPD1 shuttle facilitates transport of reducing equivalents produced in the cytosol to complex II of the electron transport chain, concomitantly regenerating oxidised cytosolic nicotinamide adenine dinucleotide (NAD<sup>+</sup>) for further redox reactions (262). High activity of this shuttle, particularly in the context of low LDH, supports the coupling of glucose to ATP generation. GPD1 can also control triglyceride and lipid synthesis by providing competition for G3P acyltransferase, which uses the same substrate (G3P) to catalyse the first, and rate-limiting, step of lipid synthesis (262).

Other shuttles also operate in  $\beta$ -cells and impact on insulin secretion. These include the malate/aspartate shuttle that primarily provides reducing equivalents from glycolysis in the cytoplasm to the mitochondria, linking glycolysis to mitochondrial metabolism. The pyruvate/malate and pyruvate/citrate shuttles are also redox shuttles that regenerate NAD<sup>+</sup> for glycolysis, further linking fuel oxidation with insulin secretion (263).

Pyruvate carboxylase recycles CO<sub>2</sub> released during oxidation of fuels by carboxylation of pyruvate to oxaloacetate to replenish the tricarboxylic acid cycle (TCA) (264). This anaplerotic activity counters removal of citrate, malate or other intermediates from the TCA, possibly for use as coupling factors in insulin secretion as well as for glucose-stimulated protein synthesis, but not for diversion to the pentose phosphate pathway, which is suppressed in  $\beta$ -cells (252, 265, 266). Cataplerosis in  $\beta$ -cells during periods of chronic fuel overload includes citrate and lipid synthesis and release, possibly playing a role in excess fuel detoxification (243).

Overall, a delicate balance between unique  $\beta$ -cell function and survival is characterised by repression of anaerobic glycolysis and reduction of ROS defences to maximise ATP production and coupling of glucose sensing to insulin secretion. In conditions of metabolic stress such as in glucolipotoxicity or T2D, function may be sacrificed in favour of survival (245). This was demonstrated by increased expression of disallowed genes such as LDH and MCT1 with correspondingly increased anaerobic glycolysis and reduced coupling of glucose metabolism to insulin secretion in a 'genetic hypoxia' mouse model described by Pullen *et al* (245). The survival versus function hypothesis suggests that reduced insulin secretion may be a consequence rather than a mechanism of disease. Regardless, normally forbidden pathways that show up-regulation in the diseased state serve as potential therapeutic targets.

#### 1.4.2 Mechanism of insulin secretion

The mechanism of glucose-stimulated insulin secretion (GSIS) is well described. Glucose is transported into the cell via the constitutively expressed glucose transporter GLUT-2 (in rodents) and phosphorylated by glucokinase. Low expression of glucose 6-phosphatase ensures that glucose

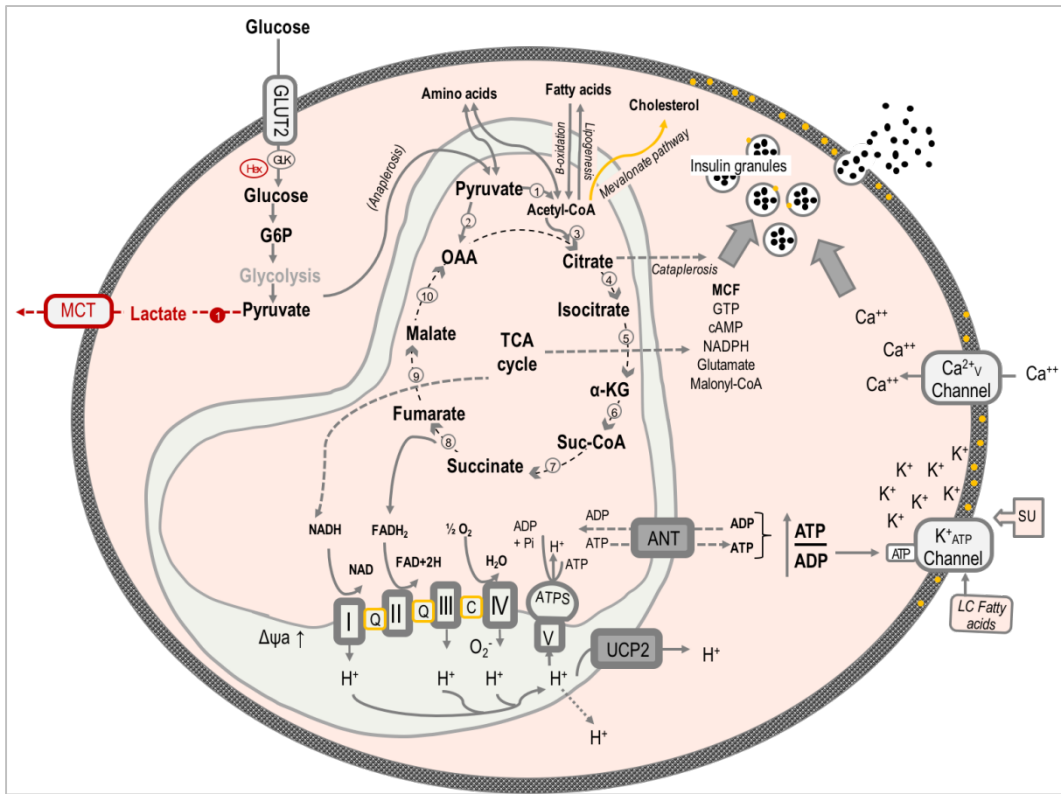


**Figure 1.3. Mitochondrial metabolism and insulin secretion in pancreatic  $\beta$ -cells.**

Products of all three major nutrient groups, carbohydrates, lipids and proteins, can undergo complete metabolism to  $\text{CO}_2$  and  $\text{H}_2\text{O}$  in the mitochondria. Pyruvate and Acetyl CoA enter the mitochondria and the TCA cycle, releasing reducing equivalents (NADPH from enzymes 1, 5, 6, and 10 and  $\text{FADH}_2$  from enzyme 8), which then enter the electron transport chain. During their re-oxidation, protons ( $\text{H}^+$ ) are pumped into the inter-membrane space as they progress through the electron transport chain consisting of NADH dehydrogenase (Complex I), succinate dehydrogenase (Complex II), cytochrome bc1 (Complex III) and cytochrome c oxidase (Complex IV). Coenzyme Q10 (Q) and Cytochrome C (C) assist by safely transporting electrons or free radicals during this process. The resulting proton gradient between the inner and outer mitochondrial membrane drives the conversion of  $\text{ADP} + \text{inorganic phosphate}$  to ATP by ATP synthase (Complex V), and ADP and ATP are exchanged between the mitochondria and cytosol by the adenine nucleotide translocator (ANT). In  $\beta$ -cells, the resulting increase in the ATP:ADP ratio causes closure of the  $\text{K}^+\text{ATP}$  channel, followed by membrane depolarisation and  $\text{Ca}^{2+}$  influx. This, in turn, facilitates fusion of insulin granules to the membrane and insulin exocytosis. Sulphonylureas (SU) are non-nutrient secretagogues that act directly on the  $\text{K}^+\text{ATP}$  channel. Long chain fatty acids may also influence closure of this ion channel. Cataplerosis, export of TCA intermediates for alternative fates, occurs largely at citrate, and produces mitochondrial coupling factors (MCF) which potentiate insulin secretion during fuel abundance. Replenishment of the TCA metabolites (anaplerosis) consequently occurs at high rates in  $\beta$ -cells, mainly entering as pyruvate. Cholesterol and other products of the mevalonate pathway (gold) are required for stabilisation of membrane proteins, as electron acceptors and antioxidants. Metabolites, transporters and enzymes in red are repressed pathways in  $\beta$ -cells that are increased in  $\beta$ -cell dedifferentiation. ① Pyruvate dehydrogenase, ② Pyruvate carboxylase ③ Citrate synthase ④ Aconitase ⑤ Isocitrate dehydrogenase ⑥  $\alpha$ -ketoglutarate dehydrogenase ⑦ Succinate thiokinase ⑧ Succinate dehydrogenase ⑨ Fumarase ⑩ Malate dehydrogenase ⑪, Lactate dehydrogenase. Adapted from Newsholme et al (267).

entering the  $\beta$ -cell does not exit after phosphorylation. It then undergoes aerobic glycolysis and, usually, complete oxidation through the mitochondrial TCA cycle, concomitantly producing ATP. The resulting increased ATP/ADP ratio stimulates closure of

ATP sensitive potassium channels ( $K^+_{ATP}$ ), causing membrane depolarisation and associated opening of voltage gated L-type calcium channels ( $Ca_v^{2+}$ ). The subsequent influx of calcium ions facilitates fusion of stored insulin granules with the membrane and, finally, exocytosis of insulin into the extracellular compartment (248, 268).

In addition to the canonical sequence of events described above, calcium-independent insulin exocytosis has been stimulated by the addition of guanine nucleotides (269), or by cell swelling caused by hypotonic media (270). Interestingly, in cells pre-depleted by 1 h of fuel-free, sulphonylurea-driven insulin secretion, further insulin amplification, also termed non-triggering stimulation, was induced by glucose (271, 272). Cytosolic acetyl-CoA, rather than energy generated by TCA oxidation, provided the signalling mechanism for this phenomenon, though other stimulus-secretion coupling factors have previously been suggested (273), as detailed in a review of insulin triggering and amplifying pathways (274).

While glucose is the most important and physiologically relevant secretagogue, other nutrient, non-nutrient and therapeutic agents can also stimulate insulin secretion, either via ATP production and the established glucose stimulus-secretion pathway, or more directly by binding to the  $K^+_{ATP}$  channel. Non-glucose nutrient secretagogues include amino acids, which enter the TCA cycle at various entry points and proceed to ATP generation, usually in conjunction with complete oxidation. For example, glutamate, glutamine, proline, histidine and arginine can be converted to  $\alpha$ -ketoglutarate, while phenylalanine and tyrosine enter the TCA cycle as fumarate (264). In addition, fatty acids can potentiate insulin secretion after esterification by various other means elaborated further below (275). Some amino acids can also stimulate insulin secretion by alternative means and are worth special mention.

Glutamine, with a blood concentration of  $\sim 0.5$  mM, is the most abundant amino acid in mammals (276). It has important roles in ammonia scavenging during the metabolism of other amino acids and redox control via its product, glutathione (277), and levels in the tissues are usually quite stable. In line with its abundance and to prevent hypoglycaemia, it does not independently stimulate insulin secretion. However, leucine allosterically activates glutamate dehydrogenase, providing a ready means of glutamine entry to the TCA cycle by conversion to  $\alpha$ -ketoglutarate via glutamate<sup>2</sup>, thereby generating ATP. Thus, at high concentrations (10 mM) L-leucine in combination with L-glutamine

---

<sup>2</sup> Glutamine is deamidated to glutamate by glutaminase, releasing ammonia. Glutamate can then be deaminated to  $\alpha$ -ketoglutarate by glutamate dehydrogenase, also releasing ammonia.



can potently stimulate insulin secretion via oxidation, ATP production, closure of the  $K^+_{ATP}$  channel, membrane depolarisation, and  $Ca^{2+}$  influx (278, 279). A similar mechanism underlies the hypoglycaemia after a protein meal in patients with gain-of-function mutations in glutamate dehydrogenase (280).<sup>3</sup>

Both glutamine and alanine are consumed at high rates in BRIN-BD11 cells (276). L-alanine increases insulin secretion in the presence of glucose. This occurs by enhancement of glucose metabolism (281). Glucose-derived glutamate pools are increased in the presence of L-alanine, and glutamate possibly acts as a metabolic coupling factor in insulin secretion (281, 282). Interestingly, a small portion (10-20%) of the stimulatory effect of L-alanine on insulin secretion can be attributed to increases in  $Ca^{2+}$  influx associated with co-transportation of  $Na^+$  (281, 283).

Insulin secretion can also be influenced by fatty acid metabolism and by signalling via metabolism-dependent and independent processes. Acetyl-CoA derived from fatty acid  $\beta$ -oxidation is used as a substrate for generation of ATP via the TCA cycle in low glucose conditions. However, free fatty acids (FFA) can further stimulate insulin secretion in high glucose states by the formation of lipid signalling molecules including long chain acyl CoA's, mono- and diacylglycerols and phosphatic acids (275, 284). Interactions between the latter and plasma membrane-bound G-protein coupled receptors (e.g. FFAR1 or GPR40) initiate a signalling cascade that ultimately activates protein kinase C or triggers  $Ca^{2+}$  release from the ER, potentiating insulin secretion (284). In contrast, long-term FFA exposure reduces insulin secretion (284, 285).

Non-nutrient secretagogues are also important in insulin stimulatory processes. Glucagon-like peptide 1 (GLP-1) is an incretin hormone secreted by intestinal L-cells that potentiates the insulin response to glucose, accounting for up to half the insulin secreted postprandially (286). Analogues of GLP-1 have recently been made available for therapeutic purposes in the treatment of T2D (287). How GLP-1 amplifies insulin secretion has been the subject of recent study, with four main mechanisms described. Firstly, GLP-1 binds to its G-protein coupled receptor expressed on the plasma membrane of  $\beta$ -cells, with subsequent signalling via adenylate cyclase leading to cyclic adenosine monophosphate (cAMP) generation and activation of protein kinase A (PKA) and the cAMP-binding protein Epac2A. This stimulates calcium release and enhanced exocytosis both directly (via synaptotagmin-7, see 288) and by binding the sulphonylurea receptor SUR1, causing  $K^+_{ATP}$  closure (reviewed in 289). Secondly, Shigeto *et al* (290) demonstrated that a further G-protein coupled link to the GLP-1 receptor resulted in activation of PKC at physiologically relevant GLP-1 and glucose concentrations (1 pM and 6 mM, respectively). This pathway accounted for ~40% of the

---

<sup>3</sup> Glutamate dehydrogenase is thought to act as an intracellular energy sensor. On one hand, it is inhibited allosterically by ATP and GTP, while ADP, GDP and L-leucine (in low phosphate potential conditions), stimulate its activity (280).

GLP-1 stimulatory effect, causing  $K^+_{ATP}$  independent calcium oscillations mediated by  $Na^+$  channels (TRPM4 and TRPM5) rather than the  $Ca_v^{2+}$  channels associated with the canonical insulin triggering pathway. They further established a third mechanism, that of GLP-1-mediated recruitment of additional  $\beta$ -cells to stimulated secretion (5% or 65% without or with GLP-1, respectively) at low GLP-1 concentrations. Fourth, there is some evidence that GLP-1 may stimulate vagal reflex pathways, initiating a neuronal-mediated insulintropic effect (291) (see also 292).

Sulphonylureas, used therapeutically to stimulate insulin secretion, bind to the SUR1 moiety of  $K^+_{ATP}$ , causing channel closure followed by membrane depolarisation,  $Ca^{2+}$  influx and insulin exocytosis (293-295). Maximal sulphonylurea-mediated channel closure requires the presence of intracellular adenosine nucleotides, in particular, ADP (294). In addition to direct action on  $K^+_{ATP}$ , many sulphonylureas (including tolbutamide and glyburide used in this study<sup>4</sup>) also bind Epac2A, similarly to GLP-1 receptor agonists. This increases  $Ca^{2+}$  influx and stimulates granule fusion and exocytosis (293). Of interest in this study, but aside from its insulin stimulating effects, sulphonylureas are also known to reduce glucagon secretion and decrease hepatic insulin clearance. Glyburide also reportedly inhibits cholesterol efflux mediated by ABCA1 (295).

An additional non-nutrient means of stimulating insulin secretion *in vitro* is by  $K^+$ -mediated depolarisation. An extracellular  $K^+$  concentration of 30 mM in the presence of diazoxide (which prevents channel closure) causes membrane depolarisation similar in amplitude to that of 10 mM glucose (296). The resulting monophasic insulin response differs from nutrient or therapeutically stimulated responses in that the effect is entirely due to membrane depolarisation, whereas nutrient or therapeutic secretagogues stimulate biphasic secretion, usually by concurrent stimulation of more than one pathway. Nevertheless, the use of depolarising concentrations of  $K^+$  is a relevant research tool, particularly to pre-trigger secretion when studying the amplifying aspect of glucose or nutrient insulin stimulation (297). Interestingly,  $K^+$  stimulates secretion at lower concentrations in conjunction with tolbutamide, a sulphonylurea, possibly due to variations in the pattern of  $Ca^{2+}$  influx stimulated by  $K^+$  alone.

The discussion above outlines various means of stimulating insulin secretion in health and disease. In T2D, additional requirements for insulin arise from the effects of peripheral insulin resistance, brought about at least in part by the diabetic environment, including dyslipidaemia.

---

<sup>4</sup> Tolbutamide, a first generation sulphonylurea, binds to the A site of SUR1 (on the eighth cytosolic loop) while glyburide (2nd generation) binds to the same site in addition to the B sites of both SUR1 and SUR2A (on the third cytosolic loop) (293).

## 1.5 The insulin/cholesterol link

Both high and low plasma cholesterol are associated with T2D. In the first instance, T2D patients have an increased risk of cardiovascular disease and obesity, over-nutrition and dyslipidaemia are risk factors for T2D. In the second instance statin use, known to effectively lower LDL cholesterol, is associated with increased risk of new onset diabetes (298). Interestingly, Mendelian randomisation studies reveal that some genetic variations of the HMGCR gene with similar LDL-lowering effects are also associated with increased risk of T2D, supporting the notion that on-target statin mechanisms are involved (205, 299-301). However, reduced insulin secretion associated with simvastatin was not rescued by the provision of DL-mevanolactone, a mevalonate synthesis activator, or the isoprenoid moieties GGPP and FPP (302). Despite this finding, it is known that protein farnesylation is required for insulin secretion induced in response to mitochondrial fuel (303), and statins (or otherwise dysfunctional HMGCR) would be expected to inhibit both farnesylation and geranylgeranylation (304). This diversity of results makes it difficult to determine whether inhibition of the cholesterol synthetic pathway is directly responsible for the diabetogenic effects of statin.

Conversely, patients with genetic variations causing familial hypercholesterolaemia, associated with higher circulating LDL cholesterol, have decreased risk of T2D (305). This suggests a complex link between insulin secretion and/or action and cholesterol, with optimal cholesterol synthesis, dietary intake and circulating plasma levels being associated with glycaemic health.

Various research endeavours have attempted to shed light on the relationship between cholesterol and insulin, with a confusing abundance of information available. The following discussion focuses on the influence of cholesterol on insulin secretion. The literature has been divided into the categories of a) membrane characteristics and associated proteins, b) metabolic pathways, c) mitochondrial function and d) ROS. For the purposes of this discussion, statin therapy is considered to be cholesterol lowering in the context of plasma LDL cholesterol (despite evidence of intracellular cholesterol enhancing effects in hepatic cells (180)), and a distinction is not specifically made between pleiotropic and direct cholesterol effects.

### 1.5.1 Membrane characteristics and associated proteins

The physicochemical effects of cholesterol on membrane characteristics provide scope for influences on the function of membrane proteins, the latter comprising ~25% of the membrane cross-sectional area (306). Proteins involved both in the processes of glucose sensing and in insulin granule exocytosis may be subject to these effects. For example, Xia *et al* (69) have demonstrated that cholesterol sequestration using M $\beta$ CD, a cholesterol sequestering agent, disrupted lipid rafts and redistributed functional membrane proteins, including those pivotal in glucose sensing, stimulus-

secretion coupling and exocytotic processes in glucose sensitive insulin secretion. The effect of high and low cholesterol on these processes is reviewed below.

#### 1.5.1.1 Glucose transporters

GLUT-1 and GLUT-2, the major glucose transporters in human and rodent  $\beta$ -cells, respectively, are not associated with lipid rafts in the cell membrane (307). On the contrary, transport to raft areas, as occurs during faulty glycosylation, is detrimental to these glycoproteins and M $\beta$ CD-mediated raft disruption is beneficial to their function (67). Based on observed effects in other cells, Wang *et al* (308) speculate that omega-3 polyunsaturated fatty acids may similarly disrupt lipid rafts, increasing glucose transport and insulin secretion. On the other hand, chronically increased fatty acid consumption can damage glycosylation processes, reducing cell surface expression and glucose uptake (309, 310). This impairment is potentially facilitated by increased ROS, discussed further in Section 1.5.3.

In apparent conflict to the pattern above, where decreased cholesterol seems to facilitate glucose transporter function, protein and mRNA expression of GLUT-2 were reduced after 48 h simvastatin treatment (2-10  $\mu$ M) in MIN6  $\beta$ -cells (68). The mechanism of this impairment is not known, and glucose uptake was not measured. In fact, this finding does not exclude the possibility of increased function, as reduced expression could potentially be a homeostatic response to prevent excessive glucose transport in the case of increased glucose uptake.

#### 1.5.1.2 Ion channels

Calcium channels ( $\text{Ca}_v^{2+}$ ) and voltage gated potassium channels ( $\text{K}_{\text{ATP}}^+$ ) are both membrane-associated proteins crucial to GSIS. Studies delineating disease mechanisms involving mutations in Kir6.2 and SUR1, that together form an important  $\text{K}_{\text{ATP}}^+$  channel in  $\beta$ -cells, reveal the key role of this ion channel in coupling metabolically derived stimulus (ATP/ADP ratio) to membrane depolarisation and insulin secretion (293, 311-313). The mechanisms of metabolic regulation of  $\text{K}_{\text{ATP}}^+$  channels are very complex and are reviewed elsewhere (314-317).<sup>5</sup>

There is debate over the location of  $\text{K}_{\text{ATP}}^+$  channels in  $\beta$ -cells, and they do not appear to be targeted to lipid rafts (69). While studies by Geng *et al* (319) demonstrate that the components of  $\text{K}_{\text{ATP}}^+$  channels, Kir6.2 and SUR1, are predominantly expressed on secretory granule membranes, electrophysiology and other functional studies clearly demonstrate a plasma membrane location (315, 320, 321). One potential explanation could be the presence of more than one type of  $\text{K}_{\text{ATP}}^+$  channel in  $\beta$ -cells, given that four isoforms of voltage-gated  $\text{K}^+$  channels are expressed in insulinoma and

---

<sup>5</sup> The  $\text{K}_{\text{ATP}}^+$  channel also senses glucose in the hypothalamus and can influence insulin action via the vagus nerve (318).

isolated islet  $\beta$ -cells (69). In contrast, the calcium channel mainly associated with GSIS,  $\text{Ca}_v$  1.3 ( $\text{Ca}_v^{2+}$ ), is targeted to lipid rafts in INS-1 cells (65).

$\text{K}_{\text{ATP}}^+$  channels are subject to functional changes in association with simvastatin treatment (68). Changes reported include up-regulation at both mRNA and protein levels and increased current density. Elsewhere, studies have implicated  $\text{K}_{\text{ATP}}^+$  in pleiotropic statin effects in several tissue types (322). Just how statins cause changes in  $\text{K}_{\text{ATP}}^+$  function, however, is not clear. Statins may pleiotropically activate  $\text{K}_{\text{ATP}}^+$  channels through inhibition of HMGCR and consequent accumulation of acetyl CoA, which may alternatively form long-chain acyl-CoA esters capable of direct interaction with the Kir6.2 unit, increasing the open probability and decreasing its sensitivity to ATP (322). Simvastatin reportedly increased the expression of the  $\text{K}_{\text{ATP}}^+$  channel, which together with decreased expression of  $\text{Ca}_v^{2+}$ , inhibited membrane depolarisation and calcium influx (68, 218). Statins may also decrease coupling by up-regulation of uncoupling protein 2 (317). Together, this could explain why tolbutamide, but not GLP-1 agonists (which additionally stimulate  $\text{K}_{\text{ATP}}^+$ -independent secretion) failed to induce insulin secretion in simvastatin-treated MIN6 cells (302).

The diabetogenicity of statins may also be related to their effect on calcium channels. Yaluri *et al* (302) found that simvastatin not only reduced insulin exocytosis in MIN6  $\beta$ -cells, but it also inhibited normal calcium influx in high glucose conditions (16.7 mM) as detected by live imaging with Fura-2-AM staining. A simvastatin-mediated effect on L-type calcium channels has also been determined in  $\beta$ -cells by alternative protocols (68, 323). Elsewhere, calcium flux was directly involved in impaired insulin secretion associated with rosuvastatin treatment, characterised by changes in calcium oscillations and accumulation of insulin granules at the plasma membrane (324).

#### 1.5.1.3 Granule fusion, SNARE proteins and exocytosis

Insulin exocytosis involves the calcium-stimulated fusion of insulin-containing granules with the plasma membrane. Several proteins that form a soluble N-ethylmaleimide sensitive fusion protein attachment protein receptor (SNARE) complex are involved in this process and include synaptosome-associated protein of 25 kD (SNAP-25), vesicle-associated membrane protein isoform 2 (VAMP2) and syntaxin-1. Cholesterol is thought to facilitate fusion, its intrinsic negative curvature providing suitable mechanical stability and lowering energy barriers for the formation of transient fusion structures (73, 325). Cholesterol also stabilises SNARE proteins within the membrane (73).

Caveolin-1 is associated with VAMP2 in  $\beta$ -cells (326) and links SNARE proteins on the membranes of the plasma to granules via its association with Cdc42, a small prenylated G-protein (327). It organises membrane domains in a cholesterol-dependent manner (328), and interestingly, also has a role in cholesterol efflux and homeostasis (329).

M $\beta$ CD-mediated cholesterol desorption increased (69, 330) or reduced (331) glucose stimulated insulin secretion (GSIS), after high (10 mM) doses in HIT-T15 or RIN-m5f  $\beta$ -cells or low (0.1 mM) doses in perfused mouse pancreas, respectively. In the latter perfused mouse pancreas study, provision of exogenous cholesterol in the perfusion media rescued insulin secretion. In INS-1 and INS-1E  $\beta$ -cells, Bacova *et al* (332) also found reduced GSIS after high dose M $\beta$ CD when expressed as a function of basal secretion, although basal secretion increased. This supports the suggestion by Vikman *et al* (331) that high dose M $\beta$ CD may impair membrane integrity, allowing unregulated insulin secretion. They found that reduced GSIS associated with cholesterol desorption in isolated mouse  $\beta$ -cells was related to relocation of SNAP-25 from the plasma membrane to cytosolic areas attendant with fewer docked insulin granules, while addition of cholesterol ameliorated these effects.

Interestingly, cholesterol reduction by statins also influences secretory granules and exocytosis. Lovastatin treatment increased the size of secretory granules but with a concomitant decrease in insulin content (71). Similarly to M $\beta$ CD treatments, pravastatin treatment also reduced insulin secretion in association with reduced expression of SNARE proteins (192).

In other secretory cells, similar exocytotic mechanisms enable further insight. For example, cholesterol content (manipulated by M $\beta$ CD or c-M $\beta$ CD) influenced the kinetics of exocytosis and the formation of fusion pores in platelets (333). While SNARE proteins were not measured directly in this study, the results align with a critical role of cholesterol in biophysical processes important for the correct function of exocytotic machinery. Likewise, reduced cholesterol levels impaired synaptic vesicle exocytosis in cultured neurons, with evidence of the involvement of SNARE protein function (334). Further, lipophilic (simvastatin and fluvastatin) but not hydrophilic (pravastatin) statins were also found to suppress the cytotoxic activity of human natural killer cells by inhibiting exocytosis (335).

Cholesterol loading experiments also suggest a direct effect of cholesterol on exocytosis. Studies by Bogan *et al* (336) and Wijesekara *et al* (337) in MIN6 cells and mouse islets, respectively, demonstrated that such loading results in cholesterol accumulation in insulin granules, a process influenced by ABCA1. This inhibited GSIS and reduced the number of fusion events, measured by fluorescently conjugated VAMP2. Interestingly, an increase in cholesterol content could also be achieved by exposure to high glucose (30 mM for 36 h), similarly resulting in increased granule size (336). This demonstrates a link between hyperglycaemia, cholesterol accumulation and changes in granule morphology that could impair exocytosis. Additionally, SNARE proteins are under-expressed in T2D (338), supporting a role for faulty exocytosis in the pathology of this condition.

Sequential exocytosis is the fusion of an insulin granule to another granule already undergoing exocytosis. This happens rarely in normal  $\beta$ -cells, may have a role in fuel sensing, and potentially

involves SNAP25. M $\beta$ CD increases the rate of this phenomenon (339), providing further evidence of the importance of cholesterol in various aspects of granule fusion and exocytosis.

In addition to cholesterol, some of its biosynthetic pathway intermediates (71) or associated lipids and their protein interactions (64) may also play a role in exocytosis regulation, secretory granule formation and GSIS. Together, these studies highlight the important role of SNARE proteins in insulin secretion, and the relationship between cholesterol and their functional regulation and cellular location.

#### 1.5.1.4 ABCA1/ABCG1 cholesterol transport

Key to cellular homeostasis of cholesterol are the cholesterol transport proteins ATP-binding cassette (ABC) transporters family A member 1 and family G member 1. ABCA1 and ABCG1 mediate cholesterol efflux in a complementary manner, binding nascent and more mature forms of HDL, respectively, for cholesterol efflux (340). Much of the cholesterol efflux research has been performed in macrophages due to their relevance in vascular disease. However, as discussed below, the role of these cholesterol transporters in the  $\beta$ -cell may be unique, a possibility emphasised by the finding that each are down-regulated in islets from T2D donors and insulin secretion is inhibited in their absence (341, 342).

$\beta$ -cell specific ABCA1 knockout in mice resulted in islet lipid accumulation, impaired glucose tolerance and reduced insulin secretion despite increased insulin content, but with normal fasting glucose levels and insulin sensitivity. In addition, ABCG1 was up-regulated, possibly to partially compensate for the loss of ABCA1 (343). To understand the mechanism of this effect of  $\beta$ -cell-specific ABCA1 knockout Kruit *et al* (341) methodically sought to identify the stage of insulin secretion that was affected in ABCA1-null islets. They determined that diminished GSIS was due to cholesterol accumulation, evidenced by decreased capacitance during membrane depolarisation (despite normal Ca<sup>2+</sup> content), alterations to Golgi structures and altered plasma microdomain organisation. Notably, insulin granule exocytosis was rescued after gentle M $\beta$ CD cholesterol depletion.

ABCG1 is expressed abundantly in pancreatic  $\beta$ -cells (342). While ABCG1-deficient mice show no changes in serum lipoprotein fractions or islet or  $\beta$ -cell total cholesterol content, they do display reduced insulin secretion and glucose intolerance *in vivo*, and reduced GSIS in isolated islets, indicating a role for ABCG1 in insulin secretion. Further, ABCG1 in  $\beta$ -cells is expressed mainly intracellularly, co-staining extensively with insulin in granules, which show enlargement and cholesterol deficiency in ABCG1 knockout cells. Importantly, cholesterol provided via c-M $\beta$ CD restored metabolic normality and granule morphology (342). ABCG1 thus emerges as a critical

regulator of cholesterol in insulin granules, in which cholesterol has for some time been known to play a regulatory role (71, 336).

From the discussion above, it is clear that both ABCA1 and ABCG1 have important influences on insulin secretion. However, while ABCA1 serves to reduce cholesterol in the plasma membrane, ABCG1 serves to increase insulin granule membrane cholesterol, the granules representing a total surface area ~4.5 times that of the plasma membrane (72, 344) and requiring a high cholesterol composition (40-50 mol%) for normal insulin secretion (71). This further emphasises the precise nature of cholesterol regulation and its importance in insulin secretion and glycaemic homeostasis. However, it also conflicts with traditional understandings of the role of ABCG1 in cholesterol efflux and it seems likely that this cholesterol transporter may have a unique, additional role in  $\beta$ -cells (342).

### 1.5.2 Mitochondrial function

Mitochondrial oxidation is linked to both insulin secretion through generation of ATP and other secretion coupling factors (263, 345), and provides numerous intermediates for multiple metabolic processes, including precursors that can be used for cholesterol synthesis. In turn, cholesterol synthesis provides various derivatives, including some that have important roles in ROS mediation and the electron transport chain (e.g. ubiquinone, haem A, FPP, GGPP, Figure 1.3). To complete the circle of influence, changes in circulating cholesterol, FFA and glucose concentrations are also linked to mitochondrial function through metabolic adaptation to glucolipotoxicity or altered nutrition, which have implications for insulin secretion (346).

As in all membranes, cholesterol is necessary in mitochondrial membranes to imbue suitable physicochemical properties. However, the mitochondrial membrane cholesterol requirement is reduced compared to other membranes, with ~ 40- and 4.5-fold lower cholesterol content than in plasma and ER membranes, respectively (347). Despite these modest cholesterol requirements, pathways exist for mitochondria to import cholesterol from all other intracellular membranes (348), ensuring its availability for mitochondrial fusion/fission, regeneration and other mitochondrial activities.

Mitochondrial morphological changes have been associated with various pathophysiological states. For example, cholesterol has been found to accumulate in cancer and Niemann-Pick disease type C (NPC) (348).  $\beta$ -cells from T2D donors and mice fed a high fat diet also have characteristic mitochondrial morphological changes, including increased mitochondrial area but not number, indicative of swelling. T2D mitochondria additionally display fragmentation with disrupted cristae (349). Interestingly, a tendency towards increased anaerobic glycolysis, a repressed pathway in  $\beta$ -cells, was reported for NPC brain cells, cancer cells and  $\beta$ -cells with engineered changes in the beta-cell fusion/ fission balance. This was not reported, however, in primary  $\beta$ -cells from T2D patients,



(348, 349) nevertheless, the latter are also known to display an altered metabolic profile, with a large increase in amino acid accumulation (350). In each case above, reduced oxidative phosphorylation and ATP production rendered the affected mitochondria less efficient.

In an animal study where hamsters were fed a diet high in cholesterol, fat and fructose, metabolic disturbances were dependent on dietary cholesterol content (351). However, cholesterol supplementation without the fructose and fatty acids did not induce dyslipidaemia or metabolic impairment, demonstrating the multifactorial nature of glucolipotoxicity and insulin resistance. Also, cholesterol loading in MIN6 cells resulted in impaired mitochondrial function characterised by reduced ATP production, basal and maximal oxygen consumption rate and reserve capacity (352).

Similarly, cholesterol loaded BRIN-BD11 cells (160  $\mu$ M c-M $\beta$ CD for 12 h) displayed decreased oxygen consumption rate, ATP production and exendin-4-stimulated insulin secretion, as well as mitochondrial morphological changes and increased ROS. Interestingly, cholesterol enrichment was also associated with impaired non-mitochondrial respiration<sup>6</sup> and extracellular acidification, representative of glycolysis (354).

In an early review of statin adverse events, and before a link between statins and T2D was made, Golomb and Evans (167) pointed out that mitochondrial defects predispose to statin adverse events and statins predispose to mitochondrial defects. Mitochondrial toxicity linked to statins has been associated with both myopathy and hyperglycaemia (167). In the first instance, this effect was studied in muscle, likely due to the higher prevalence and acute discomfort of muscle-related adverse events (355). Metabolic effects may take longer to develop, can be initially less prominent, and could be interpreted as the progression of concomitant conditions (322), thus reducing their detection. There is also increased risk in certain cohorts, including those with pre-existing risk factors for T2D, postmenopausal women and the elderly (224).

Statins have also been linked to mitochondrial dysfunction in  $\beta$ -cells and pancreatic islets. For example, reduced insulin secretion subsequent to atorvastatin but, interestingly, not pravastatin treatment (100 ng/mL) occurred in human islets and INS1  $\beta$ -cells (356). Furthermore, reduced ATP generation in atorvastatin-treated INS1  $\beta$ -cells coincided with increased ROS and reduced expression of proteins representing mitochondrial complexes I, III, IV, V and CoQ10. Cells were protected from these effects by addition of mevalonate or N-acetylcysteine, a scavenger of free radicals, further demonstrating the role of ROS in the adverse effects of atorvastatin.

---

<sup>6</sup> Non-mitochondrial respiration represents the consumption of oxygen by non-mitochondrial enzymes such as NADPH oxidases, saturases and detoxification enzymes. In some cells, such as macrophages, this can account for a significant portion of cellular oxygen uptake, while in most cells it is ~10% of total oxygen consumption (353).

An interesting observation by Chen *et al* (357) is the increase in lactate dehydrogenase (LDH) released by atorvastatin treated NIT-1  $\beta$ -cells. Their use of LDH in a cytotoxicity assay in  $\beta$ -cells is interesting, given that this is a 'prohibited pathway' in metabolically distinctive  $\beta$ -cells (see Section 1.4.1). However, it indicates that atorvastatin impairs a principal glucose homeostatic mechanism by upsetting stimulus-secretion coupling and increasing the glycolytic pathway. They also demonstrated that atorvastatin but, once again, not pravastatin, increased intracellular ROS. Moreover, in both statin treatments, autophagy was increased.

The influence of statin on mitochondrial function is thought to be at least partly via reduced CoQ10 and Haem A, the synthesis of both being dependent on the mevalonate pathway. These effects result in decreased flux through the TCA cycle with consequent decreased ATP generation and increased ROS due to decreased antioxidant capacity by the mechanism described below.

Experiments conducted by Mailloux *et al* (358) indicate that in MIN6  $\beta$ -cells and pancreatic islets, mitochondrial ROS uncouples ATP generation from glucose oxidation via up-regulation of uncoupling protein 2, thereby reducing glucose-stimulated insulin secretion (GSIS). Though statins were not used in the latter study, it supports the effect of increased ROS on mitochondrial function and insulin secretion. Together, these studies indicate that some statins may reduce insulin secretion secondary to increased ROS and consequent mitochondrial dysfunction. Interestingly, cholesterol accumulation can also increase ROS, impair mitochondrial function and blunt insulin secretion (354).

### 1.5.3 Cholesterol effects on ROS

As previously mentioned,  $\beta$ -cells have a decreased capacity to deal with excess ROS, while at the same time production of ROS is an obligatory consequence of oxidative respiration in mitochondria, a pathway used almost exclusively in these cells. It is well-known that CoQ10 transports electrons from complexes I and II to complex III. The possibility of reduced availability of CoQ10 with statin treatment potentially impacts on ATP generation and mitochondrial efficiency. Cellular damage caused by obligatory mitochondrial ROS production created during ATP synthesis is also minimised by the antioxidant activity of CoQ10 and the cellular glutathione antioxidant system (359).

Statins may also exacerbate ROS-associated dysfunction by reducing delivery of antioxidant vitamins and provitamins, which rely on lipoprotein particles for transportation. The serum concentrations of the antioxidants  $\alpha$ -tocopherol and  $\beta$ -carotene were lowered by 16% to 22% by simvastatin therapy, and this was only partially improved by increased dietary intake of  $\alpha$ -tocopherol (360).

Statins appear to reduce antioxidant potential, possibly by the mechanisms mentioned above. For example, Bouitbir *et al* (227) demonstrated a reduced GSH/GSSG ratio, indicating oxidative stress, in glycolytic but not oxidative muscle in atorvastatin-treated humans and rats. Increased H<sub>2</sub>O<sub>2</sub> and

superoxide production coinciding with atorvastatin treatment in rat myoblasts confirmed causation. They concluded that the availability of extra antioxidant resources in oxidative muscles is protective in the face of atorvastatin-associated reduction of antioxidant potential. They also demonstrated impaired mitochondrial function and reduced ATP production in atorvastatin-treated L<sub>6</sub> rat myoblasts. Similarly, Galtier *et al* (361) demonstrated statin-associated alterations in mitochondrial respiration in vastus lateralis muscle biopsies from some, but not all, healthy young volunteers after 8 weeks of high-dose simvastatin treatment.

#### 1.5.4 Other metabolic pathways

Various aspects of the link between insulin and cholesterol have been explored above, including the effect of cholesterol and cholesterol flux on a) membrane characteristics and various proteins involved in insulin stimulus/secretion coupling, b) mitochondrial function and c) the generation of ROS. A number of other observations are also relevant to understanding the relationship between these biologically important molecules, which can be demonstrated by the clinical relationship that exists between circulating cholesterol levels and glycaemia, which, in turn, is regulated by insulin (318, 362-364). While high plasma LDL cholesterol levels are a risk factor for T2D, low HDL is also associated with poorer glycaemic outcomes and obesity and provision of exogenous HDL can improve these parameters (363). Stored fat levels and plasma insulin concentrations are also positively correlated, and insulin is thought to relay adiposity signals to the brain (318, 365, 366), further demonstrating the interconnection between lipids and glucose homeostasis.

Cholesterol synthesis may be one of several mechanisms by which  $\beta$ -cells protect themselves from chronic fuel excess (243). Increased diversion of glucose carbons to triglycerides and cholesterol esters in rat islets maintained for 1 h in high glucose (16-25 mM) was demonstrated. Storage of newly synthesised cholesterol in the form of inert esters or its removal from the cell via ABCA1/ABCG1 and HDL particles was shown to be a likely means of eliminating carbons originating from glucose entry under high glucose conditions in islets. In the same study, HMG-CoA was reduced linearly as glucose concentration increased. This depletion may have been due either to consumption during cholesterol synthesis or reduced production, since HMG-CoA is an intermediate of the fatty acid oxidation/ketogenesis pathway that is reduced in elevated glucose conditions. It is not known whether inhibition of the ability to synthesise cholesterol during chronic glucose overload, as would occur in statin treatment, may increase the adverse effects of such exposure in the  $\beta$ -cell.

There is also evidence that the hexosamine biosynthetic pathway (HBP) may mitigate both glucose and lipid-induced toxicity. Increased ROS produced by hyperglycaemic conditions may redirect glucose towards the HBP (367), which is thought to function as a metabolic sensor and is well-known to be linked to insulin resistance and other complications of T2D (368, 369). Increased flux through the HBP, usually accounting for only ~3% of glucose utilisation (370), causes abnormal post-

translational *O*-linked *N*-acetylglucosamine modification of proteins. Additionally, it is responsible for altered insulin secretion (371) and plays a role in  $\beta$ -cell dysfunction via increased ROS (372). It also caused ER stress and had a dedifferentiating effect involving extracellular signal-regulated kinase (ERK) in INS-1E  $\beta$ -cells and mouse islets (373). Interestingly, increased HBP activity also augmented plasma membrane cholesterol in preadipocytes (374). Given the link between plasma cholesterol levels and insulin secretion, it would be interesting to determine whether a similar increase in plasma membrane cholesterol occurs in  $\beta$ -cells and whether it may be mechanistic in  $\beta$ -cell dysfunction and/or T2D pathophysiology.

When considering possible effects of cholesterol synthesis inhibition, the loss of post-inhibition products has been well studied, but little speculation has been given to pre-inhibition substrates or enzymes. For example, the putative accumulation of HMG-CoA and HMGCR in statin-treated tissue has received little attention. The absence of feedback regulatory signals from intermediates such as 24,25-dihydrostanosterol and squalene would both reduce HMGCR degradation and stimulate SREBP-mediated transcriptional up-regulation (49, 375). In the event of statin run-down, for example, between doses, would abundant HMG-CoA, HMGCR and acetyl-CoA supplies stimulate excessive cholesterol production? If so, would this occur in  $\beta$ -cells?

Further, acetyl-CoA, the primary substrate for cholesterol synthesis, is involved in many pathways, being a product of amino acid, fatty acid and carbohydrate catabolism, a substrate for both the TCA cycle and cholesterol synthesis, and a carbon donor for acetylation modifications of proteins and nucleic acids (376). It is not known what regulatory mechanisms determine cellular decisions about the fate of acetyl-CoA, and it is not unreasonable to speculate that a 'metabolic back-up' could overwhelm enzymes and cause accumulation of metabolites such as long chain acyl-CoAs. This may be of particular significance in the  $\beta$ -cell due to its obligatory equilibration of intra- and extra-cellular glucose (243).

A plausible example of the scenario above: it is known that long chain acyl-CoAs<sup>7</sup> directly interact with the  $\beta$ -cell  $K^+_{ATP}$  channel to increase its activity (378). This is thought to sensitise  $\beta$ -cells to changing metabolic conditions (379). Statins may thus increase  $K^+_{ATP}$  channel activation (hence reducing membrane depolarisation events) pleiotropically by the dual action of a) reduced ATP generation (due to depletion of CoQ10) and b) accumulation of acetyl-CoA, acetoacetyl-CoA and long chain acyl-CoAs (322). This, in turn, could be expected to reduce insulin secretion. Interestingly, and in support of this possibility,  $K^+_{ATP}$  channel mutations increase T2D risk (380). Metabolomic studies in statin-treated  $\beta$ -cells would be very helpful to study such effects.

---

<sup>7</sup> Interestingly, only saturated acyl-CoA esters with a chain length exceeding 12 carbons have so far been demonstrated to activate these channels (313, 377).

One further area of interest is how statins may affect central regulation of metabolic processes. In this emerging field, the hypothalamus appears to be an important central regulator of glucose metabolism and energy homeostasis. Signals from peripheral organs allow central regulation of aspects such as energy expenditure, appetite, insulin sensitivity and glucose metabolism. Faulty crosstalk can result in metabolic dysregulation (318). Statins are known to cross the blood-brain barrier (381), giving reason to anticipate a small effect. This is therefore one more avenue of investigation in the quest to understand the relationship between cholesterol metabolism and glucose homeostasis.

## 1.6 Experimental models

It is common to make use of experimental models to study the physiological effects of drugs and assess the influence of various molecules and biochemical pathways. While this is an essential strategy, it is important to be aware of certain limitations and considerations, for example, extrapolation of results and physiological relevance of drug dose. In addition, non-pharmacological agents or off-label use of pharmacological agents can sometimes be utilised to artificially model physiological conditions. The discussion in this section provides a background for models and systems applicable to studies in this thesis.

### 1.6.1 Use of statins *in vitro* and in mice

Statins are often studied *in vitro* and in animal models and differences in dose, pharmacodynamics and metabolic processes must be considered when assessing the relevance of these studies to clinical situations. The reduced complexity of *in vitro* studies is both beneficial and problematic in that systemic regulatory processes may be absent. This has obvious implications when studying complex systems such as glucose and lipid homeostasis which are regulated at both the systemic and tissue level.

Considerations of relevance to the *in vitro* statin studies later in this thesis include the absence of hepatic drug processing and the appropriate delivery of a suitable dose. Liver first-pass processing is responsible for a considerable reduction in peripheral tissue statin drug concentration (382). Several statins are also processed to metabolites of higher or lower potency by liver enzymes, mainly cytochrome CYP3A4 (154). A non-hepatic cell line such as BRIN-BD11 does not possess the cellular machinery for such processing, and the ramifications of this are unclear.

In aqueous solutions, statins are unstable. In the lactone form they are susceptible to hydrolysis, and acidic statin compounds can react with alcohols to form esters (383). Consequently, considerable variations in potency can occur, potentially leading to inter- and intra-laboratory discrepancies.

Statin drug exposure *in vitro* is also likely to be greater compared to *in vivo*, albeit more acute. The absence of hepatic or glomerular filtering means drug concentrations remain more constant. Protein binding of >95% *in vivo* must also be considered (193). In human serum, maximum plasma concentrations of 7–252 ngEq/mL (13–451 nmolEq/L) were observed in healthy adults administered atorvastatin doses of 10–80 mg/day (177). Other statins may reach 0.002–0.1  $\mu$ M over a range of experimental doses (43, 304). Tables of pharmacokinetic parameters for several statins are available in Desager and Horsmans (43). Relative to serum, the murine liver concentrates statins up to ~2-fold ( $570 \pm 543$  pmol/g (liver) vs  $221 \pm 121$  pmol/mL (serum) (384)), and in brain and muscle concentrations approximating one third those of serum have been recorded ( $64.8 \pm 69.3$  pmol/g vs  $221 \pm 121$  pmol/mL in mice, brain vs serum<sup>8</sup> (384);  $827 \pm 121$  vs  $2873 \pm 677$  ng/mL in rats, gastrocnemius muscle vs serum (385)). Comparative concentrations in other tissues are not known (193).

Cell culture doses are typically up to 1,000 times higher than those recorded in serum, being in the micromolar range; on the other hand exposure *in vivo* (and in subjects on statins) is usually for a considerably longer time. Doses of 1–10  $\mu$ M are commonly used in cell culture studies (71, 386–396), but occasionally doses up to 200  $\mu$ M have been used (397). This could be problematic, as dose-related biphasic effects on angiogenesis (176, 304) and oxidative stress (304) have been reported, and it is possible that dual effects may also occur in other physiological functions.

Similarly, high or non-pharmacological statin doses have regularly been used in animal studies. It has been suggested that high doses are tolerated in rodents because of resistance to pharmacological cholesterol-lowering effects, despite successful mevalonate pathway inhibition (193). Such resistance may be due to the induction of hepatic cholesterol synthesis through other pregnane X receptor (PXR) ligands in mice as found in a previous study (398). Well-known dissimilarities between rodent and human cholesterol metabolism (180, 399) could impact on statin efficacy in mice, and is further discussed below.

Firstly, mice do not express cholesteryl ester transfer protein (CETP), a plasma protein responsible for transferring cholesteryl ester and other neutral lipids between lipoparticles (400, 401). CETP also plays a role in the regulation of reverse cholesterol transport, the movement of cholesterol from peripheral tissue to the liver, where elimination can take place (402). In mice lacking CETP, cholesterol homeostasis in plasma is maintained during high fat diet feeding by up-regulation of bile acid synthesis to increase cholesterol elimination, with concomitant down-regulation of cholesterol synthesis (403).

---

<sup>8</sup> Brain and liver were measured by wet weight and serum by volume, both being corrected to body weight.

Furthermore, mice carry most of their circulating cholesterol in HDL and have a low LDL:HDL ratio, while in humans LDL is the major cholesterol transporter and a high LDL:HDL ratio exists (403). Mice also lack both apo(a) and lipoprotein(a) (404), while apo B-48 is expressed in the liver of mice, but not humans (403). Interestingly, and despite these lipoprotein variations, a recent study confirmed the similarity of the mouse lipoproteome to that of humans (405).

Anatomically, differences in islet architecture may influence the order in which blood passes the various endocrine cell types, influencing paracrine signalling (241, 406). While not related to cholesterol metabolism, this could also influence glycaemic responses to cholesterol therapies.

Due to these physiological and anatomical differences, the applicability of *in vitro* and animal studies to human health must be carefully considered. Nevertheless, the benefits of such studies are many, and include the freedom to use non-therapeutic agents to model physiological aspects of relevance. One such example in this thesis is the use of the cholesterol-sequestering agent methyl- $\beta$ -cyclodextrin to engineer varying cholesterol abundance in  $\beta$ -cells.

### 1.6.2 M $\beta$ CD

Methyl- $\beta$ -cyclodextrin (M $\beta$ CD) is a cone-like toroid-shaped cyclic oligosaccharide containing seven glucose units derived from amylose and containing additional methyl groups to improve aqueous solubility (407). It can form spontaneous inclusion complexes with hydrophobic molecules such as cholesterol, which fits optimally within the hydrophobic, 6-8 Å diameter cavity of M $\beta$ CD molecules (408), making them water soluble with a stoichiometry of 1:2 in the form of cholesterol<sub>1</sub>:M $\beta$ CD<sub>2</sub> (80, 407, 409). It can be used in the ‘empty’ state or pre-loaded with cholesterol to quickly sequester or donate cholesterol from/to cell membranes, respectively (409). This makes it a suitable agent for modifying membrane cholesterol content and it is commonly used to study the effect of cholesterol changes (410). Cyclodextrins are also more generally used as drug delivery agents (411) and are being investigated as pharmacologically active compounds for therapeutic use in the treatment of cholesterol storage diseases such as Niemann-Pick C disease (412) and other diseases characterised by cholesterol imbalance (407, 413).

Whether M $\beta$ CD shows specificity for cholesterol has been debated, and recent evidence that it can also sequester cholesteryl esters (414) and phospholipids (408) and form complexes with some proteins, notably insulin<sup>9</sup> (415), is of interest. Indeed, complexation with M $\beta$ CD is known to stabilise insulin. However, to my knowledge there are no reports of an influence on the measurement of insulin. Also of relevance is the oxidation protective effect of M $\beta$ CD on LDL particles and its ability to reduce LDL volume and lipid content (416). This means pleiotropic effects unrelated to membrane

---

<sup>9</sup> A complex of insulin and M $\beta$ CD increases insulin stability by 20%. There is no evidence that complexes between M $\beta$ CD and insulin form *in vivo* (415).

cholesterol concentration are possible and should be considered when utilising M $\beta$ CD *in vivo* or in complete media, both of which were avoided in this project.

The degree to which cholesterol is depleted by M $\beta$ CD *in vitro* is determined by its concentration, incubation time, temperature, cell type, and access of the agent to cells, such as might occur with increased movement (e.g. stirring), and presentation of the cells in monolayer versus suspension (410, 417). However, cholesterol extraction occurs rapidly and is time limited, with some reports suggesting that no further depletion occurs after 1 h of incubation (417).

Two pools of cholesterol, one quickly and one slowly sequestered by M $\beta$ CD, have been described (417). These pools are both thought to be located within the cell membrane. However, it is not known whether differential sequestration rates occur between the inner and outer membrane leaflet, or whether dissimilar lateral cholesterol distribution within the membrane, for example in lipid raft compared to disordered domains, gives rise to the two pools. Transbilayer cholesterol content asymmetry is known to occur (418) and has recently been quantified (59). Also, despite some reports to the contrary, M $\beta$ CD is generally thought to extract cholesterol from both lipid ordered and disordered domains (61), although its effects are specific, interrupting signalling in some pathways while leaving others intact (419).<sup>10</sup>

The mechanism of extraction is thought to be quite direct. It has been proposed that a cholesterol molecule located within the membrane diffuses directly into the cavity of a M $\beta$ CD molecule located in its immediate proximity without prior dissolution into the aqueous phase (417). In support, Liu *et al* (59) used extremely sensitive cholesterol sensors to confirm that M $\beta$ CD (5 mM) depleted cholesterol with greater efficiency from outer than inner membrane leaflets (decreases of 3.6-fold compared to 0.5-fold, respectively). However, they also discovered that cholesterol enrichment of cells by pre-loaded M $\beta$ CD may be more complex, as inner membrane leaflets were enriched effectively (73% increase) while a negligible effect was made on outer membrane leaflets in HeLa cells.

Some members of the ABC transporter family are thought to participate in the cholesterol transfer process to M $\beta$ CD, with increased extraction in the presence of ABCA1, ABCG1 and ABCG4 (420). The use of similar transporters emphasises the appropriateness of the use of M $\beta$ CD as a model for reverse cholesterol transport. Furthermore, the former two transporters, known to assist in cholesterol efflux to HDL particles (340, 421) and having specific roles in  $\beta$ -cells (see Section 1.5.1.4) are also thought to be instrumental in the maintenance of transbilayer asymmetry of plasma membrane cholesterol (59).

---

<sup>10</sup> For example, pro-survival signals from receptor tyrosine kinases to AKT via phosphoinositide 3-kinase were attenuated by 7 mM M $\beta$ CD while signals from the same receptor tyrosine kinases to extracellular signal-regulated kinase (ERK) via Ras were unaffected in several cancer cell lines (419).



Lipid rafts are disrupted by M $\beta$ CD as evidenced by reduction of fluorescent labelling of a lipid raft marker, GM1 ganglioside (422). Further evidence is found in the disrupted colocalization of caveolin (a raft protein) with insulin-like growth factor – insulin receptor (423), soluble N-ethylmaleimide-sensitive factor activating protein receptor (SNARE) proteins, and potassium and calcium channels (66). This disturbance of raft proteins important to exocytosis may be a factor in changes to secretion of glucagon and insulin in  $\alpha$  and  $\beta$ -cells, respectively, reportedly increased by M $\beta$ CD in both cell types (66, 69, 330). In contrast, insulin secretion was reduced after cholesterol loading with c-M $\beta$ CD (424).

Changes to mechanical properties caused by M $\beta$ CD include increased stiffness and rearrangement of the actin cytoskeleton, including induction of *de novo* actin polymerization in several cell types (425). Indeed, membrane-cytoskeleton adhesion is increased with cholesterol loss and decreased by cholesterol loading and this is thought to impact on the lateral mobility of membrane proteins, with cholesterol depletion being inhibitory (61). Furthermore, the area of membrane covered by lipid rafts is cholesterol dependent, with cholesterol depletion (1 mg/mL M $\beta$ CD for 10 min) reducing and enrichment (0.5 mg/mL c-M $\beta$ CD for 1 h) increasing the lipid raft area in macrophages (426). In the same study, Gaus *et al* found a reduction of lipid order in both fluid (non-raft) and raft areas after cholesterol depletion, but order was not increased by cholesterol loading.

Toxicity of M $\beta$ CD is related to its cholesterol extraction efficacy (427). It is therefore important to use a concentration/incubation period combination compatible with the cell-type and cholesterol depleting/enriching effect required. *In vivo*, M $\beta$ CD is known to cause haemolysis and morphological changes in erythrocytes (428).

### 1.6.3 BRIN-BD11 cells

Much of what is known about  $\beta$ -cells comes from work on numerous *in vitro* models. Isolated islets and pancreatic perfusion studies utilise primary cells, but there are limitations on their availability, longevity and passage length, as well as ethical considerations. To overcome these difficulties,  $\beta$ -cell lines are widely used (for example: MIN6, INS-1, NIT-1, RINm5F). These exhibit various advantages and disadvantage (reviewed in (429), see Table 1). Essential characteristics for bioenergetic relevance include functional phenotypic characteristics as outlined in Section 1.4.1, including expression of low affinity glucose transporters and glucokinase, ion channels, insulin and appropriate exocytotic machinery and absence or minimal expression of LDH and MCT1 (246).

BRIN-BD11 cells, the model used in this project, were derived by electrofusion of primary rat insulinoma and RINm5F cells. They have ~58 chromosomes, express glucose transporter 2, and glucokinase was found to be responsible for 71% of glucose phosphorylating activity, indicating appropriate glucose sensing potential (430). Although known to express other hexokinases in

addition to glucokinase (429), they have been well characterised and meet functional, metabolic, electrophysiological and calcium handling similarity requirements for suitability as a model (431). They are also demonstrably responsive to a variety of insulinotropic drugs, nutrients and other secretagogues (432-434) and metabolise amino acids at enhanced rates compared to other  $\beta$ -cell lines (281). While their precursor, RINm5F cells, are known to express high levels of LDH (247) and MCT1 (435), to my knowledge no quantitative data exists for these proteins in BRIN-BD11 cells. As for any model, due caution must be taken when extrapolating information from this model system.

## 1.7 Summary, Significance

Evidence of a link between cholesterol and glucose metabolic pathways is abundant, and is sometimes observed in concomitant pathophysiologies, such as in T2D and CVD. Furthermore, the recently described and increasingly evident association between increased onset of T2D and statin therapy has stimulated considerable research in this area. Both on-target and pleiotropic effects of statins on  $\beta$ -cells and on insulin sensitive tissue such as liver, fat and muscle, approaching the problem from both the insulin availability and insulin action sides, respectively, are under scrutiny.

It is important that the mechanism by which statin may increase the risk of T2D is understood. The potential to improve treatment, offset adverse glycaemic effects or avoid morbidity is very high in the ~1.5 million statin users in Australia, even though the number needed to harm (i.e., develop diabetes) is reasonably low (1 in 204 persons at low risk (197), and 1 in 50 over 5 years with (36) and without (196) known heart disease). Further, risk of statin-induced diabetes may be under-estimated (436), and non-adherence to statin medication regimes is high (437, 438), likely due to the high incidence of adverse events (355). Patients who may benefit from statin therapy need confidence that their treatment will not cause further morbidity. Suggestions, perhaps in jest, of the complimentary provision of statins by fast food retailers (439) demonstrates an underappreciation of the complex relationships that exist between metabolic processes, including those as fundamental as cholesterol and glucose homeostasis.

The diabetogenic effect of statins may directly relate to HMG-CoA reductase inhibition, i.e., to cellular cholesterol concentrations or to compounds such as CoQ10, which are derived from intermediates of the mevalonate pathway. These factors have potential downstream effects such as inhibition of membrane channel proteins, impaired mitochondrial function and increased ROS. To evaluate the contribution of these various potential diabetogenic mechanisms is an aim of this project.

From an experimental context, the use of M $\beta$ CD in this project, in both its pre-loaded and empty states, can help to clarify mechanisms related primarily to cholesterol abundance. For example, reduced cholesterol can cause membrane protein dysfunction, including channel proteins important to

insulin secretory processes. Insulin granule formation and fusion processes also appear to be dependent on appropriate cholesterol distribution and flux. The contribution of cellular cholesterol alone to these processes can be assessed using M $\beta$ CD, avoiding the complication of other potential statin effects.

While pleiotropic effects of statins have sometimes been enthusiastically described as beneficial, a holistic evaluation determines that this may be true in some tissues, while adverse effects, sometimes due to the same mechanism, can occur elsewhere, including in metabolically distinct  $\beta$ -cells. For example, fluvastatin was found to decrease plasma oxysterols in T2D patients and the reduced oxidation was considered to be of pleiotropic benefit (440). However, oxysterols are involved in the immune response (84), are capable of lipoprotein-independent efflux from cells (144) and some regulate HMG-CoA reductase expression (85). Therefore, a decrease in oxysterols could indicate a decreased ability to manage cholesterol levels at the cellular level, which may lead to dysfunction in  $\beta$ -cells (243). This demonstrates the importance of investigating drug effects in diverse tissue types and from different perspectives and underscores the difficulty investigators have found in drawing evidence-based conclusions to balance the risks and benefits of statin treatment (212).

The aim of this study is to contribute to the body of research assessing the complex relationship between cholesterol and glucose homeostasis. The specific aims are to:

- determine the impact of a spectrum of  $\beta$ -cell cholesterol content on insulin secretion in response to glucose and other physiological and therapeutic  $\beta$ -cell secretagogues.
- compare the influence of several statins on stimulated  $\beta$ -cell function and insulin secretion.
- assess the effect of several statins on  $\beta$ -cell energetics, mitochondrial function and stimulus/secretion coupling.
- assess the effect of changes in cholesterol on selected proteins relevant to  $\beta$ -cell function.
- determine whether glutamine is protective of statin-induced  $\beta$ -cell impairment.

In these studies, the assessment of a spectrum of cellular cholesterol concentrations using both enrichment and depletion, and in response to statins, in the same experimental model was undertaken. The use of a variety of secretagogues, both nutrient and therapeutic, assisted in exploring whether effects were similar across a range of physiological contexts. Proteomic analysis of  $\beta$ -cells that were depleted or enriched with cholesterol was undertaken to assess potential pathways of influence on insulin secretion and  $\beta$ -cell function.

In this chapter the literature has been reviewed and in Chapter 2 the effects of statins on insulin secretion in a  $\beta$ -cell model are explored. To assess whether the statin effects are related directly to

cholesterol content, and to further understand the role of cholesterol in  $\beta$ -cell function, the effect of M $\beta$ CD and c-M $\beta$ CD treatments on insulin secretion are also investigated. In Chapter 3, the effect of various statins on mitochondrial function is explored. Chapter 4 investigates the effect of cholesterol changes on several membrane proteins involved in insulin secretion using a variety of methods in a quest to generate hypotheses for future work. Chapter 5 records the metabolic effects of a combination of high fat diet and atorvastatin or pravastatin in an *in vivo* mouse study. In Chapter 6 the abundant amino acid glutamine, known to be consumed in large quantities in some physiological states (such as post-surgery, sepsis, heavy exercise) and reduced in T2D, is assessed to determine whether it is protective to statin-treated  $\beta$ -cells. Chapter 7 summarises the main findings and suggestions are made for future direction in this complex yet fascinating field of research. Figure 1.4 provides a graphic overview of the project.

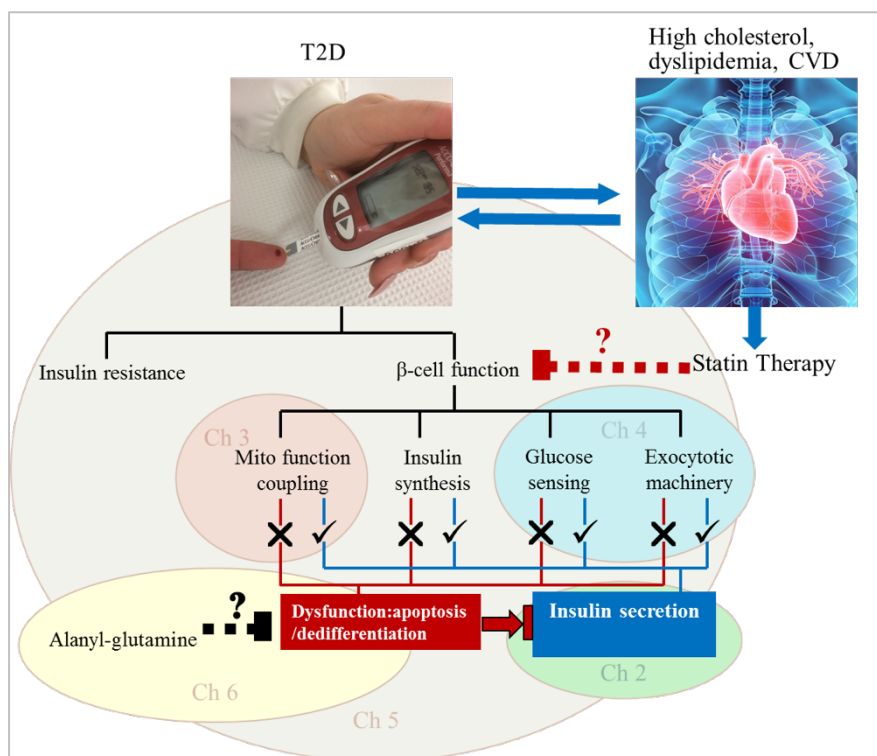


**Figure 1.4. The influence of cholesterol on  $\beta$ -cell function: A graphic project overview.**

Type 2 diabetes (T2D) and cardiovascular disease (CVD) share common risk factors and may influence each other. Statin therapy reduces serum cholesterol and is protective against CVD. However, an increased risk of T2D has been associated with statin treatment. In this project the influence of cholesterol on various aspects of  $\beta$ -cell function are explored. Altered performance of mechanisms such as mitochondrial function, glucose sensing and exocytotic machinery may lead to insulin secretion failure. The research chapters are represented by coloured ovals in the diagram. Ch 2 explores the influence of cholesterol on insulin secretion; Ch 3 investigates how statins affect mitochondrial function and stimulus/secretion coupling; Ch 4 explores the influence of cellular cholesterol on various functional proteins; Ch 5 takes a holistic view using mice fed a high fat or normal diet and treated with statins or water; and Ch 6 assesses the ability of alanyl-glutamine to rescue  $\beta$ -cells from the adverse effects of statins. CVD image from [www.nhlbi.nih.gov/news/2011](http://www.nhlbi.nih.gov/news/2011). T2D image, Gae Ellison.

## Chapter 2                      Effects of Cholesterol modification on stimulated insulin secretion

Insulin secretion is exquisitely sensitised to the glycaemic state of the organism. To achieve this, glucose uptake and metabolism must be adequately coupled to appropriate insulin secretion. The process of insulin secretion has been well described and involves closure of ATP-sensitive potassium channels ( $K^+_{ATP}$ ) located in  $\beta$ -cell membranes in response to ATP generation from the metabolism of glucose (and other substrates). This causes membrane depolarisation, opening of voltage-gated calcium channels ( $Ca^{2+}_v$ ), and subsequent calcium entry into the cytoplasm, in turn stimulating fusion of insulin granules and exocytosis.

Since the recent finding that the cholesterol-reducing statin family of drugs are linked to higher risk of new-onset Type II Diabetes (T2D) (34, 441-443), there has been speculation as to the nature of this connection. It is possible that reduced availability of membrane cholesterol caused by inhibition of cholesterol synthesis in statin therapy may hinder insulin secretion. Other studies have also shown that sub- and supra-optimal  $\beta$ -cell cholesterol levels unfavourably affect insulin secretion (336, 354, 444, 445). This project tests the hypothesis that the relationship between  $\beta$ -cell cholesterol content and stimulated insulin secretion is tri-phasic, characterised by optimal mid-range cholesterol concentration flanked by low and high cholesterol content which adversely affects insulin secretion in response to physiological and therapeutic secretagogues.

BRIN-BD11 cells have been shown to be responsive to various secretagogues including glucose, amino acids and sulphonylureas (430, 434) and were thus used as an *in vitro* model in this project. A more limited number of experiments was also attempted in freshly isolated pancreatic islets. Cholesterol was manipulated either by statin-mediated inhibition of the rate-limiting enzyme in cholesterol synthesis, 3-hydroxy-3-methylglutaryl-CoA reductase (HMGCR) or using methyl- $\beta$ -cyclodextrin (M $\beta$ CD). The latter can be used to both increase or decrease membrane cholesterol. M $\beta$ CD sequesters cholesterol from cellular membranes (410), but after pre-exposure of this agent to cholesterol (c-M $\beta$ CD) it can also act as a cholesterol donor.

Statins vary in lipophilicity and hydrophilic drugs have been deemed less likely to cause adverse pleiotropic effects due to decreased accessibility to extrahepatic tissue and intracellular compartments (170). Thus, a further hypothesis in this project states that statins will exert concentration- and lipophilicity-dependent effects on insulin secretion in response to physiological and therapeutic secretagogues. To test this, several statins were used including, in order of decreasing lipid solubility, fluvastatin, atorvastatin, simvastatin and pravastatin, the latter being considered hydrophilic (304).

## 2.1 Methods

### 2.1.1 Materials

Fetal bovine serum (FBS) was purchased from Fisher Biotech Pty Ltd and heat-inactivated before use. Ultrasensitive Insulin ELISA kits (Mercodia) and statins were purchased from Sapphire Bioscience. Amplex Red Cholesterol kits and BCA protein assay reagents were purchased from Life Technologies. All other reagents were purchased from Sigma Aldrich (Australia) unless otherwise indicated. BRIN-BD11 cells were a kind gift to my co-supervisor, P Newsholme, from Peter Flatt.

### 2.1.2 Tissue culture

BRIN-BD11 cells were cultured in RPMI medium supplemented with 1% penicillin streptomycin and 10% FBS, in 5% CO<sub>2</sub>/95% air at 37°C, and passaged at 75-80% confluence. All experiments used cells from passages 23-32.

### 2.1.3 Preparation of LPDS

Lipoprotein deficient serum (LPDS) was prepared from fetal bovine serum (FBS) using a protocol described by Goldstein *et al* (446) and others (409, 447). Briefly, the density of FBS was adjusted to 1.25 g/L using 0.354 g of NaBr per mL of serum. Aliquots were then centrifuged at 70,000 x g for 20 h at 20°C using a Sorvall T-1270 rotor in a Sorvall WX ultra centrifuge (ThermoFisher Scientific). After centrifugation, tubes were pierced at the base and the serum was allowed to flow by gravity into fresh collecting tubes. One or eight mL aliquots were collected and the protein and cholesterol content of each aliquot was measured using the Pierce BCA protein assay (ThermoFisher Scientific) and the Amplex Red Cholesterol assay (Life Technologies), respectively. Aliquots low in cholesterol were pooled and salt was removed either using a protein desalting column (ThermoFisher) or by dialysis against phosphate buffered saline (PBS, 137 NaCl, 2.7 KCl, 10 Na<sub>2</sub>HPO<sub>4</sub>, 2 KH<sub>2</sub>PO<sub>4</sub>, pH 7.4 in mM) at 4°C using three dialysate changes over 24 h with a total of at least 200 times the volume of LPDS. After dialysis, the osmolality was checked and the LPDS was filter-sterilized using a 0.2 µm syringe filter (Millipore) and assayed for protein content again. It was stored at -20°C and used at a similar concentration to 10% FBS based on protein content.

### 2.1.4 Cholesterol reduction and enhancement using cyclodextrins

Stock solutions of methyl-β-cyclodextrin (MβCD) and cholesterol loaded (c-) MβCD were prepared similarly to a previously published protocol (325) with some modifications. MβCD was prepared at 100 mM in PBS, filter sterilised and stored at -20°C. To load MβCD with cholesterol, the latter was added to 100 mM MβCD stock at 3.8 mg/mL. The mixture was mixed vigorously for 20 min then sonicated (Misonix S-4000, Qsonica) on ice at 50% amplitude for 30 min using a microtip placed directly in the mixture. The c-MβCD was then filter sterilised and stored at -20°C.

BRIN-BD11 cells were seeded at  $1 \times 10^4$  cells/well in 96-well culture plates and left to attach overnight. They were grown for a further day before they were washed once in warm ( $37^\circ\text{C}$ ) PBS and treated for 30 min, as described, with various concentrations of M $\beta$ CD or c-M $\beta$ CD prepared in Krebs-Ringer Bicarbonate Buffer (KRBB, 115 mM NaCl, 4.7 mM KCl, 2.5 mM CaCl<sub>2</sub>, 1.2 mM KH<sub>2</sub>PO<sub>4</sub>, 1.2 mM MgSO<sub>4</sub>·7H<sub>2</sub>O, 24 mM NaHCO<sub>3</sub>, 0.1% HEPES (v/v), 0.1% BSA (w/v), pH 7.4) supplemented with 1.1 mM glucose. Treatment was followed by stimulated insulin secretion tests (described below) before cells were washed twice in PBS and allowed to dry. Cholesterol was extracted using a protocol adapted from Robinet (448). Eighty microlitres of hexane:isopropanol (3:2) was added, mixed by pipetting, and the extract transferred to a v-well plate and left to evaporate, leaving a lipid film. Samples were stored at  $-20^\circ\text{C}$  until assayed for cholesterol.

A similar protocol was used to confirm that cholesterol results were not an artefact caused by non-cellular cholesterol from the c-M $\beta$ CD treatment adhering to plastic plate wells. Cells were grown in T25 flasks to 80% confluence, treated as above with M $\beta$ CD or c-M $\beta$ CD then washed and detached from the plate using 150  $\mu\text{L}$  of 0.25  $\mu\text{L}/\text{mL}$  trypsin. Cells were scraped from the flask, collected in a 1.5 mL Eppendorf tube and centrifuged at 500 x g for 3 min. The pellet was washed once with PBS and re-centrifuged before 150  $\mu\text{L}$  hexane:isopropanol (3:2) was added and mixed. Tubes were centrifuged at 4,000 x g and the cholesterol-bearing supernatant was transferred to v-well plates and allowed to evaporate to dryness. Where indicated, the pellet was prepared for DNA measurement by the addition of 100  $\mu\text{L}$  RIPA buffer and storage at  $-20^\circ\text{C}$  until being assayed.

### 2.1.5 Cholesterol reduction using statins

BRIN-BD11 cells were seeded at  $1 \times 10^4$  or  $1 \times 10^5$  cells/well in 96- or 24-well culture plates, respectively. They were left to attach overnight then treated for 24 h with 1 or 10  $\mu\text{M}$  statins as indicated. Statin stock solutions were prepared in dimethyl sulphoxide (DMSO) and stored at  $-80^\circ\text{C}$ . The final concentration of DMSO was never more than 0.01%. Statin treatments were prepared in RPMI supplemented with lipoprotein-deficient FBS (LPDS) rather than FBS. This was to remove exogenous sources of cholesterol, which could counteract the cholesterol lowering effect of the statins. Cells were then washed in PBS and cholesterol was extracted as described above.

### 2.1.6 Cholesterol measurement

Stored samples were reconstituted in isopropanol mixed in equal parts with reaction buffer (RB) supplied in the Amplex Red Cholesterol Kit (Life Technologies, A12216). Appropriate dilution of samples ensured they were within the dynamic range of the assay (0 to 8  $\mu\text{g}/\text{mL}$ ). The kit manufacturer's instructions were modified slightly by the addition of a pre-incubation step designed to digest any hydrogen peroxide (H<sub>2</sub>O<sub>2</sub>) latent in the isopropanol (448). Using a black 96-well plate, ~2 units of catalase in 10  $\mu\text{L}$  of water was added to each well with 40  $\mu\text{L}$  sample or calibrator. The

plate was then incubated for 15 min at 37°C prior to the addition of 50 µL Amplex Red working solution as per the manufacturer's instructions. H<sub>2</sub>O<sub>2</sub> controls (10 µM) with or without catalase confirmed the action of catalase in each experiment. Plates were read at excitation/emission 540/590 nm on a plate reader (EnSpire, PerkinElmer).

This enzymatic assay is based on the detection of H<sub>2</sub>O<sub>2</sub> using the fluorescent compound 10-acetyl-3,7-dihydroxyphenoxazine (Amplex® Red reagent). H<sub>2</sub>O<sub>2</sub> is generated by the oxidation of cholesterol by cholesterol oxidase. Without the catalase digestion step, all fluorescence readings were inflated and the dynamic range decreased, making accurate determinations difficult. However, as found previously (448), it was not necessary to deactivate the catalase after pre-incubation, most likely due to the far greater affinity of the detection agent (horseradish peroxidase, HRP) to H<sub>2</sub>O<sub>2</sub> compared to catalase.

### 2.1.7 Stimulated insulin secretion

Cells were grown in 96-well tissue culture plates and treated with MβCD, c-MβCD or statins as for cholesterol reduction and enhancement experiments (Sections 2.1.4 and 2.1.5). For statin experiments, an aliquot of media was collected at the end of the 24 h incubation and stored at -80°C for later measurement of longer term insulin secretion. These samples were designated 'chronic' insulin secretion samples. 'Basal' stimulation refers to low glucose (≤ 2.5 mM) controls. It is important to note that RPMI media, recommended for culture of BRIN-BD11 cells (430) and used in the majority of such studies, contains 11.1 mM glucose (449). To allow cells to consume any stored glucose that could influence secretion rates, cells were washed once in PBS and pre-incubated in KRBB supplemented with 1.1 mM glucose for 40 min before stimulation of insulin secretion. A slightly shorter pre-incubation period was carried out concurrently with the 30 min MβCD and c-MβCD treatments prior to stimulation when relevant.

After pre-incubation, the medium was replaced by various secretagogues prepared in KRBB, as indicated in the results. As is usual practice, amino acids and the GLP-1 analogue (exendin-4) were used in the presence of 16.7 mM glucose, because these secretagogues work synergistically with glucose to stimulate insulin secretion (450, 451). All sulphonylurea secretagogues were used in the presence of 2.5 mM glucose, because they induce insulin secretion even in low glucose concentrations, although their insulinotropic action is not, as is commonly thought, strictly glucose independent (452). Ethanol and DMSO were used as solvents for tolbutamide and glyburide, respectively, and control cells for these experiments were incubated in 2.5 mM glucose plus vehicle. Plates were incubated at 37°C for a further 20 min during acute insulin stimulation before media were collected and stored at -80°C for later insulin measurement. Cells were then washed in PBS and used for cholesterol and/or protein quantification as described previously (448).



### 2.1.8 Islet extraction

All animal work was performed in accordance with The Australian Code for the Care and Use of Animals for Scientific Purposes and was approved by Curtin University animal ethics committee (Approval number ARE2016-5). Pancreatic islets were extracted from 6-12 week old male Wistar rats using a protocol similar to that previously described (453-455). A cannula was inserted into the bile duct and the pancreas was perfused with 0.5 mg/mL of collagenase P (Sigma) dissolved in 10 mL of cold Hank's balanced salt solution (HBSS). After digestion at 37°C for 15 min, complete medium (RPMI 1640 supplemented with 10% FBS, 100 units/mL penicillin and 0.1 mg/mL streptomycin) was added. Histopaque (1.119, Sigma) supplemented with an electrolyte solution (5% v/v; 200 mM HEPES, 94 mM KCl, 24 mM MgSO<sub>4</sub>·7H<sub>2</sub>O, 25.6 mM CaCl<sub>2</sub>·2H<sub>2</sub>O) was used to purify islets, which were harvested by flotation to the supernatant following centrifugation for 15 min at 500 x g, with slow deceleration in a Beckman Coulter Allegra X-12 centrifuge with SX4750 rotor. Purified islets were then washed twice and plated in ultra-low adherence plates (Corning) in complete medium to recover overnight at 37°C in a 5% CO<sub>2</sub>/95% air incubator. The next day, islets were handpicked under a microscope, transferred into 6-well, ultra-low adherence treatment plates and incubated with 10 mM atorvastatin or vehicle control (DMSO) for 24 h. Groups of 15 islets were then washed twice, pre-incubated in KRBB supplemented with 1.1 mM glucose for 40 min then stimulated successively in control and stimulation conditions for 20 min each. Media were collected from the control and stimulation incubations and stored at -80°C for subsequent analysis of insulin content. Islet insulin content was subsequently measured after extraction by an overnight incubation in acid ethanol (1.5% concentrated HCl in 70% ethanol (EtOH)), as previously described (456).

### 2.1.9 Insulin ELISA

Insulin was assayed by sandwich enzyme-linked immunosorbent assay (ELISA) using an ultrasensitive or high range (for *in vitro* work and islets, respectively) Rat Insulin ELISA kit (Merckodia) as per manufacturer's instructions. Briefly, 25 µL (or 10 µL for high range kit) of appropriately diluted sample and 100 µL (or 50 µL) of enzyme conjugated detection antibody was added to wells pre-coated with capture antibodies. After 2 h of incubation at room temperature the plate was washed thoroughly with wash buffer and 3,3',5,5'-Tetramethyl-benzidine (TMB) was added. Colour was allowed to develop for 15 min then the reaction was stopped with 0.5 M H<sub>2</sub>SO<sub>4</sub>. The absorbance was read on a plate reader (EnSpire, PerkinElmer) at 450 nm.

### 2.1.10 Protein quantification

Total protein was quantified using Pierce's BCA Assay (Thermo Scientific) following manufacturer's instructions. After collection of media for insulin measurement, cells were solubilised using 25 µL RIPA buffer (140 mM NaCl, 1.0% NP-40 or Triton X-100, 0.1% sodium deoxycholate, 0.1% SDS (sodium dodecyl sulphate), 1 mM EDTA (Ethylenediaminetetraacetic acid), 0.5 mM EGTA (Ethylene

glycol-bis(2-aminoethylether)-*N,N,N,N'*-tetraacetic acid), 10 mM Tris, pH 8.0). In experiments where cholesterol had already been extracted, remaining cell debris was solubilised in 1% SDS in PBS for protein quantification.

### 2.1.11 Statistical methods

One or two-way ANOVA (as appropriate) followed by Tukey's or Dunnett's multiple comparisons test was performed using GraphPad Prism version 6.01 for Windows (GraphPad Software, La Jolla California USA, www.graphpad.com). To account for variation between individual experiments, two-way ANOVA was used with individual experiments as the row factor and treatment-secretagogue combination as the column factor. Row statistics were then used to produce figures. Statistical significance was inferred at a nominal value of  $\alpha = 0.05$ .

## 2.2 Results

Treatment with c-M $\beta$ CD resulted in substantial increases in cellular cholesterol and was associated with a concentration-dependent decrease in insulin secretion when maximally stimulated by a combination of glucose + amino acids. M $\beta$ CD had a more modest effect both on cholesterol content and insulin secretion. Both hydrophilic and lipophilic statins reduced cholesterol significantly, and maximal insulin secretion in response to glucose + amino acids was blunted, as observed for c-M $\beta$ CD treatment. Similarly, freshly isolated mouse islets treated for 24 h with atorvastatin secreted less insulin upon stimulation with high glucose + amino acids. In contrast to c-M $\beta$ CD, this statin effect was not acute, becoming significant only after extended exposure (24 h). Detailed results are outlined below.

### 2.2.1 Cholesterol absorption using c-M $\beta$ CD, but not desorption using M $\beta$ CD, blunted maximal stimulated insulin secretion.

M $\beta$ CD treatment for 30 min reduced cellular cholesterol in a dose-dependent manner ( $F(4, 52) = 8.216$ ,  $P < 0.0001$ ). Tukey's multiple comparisons test revealed significant differences in cholesterol after 30-min treatments with 2.5 and 5 mM M $\beta$ CD (25% and 28% reduction;  $P < 0.05$  and  $P < 0.01$  compared to no treatment, respectively, Figure 2.1A). There were no significant differences in cholesterol in response to 0.5 and 1 mM M $\beta$ CD treatment. Viability remained unchanged at all doses (data not shown).

Cholesterol loading with c-M $\beta$ CD resulted in highly significant increases in cell cholesterol ( $F(4, 50) = 52.89$ ,  $P < 0.0001$ , Figure 2.1B) and were of greater magnitude than that caused by M $\beta$ CD treatment, with significant increases of ~75% ( $P < 0.05$ ), ~373% ( $P < 0.0001$ ) and ~254% ( $P < 0.0001$ ) at 1, 2.5 and 5 mM concentrations, respectively.

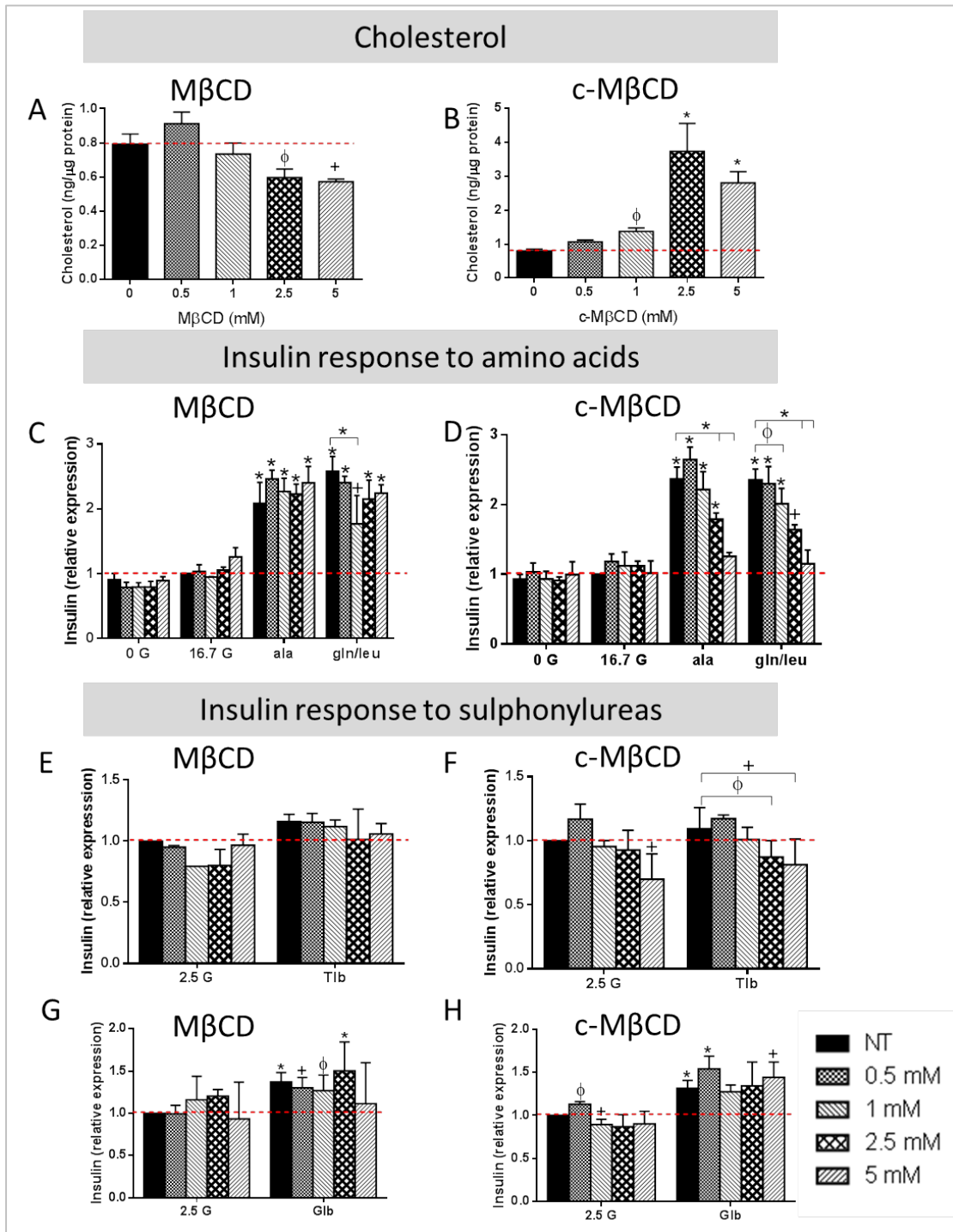


**Figure 2.1. Effects of MβCD or c-MβCD on total cellular cholesterol (A, B), and insulin secretion in response to nutrients (C,D) and sulphonylureas (E,F and G,H).**

Acute (20 min) stimulation with glucose (G, mM) ± amino acids (ala = 10 mM alanine, gln/leu = 10 mM glutamine + 10 mM leucine) (C, D), tolbutamide (tib, 200 μM) (E, F) or glyburide (glb, 20 μM) (G, H). Insulin results are expressed as relative to respective controls (0 or 2.5 mM glucose without treatment, red line) and shown as mean ± SEM. Amino acids and sulphonylureas were used in the presence of 16.7 or 2.5 mM glucose, respectively, and tolbutamide and glyburide controls also contain ethanol or DMSO, respectively. Experiments were repeated 2 (MβCD) or 3 (c-MβCD) times with 2-8 replicates per experiment. \* P < 0.001, + P < 0.01, φ P < 0.05 compared to control (untreated, 0 or 2.5 mM glucose, indicated by a red line) unless otherwise indicated.

In untreated cells, insulin secretion was marginally increased by high glucose alone (16.7 mM). Of note, in the vast majority of experiments, the BRIN-BD11 cells demonstrated little increase in insulin secretion in response to high (16.7 mM) compared to low (2.5 mM) or no glucose. However, nutrient secretagogues, including glucose + L-alanine, or glucose with the combination of L-glutamine + L-leucine (all amino acids 10 mM), the latter of which acts on glutamate dehydrogenase in an allosteric manner to enhance glutamine hydrolysis (279), stimulated a 2 to 2.5-fold increase in insulin secretion ( $P < 0.001$ , Figure 2.1C, D). Tolbutamide (200  $\mu\text{M}$ ) stimulated an  $\sim 1.1$ -fold increase in secretion above 2.5 mM glucose controls (not significant), and glyburide (20  $\mu\text{M}$ ) elicited an  $\sim 1.3$ -fold increase ( $P < 0.001$ ).

Little effect was seen on insulin secretion in BRIN-BD11 cells treated with M $\beta$ CD, whether stimulated by sulphonylureas, high glucose or amino acids in the presence of glucose. However, there were two exceptions. M $\beta$ CD (1 mM) reduced the effect of glutamine + leucine (10 mM) on insulin secretion significantly (Figure 2.1C), and higher concentrations of M $\beta$ CD (5 mM) diminished the normally significant increase caused by 20  $\mu\text{M}$  glyburide (Figure 2.1G). M $\beta$ CD tended to increase variability in stimulated insulin results, particularly for the sulphonylureas.

In contrast to the very modest effects of M $\beta$ CD, treatment with c-M $\beta$ CD was associated with a marked concentration-dependent reduction in maximal insulin secretion in response to 16.7 mM glucose + amino acids (alanine and glutamine + leucine, all 10 mM, Figure 2.1D). Control wells for tolbutamide and glyburide demonstrated more variability, possibly due to the ethanol and DMSO, respectively, although the concentration of the vehicle was no more than 0.2%. Glyburide (20  $\mu\text{M}$ ) stimulated insulin secretion but tolbutamide (200  $\mu\text{M}$ ) had little effect, at least at the concentrations used, compared to the controls: even so, c-M $\beta$ CD appeared to cause a concentration dependent decrease in insulin secretion in the presence of tolbutamide. A small, significant difference was seen in basal (2.5 mM glucose) insulin stimulation with some concentrations of c-M $\beta$ CD (Figure 2.1F). Intermediate concentrations of c-M $\beta$ CD reduced the difference between control and glyburide-stimulated insulin secretion (Figure 2.1H), though these changes are small and may be due to the general variability in these samples. Of note, few other changes were seen in basal secretion with either M $\beta$ CD or c-M $\beta$ CD treatments.

### 2.2.2 Statins reduced cellular cholesterol and adversely influenced insulin secretion

Overall, statins were very effective at reducing total cellular cholesterol in BRIN-BD11 cells. Hydrophilic and lipophilic statins were used at concentrations of 1 or 10  $\mu\text{M}$  in lipoprotein-deficient media to inhibit cholesterol synthesis in cells for 24 h before total cell cholesterol was measured (Figure 2.2 – 2.4A, Figure 2.4 D). Cell cholesterol was reduced in a dose-dependent manner in all

statins used except for fluvastatin, which showed similar decreases at 1  $\mu\text{M}$  and 10  $\mu\text{M}$  doses, although maximum reduction was at 1  $\mu\text{M}$  (Figure 2.4D).

In untreated cells, minimal sensitivity to high glucose (16.7 mM) was again observed, with an average 1.16-fold (not significant) increase in secreted insulin compared to low glucose (2.5 mM, not shown). For this reason, 16.7 mM was used in place of a low glucose control in some experiments. However, an average 2-fold change ( $P < 0.001$ ) was seen in response to 10 mM L-alanine (ala) or L-glutamine + L-leucine (gln/leu) in the presence of 16.7 mM glucose compared to 16.7 mM glucose alone (Table 2.1, Figure 2.2, Figure 2.3 and Figure 2.4). Sulphonylureas elicited a weaker stimulatory response, with 20  $\mu\text{M}$  glyburide (glb) failing to significantly increase insulin secretion. Tolbutamide (200  $\mu\text{M}$ , tlb) was more effective in these experiments, with an average 1.35-fold increase ( $P < 0.01$ ) in untreated cells. The synthetic incretin hormone exendin-4 (Ex-4), in the presence of 16.7 mM glucose, stimulated an average 1.8-fold increase ( $P < 0.001$ ) in insulin secretion.

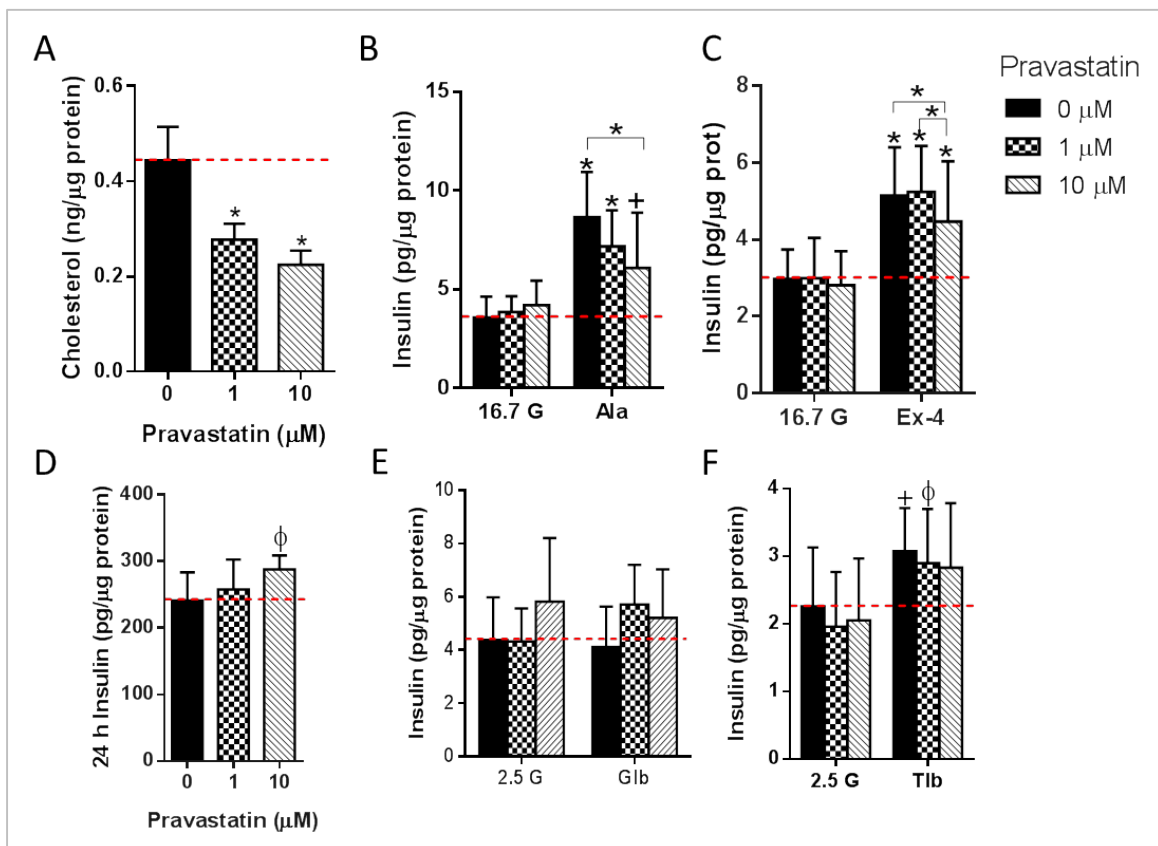


**Figure 2.2. Effects of pravastatin on cholesterol and insulin secretion in BRIN-BD11 cells.** Statins were used in lipoprotein-deficient media at 1 and 10  $\mu\text{M}$ . Cholesterol was depleted in a concentration dependent manner (A). Maximal but not basal insulin secretion was blunted after pravastatin treatment. Insulin secreted in response to glucose (G)  $\pm$  alanine (Ala, 10 mM) (B) or Exendin-4 (Ex-4, 10 nM) (C) was reduced by pravastatin treatment. However, insulin secreted in response to the sulphonylureas glyburide (Glb, 20  $\mu\text{M}$ ) (E) or tolbutamide (Tlb, 200  $\mu\text{M}$ ) (F) was minimally affected. Chronic (24 h) insulin secretion (in RPMI, 11 mM glucose) was increased in association with the higher concentration of pravastatin (D). Data is presented as mean  $\pm$  SEM.  $n=3-7$ ; \*  $P < 0.001$ ; +  $P < 0.01$ ;  $\phi$   $P < 0.05$  compared to control (red line) unless otherwise indicated.

**Table 2.1. Stimulated insulin secretion after 24 h statin treatment.**

Atorvastatin					Pravastatin				
	0 μM	1 μM	10 μM		0 μM	1 μM	10 μM		
Secretagogue	Mean ± SEM pg/μg protein	Mean ± SEM pg/μg protein	Mean ± SEM pg/μg protein	n	Secretagogue	Mean ± SEM pg/μg protein	Mean ± SEM pg/μg protein	Mean ± SEM pg/μg protein	n
2.5 G - Glb control	3.19 ± 0.72	3.53 ± 0.71	3.32 ± 1.21	3	2.5 G - Glb control	4.39 ± 1.59	4.33 ± 1.23	5.82 ± 2.38	3
Glb	3.68 ± 1.48	3.67 ± 1.40	3.67 ± 1.45	3	Glb	4.12 ± 1.52	5.71 ± 1.49	5.21 ± 1.82	3
2.5 G - Tlb control	2.40 ± 0.45	2.35 ± 0.55	2.46 ± 0.63	6	2.5 G - Tlb control	2.26 ± 0.87	1.96 ± 0.81	2.05 ± 0.91	3
Tlb	3.38 ± 0.80*	3.51 ± 0.84*	2.77 ± 0.72	6	Tlb	3.08 ± 0.64*	2.90 ± 0.80*	2.83 ± 0.96	3
16.7 G - AA control	3.78 ± 1.51	3.36 ± 1.13	3.42 ± 1.27	3	16.7 G - AA control	3.58 ± 1.05	3.86 ± 0.80	4.20 ± 1.24	3
Gln/Leu	8.65 ± 2.54*	7.04 ± 2.02*	5.28 ± 2.51	3					
Ala	7.14 ± 3.58*	6.42 ± 3.43*	4.93 ± 2.31	3	Ala	8.65 ± 2.29*	7.18 ± 1.83*	6.10 ± 2.78*	3
16.7 G - Ex-4 control	2.82 ± 0.83	2.87 ± 0.60	2.71 ± 0.77	6	16.7 G Ex-4 control	2.98 ± 0.77	3.00 ± 1.04	2.81 ± 0.88	7
Ex-4	4.67 ± 1.09*	4.56 ± 1.34*	3.90 ± 1.50	6	Ex-4	5.14 ± 1.26*	5.24 ± 1.19*	4.47 ± 1.57*	7
Fluvastatin					Simvastatin				
	0 μM	1 μM	10 μM		0 μM	1 μM	10 μM		
Secretagogue	Mean ± SEM pg/μg protein	Mean ± SEM pg/μg protein	Mean ± SEM pg/μg protein	n	Secretagogue	Mean ± SEM pg/μg protein	Mean ± SEM pg/μg protein	Mean ± SEM pg/μg protein	n
2.5 G - Glb control	3.06 ± 1.51	2.44 ± 1.19	2.79 ± 1.63	3	2.5 G - Glb control	4.49 ± 2.75	4.75 ± 0.56	4.06 ± 1.06	2
Glb	2.82 ± 1.59	2.78 ± 1.47	3.71 ± 2.31	3	Glb	3.51 ± 2.40	6.91 ± 3.07	3.49 ± 1.28	2
2.5 G - Tlb control	3.12 ± 0.95	4.43 ± 1.91	2.17 ± 0.72	3	2.5 G - Tlb control	6.00 ± 1.66	3.51 ± 0.40	5.10 ± 0.71	2
Tlb	4.63 ± 2.03*	5.48 ± 2.05*	2.95 ± 0.39	3	Tlb	6.96 ± 1.04	3.38 ± 0.25	4.47 ± 0.90	2
16.7 G - AA control	3.87 ± 0.93	5.15 ± 1.37	3.17 ± 0.97	3	16.7 G - AA control	9.21 ± 3.83	10.85 ± 3.48	7.98 ± 2.81	2
Gln/Leu	5.61 ± 2.10*	6.26 ± 2.19*	3.16 ± 0.64	3	Gln/Leu	9.52 ± 2.32	12.64 ± 6.12	7.69 ± 3.08	2
Ala	6.85 ± 1.64*	6.54 ± 1.25*	5.09 ± 1.33	3	Ala	14.26 ± 3.07	17.56 ± 5.69*	8.89 ± 0.59	2
16.7 G - Ex-4 control	3.44 ± 0.71	4.80 ± 1.80	4.58 ± 1.44	2					
Ex-4	6.94 ± 3.33	7.11 ± 3.70	5.62 ± 1.69	2					

Glb, 20 μM glyburide + 2.5 mM glucose; Tlb, 200 μM Tolbutamide + 2.5 mM glucose; Gln/Leu, 10 mM each of L-glutamine and L-Leucine + 16.7 mM glucose; Ala, 10 mM L-alanine + 16.7 mM glucose; Ex-4, 10 nM exendin-4 + 16.7 mM glucose. AA control, amino acid control (Gln/Leu and Ala). \* P < 0.05 compared to the relevant untreated control (highlighted).

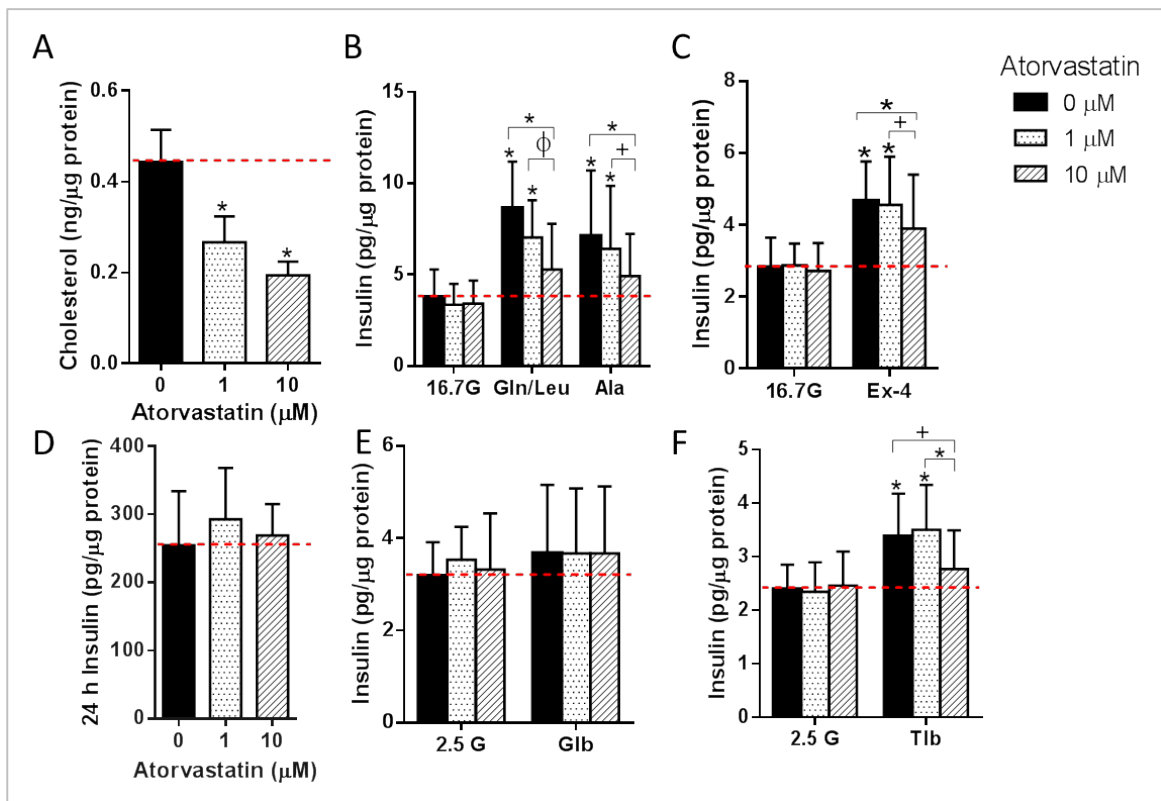


**Figure 2.3. Effect of atorvastatin on cellular cholesterol and insulin secretion.**

Cellular cholesterol was reduced in a dose-dependent manner by 24 h atorvastatin treatment (A). Insulin secreted in response to acute (20 min) stimulation by amino acids (B), Gln/Leu, 10 mM L-glutamine + 10 mM L-leucine or ala, 10 mM L-alanine) and 10 nM exendin-4 (C) but not 16.7 mM glucose (16.7G) was also reduced after atorvastatin treatment. Insulin secreted in response to the sulphonylurea tolbutamide (tlb, F) but not glyburide (glb, E) was also reduced by the higher concentration of atorvastatin. Chronic (24 h) stimulation in media containing 11.1 mM glucose was not affected by atorvastatin treatment (D). Data is presented as mean  $\pm$  SEM.  $n=3-6$ ; \*  $P < 0.001$ ; +  $P < 0.01$ ;  $\Phi$   $P < 0.05$  compared to control (red line) unless otherwise indicated.

The influence of statins on stimulated insulin secretion varied. For pravastatin- (Figure 2.2B) and atorvastatin- (Figure 2.3B) treated cells, insulin secretion stimulated by L-alanine + 16.7 mM glucose was diminished in a dose-dependent manner ( $P < 0.001$ ). This effect appeared to be stronger with atorvastatin, with the higher atorvastatin dose abrogating the stimulatory effect of the amino acid. A similar blunting was seen after gln/leu stimulation in atorvastatin-treated cells.

Likewise, exendin-4-stimulated insulin secretion was blunted by both pravastatin and atorvastatin treatment. Tolbutamide-stimulated insulin secretion also showed some blunting with pravastatin, atorvastatin and fluvastatin treatment, while in these experiments glyburide failed to stimulate insulin secretion and this was not altered by atorvastatin or pravastatin treatment.

For all acute insulin secretion experiments and across all statin treatments, no change was evident in basal (2.5 glucose) or glucose-only (16.7 mM) acutely stimulated insulin secretion.

Similarly, no change was found over 24 h of basal secretion in atorvastatin-treated cells, but surprisingly, higher dose pravastatin elicited a modest but significant increase in chronic insulin secretion (Figure 2.2 D). Further investigation in BRIN-BD11 cells treated with simvastatin and fluvastatin yielded similar results, with no change in basal insulin secretion, but blunting of stronger stimulation (Figure 2.4).

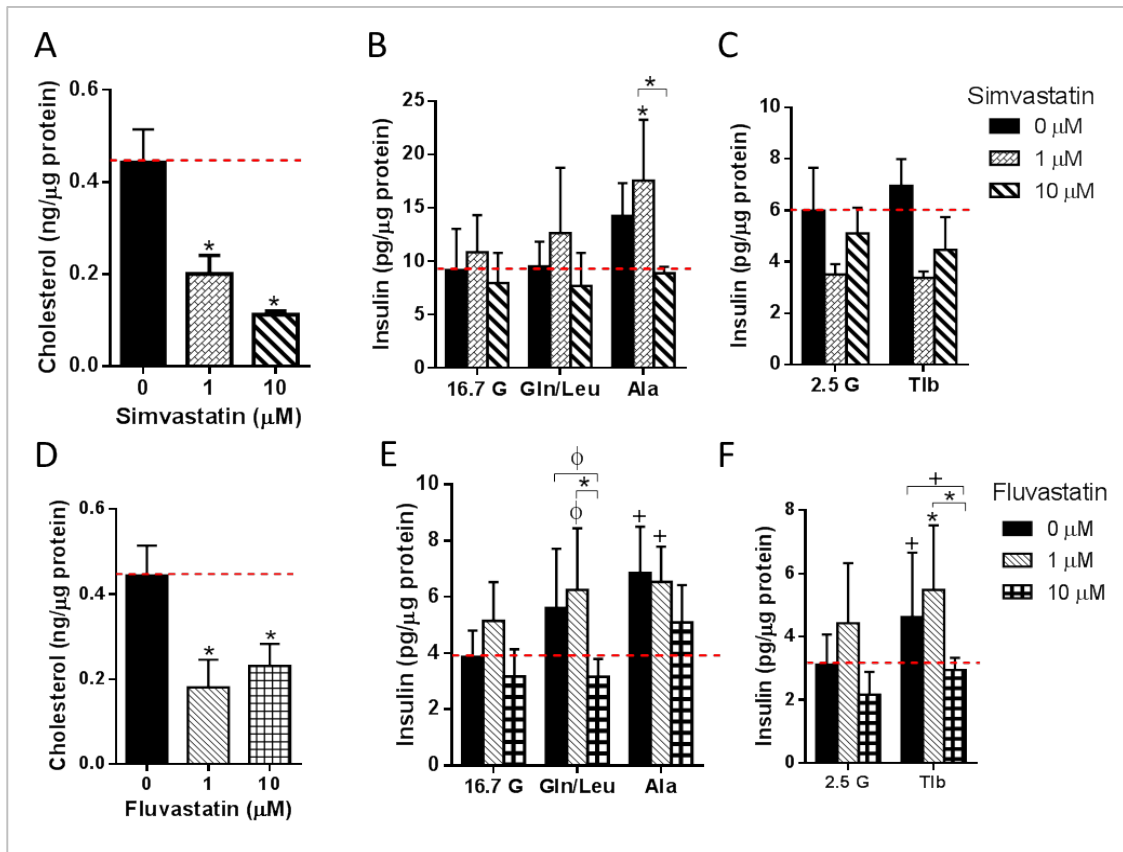


**Figure 2.4. Effect of simvastatin and fluvastatin on cholesterol and insulin secretion.** Cholesterol was reduced by simvastatin (A) and fluvastatin (D). Insulin secreted in response to acute stimulation by 10 mM L-alanine was decreased by high but not low concentrations of simvastatin (B) and fluvastatin (E). Tolbutamide-stimulated insulin secretion was also blunted by high dose fluvastatin (F) but not simvastatin (C). Data is presented as mean  $\pm$  SEM.  $n=2$  (simvastatin) or 3 (fluvastatin); \*  $P < 0.001$ ; +  $P < 0.01$ ;  $\phi$   $P < 0.05$  compared to control (red line) unless otherwise indicated.

In all experiments described above, 24 h statin treatments were followed by stimulated insulin secretion performed in the absence of statins. However, it is possible that statins could have an acute inhibitory effect, reducing insulin secretion directly by some mechanism that interferes with the secretory process. To investigate this, two different approaches were used. Firstly, insulin secretion was stimulated in the presence of 1 or 10  $\mu$ M atorvastatin, pravastatin or simvastatin in previously statin-naive cells (Figure 2.5 A, B). No acute statin influence was observed in the single experiment undertaken at each statin concentration. In the second method, cells were treated with either atorvastatin or pravastatin (10  $\mu$ M) for 24 h then stimulated to secrete insulin either in the continued presence of statins or not (Figure 2.5 C-H).



Except for tolbutamide-stimulated, pravastatin-treated cells, no difference in insulin secretion was observed based on the continued presence of statin during stimulation

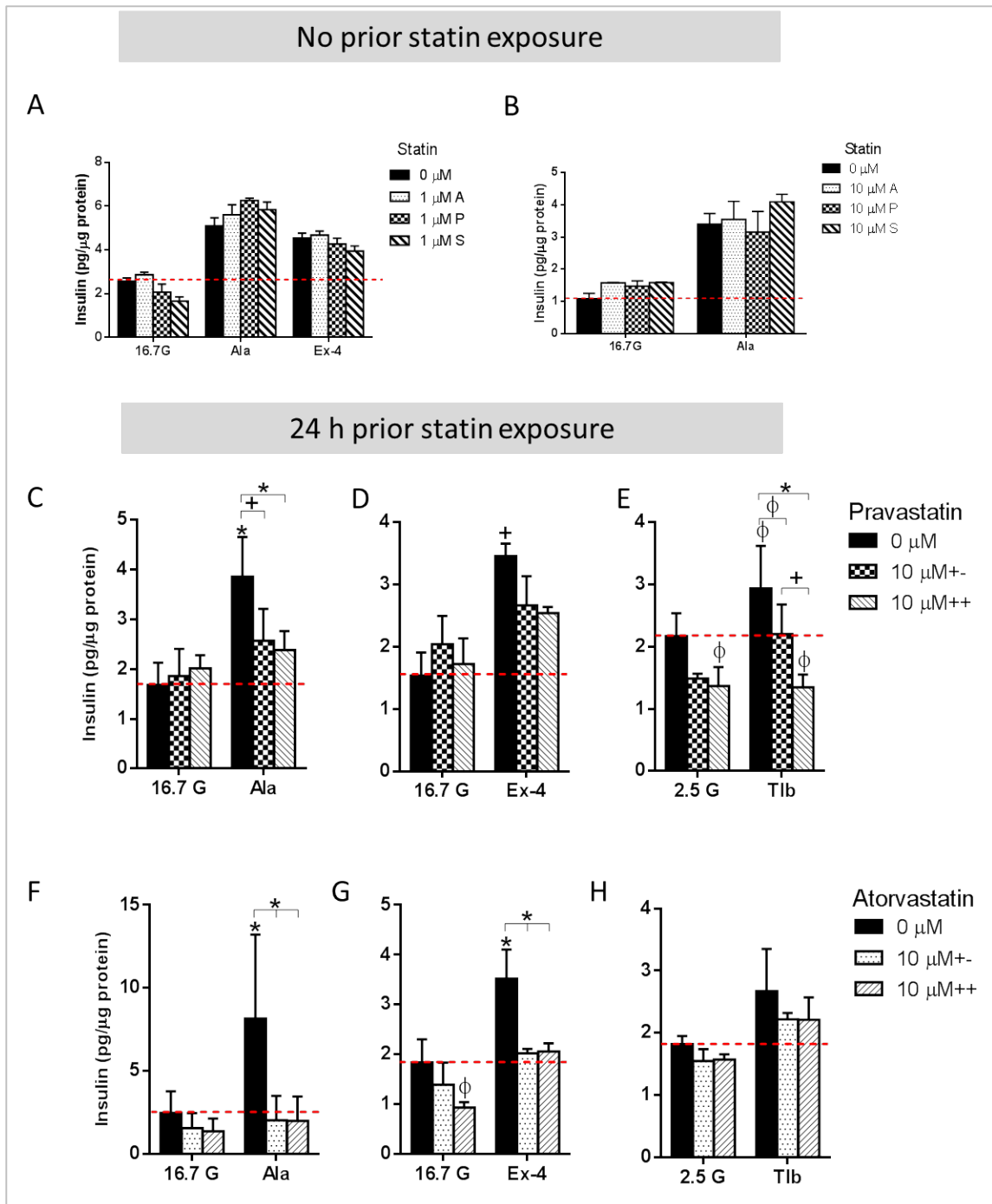


**Figure 2.5. Acute effects of statins on insulin secretion.**

The presence of low (A) or high dose (B) statins had no effect on stimulated insulin secretion in previously statin-naïve cells. The presence of statins during stimulation also had no additional effect on prior exposure (24h) to pravastatin (C-E) or atorvastatin (F-H). One exception was found in response to Tlb (E), which was further attenuated by the continuing presence of pravastatin but not atorvastatin. Data is presented as mean  $\pm$  SEM. P, pravastatin; A, atorvastatin; S, simvastatin; +-, cells treated for 24 h with statin only; ++ cells treated for 24 h with statin and stimulated to secrete insulin in the continued presence of statin. Ala, 10 mM L-alanine; Ex-4, 10 nM exendin-4; Tlb, 200  $\mu$ M tolbutamide. F, n=2, A, B, n=1 (4 replicates). All others, n=3. \*  $P < 0.001$ ; +  $P < 0.01$ ;  $\phi$   $P < 0.05$  compared to control (red line) unless otherwise indicated.

### 2.2.3 Effect of statin on stimulated insulin secretion in isolated rat islets

To assess the influence of statins on insulin secretion in primary cells, pancreatic islets were isolated from Wistar rats, treated for 24 h with 10  $\mu$ M atorvastatin *ex vivo*, and subject to acute stimulation with 16.7 mM glucose + L-alanine (Figure 2.6). When expressed in terms of insulin/islet/minute, ala-stimulated untreated, but not atorvastatin-treated, islets secreted significantly more insulin than unstimulated controls ( $P < 0.05$ , Figure 2.6 A). Islet insulin content was also measured in the same islets after stimulation tests were completed. Stimulated insulin secretion is expressed as a percentage of total insulin content in Figure 2.6 B and shows a significant difference in percent content secreted during ala stimulation between atorvastatin treatment and control groups.

The modest stimulation indices in Figure 2.6 C are indicative of islet damage during the extraction process, resulting in increased basal insulin secretion (Patrik Rorsman, personal communication, 2017). Nevertheless, a trend towards statin-mediated blunting of maximal secretion can be seen in alanine-stimulated islets and the effect can be expected to increase with improved technical expertise.

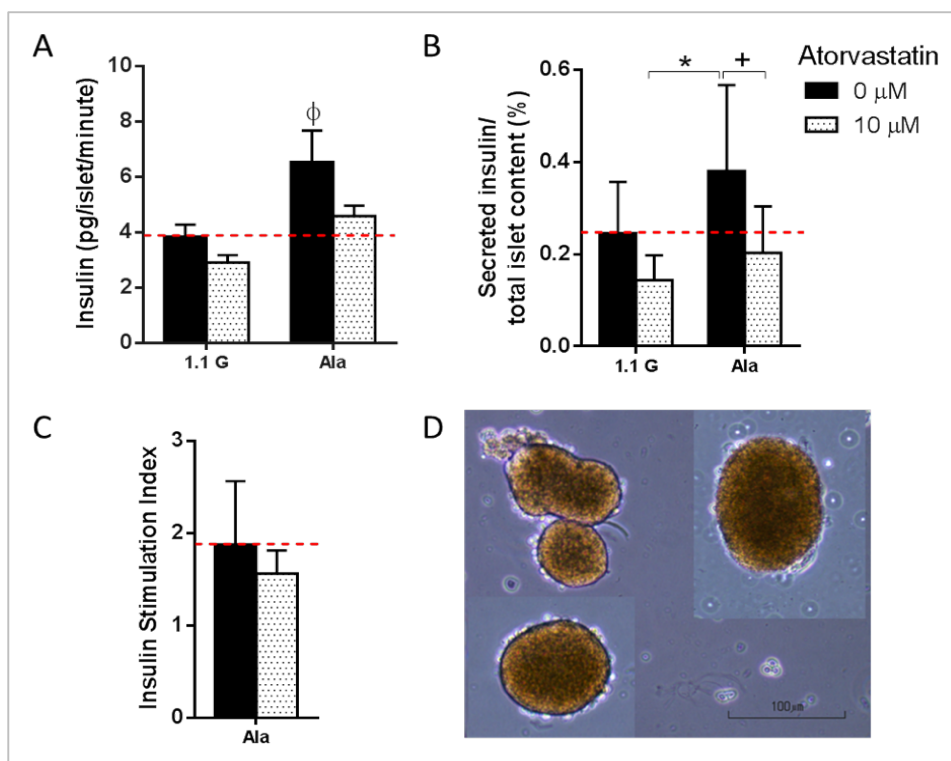


**Figure 2.6. Effect of statins on islet insulin secretion.**

Insulin from isolated islets secreted in response to acute (20 min) stimulation with 10 mM L-alanine (Ala) + 16.7 mM glucose preceded (or not) by 24 h atorvastatin treatment. **A)** Stimulated secretion per islet per min. **B)** Results expressed as a percentage of islet insulin content. **C)** Results expressed as stimulation index (stimulated secretion/unstimulated secretion in the same islets). **D)** Freshly isolated islets.  $n=6$  separate experiments with at least 4 replicates per experiment. G = glucose (mM).  $\phi$   $P < 0.05$ , +  $P < 0.01$ , \*  $P < 0.001$  compared to control (red line) unless otherwise indicated.

## 2.3 Discussion

The recently described link between increased onset of T2D and statin therapy (441) has stimulated considerable research into unknown pleiotropic actions of statins and the role of cholesterol in secretory processes. The aim of the present study was to determine whether stimulated insulin secretion, in response to a range of different secretagogues, was affected by the cholesterol-reducing effects of statin therapy, and the commonly used experimental reagents M $\beta$ CD and c-M $\beta$ CD, known to effectively modulate cell cholesterol. Statins were shown to reduce maximally stimulated insulin secretion. This could be due to drug on-target effects to inhibit cholesterol synthesis, resulting in reduced cholesterol concentrations in the cell membrane or organelles including secretory granules. It could also be related to decreases in various biologically important mevalonate pathway-derived products down-stream of HMG-CoA, or other pleiotropic statin effects. The use of M $\beta$ CD, both 'empty' and pre-loaded with cholesterol, can help to determine whether the statin effect is likely to be related to cellular cholesterol concentrations.

### 2.3.1 M $\beta$ CD-mediated cholesterol manipulation effects on insulin secretion

M $\beta$ CD sequesters cholesterol from the cell membrane, but when pre-loaded with cholesterol, can also deliver it to the cell membrane (410). The efficacy of M $\beta$ CD in cholesterol manipulation is cell type-dependent, showing altered efficiency in different cells. Our results suggest a greater impact on cholesterol loading than depletion in BRIN-BD11 cells. In fact, BRIN-BD11 cells were quite resistant to cholesterol depletion with M $\beta$ CD, yielding a 27.5% (-1.38-fold) reduction with 5 mM M $\beta$ CD over 30 min of treatment. Other cell lines in our laboratory demonstrated 56% (CHO T10), 40% (HepG2) and 23% (HSMM, with very low native cholesterol content) reduction, using the same stock preparation, dose and identical protocol and reagents (457). On the other hand, BRIN-BD11 cells were very responsive to cholesterol uptake from c-M $\beta$ CD, with a maximum 4.5-fold increase with 2.5 mM c-M $\beta$ CD treatment for 30 min. Likewise, published reports vary in their findings regarding the influence of M $\beta$ CD for a range of cell types, treatment times and doses. For example, Hissa *et al* (425) demonstrated a 4.5-fold reduction in cholesterol in immortalised mouse fibroblast cells using 5 mM M $\beta$ CD for 45 min in the absence of serum, and alveolar type II cells were depleted of 57% of their cholesterol using 3 mM M $\beta$ CD over 30 min (458). Rituper *et al* (325) achieved a 72% reduction of cholesterol in rat pituitary lactotrophs using 10 mM M $\beta$ CD for 10 min then replenished 75% of the extracted cholesterol in a further 10-min incubation with cholesterol-loaded M $\beta$ CD. Xia *et al* (66) also used 10 mM M $\beta$ CD and reported a 58% reduction in cholesterol after 30 min of treatment in  $\alpha$ TC6 (pancreatic islet  $\alpha$ -cell line) cells. Ge *et al* (333) removed 32% of cholesterol from platelets in 30 min with 10 mM M $\beta$ CD and loaded cholesterol to 131.8% with c-M $\beta$ CD. Bacova *et al* (332), who found a large difference in native

cholesterol content between INS-1 and INS-1E cell lines, reduced cholesterol to 6 and 3 % of control after 2 h of incubation in 10 mM M $\beta$ CD.

Two anomalies were seen in cholesterol manipulation with cyclodextrins. The first was a slight non-significant increase in cholesterol ( $0.8 \pm 0.1$  vs  $0.9 \pm 0.1$  ng/ $\mu$ g protein,  $P = 0.29$ , Figure 2.1C) at low concentrations of M $\beta$ CD treatment. A similar phenomenon has previously been observed (459) in T lymphocytes donated by young but not elderly participants and using the same dose (0.5 mM for 30 min) of M $\beta$ CD. The second interruption to the generally dose-dependent cholesterol curve was at 2.5 mM c-M $\beta$ CD, where cholesterol was significantly elevated compared to the 5 mM dose ( $3.74 \pm 0.17$  vs  $2.8 \pm 0.5$  ng/ $\mu$ g protein,  $P = 0.011$ ). It is not known whether some homeostatic mechanism may be responsible for these departures, or whether further replications would make them more, or less prominent. The short duration (30 min) and environment of treatment (serum-free KRBB) means cholesterol synthesis or uptake/efflux via lipoprotein particles can be ruled out as probable mechanisms of change.

Cholesterol quantification was normalised to protein content. While protein would not be expected to change over 30 min of treatment due to differential cell growth or replication, treatments could potentially compromise cell attachment to the plate. To validate whether cholesterol extraction introduced bias to measurement of protein, protein quantified in independent experiments was compared with protein quantified from cell skeletons remaining in the plate after cholesterol extraction (as in a protocol described previously (448)). There was no significant difference between the average change made by extraction to protein measures for any of the c-M $\beta$ CD treatments. Cholesterol extraction did, however, make an overall difference to protein quantification ( $P = 5.8 \times 10^{-9}$ ), with an average of 0.08 mg/mL (32%) more protein measured if cholesterol was not extracted first (results not shown). This is expected, as some proteins may be soluble in hexane/isopropanol used to extract the cholesterol. Thus, cholesterol and protein extraction carried out in successive steps should not introduce bias in protein or normalised cholesterol results.

Cholesterol depletion with M $\beta$ CD had little effect on subsequent insulin secretion, with only gln/leu-stimulated secretion showing a small decline. This is probably related to the modest cholesterol reduction caused by M $\beta$ CD. In contrast, and in keeping with its greater influence on cellular cholesterol, c-M $\beta$ CD had a significant, dose-dependent effect on subsequent amino acid-stimulated insulin secretion, with a 2.35- and 2.37-fold change stimulated by glucose + gln/leu and glucose + ala reduced to 1.15- and 1.25-fold ( $P < 0.001$ ), respectively, after 5 mM c-M $\beta$ CD treatment. Interestingly, this effect was seen only in maximally stimulated secretion, with basal or mildly stimulated insulin secretion unaffected. This may be a consequence of statistical power.

Of note, in the majority of experiments, the BRIN-BD11 cells demonstrated little increase in insulin secretion in response to high (16.7 mM) compared to low (2.5 mM) or no glucose. Although these cells are known to exhibit glucose-sensitive insulin secretion (460, 461), the effect size is small, requiring many replications to gain significance. Secretion from these cells can be variable, for example, exhibiting variable insulin secretion depending on the type of substrate (462, 463).

Given that the sulphonylureas did not demonstrate a robust stimulatory influence in proportion to the variance, the experimental design resulted in lower than expected statistical power, and more samples would need to be measured to improve the chance of determining an effect. An effect size of 0.16 was calculated (464) in statin-free controls for glyburide, 0.71 for tolbutamide and 1.18 for alanine compared to relevant controls. Thus a reduced chance of showing an effect (particularly for the glyburide experiments) could explain discrepancies in the sulphonylurea results, for example between M $\beta$ CD and statin studies.

Other studies utilising M $\beta$ CD to deplete cholesterol in  $\beta$ -cell lines have found diverse effects. For example, a significant dose-dependent decrease in glucose-stimulated insulin secretion from INS-1 and INS-1E insulinoma cell-lines was observed after 2 h of treatment with 10 mM M $\beta$ CD (332). Conversely, a significant increase in insulin secreted by HIT-T15 cells was associated with 10 mM M $\beta$ CD treatment for 30 min when stimulated with 10 mM glucose for 1 h (69). These studies used a higher dose and/or time than was used in the present study and cholesterol was reduced to a greater extent, which may account for the difference. There may also have been influences on membrane integrity as discussed below. Indeed, the study in INS-1 and INS-1E cells mentioned above reported insulin secretion as % of basal, due to the greatly increased basal secretion in cholesterol depleted cells. Basal secretion was not measured in the HIT-T15 study, which may account for the different result.

Cholesterol loading caused significant blunting of maximally stimulated insulin secretion in the current study. Elsewhere, LDL receptor knockout mice with resulting high cholesterol content in islets had reduced insulin response to glucose stimulation. This was accompanied by decreased intracellular calcium, observed by changes in Fura-2/AM fluorescence in association with intracellular calcium concentrations. In the same study, reduction of cholesterol to levels consistent with wild-type using M $\beta$ CD treatment returned GSIS to normal. At the same time, reduction of cholesterol with M $\beta$ CD in wild type islets also reduced intracellular calcium concentrations and GSIS, except at high M $\beta$ CD concentrations (10 mM), when membrane integrity was compromised and insulin secretion greatly increased (444).

Extensive studies on the effect of cyclodextrins in exocytosis include findings that cholesterol reduction caused lipid raft disassembly, along with loss of channel proteins (such as Ca<sub>v</sub>1.2) and fusion proteins (such as SNAP25, syntaxin-1A and VAMP2) from lipid rafts (69, 73), and

reduced granule fusion (331). These effects have been attributed partly to the physical properties of cholesterol on membranes such as curvature and fluidity (327). Loss of hypotonicity-stimulated insulin secretion has also been attributed to rigidity caused by cholesterol loading (332).

### 2.3.2 Statins reduced cholesterol and blunted maximal insulin secretion

Statin treatment in lipoprotein-deficient media, regardless of the specific statin, was very effective in reducing total cellular cholesterol. In the absence of lipoprotein-mediated flux, this change must be mainly a result of reduced cholesterol synthesis. It is interesting to note the implication this has for the rate of cholesterol synthesis and the rapidity with which cholesterol is diminished from  $\beta$ -cells in the absence of lipoprotein-mediated efflux, with 47.5% – 72% cholesterol reduction with different statins over a 24-h period. Some of this ‘loss’ could be associated with cell proliferation. BRIN-BD11 cells are known to divide approximately every 20 h (430). Existing cholesterol would thus be reduced in comparison to protein content of the population unless *de novo* synthesis could match this demand.

Another consideration is the role of cholesterol in the insulin granule membrane, the fate of which is not fully elucidated. It is known that the total surface area of insulin granules (at least in rabbits) is ~4.5-fold that of the plasma membrane, having similar cholesterol concentration (344). This represents a considerable pool of cholesterol, which is assumed to be cycling between insulin granules and plasma membranes. The possibility that some could be lost during exocytosis somewhat depends on the nature of fusion, release and membrane retrieval. Imaging analysis has demonstrated that insulin granules are created *de novo* in the Golgi and are not rapidly recycled in ‘kiss-and-run’ events (465). A review of this and other possible models is available elsewhere (466). Consistent with the *de novo* granule synthesis model,  $\beta$ -cells possess enzymes for lipogenesis and their inhibition is linked to reduced insulin secretion, leading to the proposal that mitochondrial biosynthesis may provide substrates for lipid synthesis, at least partially to supply granule membrane lipids (467). Conversely, studies in calf chromaffin cells and MIN6  $\beta$ -cells have reported data suggesting a link between rates of exocytosis and endocytosis, supporting the concept of a membrane cycling mechanism (468, 469). Thus, the extent of potential cholesterol loss to cells during exocytosis, if any, remains unclear.

Regardless of the mechanism of cholesterol loss or its alternative fate during inhibition of synthesis, the effects on robustly stimulated insulin secretion are similar to that found after cholesterol loading by c-M $\beta$ CD. Statin-treated cells had a reduced insulin response when acutely stimulated by potent secretagogues including gln/leu, ala, and ex-4, and in some cases, tolbutamide. A similar result was produced in atorvastatin-treated islets. In studies elsewhere, rosuvastatin (470) and simvastatin but not pravastatin (302) reduced glucose-stimulated insulin secretion in INS-1 832/13 and MIN6 cells, respectively. Cellular cholesterol was not measured

in the latter study so it is not possible to assess the effectiveness of HMG-CoA inhibition. An insulin secretion rate-attenuating effect was found in  $\beta$ -cells from human islets treated with 100 nM atorvastatin, pravastatin, rosuvastatin and pitavastatin (471). In islets isolated from rosuvastatin-treated mice on a normal diet, insulin secretion in response to high glucose (> 11.1 mM) or potassium-stimulated insulin secretion was also reduced (324). Interestingly, basal insulin secretion was not affected.

The lack of effect produced by glyburide or basal stimulation in this study contrasts with the results above, possibly due to effect size and statistical power. When cholesterol is plotted against glucose + alanine-stimulated insulin secretion across atorvastatin, pravastatin and c-M $\beta$ CD treatment, a pattern emerges where the highest secretion is at untreated levels, and deviations in cell cholesterol, either up or down, are associated with reduced insulin secretion (Figure 2.7). This supports the stated hypothesis, at least for secretagogues that stimulate a robust insulin response.

Similar effects on the blunting of maximal insulin secretion of both cholesterol depletion and overload could result from either similar or diverse mechanisms which have similar outcomes. For example, mitochondrial insufficiency could reduce maximal insulin secretion similarly to effects on membrane characteristics limiting exocytosis. Evidence supporting these examples include the rescue of GSIS impaired by lovastatin by the addition of mevalonate, postulated in that study to be due to the restoration of the prenylation of small GTP-binding proteins (472, 473). Elsewhere, Xu *et al* postulated that fewer insulin granule fusion events take place in cholesterol loaded cells (5 mM c-M $\beta$ CD for 30 min), accompanied by changes in the nature of those events (474). Mechanisms of cholesterol modulation-induced insulin blunting may thus be varied and may be cumulative.

Like glucose, nutrient secretagogues such as L-alanine and L-glutamine undergo complete hydrolysis in the TCA cycle and electron transport chain to produce H<sub>2</sub>O, CO<sub>2</sub> and ATP (264). ATP is coupled to insulin secretion via K<sup>+</sup><sub>ATP</sub> channels and the subsequent processes of insulin secretion. Sulphonylureas such as tolbutamide, on the other hand, bind directly with the SUR entity of the K<sup>+</sup><sub>ATP</sub> channel, causing it to close independently of metabolic processing and the ATP:ADP ratio. Given that both tolbutamide and nutrient secretagogue-stimulated insulin secretion were affected by statin-induced cholesterol changes, it seems probable that cholesterol content-related mechanisms are at least partially, and possibly mainly, involved, as suggested elsewhere (205, 299-301, 323).

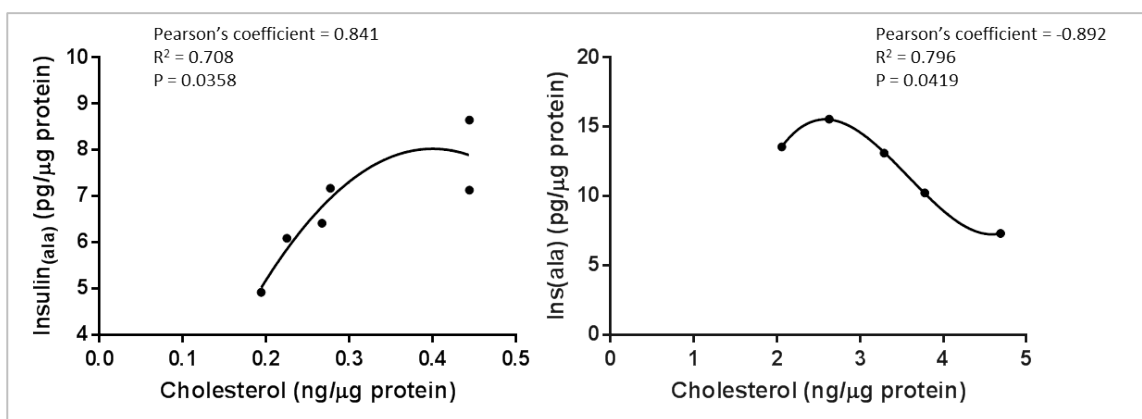


**Figure 2.7. Correlation between cholesterol and Insulin.**

Insulin secreted in response to L-alanine was plotted against cholesterol values for different concentrations of statins (pravastatin and atorvastatin, LHS) and c-MβCD (RHS). A polynomial correlation curve was fitted to the data.

A greater insulin inhibiting effect that was seen after nutrient or exendin-4 stimulation could be due to secretagogue dose equivalence, and indeed this is most likely the case for glyburide, which, in statin experiments, failed to stimulate insulin secretion even in untreated cells in some experiments. However, there are other factors such as metabolic coupling factors (MCF) and inhibition of cholesterol intermediates involved in metabolic and secretory processes, that may contribute to nutrient-secretagogue failure after cholesterol inhibition and these will be explored in more detail in later chapters.

### 2.3.3 Lipophilic vs hydrophilic statins

Pravastatin is a hydrophilic statin while atorvastatin is lipophilic. It is anticipated that this physicochemical characteristic would differentially influence the intracellular permeability of the two statins. In support, many studies have found reduced pleiotropy with pravastatin compared to atorvastatin or other lipophilic statins (212, 357, 475). In the current study both statins effectively reduced cellular cholesterol and impaired robustly stimulated insulin secretion, but pravastatin had a somewhat milder effect than atorvastatin, demonstrated by smaller differences in stimulated insulin secretion with or without high dose (10 μM) statin. For example, the 10 μM pravastatin dose was not different from the 1 μM dose in its effect on insulin stimulated by 16.7 mM glucose + alanine, while the same doses in atorvastatin caused a significant difference.

There are two factors affecting lipophilicity-related variability that differ in this study from the *in vivo* situation. Firstly, variances between lipophilic and hydrophilic statins in first-pass hepatic uptake and cytochrome P450 processing have been described (169), however, no hepatic processing occurs in *in vitro* studies such as the current one. Pravastatin is not metabolised enzymatically and largely undergoes extraction via the bile/faecal route or glomerular filtration in a similar form to that which is ingested, although acids can catalyse the



formation of isomers, which are similarly excreted (476). In contrast, atorvastatin undergoes metabolism by CYP3A4 and metabolites are eliminated via the bile (172).

Secondly, the use of DMSO as the solvent may increase the intracellular penetration of pravastatin, as it is known to do with other substances (477). This possibility was suggested by reduced efficacy to inhibit cholesterol synthesis and interfere with insulin secretion when pravastatin was dissolved directly in water (results not shown), however, other factors may have contributed to this effect and further study would be necessary.

For the reasons outlined above, differences between lipophilic and hydrophilic statins may have been minimised in the current study compared to the *in vivo* situation. Results reported here do not negate the possibility that lipophilic statins may confer greater pleiotropy than their hydrophilic counterparts. Further studies with greater power, the use of additional hydrophilic statins (e.g. pitavastatin) and addressing the issues above would be necessary to conclusively compare the effects of statins on  $\beta$ -cell function based on their lipophilicity.

#### 2.3.4 Atorvastatin does not acutely affect insulin secretion

An acute effect of statin has been recently documented, where an elegant single islet imaging protocol was used to demonstrate that stimulated insulin secretion was rapidly inhibited by co-incubation with simvastatin (478). If accurate, this would indicate that processes other than inhibition of cholesterol or its intermediates, which would require hours rather than minutes of statin exposure, were implicated mechanistically.

In contrast to the report mentioned above, no acute effect of atorvastatin on insulin secretion was found in this study, either when added to stimulation media in untreated cells, or characterised by further changes effected by ongoing atorvastatin treatment during stimulation (Figure 2.5). The acute effect reported by Scattolini *et al* could have been due to differences between simvastatin and atorvastatin, or it could be artefactual; insulin was not measured directly, but by fluorescence of a zinc fluorophore, zinc being co-secreted with insulin in a stoichiometric manner (479-481). However, no controls were used to assess whether simvastatin could potentially affect fluorescence independently, such as by formation of salts with zinc, with the statin binding to zinc in competition with the fluorophore (as is a known possibility, (482) see Example 6). Results in the current study suggest that acute effects such as direct interference with ion channels are unlikely. However, GSIS was previously found to be decreased after just 2 h of 1  $\mu$ M simvastatin treatment, but not by inhibition of cholesterol downstream of farnesyl pyrophosphate, indicating that isoprenylation intermediates may have a role in the statin-mediated attenuation of GSIS (483).

### 2.3.5 Conclusion

Both c-M $\beta$ CD treatment, which significantly increased cellular cholesterol via membrane-associated cholesterol loading, and statin treatment, which decreased cellular cholesterol by inhibiting its synthesis, were associated with blunting of maximal insulin secretion. Pravastatin (hydrophilic) and atorvastatin (lipophilic) were the main statins under investigation in this project, but similar results were also found with fluvastatin and simvastatin (both lipophilic). Taken together, it appears that potency to modulate cholesterol content has a greater impact on the risk of blunted insulin secretion than lipophilicity, the direction of cholesterol modification, i.e., whether it is increased or decreased, or the mode of cholesterol manipulation i.e., whether it is modified via membrane loading or sequestration or by HMGCR inhibition. One exception to this was an anomaly in cholesterol loading using c-M $\beta$ CD where the 2.5 mM dose exceeded the 5 mM dose in post-treatment cellular cholesterol measurements.

These results support the hypothesis that the relationship between  $\beta$ -cell cholesterol content and stimulated insulin secretion is tri-phasic, characterised by optimal mid-range cholesterol concentration flanked by low and high cholesterol content which reduces insulin secretion in response to robust stimulation with physiological and therapeutic secretagogues, but does not affect acute basal secretion. Chronic basal secretion may be increased, at least by some statins (pravastatin), possibly due to membrane damage, but further investigation would be necessary to confirm this. Increased LDHA activity in the media of atorvastatin treated cells was recently reported in another  $\beta$ -cell line (NIT-1), suggesting membrane damage (357).

These results also support the hypothesis that statins exert concentration-dependent effects on insulin secretion, and this is more closely linked to the extent to which they modify cholesterol content rather than lipophilicity, at least in an *in vitro* context. The lipophilic statins, however, were more likely to reduce viability at higher concentrations and atorvastatin exerted a stronger adverse influence on insulin secretion than pravastatin.

Nutrient and therapeutic secretagogues used in this project stimulate insulin secretion either directly by binding to the K<sup>+</sup><sub>ATP</sub> channel to facilitate its closure or via the TCA cycle, being coupled to insulin secretion via ATP and various other metabolic coupling factors. However, insulin blunting seemed more related to the capacity to stimulate secretion rather than the mechanism of stimulation, with more robust stimulation more greatly affected than low-level stimulation and basal stimulation not affected.

### 2.3.6 Limitations and future directions.

While BRIN-BD11 cells are reportedly responsive to glucose stimulation (461), the effect size is small, reducing the statistical power of insulin stimulation experiments. This cell line does, however, demonstrate appropriate glucose metabolism (460, 484) and insulin responsiveness to

amino acids (450) and is thus considered an appropriate model. However, the minimal size of the response to glucose observed in the present study is a limitation.

Islet results are expected to show greater stimulation indices than were produced here. Our group is in the process of learning the technically difficult skill of successful islet isolation and, while to the best of my knowledge the results reported here are reliable, it is expected that, with time and practice, more convincing results will be produced.

This study demonstrates the effectiveness of HMGCR inhibition by statins in a tissue type neither specifically targeted by these drugs nor usually associated with large cholesterol flux. It is known that lipophilic statins are metabolised by hepatic enzymes (172), which are not available in this *in vitro* system. The difference in impact between the original drug and its post-hepatic metabolites is not known. At the very least, first-pass hepatic processing would be expected to reduce the statin concentration reaching the  $\beta$ -cells *in vivo*. However, details of expected exposure of  $\beta$ -cells to statins or their metabolites, and how closely this *in vitro* study replicates the conditions *in vivo* is unknown. This is a limitation of this study.

Further study that would support this body of research would be to conduct rescue experiments, where cholesterol depletion is rescued by cholesterol loading. Preliminary work has been done on such a study and is available in Appendix A.1.

The fate of cholesterol in  $\beta$ -cells is not fully understood, and it would be useful to trace cholesterol in a closed *in vitro* system. In addition, tracing labelled cholesterol provided to replete severely cholesterol-depleted cells, with reference to potential insulin secretion rescue, would be useful in determining mechanisms of statin-mediated insulin blunting.

This project supports existing research demonstrating that there is a clear link between cellular cholesterol and insulin secretion, but the nature of this link is not fully understood. The influence of lipoprotein particles in moderating statin effects in islets is also not fully understood, and to remove the possibility of any such influence, this study was performed in their absence. However, the *in vivo* situation is further complicated by the presence of lipoprotein particles, which will vary in concentration and ratio of constituents between species and between individuals. Further research would be helpful to address these topics.

## Chapter 3      Metabolic effects of statins in $\beta$ -cells

In the previous chapter, maximal insulin secretion was blunted by both cholesterol-reducing statin medication and cholesterol-enhancing c-M $\beta$ CD treatment in BRIN-BD11 cells. These effects may be directly due to modified cholesterol levels or they may be caused by pleiotropic mechanisms including diminished concentrations of biologically active intermediates downstream of HMG-CoA in the cholesterol synthetic pathway.

HMG-CoA reductase inhibitors reduce the synthesis not only of cholesterol, but also of products derived from intermediates of the mevalonate pathway. Some of these, such as Coenzyme Q10 and haem-A, have important functions in normal cell metabolism, particularly in mitochondrial oxidative phosphorylation. In  $\beta$ -cells, glucose metabolism is tightly coupled to insulin secretion, with the production of ATP through oxidative phosphorylation being central to the process. In this chapter, the primary aim was to characterise the metabolic effects of statin treatment on mitochondrial function in BRIN-BD11 cells. A phenotypic switch from obligatory aerobic respiration to a more glycolytic metabolic profile was found. This was not accompanied by changes in glucose uptake, and an investigation exploring possible changes in the expression profile of a panel of glycolytic enzymes found an increase in hexokinase I expression and phosphorylation of glycogen synthase kinase  $\beta$  at serine 9. How these effects might reduce the capacity to secrete insulin and increase the risk of T2D is discussed.

### 3.1 Background

#### 3.1.1 $\beta$ -cell metabolism

Pancreatic  $\beta$ -cells possess unique features, such as expression of a high  $K_m$  form of glucose transporter (GLUT2) and hexokinase (glucokinase) and low expression of glucose-6-phosphate phosphatase, to support their important physiological role in providing insulin in a fuel-dependent manner to ensure systemic glucose homeostasis (described in Section 1.4.1). However, this also exposes the  $\beta$ -cell to increased metabolic vulnerabilities as they lack the capacity of other cell types to moderate metabolic risk. For example, constitutive expression of glucose transporters (485) means they are unable to reduce glucose uptake in a high glucose environment (243).

Under normal conditions, 80-90% of glucose entering the  $\beta$ -cell is committed to complete hydrolysis to carbon dioxide and water (247, 252). Metabolic coupling factors (MCF) such as ATP, NADPH, malonyl-CoA, fumarate, malate and citrate/isocitrate ensure that insulin secretion is balanced to nutrient load (77, 243, 486, 487). Reduced responsiveness to glucose in metabolic disturbance, such as metabolic syndrome or type 2 diabetes (T2D) is, in part, due to insulin resistance, but insulin secretion coupling, the capacity to secrete insulin in response to

plasma glucose concentration changes, also plays a role, particularly in later stages of disease (488, 489).

Glucose toxicity occurs when chronically elevated glucose increases mitochondrial ROS production, and insulin secretion is inadequate due to reduced insulin gene expression and increased  $\beta$ -cell apoptosis (490), also referred to as  $\beta$ -cell fatigue.  $\beta$ -cells possess excess fuel detoxification pathways, which are mobilised under high glucose load. These operate when glucose exceeds  $\beta$ -cell saturation (16 mM in rat islets, (243)) and result in reduced insulin secretion coupling. Beyond this, glucose utilisation proceeds to fuel detoxification pathways including futile cycling and synthetic pathways to form metabolites such as citrate, glycerol, triglycerides, fatty acids and cholesterol, providing alternative glucose disposal routes (243). Indeed, under chronic glucotoxic conditions, it has been postulated that  $\beta$ -cells can reduce stress by dedifferentiation, thereby exchanging functional uniqueness, including insulin secretion coupling, for increased chance of survival (245, 491).

Dedifferentiation, thought to be initiated by glucotoxicity, is a state whereby the  $\beta$ -cell devolves towards a progenitor-like or otherwise altered phenotype, characterised by a loss of metabolic specificity and insulin secretion dysfunction (492). An increase in the expression of normally suppressed genes such as LDHA, the monocarboxylate transporter MCT1, and hexokinase I, concomitant with a reduction in the expression of specifically preferential genes such as those for insulin, GLUT2, glucokinase, mitochondrial glycerol phosphate dehydrogenase, pyruvate carboxylase and ion channels have been reported (493, 494). Changes in expression or activation of  $\beta$ -cell-enriched transcription factors also occur (248, 495, 496). Increased lactate production, reduced insulin secretion and a switch towards a more anaerobic phenotype are all manifestations of these adaptations (497). Importantly, similar transcriptional changes and clinical characteristics are observed in T2D patients (498). Dedifferentiated  $\beta$ -cells appear to have the capacity to re-differentiate under favourable conditions (499).

### 3.1.2 Metabolic implications in statin treatment

Statin-related myotoxicity occurs in ~10% of patients (36, 196), prompting research into its metabolic effects. *In vivo* studies report decreased oxidative phosphorylation in muscle (500), adverse changes in indices of systemic insulin resistance (501), and increased incidence and progression of T2D with statin therapy (See Table 1.1).

Several potential mechanisms of statin-mediated metabolic risk have been postulated, but no consensus has been reached to date. Statin treatment inhibits not only cholesterol synthesis but also intermediates of the mevalonate pathway and their products, some of which are known to be important in metabolic processes as reviewed in Chapter 1. For example, coenzyme Q10 is important for its redox function and involvement in the mitochondrial electron transport chain

(ETC) (76) (See Figure 1.3). Similarly, the farnesyl and geranylgeranyl isoprenoids act as donors of a hydrophobic prenylation moiety to small signalling G-proteins, controlling their localisation and function (502). These intermediate products are essential in signalling processes linked to insulin secretion (503). Thus, it is reasonable to consider the possibility of metabolic disruption by statin treatment in the search for mechanisms by which statins are linked to new onset and progression of T2D.

In summary, compelling reasons to assess the effect of statin treatment on metabolic function in highly metabolic  $\beta$ -cells include a) the known effects of statins on metabolic function in tissues other than  $\beta$ -cells; b) the postulation of several potential mechanisms by which statins may affect  $\beta$ -cell metabolic function; c)  $\beta$ -cells' specific susceptibility to metabolic stresses; and d) the importance of metabolic stimulus-secretion coupling to insulin sufficiency and whole-body glucose homeostasis.

## 3.2 Methods

### 3.2.1 Cells and reagents

The BRIN-BD11 cell line was a kind gift to Philip Newsholme from Peter Flatt (School of Biomedical Sciences, Ulster University). Seahorse consumables were obtained from In Vitro Technologies, Australia. Antibodies were supplied by Cell Signalling or Abcam and other Western blotting reagents were obtained from BioRad. Statins were purchased from Sapphire Biosciences. All other kits and reagents were supplied by Sigma (Australia).

### 3.2.2 Tissue culture and LPDS preparation

BRIN-BD11 cells (passage 22-32) were grown in RPMI-1640 supplemented with 1% penicillin / streptomycin and either 10% foetal bovine serum (FBS) or the equivalent volume of bovine lipoprotein deficient serum (LPDS), based on protein content. They were cultured at 37°C in a humidified 5% CO<sub>2</sub>/95% air environment. LPDS was prepared as described in Section 2.1.3.

### 3.2.3 Mitochondrial and Glycolytic stress tests.

Anaerobic glycolysis and oxidative phosphorylation represent the two main energy-producing pathways of mammalian cells (504). Oxygen consumption rate can be measured directly, and glycolysis can be measured indirectly via extracellular acidification as an indication of lactate production. These measures can then be used to assess the metabolic profile of cells. This technique is facilitated by the Seahorse extracellular flux analyser that can measure both parameters simultaneously, often in the context of the mitochondrial and glycolytic stress tests. Both stress tests use a succession of agents to allow analysis of the mitochondrial or glycolytic function of the sample cells.

The Mito Stress Test includes injections of oligomycin, carbonyl cyanide-4-(trifluoromethoxy) phenylhydrazone (FCCP) and a mixture of rotenone and antimycin A, delivered in that order. These drugs, respectively, inhibit ATP synthase, uncouple respiration from ATP synthesis by allowing  $H^+$  ions to move unchecked across the mitochondrial membrane, and inhibit complexes I and III of the electron transport chain. Oxygen consumption rate (OCR) data collected throughout the test allows quantification of basal respiration, ATP production and maximal respiration. Proton leak, spare capacity and non-mitochondrial respiration can also be calculated, as represented in Figure 3.1A and Table 3.1.

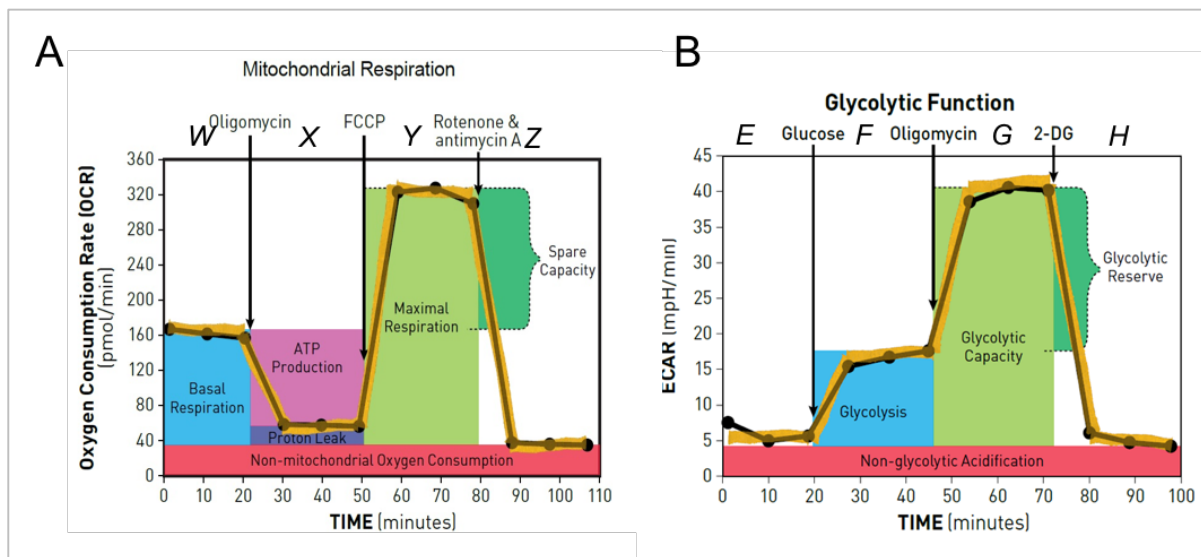


**Figure 3.1. Stress test kinetics.**

A: Diagram representing Mito Stress Test kinetics showing how different respiratory parameters can be calculated. B: Diagram representing glycolytic stress test kinetics showing how different glycolytic parameters can be calculated. Images adapted from Agilent.

The glycolytic stress test involves injecting glucose, followed by oligomycin and 2-deoxyglucose (2DG), which inhibits glycolysis. The pH of the medium in the immediate vicinity of the sample is measured concurrently with the OCR and is calculated as extracellular acidification rate (ECAR). Increased ECAR is known to be a direct result of lactate accumulation, provided  $CO_2$ -related acidification is taken into account (505). From the resulting ECAR data it is possible to calculate glycolysis, glycolytic capacity, glycolytic reserve and non-glycolytic acidification (Figure 3.1 and Table 3.1). Note that the 2DG injection is not required to obtain data for glycolytic parameters. The injection protocol in these experiments combined elements of both assays, utilising the maximum number of injections (4) to allow analysis of both mitochondrial and glycolytic function simultaneously.

**Table 3.1. Table of equations for mitochondrial and glycolytic parameters**

Letters in bold italics refer to values in the corresponding area of Figure 3.1. Min = minimum value; Max = maximum value; numbers refer to the measurement number: For example, Y (Max) = the highest value within the Y region; W (3) = 3<sup>rd</sup> measurement within the W area (immediately before the oligomycin injection). Sourced from Agilent.

	Parameter	Equation
<b>Mitochondrial Respiration</b>		
NMR	Non-mitochondrial oxygen consumption	Z (Min)
BR	Basal respiration	W (3) – Z (Min)
MR	Maximal respiration	Y (Max) – Z (Min)
PL	Proton (H <sup>+</sup> ) leak	X (Min) – Z (Min)
AP	ATP production	W (3) – X (Min)
SRC	Spare respiratory capacity	MR – BR
SRC%	Spare respiratory capacity %	MR/BR x 100
CE	Coupling efficiency	AP/BR x 100
<b>Glycolytic Function</b>		
Glyc	Glycolysis	F (Max) – E (3)
GC	Glycolytic capacity	G (Max) – E (3)
GR	Glycolytic reserve	GC – Glyc
GR%	Glycolytic reserve as %	GC/Glyc x 100

Cells were seeded in 96-well Seahorse culture plates at  $1 \times 10^5$  cells per well in RPMI medium supplemented with LPDS and antibiotics as described above, and left to attach overnight. They were then treated with 1 or 10  $\mu\text{M}$  atorvastatin calcium salt, pravastatin sodium salt, simvastatin, fluvastatin sodium hydrate or vehicle control (DMSO) for 24 h. The Seahorse extracellular flux analyser was pre-warmed and the Seahorse cartridge hydrated for 24 h before the assay as per commercial instructions. Before the assay, media were changed to unbuffered Seahorse medium containing 2.5 mM glucose to facilitate accurate measurement of minute pH changes in the extracellular environment. The cells were incubated for 1 h without CO<sub>2</sub> prior to beginning the assay.

The instrument protocol consisted of basal readings, 12 min; injection A: 2.5 or 25 mM glucose, 20 min; injection B: 2  $\mu\text{M}$  oligomycin, 20 min; injection C: 0.2  $\mu\text{M}$  FCCP, 20 min; injection D: 1  $\mu\text{M}$  each of rotenone and antimycin A, 12 min. Each experiment was repeated three times with four replicates in each experiment.

### 3.2.4 Glucose uptake and mitochondrial function by alamar blue assay

Glucose uptake was estimated in BRIN-BD11 cells by measuring a fluorescently labelled glucose analogue by flow cytometry. Cells were seeded in T75 flasks at  $4 \times 10^6$  cells per flask



and grown to 70% confluence in RPMI supplemented with FBS as outlined above. They were then washed twice in warm phosphate buffered saline (PBS) and medium was replaced with RPMI supplemented with LPDS and either 10  $\mu$ M atorvastatin, pravastatin or DMSO as vehicle control. After a 24 h incubation medium was removed, cells were washed once in PBS, trypsinised and transferred to microcentrifuge tubes. Cells were centrifuged at 700 x g for 3 min, and 20  $\mu$ M of the glucose analogue 2-(N-(7-Nitrobenz-2-oxa-1,3-diazol-4-yl)amino)-2-Deoxy-D-glucose (2-NBDG, ThermoFisher Scientific) was added in glucose free medium for 30 min. Cells were washed once in PBS then resuspended in PBS and kept on ice. Propidium iodide was added to a final concentration of 0.5  $\mu$ g/mL to detect dead cells before analysis on a BD LSR Fortessa flow cytometer (excitation/emission 496/636 and 465/540 for propidium iodide and 2NBDG, respectively).

Alamar blue (Life Technologies, 10% of the media volume) was added to the media of treated cells, which were incubated at standard culture conditions for a further 4 h. Fluorescence was determined in a plate reader (EnSpire, PerkinElmer) at 570/585 nm excitation/emission and normalised to wells containing media and alamar blue reagent but no cells.

### 3.2.5 Whole cell ATP/ADP assessment

Cells were seeded in 96-well plates at  $1 \times 10^4$  cells per well and treated with 10  $\mu$ M atorvastatin or pravastatin for 24 h in RPMI supplemented with LPDS as described above. Cells were washed once with PBS and pre-incubated in Krebs–Ringer Bicarbonate Buffer (KRBB) supplemented with 1.1 mM glucose for 40 min before being stimulated for 20 min using 16.7 mM glucose plus 10 mM L-alanine (Ala) in KRBB. Media were then removed and cells were immediately lysed using ATP reagent from a commercial ADP/ATP Ratio Assay Kit (Sigma-Aldrich, catalogue number MAK 135) following kit instructions. Briefly, lysates were placed in a white 96-well plate and luminescence was measured after 1 min using a microtitre plate reader (EnSpire, Perkin Elmer, USA). The plate was incubated at room temperature for a further 10 min, then the luminescence was measured again. This reading was considered the residual background luminescence for the ADP reading that followed. ADP reagent (5  $\mu$ L) was added to each well to convert ADP to ATP, and the luminescence was measured for the third time after 1 min. ADP was calculated by subtracting reading 2 from reading 3, and the ATP/ADP ratio calculated by dividing reading 1 by the difference between readings 3 and 2.

### 3.2.6 Quantification of glycolytic proteins by Western Blotting

Cells were grown to 80% confluence in T75 flasks. They were treated with 10  $\mu$ M atorvastatin, pravastatin or DMSO for 24 h before being pre-incubated for 40 min in KRBB with 1.1 mM glucose and stimulated with 16.7 mM glucose + 10  $\mu$ M L-alanine for 20 min as described above. Cells were then scraped from the flask and collected in 15 mL centrifuge tubes, centrifuged at 300 x g for 5 min, washed once in PBS, and re-suspended in 150  $\mu$ L ice-cold

lysis buffer (50mM Tris, pH 7.5, with 0.5mM EDTA and 20% glycerol + phosphatase/protease inhibitors). Cells were then incubated on ice for 20 min with occasional mixing before being sonicated on ice at 50% amplitude twice for 10 s with 5 s between bursts, using a probe sonicator with microtip attachment (Misonix s-4000, QSonica). Lysates were centrifuged at 800 x g for 10 min at 4°C. Supernatants were collected and the pellets washed in a further 100 µL of lysis buffer and re-centrifuged. Wash supernatants were pooled with the original supernatant collected from the same tube and protein was estimated using the BCA assay (Pierce, BioRad). Lysates were stored at -80°C until used for Western blotting.

Protein samples were run on precast 4-12% acrylamide gels (Bolt™, Life Technologies) using 15 or 30 µg protein per well under reducing conditions (50 mM dithiothreitol, Bolt™ Sample Reducing Agent, Life Technologies) for ~50 min at 120 volts. Proteins were then transferred to nitrocellulose membranes using the iBlot system and a 7-min dry transfer protocol. Transfer stacks were obtained from Life Technologies. Membranes were blocked in blocking buffer (3% bovine serum albumin (BSA) in TBST: 0.1% Tween 20, 137 mM NaCl, 2.7 mM KCl, 19 mM Tris base, pH 7.4) for 1 h at room temperature, then cut and incubated in the relevant primary antibody diluted to appropriate concentrations (see Table 4.1) in blocking buffer overnight at 4°C with gentle rocking. Appropriate horseradish peroxidase (HRP)-conjugated secondary antibodies (rabbit, mouse or goat) were used for 1 h at room temperature and membranes were washed three times for 5 min in blocking buffer. Membranes were incubated in enhanced chemiluminescence (ECL) Prime Western Blotting Detection Reagent (GE Healthcare Lifesciences) for 2 min before being detected using a BioRad ChemiDoc imaging system and analysed using Image Lab 6.0 software.

### 3.2.7 Statistical Analysis

Seahorse data was collected and organised using dedicated report making software (Wave, Agilent Technologies, version 2.4.0) then analysed using two-way ANOVA followed by Tukey's multiple comparisons test in GraphPad Prism version 6.01 for Windows (GraphPad Software, La Jolla California USA, www.graphpad.com). For Seahorse data requiring calculations (mean of measure A – mean of measure B, for example) the error was calculated using the formula  $\sqrt{(a^2 + b^2)}$ , where a is the standard deviation (SD) or standard error of the mean (SEM) of measure A and b is the SD or SEM of measure B. Flow cytometry data was analysed using FlowLogic (Version 2.2, Inivai) and Western blot densitometry was performed using Image Lab 6.0 software. Statistical significance was calculated using one- or two-way ANOVA followed by Dunnett's multiple comparisons test in GraphPad Prism. Statistical significance was inferred at a nominal value of  $\alpha = 0.05$ .

## 3.3 Results

### 3.3.1 Mitochondrial function

Oxygen consumption (OCR) and extracellular acidification (ECAR) rates were measured simultaneously using the Seahorse extracellular flux analyser after 24 h statin treatment at 1 or 10  $\mu\text{M}$  as indicated (See Figure 3.2). A class effect was observed whereby all statins tended towards reduction of basal and maximal oxygen consumption rates, with reduced ATP production. At the same time, an increase in glycolysis was observed.

### 3.3.2 Oxygen Consumption Rate (OCR)

Atorvastatin was found to have a greater adverse effect on OCR than pravastatin at the same concentration (10  $\mu\text{M}$ ). Simvastatin (1  $\mu\text{M}$ ) similarly tended towards reduced OCR, though not significantly. Basal respiration was reduced in all statins, though this was significant only in atorvastatin ( $69 \pm 5\%$  of vehicle control (VC),  $P < 0.01$ ) and 10  $\mu\text{M}$  simvastatin ( $28 \pm 10\%$  of VC,  $P < 0.001$ ) treatment groups. Maximal respiration (MR) was reduced to  $80 \pm 11\%$  and  $65 \pm 4\%$  ( $P < 0.05$ ,  $P < 0.001$ ) for pravastatin- and atorvastatin-treated cells, respectively, compared to the vehicle-treated group. ATP production (AP) was reduced to  $61 \pm 8\%$  in atorvastatin-treated cells ( $P < 0.05$ ) but was not significantly different from vehicle-treated controls in response to pravastatin treatment. Proton leak (PL) and non-mitochondrial oxygen consumption were not affected by statin treatment. Respiratory capacity percent (RC%) and coupling efficiency, calculated as per Table 3.1, were likewise unaffected by statin treatment. Spare respiratory capacity was significantly different for 10  $\mu\text{M}$  simvastatin, ( $P < 0.001$ ) and as a class there was a difference between statin treated and non-treated cells ( $P < 0.01$ ).

Simvastatin was found to be highly toxic to mitochondria at 10  $\mu\text{M}$ , with very low oxygen consumption rates across the entire protocol. Nevertheless, there was little evidence of increased death in 10  $\mu\text{M}$  simvastatin-treated cells in a parallel experiment where cells were stained with trypan blue (Figure 3.6), though morphologic changes showed a rounding of cells with greatly reduced surface area of attachment. Other statins caused similar morphological changes in a dose-dependent manner, but cell death was not greatly increased.

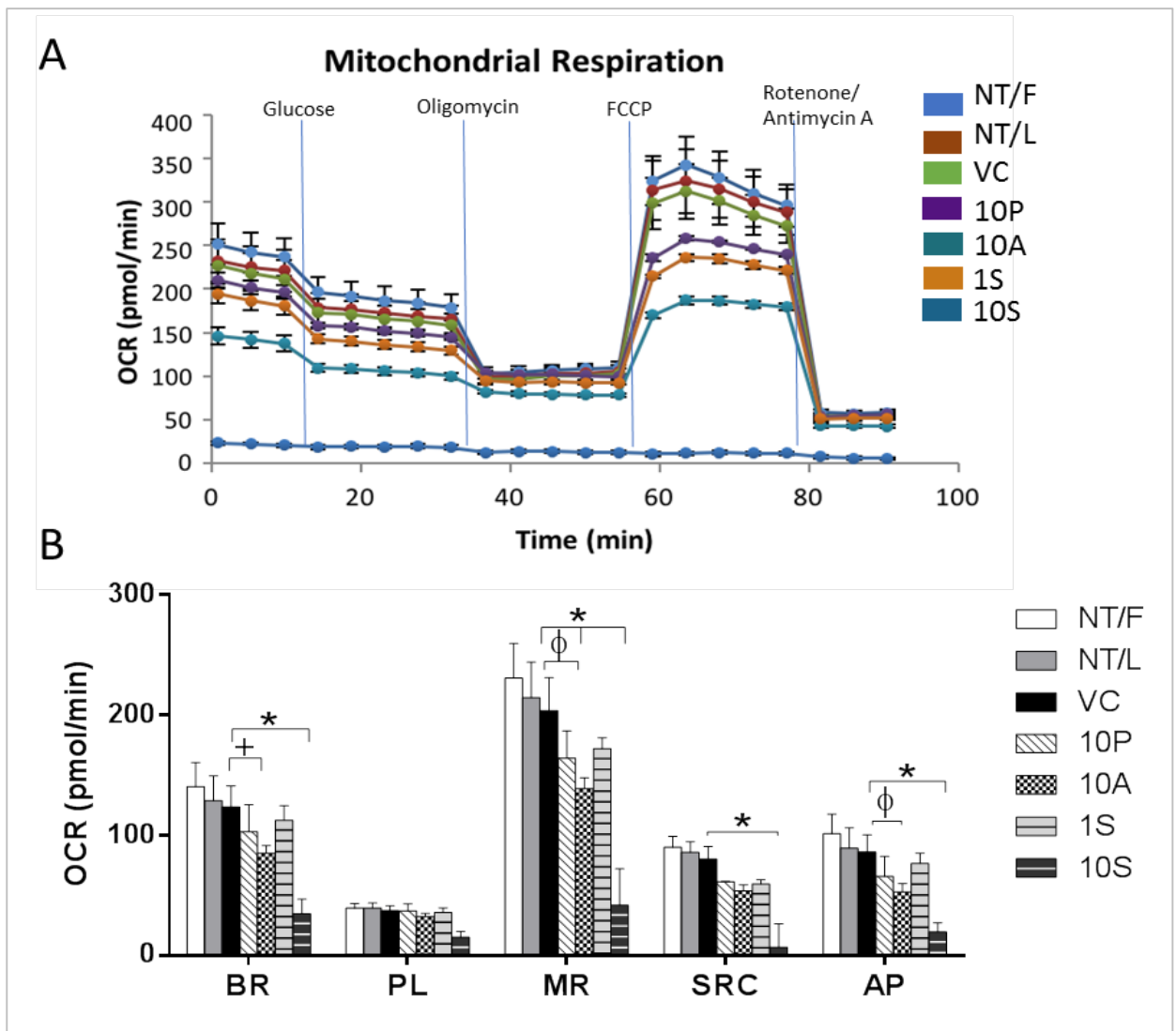


**Figure 3.2. Mitochondrial stress test kinetics.**

**A.** A representative example of mitochondrial oxygen consumption rate (OCR) with or without statin treatment. **B.** Pooled data from three separate experiments, each with four replicates, indicated a trend towards a statin class effect characterised by reduced maximal respiration (MR), basal respiration (BR) and ATP production (AP). Proton leak (PL) was not affected by statin treatment. Spare respiratory capacity (SRC), calculated by MR – BR tended towards a statin effect, with reduced respiration in statin-treated compared to non-statin-treated cells ( $P < 0.05$ ), though not significant for any statin individually. NT/F, untreated and supplemented with foetal bovine serum (FBS) rather than lipoprotein deficient serum (LPDS), used for all other samples; NT/L, untreated and supplemented with LPDS; VC, vehicle control (DMSO); 10P, 10  $\mu\text{M}$  pravastatin; 10A, 10  $\mu\text{M}$  atorvastatin; 1S, 1  $\mu\text{M}$  simvastatin; 10S, 10  $\mu\text{M}$  simvastatin.  $n=3$ ;  $\Phi$   $P < 0.05$ ; +  $P < 0.01$ ; \*  $P < 0.001$ . Data is presented as mean  $\pm$  SEM.

### 3.3.3 Extracellular Acidification Rate (ECAR)

During glycolysis, the extracellular environment is acidified due to proton efflux from the cell when glucose is metabolised to pyruvate and then lactate, which is secreted. The extracellular acidification rate can thus be measured as a proxy for glycolysis (505). It has previously been confirmed that BRIN-BD11 cells also secrete lactate during anaerobic glycolysis, which can

reliably be measured in this manner (506), unlike primary  $\beta$ -cells that do not possess the enzymes and monocarboxylate transporters required for this process.

A significantly higher acidification rate, representing increased glycolysis, was measured in cells treated with statins, apart from 10  $\mu$ M simvastatin, which was found to be toxic to both aerobic and anaerobic energy-producing pathways in BRIN-BD11 cells (Figure 3.3).

Glycolysis in pravastatin-, atorvastatin- and simvastatin- (1  $\mu$ M) treated cells was  $135 \pm 30\%$ ,  $143 \pm 29\%$  and  $142 \pm 28\%$  that of vehicle-treated cells ( $P < 0.05$ ,  $P < 0.01$  and  $P < 0.01$ ), respectively. While glycolytic capacity did not change, statin-treated cells were functioning at maximum glycolytic capacity due to their high glycolytic rate, while untreated cells had the capability to increase glycolysis by  $\sim 50\%$ . This is illustrated by severely reduced glycolytic reserve (GR) in statin-treated cells.

To assess the cumulative effect of statin treatment on both major pathways of energy production, glycolysis and oxidative phosphorylation (OxPhos), values for maximum respiration and glycolytic capacity were calculated as a percentage of control and stacked (Figure 3.4A). A slight decrease in total energy production capacity was observed in statin treated cells compared to the control. However, the cumulative reserve capacity of both OxPhos and glycolysis was severely impaired in statin-treated cells, due mainly to decreased glycolytic reserve (Figure 3.4B). These cells appeared to be working at maximum glycolysis after statin treatment with high glucose stimulation, whereas untreated cells maintained some reserve capacity.

### 3.3.4 Alamar blue mitochondrial function assay

As a further assessment of mitochondrial function, an alamar blue assay was used to observe the reduction of resazurin to resorufin. In healthy cells this is a continuous process after the addition of alamar blue reagent and is often used to assess cell proliferation and cytotoxicity (507). In accordance with extracellular flux assays, 10  $\mu$ M atorvastatin and simvastatin demonstrated reduced mitochondrial reduction of resazurin after 4 h incubation with 10% alamar blue (Figure 3.5A).

### 3.3.5 Quantifying ATP/ADP Production

An alternative method of ATP measurement was undertaken to compare with the indirect measurement of ATP production as a function of oxygen consumption using the Seahorse extracellular flux analyser as indicated above. ATP was measured directly in whole cell lysates using a luciferin substrate reaction. As a second step, cellular ADP was converted to ATP enzymatically and measured. Both ATP and ADP luminescence was slightly reduced in atorvastatin treated cells, but no significant difference was observed between vehicle- and statin- treated cells in ATP, ADP or the ratio of ATP:ADP.

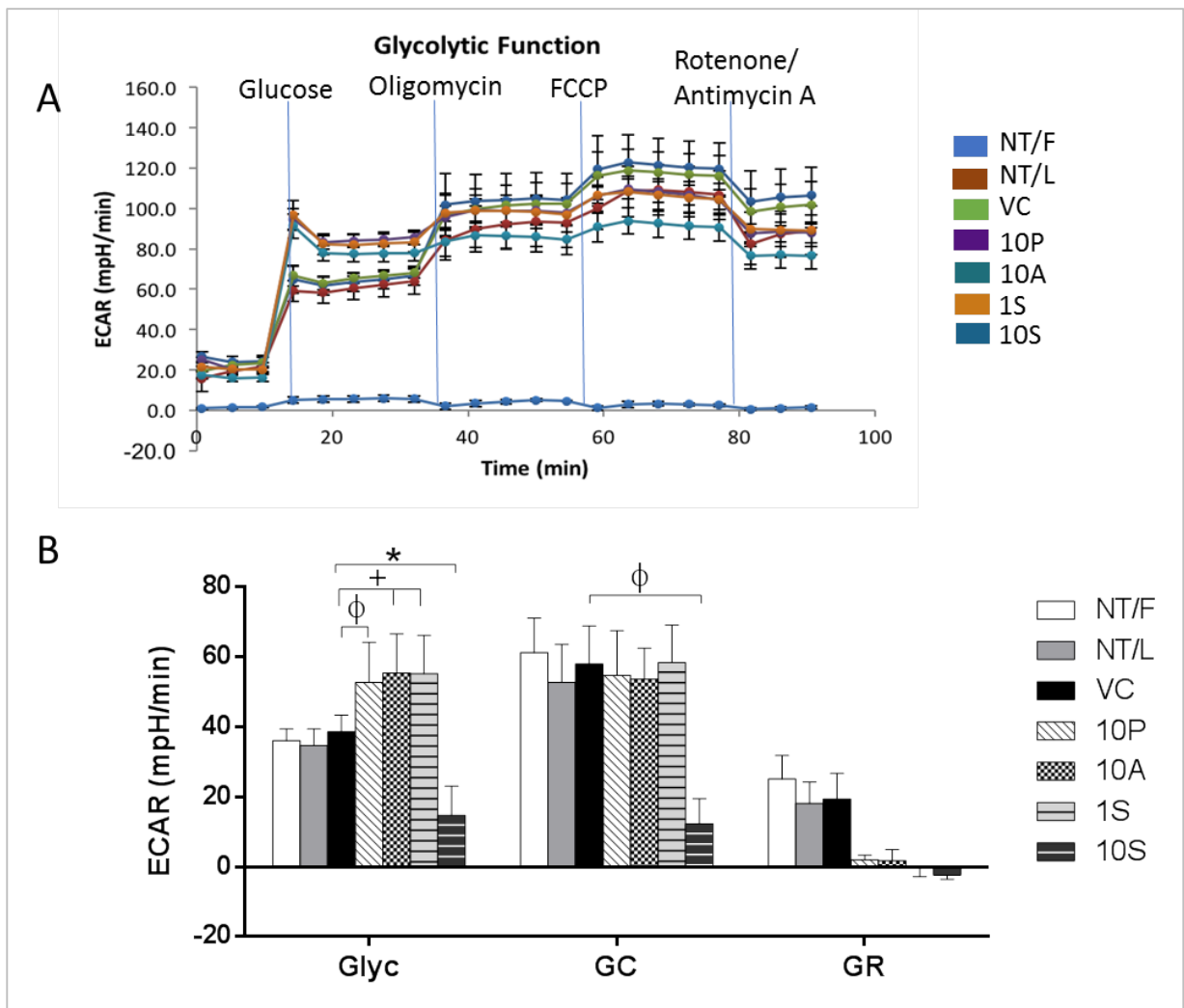


**Figure 3.3. Glycolytic function analysis.**

**A.** A representative example of glycolysis kinetics demonstrating extracellular acidification rate (ECAR) with and without statin treatment. **B.** Pooled data from three separate experiments, each with four replicates indicated a class effect of statins to increase glycolysis (Glyc). Glycolytic capacity (GC), however, was not altered. Glycolytic reserve (GR) calculated by GC – Glyc, was decreased in statin treated cells in proportion to the increase in glycolysis. NT/F, untreated and supplemented with foetal bovine serum (FBS) rather than lipoprotein deficient serum (LPDS), as for all other samples; NT/L, untreated and supplemented with LPDS; VC, vehicle control (DMSO); 10P, 10  $\mu$ M pravastatin; 10A, 10  $\mu$ M atorvastatin; 1S, 1  $\mu$ M simvastatin; 10S, 10  $\mu$ M simvastatin. The data represents mean  $\pm$  SEM.  $\Phi$   $P < 0.05$ ; +  $P < 0.01$ ; \*  $P < 0.001$ .

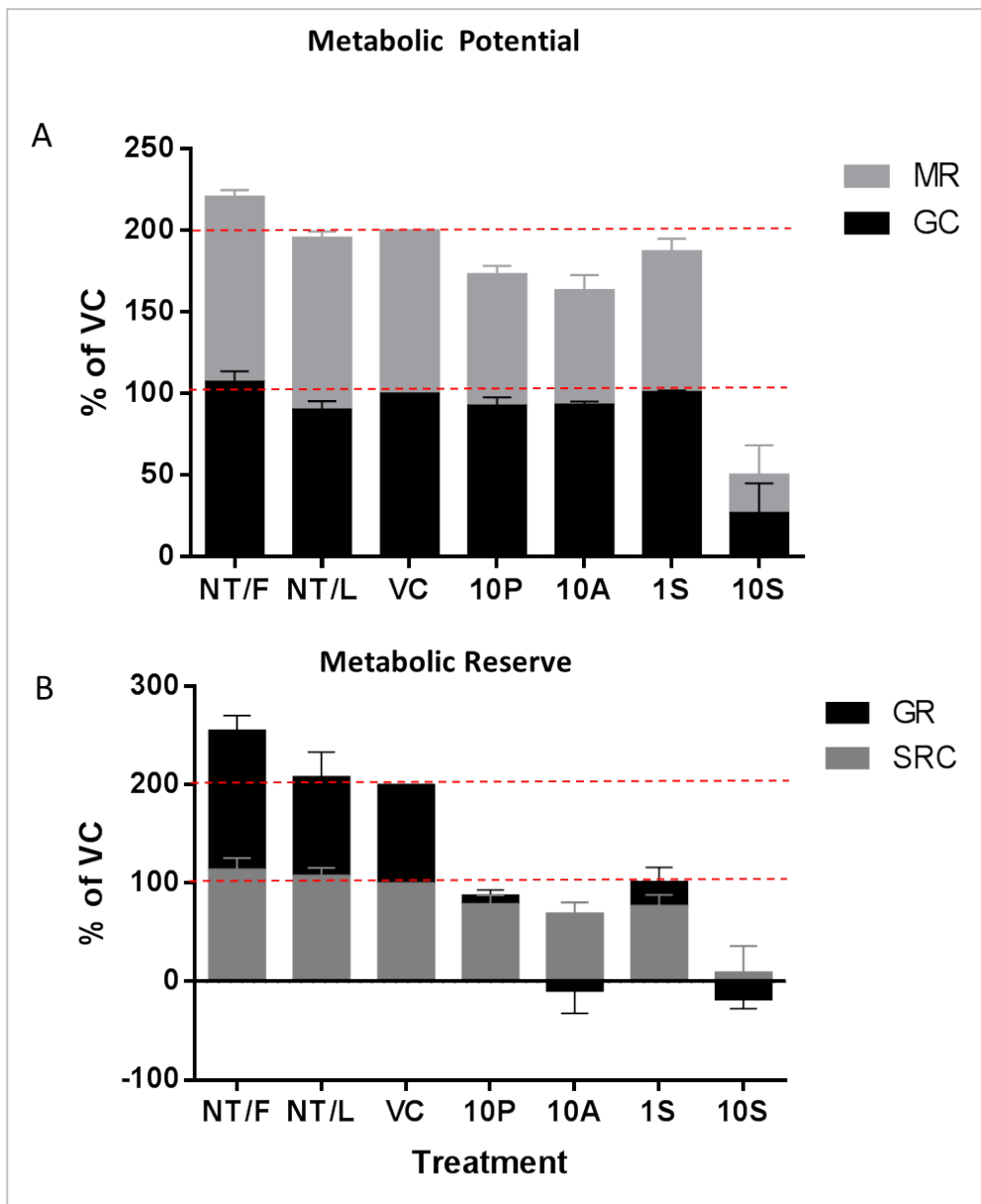


**Figure 3.4. Metabolic potential and reserve.**

Data was collated from both oxidative phosphorylation (grey) and glycolysis (black) for further comparison. **A.** Maximal respiration (MR) and glycolytic capacity (GC) values were recorded as % of control and then stacked. Together they demonstrate that the total capacity for glucose oxidation changed little. **B.** Similarly, stacked data representing glycolytic reserve (GR) and spare respiratory capacity (SRC) demonstrates that statin treated cells had reduced capacity to increase glucose oxidation by either pathway. Rather, statin treatment increased the relative contribution of anaerobic glycolysis to glucose oxidation and little further capacity existed. Data is represented as mean  $\pm$  SEM of three separate experiments, and red lines indicate control values. NT/F, untreated and supplemented with FBS; NT/L, untreated and supplemented with LPDS (as for all other groups); VC, vehicle control; 10P, 10  $\mu$ M pravastatin; 10A, 10  $\mu$ M atorvastatin; 1S, 1  $\mu$ M simvastatin; 10S, 10  $\mu$ M simvastatin.

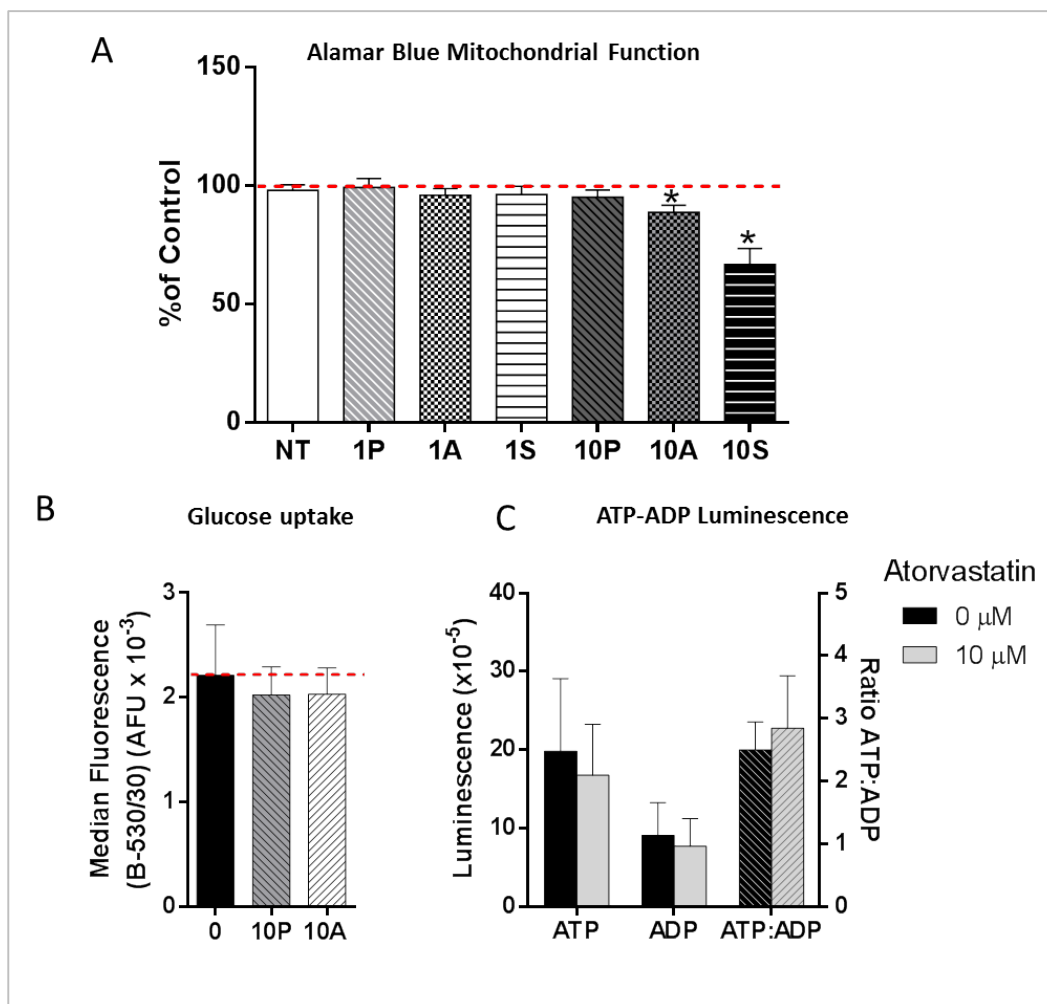


**Figure 3.5. Further metabolic assessment of statins in BRIN-BD11 cells.**

**A.** An alamar blue assay demonstrated reduced mitochondrial reduction of resazurin to resorufin in cells treated with 10  $\mu\text{M}$  concentrations of atorvastatin (A) and simvastatin (S) but not pravastatin (P) or lower dose (1  $\mu\text{M}$ ) of either statin. Data is expressed as % of vehicle control (VC), represented by the red line. NT, no treatment.  $n=6$ . **B.** Glucose uptake measured by flow cytometry after 30 min incubation with a fluorescent glucose analogue demonstrated no changes after statin treatment. **C.** Total cellular ATP and ADP were not affected by 10  $\mu\text{M}$  atorvastatin assessed by luminescence assay. ATP:ADP ratio (hatched bars, read from the right y-axis) was also unaffected. B and C,  $n=3$ . Flow cytometry data (B) is represented as median fluorescence  $\pm$  SEM (arbitrary fluorescent units (AFU), scale  $\times 10^{-3}$ ) and all other data represents mean  $\pm$  SEM. \*  $P < 0.001$ .

### 3.3.6 Glucose Uptake

Having observed an increase in glycolysis after statin treatment, it was of interest to determine whether increased glucose uptake contributed to this metabolic change. This was determined by flow cytometric analysis using a fluorescently labelled deoxyglucose (2NBDG). Dead cells were gated out based on permeability to propidium iodide. No difference was found between cells treated with vehicle only and those treated with 10  $\mu\text{M}$  pravastatin or atorvastatin, indicating that increased glycolysis associated with statins was not accompanied by increased glucose uptake (Figure 3.5C).



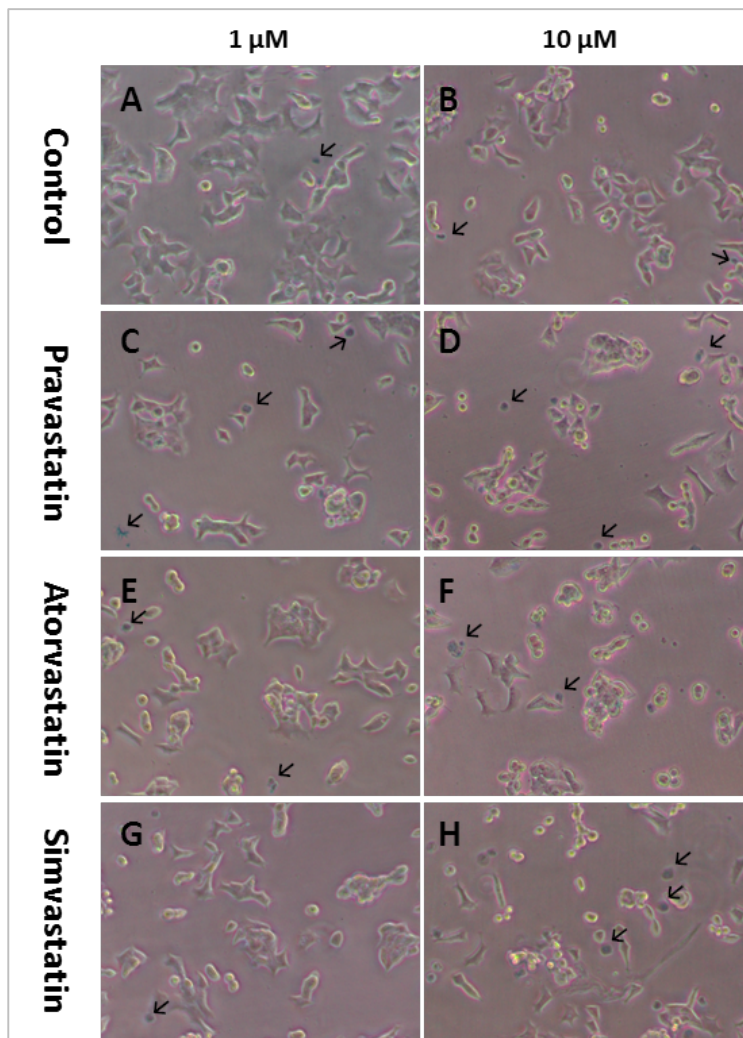


**Figure 3.6. The effect of statins on cell death as assessed by trypan blue exclusion.** Cells treated with 1 or 10  $\mu$ M statin for 24 h were stained with trypan blue. This stain is taken up only by cells with compromised membranes, indicating cell death (arrows indicate examples only). **A)** No treatment; **B)** DMSO control; **C-H)** statins and concentrations as shown. Several cells within each treatment group were positive for trypan blue uptake, with slightly more in the 10  $\mu$ M simvastatin group (**H**).

### 3.3.7 Influence of statins on selected glycolytic enzymes

To investigate the possibility that phenotypic changes were accompanied by changes in the expression of glycolytic enzymes, statin-treated BRIN-BD11 cells were stimulated with high glucose (16.7 mM) + alanine for 20 min before being harvested for Western blot interrogation using a glycolytic enzyme antibody panel standard to our laboratory.  $\beta$ -actin was used as a loading control. Increased expression of hexokinase I (1.4-fold,  $P < 0.05$ ) in atorvastatin treated cells was observed. No changes in expression were demonstrated in the other enzymes investigated (Figure 3.7). However, there was an increase in the inhibitory phosphorylation of glycogen synthase kinase (pGSK3 $\beta$ ) at serine 9 associated with atorvastatin treatment (1.45-fold,  $P < 0.01$ ). A table outlining the role of these enzymes in glycolysis is available in Appendix A.2.

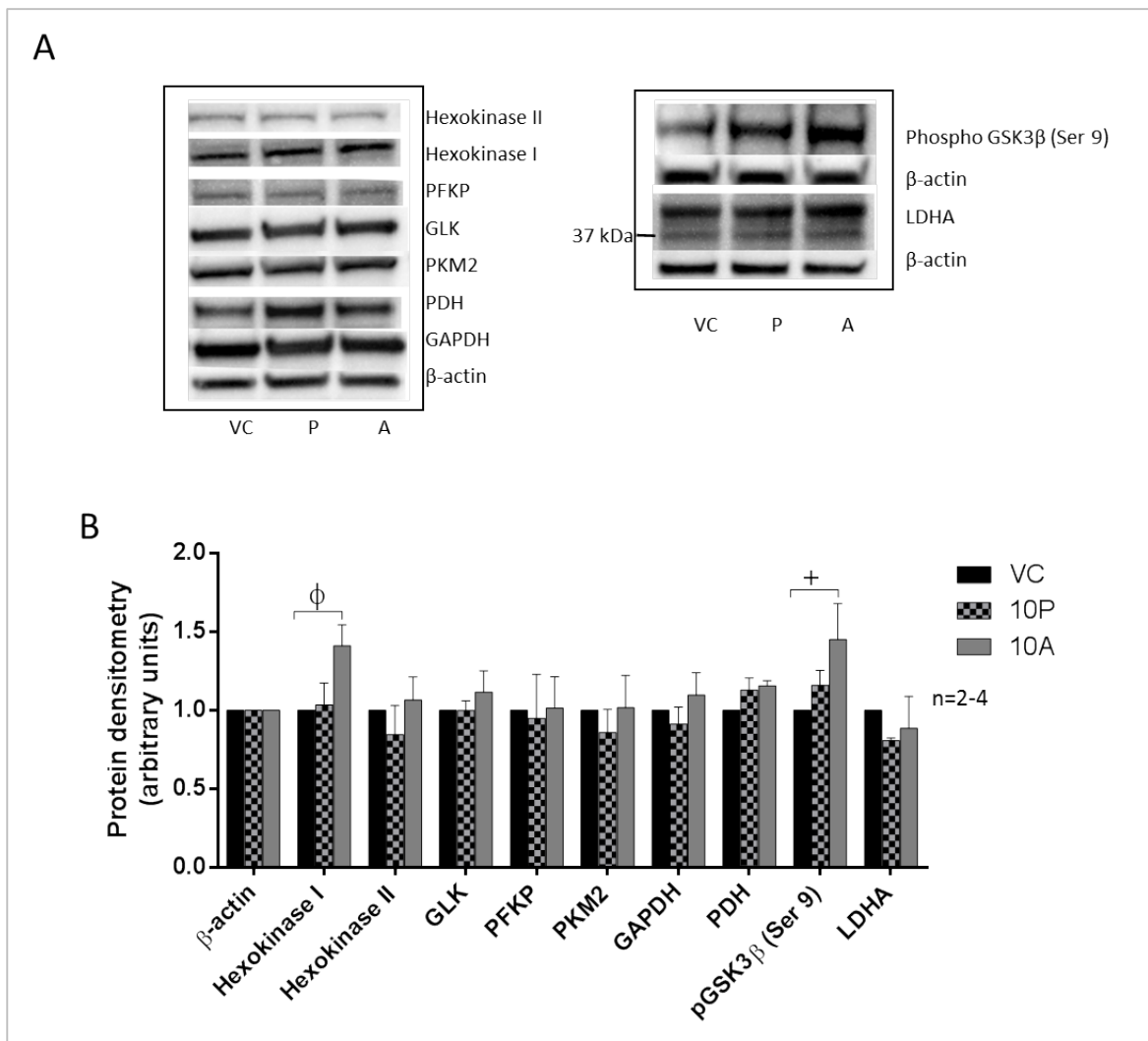


**Figure 3.7. The effect of statins on glycolytic enzyme expression.**

**A)** Representative blots and **B)** densitometric analysis of glycolytic enzymes in BRIN-BD11 cells treated for 24 h with 10  $\mu$ M pravastatin (10P), atorvastatin (10A), or vehicle control (VC, DMSO) and stimulated for 20 min with 16.7 mM glucose + 10 mM alanine immediately before lysis demonstrated few changes in expression. The exceptions were hexokinase I and glycogen synthase kinase (pGSK3 $\beta$ ) phosphorylated at serine 9, both exhibiting increased expression with 10  $\mu$ M atorvastatin treatment. BRIN-BD11 cells showed considerable expression of a protein recognised by the lactate dehydrogenase (LDHA) antibody, though only a small band was found at the expected molecular weight of 36 kDa. Data is shown as the mean  $\pm$  SEM of 2-4 individual experiments. GLK, glucokinase (hexokinase IV); PFKP, phosphofructokinase; PKM, pyruvate kinase (muscle 2); GAPDH, glyceraldehyde-3-phosphate dehydrogenase; PDH, pyruvate dehydrogenase.

### 3.4 Discussion

ATP generation through oxidative phosphorylation is important for coupling metabolism with insulin secretion. Thus, mitochondrial dysfunction could contribute to the diabetogenic effect of statins. Furthermore, statin-related adverse effects in muscle have been associated with mitochondrial dysfunction (167), and an influence of statins on mitochondrial function has been demonstrated in human muscle and C2C12 cells (mouse myoblast) (361, 508, 509), rat liver (510) and HepG2 cells (human hepatoma) (511). Few studies, however, have focused on the

effect of statins on mitochondrial function in  $\beta$ -cells. Sadighara *et al* (512) studied the effect of atorvastatin on isolated mitochondria from whole rat pancreas but used concentrations of the drug that were found to be toxic to  $\beta$ -cells in the current study. Additionally, while several effects including decreased mitochondrial membrane potential and increased ROS were reported, any effect specifically on  $\beta$ -cell mitochondria would likely be masked by the far more abundant exocrine-derived organelles. The present study thus provides important information regarding possible statin-related mitochondrial effects.

### 3.4.1 Statins induced a shift to glycolysis and reduced respiration

Glycolytic stress test results in this study show that 24-h statin treatment (atorvastatin, pravastatin and simvastatin) induced a glycolytic phenotype in BRIN-BD11 cells. Respiration rates in  $\beta$ -cells are usually high, as these cells are active with a very high aerobic to anaerobic ratio. The main effect of statin treatment was to reduce MR by 23 – 35 % ( $P < 0.05$ ) while increasing anaerobic glycolysis by 35 – 43% ( $P < 0.05$ ). In addition, atorvastatin treatment reduced basal respiration and ATP production rates by 31% and 39% ( $P < 0.01$ ,  $P < 0.05$ ), respectively. This suggests a Warburg-like metabolic phenotypic switch and could explain the blunted maximal insulin secretion observed in statin treated cells (see Chapter 2), at least in part.

Statin-treated BRIN-BD11 cells were found to be functioning close to their maximal metabolic capacity with little reserve, possibly to compensate for the reduced efficiency of the glycolytic phenotype to generate ATP. The diminished maximal respiration was reflected in the reduced spare respiratory capacity (calculated by maximal respiration – basal respiration) of statin treated cells. Glycolytic reserve, not expected to be large in  $\beta$ -cells, was also reduced, although this did not reach statistical significance in individual treatments. When considered together, reduced spare respiratory capacity and glycolytic reserve would greatly reduce the overall metabolic potential of the cells.

Maintenance of a reasonable bioenergetic reserve capacity has been flagged as a signature of healthy mitochondria (352, 513). The reduction of bioenergetic reserve capacity, both from aerobic (spare respiratory capacity) and anaerobic respiration (glycolytic reserve) (Figure 3.4) could mean that cumulative stress in the presence of additional stressors, such as hyperglycaemia and/or hyperlipidaemia, would have the potential to cause mitochondrial failure and further stimulus-secretion disconnection in  $\beta$ -cells. This could explain the increased risk of new onset T2D associated with statin therapy in patients with pre-existing risk factors for metabolic health (33, 219).

A similar shift towards anaerobic glycolysis was seen in the erythrocytes of simvastatin-treated rats (514), accompanied by greatly increased production of lactate and pyruvate, increased

uptake of a fluorescent glucose analogue and increased glucose-6-phosphate dehydrogenase activity. The latter two observations may compensate for the reduced energy efficiency of the anaerobic pathway.

### 3.4.2 Glucose uptake

Contrary to the increased glucose uptake in erythrocytes in response to simvastatin mentioned above, statins have also been shown to decrease glucose uptake in a variety of insulin-responsive tissue types such as liver (515), adipocytes (515, 516) and skeletal muscle (471, 515). In addition, expression of the glucose transporter GLUT2 was suppressed in a concentration-dependent manner in response to atorvastatin and pravastatin treatment in human  $\beta$ -cells (471). In BRIN-BD11 cells in this study, statins had no effect on glucose uptake. The increase in glycolysis (Figure 3.5C) therefore cannot be explained by an increase in glucose uptake. This supports the conclusion that glucose metabolism is re-routed from the aerobic to the anaerobic pathway in response to statin treatment. Without compensatory increased glucose uptake to maintain ATP production at levels similar to non-treated cells, reduced insulin secretion in response to glucose stimulation can be predicted.

### 3.4.3 ATP production

While there is an atorvastatin-related decrease in ATP production as measured by the Mito Stress Test as indicated above, total cellular ATP did not change with statin treatment, according to results obtained using a whole cell ATP/ADP assay. It should be noted that the two assays differ in that the former measured the rate of ATP generation and the latter measured total ATP at a given timepoint. The ATP measured in the Mito Stress Test is an indirect rate measure, contrasting with the direct measurement of ATP by luciferase luminescence. Others have also found differences between measures of ATP using similar assays (243).

The ATP/ADP ratio is known to have a direct effect on insulin secretion, being responsible for closure of ATP-sensitive potassium channels ( $K^+_{ATP}$ ), which then causes depolarisation, opening of calcium channels and consequent secretory granule/membrane fusion and exocytosis (517). The ATP/ADP ratio measured by luminescence did not change with statin treatment in this project. However, mitochondrial stimulus-secretion coupling factors other than ATP/ADP ratio, including citrate, 2-oxoglutarate and associated glutamate, malate and NADPH, may be reduced due to depressed mitochondrial function. The effect of statins on these coupling factors remains to be determined.

### 3.4.4 Expression of enzymes dictating the fate of glucose

It is unclear whether decreased aerobic capacity may precipitate the switch to a glycolytic phenotype or whether it is driven by changes in the expression of glycolytic enzymes stimulated by alternative mechanisms. In tumorigenesis, the Warburg effect is initiated, at least in part, by

pyruvate kinase (PK) (518). PKM2, the isoform found mainly in islets, is translocated to the nucleus after being phosphorylated at serine 37 by extracellular signal-regulated kinase (ERK) 1/2. It then acts as a transcription factor to regulate its own expression and that of other rate-limiting glycolytic enzymes such as glucose transporter 1 (GLUT 1) and lactate dehydrogenase (LDHA). High affinity hexokinases I & II are also an early marker of malignancy in liver and pancreas, with a concomitant silencing of glucokinase (GLK) (519).

Similar mechanisms could potentially drive the change towards a more glycolytic phenotype observed in this study. Alternatively, hypoxia in  $\beta$ -cells strongly induces LDHA, pyruvate dehydrogenase kinase 1 (PDK1), GLUT1 and monocarboxylate transporter (MCT) 1 or 4 (497, 520). These adaptations, mediated by the activation of hypoxia inducible factor (HIF)1 $\alpha$ , facilitate the anaerobic pathway of glucose metabolism that is normally repressed in  $\beta$ -cells.

To further characterise changes in the metabolic phenotype of statin-treated BRIN-BD11 cells, Western blot analysis was performed for a small panel of glycolytic enzymes to assess potential expression changes. These included enzymes such as hexokinase I and LDHA, known to be down-regulated in primary  $\beta$ -cells, but which are implicated in the phenotypic switch towards anaerobic glycolysis. A summary of the role of enzymes included in the panel is available in Appendix A.2.

The two significant changes observed in this study were an increased expression of hexokinase I and increased inhibitive phosphorylation at serine 9 in GSK3 $\beta$ . While no changes were seen in the expression of the other enzymes (hexokinase II, GLK, phosphofructokinase-platelet (PFKP, the isoform found in  $\beta$ -cells), pyruvate kinase (PK) M2, glyceraldehyde 3-phosphate dehydrogenase (GAPDH), pyruvate dehydrogenase (PDH) and LDHA), gene upregulation and activation studies would present a more complete picture of how they may respond to statin treatment.

### *Hexokinase I*

Hexokinase I is selectively repressed in  $\beta$ -cells and liver (245), although it is expressed in BRIN-BD11 cells; a phenotypic shift to low affinity hexokinases is commonly observed during the first 20 passages in the establishment of  $\beta$ -cell cultures (429). Other stressors such as high sucrose consumption (521) and hyperglycaemia following partial pancreatectomy (493, 494) are also associated with enhanced hexokinase I expression in islets. MIN6 cells exhibited increased hexokinase I expression and decreased GLK expression over time and this was relative to loss of GSIS (522). In other tissues, hexokinase I transcription, along with other glycolytic genes, was increased in patients with impaired respiration related to genetic mitochondrial disease (523), demonstrating a link between impaired mitochondrial function and hexokinase I upregulation.

### *GSK3 $\beta$*

The role of glycogen synthase kinase 3 $\beta$  (GSK3 $\beta$ ) in  $\beta$ -cells is complex. GSK3 $\beta$  is a kinase involved in several signalling pathways, including insulin. It is named for its function of inactivating glycogen synthase (87), but has more predicted substrates than any other kinase (524, 525), including numerous transcription factors, implicating a widespread influence on gene expression (525). It has the unusual characteristic of constitutive activity but can also be phosphorylated at tyrosine 216 for maximal activation or at serine 9 for inhibition of many, but not all, of its phosphorylating activities (525, 526).

Among other actions, GSK3 $\beta$  phosphorylates the transcription factor promoting insulin gene transcription, pancreatic duodenal homeobox-1 (PDX-1), triggering its proteasomal degradation in low glucose (527). Phosphorylation of GSK3 $\beta$  at serine 9 by Per-Arnt-Sim domain-containing kinase (PASK) inactivates it, stabilising PDX-1 in high glucose conditions. Increased activation of GSK3 $\beta$  has been associated with several diseases, including T2D (528-531). Inhibitors of GSK3 $\beta$  are consequently being investigated for their therapeutic potential (528, 529, 532).

The significant increase in phosphorylation of GSK3 $\beta$  (Ser 9) observed in the current study would be expected to inhibit GSK3 $\beta$  action, thereby paradoxically stimulating insulin secretion. Despite this expected effect on insulin secretion, however, inhibition of this enzyme may have unexpected consequences. This is supported by a recent study using mice expressing mutant GSK3  $\alpha$  and  $\beta$  that could not be phosphorylated at serine 21 or 9, respectively, and thus were continuously active (uninhibited) (533). In wild type controls fed a high fat diet, GSK3 inhibition by serine phosphorylation was strongly stimulated. Metabolic syndrome, characterised by enhanced insulin secretion, hyperglycaemia, obesity and insulin resistance in control animals was found to be mediated through enhanced expression of adiponectin, related to inhibition of GSK3 activity in these animals. In contrast, the mice expressing continuously active mutant GSK3 were protected against obesity, metabolic syndrome, and diabetes, suggesting that inhibition of GSK3 may have a role in the development of these adverse events, potentially via loss of adiponectin secretion from adipose tissue.

Contradictory to results reported in the current study, simvastatin and atorvastatin were recently respectively shown to decrease GSK3 $\beta$  serine 9 phosphorylation in L6 myotubes (534) and, in our laboratory, human skeletal muscle cells and myoblasts (HSMM, T. Sabapathy, unpublished data). This discrepancy could be due to different actions of GSK3 $\beta$  in various tissue types, as others have noted (528). Differences in exposure could also result in varying effects, which could reflect a time course of progressive adaptations.

Elsewhere, studies have suggested that GSK3 $\beta$  inhibition may increase survival. For example, it is thought to confer resistance to cisplatin, a chemotherapeutic drug used against ovarian

cancer, and works through stabilisation of the apoptotic protein P53 (535). In addition, Marchand *et al* (536) discovered that the autophagy facilitated by GSK3 inhibition counterintuitively supported pro-survival in pancreatic cancer cells, and preventing inhibition of GSK3 sensitised cells to apoptosis. As pro-survival agents, GSK3 $\beta$  inhibition and hexokinase I expression may mutually support  $\beta$ -cell survival when under duress, such as during exposure to statins.

Interestingly, hexokinase I and GSK3 $\beta$  may be linked through a common ability to bind the voltage dependent anion channel (VDAC) on the outer mitochondrial membrane (537). Further, GSK3 $\beta$  appears to regulate the binding of hexokinase I to VDAC in cancer cells, and their association in this context is related to cholesterol accumulation in the mitochondrial membrane (348). Increased hexokinase binding to VDAC is also known to protect mitochondria against apoptosis (537). Intriguingly, these processes are linked to the Warburg effect in cancer cells, suggesting metabolic adaptation is associated with these enzymes and their interaction.

#### 3.4.5 Putative mechanism of statin-related mitochondrial dysfunction

Based on results in this study and evidence from the literature, mitochondrial dysfunction related to statin therapy could be due to stimulus-secretion uncoupling secondary to CoQ10 deficiency or increased glycolytic activity causing reduced flux through oxidative phosphorylation. This mechanism is explored further below.

There is evidence that statins reduce plasma coenzyme Q10 (CoQ10, also called ubiquinone) (538, 539) and that exogenous CoQ10 relieves statin-associated CoQ10 deficiencies, and has beneficial effects on pancreatic  $\beta$ -cell function (301, 540). In particular, the potential effect of CoQ10 depletion on mitochondrial function has been proposed as a mechanism for statin-related mitochondrial dysfunction in skeletal muscle (500) and has also been mooted for  $\beta$ -cells (34, 443), though this still remains to be determined (218). CoQ10, a flexible electron carrier with the capacity to be partially or fully reduced, is a component of the electron transport chain and thus involved in insulin stimulus-secretion coupling in  $\beta$ -cells. A deficiency of CoQ10 could therefore reduce coupling and hence insulin secretion, potentially characterised by blunted maximal secretion when ATP production is limited by the deficiency, as observed in this study (see Chapter 2). However, coupling efficiency (CE) was not influenced by statins in the current study and further assessment of coupling efficiency by other methods would be helpful.

Interestingly, a higher lactate:pyruvate ratio in plasma was found to be associated with reduced plasma CoQ10 in statin-treated patients (541). This supports the findings in this study of increased anaerobic respiration in response to statins. However, it should be noted that the

lactate:pyruvate ratio, used clinically to diagnose mitochondrial cytopathies (542, 543), represents whole body respiratory inadequacy and not  $\beta$ -cells specifically.

Reduced metabolic flexibility intrinsic to  $\beta$ -cells can be reversed under adverse conditions, for example, when stressed by hypoxia and glucotoxicity (245, 544, 545). By this means  $\beta$ -cells, at least in some circumstances, can prevent demise by sacrificing their unique function and allowing the strongly repressed pathway of anaerobic glycolysis. This phenomenon is known as  $\beta$ -cell dedifferentiation and is characterised by loss, at least to some extent, of glucose sensitive insulin secretion (545) and increased glucagon secretion (546), possibly due to transdifferentiated  $\beta$ -cells taking on  $\alpha$ -cell characteristics (491) in the absence of apoptosis (373). Reduced expression of transcription factors such as MafA, PDX-1, Nkx6.1, Pax6, HNF3b, HNF4a, and HNF1a, along with upregulation of c-Myc (492, 494), instigate upregulation of genes that are normally repressed in  $\beta$ -cells (such as LDHA, hexokinase I, monocarboxylate transporters and glucose-6-phosphate) and downregulation of  $\beta$ -cell specific proteins (such as insulin, Glut-2, glucokinase, mitochondrial glycerol-3-phosphate dehydrogenase and pyruvate carboxylase) (492). This may be in response to increased flux through the hexosamine biosynthetic pathway (373), endoplasmic reticulum stress and ROS (490), induced by glucotoxicity.

Whether increased anaerobic glycolysis is a compensatory mechanism subsequent to mitochondrial dysfunction or whether decreased entry into the TCA cycle is secondary to upregulated anaerobic pathways is unclear. However, it is tempting to suggest that statin-induced mitochondrial stress may contribute towards such a switch, particularly when combined with additional stressors such as chronic hyperglycaemia/hyperlipidaemia. The dedifferentiation process would be expected to lift the embargo on anaerobic respiration found in healthy  $\beta$ -cells, allowing increased flux through anaerobic glycolysis at the expense of insulin stimulus-secretion coupling, a result demonstrated in response to statins in this project. Up-regulation of hexokinase I supports this possibility. Possibly supportive but requiring further investigation is the trend towards inhibition of GSK3 $\beta$  by serine 9 phosphorylation, and not supportive is the lack of expression changes in other glycolytic enzymes including LDHA, PDH, PKM2 or GLK, known to be associated with hypoxia and/or the Warburg effect. However, activity status or kinetic studies of these glycolytic enzymes have yet to be undertaken. Increasing the time of statin exposure beyond 24 h would also be helpful to further assess a putative trend towards  $\beta$ -cell dedifferentiation suggested by these results.

### 3.4.6 Further work and limitations

Primary  $\beta$ -cells, with their phenotypic 80-90% rate of glucose carbon conversion to CO<sub>2</sub> (252, 547), and suppressed glycolytic machinery including monocarboxylate transporters and LDHA (435, 548), could be considered unsuitable subjects for ECAR measurements using the Seahorse



extracellular flux analyser. Furthermore, a glycolytic stress test performed in dispersed islet cells in our laboratory showed very little glycolysis or glycolytic capacity (Carlessi, unpublished). BRIN-BD11 cells, like all immortal cell lines, demonstrate some divergence from the primary  $\beta$ -cell phenotype and may not be an accurate model. They may have altered coupling efficiency compared to primary  $\beta$ -cells due to increased expression of hexokinases I and II, monocarboxylate transporters and LDHA (see Chapter 4); however, this would not explain the effect of statins in this study. Nonetheless, caution is necessary in extrapolation of these results to primary  $\beta$ -cells, and further work in islets and primary  $\beta$ -cells is warranted.

A further limitation in the determination of maximal respiration using the mitochondrial stress test in  $\beta$ -cells is potential ATP depletion (246). Glycolytic ATP generation is required for the maintenance of cellular ATP levels after shutting down ATP synthase with oligomycin. In  $\beta$ -cells, where the glycolytic pathway is restricted, subsequent glycolysis (which requires an initial investment of ATP) may be limited by ATP depletion, thereby affecting the measurement of maximal respiration after metabolic uncoupling using the protonophore FCCP. A recommendation has been made to use oligomycin and FCCP together in a separate experiment in  $\beta$ -cells to avoid ATP depletion and more accurately record maximal respiration (246). It is possible that BRIN-BD11 cells are not as limited in glycolytic ATP production as primary  $\beta$ -cells, however an assessment is yet to be carried out.

Proton leak, determined by the difference in oxygen consumption rate during ATP synthase versus total mitochondrial inhibition, was not affected by statin treatment. However, extracellular acidification rate measured in the same experiment increased further when mitochondrial uncoupling took place after the addition of FCCP. Mitochondrial  $\text{CO}_2$  produced during oxidative phosphorylation could potentially contribute to this acidification. To account for possible confounding factors, an additional method should be used to measure acidification resulting from oxidative phosphorylation. This is a limitation of the present study and will be further examined using the recent protocol developed by Agilent for improving the quantification of cellular glycolytic rate (505).

Further investigation of glycolytic enzymes would be helpful. As mentioned above, phosphoproteomic or enzyme kinetic studies would provide additional information on the stimulation of glycolytic pathways. PKM2 (549, 550) and LDHA tyrosine phosphorylation (551, 552) is associated with the Warburg effect and it would be interesting to assess whether similar processes are at work in the statin-treated  $\beta$ -cell model used in this study. Glucose disposal could be further investigated by the study of other pathways such as flux through the hexosamine biosynthetic pathway and lipogenesis in the context of statin treatment. In addition, it would be interesting to investigate potential changes in the expression and subcellular localisation of transcription factors such as FOXO1, HIF1 $\alpha$ , MAFA and PDX1, known to be

representative of  $\beta$ -cell dedifferentiation and to precede the onset of T2D (491, 497, 553). The mutually exclusive proliferative or mature  $\beta$ -cell phenotype is also distinguishable by expression of these transcription factors (238).

### 3.4.7 Conclusion

Statin treatment decreased ATP production and maximal respiration with a concomitant increase in glycolysis but not glucose uptake in BRIN-BD11 cells. A possible mechanism for these findings is as follows: reduced mitochondrial CoQ10 content reduces the ability to produce ATP via oxidative phosphorylation, thus limiting maximal stimulated insulin secretion. To compensate, glucose is directed towards anaerobic glycolysis, a pathway usually disallowed in  $\beta$ -cells, and stimulus/secretion coupling is attenuated. This may be a  $\beta$ -cell pro-survival mechanism, and further research will be required to assess whether this results in  $\beta$ -cell dedifferentiation akin to what has been described in T2D.

## Chapter 4      Effects of cholesterol manipulation on selected proteins central to $\beta$ -cell function

Following the observations of cellular cholesterol-associated changes on insulin secretion and  $\beta$ -cell bioenergetics, it was of interest to ascertain whether the function or regulation of various additional proteins may be altered by changes in cellular cholesterol concentrations. Of particular interest were those having a role in glucose sensing or insulin secretion, often located on or near cholesterol-rich plasma membranes. Cholesterol endows cell membranes with physical attributes essential for the optimal function of some resident proteins, and is a factor in membrane organisation into lipid raft micro-domains. The specific aim of this work was to assess the effect of changes in cholesterol on selected proteins central to  $\beta$ -cell function, additional to the glycolytic proteins assessed previously.

To this end, BRIN-BD11 cells were examined to assess whether statins had an influence on selected proteins related to oxidative stress and cell signalling. The sub-cellular location of a limited number of targeted proteins, some of which appear to be exclusive to  $\beta$ -cells, in line with potentially unique functions in these cells, was also assessed by immunoblotting. A more generalised protein snapshot was presented by isobaric tags for relative and absolute quantitation (iTRAQ) proteomics after M $\beta$ CD- and c-M $\beta$ CD- associated cholesterol adjustment. Some additional observations from flow cytometric techniques were also made. Not all proteins were examined in the same way, partly due to the breadth of the study, together with time and technical limitations. However, an attempt has been made to bring several strands of evidence together to consolidate an understanding of the influence of cholesterol on specific insulin secreting processes in the context of stimulated insulin secretion. Accordingly, results presented here are the sum effect of cholesterol-adjusting treatment and stimulation by high glucose and L-alanine.

Among proteins pertinent to cell signalling, atorvastatin treatment resulted in upregulation of mTOR expression and increased phosphorylation of the insulin receptor. A trend towards upregulation of ABCA1 was also observed in the membrane fraction of alanine stimulated, atorvastatin-treated BRIN-BD11 cells. Interestingly, caveolin 1 and ABCG1 were located in the cytosolic and mitochondrial fractions, respectively, unlike what may be expected in other cell types. No changes were observed in expression or cellular location after M $\beta$ CD or c-M $\beta$ CD treatment in proteins selected for Western blotting analysis, however iTRAQ proteomics analysis of a specific cell fraction revealed several changes in protein abundance, with more changes occurring in the c-M $\beta$ CD than the M $\beta$ CD treatment group, consistent with results elsewhere in this project. Flow cytometry revealed autofluorescence changes

accompanying cholesterol modifying treatment, with increased and decreased autofluorescence associated with reduced and increased cholesterol, respectively. However, a possibility that cholesterol content may affect fluorescence detection was flagged, and further work will be necessary to assess the reliability of this method for quantitation of immunostained proteins. Flow cytometry was nevertheless useful for detecting changes in cell size and complexity, the former being increased with both c-M $\beta$ CD and atorvastatin treatment, and the latter changing inversely with cholesterol abundance, increasing with M $\beta$ CD and atorvastatin treatment and decreasing with c-M $\beta$ CD treatment. The data in this chapter informed the development of five testable hypotheses to establish promising lines of enquiry for future exploration of potential mechanisms by which cholesterol content may influence  $\beta$ -cell function, summarised in Section 4.5.

## 4.1 Background

The cell membrane, with cholesterol contributing ~10 – 45% of its total lipids (59, 61, 554), and usually accounting for ~64 – 90% of cellular cholesterol (61, 555), is a dynamic, functional lipid bilayer responsible for communication with the extracellular environment and has selective permeability to molecules between intra- and extra-cellular compartments. A widely understood hypothesis with strong supporting evidence (albeit not universally accepted, see (306, 556)) suggests that lipid raft micro-domains, characterised by increased order, facilitate the organisation of many transmembrane proteins (61, 338, 557). Several processes important to glucose sensing and insulin secretion are dependent on raft-embedded proteins for optimal function. For example, calcium influx leading to insulin granule fusion is facilitated by voltage gated calcium channels ( $\text{Ca}^{2+}_v$ ) located in lipid rafts (65). Also, SNARE proteins including vesicle-associated membrane protein isoform 2 (VAMP2) and the 25 kDa synaptosomal protein (SNAP-25) (69, 558), are transmembrane proteins whose location within lipid rafts is important to their effective function in granule fusion. In addition, glucose transporter 2 (GLUT-2) and ATP sensitive potassium channels ( $\text{K}_{\text{ATP}}$ ), which function optimally in non-raft membrane areas (67), are responsible for glucose uptake and membrane depolarisation, respectively, in the rodent  $\beta$ -cell.

Specific membrane characteristics such as thickness, flexibility, order and phase behaviour are known to facilitate the function of membrane proteins involved in glucose sensing and insulin secretion, and these properties are largely bestowed by the physicochemical characteristics of the nonpolar cholesterol molecule (64, 306, 333, 418). Therefore, changes in membrane cholesterol content mediated by statins or M $\beta$ CD may negatively impact glucose homeostasis.

Furthermore, isoprenoids are products of the mevalonate pathway of cholesterol synthesis and are involved in prenylation of signalling molecules such as small G-proteins, a process that

enables their recruitment to the cell membrane due to increased hydrophobicity (reviewed in 559). Ras-related C3 botulinum toxin substrate 1 (Rac1) is one such protein that relies on geranylgeranylation for appropriate membrane recruitment and is known to be involved in GSIS stimulus-secretion coupling, probably via membrane remodelling (78, 560).

Evidence thus suggests that cholesterol and/or intermediates within its biosynthetic pathway provide several potential mechanisms by which M $\beta$ CD or statins could interfere in processes necessary for insulin secretion and glucose homeostasis. In response to this, representative proteins were investigated in BRIN-BD11 cells for changes in expression and cell compartment localisation after cholesterol manipulation with c-M $\beta$ CD and statins in this hypothesis-generating project. Table 4.2 lists the proteins examined, provides a rationale for their inclusion by way of a brief statement about function, and summarises relevant results. Proteins were chosen from five functional areas: a) glucose homeostasis, b) lipid homeostasis, c) insulin secretion, d) oxidative stress and e) signalling.

## 4.2 Methods

Two methods of cholesterol manipulation were employed as described previously: loading and sequestration by M $\beta$ CD (preloaded or not with cholesterol), and inhibition of synthesis by atorvastatin or pravastatin. Not all treatment groups were assessed by all methods for relevance or technical reasons. Generally, after treatment BRIN-BD11 cells were stimulated with 10 mM alanine and 16.7 mM glucose for 20 minutes immediately prior to harvest.

Western blotting with or without separation into cytosolic, membrane and mitochondrial fractions (as described), flow cytometry and iTRAQ proteomic analysis were used to identify cell localisation and determine changes in abundance of specific proteins. Flow cytometry was investigated to explore whether the single cell, quantitative nature of this technique could be useful to assess intracellular protein changes in the context of statin, M $\beta$ CD or c-M $\beta$ CD treatment. The latter work provided some interesting observations relevant to this chapter, although its suitability for quantitative protein analysis in this context was found to be questionable. An overview of the experiments in this chapter and the questions they address is available in Figure 4.1.

### 4.2.1 Cell culture

BRIN-BD11 cells were grown in RPMI supplemented with 10% FBS (or the protein equivalent of LPDS for statin-treated cells, see Section 2.1.3) and 1% penicillin/streptomycin in T75 tissue culture flasks. For statin experiments cells were grown to approximately 50% confluence, and then treated for 24 h with or without pravastatin or atorvastatin as described in Section 2.1.5. For M $\beta$ CD experiments cells were grown to ~70% confluence, washed twice in PBS then treated with 5 mM c-M $\beta$ CD or M $\beta$ CD for 30 min in RPMI without FBS for flow cytometry or

in Krebs' Ringer Bicarbonate Buffer (KRBB) supplemented with 1.1 mM glucose for analysis by Western blotting. The protocol for the preparation of KRBB and treatments is described in full in Section 2.1.4.

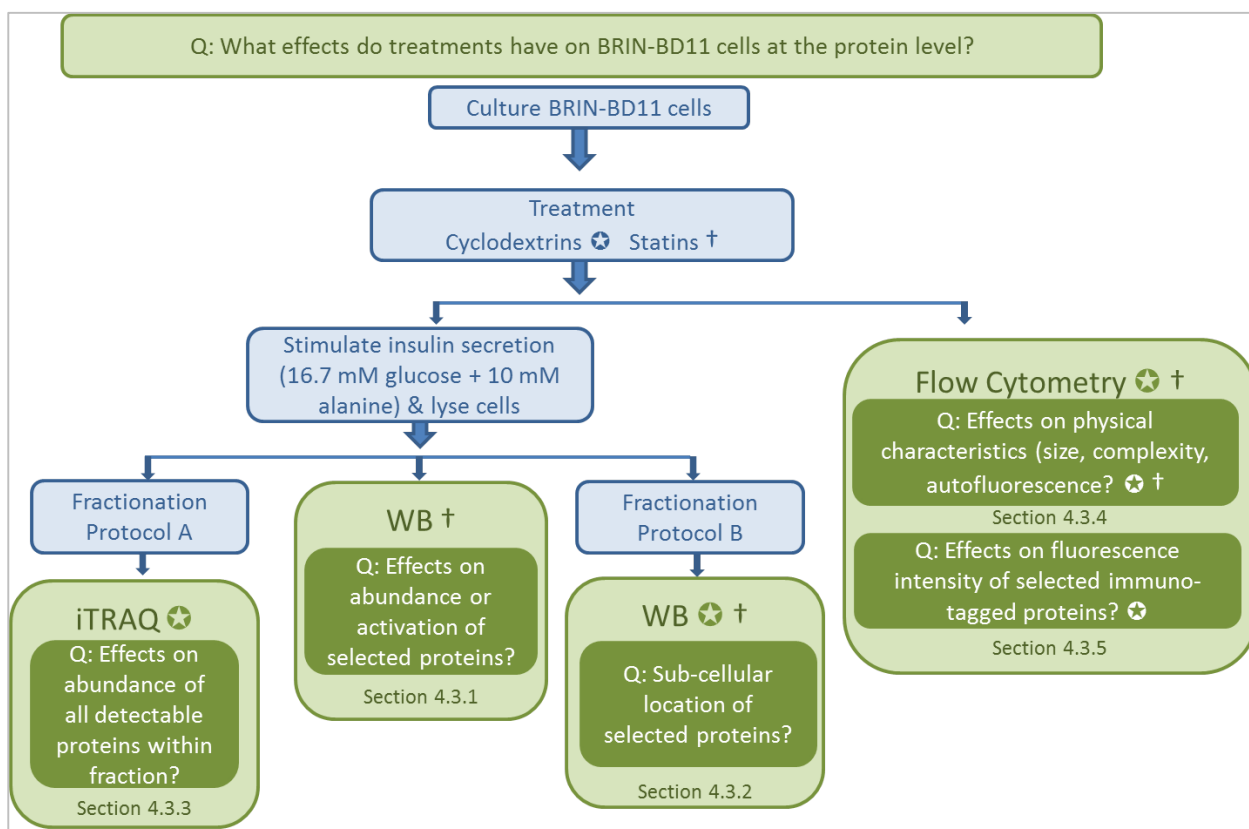


**Figure 4.1. Overview of techniques and research questions in Chapter 4.**

Note that not all treatments were explored using all techniques. Symbols for cyclodextrin treatments (both M $\beta$ CD and c-M $\beta$ CD; ★) and statins (†) indicate which treatment effects were studied.

#### 4.2.2 Cell lysate preparation for Western Blot analysis

BRIN-BD11 cells were grown in T175 flasks and treated as described above. Before harvesting, cells were starved for 40 min in KRBB supplemented with 1.1 mM glucose. Alternatively, when using c-M $\beta$ CD and M $\beta$ CD, treatment and starvation were performed for 30 min simultaneously. Cells were then stimulated in KRBB supplemented with 16.7 mM glucose and 10 mM alanine for 20 min before being washed in cold PBS, scraped into 15 ml centrifuge tubes, pelleted by centrifugation at 500 x g for 5 min and lysed in RIPA buffer supplemented with a phosphatase/protease inhibitor cocktail (Cell Signaling Technology). Samples were stored at -80°C prior to analysis. For samples destined for membrane and cytosolic fractionation, starting buffer (SB; 225 mM mannitol, 75 mM sucrose, 30 mM Tris-HCl, pH 7.4) prepared freshly on the morning of protein harvest as per Suski *et al* (561) was used in place of RIPA buffer.

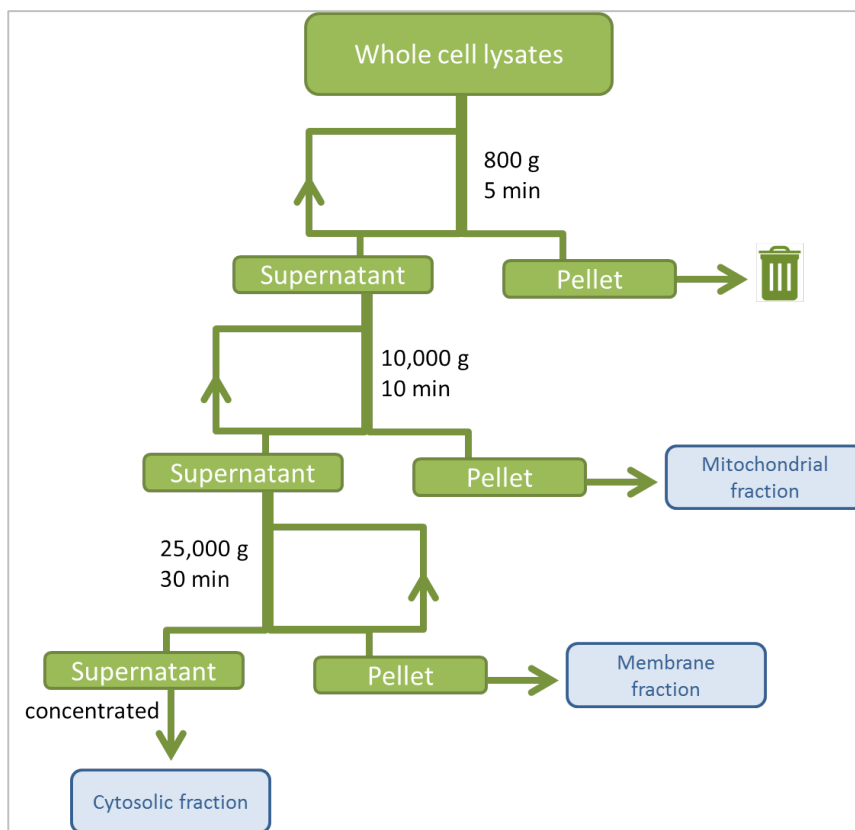


**Figure 4.2. Flow diagram of fractionation B protocol for sub-cellular protein location analysis by Western blot.**

#### 4.2.3 Cell fraction preparation for Western Blot analysis

Membrane fractions were isolated from freshly prepared lysates as described (561). Briefly, cell pellets pooled from 2 (statin) or 3 (M $\beta$ CD) T175 flasks were resuspended in 4 ml SB supplemented with protease/phosphatase inhibitors and homogenised using 16 strokes of a 10 ml glass/PTFE Potter-Elvehjem dounce homogeniser with a medium fit pestle. Samples were kept on ice or at 4°C throughout the procedure. Sub-cellular fractions were prepared as follows (see Figure 4.2). The homogenate was transferred to a 15 ml centrifuge tube and centrifuged at 800 x g for 5 min to precipitate nuclei and cell debris. The pellet was discarded and centrifugation of the supernatant was repeated. The supernatant was collected into an ultracentrifuge tube and centrifuged for 10 min at 10,000 x g in a Beckman Coulter Optima XE-100 ultracentrifuge paired with a 70.1 TI fixed angle rotor. For M $\beta$ CD experiments, pellets (representing the mitochondrial fraction) were resuspended in 45  $\mu$ L of SB buffer supplemented with 1% SDS and stored. Mitochondrial yield was lower in the statin experiments due to the preparation of fewer flasks of cells, thus mitochondrial pellets were not visible and were not collected. The supernatant was placed in a fresh ultracentrifuge tube and the procedure was repeated to remove any remaining mitochondrial contamination, then centrifuged in a new tube at 25,000 x g for 30 min. This yielded a ‘cytosolic fraction’ (supernatant), which was collected and stored, and subsequently concentrated using a 1 kD pore-size protein concentrating centrifuge column (Pall). The ‘membrane fraction’ (pellet) was washed in 3 mL SB and

centrifuged again at 25,000 x g for 30 min before resuspension in 50  $\mu$ L of SB buffer and storage at  $-80^{\circ}\text{C}$  for future use. All fractions were quantified for protein using a Pierce BCA assay (ThermoFisher Scientific) as per manufacturer's instructions.

#### 4.2.4 Protein quantitation by Western Blot analysis

Within any experiment, equivalent amounts of protein from whole cell lysates or fractioned samples were prepared in Laemmli sample buffer (BioRad) and Bolt reducing agent (Life Technologies). Samples were denatured for 10 min at  $98^{\circ}\text{C}$  (except when probing for  $\text{Na}^{+}\text{K}^{+}\text{ATPase}$ ) and loaded on a 4-12% precast Bis-Tris gradient gel (Biorad) for separation by SDS-PAGE at 120 V for approximately 50 min. Proteins were transferred to a nitrocellulose membrane using the iBlot semi-dry system (Life Technologies) on a 7 min transfer program. Membranes were incubated in blocking buffer (BB; 3% BSA in TBST) for 1 h at room temperature before being probed overnight at  $4^{\circ}\text{C}$  using various antibodies prepared in BB as per Table 4.1. Horseradish peroxidase (HRP)-conjugated secondary antibodies were prepared in BB and membranes were incubated for 1 h at room temperature, washed three times in BB for 5 min then imaged using the ChemiDoc™ MP System (Bio-Rad) imaging system and Amersham ECL Prime Western Blotting Detection Reagent (GE Healthcare Lifesciences). When multiple probing was done on the same membrane a mild stripping buffer was used as described in the protocol published by Abcam. Briefly, membranes were incubated twice for 10 min each in stripping buffer (1.5% (w/v) glycine, 0.1% (w/v) SDS, 1% (v/v) Tween 20, pH 2.2), then twice for 10 min in TBS and twice for 5 min in TBST before blocking as above. They were then probed with primary antibodies for 2 h followed by secondary antibodies for 1 h, both at room temperature, and then washed and detected as above. Densitometry analysis was performed using Image Lab 6.0 software.

#### 4.2.5 Protein quantitation by iTRAQ analysis

BRIN-BD11 cells were grown, treated with  $\text{M}\beta\text{CD}$  or  $\text{c-M}\beta\text{CD}$  and stimulated for 20 min with 10 mM alanine and 16.7 mM glucose as described above. Cells were scraped from the flask in ice-cold PBS and pelleted by centrifugation at 500 x g for 3 min. Cells were re-suspended in ice-cold lysis buffer (400  $\mu$ l containing 50 mM Tris, pH 7.5, 0.5 mM EDTA, 20% glycerol, 1 x protease/phosphatase inhibitors) and sonicated on ice as described (562), using 2 x 10 sec bursts with 5 sec between using an immersion microtip and an amplitude of 50% (Misonix s-4000, QSonica).

To avoid diluting out the less abundant membrane proteins, including those relevant to  $\beta$ -cell function, by high relative abundance of cytosolic proteins, membrane enriched fractions were prepared by ultracentrifugation using a simplified fractionation protocol. A clarification centrifugation at 800 x g for 10 min was undertaken, the pellet was resuspended in 400  $\mu$ l of fresh lysis buffer, then re-centrifuged as above. The supernatants from both steps were



combined for each sample and ultracentrifuged at 100,000 x g for 1 h using an Optima Max-XP ultracentrifuge and fixed angle TLA 120.1 rotor. The supernatant ('S' fraction) was stored at -20°C and the pellet ('P' fraction) was resuspended in 150 µl lysis buffer. Samples from both fractions were diluted 1 in 4 to reduce glycerol interference in the assay and quantified using a BCA assay. 150 µg of protein from each 'P' fraction sample was placed in 1.5 ml centrifuge tubes and 600 µl ice cold acetone was added. 'P' fraction samples were incubated at -20°C to precipitate overnight then transported on ice for iTRAQ analysis by a research provider, Proteomics International.

iTRAQ analysis was undertaken as previously described (563). Briefly, samples were trypsin digested, labelled with isobaric tags, pooled and separated by strong cation exchange liquid chromatography. 'P' fractions were analysed by electrospray ionisation mass spectrometry and spectral data was analysed against *Rattus norvegicus* using the SwissProt database, downloaded in April 2016, facilitated by ProteinPilot™ software (Casey, 2016, Proteomics International results report, Appendix B).

#### 4.2.6 Flow cytometry

After treatment, cells were washed once in ice-cold PBS, scraped into 15 ml centrifuge tubes and centrifuged at 500 x g for 3 min. Pellets were resuspended in 1300 µL PBS and 100 µL aliquots (~1 million cells per well) were placed into a round-bottom 96-well plate. All subsequent procedures were undertaken in the dark at 4°C or on ice. The samples were centrifuged at 500 x g for 3 min. The supernatant was removed and cells were stained with 100 µL ZombieNIR™ near-infrared (NIR) fixable viability dye (BioLegend) for 20 min. The stain was removed and cells were fixed in 0.5% paraformaldehyde (PFA) for 10 min. Cells were washed twice then permeabilised and blocked for 20 min in permeabilisation buffer (PB; 5% FBS, 2% BSA, 0.1% saponin, 0.3 M glycine in PBS). For samples undergoing antibody staining, cells were incubated for 30 min with primary antibodies prepared in PB as per results, washed three times, then for a further 30 min with secondary antibodies conjugated to various fluorophores also prepared in PB, as per results. Finally, cells were washed three times and stored at 4°C overnight before being analysed on a BD LSR Fortessa flow cytometer. Table 4.1 records the various antibodies and concentrations used.

The gating hierarchy used was as follows: P1 > Singlets > Live singlets (LS) > Viable (Figure 4.3). The cell population (P1) was identified in a forward scatter area (FSC-A) vs side scatter area (SSC-A) scatter plot, gated to exclude subcellular events. The P1 population was then gated to include single cells (singlets) using FSC height vs area. Dead cells were excluded from the singlet population based on fluorescence from ZombieNIR™ staining, yielding the LS population. Detector channels not used for fluorophores were left open to gain extra information about the effect of treatments on cellular autofluorescence. Although the source of

intrinsic autofluorescence was not explored, noting differences between treatments/conditions compared to untreated/control samples enabled further differentiation. Consequently, due to the observation that a population of cells staining positively for insulin could also be differentiated independently of insulin staining using signals from autofluorescence and ZombieNIR™ collected in the emission filters (525/50) from violet laser (405 nm) excitation (V(525/50)) and (780/60) from red laser (640 nm) excitation (R(780/60)), respectively, active cells (designated ‘viable’) were gated and this population was subsequently used (see Figure 4.9).

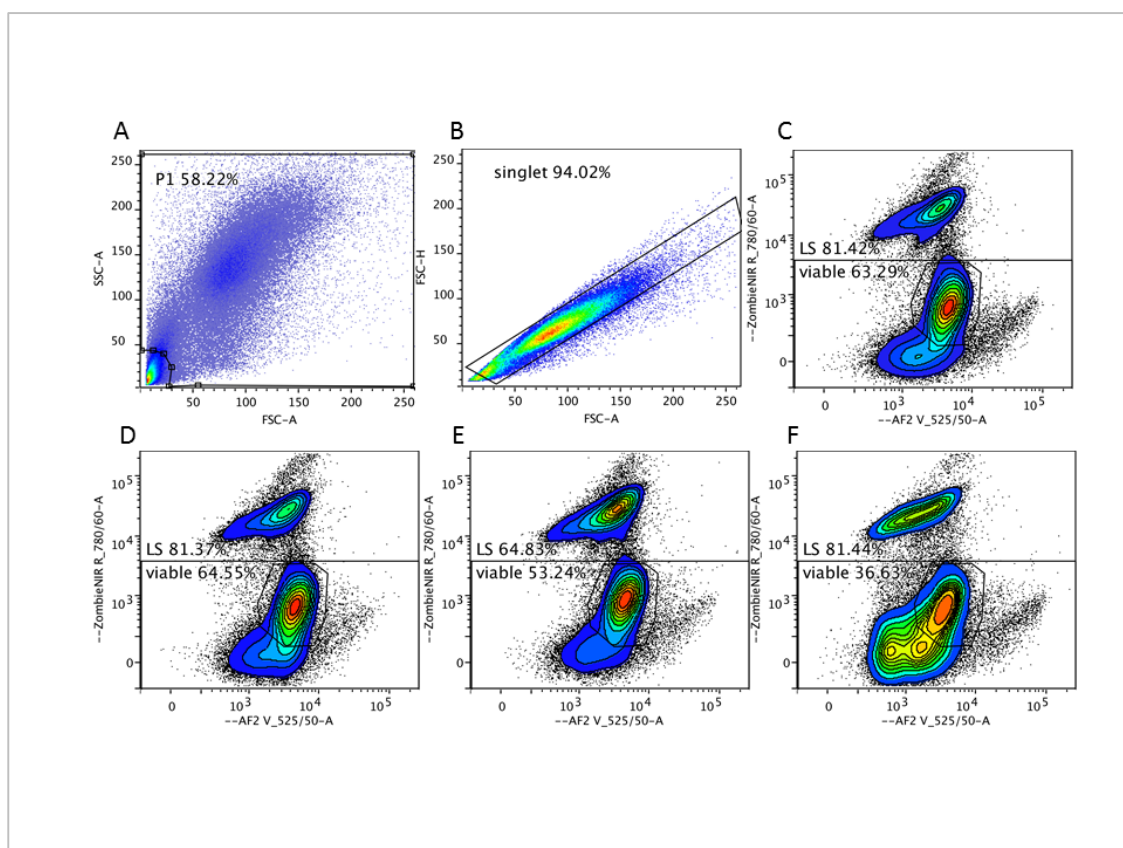


**Figure 4.3. Gating hierarchy for flow cytometry.**

**A:** Debris was gated out, leaving whole cells in the P1 population (within the black gate). **B:** doublets or grouped cells were gated out by a size exclusion gate based on forward scatter, leaving the single cell population within the gated area. **C:** Dead cells that took up the live/dead ZombieNIR™ stain were excluded, leaving the live singlets (LS, lower rectangular gate). A subset of the LS population was selected as the ‘viable’ population (simple closed curve) based on fluorescence in the red R(780/60) and violet V(525/50) channels. Insulin staining was found to correlate with autofluorescence in this channel (see also **Figure 4.9**). **D, E** and **F** show representative examples of control, MβCD-treated and c-MβCD-treated samples, respectively. The populations were colour-coded according to number of events, with black representing the fewest events, then progressing through blue, green and yellow, with red showing the highest number of events. c-MβCD treatment typically reduced autofluorescence, leaving fewer cells in the viable gate.

**Table 4.1. Antibodies used in Western Blot and Flow Cytometry experiments**

Category/Supplier	Cat. #	Target	Expected MW	WB		Flow Cytometry		
				Concentration	HRP-Secondary	1 <sup>o</sup> Conc	Secondary	2 <sup>o</sup> Conc
<b>Lipid Homeostasis</b>								
Abcam	ab52629	SR-B1	80	1 in 2,000	R-1 in 5,000	na		
Abcam	ab174830	HMGCR	97	1 in 5,000	R-1 in 5,000	1 in 200	R-488	1 in 2,000
Abcam	ab66217	ABCA1	254	1 in 200 or 500	M2-1 in 5,000	1 in 200	M2-647	1 in 2,000
Abcam	ab30532	LDLr	100-160	1 in 150	R-1 in 5,000	1 in 100	R-488	1 in 2,000
Abcam	ab28482	SREBP2	68, 120	1 in 500	R-1 in 5,000	1 in 200	R-488	1 in 2,000
<b>Glucose Sensing/ Ins secretion</b>								
Abcam	ab7842	Ins	12	na		1 in 250	GPg-647	1 in 2,000
Abcam	ab70222	VAMP2	18	1 in 1,000	R-1 in 5,000	1 in 200	R-488	1 in 2,000
Abcam	ab18199	Caveolin1	20	1 in 400	R-1 in 5,000	na		
Abcam	ab31281	SNAP25	22	1 in 500	Gt 1 in 10,000	na		
Abcam	ab37796	GLK	52	1 in 500	R-1 in 5,000	1 in 100	R-488	1 in 2,000
Abcam	ab54460	GLUT2	57	1 in 1,000	R-1 in 5,000	1 in 100	R-488	1 in 2,000
Abcam	ab15272	IAPP	87	1 in 1,000	R-1 in 5,000	1 in 200	R-488	1 in 2,000
Abcam	ab32844	SUR1	175	1 in 500	R-1 in 5,000	1 in 50	R-488	1 in 2,000
Abcam	ab85491	CaV1.3	245	1 in 1,000	M2-1 in 5,000	1 in 100	M2-PE	1 in 200
<b>Oxidative Stress</b>								
Abcam	ab2302	Active Caspase 3	17	1 in 200	R-1 in 5,000	1 in 100	R-488	1 in 2,000
Abcam	ab185962	HSP70	94-110	1 in 2,000	R-1 in 5,000	1 in 200	R-488	1 in 2,000
Abcam	ab136918	iNOS	131	1 in 2,000	R-1 in 5,000	1 in 500	R-488	1 in 2,000
<b>Signaling</b>								
Jomar	ARC03	Rac1	21	1 in 500	R-1 in 5,000	na		
Cell Signaling	#13038	pAKT (Thr-308)	60	1 in 1,000	R-1 in 5,000	na		
Cell Signaling	#3023	pIR (Tyr1361)	170	1 in 500	R-1 in 5,000	na		
Cell Signaling	2983	mTOR	289	1 in 1,000	R-1 in 5,000	na		
Abcam	ab983	Irb	95	1 in 500	M2-1 in 5,000	1 in 50	M2-647	1 in 2,000
<b>Control</b>								
Abcam	ab8245	GAPDH	36	1 in 5,000	M1-1 in 5,000	na		
Abcam	ab8229	β-actin	42	1 in 5,000	Gt 1 in 10,000	na		
Abcam	ab139181	SDHA	70	1 in 1,000	R-1 in 5,000	na		
Abcam	ab176333	KDEL [EPR12668]	observed at 57	1 in 10,000	R-1 in 5,000	na		
Abcam	ab76020	Na+/K+ ATPase	100	1 in 10,000	R-1 in 5,000	na		
<b>Glycolytic</b>								
Abcam	ab8245	GAPDH	36	1 in 1,000	R-1 in 5,000	na		
Cell Signaling	3582	LDHA	36	1 in 1,000	R-1 in 5,000	na		
Cell Signaling	5558	pGSK3β (Ser9)	47	1 in 1,000	R-1 in 5,000	na		
Cell Signaling	3205	PDH	49	1 in 1,000	R-1 in 5,000	na		
Cell Signaling	3190	PKM1/2	58	1 in 1,000	R-1 in 5,000	na		
Cell Signaling	4053	PKM2	58	1 in 1,000	R-1 in 5,000	na		
Cell Signaling	8164	PFKP	86	1 in 1,000	R-1 in 5,000	na		
Cell Signaling	2024	Hex I	102	1 in 1,000	R-1 in 5,000	na		
Cell Signaling	2867	Hex II	102	1 in 1,000	R-1 in 5,000	na		
Cell Signaling	2983	mTOR	289	1 in 1,000	R-1 in 5,000	na		
<b>Isotype control</b>								
Abcam	ab14917	LYVE-1 (Rabbit)			Matched relevant concentration	R-488		1 in 2,000
Life Technologies	#02-6300	Mouse IgG2b isotype control			Matched relevant concentration	M2-647		1 in 2,000
Santa Cruz Biotechnology	sc-2711	Guinea pig IgG isotype control			Matched relevant concentration	GPg-647		1 in 2,000
Life technologies	#02-6102	Rabbit IgG isotype control			Matched relevant concentration	R-488		1 in 2,000
<b>Secondary Abs &amp; dyes</b>						<b>Abbreviation</b>		
Abcam	ab150113 or ab150077	Goat Anti-Mouse IgG H&L (Alexa Fluor® 488)				R-488		
BioLegend	406708	Rat anti-mouse IgG2b (PE)				M2-PE		
Abcam	ab150187	Goat Anti-Guinea pig IgG H&L (Alexa Fluor® 647)				GP-647		
Abcam	ab172327	Rat monoclonal (SB74g) Anti-Mouse IgG2b (AlexaFluor 647)				M2-647		
Abcam	ab6721	Goat Anti-Rabbit IgG H&L (HRP)				R		
Abcam	ab6789	Goat Anti-Mouse IgG H&L (HRP)				M2		
Abcam	ab6908	Goat Anti-Guinea pig IgG H&L (HRP)				GP		
Abcam	ab6741	Rabbit Anti-Goat IgG H&L (HRP)				Gt		
BioLegend	423105	Zombie NIR fixable viability dye						

## 4.3 Results

### 4.3.1 Statin-associated changes in proteins involved in oxidative stress and signalling

To evaluate whether statins were associated with changes in the expression of selected proteins involved in  $\beta$ -cell function, Western blots were performed on whole cell lysates from statin-treated BRIN-BD11 cells immediately after stimulation with high glucose and alanine. Since statins may influence insulin secretion via an increase in reactive oxygen species (356) (also see Section 1.5.3), proteins pertinent to oxidative stress were investigated. Changes in cell signalling in response to statins may also interfere with insulin secreting processes, thus several signalling proteins relevant to  $\beta$ -cell function were examined. All proteins interrogated in this chapter are included in Table 4.2, where a brief description of their function provides a rationale for their inclusion.

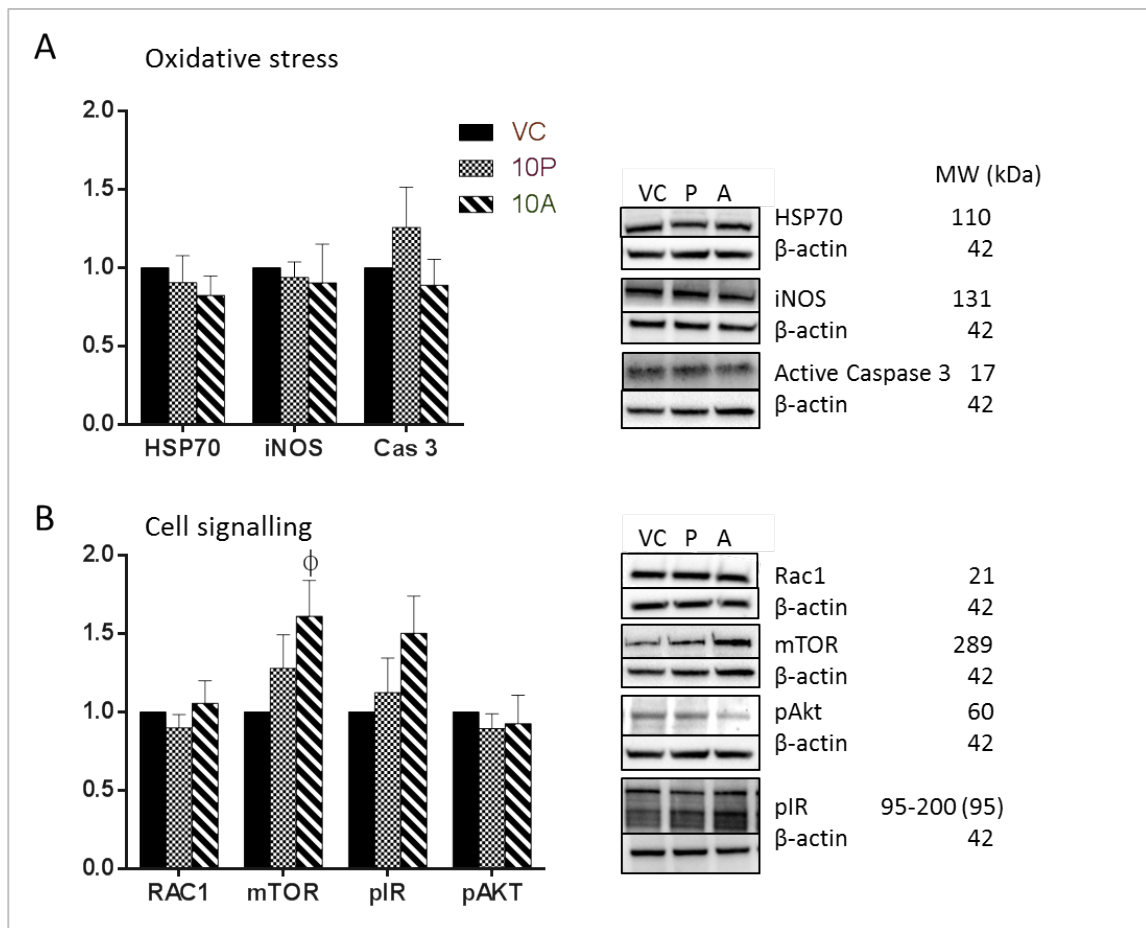


**Figure 4.4. Western blot assessment of the effect of statins on selected proteins related to oxidative stress (A) and signalling (B).**

Representative blots are shown and graphs include densitometry data (mean  $\pm$  SEM) from at least three separate experiments except pAkt, which is from two experiments. Density values were normalised to both the housekeeping protein  $\beta$ -actin and the vehicle control (VC). P, 10  $\mu$ M pravastatin; A, 10  $\mu$ M atorvastatin. The observed molecular weights (MW) are shown. Where this differs from the expected MW, expected values are in parentheses.  $\phi$ ,  $P < 0.05$  compared to VC.

Proteins representing the oxidative stress pathway included heat shock protein 70 (HSP70), inducible nitric oxide synthase (iNOS), and active caspase 3 (Cas 3). There were no significant changes in expression in this group (Figure 4.4A).

Signalling proteins assessed included Ras-related C3 botulinum toxin substrate 1 (RAC1), mammalian target of rapamycin (mTOR), insulin receptor (pI-R) phosphorylated at tyrosine 1361 and AKT (pAKT) phosphorylated at threonine 308 (Figure 4.4B). Of these, mTOR was upregulated with atorvastatin treatment by >50% ( $P < 0.05$ ), and there was a similar trend for pI-R ( $P = 0.14$ ).

There was a general overall trend towards a greater influence on protein expression by atorvastatin compared to pravastatin. This is consistent with its greater impact on  $\beta$ -cell energetics and insulin secretion as described in previous chapters.

#### 4.3.2 Determination of the cellular localisation of specific proteins

Since cholesterol and some products of its synthesis stabilise some proteins to the membrane, it is possible that alterations in cholesterol content or inhibition of cholesterol synthesis could affect the sub-cellular localisation of some proteins pertinent to  $\beta$ -cell function. To examine this, Western blot analyses were undertaken using cell lysates that had been separated into cytosolic and membrane fractions as previously described (561). A mitochondrial fraction was additionally collected in experiments assessing the influence of c-M $\beta$ CD and M $\beta$ CD. This simultaneously allowed for the clarification of previous reports regarding the potential  $\beta$ -cell-specific location of caveolin 1 and ABCG1.

The cell fraction markers GAPDH, Na<sup>+</sup>K<sup>+</sup>ATPase and Succinate Dehydrogenase Complex Subunit A (SDHA) were predominantly associated with the cytosolic, membrane and mitochondrial fractions, respectively, as expected (Figure 4.5).  $\beta$ -actin was most strongly associated with the cytosolic fraction but was also found in mitochondrial fractions and exhibited greater variability than the other cytosolic marker. This may be due to it being bound to organelles and, hence, purified with them as well as being freely soluble in the cytosol. It was deemed a less reliable marker than GAPDH, which was subsequently used as a loading control for cytosolic fractions (Figure 4.5B). In line with previous observations in primary  $\beta$ -cells (69, 564) and MIN6 cells (326) but contrary to its widely understood function in membrane caveolae formation, caveolin-1 strongly associated with cytosolic but not membrane fractions. Proteins that partitioned preferentially to the membrane fraction, along with the relevant loading control, Na<sup>+</sup>K<sup>+</sup>ATPase, included ABCA1, SUR1 and RAC1 (Figure 4.5C). ABCG1 and Glut-2 partitioned into the mitochondrial fraction with the relevant marker, SDHA (Figure 4.5A). No proteins studied were found to change significantly in abundance or cellular

compartmentalisation with M $\beta$ CD or c-M $\beta$ CD treatment, relative to the reference proteins for the fractions studied.

**Table 4.2. Summary of the influence of M $\beta$ CD (M), c-M $\beta$ CD (C), atorvastatin (A) or pravastatin (P) on BRIN-BD11 protein expression as measured by Flow Cytometry and Western Blotting (WB)**

	Protein	Full name	Function*	Expected Cell compartment localisation	Results	
					Flow cytometry	WB
Lipid homeostasis	ABCA1	ATP-binding Cassette Subfamily A Member 1	A cholesterol pump responsible for cholesterol efflux.	PM	M $\uparrow$ C $\downarrow$	M $\leftrightarrow$ C $\leftrightarrow$ A $\uparrow$ P $\leftrightarrow$
	ABCG1	ATP-binding Cassette Subfamily G Member 1	Cholesterol transporter, may work cooperatively with ABCA1 in cholesterol efflux but appears to have unique functions in $\beta$ -cells.	Mito	M - C -	M $\leftrightarrow$ C $\leftrightarrow$ A - P -
	LDLr	Low Density Lipoprotein receptor	Binds LDL, facilitating cholesterol flux into the cell.	PM	M $\leftrightarrow$ C $\downarrow$	M - C - A $\uparrow$ P $\leftrightarrow$
	SREBP2	Sterol Regulatory Element Binding Transcription Factor 2	A transcriptional activator controlling lipid synthesis including cholesterol and fatty acids and LDL receptor expression.	cyto	M $\leftrightarrow$ C $\downarrow$	M - C - A $\leftrightarrow$ P $\leftrightarrow$
Glucose homeostasis	GLUT2	Glucose Transporter Type 2, Liver	Responsible for glucose uptake in $\beta$ -cells and liver, having low glucose affinity to facilitate its function as a glucose sensor.	Mito/PM	M $\leftrightarrow$ C $\downarrow$	M $\leftrightarrow$ C $\leftrightarrow$ A $\leftrightarrow$ P $\leftrightarrow$
	GLK	Glucokinase See Ch 3, Fig. 3.7	Phosphorylates glucose to glucose-6-phosphate specifically in $\beta$ -cells and liver in the first step in the glucose metabolism.	Mito	M - C -	M - C - A $\leftrightarrow$ P $\leftrightarrow$
	Irb	Insulin Receptor $\beta$	A receptor with kinase function that binds insulin and begins the insulin signalling process.	PM	M $\leftrightarrow$ C $\downarrow$	M - C - A - P -
	INS	Insulin	A hormone that stimulates glucose uptake in responsive tissues. Increases glycogen synthesis and reduces gluconeogenesis.	cyto	M $\downarrow$ C $\downarrow$	M - C - A - P -
Insulin secretion	Cav 1.3	Voltage-Gated Calcium Channel Subunit Alpha	Mediates calcium influx in response to membrane depolarisation. Stimulates insulin exocytosis.	PM	M $\downarrow$ C $\downarrow$	M - C - A - P -
	SUR1	Sulfonylurea Receptor 1	Forms a part of the ATP-sensitive potassium channel involved in stimulating membrane potential changes that end in insulin secretion in response to changes in ATP/ADP ratio.	PM	M - C -	M $\leftrightarrow$ C $\leftrightarrow$ A $\leftrightarrow$ P $\leftrightarrow$
	VAMP2	Vesicle Associated Membrane Protein 2	A component of the docking and fusion complex between insulin granules and the plasma membrane.	PM/granules	M $\leftrightarrow$ C $\downarrow$	M - C - A - P -
	Caveolin 1	Caveolin 1	Scaffolding protein usually found in the plasma membrane but may have a different role in $\beta$ -cells.	PM (but found in cytosol here)	M - C -	M $\leftrightarrow$ C $\leftrightarrow$ A $\leftrightarrow$ P $\leftrightarrow$
Oxidative stress	HSP70	Heat Shock Protein Family A Member 4	Has a protective role in stresses such as oxidative stress.	cyto	M - C -	M - C - A $\leftrightarrow$ P $\leftrightarrow$
	iNOS	inducible Nitric Oxide Synthase	responds to stress to produce nitric oxide. Enhances synthesis of proinflammatory cytokines.	cyto	M - C -	M - C - A $\leftrightarrow$ P $\leftrightarrow$
	Cas 3	Active Caspase 3	A protease involved in apoptosis.	cyto	M - C -	M - C - A $\leftrightarrow$ P $\leftrightarrow$
Signalling	RAC1	Rac Family Small GTPase 1	Is activated by GTP binding and inactivated by GDP binding, associates with the membrane and regulates several cellular functions, including insulin secretion.	PM	M - C -	M $\leftrightarrow$ C $\leftrightarrow$ A $\leftrightarrow$ P $\leftrightarrow$
	mTOR	Mammalian Target Of Rapamycin Kinase	A kinase that regulates many cellular functions (phosphorylates at least 800 proteins) in response to signals such as stress, hormones and nutrients.	cyto	M - C -	M - C - A $\uparrow$ P $\uparrow$
	pIR	phospho Insulin Receptor	Insulin receptor that has been phosphorylated to its active form. Responsible for signal	PM	M - C -	M - C - A $\uparrow$ P $\leftrightarrow$
	pAKT	phospho AKT	A kinase with broad function, including insulin signalling.	cyto	M - C -	M - C - A $\leftrightarrow$ P $\leftrightarrow$

PM-plasma membrane, cyto-cytosolic, mito-mitochondrial, M-M $\beta$ CD, C-c-M $\beta$ CD, A-atorvastatin, P-pravastatin

- not reported  $\leftrightarrow$  no change  $\uparrow$  trend towards increase  $\uparrow$  increase (P<0.05)  $\downarrow$  decrease (P<0.05)

\*Source: <http://www.genecards.org/>

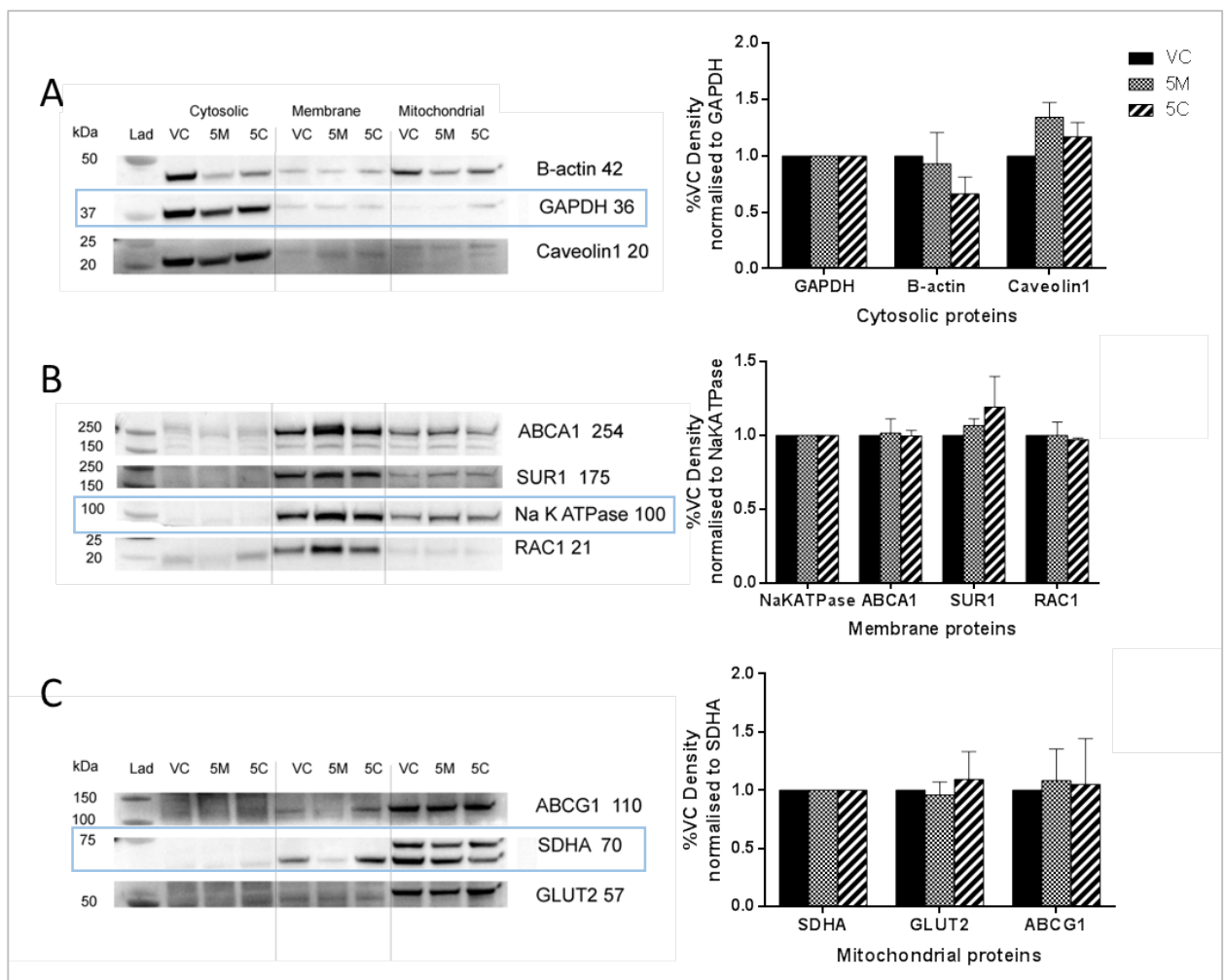


**Figure 4.5. Cellular localisation of proteins from MβCD treated cells.**

**A.** Proteins that separated with the cytosolic marker Glyceraldehyde-3-Phosphate Dehydrogenase (GAPDH) included B-actin and Caveolin1. **B.** Proteins that separated into the membrane fraction using sodium potassium ATPase ( $\text{Na}^+\text{K}^+\text{ATPase}$ ) as a marker included ABCA1, SUR1 and RAC1. **C.** Proteins that separated with the mitochondrial fraction included ABCG1 and GLUT2. Succinate Dehydrogenase Complex Subunit A (SDHA) was used as the mitochondrial marker. There was no significant difference between treatments in band density, normalised to marker proteins (rectangle) in each fraction. Representative blots are shown and graphs include densitometry data from three repeats, representing the mean  $\pm$  SEM.

Similarly to c-MβCD treatments, there were no significant changes in proteins measured in various sub-cellular fractions after pravastatin or atorvastatin treatment (Figure 4.6). However, an atorvastatin-associated trend towards increased ABCA1 was evident, though variable, with a  $68 \pm 40\%$  increase compared to control ( $P = 0.07$ ). There was also increased accumulation of membrane proteins overall with atorvastatin treatment (1 vs  $1.4 \pm 0.2$  by ANOVA, treatment effect, for control vs atorvastatin, respectively,  $P = 0.02$ ).

It cannot be ruled out that this overall increase in the membrane fraction of the atorvastatin group may be indicative of treatment-induced changes in  $\text{Na}^+\text{K}^+\text{ATPase}$  itself, which was used as a loading control.  $\text{Na}^+\text{K}^+\text{ATPase}$  has been linked with cholesterol regulation (135) and a decrease in its activity was seen in peripheral blood mononuclear cells in dyslipidemic, diabetic

humans compared to healthy controls (565), but it is not known whether this was cell specific or related to expression profiles or function only. However, similar changes were seen in RAC1 and ABCA1 in other experiments not normalised to Na<sup>+</sup>K<sup>+</sup>ATPase, so this is unlikely.

Cytosolic accumulation of Rac1 was previously noted during inhibition of prenylation (566), an effect which may be expected to occur during inhibition of cholesterol synthesis with statins. However, this was not observed in the current study.

Interestingly, ABCG1 and GLUT2, which associated strongly and almost exclusively with the mitochondrial fraction in the MβCD samples, were not detectable in the statin samples in which no mitochondrial sample was collected due to the small fraction size and lack of visibility (data not shown), confirming their exclusive location in the mitochondrial fraction.

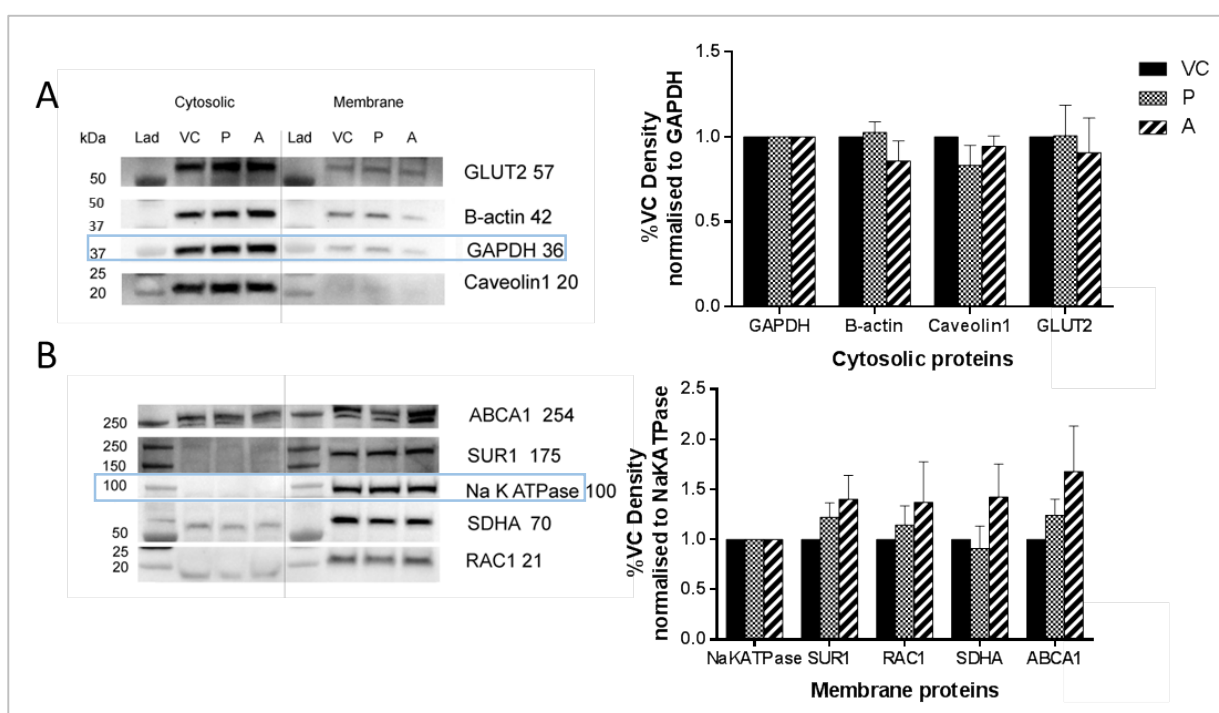


**Figure 4.6. Cellular localisation of proteins from statin-treated cells.**

**A;** Proteins that separated with the cytosolic marker Glyceraldehyde-3-Phosphate Dehydrogenase (GAPDH) included B-actin and Caveolin1. No mitochondrial fraction was retained for these samples and the light band of GLUT2 was associated mainly with the cytosolic fraction. **B;** Proteins that separated into the membrane fraction using sodium potassium ATPase (Na<sup>+</sup>K<sup>+</sup>ATPase) as a marker included ABCA1, SUR1 and RAC1. A band at approximately 60 kDa was evident after incubation with the mitochondrial marker, anti-SDHA antibody. A similar band was seen in the MβCD fractions in addition to the band representing SDHA at 70 kDa. There was no significant difference between treatments in band density, normalised to marker proteins in each fraction. However, ABCA1 displayed a tendency toward increased expression with atorvastatin treatment (P = 0.07). Representative blots are shown and graphs include densitometry data from three separate experiments. Error bars are ± SEM.



In a similar vein to the Western blot analysis, but aimed at a global perspective rather than being limited to selected proteins, iTRAQ proteomic analysis was undertaken to further study potential changes in relative abundance of proteins in response to the cholesterol sequestering or loading agents M $\beta$ CD or c-M $\beta$ CD, respectively. The opportunity to complete this study arose within a limited time frame and iTRAQ was used as a screening tool to identify proteins or functional groups of proteins which changed significantly in expression with cholesterol abundance. This data is preliminary, and further biological replicates are necessary to confirm these results. Samples were trypsin digested and labelled with iTRAQ reagents then subjected to electrospray (LC-MS/MS) mass spectrometry. Digested peptides were quantified by means of iTRAQ and identified against the SWISS-PROT protein sequence database.

To characterise the supernatant (S) and pellet (P) fractions prepared by ultracentrifugation, samples were analysed by Western blot analysis, and probed with antibodies against protein marker proteins for cytosolic (GAPDH and  $\beta$ -actin), mitochondrial (SDHA), endoplasmic reticulum (KDEL) and plasma membrane (Na<sup>+</sup>K<sup>+</sup>ATPase) proteins. All markers except KDEL showed stronger bands in the ‘S’ fraction (Figure 4.7), suggesting it contained cytosolic, plasma membrane and mitochondrial fractions. It was concluded that the ‘P’ fraction was likely to be enhanced for endoplasmic reticulum. This is in line with protocols to isolate a microsomal fraction using ultracentrifugation (567, 568), however, the omission of intermediate centrifugation steps normally present in the standard protocol led to the expectation that mitochondrial and plasma membrane components may also be constituents of the ‘P’ fraction.

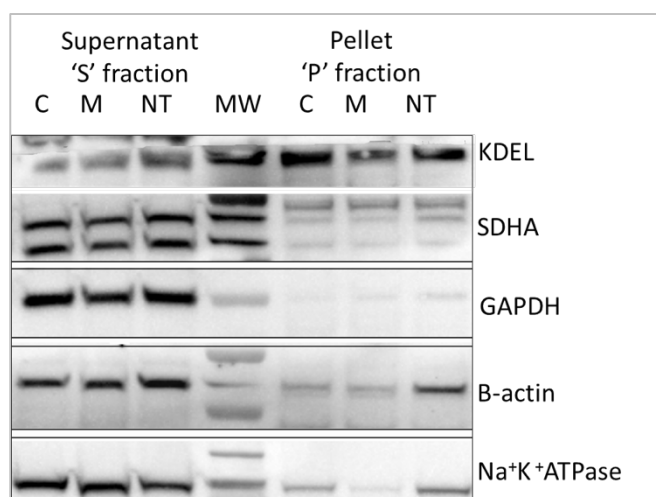


**Figure 4.7. Characterisation of iTRAQ protein samples.**

Western blot analysis showed that the pellet samples used for iTRAQ were enhanced for the endoplasmic reticulum marker (KDEL) and contained few cytosolic (GAPDH,  $\beta$ -actin) proteins. Some plasma membrane (Na<sup>+</sup>K<sup>+</sup>ATPase) and mitochondrial (SDHA) marker were present.

As mentioned above, only the ‘P’ fraction was examined by iTRAQ, which identified a total of 1049 proteins. Thirty-four were not identified in every treatment group and were not compared, leaving 1015 proteins identified in all samples at >95% confidence. Of these, 61 proteins were

significantly up- or down-regulated compared to control. However, 22 of these were found to have inconsistent results in the two non-treated controls, and were excluded from further consideration, leaving 16 and 24 differentially expressed proteins associated with M $\beta$ CD or c-M $\beta$ CD treatment, respectively, including one protein (protein disulfide-isomerase) that was up-regulated in both treatments. Figure 4.8 provides a graphic representation of differentially expressed proteins while Table 4.3 and Table 4.4 provide a summary of the names and functions of proteins with changed abundance in response to M $\beta$ CD and c-M $\beta$ CD, respectively.

Genecards ([www.genecards.org](http://www.genecards.org)) and Rat Genome Database ([rgd.mcw.edu](http://rgd.mcw.edu)) were searched to identify the function of differentially expressed proteins, which were then classified into 8 functional categories as listed in Tables 4.2 and 4.3 and Figure 4.8. Overall, more proteins related to protein synthesis were up- or down-regulated compared to other categories. These included 5 and 2 that were found to be more, or less, abundant, respectively, after M $\beta$ CD treatment, and 3 and 7 found to be more, or less abundant, respectively, after c-M $\beta$ CD treatment.

The second largest functional category in the 'P' fraction affected by c-M $\beta$ CD or M $\beta$ CD was comprised of six proteins involved in metabolism, including  $\beta$ -oxidation. These are usually found in the mitochondria or cytosol, and were all down-regulated except for LDHA, which was up-regulated in the c-M $\beta$ CD group. In addition, 3 stress-related proteins usually found in the ER or mitochondria were up-regulated, while 4 transport related, 2 signalling and 1 structural protein were also affected, some by up- and others by down-regulation.

Two proteins were placed in the 'other' category, including a zinc finger domain protein for which there is little information on specific function, and ectonucleotide pyrophosphatase/phosphodiesterase 1, a transmembrane enzyme found in the plasma membrane and the endoplasmic reticulum that hydrolyses ATP and other nucleosides and may have a role in the modulation of insulin sensitivity and function (<http://www.genecards.org/>, Weizmann Institute). Interestingly, it is elevated in people who are insulin resistant and in obesity, and translocates rapidly to the plasma membrane from intracellular sites in the presence of insulin (569). It was upregulated in association with c-M $\beta$ CD treatment.

Of the 12 proteins investigated by Western blot in this chapter, five were also detected by iTRAQ analysis, including the cytosolic, plasma membrane and mitochondrial fraction markers GAPDH, Na<sup>+</sup>K<sup>+</sup>ATPase and SDHA respectively, and the signalling proteins mTOR and RAC1. The granule fusion proteins SNAP-25 and VAMP2 were also identified by iTRAQ, along with the LDLr. None of these were found to be significantly up- or down-regulated by the cyclodextrin treatments used, at least in the 'P' fraction examined. Marker proteins are considered to have stable expression, and as expected, no change was discerned. However, the iTRAQ results confirm their presence in BRIN-BD11 lysates from the 'P' fraction. As found in

the Western blot results, RAC1 was also unaffected by M $\beta$ CD and c-M $\beta$ CD treatments. Detection of the monocarboxylate transporter 1 and LDHA in BRIN-BD11 cell lysates is interesting, given that expression of these proteins is usually strongly repressed in primary  $\beta$ -cells (see Section 1.4.1). Also of interest is the downregulation by 2.5-fold ( $P < 0.01$ ) of hexokinase II in association with M $\beta$ CD treatment. Hexokinases other than glucokinase (hexokinase IV) are likewise repressed in primary  $\beta$ -cells as discussed in Section 1.4.1. However, BRIN-BD11 cells do express some normally repressed proteins due to their origin, being transformed cells with some tumour-like phenotypic adaptations. An effect on hexokinases, albeit in the opposite direction, was earlier found in association with atorvastatin treatment, where hexokinase I was upregulated while hexokinase II was not affected (Section 3.4.4), and such changes have the capacity to alter stimulus-secretion coupling.

Several caveats apply to this iTRAQ data. Only one experiment was conducted, and the results therefore need further validation; the value of running replicates has been stressed in a recent study (563). In addition, the opportunity to conduct this experiment was time-restricted and characterisation of prepared cell fractions followed rather than preceded iTRAQ analysis. Consequently, the fraction analysed did not meet expectations in terms of plasma membrane content. Further, it would be expected that some cholesterol-related changes in protein expression may be in opposite directions with cholesterol loading and depletion, but this was not the case.

In accordance with the higher impact of c-M $\beta$ CD treatment on insulin secretion reported in Chapter 2, more proteins were differentially expressed after cholesterol loading than depletion, and several pathways involved in metabolism and insulin secretion were up or down-regulated or displaced. The full report is included in Appendix B.

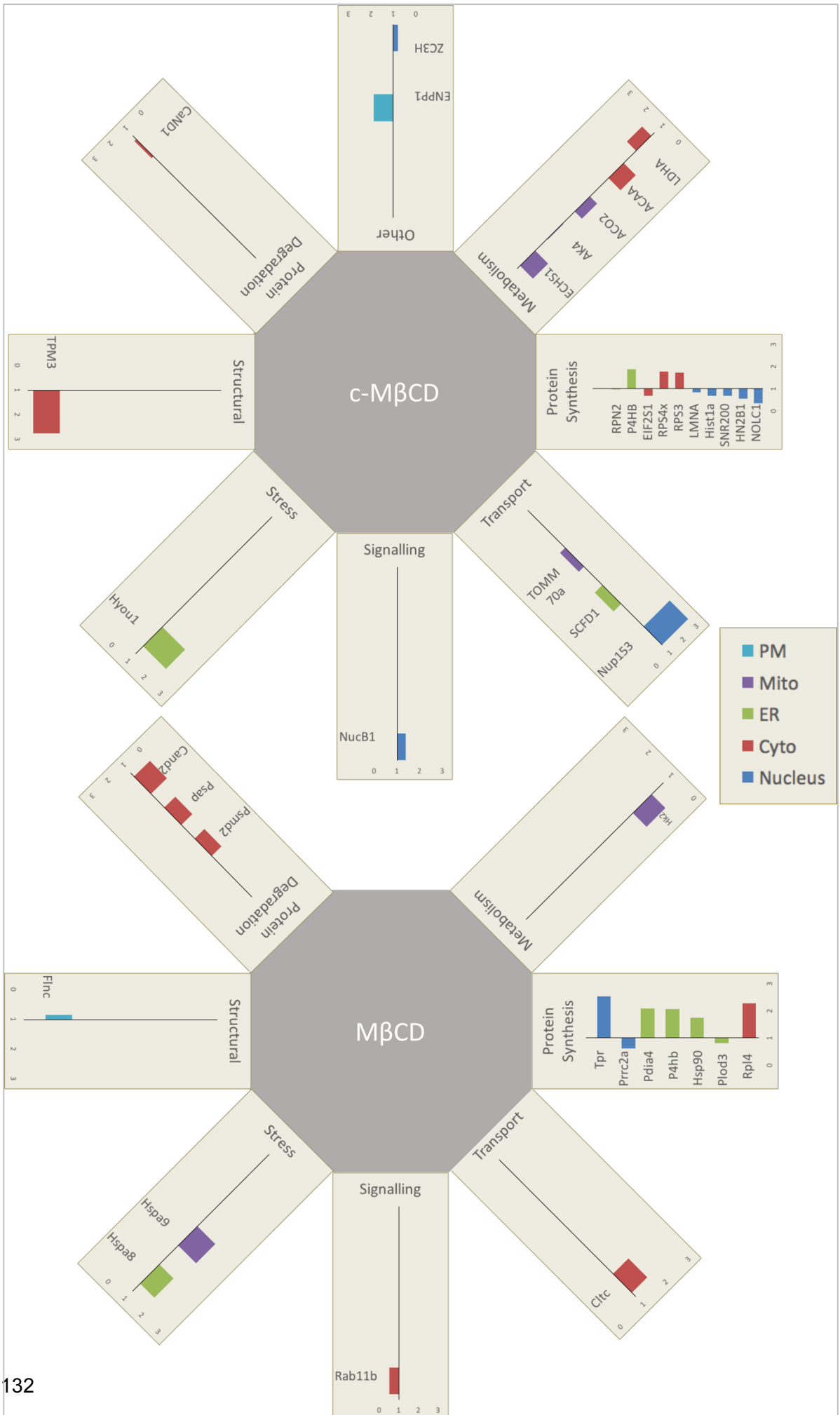


**Figure 4.8. iTRAQ analysis of 'P' fractions from BRIN-BD11 cells treated with M $\beta$ CD or c-M $\beta$ CD.**

The figure is arranged by functional categories of proteins found to be significantly up- or down-regulated ( $P < 0.05$ ). Bars are colour-coded according to the cell compartment to which the reported protein is usually recruited and height signifies the degree of variation from control. Bars to the right of the axes show up-regulation and those to the left, down-regulation. A value of 1.0 (and location of the x-axis) represents no change,  $> 1.0$  represents upregulation, and  $< 1.0$ , downregulation. **Table 4.3** (M $\beta$ CD) and **Table 4.4** (c-M $\beta$ CD), containing full names and a brief description of the function of all proteins included in this figure can be found below.

**Table 4.3. Proteins from 'P' fractions after M $\beta$ CD treatment.**

M $\beta$ CD-associated protein abundance changes						
	Protein	Full name	*Function	Expected localisation	Changes with treatment	
					UP	DOWN
Protein Synthesis	Rpl4	60S ribosomal protein L4	Ribosomal protein involved in mRNA translation	Cyto	2.27	
	Plod3	Procollagen-lysine,2-oxoglutarate 5-dioxygenase 3	Catalyses the synthesis of attachment sites for carbohydrates in collagen - intermolecular crosslinks/stability	ER		0.80
	Hsp90b1	Endoplasmic	Molecular chaperone/ protein folding. Associated with pathogenic states.	ER	1.74	
	P4HB	Protein disulfide-isomerase	Forms/rearranges disulfide bonds. Also participates in ER-associated degradation pathway	ER	2.05	
	Pdia4	Protein disulfide-isomerase A4	Protein folding and thiol-disulfide interchange. Antibody assembly, insulin secretion.	ER	2.07	
	Prrc2a	Protein PRRC2A	Associated with $\beta$ -cell destruction in T1DM.	Nucleus, Cyto, PM		0.61
	Tpr	Nucleoprotein TPR	Transport and quality control of mRNA	Nucleus	2.51	
Protein Degradation	Psm2	26S proteasome non-ATPase regulatory subunit 2	ATP-dependent degradation of ubiquitinated proteins, and is involved in TNF signalling.	Cyto		0.41
	Cand2	Cullin-associated NEDD8-dissociated protein 2	Assembles ubiquitin ligase complexes	Cyto, nucleus		0.01
	Psap	Prosaposin	Cleaved to generate saposins A-D, involved in the lysosomal degradation of sphingolipids	Cyto		0.31
Metabolism	Hk2	Hexokinase-2	Insulin responsive glucose kinase	Mito		0.40
Stress	Hspa8	Heat shock cognate 71 kDa protein	Protein quality control, chaperone and protection of the proteome from stress	ER	1.85	
	Hspa9	Stress-70 protein, mitochondrial	Cell proliferation, stress response and mitochondrial maintenance	Mito	2.07	
Signalling	Rab11b	Ras-related protein Rab-11B	regulating exocytotic and endocytotic pathways including membrane recruitment, recycling of transmembrane proteins such as Ca and K channels and possibly insulin granule exocytosis.	Cyto		0.51
Structural	Finc	Filamin-C	Crosslinks actin filaments and membrane protein anchoring. May reorganise the cytoskeleton during signalling events.	PM		0.84
Transport	Cltc	Clathrin heavy chain 1	Intracellular trafficking of receptors and endocytosis of a variety of macromolecules. Involved in early autophagosome formation.	Cyto	1.69	
PM-Plasma Membrane, Cyto-Cytosolic, Mito-Mitochondrial, ER-Endoplasmic Reticulum						
*Source: <a href="http://www.genecards.org/">http://www.genecards.org/</a>			$\gg P < 0.05$ for all measures			

**Table 4.4. Proteins from 'P' fractions after c-M $\beta$ CD treatment.**

c-M $\beta$ CD-associated protein abundance changes						
	Protein	Full name	*Function	Expected Cell compartment localisation	Changes with treatment	
					UP	DOWN
Protein Synthesis	RPS3	40S ribosomal protein S3	Initiation of mRNA translation. Also involved in UV-induced DNA damage repair	Cyto	1.7061	
	RPS4x	40S ribosomal protein S4, X isoform	Catalyses protein synthesis	Cyto	1.7701	
	EIF2S1	Eukaryotic translation initiation factor 2 subunit 1	Promotes the binding of the initiator tRNA to the ribosome	Cyto		0.6668
	P4HB	Protein disulfide-isomerase	Forms/rearranges disulfide bonds.	ER	1.8535	
	RPN2	Dolichyl-diphosphooligosaccharide--protein glycosyltransferase subunit 2	Links mannose oligosaccharides to asparagine residues in newly synthesised polypeptides.	ER		0.955
	NOLC1	Nucleolar and coiled-body phosphoprotein 1	Regulates RNA polymerase I by the linking of ribosomal enzymes	Nucleus		0.3373
	HN2B1	Heterogeneous nuclear ribonucleoproteins A2/B1	Sorting, regulating and packaging pre-mRNAs.	Nucleus		0.5395
	SNR200	U5 small nuclear ribonucleoprotein 200 kDa helicase	Pre-mRNA splicing and spliceosome formation.	Nucleus		0.6607
	Hist1a	Histone H1.1	Necessary for the organisation of chromosomes in chromatin. Regulates gene transcription through DNA methylation.	Nucleus		0.673
	LMNA	Prelamin-A/C	Nuclear stability and gene expression. Protective fibrous layer on nuclear membrane. Implicated in premature senescence.	Nucleus		0.8241
Protein Degradation	CaND1	Cullin-associated NEDD8-dissociated protein 1	Regulates (inhibitory) ubiquitinylation of proteins destined for degradation by the ubiquitin proteasome system.	Cyto	1.1272	
Metabolism	LDHA	L-lactate dehydrogenase A chain	Catalyzes the final step in anaerobic glycolysis, the conversion of L-lactate and NAD to pyruvate and NADH.	Cyto	1.5704	
	ACAA	3-ketoacyl-CoA thiolase A, peroxisomal	Involved in $\beta$ -oxidation in peroxisomes.	cyto		0.2655
	ACO2	Aconitate hydratase, mitochondrial	An enzyme in the TCA cycle.	Mito		0.5598
	AK4	Adenylate kinase 4, mitochondrial	Homeostasis of adenine nucleotide ratios.	Mito		0.9727
	ECHS1	Enoyl-CoA hydratase, mitochondrial	An enzyme in the mitochondrial fatty acid $\beta$ -oxidation pathway	Mito		0.2228
Stress	Hyou1	Hypoxia up-regulated protein 1	Has a cytoprotective role in hypoxia and is induced by stress. Involved in protein folding and secretion.	ER	2.3988	
Signalling	NucB1	Nucleobindin-1	Involved in Golgi calcium homeostasis and calcium signalling.	Nucleus	1.3677	
Structural	TPM3	Tropomyosin alpha-3 chain	Stabilises actin filaments in the cytoskeleton.	Cyto	2.7542	
Transport	SCFD1	Sec1 family domain-containing protein 1	Has a role in vesicle-based transport between the ER and Golgi.	ER		0.413
	TOMM70a	Mitochondrial import receptor subunit TOM70	Imports mitochondrial precursor proteins.	Mito		0.5916
	Nup153	Nuclear pore complex protein Nup153	A component of the nuclear pore complex that facilitates transport across the nuclear membrane.	Nucleus	2.9376	
Other	ZC3H	Zinc finger CCCH domain-containing protein 18	Function unknown.			0.7798
	ENPP1	Ectonucleotide pyrophosphatase/phosphodiesterase family member 1	Hydrolyzes ATP and other nucleosides. Is thought to modulate insulin sensitivity and function.	ER, PM	1.8535	

PM-Plasma Membrane, Cyto-Cytosolic, Mito-Mitochondrial, ER-Endoplasmic Reticulum

\*Source: <http://www.genecards.org/>

$\geq P < 0.05$  for all measures

### 4.3.3 The influence of M $\beta$ CD, c-M $\beta$ CD and atorvastatin on physical characteristics of BRIN-BD11 cells

Flow cytometry has several advantages over Western blotting due to its ability to interrogate single, whole cells as opposed to lysates. During preliminary flow cytometry work, an observation was made that treatments appeared to affect certain physical characteristics of cells. To examine this further, BRIN-BD11 cells treated with c-M $\beta$ CD, M $\beta$ CD or atorvastatin were assessed for changes in size, complexity and autofluorescence. The parameters of forward scatter (FSC), side scatter (SSC) and autofluorescence in the violet range (V525/50), respectively, were used to this end. Changes due to cell death or temperature variations were eliminated by excluding cells that stained positively for ZombieNIR™, which is only taken up by dead cells, and by fixing in 0.5% paraformaldehyde, respectively. The gating hierarchy used in all flow cytometry experiments is illustrated in Figure 4.3.

Autofluorescence excited by the violet laser (excitation 405 nm, emission detected at 525/50 nm) was found to correlate positively with insulin content assessed using insulin targeted antibodies. A small population of viable cells with low insulin content was consistently observed (12-20%), and these were excluded by gating for high autofluorescence in conjunction with appropriate fluorescence from ZombieNIR™. While the source of autofluorescence was not investigated in these studies, previous findings have linked autofluorescence in certain wavelengths to metabolic processes<sup>1</sup>. Data was collected across all channels and autofluorescence was found to be highest in the violet 525/50 channel. A viable cell population known to be positive for insulin content was subsequently assessed.

To be sure that only functional  $\beta$ -cells were included in the analysis, a combination of signals for cellular autofluorescence and ZombieNIR™ collected in the V(525/50) and R(780/60) channels, respectively, enabled an insulin-positive population to be predicted even in the absence of insulin staining, and this was verified by insulin staining. Figure 4.9 demonstrates the correlation between autofluorescence and insulin positive cells, and provides examples of typical populations treated or not with M $\beta$ CD or c-M $\beta$ CD.

---

<sup>1</sup> It has long been understood that metabolic processes, particularly those relating to production of NADH and NADPH are associated with autofluorescence (reviewed in (570)). Intrinsic fluorescence from these two molecules is identical, with absorption and emission peaks at 340 and 460 nm, respectively. Being indistinguishable, fluorescence arising from both molecules is termed NAD(P)H and recognised as the sum of fluorescence from both sources. In addition, the cellular electron transporter flavine adenine dinucleotide (FAD) has also been recognised as an intrinsic source of fluorescence (571). It is typically excited at 488 nm and emits between 510 and 550 nm. Protocols have been published to use autofluorescence to monitor the redox state of cells and tissue, including islets (572) and to distinguish  $\beta$ -cells from other cells in dispersed islets using flow cytometry (455, 571, 573). A method has even been devised to distinguish between NADH and NADPH as fluorescence sources in  $\beta$ -cells using 2-photon and confocal imaging, by exploiting the metabolic uniqueness of  $\beta$ -cells that prevents the use of exogenous pyruvate as ATP fuels (574, 575).

Autofluorescence was assessed using cells included in the ‘live singlets’ (LS) gate, while the ‘viable’ population was assessed for size and complexity. The reduced autofluorescence of c-M $\beta$ CD-treated cells meant that fewer cells selected as singlets were included in the ‘viable’ population, with  $42 \pm 6\%$  of the parent population compared to  $54 \pm 1\%$  and  $69 \pm 2\%$  for C, M and NT (controls), respectively, (mean  $\pm$  SD,  $P < 0.0001$  for all comparisons). Cholesterol sequestration from cell membranes using a 30 min, 5 mM M $\beta$ CD treatment was associated with a small but significant increase in autofluorescence (1.06-fold increase,  $P < 0.05$ ), forward scatter (FSC, 1.03-fold increase,  $P < 0.001$ ) representing size, and side scatter (SSC) representing cell complexity (1.06-fold increase,  $P < 0.001$ ) (Figure 4.10). In contrast, when cholesterol was loaded into cells using c-M $\beta$ CD treatment under equivalent conditions, larger scale changes were seen in all parameters measured. These included decreases in autofluorescence (1.7-fold decrease,  $P < 0.001$ ) and complexity (1.5-fold decrease,  $P < 0.001$ ) and an increase in cell size (1.12-fold increase,  $P < 0.001$ ).  $\beta$ -cells treated with c-M $\beta$ CD exhibited two peaks in autofluorescence in the LS population, both with lower median fluorescence intensity than other cells, which all displayed one peak.

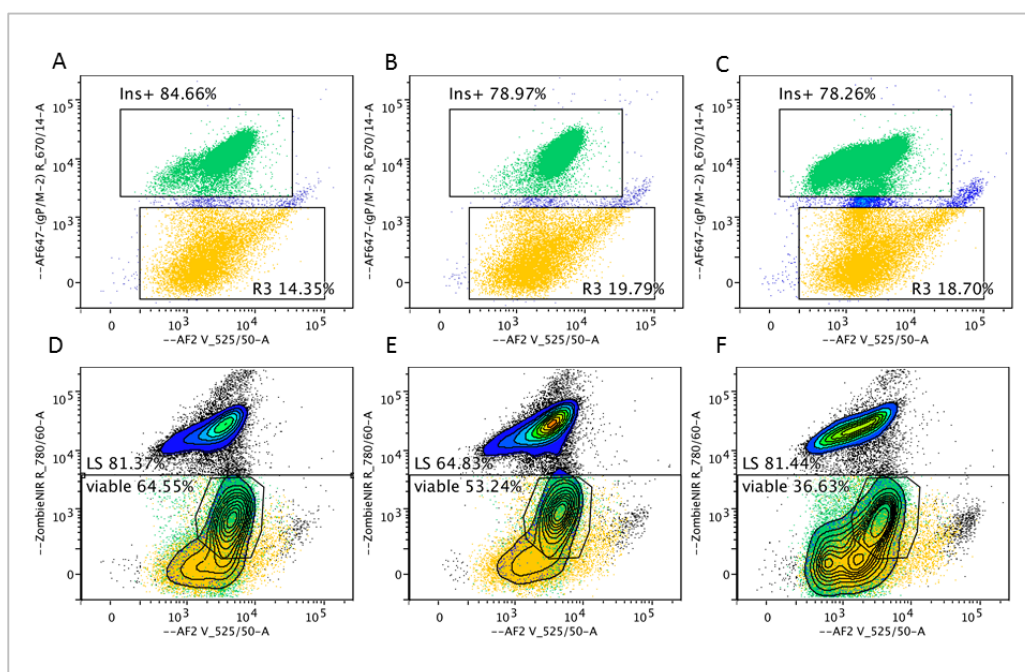


**Figure 4.9. Autofluorescent characteristics of BRIN-BD11 cells aids in differentiating insulin positive and negative cells.**

**A-C:** Insulin positive (green) and negative (yellow) cells are shown in the live singlet (LS) population and **(D-F)** back-gated in the singlets population, which also shows dead cells (blue). They can be reasonably well differentiated independently of insulin staining in a dot plot recording fluorescence from live/dead stain (ZombieNIR™) uptake vs autofluorescence (AF) in the violet V(525/50) channel. **A,D:** Insulin positive cells (green, shown in the LS population in A) tended towards the centre of a ZombieNIR™ vs autofluorescence dot plot in control cells (D), and in M $\beta$ CD-treated cholesterol depleted cells (**B,E**). c-M $\beta$ CD-treated, cholesterol loaded cells (**C,F**) exhibited reduced autofluorescence (see also **Figure 4.10**), and insulin-positive cells were spread through a wider range in the ZombieNIR™ vs AF plot. Regardless, an insulin-positive population fell nicely within the ‘viable’ gate, a subset of the ‘live singlet’ (LS) population based on these two parameters.



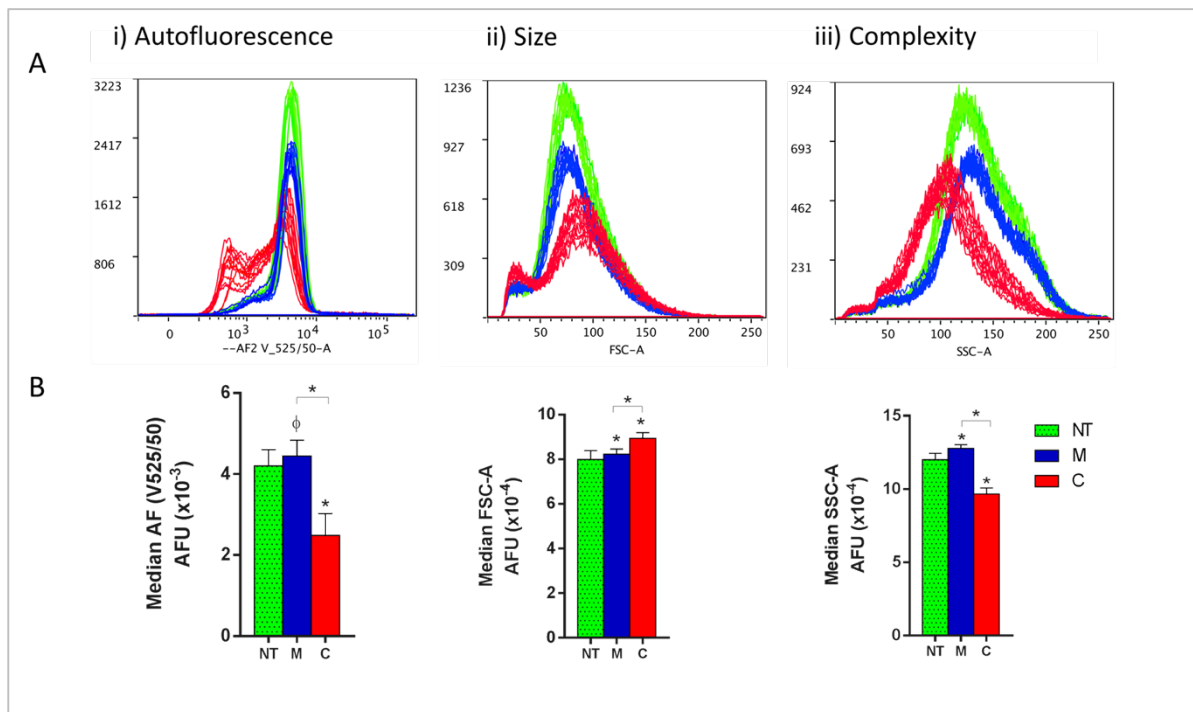


**Figure 4.10. Changes in physical characteristics of BRIN-BD11 cells associated with M $\beta$ CD treatment.**

**A:** Histograms of representative samples showing **i)** autofluorescence in the violet channel (V525, bandwidth 50), LS population; **ii)** forward scatter – area (FSC-A) representing cell size of viable cells; and **iii)** side scatter – area (SSC-A) indicating the degree of complexity of viable cells. **B:** Data for the graphs was compiled from 4 individual experiments (9-12 samples containing > 40,000 cells per condition per experiment). Scale on the bar graph y-axis is **i)**  $\times 10^{-3}$ , **ii)** and **iii)**  $\times 10^{-4}$  arbitrary fluorescent units. NT, no treatment; M, M $\beta$ CD; C, c-M $\beta$ CD. Results in the graphs represent the mean  $\pm$  SEM.  $\Phi$   $P < 0.05$ , \*  $P < 0.001$

Inhibition of cholesterol synthesis by 24 h atorvastatin treatment (10  $\mu$ M) exhibited some similarities to M $\beta$ CD-mediated cholesterol sequestration, including increased autofluorescence of LS-gated cells ( $P < 0.001$  and  $P < 0.0001$  compared to vehicle control and no treatment, respectively; 12 samples per group, each with > 40,000 events in the LS gate, in one experiment). Again similarly to M $\beta$ CD, both cell size measured by FSC and complexity measured by SSC were also significantly increased by atorvastatin ( $P < 0.0001$  compared to both vehicle control (VC) and no treatment (NT)) (Figure 4.11 (ii & iii)). Compared to NT, VC slightly but significantly decreased complexity ( $P < 0.001$ , Figure 4.11 (iii)). The number of cells selected in the ‘viable’ gate from the ‘singlets’ gate was  $47 \pm 1\%$ ,  $68 \pm 2\%$  and  $74 \pm 2\%$  (mean  $\pm$  SD) for atorvastatin, VC and NT respectively, ( $P < 0.0001$  for all comparisons, not shown). This was almost entirely due to increased permeability to ZombieNIR<sup>TM</sup> stain, demonstrating a decline in viability with atorvastatin treatment. An increase in apoptosis is usually associated with a decrease in size (FSC) and an increase in complexity (SSC) (576), therefore apoptosis is unlikely to explain the increase in complexity observed in atorvastatin treated cells.

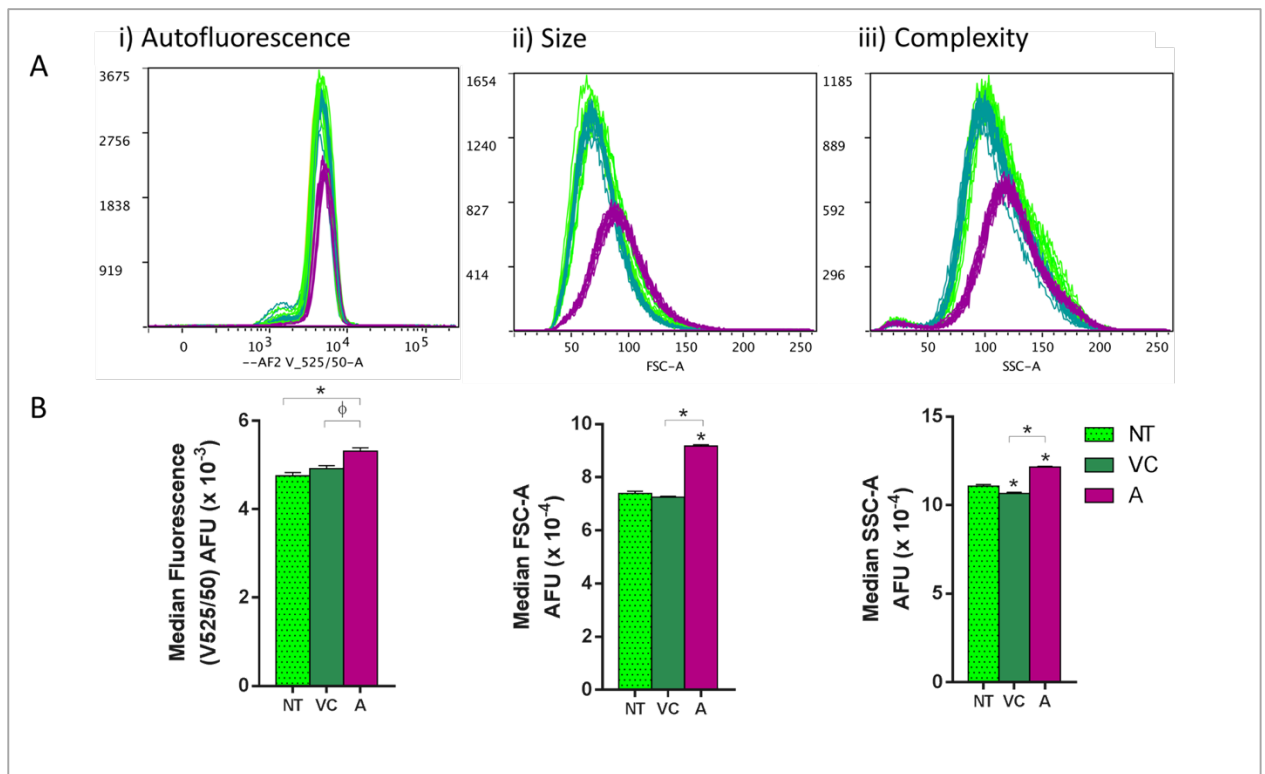


**Figure 4.11. Changes in physical characteristics of BRIN-BD11 cells associated with atorvastatin treatment.**

**A:** Histograms showing i) autofluorescence in the violet channel (V525, bandwidth 50), ii) forward scatter (area) representing cell size of viable cells, and iii) side scatter (area) indicating the degree of complexity of viable cells. Note there were fewer cells in the atorvastatin group (cerise) due to reduced viability. **B:** Median fluorescence (data from one experiment, 12 samples per condition, > 40,000 events per sample). Scale on the y-axis is i)  $\times 10^{-3}$ , ii) and iii)  $\times 10^{-4}$  arbitrary fluorescent units (ABU). NT, no treatment; VC, vehicle control; A, 10  $\mu$ M atorvastatin. Results in the graphs represent the mean  $\pm$  SEM. \*  $P < 0.001$

#### 4.3.4 Flow cytometric analysis of the effects of c-M $\beta$ CD and M $\beta$ CD on selected proteins

Flow cytometry was used to investigate the effects of short, cholesterol-manipulating M $\beta$ CD and c-M $\beta$ CD treatments on selected proteins related to lipid and glucose homeostasis and insulin secretion. While more often used to detect cell surface targets, saponin-based permeabilisation protocols allow successful interrogation of intracellular and even intra-nuclear targets (577). Hence flow cytometry was used in a similar way to Western blot analysis, though different target proteins were assessed, mainly due to time and technical constraints.

Isotype controls and secondary antibodies alone were used to ensure specificity of binding (Figure 4.12). An antibody raised in rabbit against LYVE1, a protein not expressed in  $\beta$ -cells, was used in place of the rabbit isotype control, which showed high non-specific binding. Other isotype controls confirmed acceptable specificity at relevant concentrations.

Antibodies were used against proteins involved in lipid homeostasis (ABCA1, LDLr, SREBP2), glucose homeostasis (GLUT2, IRb, GLK and INS) and insulin exocytosis (Cav1.3, VAMP2). For a summary of the function of these and other proteins used in this chapter, see Table 4.2. Details of antibodies are listed in Table 4.1.

The treatment associated with the greatest overall changes in BRIN-BD11 cells was c-M $\beta$ CD, with fewer effects accompanying M $\beta$ CD and atorvastatin treatment (Figure 4.13). There was a significant reduction in immunostaining intensity for all aforementioned protein targets with c-M $\beta$ CD treatment. In contrast, only insulin and calcium channel (Cav1.3) immunostaining was reduced in response to M $\beta$ CD treatment ( $P < 0.01$  and  $P < 0.001$ , respectively). These results correspond with the scale of adverse effects on maximal insulin secretion of c-M $\beta$ CD (substantial) compared to M $\beta$ CD (minimal) reported in Chapter 2, however, there is reason to suspect artefactual interference, as the uniformity of changes across all targets in the c-M $\beta$ CD group is unexpected and may be due to technical artefacts accompanying cholesterol loading as discussed below.

Potential explanations for generalised reduced fluorescence in c-M $\beta$ CD treated cells include a) permeabilisation failure, b) decreased epitope expression, c) decreased receptor binding or d) an influence of cholesterol to block fluorescence from intracellular targets. Possibility a) would be expected to similarly affect both c-M $\beta$ CD and M $\beta$ CD results, which was not the case, making it less likely. Possibility b) is unlikely due to discrepancies between flow cytometry and WB results, although access to epitopes may be affected by cholesterol abundance, and may be related to possibility c). Indeed, decreased I-R immunostaining associated with c-M $\beta$ CD is concordant with results from insulin/insulin receptor binding studies previously performed in our laboratory (457). This was observed not only in a variety of cells but also in virus-like particles, a cell membrane model, possibly explained by cholesterol-associated changes in membrane structure limiting accessibility to relevant epitopes. Autofluorescence data was collected in the violet channel, unlike the immunostaining data, and would not influence other results.

The best consensus with observations is thus the possibility that cholesterol is associated with interference of intracellular fluorescence signals (see d) above), given that it can also explain both reduced immuno- and auto- fluorescence. The use of forward scatter (FSC) and side scatter (SSC) to estimate cell size and complexity has been well described (578) and is commonly used for these parameters. However, it is well-known that scatter measurements can be affected by differences in the refractive index of liquids, cells and particles as well as by cellular constituents. There is little information available on the effect of changes in cellular cholesterol abundance on light scatter such as is collected in flow cytometry analysis or whether it may change the refractive or fluorescent characteristics of cells or cell particles. Interestingly,

in tissue clearing experiments for 3-dimensional confocal microscopy, lipid-rich regions were found to remain opaque, indicating higher refraction of light (579). Cholesterol-related ‘opacity’ could potentially reduce autofluorescence and side-scatter, at the same time increasing forward-scatter. Though this aspect is beyond the scope of the present study, the possibility that this could account for some of the changes observed, particularly with c-M $\beta$ CD treatment, should be acknowledged.

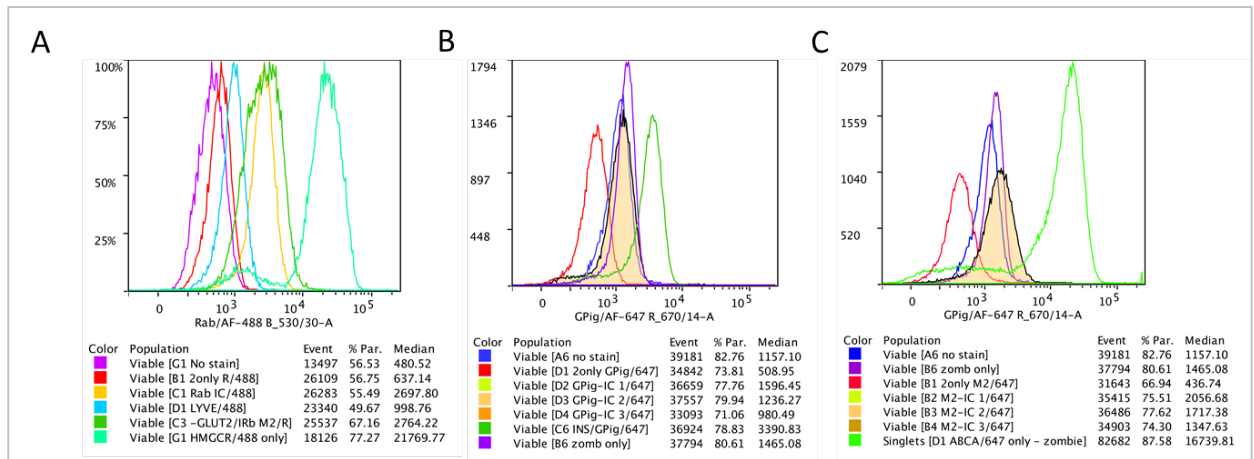
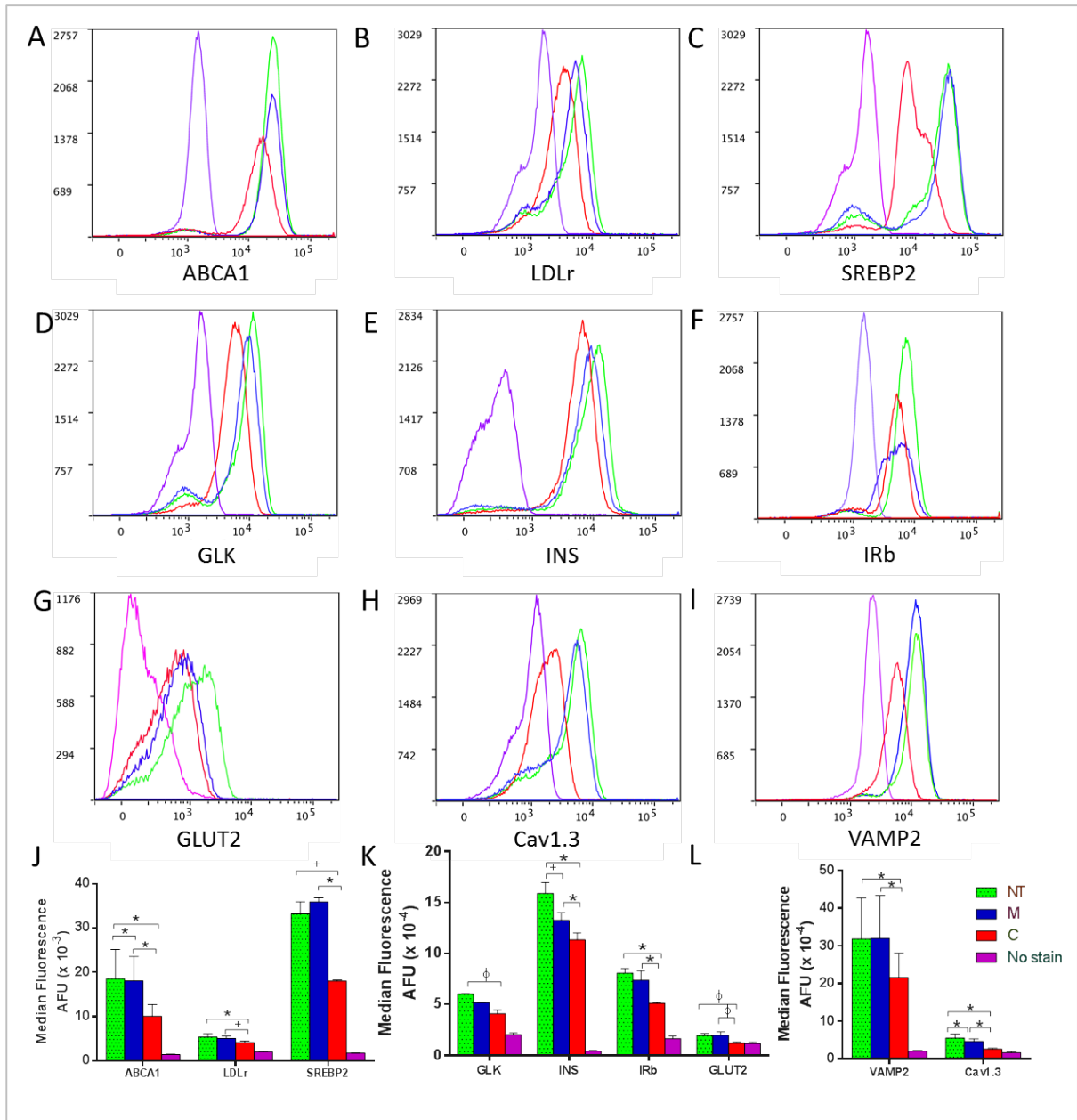


**Figure 4.12. Isotype controls for flow cytometry.**

**A.** Secondary antibodies to rabbit immunoglobulin (Ig) G conjugated to Alexa Fluor 488: There was high non-specific binding with the rabbit isotype control (yellow). Specificity was established for our rabbit antibodies by using a primary antibody to a cell marker known to be absent in pancreatic  $\beta$ -cells (anti LYVE, turquoise). Bright and pale green plots represent low (Glut-2) and high (HMGCR) fluorescence from rabbit positive antibodies, respectively. Secondary antibodies to guinea pig IgG (**B**) and Mouse IgG isotype 2 (**C**), both conjugated to Alexa Fluor 647, demonstrated specificity to isotype control (highlighted) at a concentration equivalent to primary antibodies used. Controls for tests include no stain (dark blue) ZombieNIR™ only (cerise) and secondary only (red). Green shows an appropriate positive control.



## 4.4 Discussion

Lipids are known to influence exocytotic processes including insulin secretion (64, 331). Among the many lipids, cholesterol is thought to be singularly important due to its influence on biophysical characteristics of the cell membrane (333, 425), including characteristics such as negative curvature (73), rigidity, fluidity, and membrane thickness and permeability (580). Consequently, cholesterol is required for normal secretion and its depletion or absence inhibits secretory processes. On the other hand, an accumulation of cholesterol can also be detrimental to secretion, including that of insulin (343). However, its exact role in insulin secretion and the influence of changes in cholesterol on insulin secretion are not yet clear.

In this hypothesis-generating chapter, evidence of the effect of cholesterol-modifying treatments on BRIN-BD11 cell proteins was sought. Selected proteins having functional significance in  $\beta$ -cells were assessed by Western blot and flow cytometry for changes in expression and/or cell compartment localisation to further understand the role of cholesterol disturbance in insulin secretion. In addition, a proteomics technique allowed a more general, albeit preliminary evaluation of protein abundance changes. A series of testable hypotheses informed by results in this and previous chapters have been generated to establish further lines of investigation into the role of cholesterol in  $\beta$ -cell function and insulin secretion. Table 4.2 summarises the function of specific proteins to highlight their relevance to this study and includes Western blot and flow cytometry results.

### 4.4.1 The influence of cholesterol manipulation on protein localisation

A commonly recognised role of cholesterol within cell membranes relates to the organisation of membrane proteins into specific domains. Displacement of proteins to different cellular compartments or laterally into or out of lipid raft domains (61, 69, 557, 581) or failure to translocate on a physiological stimulus (582) can cause dysfunction. In addition, products of mevalonate pathway intermediates (e.g. farnesyl pyrophosphate and geranylgeranyl pyrophosphate) are involved in the membrane localisation and stabilisation of some proteins. For example, prenylation is required for the signalling activity of small G-proteins such as Rac1 (559, 560). Insulin granule size and docking is also affected by cholesterol accumulation (336). In this project, several methods were used to gather information regarding the effect of cholesterol on the expression and cellular localisation of specific proteins and a snapshot of proteomic changes that occurred within a selected cellular fraction after M $\beta$ CD or c-M $\beta$ CD treatment was provided by iTRAQ data.

Pancreatic  $\beta$ -cells appear to be unique in the cellular localisation of two proteins investigated, caveolin 1 and ABCG1. Western blot analysis of subcellular fractions indicated that these proteins separated with the cytosolic and mitochondrial markers, respectively.

Caveolin-1 is known to participate in cholesterol binding and the formation of caveolae on plasma membrane surfaces in other cells, but its absence from the membrane fraction suggests its role in  $\beta$ -cells may be unique. Instead, caveolin-1 separated with the cytoplasmic markers GAPDH and  $\beta$ -actin. This is consistent with its involvement in insulin receptor trafficking in the presence of insulin, contributing to autocrine insulin signalling (564). It has also been implicated in IL-1 $\beta$ -induced nitric oxide release (583), prevention of inappropriate insulin release (326, 584) and intracellular cholesterol homeostasis (329).

Rac1, SUR1 and ABCA1 separated with the membrane marker, Na<sup>+</sup>K<sup>+</sup>ATPase, as expected, and GLUT2 and ABCG1 were associated with the mitochondrial marker, SDHA. While the function of ABCG1 in  $\beta$ -cells is not well understood, in macrophages (340) and endothelial cells (585) it is involved in cholesterol efflux to HDL particles. In the former it also has a role in trans-cellular transport of cholesterol (586). Its cellular location is disputed (97), with some studies citing evidence of its location at the plasma membrane (420, 587) and others finding it to be absent from the latter, rather having an intracellular function and location (588). Völgyi *et al* (589) identified ABCG1 in mitochondrial-associated endoplasmic reticulum membrane fractions in mouse cerebral cortex tissue<sup>1</sup>, which agrees with the location revealed in this study. However, in MIN6 and primary mouse  $\beta$ -cells, ABCG1 was found to be localised primarily to insulin granules (342). Sturek *et al* (342) demonstrated that insulin granule morphology was changed, granule cholesterol content reduced and insulin secretion attenuated in the absence of ABCG1 in  $\beta$ -cells, consistent with evidence of a role in the synthesis of insulin granules (72). Insulin granules are expected to be located in the post-mitochondrial supernatant (590), equating with the cytosolic fraction in the protocol used in the current study. However, a longer, faster centrifugation protocol employed in the current study may mean the insulin granules separated with the mitochondrial fraction. Regardless, the localisation debate continues, potentially partly due to cell-type specificity in the function and localisation of this sterol transporter. It would be helpful to probe for ABCG1 in similarly prepared fractions from several different cell types to assess the uniqueness of its cellular localisation in  $\beta$ -cells.

No major compartment changes accompanied the cholesterol modifying treatments among the proteins examined. Some changes were evident within fractions other than the major intracellular location for a given protein, but further study would be required to assess whether this represented true localisation changes. Lateral movement into or out of lipid raft regions within membranes has been known to occur with cholesterol depletion and is thought to impact insulin secretion (69). Further study to assess this phenomenon in cholesterol loading and statin treatment would be of interest.

---

<sup>1</sup> Interestingly, it was drastically downregulated in a pre-symptomatic Alzheimer's Disease mouse model.

The results from iTRAQ proteomics demonstrated that there were more proteins with variant expression in the c-M $\beta$ CD group, with 1.4% or 2.2% of all proteins identified as having significantly different expression in M $\beta$ CD or c-M $\beta$ CD treatment groups, respectively. This suggests that cholesterol loading created greater disruption to cellular processes than cholesterol depletion and is consistent with greater disturbance in insulin secretion (Chapter 2) and mitochondrial function (Chapter 3) associated with c-M $\beta$ CD compared to M $\beta$ CD treatment.

In both treatments, the main effects seen within the 'P' fraction assessed by iTRAQ analysis appeared to include early preparation for protein synthesis, protein degradation, stress mediation, some structural impact and metabolic consequences. The greatest effect of both cholesterol loading and sequestration was within the protein synthesis functional category, with changes in 10 (3 up, 7 down) and 7 (5 up, 2 down) proteins with c-M $\beta$ CD and M $\beta$ CD treatment, respectively. These include several proteins influencing transcription and could indicate an early response towards regulatory protein synthesis. Upregulation of several heat shock proteins is a well-known response consistent with acute stress (591, 592).

To understand changes in insulin secretion with cholesterol manipulation found in Chapter 2, notice was taken of the functional categories represented by proteins affected by M $\beta$ CD or c-M $\beta$ CD treatment. Those related to stress response, regulation of protein synthesis and metabolism are potential mechanisms for disturbance of insulin secretion, with proteins involved in metabolism theoretically having the most direct affect. Interestingly, 5 proteins related to metabolic processes were affected by c-M $\beta$ CD treatment compared to one with M $\beta$ CD. The latter was associated with downregulation of hexokinase II, linked to glycolysis, and likely to support rather than diminish insulin secretion coupling (see Chapter 3). The former included downregulation of ACAA and ECHS1, proteins involved in fatty acid oxidation, aconitase 2 (an enzyme in the TCA cycle), and a very small (3%) decrease in adenylate kinase 4, involved in homeostasis of nucleotide ratios. There was also a 57% increase in LDHA, involved in anaerobic glycolysis, a prohibited pathway in  $\beta$ -cells, and reduced expression of a mitochondrial import protein (TOM70a, listed among the transport proteins).

Mitochondrial function impairment was found to be a likely factor relating intracellular cholesterol changes to insulin secretion (discussed in Chapter 3). This proteomics data supports a case for the damaging potential of c-M $\beta$ CD-associated cholesterol loading on mitochondrial function. For example, LDHA upregulated by c-M $\beta$ CD treatment is consistent with secretion-coupling dysregulation (548) and  $\beta$ -cell dedifferentiation (494). Further, aconitase 2 (ACO2) catalyses the conversion of citrate to isocitrate in the 2<sup>nd</sup> step of the TCA cycle (Genecards). Downregulation by 44% is likely to affect mitochondrial ATP production, again potentially affecting  $\beta$ -cell secretion-coupling. Downregulation of enzymes necessary for  $\beta$ -oxidation in peroxisomes (ACAA) & mitochondria (ECHS1) of ~80% could also impact on generation of



ATP from fatty acids, as could the 41% downregulation of TOM70, a protein transporter supporting mitochondrial import of precursor proteins.

Downregulation of HexII with membrane cholesterol depletion conflicted with the trend towards upregulation of Hex I, observed in association with atorvastatin treatment in Chapter 3, however the two responses may be complementary or compensatory. Also, though both treatments result in decreased total cholesterol, the mechanisms by which insulin secretion is affected may differ between the two cholesterol depletion methods. This is in concordance with the greater adverse effect of atorvastatin on insulin secretion compared to M $\beta$ CD (Chapter 2).

Flow cytometric analysis of cyclodextrin-treated BRIN-BD11 cells in the current study demonstrated significant changes in protein targets relevant to stimulus-secretion coupling after cholesterol loading but not depletion. Western blotting of a few targets in cytosolic, membrane and mitochondrial fractions in c-/M $\beta$ CD-treated cells gave little evidence of protein movement between compartments, though lateral movement in/out of rafts was not studied.

While further evidence would be required to determine how individual changes in protein expression with cholesterol manipulation affect  $\beta$ -cells, there is enough evidence to propose that *cholesterol manipulation, particularly loading, leads to some degree of protein disruption in  $\beta$ -cells, with consequences that include metabolic impairment and reduced insulin secretion. It is not clear whether this is due to organisational changes including cellular compartment changes, or rapid expression changes in response to cholesterol loading or depletion.*

#### 4.4.2 Does cholesterol flux have a role in insulin secretion?

In addition to the biophysical properties of cholesterol and its role in supporting membrane protein function, cholesterol flux itself may be important in glucose homeostasis. Studies have implicated genes whose products are involved in both efflux and influx of cholesterol, in T2D pathology (reviewed in 593).

Cholesterol influx via the low density lipoprotein receptor (LDLr) has been recognised as an important regulator of cholesterol homeostasis and may be associated with T2D risk (305, 594, 595). Upregulation of the LDL receptor is central to the mechanism by which statins reduce serum cholesterol (102, 103, 184, 186, 596, 597), although a 1.3-fold increase in  $\beta$ -cells in response to atorvastatin found in preliminary work for the current study failed to reach statistical significance ( $P = 0.19$ , not shown). SREBP2 is a key regulator of the cholesterol biosynthetic pathway and is responsible for facilitating the upregulation of LDLr and cholesterol synthetic pathways including HMGCR (594). There are two other isoforms, SREBP1a and SREBP1c which primarily regulate fatty acid synthesis (123), though the former can also control cholesterol synthesis (598).

Interestingly, familial hypercholesterolaemic patients with severely reduced LDLr-mediated cholesterol flux have a reduced risk of T2D (305). In contrast, increased cholesterol uptake during statin therapy is associated with increased T2D risk, and a hypothesis linking transmembrane cholesterol transport to T2D development has been proposed (305).

This does not contradict observations that circulating LDL concentrations may be associated with T2D risk, with high LDL being detrimental and low, beneficial. Rather, it shifts the focus of potential harm from circulating cholesterol levels to cellular cholesterol levels or cholesterol transport itself. Furthermore, cholesterol efflux may also be important, particularly in the context of over-nutrition. For example, cholesterol and cholesterol ester synthesis, in addition to that of glycerol and other lipids, was found to be an important fate of glucose carbons, acting as an excess energy 'exhaust' for  $\beta$ -cells chronically stimulated with high glucose (243).

Components of the cholesterol efflux machinery such as ABCA1 have been positively associated with insulin secretion and glucose homeostasis (343, 599). Interestingly, and somewhat counterintuitively, Western blot results in the current study suggest that upregulation of ABCA1, at least in the membrane fraction, may be associated with atorvastatin treatment in stimulated  $\beta$ -cells. An increase in ABCA1 would be expected to increase cholesterol efflux through HDL (421, 600, 601), an unexpected consequence of cholesterol synthesis inhibition, but nevertheless a clinically documented phenomenon (602-604). This could possibly be due to homeostatic mechanisms, with the statin-induced increased cholesterol uptake via LDLr being countered, at least initially, by measures designed to increase efflux, such as ABCA1 upregulation: except that in the model system used here, LDL was not available. These results are contrary to a studies in macrophages in which reduced ABCA1 mRNA was associated with pravastatin treatment (605, 606). However, in the former study, Ando *et al* found that ABCA1 mRNA expression measured in mouse hepatic tissue increased with pravastatin treatment after 24 h but not 2 weeks, suggesting that the effects may be time- and tissue-dependent. Further study is necessary, including an assessment of SR-B1, SREBP2, 1a and 1c, and involving kinetic studies and various statin treatment lengths.

Studies in the literature of the effect of statins on ABCA1 and cholesterol efflux are conflicting. Although no other studies in  $\beta$ -cells could be found, varying effects have been observed in hepatocytes and macrophages. In hepatocytes, there are reports of increased cholesterol efflux (601) and synthesis (180), ABCA1 mRNA (606, 607) and protein (608) in association with selected statins. No effect was found with atorvastatin in one of the studies (608) or, in another study, pravastatin (605). Additionally, statins (atorvastatin or simvastatin) induced an increase in mRNA abundance of ABCA1 in human macrophages *ex vivo* (609) and *in vivo* (604), although considerable evidence from other studies (606, 610-613) demonstrated a statin-associated decreased expression of ABCA1 protein or mRNA in human and mouse

macrophages and several macrophage cell lines. The discrepancies in macrophage studies could potentially be explained by cellular cholesterol status and macrophage differentiation (133).

Despite conflicting results, the mechanism of statin influence in macrophages appears to be via the induction of micro RNA33, which downregulates ABCA1 in peripheral tissue. In contrast, tissue-specific ABCA1 regulation in the liver results in differential statin effects between the two sites (614). In a study utilising  $\beta$ -cell specific ABCA1 knockout mice it was determined that ABCA1 plays a role different to that in liver and influences both cholesterol and glucose homeostasis in mouse  $\beta$ -cells (343). Although the effect of statin in ABCA1 knockout mice was not included in the study, it demonstrates that tissue-specific variations may be anticipated.

It is also possible that there are species-specific differences. It is well-known that differences exist in plasma circulation of lipoproteins between mouse and man (615). For example, in rodents HDL carries most of the plasma cholesterol, unlike in humans (194, 405). Given that a) there is a precedence for tissue specificity occurring in ABCA1 function and regulation, b) inconsistencies exist between reports of the effects of statins on cholesterol transport via ABCA1, and c) the metabolic implications of changes in ABCA1-mediated cholesterol transport are not well understood, further investigation of the effects of statins on ABCA1 and cholesterol efflux in  $\beta$ -cells is required to better comprehend its influence on insulin secretion and  $\beta$ -cell function.

Despite gaps in our knowledge, the importance of cholesterol efflux, influx or both in the relationship between cholesterol and insulin secretion or action is clear, and leads to the following hypothesis: *Cholesterol efflux, influx or both via lipoprotein-mediated cholesterol transport pathways is important in  $\beta$ -cell function and insulin secretion, with imbalance or functional loss of cholesterol flux being detrimental. Net direction of flux may also be important for glycaemic health.*

#### 4.4.3 Regulatory modifications resulting in blunting of maximal insulin secretion may be associated with upregulation of mTOR and I-R activation

The insulin signalling cascade is well-described and involves several pathways leading to diverse effects including glucose transport, glycogen synthesis, and protein synthesis and growth (reviewed in 616, 617). Besides being important in insulin-sensitive tissues such as liver, adipose and muscle, insulin autocrine signalling is likely to be important in maintaining  $\beta$ -cell mass and function (618), though uncertainty about the nature of autocrine signalling persists (619). Several proteins involved in the insulin signalling pathway, including insulin receptor (I-R), Akt, also known as protein kinase B, and mechanistic target of rapamycin (mTOR), were assessed to determine the effect of pravastatin and atorvastatin on insulin signalling in  $\beta$ -cells. Interestingly, very recently (and after the work described here was

underway), insulin receptors were found to largely reside in intracellular rather than plasma membranes in  $\beta$ -cells (564). In conjunction with this phospho-caveolin 1-mediated insulin receptor internalisation, insulin signalling was found to be biased towards the Erk pathway and away from the Akt pathway in  $\beta$ -cells. This indicates that the role of insulin autocrine signalling may be more mitogenic than metabolic, given that the two insulin signalling pathways have divergent downstream effects (617).

The most significant changes found by Western blot analysis were upregulation of pI-R and mTOR associated with atorvastatin treatment. Interestingly, these proteins have previously been linked to the development of T2D (620, 621).

mTOR is a serine/threonine kinase with regulatory involvement in multiple processes, mainly governing cell growth, maturation, proliferation and survival (reviewed in 622, 623). It is a key environmental sensor that allows cells to maintain homeostasis in a dynamic milieu of extracellular signals, and is involved in the insulin signalling pathway. A link between dysregulation of mTOR and disease states including T2D is reviewed by Saxton and Sabatini (624). Possible mechanisms include the ability of mTOR, in the complex mTORC1, to control a shift in glucose metabolism from oxidative phosphorylation to glycolysis, or, via independent SREBP activation, increased flux through the pentose phosphate pathway thereby utilising glucose carbons in NADPH and other intermediate metabolites rather than ATP production. This is of interest considering the influence of atorvastatin to both increase mTOR expression and provoke a more glycolytic phenotype in BRIN-BD11 cells as demonstrated in Chapter 3. Either metabolic shift in the  $\beta$ -cell has the potential to interfere with stimulus-secretion coupling. Furthermore, pancreatic  $\beta$ -cell function is regulated in part by mTORC1 signalling, with hyper-activation initially improving glucose tolerance due to  $\beta$ -cell mass and insulin secretion increase, followed by  $\beta$ -cell exhaustion and hyperglycaemia (see Mori 2009 and Shigeyama 2008 in (624)). mTORC2, a second complex involving mTOR, is primarily a downstream effector of insulin signalling through phosphoinositide 3-kinase (PI3K) (624). Chronic mTOR inhibition, such as is used in some cancer therapies, can disrupt insulin signalling through inactivation of mTORC2, resulting in an increased risk of new onset T2D (reviewed in 625). Interestingly, physiological outcomes from both hyper- and hypo-activation of mTOR can be similar, effected by either mTORC1 or mTORC2, respectively (624).

Cholesterol trafficking was recently shown to be a requirement for mTOR activity, at least in endothelial cells (626), and hepatic LDL receptors are regulated by mTOR complex 1 via PCSK9 subsequent to insulin signalling (627), indicative of the involvement of mTOR in cholesterol homeostasis. The precise nature of the relationship and how statins may affect it, however, is unclear. For example, contradictory changes in mTOR activity have previously been associated with statins in HepG2 cells, where both increased (628) and decreased (629)

mTOR phosphorylation have been reported. Activation of key signalling proteins of the PI3K/Akt/mTOR and Akt/GSK-3 $\beta$  signalling pathways by atorvastatin has also been determined in cerebral cortical rat neurons (630). The phosphorylation status of mTOR was not examined in this study, though mTOR itself was increased, and pGSK-3 $\beta$  (serine 9) but not pAkt was increased after atorvastatin treatment (Figure 3.7, Figure 4.4, respectively).

Upregulation of phosphorylated insulin receptor (pI-R) was induced by atorvastatin, in contrast to the decreased phosphorylation previously associated with simvastatin in MIN6  $\beta$ -cells (302). mTOR and I-R have a complex relationship, with both downstream and upstream influences on each other via various feedback mechanisms involving I-R substrate (I-RS) and the PI3K/AKT and the Tuberous sclerosis proteins 1 and 2 (TSC1/2)/mTOR pathways (reviewed in 631, 632). Many insulin-dependent processes related to metabolic regulation, energy storage and growth may be implicated and further investigation would help to understand the consequences of upregulation of these two regulatory proteins. Whether functional changes such as are described in Chapters 2 and 3 could be linked to this finding could be the focus of future work, based on the hypothesis that *reduced mitochondrial coupling and attenuation of maximal stimulated insulin associated with atorvastatin occur through an mTOR- and I-R-dependent mechanism.*

#### 4.4.4 Cholesterol manipulation affects cell granularity

Complexity, as indicated by side scatter (SSC) in flow cytometry, was reduced in cholesterol loaded cells but increased in cells depleted of cholesterol by either M $\beta$ CD or atorvastatin treatment. Intracellular structures such as granules, organelles and roughness of surface or intracellular membranes can contribute to increased SSC (578).

Apoptosis is known to increase cell granularity but in this case it is unlikely to be the cause, being inconsistent with viability studies conducted in this project (see Chapter 2). The most common cytosolic granular structures in  $\beta$ -cells are insulin granules. A large treatment-induced increase in insulin granule number would be unlikely during a 30 min M $\beta$ CD treatment and insulin immunostaining was decreased by both M $\beta$ CD and c-M $\beta$ CD treatment, suggesting reduced insulin content. However, excess cholesterol delivered by c-M $\beta$ CD or acetylated LDL is known to accumulate in secretory granules in various  $\beta$ -cell lines, causing an increase in their size (336), and the effect of this on granularity is not known. Interestingly, lovastatin also caused an increase in secretory granule size with a concomitant reduction in mature granule density and insulin content (71).

A possible membrane smoothing effect of cholesterol due to its lipid ordering influence (61) could potentially explain the changes observed in granularity. Interestingly, a large increase in the size and visibility of the mitochondrial fraction in the c-M $\beta$ CD group during fractionation,

despite similar protein concentrations, was noted anecdotally (but not measured).

Mitochondrial cholesterol accumulation occurs in brain and liver cells, where it results in altered metabolic function, and possibly increases hexokinase translocation to the mitochondria (reviewed in 348).

Additional study would be required to confirm the nature of the increase in complexity associated with cholesterol depletion and reciprocal decrease with cholesterol loading, and whether *changes in granularity are linked to changes in  $\beta$ -cell function associated with intracellular cholesterol manipulation*. If this hypothesis was found to be correct it could provide the foundation for additional methods of evaluating  $\beta$ -cell cholesterol and/or functional status.

#### 4.4.5 Cell swelling is associated with cholesterol loading and depletion

Size, indicated by forward scatter (FSC) in flow cytometry, was significantly increased in both c-M $\beta$ CD and atorvastatin (by ~12.5 and 20%, respectively) but not M $\beta$ CD treatments. This suggests a possible relationship between cell size and  $\beta$ -cell function, considering that maximal insulin secretion was blunted and mitochondrial function was adversely affected by the same treatments that were associated with increased cell size (as reported in Chapters 2 and 3).

The increase in size observed in c-M $\beta$ CD and atorvastatin-treated cells indicates the possibility that they could be subject to swelling-induced rather than or as well as secretagogue-induced insulin secretion. Osmotically induced cell swelling can stimulate insulin secretion independently of secretagogues via a calcium-independent pathway (270, 633, 634). Since the insulin secretion pathway in swelling-induced secretion does not involve changes in ADP/ATP ratios, it is not coupled to glucose metabolism, which could account for reduced sensitivity to secretagogues as reported in Chapter 2. However, it is not known whether swelling and glucose stimulation pathways are mutually exclusive, as experiments in the hypotonic cell-swelling studies did not include secretagogues together with swelling. Hence, further study would be required to test the hypothesis that *cell swelling associated with c-M $\beta$ CD and atorvastatin treatment results in uncoupled insulin secretion via a calcium- and ADP/ATP- independent pathway similar to osmotically induced insulin secretion*.

#### 4.4.6 Notes regarding the use of flow cytometry in this project

Flow cytometry has been used to stain intracellular targets, including islet hormones, for some time (635), and some results presented in this chapter trial the use of intracellular immunostaining with flow cytometric analysis as an alternative method for assessing protein changes. However, there is a possibility that the results were affected by artefacts, potentially due directly to changes in the cholesterol content. However, some interesting observations made during this process include: a) size and complexity measurements showed interesting

changes not only with M $\beta$ CD and c-M $\beta$ CD treatment, but also in atorvastatin-treated cells and, to the best of my knowledge, this has not been previously reported; b) c-M $\beta$ CD had major effects on fluorescence, including autofluorescence; this may be a result of cholesterol-induced disturbances within the cell, or cholesterol loading may change the light scattering properties of the cells as discussed in Section 4.3.4; c) the population of  $\beta$ -cells is heterogeneous, based on insulin content and autofluorescence, even in a cell line such as BRIN-BD11, with ~12-20% of cells consistently showing reduced fluorescence from endogenous sources and from insulin staining. The latter observation is discussed in further detail below.

Heterogeneous  $\beta$ -cell populations have been described previously, with classifications based on glucose sensing ability (236, 237), insulin mRNA expression abundance (233), mature vs proliferative (238), or dedifferentiated cells (491, 492, 498, 545). Furthermore, ‘pacemaker’ cells, also known as ‘hubs’, with specific characteristics and a role in initiating pulsatile waves and coordinating the glucose response from the islet have been described (239). Further characterisation may enable an assessment as to whether the smaller yet viable cells with reduced insulin expression and autofluorescence that consistently made up 12-20% of the population in the current study could be identified as one of the groups classified in the literature.

#### 4.4.7 Summary

Overall, there was concordance between the extent of protein changes in the different treatments and functional effects reported in Chapters 2 and 3, identified by iTRAQ and Western blots. For example, atorvastatin and c-M $\beta$ CD, the treatments noted earlier for having greater cholesterol changing capacity and larger adverse effects in insulin secretion and mitochondrial function, generally showed greater changes from control than the other treatments. Potential mechanisms for adverse effects involving mTOR, insulin signalling, and ABCA1 were indicated by Western blot analysis. Although major compartment changes for selected targeted proteins were ruled out as a response to cholesterol loading or depletion, identifying the main cellular location of various proteins of interest was noteworthy in developing a better understanding of the function of caveolin 1 and ABCG1 in  $\beta$ -cells, which may differ from their function in other cell types. An association between metabolic activity and cholesterol loading was indicated by the number of up- or down- regulated metabolic proteins identified by iTRAQ analysis. Unexpected effects such as changes in autofluorescence, granularity and cell size indicated by light scatter in flow cytometric analysis provide new insights and, potentially, a foundation for new tools to examine the influence of cholesterol and  $\beta$ -cell function. Despite some confounding technical considerations and caveats as described, experimental data presented in this chapter provide an insight into areas that might hold promise for future investigation into the mechanisms linking cholesterol changes with mitochondrial function and insulin secretion.

## 4.5 Future direction

Areas of interest for follow-up enquiries relate to hypotheses generated in this project:

1. Cholesterol manipulation, particularly loading, leads to some degree of protein disruption in  $\beta$ -cells, with consequences that include metabolic impairment and reduced insulin secretion. It is not clear whether this is due to organisational changes including cellular compartment changes, or rapid expression changes in response to cholesterol loading or depletion.
2. Cholesterol efflux, influx or both via lipoprotein-mediated cholesterol transport pathways is important in  $\beta$ -cell function and insulin secretion, with imbalance or functional loss of cholesterol flux being detrimental. Net direction of flux may also be important for glycaemic health.
3. Reduced mitochondrial coupling and attenuation of maximal stimulated insulin associated with atorvastatin occur through an mTOR- and I-R-dependent mechanism.
4. Changes in granularity associated with intracellular cholesterol manipulation are linked to changes in  $\beta$ -cell function.
5. Cell swelling associated with c-M $\beta$ CD and atorvastatin treatment results in uncoupled insulin secretion via a calcium- and ADP/ATP- independent pathway similar to osmotically induced insulin secretion.

Further studies could include iTRAQ investigations in atorvastatin-treated BRIN-BD11 cells or dispersed islets from statin-treated mice.

An important secretion-related function of cholesterol is its role in the organisation of crucial proteins within lipid rafts (61, 338, 557, 581) spanning those involved in glucose sensing through to exocytosis of insulin. Raft-associated proteins of interest in insulin secretion include ATP dependent potassium channels ( $K^+_{ATP}$ ), voltage-gated calcium channels ( $Ca^{2+}_v$ ) and granule docking proteins such as SNAP-25 and VAMP2 (65, 69, 558). Interruption of lipid rafts by cholesterol sequestration has consequences for both raft-associated and non-raft-associated membrane proteins such as Glut-2 (331, 425). However, cholesterol loading may have even greater disruptive consequences for protein in  $\beta$ -cells as evidenced by the flow cytometry and iTRAQ results in this chapter and the insulin secretion results in Chapter 2. Further analysis of detergent soluble and insoluble membrane fractions by Western blot could also help to assess potential protein displacement by cholesterol treatments. This could be supported by further experiments using an interesting flow cytometry technique described elsewhere that uses lipid raft proteins as markers for raft disruption to assess raft proteins of



interest tagged by antibodies specific to extracellular surface epitopes (636). Further, protein crosslinking prior to lysis and protein precipitation has been used as a novel method of studying proteins co-precipitated with known raft proteins (67). Immunocytochemistry investigation would also be an important method of assessing cellular location of proteins with and without cholesterol modification.

## Chapter 5      The metabolic effects of statins in mice

While *in vitro* investigations are useful and can assist in exploring mechanisms in a relatively simple biological context, the *in vivo* environment is far more complex, and extrapolation of knowledge from the former to the latter context requires extra scrutiny. In the case of drugs such as statins, hepatic processing and  $\beta$ -cell drug exposure are just two of many variables that differ between the *in vivo* and *in vitro* context. The object of this study<sup>1</sup> was to see how the responses to cholesterol manipulation in  $\beta$ -cells observed in *in vitro* studies in earlier chapters are reflected in the *in vivo* context. Thus, the aim was to evaluate the effect of statins on glucose homeostasis in mice, with or without pre-existing obesity and insulin resistance induced by HFD feeding.

Two members of the statin family, pravastatin and atorvastatin, were used to inhibit cholesterol synthesis. In addition, a high fat diet (HFD) was used to model excess nutrient intake and an insulin resistant state. Originally, the collection of insulin secretion data from stimulated islets *ex vivo* was expected to be an important measure. Unfortunately, technical difficulties related to extraction of healthy, intact islets thwarted these goals. Some interesting observations were nevertheless made, and main measures reported here include an oral glucose tolerance test, weight change, plasma cholesterol, fasting blood glucose, fasting plasma insulin, and importantly, fasting plasma glucagon, which has not previously been investigated in this context.

### 5.1 Abstract

In previous chapters, statins were shown to impair  $\beta$ -cell mitochondrial ATP production and diminish insulin secretion in response to robust stimulation in the *in vitro* context. To determine whether statins may also influence  $\beta$ -cell function and glucose homeostasis in healthy and insulin resistant mice, male C57Bl/6J mice were fed a high fat (HFD) or normal (ND) diet and treated with pravastatin (P), atorvastatin (A) (10 mg/kg/day) or water (V) for 12 weeks by gastric gavage. As expected, weight and plasma cholesterol were significantly increased by the HFD. Interestingly, neither pravastatin nor atorvastatin had any effect on plasma cholesterol. The HFD also increased fasting plasma glucose, insulin and glucagon as well as insulin resistance (HOMA-IR). Overall, atorvastatin had a greater influence than pravastatin, demonstrating the differential effects of different members of the statin family. The main effect of atorvastatin was to significantly increase HOMA-%B, an index of  $\beta$ -cell function, in the ND cohort. This was due to the combined effect of non-significant trends towards increased fasting

---

<sup>1</sup> See the note at the front of this thesis for a list of contributors to this study.

plasma insulin and decreased fasting blood glucose. Statins were not associated with other statistically significant influences within diet groups. However, other subtle trends were diet-dependent and included a tendency for atorvastatin to ameliorate HFD-related elevations in fasting plasma insulin and insulin resistance and exacerbate the effect of the HFD in elevating fasting plasma glucagon and adversely influencing blood glucose recovery following a glucose challenge.

## 5.2 Background

Type 2 diabetes (T2D) increases the risk of death from heart disease and comorbidity with cardiovascular disease (CVD) is very common among diabetics. For this reason, the statin family of cholesterol-lowering drugs is often prescribed for patients with T2D or who have increased risk of T2D, as well as diabetes-free patients who present with cardiovascular symptoms or dyslipidaemia. While these drugs are effective in protecting patients from adverse cardiovascular events, they have also been associated with a higher risk of progression and new onset of diabetes. Several explanations for this have been proposed, but the mechanism by which statins contribute to insulin resistance and T2D has not yet been definitively determined.

Statins range in lipophilicity (637), a characteristic that is likely to affect non-hepatic uptake and pleiotropy, both favourable and otherwise. Lipophilic statins such as atorvastatin are more likely to pass through cell membranes and reduce cholesterol synthesis in non-hepatic tissue. Conversely, hydrophilic statins such as pravastatin require transporters (e.g., organic anion transporting polypeptide, OATP, expressed in the liver), to navigate the barrier presented by the phospholipid bilayer and are thus more hepatic selective (170).

Pleiotropy has been widely studied in statins and both beneficial (e.g., reduced inflammation) (211, 638) and detrimental (e.g., reduced insulin secretion) (208, 639) effects have been reported. While many of these effects are still under investigation, the potential complexity of examining the consequences of inhibiting a process as basic as cholesterol synthesis needs to be appreciated. This complexity is particularly evident given that a) all nucleated mammalian cells are provided with the machinery to manufacture cholesterol, suggesting a highly conserved and thus important biological process; b) cholesterol has important functions in cell membrane organisation and fluidity (640) and thus membrane transport and cell signalling (61, 74, 333) and c) statins inhibit the early steps in the mevalonate pathway of cholesterol synthesis, thus also contributing to depletion of biologically important intermediate products such as isoprenoids and CoQ10, some of which affect membrane localisation of metabolites and ATP production (78, 359, 559, 641). It is thus easy to conceive that pleiotropy could be complex and extensive. Furthermore, differences in age and pre-existing metabolic risk factors such as

obesity and insulin resistance (33, 218, 219, 642) have also been found to alter the risk of statin-associated new-onset T2D.

Cell-based studies are inadequate when considering the complexity of whole body physiology and its capacity to affect the action of statins on glucose homeostasis, particularly over the long term. Firstly, lipid homeostasis is affected by intestinal lipid uptake and trans-intestinal cholesterol excretion (TICE), circulating lipoproteins, bile acid secretion, cholesterol synthesis and synthesis of cholesterol products such as steroid hormones, and vitamins D and K. Secondly, glucose homeostasis is affected by factors such as diet, insulin sensitivity, and regulatory and counter-regulatory hormones such as insulin, glucagon, somatostatin (reviewed in 643) and the incretin hormones glucagon-like peptide 1 and glucose-dependent insulinotropic polypeptide (reviewed in 644). Physiological relevance thus requires the context of whole body physiology when assessing the pleiotropic effects of statins on glucose homeostasis.

Glucagon is secreted by pancreatic islet  $\alpha$ -cells when blood glucose concentrations decline. The mechanism is reviewed by Briant *et al* (643) and is thought to have both intrinsic and paracrine regulatory influences. Intrinsic regulation is by means of high-voltage action potentials, intensified by the opening of voltage-gated sodium and calcium channels, that cause calcium channels responsive only to high voltages (P/Q-type voltage gated calcium channels) to open. Calcium influx triggers glucagon granule exocytosis. During high glucose conditions, ATP generation drives membrane depolarisation due to closure of the same type of  $K^+$ <sub>ATP</sub> channels that are found in  $\beta$ -cells, leading to membrane depolarisation. However, this action is inhibitory in  $\alpha$ -cells due to the consequent inactivation of voltage-regulated sodium channels required for the amplification of the action potential, which is subsequently inadequate to open the P/Q-type calcium channels coupled tightly to the exocytotic machinery of  $\alpha$ -cells. These events have several factors in common with insulin exocytosis and may equally be affected by changes in cellular cholesterol concentrations. While insulin has been more frequently studied, statin influences on glucagon secretion may contribute to the diabetogenicity of these widely-used drugs, and has not previously been studied in the context of the influence of statins.

To augment studies in previous chapters, an *in vivo* model, which provides the opportunity to investigate how all relevant influences including insulin and glucagon work together, was chosen to further understand the metabolic influence of statins. Atorvastatin and pravastatin were chosen to represent chronic lipophilic and hydrophilic statin therapy in male C57Bl/6J mice pre-fed for four weeks with either a normal or high fat diet. The purpose of pre-feeding was to model variations in risk factors for metabolic well-being, such as insulin resistance and obesity, and early obesity-related symptoms are present in this mouse model after four weeks (645). More specifically, the aim of this study was to observe whether statin treatment influences glucose tolerance or fasting plasma glucose, insulin or glucagon levels, and whether

these influences are variable based on pre-existing risk factors such as obesity and insulin resistance.

## 5.3 Methods

### 5.3.1 Mice and diets

C57Bl/6J male mice 8 weeks of age were obtained from the Animal Resources Centre (ARC), Murdoch, Australia (JAX stock #000664, <https://www.jax.org/strain/000664>). They were fed *ad libitum* on normal rodent chow (ND) or a diet formulated to provide 59% of total digestible energy (22.8 MJ/kg) from lipids and 15% from protein (HFD), obtained from Specialty Feeds, Glen Forrest, Western Australia. The sole source of carbohydrate in the HFD diet was sucrose. A detailed description of each diet is available in Appendix C. Animals were maintained in a quarantined environment on a 12 h light–dark cycle, had constant access to water and were monitored weekly for weight gain. Animals were kept in groups of three or four, two cages per condition.

The HFD preparation was stored at  $-20^{\circ}\text{C}$ , or at  $4^{\circ}\text{C}$  for up to one week, and was provided fresh every 2<sup>nd</sup> day to avoid the consumption of oxidised fats. All experiments were performed according to the Australian Code of Practice for the care and use of animals for scientific purposes and were approved by the Curtin University Animal Ethics Committee (approval number AEC\_2016\_17).

### 5.3.2 Treatments

Mice received ND or HFD (21 mice per diet) for 4 weeks prior to being allocated into three groups per diet (7 mice per group) and treated with 10 mg/kg/day pravastatin (P), atorvastatin (A), or water control (V), making 6 groups altogether: V-ND, A-ND, P-ND, V-HFD, A-HFD and P-HFD. Atorvastatin (calcium salt) and pravastatin (sodium salt) were purchased from Sellex Chemicals, USA, and were suspended or dissolved, respectively, in water. Doses of 200  $\mu\text{l}$  were administered for 12 weeks by gastric gavage at the same time each day ( $\pm 1$  h) using stainless steel gavage tubes (Walker Scientific).

### 5.3.3 OGTT

During the last week of statin treatment and after 15 weeks on the diets, mice were fasted for 6 h in the morning and subjected to an oral glucose tolerance test (OGTT). An initial blood glucose reading was taken using a hand-held glucometer (OneTouch Verio IQ) and a drop of blood collected from a small nick in the tail vein. A bolus of glucose (2 g/kg) (646) was then administered by gastric gavage and blood glucose levels were monitored over a period of 2 h using blood collected at intervals from the tail vein.

### 5.3.4 Organ retrieval

After 12 weeks of statin treatment and 16 weeks on the diets, mice were again fasted for 6 h in the morning before being sacrificed. Blood was collected by cardiac puncture using needles and syringes pre-coated with 2.4% EDTA solution and fasting blood glucose was measured as previously described. Blood samples were immediately centrifuged at 2,000 x g for 10 min at 4°C to separate the plasma. A 100 µl aliquot of plasma was immediately transferred to a 0.5 ml microfuge tube containing 1 µl of protease inhibitor, mixed by pipetting, then a 50 µl aliquot was placed in a second microfuge tube. These aliquots were kept on ice and stored at -80°C within 1 h for subsequent measurement of glucagon. The remaining plasma was likewise stored at -80°C to be used for insulin and cholesterol assays.

The pancreas was perfused with collagenase P via the common bile duct and removed for islet extraction as previously described (454) (see Section 2.1.8). Several additional organs were also harvested for use in other collaborative projects.

### 5.3.5 Calculation of Insulin Sensitivity

To determine the most appropriate measure of insulin resistance and its reciprocal, insulin sensitivity, in the mouse cohort in this study, three different algorithms were used; Homeostasis Model Assessment of Insulin Resistance and Sensitivity (HOMA-IR and HOMA-%S, respectively) and Quantitative Insulin Sensitivity Check Index (QUICKI). In addition, beta cell function was estimated using HOMA-%B. HOMA-%B is a standard indicator of β-cell function or activity validated against the hyperinsulinaemic/euglycaemic clamp and other robust measures from which β-cell function can be assessed (647). All HOMA scores were calculated from measures of plasma insulin and glucose during the fasting state (Table 5.1, Equations 2, 5).

Insulin was measured in µg/L. The World Health Organisation (WHO)-established conversion factor of 1 IU = 0.0347 mg of insulin was used in calculations (648). This is based on human recombinant insulin but an equivalent for mouse insulin was not available.

The most recent version of HOMA, HOMA2, can be computed using an online calculator provided by Oxford University for calculation of human β-cell function (%B), insulin sensitivity (%S) and insulin resistance (IR) (649). However, to better reflect species distinctiveness, the HOMA-IR calculation was modified as previously described (650).

HOMA-IR was calculated according to Equation 2 and  $\log_{10}$  transformed (651). In humans, this measure of insulin resistance is calibrated to equate with 1 in normal healthy individuals (651). The calibration constant for mice in this study was calculated by multiplying median fasting glucose (FG) and fasting insulin (FI) values from control ND mice (Equation 1), which was then used as the denominator for the HOMA-IR calculation (Equation 2). To calculate β-cell function at 100% (%B), an assumption was made, as previously elucidated (650), that the linear

regression describing 100%B passes through the median FI point for the control mice, representing the best fit for the FG and FI values for the 7 control mice. Thus, Equation 5 was deduced, providing the *a* and *b* values for Equation 4 (%B). HOMA-IR values were further log transformed, as recommended (651). Quantitative insulin sensitivity check index (QUICKI) was calculated as described previously (652, 653) using Equation 7. These and various other methods of evaluating insulin resistance have recently been reviewed (654).

**Table 5.1. Equations used in insulin sensitivity calculations**

Calibration constant (CC)	$CC = [Med\ FG][Med\ FI] = 12.2 \times 5.68 = 69.3$	Equation 1
Homeostatic model assessment	$HOMA-IR = \frac{[FG][FI]}{69.3}$	Equation 2
Insulin sensitivity	$\%S = \frac{1}{HOMA-IR} 100\%$	Equation 3
Line of best fit	$y = 1.625x - 14.15$	Equation 4
$\beta$ -cell function	$\% \beta = \frac{\frac{1}{a} \times [FI]}{([FG] - \left  \frac{b}{a} \right )} 100\%$	Equation 5*
Specific $\beta$ -cell function (used in this study)	$\% \beta = \frac{0.61 \times [FI]}{([FG] - 8.7)} 100\%$	Equation 6
QUICKI	$\frac{1}{[\log(FG) + \log(FI)]}$	Equation 7

Notes: Eq. 1: Med FG is median fasting glucose of the control group (mmol/L)

Med FI is median fasting insulin of the control group (mU/L)

Eq. 2: FG is individual fasting glucose (mmol/L)

FI is individual fasting insulin (mU/L)

Eq. 5: *a*=slope of the line of best fit (Equation 4)

*b*=y-intercept of the line of best fit (Equation 4)

Eq. 7: FG is fasting plasma glucose (mg/dL)

FI is fasting plasma insulin ( $\mu$ IU/L)

values below 0.339 indicate insulin resistance.

\* The absolute value brackets around  $\frac{b}{a}$  were added in Equation 5, since in van Dijk (650) the subsequent use of their equivalent equation required it.

### 5.3.6 Statistical analysis

One or two-way ANOVA (as appropriate) followed by Tukey's or Dunnett's multiple comparisons test and correlations were performed using GraphPad Prism version 6.01 for Windows, GraphPad Software, La Jolla California USA. Statistical significance was inferred at a nominal value of  $\alpha = 0.05$ . Where necessary, data was  $\log_{10}$  transformed to meet assumptions of normality. In figures where statistical significance was of interest in the relationship of each group compared to every other group, superscripts indicating similarity (rather than difference) are used. This is standard practice in many disciplines, and statistical difference at  $P < 0.05$  is indicated between groups that do not share a letter in common. When used, this is indicated in the figure legend. These annotations were prepared using the superscript generator available online (655).

Tukey's box and whisker plots are used to present much of the data in this chapter. The box represents the 25<sup>th</sup> to 75<sup>th</sup> percentile with a line denoting the median. The upper whisker extends to the largest value that is less than or equal to 1.5 times the inter-quartile range (75<sup>th</sup> – 25<sup>th</sup> percentile) beyond the 75<sup>th</sup> percentile. Any values greater than this are plotted as individual points. Similarly, the lower whisker extends below the box to the value that is greater than or equal to the 25<sup>th</sup> percentile minus 1.5 times the inter-quartile range. Any values beyond this are plotted individually (656). Means are indicated by a '+' sign.

## 5.4 Results

Overall, a HFD induced a glucose intolerant state with increased fasting glucose and insulin. This was slightly ameliorated by statins in the HFD cohort, although fasting glucagon was elevated significantly by atorvastatin, and a trend towards reduced glucose tolerance was noted in the statin-treated, HFD-fed animals. Amongst the mice given the ND, statins, particularly atorvastatin, tended to increase insulin resistance and significantly increased  $\beta$ -cell function estimated by HOMA-%B ( $P < 0.01$ ) but had no influence on glucagon secretion in this diet group.

### 5.4.1 Weight & food consumption

Mice were randomly allocated to treatment groups on arrival and were not found to have significant differences in weight at baseline ( $24 \pm 1$  g, all results given as mean  $\pm$  SEM). Mice on ND consumed an average of  $41.6 \pm 1.5$  kJ/animal/day over 16 weeks, ranging from  $41.2 \pm 1.4$  to  $49.1 \pm 3.3$  kJ/animal/day in weeks 3 and 16, respectively. The diet provided 12.8 kJ/g of digestible energy, of which 14% was from lipids and 19% from proteins. The ND groups consumed food at a steady rate over the period of the study, with a tendency for atorvastatin-treated animals to consume less food in the latter weeks despite increased body mass compared to other ND groups ( $P < 0.001$ ). Over both diet groups, a change in the gradient



of the weight curve was discernible soon after treatment commenced. To quantify this, weight change over experiment weeks 2-4 (10-12 weeks of age) was compared with weight change over weeks 7-9 (see Figure 5.1B). A 2-way ANOVA indicated an overall significant difference ( $P < 0.001$ ) between weight gain in the pre- and mid-treatment time periods, the difference being greatest in the A-HFD group (a difference of 2.1 g in weight gain over 2 weeks,  $P < 0.001$ ) and least in the V-ND group (0.8 g difference in 2 weeks, ns). This was not reflected in a change in food consumption and is not expected to be a factor of age, as C57Bl/6J mice are known to gain weight more slowly between two periods of faster growth in weeks 5-9 and 21-25 (657).

Mice on the HFD consumed 27% less food daily (by weight) than the ND controls ( $2.4 \pm 0.2$  vs  $3.3 \pm 0.2$  g/animal/day,  $P < 0.001$ ). Energy intake in the HFD group ranged from  $45 \pm 2$  to  $66 \pm 3$  kJ/animal/day in weeks 3 and 16, respectively (Figure 5.2A). A period of diet adjustment appears to have occurred immediately after the change to HFD. Over the initial three weeks, food consumption decreased steadily before its subsequent stabilisation. The atorvastatin HFD group also showed decreased food consumption together with plateaued weight gain over three weeks at commencement of gavage.

There was an inverse relationship between weight gain and the mass of food consumed between the two diet groups, but this was more than countered by the extra energy available in the HFD (22.8 kJ/g vs 12.8 kJ/g) (compare Figure 5.1A with Figure 5.2A). As expected, HFD animals gained weight more rapidly than their ND counterparts, even during the initial 3 weeks of the diet when consumption was decreasing and energy consumption declined to similar levels to that of the ND groups. By week 4 a significant weight difference between the groups had been established and this persisted to the end of the experiment.

The amount of digestible energy (kJ) consumed daily varied with the diet. Animals fed a HFD consumed an average of  $\sim 10 - 16$  kJ/day ( $31 \pm 12\%$  over 15 weeks,  $P < 0.001$ ) more than control groups. Weight gain was plotted with respect to total energy consumed/animal over 15 weeks in Figure 5.2B. Among the ND groups, animals treated with atorvastatin consumed  $\sim 3$  kJ/day less than the pravastatin group ( $P < 0.05$ ). Among the HFD groups, atorvastatin- and pravastatin-treated mice consumed  $\sim 3$  kJ/day ( $P < 0.05$ ) and  $\sim 2.3$  kJ/day (ns) less, respectively, than those receiving no statin.

Statins appeared to affect the relationship between energy intake and weight gain. Across both diets, there were significant differences between all treatments for weight gain. Despite the fewer kilojoules consumed, the A-ND group gained more weekly weight than the vehicle or pravastatin groups eating the normal diet ( $P < 0.001$ ). Among the HFD groups, however, atorvastatin-treated animals gained less average weight weekly than the vehicle and pravastatin groups ( $P < 0.01$ ). A positive correlation between energy consumed and weight gain was found

in the V-HFD and P-HFD groups, but not the A-HFD or ND groups (Pearsons  $r = 0.6$ ,  $P < 0.05$ ;  $r = 0.65$ ,  $P < 0.01$ ;  $r = 0.43$ , ns for V-HFD, P-HFD and A-HFD, respectively).

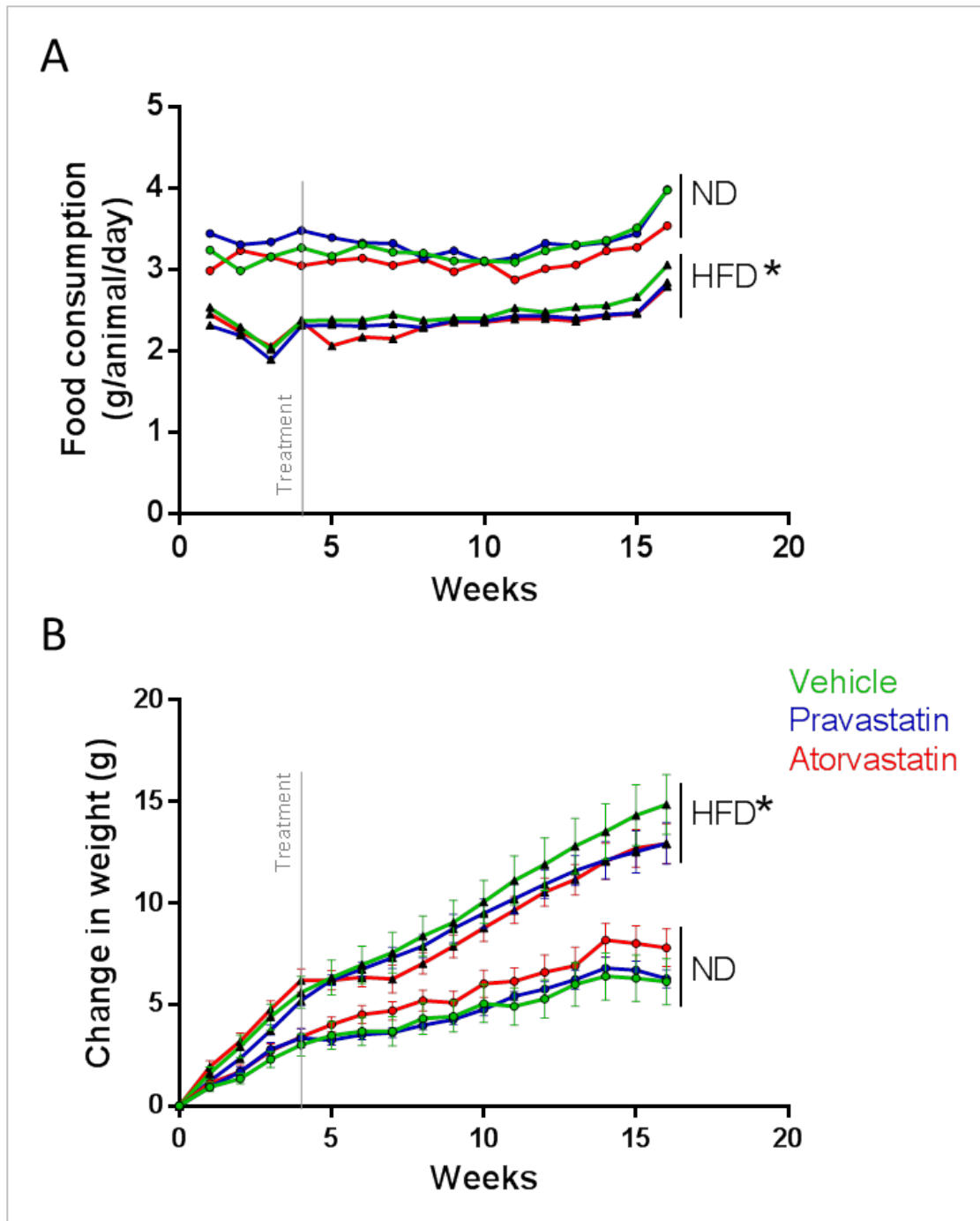


**Figure 5.1. Effect of diet and statins on weight gain and food consumption.**

**A.** Mice fed the HFD consumed approximately one third less (by weight) than control groups ( $P < 0.001$ ). **B.** Groups were differentiated by weight gain within four weeks of beginning the diets, with HFD groups quickly exceeding weight gained by individuals on the control diet. A 2-way Repeated Measures ANOVA indicates a significant difference in weight between the diets ( $P < 0.001$ ). Data in B is shown as mean  $\pm$  SEM.  $n=7$  mice per group. \*  $P < 0.001$

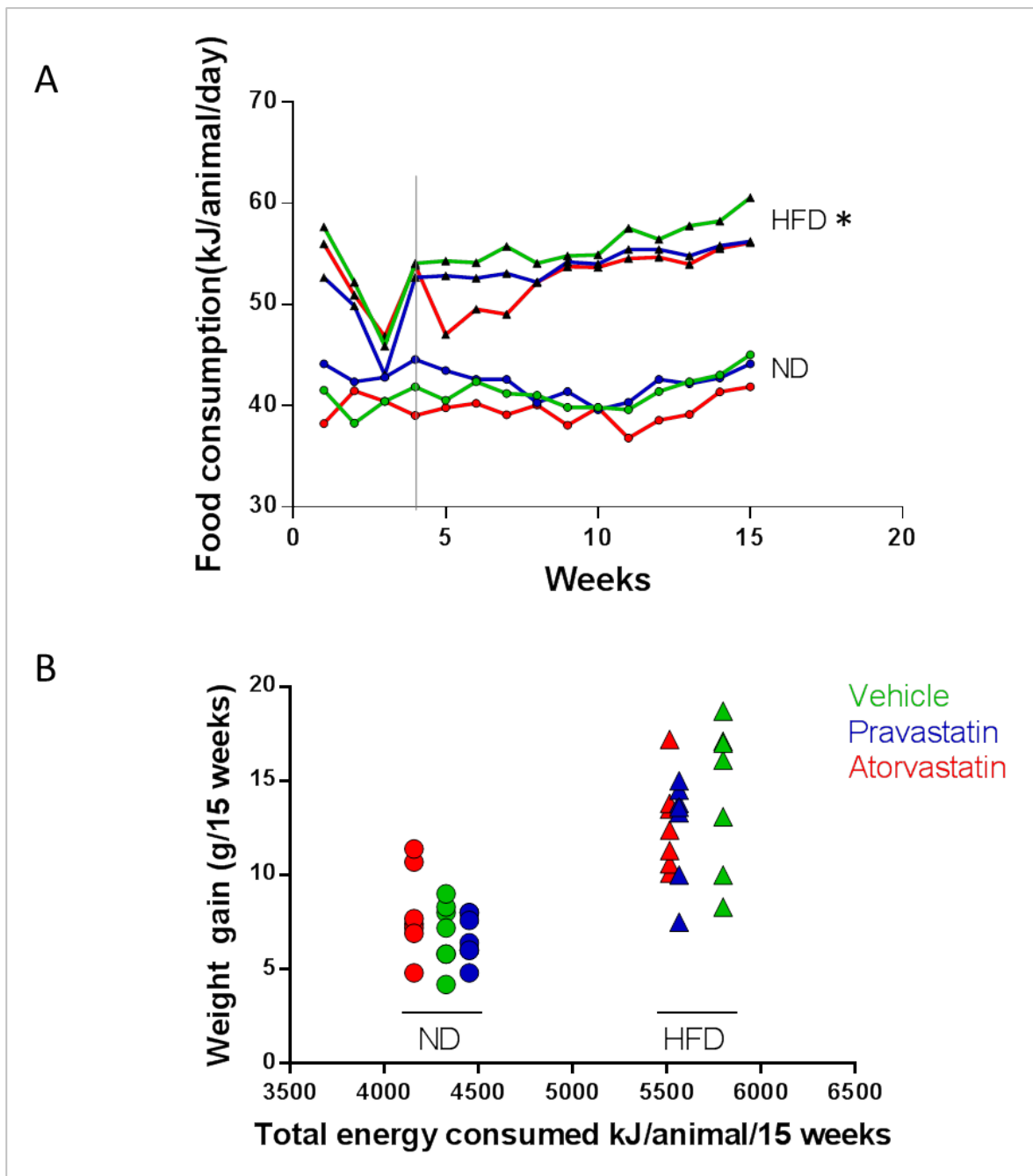


**Figure 5.2. Effect of diet and statins on energy consumption.**

**A.** The amount of digestible energy (kJ) consumed daily varied per the diet, with ~30% less consumed by the ND animals each day ( $P < 0.001$ ). **B.** Weight gain is plotted with respect to total energy consumed. Each circle (ND) or triangle (HFD) represents one mouse. Within both diet groups, least energy was consumed by animals given atorvastatin, however this was not reflected in lighter weight.  $n=7$ . \*  $P < 0.001$

#### 5.4.2 Metabolic parameters

Metabolic parameters assessed included glucose tolerance, measured by means of an oral glucose tolerance test (OGTT), and fasting plasma levels of glucose, insulin, glucagon and cholesterol (Figure 5.3, Figure 5.5). Overall, greater effects were elicited by diet rather than statins. Statins exacerbated diet-related variation for the OGTT and glucagon measures, but a larger diet effect was found in the treatment control groups (V) for all other parameters. Group data is presented in Figure 5.4 and Figure 5.3. and data from individual mice is provided in the heat-map (Figure 5.5). Correlations between parameters are presented in Figure 5.6.

**Fasting Glucose (FG) and glucose tolerance (OGTT):** There was a significantly different effect on FG in response to the two diets, both overall and within each treatment group (Figure 5.3A), with HFD groups having  $\sim 3.1 - 4.2$  mmol/L higher FG than their ND counterparts ( $P < 0.001$ ). However, there was no difference between V-ND and the statin-treated HFD groups, suggesting a beneficial effect of statins. Atorvastatin appeared to have a mild FG-lowering effect in the ND group, but it was not statistically significant ( $P = 0.2$ ).

When subjected to a glucose challenge (2 mg/kg by gastric gavage) after 11 weeks of statin treatment and 15 weeks of diet (Figure 5.4), statins increased the difference in plasma glucose between the two diets, both lowering blood glucose concentrations in the ND groups and elevating glucose in the HFD groups (relative to vehicle controls). Consequently, there was a significant difference in the AUC between the two diets for pravastatin- (P-ND vs P-HFD,  $P < 0.01$ ) and atorvastatin-treated (A-ND vs A-HFD,  $P < 0.001$ ), but not vehicle-treated mice (A-ND vs A-HFD,  $P = 0.2$ , Figure 5.4B). No difference was seen between vehicle or statin groups fed the same diet, but the AUC for A-HFD was significantly larger than that for V-ND ( $P < 0.05$ ).

In humans, a delayed post-challenge peak glucose concentration has been associated with declining  $\beta$ -cell function and poorer glucose tolerance (658, 659). In most mice, the peak glucose concentrations were observed 10 minutes after the glucose challenge. However, peak glucose concentrations for five of the seven mice in the A-HFD group were observed 20 minutes after the challenge or later, compared to three of seven (P-HFD) and one of seven (V-HFD) delayed peaks in other HFD groups.

Additional subtle differences were also observed. At time-point 1, 10 minutes after the glucose challenge, atorvastatin-treated mice on the HFD had significantly higher blood glucose than their ND counterparts ( $P < 0.05$ ). This difference was not resolved until 2 h post-glucose. At 20 and 30 min post-challenge, the A-HFD group demonstrated elevated glucose compared to the V-ND group ( $P < 0.01$  and  $P < 0.05$ , respectively) and V-HFD group ( $P = 0.07$  and  $P < 0.01$ , respectively). Pravastatin-treated, HFD animals also had significantly higher blood glucose at

20 and 60 min post-glucose compared to their ND counterparts (both  $P < 0.05$ ) and the V-ND group ( $P < 0.05$  at 60 min). An overall difference between dietary groups persisted ( $P < 0.001$ ).

**Fasting insulin (FI):** There was a HFD-associated increase in FI ( $P < 0.001$ ) in mice not treated with statins, but no change between HFD and ND in mice on statins. This was partly due to a non-significant increase in FI in atorvastatin-treated mice on the ND (~33% increase,  $P = 0.2$ ), while in the HFD groups statins appeared to have had an attenuating effect. This was, however, punctuated by extremes. An individual mouse in the A-HFD group was found to have very high FI (Figure 5.3B and Appendix A.3). If this individual is a true outlier, then its exclusion from the data would result in the A-HFD and V-ND groups being statistically similar.

**Fasting glucagon:** Analogous to FG and FI, fasting glucagon (Figure 5.3C) was increased in the HFD groups overall ( $P < 0.001$ ). However, individually the effect became statistically significant only in the atorvastatin, but not vehicle or pravastatin, groups ( $P < 0.01$ , A-ND vs A-HFD). There was also a significant difference between V-ND and both HFD-statin groups ( $P < 0.05$  and  $P < 0.01$  for V-ND vs P-HFD and A-HFD, respectively).

**Homeostatic model assessment (HOMA):** Insulin resistance was determined by HOMA-IR (see Section 5.3.5). The HFD significantly increased insulin resistance. This was true both overall ( $P < 0.001$ ) and for mice fed the HFD with or without statin treatment when compared to V-ND ( $P < 0.05$  with statins,  $P < 0.001$  without statins), but there was no difference between diets when mice were given statins (P-ND vs P-HFD and A-ND vs A-HFD, Figure 5.3E). If the potential outlier with high insulin is excluded, the effects described above remain unchanged, however, a trend towards an insulin resistance-ameliorating effect of atorvastatin emerges in the HFD-fed mice ( $P = 0.09$ , V-HFD vs A-HFD, see Appendix A.3). Similar results were obtained using QUICKI, and measures of insulin sensitivity and resistance are compared in Figure 5.8. As for HOMA-IR, there is a significant difference between diets for the statin-naïve groups but statins had a non-significant, diet-dependent influence, decreasing sensitivity in the ND cohort and increasing it in the HFD cohort, ultimately ameliorating the dietary influence on insulin sensitivity.

HOMA-%B, a model of  $\beta$ -cell function, was also calculated (Figure 5.3F). Interestingly,  $\beta$ -cell function was significantly increased in the A-ND and V-HFD groups compared to V-ND ( $P < 0.01$  and  $P < 0.05$ , respectively), while, conversely, A-HFD and P-HFD were not significantly different from V-ND or their respective ND counterparts. The influence of atorvastatin to elevate HOMA-%B in healthy mice has not previously been reported.

Statins overall, and atorvastatin in particular, appears to exacerbate the glycaemic stress imposed by a HFD in terms of glucose tolerance and glucagon secretion, while slightly attenuating (but not significantly) the insulin resistance imposed by the HFD.

**Plasma and liver cholesterol:** As expected, HFD increased plasma cholesterol (PC,  $P < 0.05$ , Figure 5.3D), however, neither statin reduced plasma cholesterol, irrespective of diet. Interestingly, results from another project in the laboratory indicated that while the high fat diet did not influence liver cholesterol content, atorvastatin treatment was associated with a significant increase in hepatic cholesterol in both diet groups (Figure 5.7, Sabapathy, personal communication). Livers from the HFD-fed mice were paler than those from ND groups, suggesting higher fat loading, however colour offers poor correlation to liver fat content, and can be prone to error (660). The influence of pravastatin on liver cholesterol was not examined.

**Metabolic correlations:** A moderate but highly significant positive correlation was evident between log transformed FI and both FG and fasting glucagon across all diets and treatments both including, and excluding, the potential outlier (Figure 5.6A). This may at first appear somewhat surprising, because an inverse correlation would normally be expected between insulin and both glucose and glucagon (661). Under normal conditions insulin exerts an inhibiting paracrine influence on glucagon secretion, possibly by altering the sensitivity of  $\alpha$ -cell  $K^+_{ATP}$  channels to ATP (662). However, in some contexts (including diabetes and dispersed  $\alpha$ -cells), paradoxical stimulation of glucagon by glucose (663, 664) and, possibly, insulin (665) occurs. Mathematical modelling has successfully reproduced this high glucose stimulation phenomenon when accounting for the involvement of dysregulated somatostatin secretion and both paracrine and intrinsic influences (643, 666).

When fasting insulin and glucose were plotted against cholesterol, a significant correlation was found. However, no correlation was found between cholesterol and fasting glucagon (Figure 5.6B).

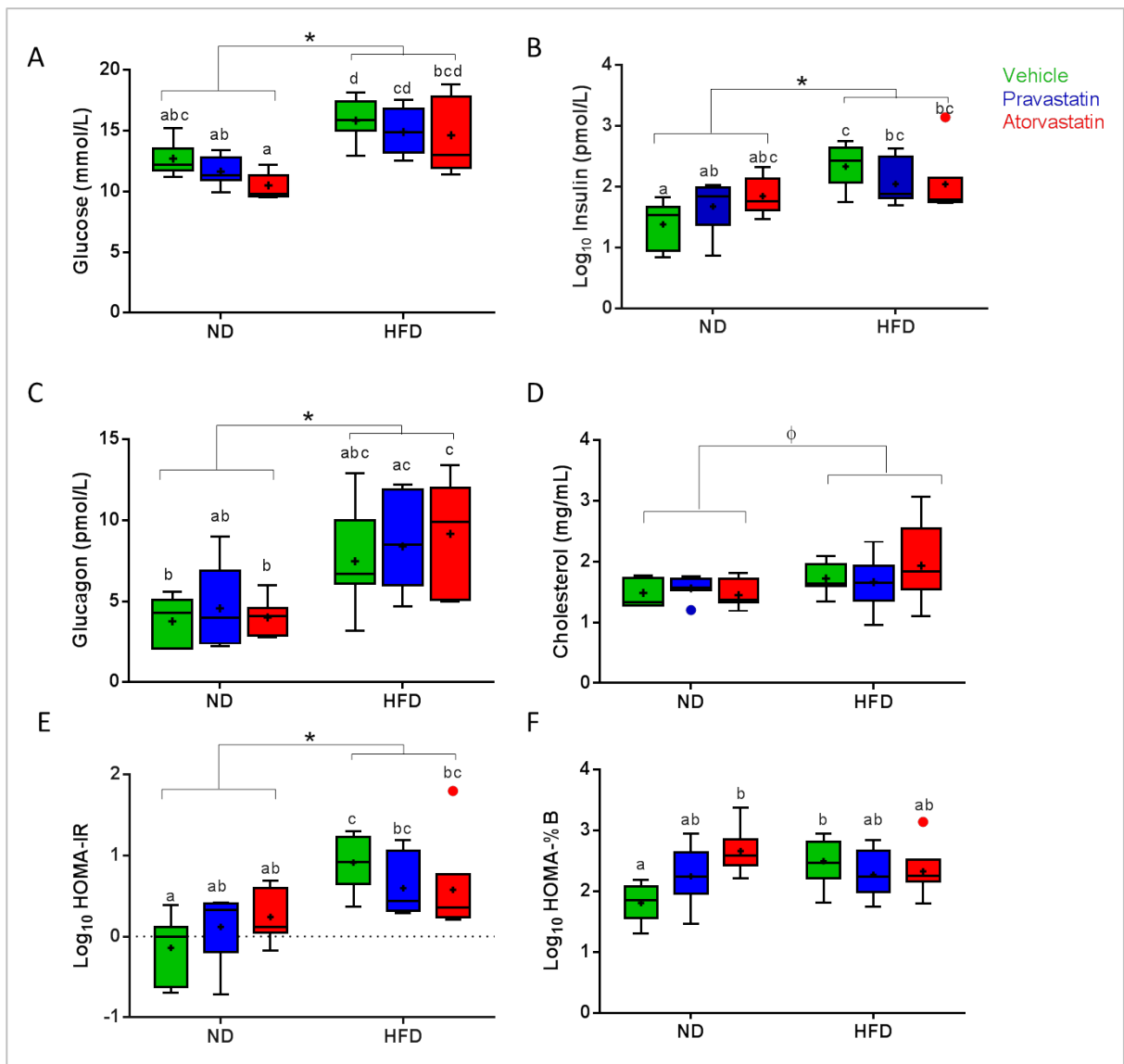


**Figure 5.3. The effect of diet and statins on metabolic parameters.**

There was significant variation in metabolic parameters between diets but less between treatment groups. Statins slightly attenuated the effects of HFD on fasting glucose (A) and insulin (B), but tended to exacerbate the effect of the HFD on fasting glucagon (C), while having no effect on cholesterol (D). A slight attenuation of insulin resistance by statins was indicated by HOMA-IR (E), although the HOMA-%B measure of  $\beta$ -cell function indicated that  $\beta$ -cell function in mice on the ND was increased with atorvastatin treatment (F). Data is presented as Tukey box plots and represents data from 7 mice per group. Means with superscripts in common are not significantly different from each other (2way ANOVA with Tukey's multiple comparisons test,  $P < 0.05$  indicating significance). ND, Normal diet; HFD, High fat diet.  $\Phi$ ,  $P < 0.05$ ; \*,  $P < 0.001$ .

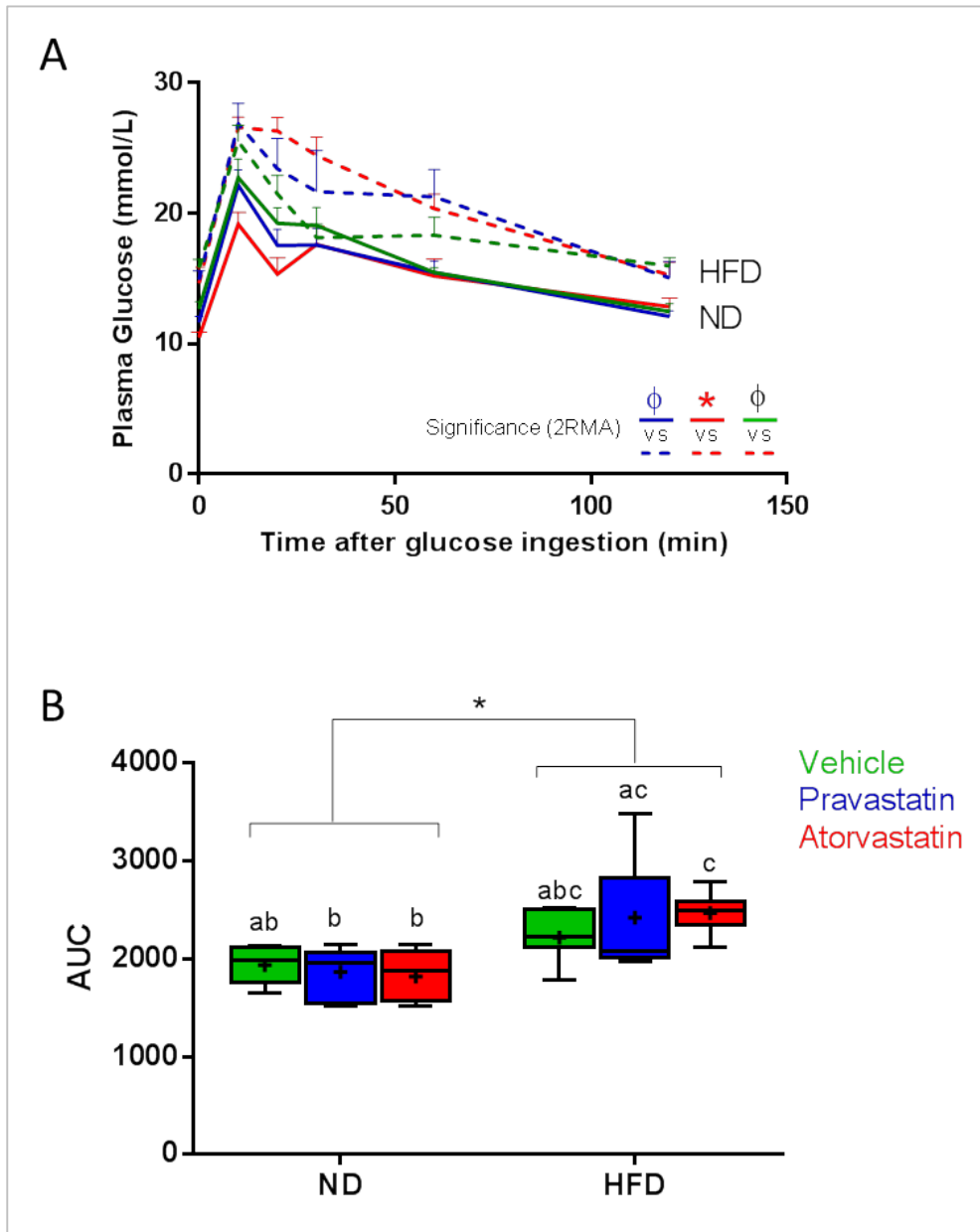


**Figure 5.4. The effect of diet and statins on glucose tolerance (OGTT).**

**A.** Plasma glucose was measured after a 6 h fast, and at time points (10, 20, 30, 60 and 120 min) after a 2 g/kg bolus of glucose. Results are shown as the mean  $\pm$  SEM of 7 individual mice per group. Lower error bars are omitted for clarity. Significance was determined using 2-way repeated measures ANOVA (2RMA) (P-ND vs P-HFD ( $\phi$ ), A-ND vs A-HFD ( $*$ ) and V-ND vs A-HFD ( $\phi$ )). **B.** OGTT data is shown as area under the curve. Means with superscripts in common are not significantly different from each other (2-way ANOVA, Tukey's multiple comparisons test,  $P < 0.05$ ). ND, Normal diet; HFD, High fat diet.  $n = 7$  mice per group.  $\phi$ ,  $P < 0.05$ ; \*,  $P < 0.001$  Symbols in black are compared to V-ND (solid green), unless indicated otherwise. Coloured symbols represent differences between HFD and ND within the same statin treatment group, indicated by the colour.



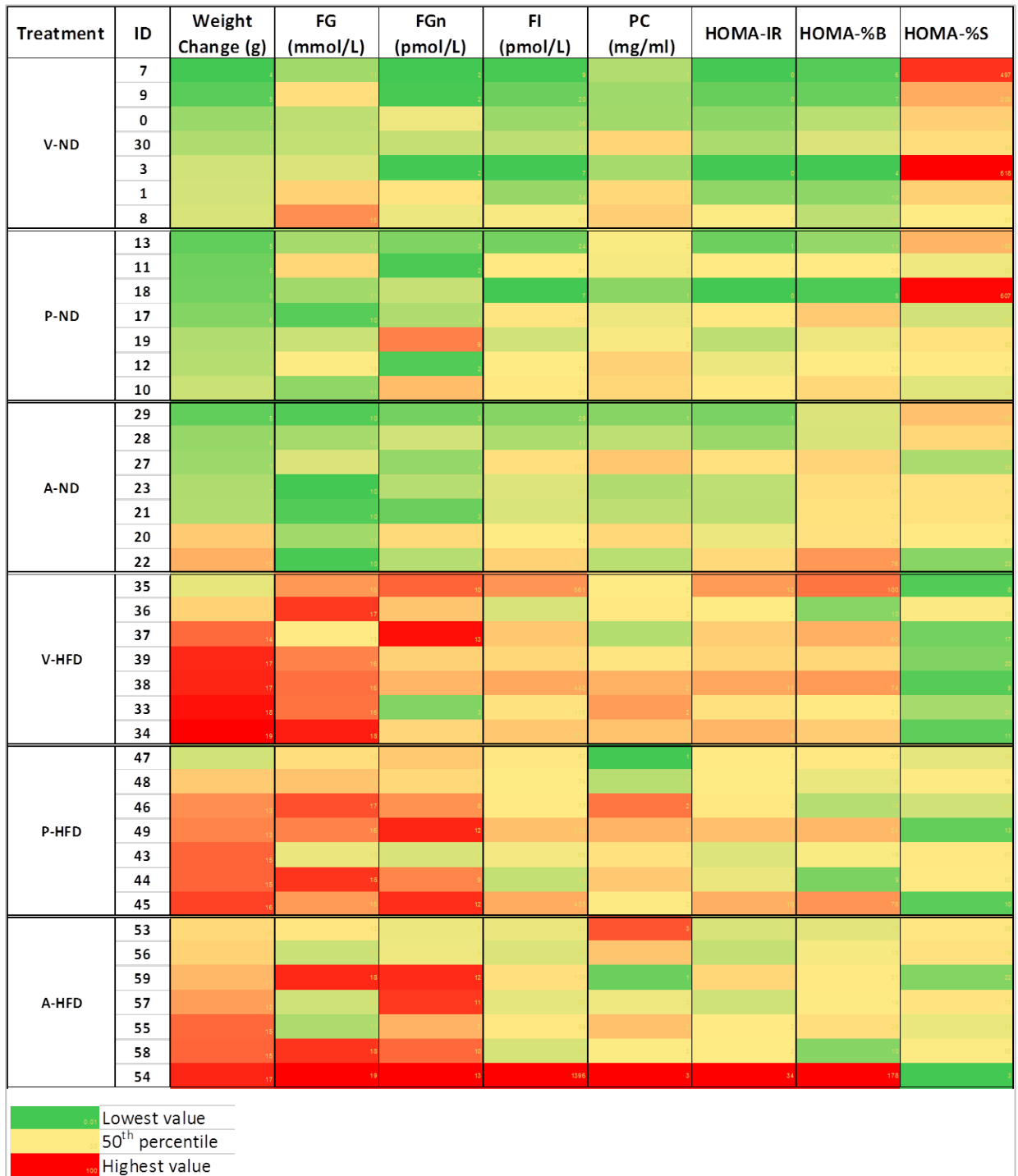


**Figure 5.5. Heat-map of metabolic parameters.**

FG, fasting blood glucose; FGn, fasting plasma glucagon; FI, fasting plasma insulin; PC, plasma cholesterol; V, vehicle; P, pravastatin; A, atorvastatin, both at 10 mg/kg/day; ND, normal diet; HFD, high fat diet.

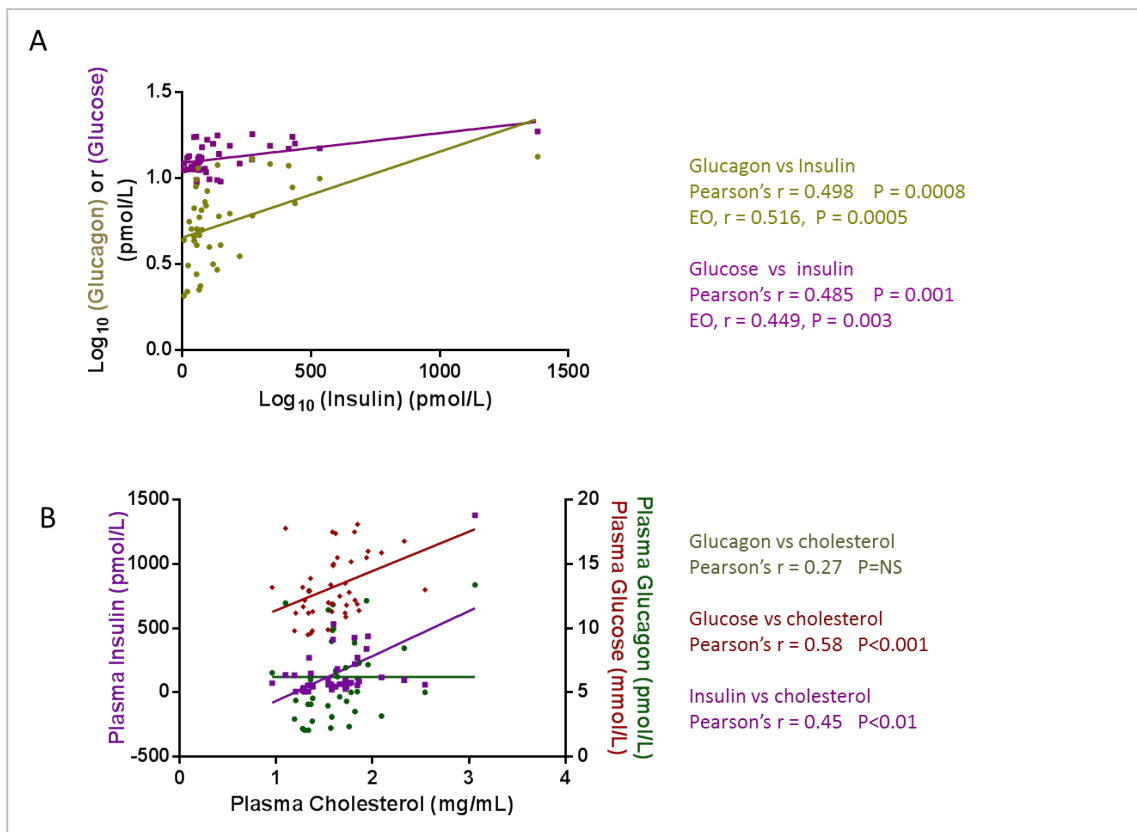


**Figure 5.6. Correlations between insulin or cholesterol and other metabolic parameters.**

**A.** Log transformed fasting glucagon or glucose across all treatment groups was plotted against log transformed fasting insulin and a medium, significant correlation was observed between these data sets, both including and excluding the outlier. This is driven mainly by the HFD groups, for without them the correlations do not exist. **B.** Data for fasting plasma insulin and glucose but not glucagon across all treatment groups correlated significantly with plasma cholesterol. EO, excluding outlier.

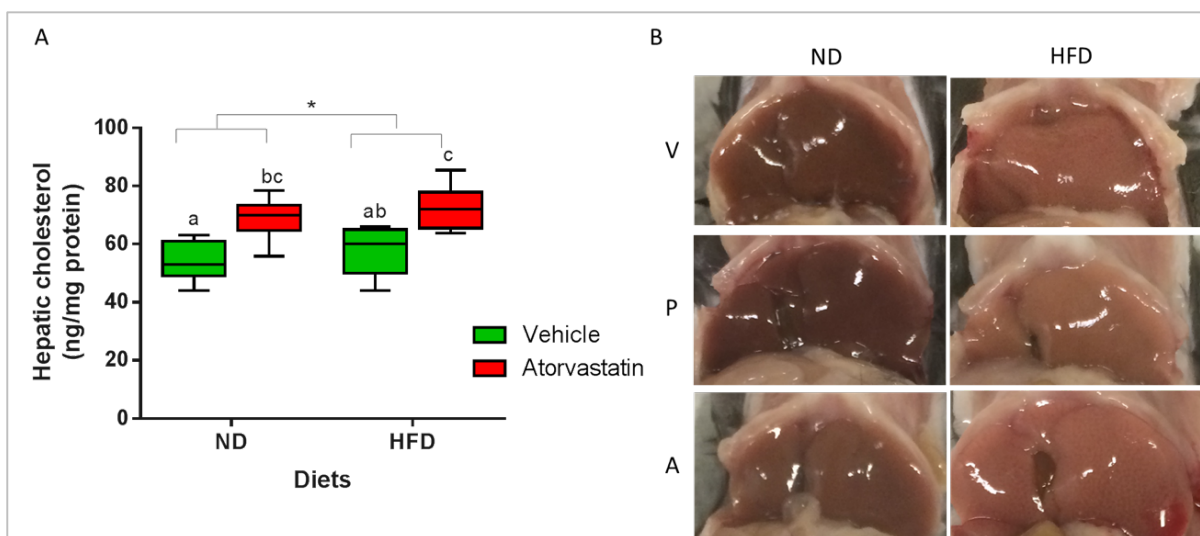


**Figure 5.7. Effect of diet and atorvastatin on hepatic cholesterol.**

**A.** Cholesterol measured in liver samples was influenced by treatment but not by diet. Atorvastatin increased hepatic cholesterol significantly. n = 7 mice. Modified from (457). **B.** Representative liver samples from the 6 groups of mice. HFD affected the liver colour in all mice, although this may be a poor indicator of fat accumulation. Letters signify statistical similarity (2-way ANOVA with Sidak's multiple comparisons test, P < 0.05 indicating significance) V, vehicle; P, pravastatin; A, atorvastatin; ND, normal diet; HFD, high fat diet; \*, P < 0.001.

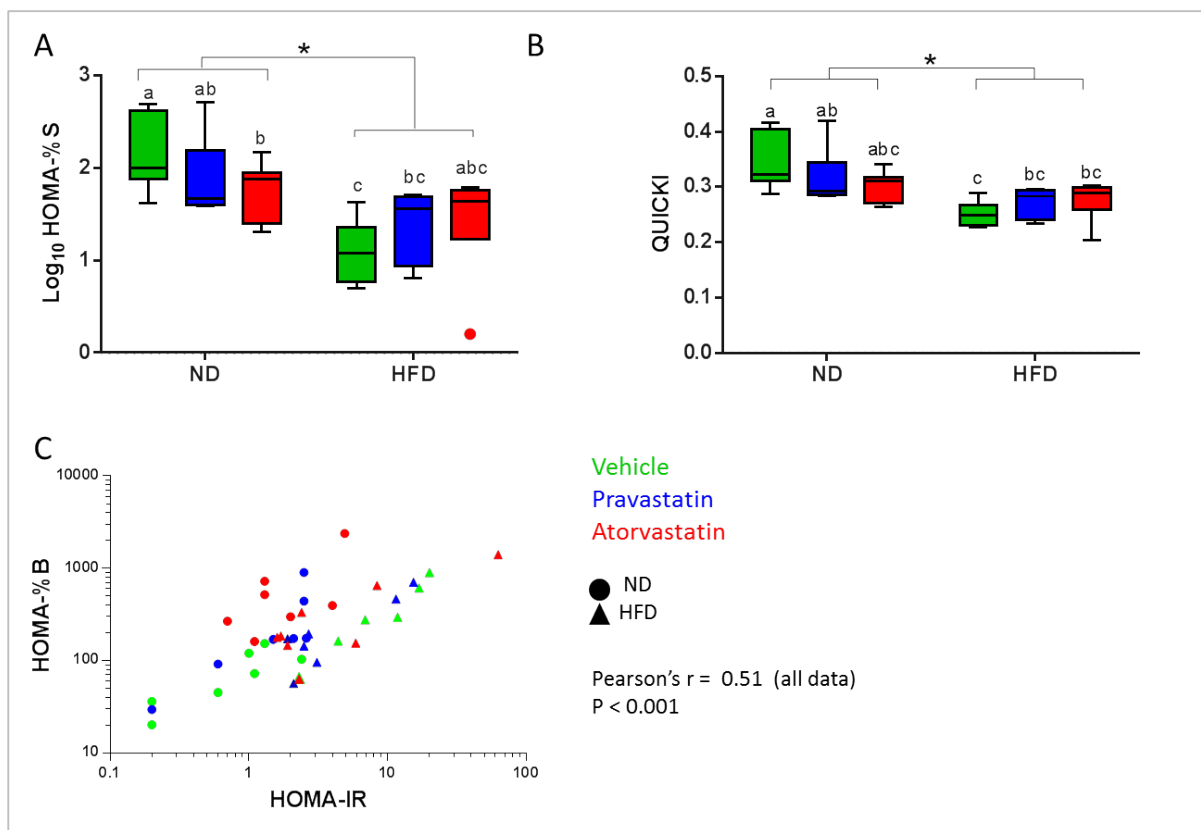


**Figure 5.8. Measures of Insulin sensitivity compared.**

(A), HOMA-%S (B), QUICKI (C) As expected, there is a correlation between HOMA-IR and other derivations of insulin sensitivity. ND, Normal diet; HFD, High fat diet. Letters signify statistical similarity: subscripts in common are not significantly different (2way ANOVA with Tukey's multiple comparisons test,  $P < 0.05$  indicating significance). ND, Normal diet; HFD, High fat diet. \*,  $P < 0.001$ .

## 5.5 Discussion

The aim of this study was to explore the effect of statins on glucose homeostasis in mice, with or without pre-existing obesity and insulin resistance induced by HFD feeding. In line with the large body of evidence available, results in this study demonstrate the deleterious effect of a HFD on insulin resistance and glucose homeostasis in C57Bl/6J mice. Statins exacerbated the dietary influence on glucose normalisation during an OGTT, discussed below, but a greater impact was imposed by diet. B-cell function (HOMA-%B) was significantly elevated by atorvastatin in the ND group, in association with increased fasting plasma insulin and decreased fasting glucose in this group, though not to statistical significance in the latter two parameters. A novel finding associating atorvastatin with exacerbation of elevated fasting plasma glucagon in the HFD group was also made.

As has been previously observed (212, 357), the influence of pravastatin was minimal compared to that of atorvastatin. Pravastatin appears to influence various outcomes in a similar direction

to atorvastatin, but to a lesser degree than atorvastatin, and was therefore less likely to yield statistically significant differences. This may be due to the difference in lipophilicity between the two drugs, pravastatin being considered hydrophilic and atorvastatin lipophilic (637). Hydrophilic statins are thought to have reduced systemic diffusion compared to their lipophilic counterparts due to the phospholipid plasma membrane barrier.

### 5.5.1 The influence of diet and statins on weight

Diets were commenced four weeks prior to commencement of statin treatment to induce obesity and increase insulin resistance. A period of reduced food consumption observed over the initial three weeks of HFD could be due to a dislike for the taste, or to increased satiation due to fat content. These mice are known to strongly prefer sweet tastes (667). The atorvastatin HFD group also showed decreased food consumption together with plateaued weight gain immediately on commencement of treatment. It is not known why this occurred. It is unlikely to be related to commencement of gavage, as the procedure was initiated in all groups simultaneously. It could have been taste-related, due to traces of atorvastatin remaining in the buccal cavity, but was not noticed in the ND group. Several reports of increased irritability during statin treatment may hold clues to this observation (668, 669), though more research would be necessary to make a conclusion.

The atorvastatin-associated weight gain independent of food intake observed in ND animals in this study has previously been observed in male (629) and female (670) C57Bl/6J mice and humans (671). It was attributed to increased hepatic gluconeogenesis, as evidenced by increased expression of gluconeogenic genes (glucose-6-phosphatase and phosphopyruvate carboxylase) in the former study. Additional considerations proposed in the latter two studies include a statin-associated adjustment in gut microbiota towards species with an increased capacity to harvest energy, and dietary relaxation associated with statin therapy in the human study. Activity levels were not measured in this or the other studies mentioned, but an increase in sedentary behaviour could be investigated as an alternative explanation for this observation. In humans, statin treatment has often been associated with muscle pain and reduced activity (361).

### 5.5.2 The influence of diet and statins on glucose homeostasis

Overall, animals fed a HFD in the current study exhibited significantly elevated fasting plasma glucose, insulin and glucagon compared to ND groups but statins did not cause further elevation compared to the vehicle controls (Figure 5.3). However, each treatment group (statins or vehicle) had significantly elevated fasting glucose when fed a HFD compared to animals fed a ND with the same treatment.

Statins had no effect on fasting glucagon among the ND animals. However, the atorvastatin HFD group displayed significantly increased fasting glucagon compared to all animals fed a ND independent of statin treatment (i.e., V-ND, P-ND and A-ND). Glucagon excess would be expected to increase hepatic glucose release, and in the A-HFD group, higher glucagon concentrations would antagonise secreted insulin after a glucose challenge. Indeed, in an earlier study, glucagon knock-out mice were resistant to HFD-related hyperglycaemia (672). The influence of atorvastatin was only apparent in the context of a HFD, and neither glucagon nor insulin were significantly different between A-HFD and the vehicle-treated HFD control.

Plasma glucagon is dysregulated in diabetes such that it is inappropriately elevated in hyperglycaemia, and insufficient during hypoglycaemia (643). This occurs in conjunction with diminished  $\beta$ -cell mass and increased  $\alpha$ -cell mass (673), perhaps due, at least in part, to expression of glucagon by  $\beta$ -cells (674), although complete transdifferentiation of  $\beta$ -cells into  $\alpha$ -cells has been refuted by lineage tracing analysis (499). Glucagon activity has been largely overlooked in diabetes therapy but it is increasingly evident that its dysregulation contributes significantly to the pathophysiology of this disease (673, 675). New therapies targeting the glucagon receptor (676-678) are under development and show promise, although total  $\alpha$ -cell disruption does not improve glucose tolerance in T2D (679). The effect of atorvastatin to elevate fasting plasma glucagon on a background of HFD feeding reported in the current study is a novel finding which is of interest, given the attention on glucagon as a pathophysiological mechanism and potential therapeutic target in T2D.

The OGTT demonstrated that a prolonged HFD increases the peak level of glucose and length of time to normalise after a glucose challenge. Statins, particularly atorvastatin, affected blood glucose concentrations in a diet-dependent manner after a bolus of glucose, being associated with a trend towards diminished blood glucose in the ND cohort ( $P = 0.2$ ) but elevated blood glucose in the HFD cohort, particularly between 20 and 60 min post-challenge in the A-HFD group ( $P < 0.05$  vs V-ND) and at 60 min post-challenge in the P-HFD group ( $P < 0.01$  vs V-ND). The trend ( $P = 0.2$ ) to lower fasting glucose and reduced peaks after the glucose challenge in the A-ND mice could be due to the tendency ( $P = 0.2$ ) for higher fasting insulin levels found in association with atorvastatin, and is in line with the significantly higher ( $P < 0.01$ ) HOMA-%B scores calculated for this group. This is in agreement with the known effect of statins to increase plasma insulin, which can occur even in the absence of hyperglycaemia, and may precede the development of diabetes (298). For the HFD groups, there was no evidence in this study that the contrasting effect of statins to elevate blood glucose at 10 – 60 min post-challenge was due to changes in insulin or glucagon, though only fasting concentrations of the hormones were recorded.

In a study by Salunkhe *et al* (324) in mice on a normal diet, a similar statin-associated decrease in blood glucose occurred during an OGTT after 4 weeks of rosuvastatin treatment.

Interestingly, the rosuvastatin effect was diminished after a further 4 weeks, suggesting compensatory mechanisms may reduce the statin effect on glucose response over time. In the same study but in animals fed a high fat diet, rosuvastatin had little effect on blood glucose in response to a glucose challenge. Elsewhere, the response to an OGTT was not influenced by pravastatin or atorvastatin in HFD-fed, male, C57Bl mice, but a comparison with mice fed a normal diet was not made (629). In agreement with the trend found in the current study, atorvastatin and pravastatin treatment resulted in higher fasting blood glucose concentrations compared to HFD controls after 16 weeks on a HFD. In the same study, serum cholesterol was reduced by rosuvastatin and fluvastatin but, as in our study, not by pravastatin and atorvastatin treatment. The increased statistical significance compared to the current study may be due to the higher statin dose used (0.01%, w/w of diet), approximately equivalent to a 4-fold higher dose than was used in the current study.

### 5.5.3 Further influences on Insulin sensitivity

Insulin sensitivity and insulin resistance are reciprocal terms denoting the effectiveness of insulin in stimulating glucose uptake. It is an important parameter in metabolic health and can be estimated by several methods as a more practical substitute for the invasive hyperinsulinaemic/euglycaemic clamp, which is generally considered the gold standard (653, 680, 681). HOMA modelling is based on measures of fasting glucose and fasting insulin (682). Approximations are often calculated using a linear equation provided by the authors as an alternative to the more complex computer modelling. The model was updated (683) when computers became readily available and was subsequently made available to clinicians and researchers in 2004 by Oxford University at <https://www.dtu.ox.ac.uk/homacalculator/>. The model is calibrated to give values of 100% in healthy young adults (651), which suggests that a recalibration for meaningful application to laboratory animals would be appropriate. This was done by van Dijk *et al* (650), and a similar method based on their work has been used in this study.

An increase in insulin resistance with HFD is expected in C57Bl/6J mice. This in-bred strain lacks an inner mitochondrial integral membrane protein known as nicotinamide nucleotide transhydrogenase (Nnt), associated with impaired glucose homeostasis and insulin secretion when fed a HFD (684). The diet effect was considerably greater than any statin effect. However, statin-treated mice showed some differences from control mice, outlined below.

As expected, the V-HFD group demonstrated a significant increase in insulin resistance as calculated by HOMA-IR compared to their ND-fed counterparts ( $P < 0.001$ ). Within diet groups, statins did not significantly alter insulin resistance, and slight statin-associated increases

and decreases in insulin resistance among the ND and HFD groups, respectively, meant that pravastatin- and atorvastatin-treated mice on the HFD were not significantly more resistant than their ND-fed counterparts (P-ND vs P-HFD and A-ND vs A-HFD) despite an overall increase in the HFD cohort. This result is supported by the findings of a colleague who assessed insulin action in the livers of mice in this study. He found decreased expression of insulin receptors and insulin-specific binding in HFD animals ( $P < 0.01$ ) compared to those on a ND, which could explain the reduced insulin sensitivity in the HFD cohort. However, the total number and phosphorylation of insulin receptors and insulin-specific binding was greatly increased in atorvastatin-treated, HFD-fed animals compared to statin-naïve animals on the same diet ( $P < 0.001$ ). By contrast, no such effects of atorvastatin on insulin receptor expression, activation or binding were observed in the ND groups (457). This suggests that atorvastatin may be associated with a diet-dependent effect to reduce insulin resistance by increasing insulin receptor expression and affinity to insulin in HFD mice.

The trend described above does not appear to support clinical evidence of increased risk of statin-related diabetes in persons with pre-existing metabolic risk factors, although taken together with the adverse influence of atorvastatin on OGTT performance, this may be misleading. Individual potential to compensate for statin-related changes may affect the development of insulin resistance and hyperglycaemia, and is discussed further below.

HOMA-%B, a measure related to HOMA-IR, does not empirically reflect the capacity of  $\beta$ -cells to mount a postprandial response, being calculated from measures of plasma insulin and glucose during the fasting state (Table 5.1, Equation 5); nevertheless, it is a useful indicator. The increase in HOMA-%B associated with the HFD may reflect a compensatory increase in insulin secretion due to increased insulin resistance in the statin-naïve groups. Statins were not associated with further HOMA-%B changes in the HFD cohort. However, in animals fed the ND, a significant increase was calculated for HOMA-%B in the atorvastatin group. This indicates that  $\beta$ -cells may have increased basal activity in response to atorvastatin treatment, as demonstrated by modestly (but not significantly) reduced glucose and increased insulin and insulin resistance. *In vitro* studies in this project were inconclusive on the association of statins with increased chronic insulin secretion. This is discussed further in Section 6.4. Interestingly, compensatory hypersecretion of insulin was found to precede  $\beta$ -cell failure in mice, at least when driven by over-nutrition (685), and this may also occur in statin-induced diabetes (298). Further work would be necessary to determine whether the increased  $\beta$ -cell function indicated by HOMA-%B in A-ND mice was compensatory or indicative of  $\beta$ -cell stress. Also of interest is the indication of a greater effect of atorvastatin on  $\beta$ -cell function for mice on the ND than those fed a HFD. Indeed, an effect equivalent to that of a HFD in the vehicle group was evident, although insulin resistance was not as elevated in this group. An alternative

explanation could concern cell membrane disruption or damage and subsequent insulin ‘leak’ due to reduced cholesterol, but further evidence would be required to assess this.

The current study demonstrates that atorvastatin may be associated with hyperglucagonaemia when combined with a HFD while trending towards hyperinsulinaemia in the ND group. This, together with the impact of atorvastatin on the OGTT and IR, supports an evidence-based conclusion that the numbers needed to treat (NNT) data is unfavourable towards preventative statin prescription in a cohort at low-risk of CVD (197, 686).

#### 5.5.4 Other observations

**Individual variation.** One mouse in the A-HFD group was more adversely affected by atorvastatin, potentially representing a statistical outlier (discussed below). Excluding this animal, atorvastatin appeared to benefit those fed a HFD in terms of insulin resistance. For example, excluding the outlier, the HOMA-IR measure of insulin resistance showed no significant difference between mice in the V-ND and A-HFD groups, whereas other HFD groups had significantly increased ( $P < 0.05$ ) insulin resistance (Appendix A.3). Similarly, a 2-way ANOVA showed significantly reduced fasting insulin for A-HFD compared to V-HFD, but no difference between the former and V-ND (again, excluding the outlier). Chen *et al* (687) report similar preservation of  $\beta$ -cell function from 30 mg/kg/day treatment with atorvastatin for 58 days in obese mice. It is not understood why atorvastatin appears to interact differentially with different diets.

Mouse 54 in the A-HFD group did not benefit from atorvastatin (see Figure 5.5), and the possibility that parallels may exist with some individuals who are statin-intolerant warrants a brief discussion of this mouse. It had the highest recorded measurements within the entire cohort for serum cholesterol, fasting plasma glucose, glucagon and insulin. Indeed, the log transformed FI value was 3 standard deviations above the total mean, making it a statistical outlier. It also had the highest mass amongst members of the A-HFD group, though two individuals in the V-HFD group were heavier. It is well known that significant variation occurs in mouse data, even with inbred mice of the strain used in this study, demonstrating differences in insulin sensitivity and secretion (688, 689). Further experiments with greater statistical power would allow categorisation of mice into high and low responders similar to previous studies (690, 691) to give more insight into phenotypic variability. Metabolic vulnerability in this individual may have been induced by atorvastatin, perhaps interacting with diet. Alternatively, it may be a phenotypic outlier in response to diet alone, or, given that  $n=1$  in this case, its results may be meaningless to the discussion at hand.

A similar vulnerability to statin adverse effects has been experienced by a minority of patients, including myositis and adverse immune reactions (692-697), unexpected lipid-associated



outcomes (698), reduced cognitive ability (699) and metabolic effects (700). Thus, a personalised approach may be helpful in deciding on the appropriateness of statin therapy to meet individual requirements. For example, variations in some cytochrome P450 genes involved in the hepatic processing of selected statins may predispose to adverse effects of certain statins (175). Statins are metabolised differentially, ranging from alternative hepatic enzymes involved in processing (e.g., atorvastatin and fluvastatin are principally metabolised by the CYP3A4 and CYP2C9 isoenzymes, respectively (169)) to no hepatic processing for pravastatin (see Sections 1.3, 7.2) and thus patients may respond differently according to phenotypic variation. Low activity of metabolising enzymes may result in higher statin accumulation in tissue and an associated increase in toxicity (701). Genetic variations in some muscle enzymes (209) and concomitant use of certain medications (165) also increase the risk of statin-induced myopathy.

Statin are considered to be mitochondrion-toxic (702) and are thus prescribed with caution for patients with mitochondrial disorders (703). Further research in the field of individualised medicine and predisposing factors leading to statin-related adverse events will be beneficial in reducing the incidence of these events.

***Statin dose and efficacy in cholesterol reduction in mice*** The statin dose used in this study (10 mg/kg/day) was equivalent to 8-10 times that commonly used therapeutically in humans. However, statin is metabolised more quickly in rodents (704), reducing exposure. The latter study estimated that a 13 mg/kg/day dose represented a similar exposure to that regularly used in humans. The dose used here was previously used by collaborators and will allow future comparison of the two studies (670). Other studies have used doses ranging from 1-500 mg/kg (193). For example, Lorza-Gil *et al* (192) used 40 mg/kg/day, though the delivery of pravastatin in drinking water means the dose was estimated.

Mice fed a HFD showed increased plasma cholesterol concentrations. The statin dose used failed to reduce plasma cholesterol levels in statin treated animals irrespective of diet (Figure 5.3A). A similar result has been documented elsewhere (193, 670). Indeed, it has been suggested that mice can tolerate very high statin doses because of their resistance to its pharmacological effects (193), and a systematic review found no statistically significant effect of statins on total cholesterol in C57Bl/6 mice (705). In contrast, rosuvastatin (191) and very high-dose pravastatin (approximately 40 times higher than used in humans) (192) did significantly reduce plasma cholesterol in LDL receptor (LDLr) knockout mice. This is interesting, since the mechanism by which statins are thought to reduce plasma cholesterol is via increased LDLr expression (via sterol regulatory element-binding protein, SREBP2), thereby increasing tissue uptake of cholesterol while concurrently removing it from circulation (102, 596, 597). In the absence of LDLr there must be another mechanism for reducing plasma

cholesterol, a hypothesis supported by Schonewille *et al* (180), who found evidence for cholesterol efflux pathways via bile acid and faecal excretion. They also found that plasma cholesterol was decreased by atorvastatin and lovastatin but not rosuvastatin.

Although the mice in the current study were resistant to the serum cholesterol depletion effects of statins, there is evidence of a response to mevalonate pathway inhibition, similarly to the observations of Bjorkhem-Bergman *et al* (704) using a dose estimated to be ~13 mg/kg/day delivered via the diet. Hepatic cholesterol was measured by a fellow PhD student in our research group and found to be paradoxically increased with atorvastatin treatment, both in ND and HFD animals ( $P < 0.01$ ) (457) (Figure 5.7). Further, the liver plasma membrane cholesterol and cytosolic fractions were significantly different between both diets and treatments, with atorvastatin fractions having higher cholesterol content. Conversely, the plasma associated membrane (PAM) fraction from atorvastatin-treated animals was significantly lower in cholesterol for both diets, and the mitochondrial fractions were not different. A similar hepatic cholesterol increase in response to statin treatment was also found previously (180), though plasma cholesterol was slightly reduced in the two-week treatment time. An ~10-fold increase in hepatic cholesterol synthesis over 72 h was due to SREBP2-mediated upregulation of HMGCR and other cholesterol synthetic genes.

Measurements of HMGCR protein and mRNA will be undertaken in liver samples in future studies to further explore mevalonate pathway inhibition. It is likely that a new cholesterol synthesis equilibrium may have been reached during the 12 weeks of treatment.

Schonewille *et al* (180) demonstrated that, after two weeks of statin treatment, hepatic HMGCR and its substrate accumulates and may out-compete statin inhibition of the enzyme. This seems a likely prospect, and potentially results in new 'normal' levels of cholesterol intermediates after an initial period of adaptation in statin treated animals.

### 5.5.5 Limitations and future studies

Given that pravastatin showed similar trends but smaller effects than atorvastatin, increasing the power of the study by using more animals per group may have enabled higher statistical significance and greater certainty of the effects of diet and statins.

Many studies of statins and their effects, such as the present study, use mice or rats as model organisms (706) and mice are a very amenable model for studies for several reasons. Logistical considerations include ease of husbandry, ready access to suitable housing arrangements and cost effectiveness, as well as the availability of species-specific antibodies and various analysis kits. In the current study the spontaneous progression of C57Bl/6J mice towards insulin resistance upon HFD feeding provides a model of increased T2D risk factors, and the availability of comparative studies in the same strain made the choice attractive. Interestingly,

C57Bl/6 mice were found to more closely represent human plasma lipid profiles over eight major lipid fractions than several commonly used transgenic mice (707). Other studies also support the use of mice in plasma lipid studies (405, 706). However, differences in the lipid transport systems between rodent models and humans must be taken into consideration (see Section 1.6.1) and may contribute to failure to replicate results in clinical trials of prospective lipid-related drugs (707). For example, when fed a HFD, mice downregulate cholesterol synthesis and upregulate bile acid synthesis to dispose of excess cholesterol, hence maintaining cholesterol homeostasis in plasma (403). In the current study, it is highly probable that pharmacological failure of statins in lowering plasma cholesterol is due to species differences (193).

Guinea pigs have been mooted as a more appropriate model of human CVD and statin studies have found them to have similar responses to statin, with upregulated LDLr and decreased plasma LDL (708). They are also susceptible to streptozotocin-induced diabetic syndrome (709), however, a HFD may not induce insulin resistance in this species (710). Insulin storage and the molecular structure of insulin also varies in guinea pigs, characterised by the absence of zinc (711). In humans and many other species, zinc is co-secreted with insulin in a ratio of 1:3 and has roles in signalling, storage and secretion of insulin (712). Nevertheless, it would be valuable to assess guinea pigs, among other species, as alternative models for the study of the effect of cholesterol manipulations on  $\beta$ -cell function.

In an animal model in which plasma cholesterol is reduced, further studies could compare pravastatin and atorvastatin at effective equivalent doses once their efficacy within the model is established. This would accurately address the question of the effect of changes in cholesterol on glucose metabolism in the context of lipophilic vs hydrophilic statins.

Apart from alternative animal models, it would be particularly useful to see whether age is a factor in adverse pleiotropic effects of statins related to metabolic health. In meta-analyses of random controlled trials, elderly subjects were at greater risk of new onset diabetes than their younger counterparts (224, 298). Thus, it would be appropriate to run a similar study in elderly versus young animals. In addition, this study could be improved by including an assessment of metabolic parameters at an earlier time-point to study events during a putative metabolic reprogramming phase.

GSIS studies in isolated islets are a valuable tool for describing functional metabolic consequences of various treatments. For example, pravastatin treatment over 12 or 16 weeks was found to reduce both plasma cholesterol and, insulin secretion in islets isolated from LDLr knockout mice (192). In the current study, islets were isolated and experiments completed for *ex vivo* GSIS investigation, however, technical difficulties rendered these studies unsuitable, and they are being planned for a future study.

An elegant study in which an isoglycaemic, hyperinsulinaemic clamp was used in newly diagnosed T2D humans or healthy controls to observe the effect of insulin resistance on  $\beta$ -cell function, including GSIS, was able to distinguish between exogenous and endogenous insulin (713). A similar technique, potentially including additional secretagogues other than glucose, could be done after statin therapy in rats to further measure the influence of statins on  $\beta$ -cell function *in vivo*. Finally, somatostatin, another islet hormone, has also been shown by mathematical modelling to play a regulatory role in insulin and glucagon secretion in health and T2D (643) and this could be assessed in future studies.

## 5.6 Conclusion

The main results of this study include the greater impact of atorvastatin compared to pravastatin, the increase in fasting glucagon associated with atorvastatin and a HFD, the ameliorating effect of atorvastatin on insulin resistance in the HFD fed mice and the trend towards an increase in fasting glucose and insulin in response to atorvastatin in the ND cohort, indicative of increased  $\beta$ -cell function index (HOMA-%B). These results suggest a complex relationship between cholesterol and metabolic processes, as indeed is to be expected. This is further exemplified by discrepant views in the literature. For example, some animal studies report improved insulin sensitivity (501) and expanded  $\beta$ -cell mass (687) in response to statins while others describe adverse effects such as reduced GSIS (192) and exacerbated hyperglycaemia in diabetic rats (714). Human studies also show diverse outcomes (collated in 212, see Table 1). This can be explained in part by dissimilar conditions used in these studies, including statin type, dose, duration of treatment, and cohort, including pre-existing conditions of subjects (e.g. age, gender, obesity, T2D, familial hypercholesterolaemia, insulin resistance etc.). While contradictions persist, the mounting body of evidence from powerful meta-analyses and randomised controlled trials has established a persistent, though small diabetogenic effect of statins, possibly being context-dependent. An even stronger effect is reported from a meta-analysis of observational studies (436). The current study contributes by highlighting the diet-based differential outcomes on insulin resistance and insulin secretion associated with atorvastatin and the association of atorvastatin with hyperglucagonaemia only in mice fed a HFD. Evidence from this study indicates that atorvastatin has a small diabetogenic effect in mice fed both a ND and a HFD, the former implied by increased  $\beta$ -cell secretion (indicated by HOMA-%B) and the latter by OGTT performance, though this was offset by a beneficial effect on insulin resistance.

## Chapter 6      Statin-Glutamine Interactions in the $\beta$ -cell

Glutamine serves numerous functions: in addition to being a component of proteins and a precursor for purine and pyrimidine synthesis, it contributes to redox homeostasis via provision of glutamate for glutathione synthesis and has a beneficial influence on  $\beta$ -cell function (715). It is a mitochondrial substrate, being partially oxidised in the TCA cycle, is a nitrogen donor via glutamate formation and insulin secretagogue in the presence of leucine (715, 716). As outlined in previous chapters, statins have been found to reduce maximal mitochondrial respiration and insulin secretion. The aim of this chapter was to assess whether glutamine, in the form of a chemically stable dipeptide with alanine (Ala-Gln), could ameliorate the adverse effects of atorvastatin on maximally stimulated insulin secretion and mitochondrial function (reported in Chapters 2 and 3). My results have demonstrated that this was not the case, nevertheless this work facilitates a deeper understanding of the effect of atorvastatin in the context of Ala-Gln availability in  $\beta$ -cells.

### 6.1 Background

Glutamine is the most abundant amino acid in the body (277, 717) and is considered conditionally essential in humans due to its high consumption in catabolic states, where plasma glutamine is lowered to a critical level, below 0.4 mM (718, 719). It has a beneficial effect on insulin action and glycaemic control in a variety of clinical situations associated with insulin resistance, including surgery, trauma and sepsis (3, 720). A significant reduction in circulating glutamine concentrations is also associated with T2D (721, 722), and oral glutamine supplementation is beneficial in maintaining glucose homeostasis (723). This may be mediated directly by entry of glutamine carbon into the TCA cycle (in the presence of leucine) and thus energy generation or indirectly via a balancing influence on immune function (724), GLP-1 stimulation, or antioxidant action (3, 725). Beneficial effects of glutamine on gut microbiota have also been observed in obese subjects, with a short oral supplementation program influencing alterations in species composition similar to those obtained in weight loss programs (726). Metabolomic profiling of statin users demonstrated no effect on circulating amino acid concentrations (727).

Cells in culture are known to require glutamine in excess of other amino acids (728) and  $\beta$ -cells, including BRIN-BD11 cells, consume glutamine at high rates (715) (276), partly for pyrimidine and purine synthesis (728, 729). Among the many functions of glutamine in cell metabolism, proliferation, protein synthesis and degradation, cell defence and repair, specific to glucose homeostasis is its role in insulin action, and in  $\beta$ -cells exclusively, in insulin secretion (730). For example,  $^{13}\text{C}$  NMR analysis has indicated that besides supplying carbons for the TCA, the

main fate of glutamine in BRIN-BD11 cells is generation of stimulus-secretion coupling factors and glutathione synthesis for redox functions (715). Paradoxically, glutamine can also induce insulin resistance in insulin-sensitive tissue by mediating flux through the hexosamine biosynthetic pathway via the rate-limiting enzyme glutamine:fructose-6-amidotransferase (GFAT) (370), demonstrating its potential for opposing influences on glucose homeostasis.

Both alanine and glutamine can supply carbons for entry to the TCA cycle and thus contribute to the production of ATP (715). Conversely, they can also stimulate fatty acid synthesis in BRIN-BD11 cells by upregulating enzymes (ATP citrate-lyase and acetyl-CoA carboxylase, respectively) that provide both the substrate (via citrate conversion to acetyl-CoA) and enzymatic activity for fatty acid synthesis (717), potentially diverting carbons from ATP production.

Stimulation of insulin secretion by pathways other than via ATP generation are not well understood (715, 717, 731). Apart from possible stimulus-secretion products that amplify insulin secretion, orally administered glutamine slows gastric emptying and influences an increase in insulin secretion via stimulation of incretin hormones in the gastrointestinal tract (725). Interestingly, in adolescents with Type I diabetes (where destruction of  $\beta$ -cells has occurred), oral glutamine supplementation increased the risk of hypoglycaemia after exercise without altering insulin sensitivity (732). The mechanisms of this effect have not yet been elucidated.

Glutamine is also well-known as a transporter of nitrogen (733, 734), which is critical in the formation of  $\text{NH}_3$  in the kidney, as  $\text{NH}_3$  accepts a proton to become  $\text{NH}_4^+$ , and for its contribution to redox processes through the synthesis of glutathione and its glutaredoxin activity, molecules on which  $\beta$ -cells have an increased dependence (735). Several enzymes are required for these processes, including glutaminase, glutamine synthase (GS), glutathione peroxidase (GPx), glutathione reductase (GTR) and glutamate dehydrogenase (GDH). Glutaminase and GS affect the conversion of glutamine to glutamate and ammonia and vice versa, with an ATP requirement for the reverse conversion (280). GPx and GTR convert glutathione between its reduced and oxidised forms, respectively, with the associated removal or production of hydrogen peroxide. In agreement, glutamine feeding was accompanied by an increase in plasma glutathione peroxidase (GPx) activity and improved total antioxidant status in dairy cows (736). Glutathione is also capable of non-enzymatic interaction with ROS species (737). GDH is the catalyst for the  $\text{NAD(P)H}^+$ -dependent conversion of L-glutamate to  $\alpha$ -ketoglutarate and is allosterically activated by L-leucine. GDH also potentially acts as an energy sensor, turning off leucine-stimulated insulin secretion in high ATP or GTP conditions, and turning it on in low fuel conditions (280).

Oxidative stress occurs when the production of oxidised products of metabolism exceeds the capacity of antioxidants to neutralise them, and free radicals such as superoxide and hydrogen peroxide are formed. Nitrosative stress is similarly caused by excessive production of reactive nitrogen species from nitric oxide, such as peroxynitrite, ammonia and others. These molecules can oxidise other biological molecules, producing changes in structure and function. Glutamine is normally protective of mitochondrial oxidant injury (277) but excessive quantities can also increase oxidative/nitrosative stress due to hydrolysis in the mitochondria and the production of glutamate and ammonia (738).

Glutathione and its associated redox systems may also have a role in the control of exocytosis, including that of insulin (735). Glutaredoxin and thioredoxin were found to be essential for amplification of insulin secretion in the presence of glucose. Thus, ROS management, fuel sensing and coupling of mitochondrial metabolism with insulin secretion are specific roles of glutamine in  $\beta$ -cells.

Earlier studies demonstrated that statins reduced maximal ATP production and insulin secretion. The question of interest in this chapter was whether glutamine (in its more stable dipeptide form with alanine) could moderate statin effects on mitochondrial function and insulin secretion in  $\beta$ -cells.

## 6.2 Methods

BRIN-BD11 cells were seeded at  $1 \times 10^4$  cells/well in 96-well plates and cultured in the presence or absence of 2 mM alanyl-glutamine (Ala-Gln) and 10  $\mu$ M atorvastatin or vehicle control. Additional concentrations of Ala-Gln were used initially to determine the optimal concentration. Acute and chronic insulin secretion was measured as described in Chapter 2. After 24 h, medium was removed and collected for measurement of chronic insulin secretion, cells were washed and then starved for 40 min in KRBB supplemented with 1.1 mM glucose. They were then stimulated with secretagogues prepared in KRBB as indicated in the Results for 20 min, followed by collection of media for measurement of stimulated insulin secretion. Cells were then lysed with RIPA buffer and assayed for protein content, determined using the BCA assay for protein. Insulin was assayed using an ultrasensitive insulin ELISA kit (Mercodia) using the published protocol as previously described (Section 2.1.9).

To determine the metabolic effects of Ala-Gln, with or without atorvastatin treatment, cells were seeded into Seahorse 96-well plates and allowed to attach overnight. Medium was removed and cells were treated with or without Ala-Gln and 10  $\mu$ M atorvastatin for 24 h before media were changed to unbuffered Seahorse medium (DMEM base medium supplemented with phenol red, 2.5 mM glucose, 1 mM sodium pyruvate,  $\pm$  2 mM Ala-Gln (all from Sigma-Aldrich), pH  $7.35 \pm 0.05$  at  $37^\circ\text{C}$ ); the cells were incubated in air at  $37^\circ\text{C}$  for 1 h to stabilise the

pH before assay. The injection protocol was as follows: A, 25 mM glucose; B, 2  $\mu$ M oligomycin; C, 0.3  $\mu$ M FCCP; D, 1  $\mu$ M rotenone + 1  $\mu$ M antimycin A. Following this assay, the cells were lysed in RIPA and DNA was quantified using a PicoGreen fluorescence assay (Life Technologies), as per manufacturer's instructions. DNA content was used to normalise oxygen consumption rate (OCR) and extracellular acidification rate (ECAR) results.

Statistical analysis was performed using GraphPad Prism version 6.01 for Windows, GraphPad Software, La Jolla California USA. One or two-way ANOVA (as appropriate), followed by Tukey's or Sidak's multiple comparisons test were used to determine significance, which was inferred at a nominal value of  $\alpha = 0.05$ .

### 6.3 Results

Stimulated insulin secretion was reduced when Ala-Gln was absent during the 24 h culture preceding acute insulin stimulation with secretagogues. This decline was greater in cells concurrently treated with 10  $\mu$ M atorvastatin (A), with stimulated insulin secretion reduced to approximately half that of vehicle-treated cells. For example, at 2 mM Ala-Gln, the ratio of insulin secreted in response to the secretagogue in cells pre-treated with 2 mM compared to no Ala-Gln was  $3.4 \pm 0.5$  pg/ $\mu$ g protein compared to  $1.7 \pm 0.4$  pg/ $\mu$ g protein for vehicle or 10A, respectively ( $P < 0.01$ , Figure 6.1). A dose-response curve shows little change between Ala-Gln concentrations of 1 to 4 mM (Figure 6.1), and 2 mM was chosen for future experiments. This is a commonly used concentration of glutamine and is the concentration used in commercial media, and used during experiments in previous chapters. L-alanine, however, is not added to the RPMI medium purchased by our lab (449). At high concentrations of Ala-Gln (8 mM), cells not treated with atorvastatin were associated with reduced stimulated insulin secretion.

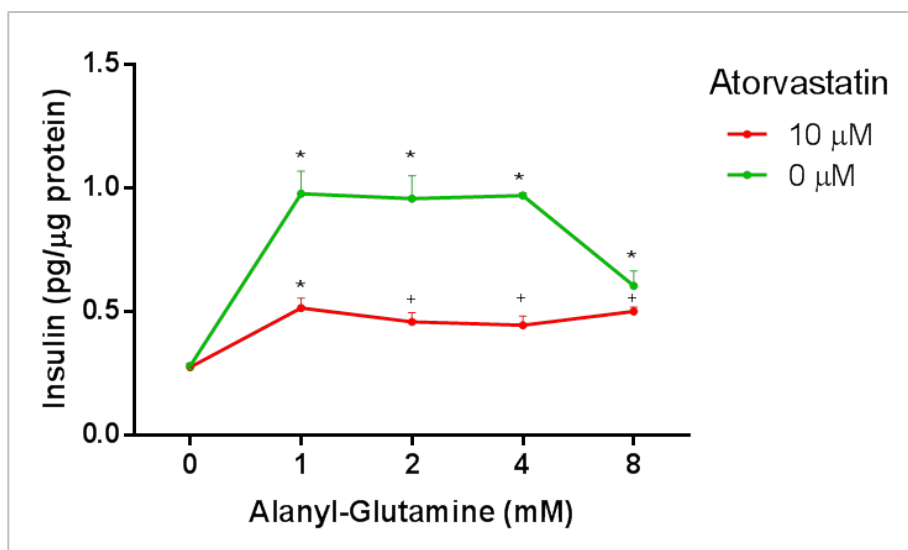


**Figure 6.1.** Dose-response of Ala-Gln pretreatment on insulin secretion stimulated by high glucose (16.7 mM) + 10 mM L-alanine.



No difference was seen between 1 and 4 mM Ala-Gln, but no Ala-Gln or high Ala-Gln reduced acutely stimulated insulin secretion. This data was from one experiment with 4 replicate wells. Error bars SEM. +  $P < 0.01$ , \*  $P < 0.001$  compared to 0 mM Ala-Gln in the same treatment group.

In agreement with earlier studies (Chapter 2), pravastatin and atorvastatin were associated with a reduction in insulin secretion but secretion was not restored by Ala-Gln. The absence of Ala-Gln had a similar influence to the deleterious effect of statins on insulin secretion (Figure 6.2A). Chronic (24 h) insulin secretion was slightly increased with Ala-Gln ( $P < 0.01$ , Figure 6.2B), especially when combined with atorvastatin treatment.

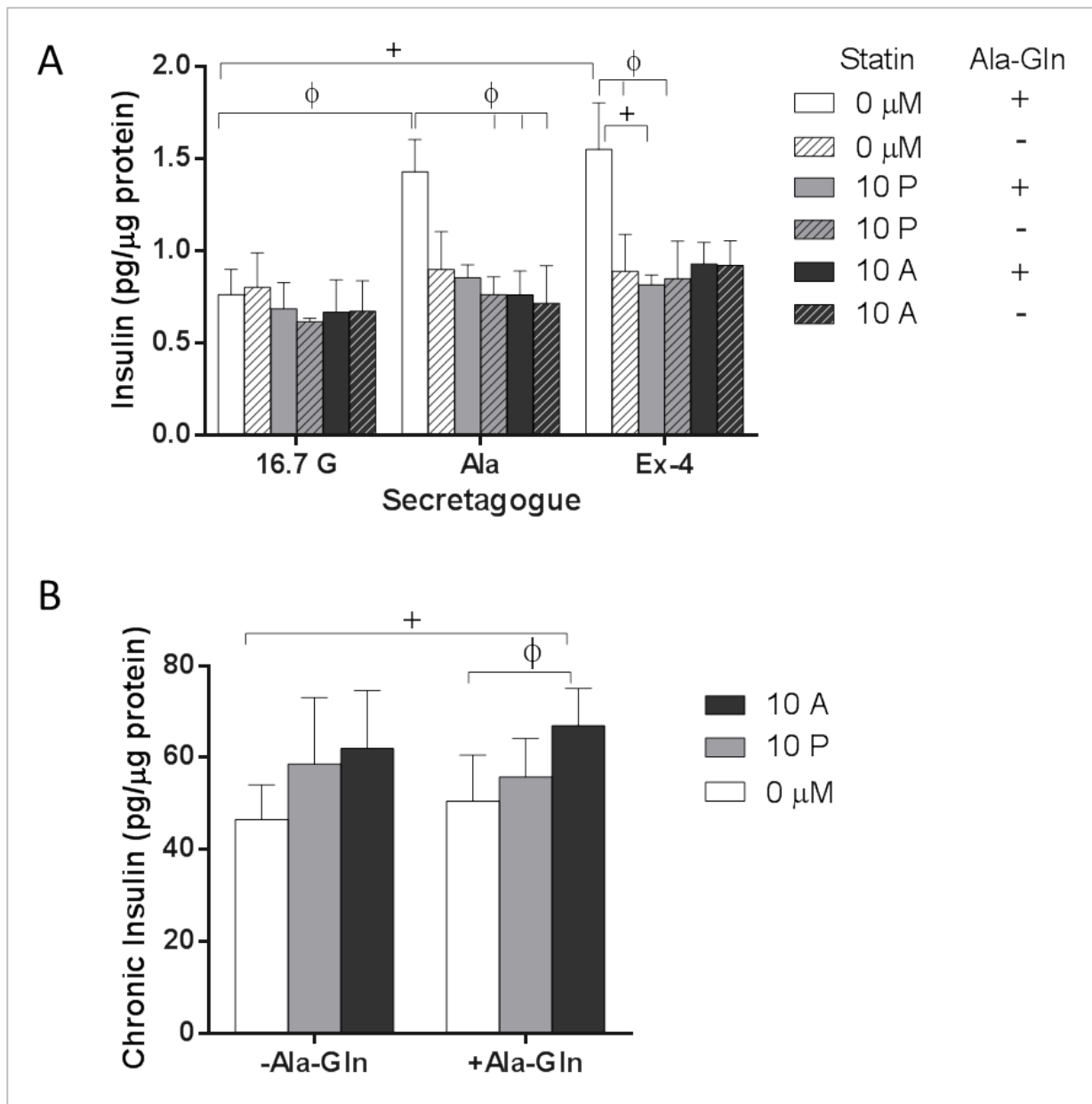


**Figure 6.2. Effect of alanyl-glutamine (Ala-Gln) on acute and chronic insulin secretion.**

**A.** Acute insulin secretion in BRIN-BD11 cells stimulated by 16.7 mM glucose (G) alone or with 10 mM alanine or 10 μM exendin-4 after 24 h incubation with or without 10 μM atorvastatin or pravastatin and/or Ala-Gln. **B.** Chronic (24 h) insulin secretion with or without atorvastatin, pravastatin and Ala-Gln. 10 A, 10 μM atorvastatin; 10 P, 10 μM pravastatin. Error bars ± SEM; n=3; +,  $P < 0.01$ ; φ,  $P < 0.05$ .

To determine whether the insulin secretion effects described above were related to mitochondrial function, studies were conducted using the Seahorse extracellular flux analyser. In the absence of statins, Ala-Gln starvation reduced basal respiration (BR,  $P < 0.01$ ) and ATP production (AP,  $P < 0.01$ ), but, interestingly, it did not affect maximal respiration (MR), and hence increased spare respiratory capacity (SRC), calculated as the difference between MR and BR (Figure 6.3A). In cells supplied with Ala-Gln and as seen previously (see Chapter 3), atorvastatin treatment reduced BR ( $P < 0.05$ ), MR ( $P < 0.001$ ) and AP ( $P < 0.05$ ) compared to control cells. The effect of the presence or absence of Ala-Gln in atorvastatin-treated cells was generally smaller than in statin-free controls, significantly affecting only MR and SRC, with Ala-Gln provision paradoxically decreasing these related measures (see Table 3.1, Chapter 3 for the method of calculating the various parameters). In statin-free cells, Ala-Gln also produced an increase in basal oxygen consumption rate (BR,  $P < 0.01$ ) and ATP production (AP,  $P < 0.01$ ). The presence of Ala-Gln did not ameliorate atorvastatin-related oxygen consumption effects.

A general reduction in extracellular acidification rate (ECAR) was seen with Ala-Gln deficiency (Figure 6.3B). Amongst the metabolic parameters calculated from ECAR, the most affected by Ala-Gln was glycolytic capacity (GC) which was significantly reduced ( $P < 0.001$ ) in the absence of the dipeptide in both control and atorvastatin-treated cells. Its related function, glycolytic reserve (GR), was also reduced by Ala-Gln absence in statin-free cells ( $P < 0.01$ ).

Reduced SRC % when Ala-Gln was available during cell incubation was compensated by increased GR% in statin-free cells (Figure 6.3C). In atorvastatin-treated cells, the combined effect of reduced SRC and GR resulted in a small reduction in total energetic reserve. While glycolytic reserve % was increased in the presence of Ala-Gln ( $P < 0.01$ ), spare respiratory capacity % was reduced to an even greater extent ( $P < 0.001$ ), resulting in a small overall decrease in reserve (sum of GR% and SRC%) in the presence of Ala-Gln (Figure 6.3C).

When OCR was plotted in terms of ECAR (Figure 6.4), a tendency towards a more energetic phenotype was noted in Ala-Gln supplemented cells. Atorvastatin had no significant effect on aerobic phenotype, although there was a slight influence to reduce the aerobic capacity of the cells.

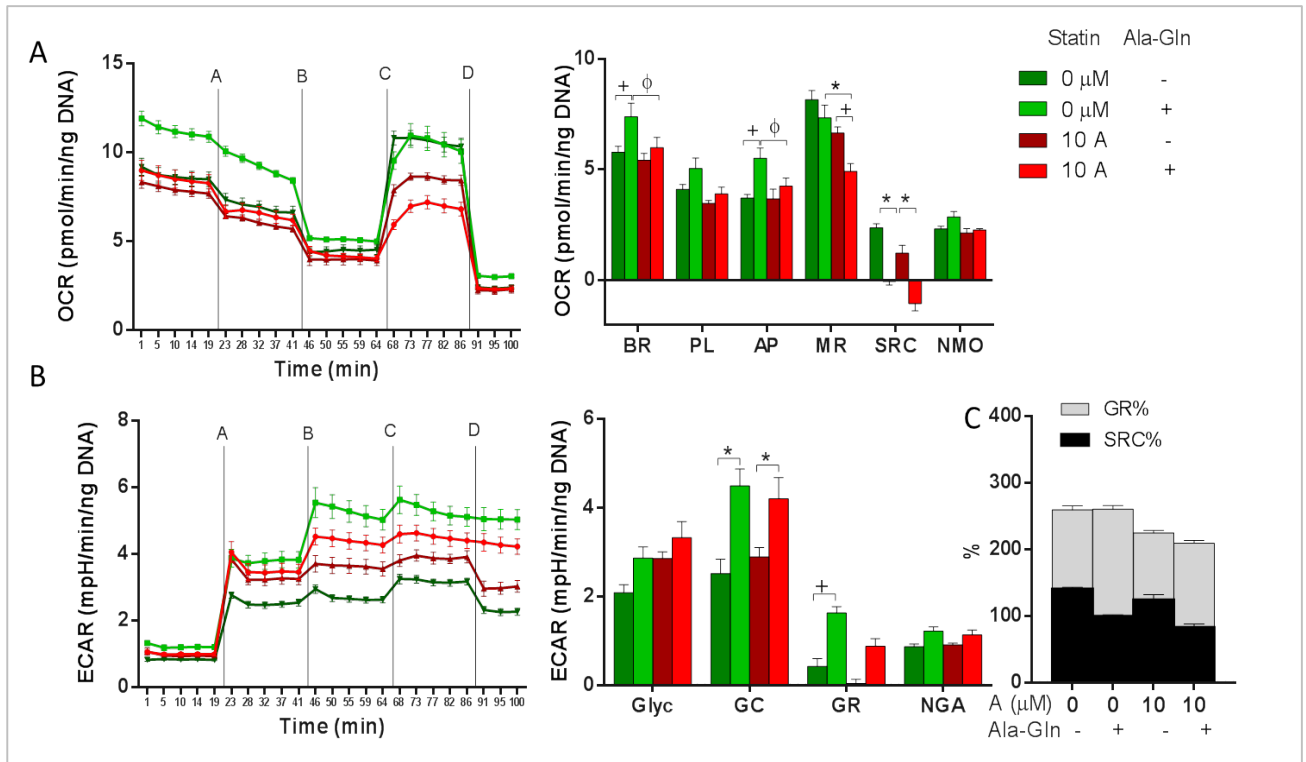


**Figure 6.3. Metabolic effects of Ala-Gln in combination with atorvastatin.**

**A) OCR and B) ECAR of BRIN-BD11 cells with or without 10  $\mu$ M atorvastatin and Ala-Gln. C. Stacked graph showing the influence of atorvastatin with or without Ala-Gln on mitochondrial capacity represented by GR% and SRC%.**

10A, 10  $\mu$ M atorvastatin; Ala-Gln, alanyl-glutamine. Representative experiment with 6 replicates. BR, basal respiration; PL, proton leak; AP, ATP production; MR, maximal respiration; SRC, spare respiratory capacity; NMO, non-mitochondrial oxidation; Glyc, glycolysis; GC, glycolytic capacity; GR, glycolytic reserve; NGA, non-glycolytic acidification. \*  $P < 0.001$ , +  $P < 0.01$ ,  $\phi$   $P < 0.05$ . Error bars  $\pm$  SEM.

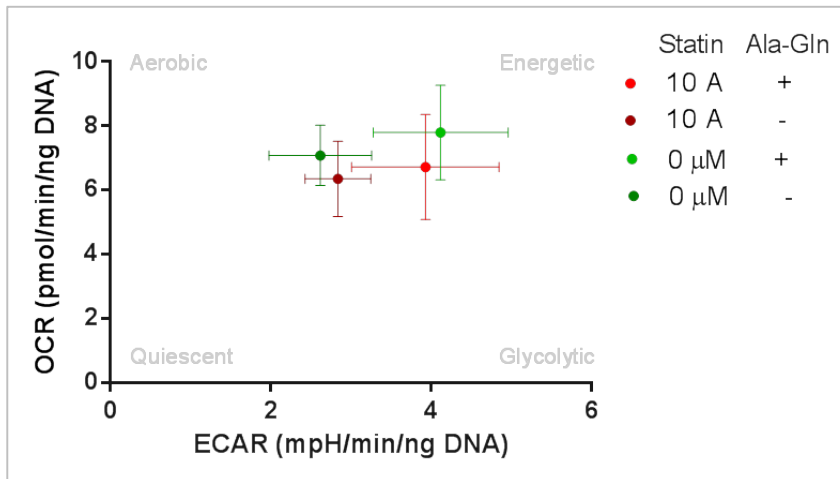


**Figure 6.4. Effect of Ala-Gln and atorvastatin on energetic state of BRIN-BD11 cells.**

The relationship between OCR and ECAR gives an overview of the energetic state of the cells after the various treatments. Ala-Gln moved the phenotype slightly towards an energetic state both with and without atorvastatin treatment (not significant). Atorvastatin, both with and without Ala-Gln, moved the cells slightly towards a more glycolytic phenotype (not significant). Error bars  $\pm$  SD.

## 6.4 Discussion

Glutamine is the most abundant amino acid in the human body; average extracellular concentrations are ~0.7 mmol/L while intracellular concentrations vary between 2 and 20 mmol/L, depending on cell type (717). Normal daily dietary intake is <10 g and humans produce 40-70 g/day endogenously (739). However, in insulin resistant states, including in T2D, an increased tissue requirement for glutamine often results in low plasma levels (723). The aim of this study was to determine the influence of glutamine (as alanyl-glutamine) on atorvastatin-treated BRIN-BD11 cells; specifically, to assess its potential to ameliorate the adverse effects of atorvastatin on mitochondrial function and insulin secretion as reported in Chapters 2 and 3. The results clearly show that Ala-Gln could not ameliorate these deleterious effects of atorvastatin. In fact, an adverse effect of Ala-Gln in statin-treated cells was observed on maximal respiration and spare respiratory capacity.

The absence of Ala-Gln had a similar influence to the deleterious effect of atorvastatin in blunting stimulated insulin secretion, and the addition of Ala-Gln could not restore the detrimental effect of atorvastatin at any of the concentrations used, including 2 mM, typically present in culture media (Figure 6.1). Interestingly, stimulated secretion was blunted in control cells pre-incubated with the highest Ala-Gln concentration (8 mM). Similarly to results reported in Chapter 2, insulin secretion was blunted by statins when acutely stimulated with high glucose and alanine or exendin-4, and this was not restored by Ala-Gln (Figure 6.2A).

Furthermore, atorvastatin-induced changes in mitochondrial function were not restored by Ala-Gln supply. Rather, there was an overall decrease in respiratory reserve (sum of GR% and SRC%) (Figure 6.3C). In addition, maximal respiration, which, similarly to previous findings (see Figure 3.1), was reduced with atorvastatin treatment (-1.2-fold,  $P = 0.01$ ), was further reduced with simultaneous Ala-Gln treatment (-1.5-fold,  $P < 0.0001$ ). Also similar to previous findings, ATP production was diminished by atorvastatin treatment ( $P < 0.05$ , compare Figure 6.3A and Figure 3.1), but this was not rescued by the addition of Ala-Gln. Thus, while mitochondrial changes induced by atorvastatin treatment were consistent with previous findings, they were not reversed by Ala-Gln treatment.

A possible reason for the failure of glutamine to completely restore maximal stimulated insulin secretion in atorvastatin-treated cells could relate to oxidative stress induced by this statin, keeping in mind that glutamine is a key player in regulating antioxidant defences. The effect of statins on oxidative stress is under considerable debate, as discussed in Section 1.3.4.3. Statins have been associated with both increased and decreased ROS, mainly via changes in the availability of isoprenoid intermediates of cholesterol synthesis. HMGCR inhibition depletes isoprenoid intermediates along with cholesterol, including geranylgeranyl pyrophosphate

(GGPP) and farnesyl pyrophosphate (FPP) (304). GGPP and FPP prenyl groups post-translationally bind to signalling proteins such as the rho family of small G proteins, thereby recruiting them to membranes; reduced signalling can sometimes reduce ROS, as when recruitment of subunits including prenylated Rac1 are required for nicotinamide adenine dinucleotide phosphate oxidase (Nox) activation at the membrane. Decreased endoplasmic reticulum and LDL-related oxidative stress have also been associated with statin therapy (reviewed in 210). On the other hand, unmitigated mitochondrial ROS generation due to ubiquinone (CoQ10) deficiency after statin therapy was associated with ROS increases (40). A recent study in human islets and INS-1 cells demonstrated that atorvastatin (100 nM) is associated with mitochondrial dysfunction characterised by diminished CoQ10, other complexes of the respiratory electron transport chain, and ATP production, resulting in increased ROS and reduced stimulated insulin secretion (356). It is possible that ROS arising from different cellular compartments has different effects on metabolism and insulin secretion, as reported by Mailloux *et al* (358). In the current study, atorvastatin was clearly associated with reduced insulin secretion and mitochondrial dysfunction which was not rescued by alanyl-glutamine, and more work is needed to clearly specify the mechanisms.

While glutamine, as a substrate for glutamate and thus glutathione synthesis, is important in decreasing mitochondrial ROS via the glutathione redox system and may thus be expected to ameliorate statin-induced ROS increases, there are three considerations in the context of this study which may limit, or even reverse, any beneficial effects: a) glutamine oxidation *per se* can add to respiratory ROS production (740, 741), b)  $\beta$ -cells are known to be sensitive to ROS because of their relatively low redox capacity (490, 742); and c) glutathione peroxidase synthesis may be inhibited by statins (40, 743, 744). These factors make it less likely that glutamine-dependent antioxidant processes would be able to restore oxidative balance.

Interestingly, increased glutathione peroxidase activity together with increased superoxide dismutase and glutathione reductase activity and glutathione concentration was reported by Mikasinovich & Belousova (514) using simvastatin-treated rats. They suggested this may be indicative of hypoxic adaptation due to simvastatin-related hypoxia. The mitochondrial switch towards glycolysis as described in Chapter 3, and, to a lesser extent, this chapter, would support this conclusion.

High levels of ROS products may lead directly to mitochondrial impairment, but observed changes in insulin secretion and mitochondrial function could also be explained by mitochondrial uncoupling, for example by uncoupling protein 2 (UCP-2), which could mediate damage from ROS (267, 358, 745). Interestingly, a link between glutamine and mitochondrial uncoupling exists in the recent discovery that glutathionylation of UCP-2 inhibits proton leak and amplifies GSIS, while ROS-mediated reversal of glutathionylation of UCP-2 establishes

proton leak and decreases GSIS (358). Hence the presence of glutamine, a substrate for glutathione, could be expected to attenuate proton leak through UCP-2 and would thus increase GSIS in the absence of ROS. Interestingly, high glutamine concentrations were found to increase uncoupling in myocytes and differentiated myotubes (741). Whether statins affect UCP may be an interesting question. In adipocytes, atorvastatin had no effect on UCP-1 expression in one study (746). In contrast, elsewhere HMG-CoA synthase 2 (HMGCS2), an enzyme involved in HMGCR synthesis, strongly correlated with UCP1 expression and was reduced significantly by HMGCS2 knockdown and simvastatin treatment (747). Decreased UCP-2 was also found in a model of intermittent hypoxia similar to sleep apnoea (748). If, as discussed above, statin treatment is linked to hypoxic stress, a change in UCP-2 could be anticipated. A literature search was unable to uncover information on the status of UCP-2 in  $\beta$ -cells treated with statins, making this a potentially unexplored area of study. This is an area of potential interest, given that the mevalonate pathway, and more specifically, the prenylation of small GTP-binding proteins, is thought to regulate adipocyte browning, while statins reduce UCP1 expression in brown adipocytes (747).

Glutamine can supply carbons for entry to the TCA cycle in the presence of leucine and thus contribute to the production of ATP (715), which may account for the trend towards a more 'high energy' phenotype in the presence of glutamine (Figure 6.4). This, in turn, could be expected to increase insulin secretion in  $\beta$ -cells. Both increased ATP production and insulin secretion were observed in statin-naïve cells, but not in the presence of atorvastatin, potentially suggesting a different fate of glutamine in statin-treated cells, which may be due to direct toxicity or compensatory mechanisms.

Of interest to this study, a hypothesis that hypoglutaminaemia may be an adaptive mechanism to maximise metabolic efficiency in acute stress such as critical illness has been suggested (741). Krajcova *et al* reported an optimal efficiency of aerobic phosphorylation at 300  $\mu$ M glutamine supplementation (15% of the glutamine available in most media and ~40-60% of physiological plasma concentrations (715)) in myoblasts and myotubes. Higher concentrations reduced efficiency via respiratory uncoupling. Whether similar efficiency changes are linked to glutamine in  $\beta$ -cells would need to be assessed, as the metabolic fate of glutamine may be tissue-specific.

Chronic insulin secretion measured over 24 h was similar in statin-naïve cells with or without Ala-Gln, suggesting that basal insulin secretion was not dependent on the presence of Ala-Gln. This is perhaps surprising, considering that a recent study found that the absence of Ala-Gln reduced 24 h insulin secretion by 78% in BRIN-BD11 cells (749). It is unclear why there was a difference in results, but it is quite likely related to differences in incubation conditions, including the use of DMEM culture medium as opposed to RPMI.

Atorvastatin was associated with increased chronic insulin secretion, but only in the presence of Ala-Gln. It is likely that this difference is due to the statistical power of the experiment, as a similar trend is apparent in the Ala-Gln negative group. There was a similar small but significant increase in chronic insulin secretion observed with pravastatin (but not atorvastatin) treatment reported in Chapter 2, in which normal media containing 2 mM glutamine was used. It is not known why a discrepancy exists over which statin is associated with this effect, but hydrophilicity and the binding of statins to serum protein may influence their ability to block  $K^+_{ATP}$  channels, causing hypersecretion (750). Also, it should be remembered that both amino acids in the dipeptide, which was used because of its superior stability and common use in therapeutic contexts compared to pure glutamine (751), may have an influence on insulin secretion. L-alanine is known to stimulate insulin secretion directly but L-glutamine does not except in combination with other amino acids, particularly L-leucine (244). Indeed, both L-alanine and L-glutamine (in combination with L-Leucine) were used as secretagogues in previous experiments (see Chapter 2). This presents a possible explanation for increased chronic insulin secretion over 24 h in atorvastatin-treated cells in the presence of Ala-Gln. However, it does not explain the difference between long-term secretion in statin- and vehicle-treated cells.

Another possible cause for increased chronic insulin secretion is leakage due to cell enlargement or other changes in cell membrane composition. Cholesterol deficiency could potentially influence membrane integrity and thus insulin 'leak'. Cell swelling associated with atorvastatin treatment could also play a role. An increase in cell size observed in relation to atorvastatin treatment was reported in Chapter 4. It is known that cell swelling induces insulin secretion (270, 633, 634). However, the latter work was in the context of osmotically induced swelling and demonstrated that this invokes a calcium-independent pathway of exocytosis. Whether atorvastatin-related cell enlargement (see Section 4.4.5) has similar characteristics is unknown.

#### 6.4.1 Summary and future directions

There are few studies on the effects of glutamine in combination with statins in  $\beta$ -cells. In the current study glutamine, provided in the form of Ala-Gln, was found to have little ameliorating effect on reduced insulin secretion or metabolic changes associated with pravastatin or atorvastatin treatment, although it greatly improved insulin secretion response and ATP production in otherwise glutamine deprived cells without statins. Some parameters actually demonstrated poorer outcomes with availability of the dipeptide. This is despite the expectation that glutamine may protect mitochondrial structure and function in oxygen toxicity (752).

There is a physiological basis for the hypothesis that the presence of supra-physiological glutamine concentrations in atorvastatin-treated cells may increase mitochondrial ROS. In summary, statin-induced inhibition of ubiquinone and glutathione peroxidase synthesis together

with glutamine-induced increases in ROS-generating flux through the TCA cycle could overwhelm the capacity of the glutathione redox system in  $\beta$ -cells, known for their relatively low redox potential, to maintain homeostasis. This would result in inadequate mediation of UCP-2 via glutathionylation and potential oxidative damage, reducing the capacity to secrete insulin in a fuel-sensitive manner.

Interestingly, a clinical trial is currently under way to study the effect of oral L-glutamine supplementation on mitochondrial function in patients with chronic kidney disease (<https://clinicaltrials.gov/ct2/show/NCT02838979>). While this trial is not related to statin therapy, it is specifically targeting mitochondrial function with L-glutamine and the results will be interesting to consider in the context of mitochondrial impairment, including that caused by statins.

The shortage of experimental evidence of the effects of statins in ROS processes in  $\beta$ -cells, with only one published study to the best of my knowledge, leaves much room to explore this topic further. Modification of the redox potential by addition of CoQ10 or another antioxidant, together with Ala-Gln, would assist in clarifying the mechanistic role of ROS in the influence of glutamine as reported here. The possibility of UCP-2 involvement via its glutathione link is unexplored. In addition, the interaction between statin and glutamine metabolism in the  $\beta$ -cell context is an interesting, novel opportunity.



## Chapter 7 Conclusion

This project examined the influence of changes in intracellular cholesterol on  $\beta$ -cell function, including insulin secretion. This is of significance in the context of an association between the widely-used class of cholesterol lowering agents, the statins, and increased risk of diabetes. The preceding chapters address the aims of this Thesis using an *in vitro* model of  $\beta$ -cells supported by some work with rat islets and a mouse model in both health and a diet-influenced insulin resistant state. The aims and principal findings are summarised below.

The first aim, addressed in Chapter 2, was to determine the impact of  $\beta$ -cell cholesterol content on insulin secretion in response to glucose and other physiological and therapeutic  $\beta$ -cell secretagogues. Two different means of altering cell cholesterol content were used: a) inhibition of cholesterol synthesis using statins, or b) delivery or sequestration of cholesterol by M $\beta$ CD in its cholesterol loaded or naked forms, respectively. Both cellular cholesterol enhancement using c-M $\beta$ CD and depletion using statins reduced robust stimulation of insulin secretion using a combination of high glucose (16.7 mM) plus either L-alanine or glutamine and L-leucine (all 10 mM) in a dose-dependent manner. M $\beta$ CD had a weaker influence than statins in reducing  $\beta$ -cell cholesterol and a weaker influence than both statins and c-M $\beta$ CD on subsequent attenuation of insulin secretion. Similarly, insulin secretion from rat islets stimulated with high glucose (16.7 mM) plus L-alanine (10 mM) was attenuated by 24 h treatment with 10  $\mu$ M atorvastatin. Little influence was seen on basal insulin secretion, although chronic secretion over 24 h was elevated in some instances. The differential effects according to the strength of stimulation may be due to a variety of reasons, discussed further below.

Tolerability of statins and differential pleiotropic effects in the clinical setting have been attributed to differences in permeation into non-hepatic tissue due to variations in lipophilicity between members of the statin family (170, 637). The second, and related aim, addressed in Chapter 2 and indeed throughout the project, was to compare the influence of several statins on  $\beta$ -cell function and insulin secretion. Pravastatin and atorvastatin, lipophilic and hydrophilic statins, respectively, were the main statins used throughout this work, in both *in vitro* and *in vivo* contexts. Several other statins of varying lipophilicity were additionally used to support the main findings. Studies reported in this work support clinical findings of reduced adverse effects for pravastatin compared to atorvastatin on  $\beta$ -cell function (753), although whether this is due to differences in lipophilicity has not been investigated. Several considerations related to this are discussed below. This is a clinically relevant finding, and supports several meta-analyses revealing a lower risk of T2D, or adverse events generally, associated with pravastatin compared to atorvastatin (754-756).

The reduced insulin secretion observed in Chapter 2 may be due to a variety of reasons, including stimulus/secretion coupling, to which the production of ATP through glycolysis and oxidative phosphorylation is central. The third aim, explored in Chapter 3, therefore examined whether changes in cell cholesterol influenced  $\beta$ -cell energetics, mitochondrial function and stimulus/secretion coupling. Statins were found to reduce ATP production and maximal respiration while, at the same time, increasing glycolysis. These effects represent a potential mechanism by which robust insulin secretion is diminished by statins. Metabolic reserve, indicated by glycolytic reserve and spare respiratory capacity, was also attenuated by statins, possibly providing a clue to the differential effect of statins on basal vs robustly stimulated insulin secretion. As anticipated from insulin secretion studies, pravastatin had a more modest effect on  $\beta$ -cell mitochondrial function than that of atorvastatin or simvastatin.

In the fourth aim, the influence of cholesterol on selected proteins relevant to  $\beta$ -cell function was investigated. Thus in Chapter 3, a panel of glycolytic enzymes was assessed by Western blot to determine whether increased glycolysis was associated with their differential regulation. In addition, selected proteins related to oxidative stress, lipid homeostasis and metabolic or mitogenic signalling were examined by Western blot in Chapter 4. In the same chapter, results generated through an opportunity to use a proteomics approach to obtain an overview of changes elicited by M $\beta$ CD and c-M $\beta$ CD were presented. The main findings from these various investigations were an increase in hexokinase I, ABCA1 and mTOR expression, stimulated by atorvastatin but not pravastatin. There was also increased phosphorylation of GSK3 $\beta$  and the insulin receptor in atorvastatin-treated BRIN-BD11 cells. These changes support the alterations in metabolic profile demonstrated by mitochondrial function assessments and suggest increased autocrine signalling, possibly with a more mitogenic rather than metabolic role, as discussed in Chapter 4. The iTRAQ proteomics study confirmed a greater modifying influence from c-M $\beta$ CD than M $\beta$ CD treatment, mainly on proteins in three functional categories including metabolism, protein synthesis and transport. However, there are several caveats to this work (discussed in Chapter 4) related to the sample preparation and possible replication issues as seen in differences between the two control samples. The iTRAQ work is based on just one experiment; hence further validation is required. These influences on various functional proteins have been discussed in the context of the available literature and provide a basis for further research into the mechanisms by which cellular cholesterol changes may impact  $\beta$ -cell function.

Flow cytometry was also used to investigate selected proteins in a whole, single cell context. However, the results appear to be subject to artefacts, possibly directly due to cholesterol effects on light scatter, permeabilisation and/or binding as discussed in Chapter 4.

An interesting incidental finding from flow cytometry analysis revealed that cell size, complexity and autofluorescence were significantly increased by atorvastatin, the increase in size reaching ~24%. This may be related to cholesterol content reduction, as M $\beta$ CD caused similar, though more modest increases in size, complexity and autofluorescence in line with its more modest effect on cholesterol depletion. In contrast, c-M $\beta$ CD, which effectively increased cellular cholesterol, was associated with the greatest changes in two of these parameters, considerably reducing complexity by ~20% and autofluorescence by ~40% in the appropriately gated group. However, cell size was modestly increased (by ~12%) by c-M $\beta$ CD treatment. Autofluorescence, thought to be associated with FAD and NAD(P)H activity (573), appeared to correlate with insulin content, so this could indicate metabolic alterations, though reduced autofluorescence may also be related to similar artefacts as those suspected to have influenced immunofluorescent studies and further investigation is required to more fully appreciate the potential ramifications of these observations.

The relevance of *in vitro* studies to the *in vivo* context is an important aspect, and the fifth aim and focus of Chapter 5 was to evaluate the effect of statins on glucose homeostasis in mice, with or without pre-existing obesity and insulin resistance induced by HFD feeding. C57Bl/6J mice, pre-fed or not with a high fat diet, were administered atorvastatin or pravastatin for 12 weeks. Mice on a high fat diet were heavier, more insulin resistant and less glucose tolerant, and atorvastatin exacerbated the glucose intolerance (OGTT) but not insulin resistance (HOMA-IR). Fasting glucagon was also increased in the insulin-resistant, statin-treated animals. In healthy mice, atorvastatin was associated with increased  $\beta$ -cell activity and a trend towards increased insulin resistance. Pravastatin followed similar trends to atorvastatin in both healthy and insulin resistant mice, but to a lesser extent. Statins did not influence glucose tolerance in healthy animals.

Studies in our laboratory and as described in Chapter 1 suggested that glutamine supplementation may be critical to  $\beta$ -cell health, and thus insulin secretion. The sixth aim, addressed in Chapter 6, was therefore to determine whether glutamine is protective of statin-induced impairment of  $\beta$ -cells. Results demonstrated that glutamine, introduced as a dipeptide with L-alanine (alanyl-glutamine), did not rescue, and if anything, exacerbated statin effects in  $\beta$ -cells, including reducing ATP production and insulin secretion.

Discussions throughout this project relate to the observations made and to the aims, summarised above. Novel aspects include the comprehensive study of insulin secretion in BRIN-BD11 cells after manipulation of cholesterol content across a wide range, including both cholesterol enrichment and depletion; the study of the effect of statins on mitochondrial function using the Seahorse extracellular flux analyser; the mouse study of statins in the context of a diet-induced insulin resistant state, including fasting glucagon measures; the study assessing whether alanyl-

glutamine could be beneficial in ameliorating some effects of statins; the studies on the effect of statins on some physical cell characteristics by flow cytometry; and the iTRAQ proteomics study, which has never been examined before (though still requiring validation). A broader discussion linking some of the ideas in this project follows.

For some time, evidence pointing to a diabetogenic effect of statins has been accumulating. Many putative mechanisms for this influence have been postulated, including those relating to products of the mevalonate pathway or cholesterol itself, and those relating to other pleiotropic effects, such as an influence on ion channels or granule fusion events. Those related to  $\beta$ -cell function are summarised in Figure 7.1.

Thus far, and on the basis of *in vitro* studies in BRIN-BD11 cells, it has been established, through both the use of statins and c-M $\beta$ CD, that cellular cholesterol changes do affect insulin secretion in response to robust stimulation. Further, this effect is similar with both increased and decreased cellular cholesterol levels, and is relative to both the magnitude of the change in cholesterol concentration and the strength of insulin secretion stimulus. In addition, the mouse study also demonstrated that a diet-induced insulin resistant state can modify the diabetogenic influence of statins in mice and the studies in Chapter 3 suggest that mitochondrial function may be one possible mechanism by which cholesterol changes affect  $\beta$ -cell function. Indeed, it is likely that several effects of the inhibition of cholesterol synthesis work synergistically or in opposition in  $\beta$ -cells, interacting with environmental (e.g. hormones, statin dose, ROS, nutrient milieu) and phenotypic factors (e.g. redox potential, enzyme expression, oxidative phosphorylation capacity). Evidence of such interactions observed in this project are, for example, the diet-dependent effects on insulin resistance and glucagon. This is not surprising, given that cholesterol synthesis and glucose metabolism are such fundamental, closely regulated cellular and systemic processes. A high degree of complexity is supported by the large variability in individual response to statins found in clinical trials, which can range from 70% LDL cholesterol reduction to 10% increase (137), and which was reflected in some individuals in the animal study in Chapter 5.

The current project suggests that changes in cholesterol content influence  $\beta$ -cell function, and the mechanisms of statin-associated diabetogenicity are a) likely to be associated with cholesterol changes in  $\beta$ -cells, b) differential based on specific statins, c) secondary, at least in part, to mitochondrial impairment, d) affected by environmental factors such as diet, and e) associated with complex metabolic and phenotypic changes, including increased glycolysis in  $\beta$ -cells, and, at least to some extent, compromise of native  $\beta$ -cell characteristics to support pro-survival adaptations. These aspects are discussed further below. To keep the literature up-to-date in a burgeoning research area, many of the articles quoted in this thesis were written after commencement of the project, and in some cases, after completion of experiments.

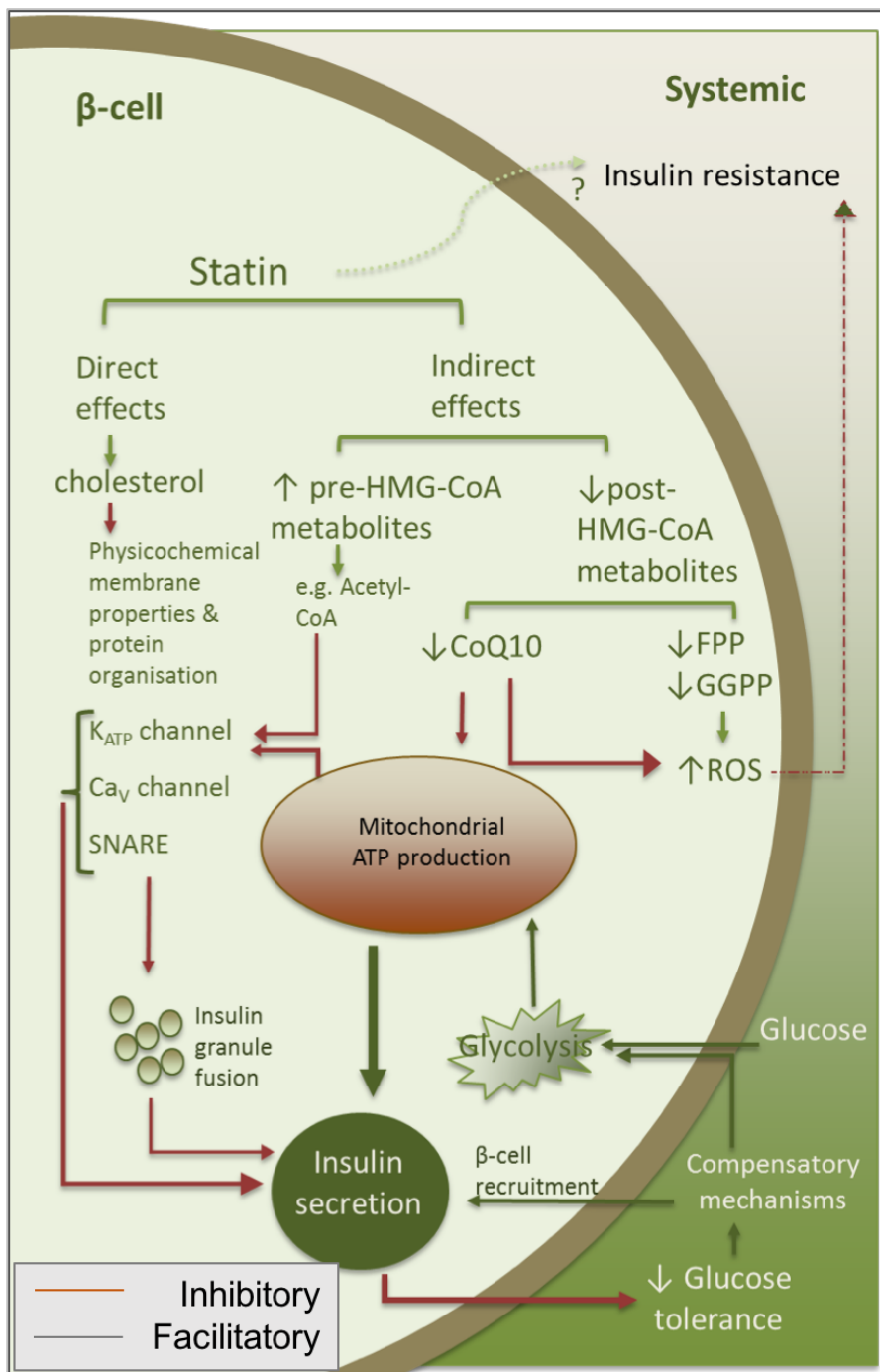


**Figure 7.1. Potential hypoinsulinaemic mechanisms of statins in  $\beta$ -cells**

Statins potentially exhibit adverse effects on  $\beta$ -cell function directly by on-target cholesterol depletion or by indirect effects. Reduced cholesterol synthesis may deplete membrane cholesterol, affecting the physicochemical properties of cell membranes and those of insulin granules. In turn, this may influence the function of membrane proteins such as ion channel proteins, and those involved in glucose sensing and granule fusion. Indirect effects include those relating to both increased pre-HMG-CoA metabolites and decreased post-HMG-CoA metabolites. For example, elevated cellular long-chain fatty acids resulting from accumulation of acetyl-CoA can influence  $K_{ATP}$  channel function. Reduced mevalonate pathway products such as CoQ10 and prenylation moieties may influence mitochondrial function and the cellular redox capacity. Compensatory mechanisms may reduce stimulus-secretion coupling and lead to  $\beta$ -cell dedifferentiation and reduced capacity to secrete insulin. Statins may have additional influences on insulin resistance beyond the scope of this study.

## 7.1 Cellular cholesterol changes intrinsically influence $\beta$ -cell function.

Cellular cholesterol changes appear to have an intrinsic influence on the function of  $\beta$ -cells. This is evidenced by the amelioration of insulin secretion by both statin-mediated inhibition of cholesterol synthesis and desorption or loading of cholesterol by M $\beta$ CD in its naked or pre-loaded forms, respectively. Potential mechanisms of this effect include interruption of lipid rafts and attendant failure of ion channels, granule fusion processes and membrane-associated transport proteins (69, 73, 331).

Alanine plus high glucose-stimulated insulin secretion in this study was found to support the hypothesis that the relationship between  $\beta$ -cell cholesterol content and stimulated insulin secretion is tri-phasic, characterised by optimal mid-range cholesterol concentration flanked by low and high cholesterol content which reduces insulin secretion (Chapter 2 Figure 2.7). Less robust stimulation or basal secretion was mostly not affected by cholesterol changes. Putative reasons for this difference could be differential mechanisms involved in stimulated vs basal insulin secretion, reduced reliance on metabolic coupling factors, which could be affected by modified cellular cholesterol levels, a rate-limiting effect of cholesterol changes in some unidentified process involved in secretion, for example, granule fusion, ATP production (due to reduced maximal respiration), or ion channel opening such that it is not affected at basal secretion rates but cannot maintain a suitable velocity for higher secretion rates. Differential effects may also be due to reduced power to determine a smaller effect, although similar differences have also been reported elsewhere (354).

There is an established association between cholesterol and glucose homeostasis. This is evident in the high rate of concomitant diabetes and hyperlipidaemia. A recent study demonstrated that the association may be more direct than previously understood. In streptozotocin-treated, recently diabetic rats, Romano *et al* (757) discovered alterations in steroidogenesis and cholesterol homeostasis, and defects in mitochondrial function in the hippocampus. This demonstrates the possibility that glycaemia may influence cholesterol metabolism, rather than or in addition to dyslipidemia leading to diabetes, as is commonly understood. It has also recently been noted that cholesterol can be protective against oxidative stress and  $\beta$ -amyloid activity in neuronal cells (758), revealing a new role for this sterol more often associated with adverse effects.

One could also surmise as to whether cholesterol flux rather than (or as well as) its overt presence in sufficient quantities could be beneficial in insulin secretion. Several studies demonstrate the importance of various cholesterol transporters such as ABCA1 (72, 337, 341, 343, 599), ABCG1 (72, 97, 342, 599), and HDL (91, 611), to insulin secretion and glycaemic

health. In addition, a recent study established lipogenesis, including cholesterol synthesis, as a carbon ‘exhaust’ mechanism in  $\beta$ -cells in the context of chronic over-nutrition (243). Statins can affect cholesterol flux both by its impact on the function of cholesterol transporters (759, 760) and by inhibiting cholesterol synthesis, potentially producing a smaller cholesterol pool. While changes in ABCA1 expression were observed in the current study, the direct impact of statin-induced changes in cholesterol flux on insulin secretion would make an interesting study.

## 7.2 Differential effects of statins

Results of insulin secretion and mitochondrial function experiments as well as Western blots and the animal study all demonstrated differential effects between pravastatin and atorvastatin, with atorvastatin almost always causing a more marked deviation from the control and pravastatin having an intermediate effect. The regularity of this pattern over a variety of different approaches in this project was quite remarkable, but has also been demonstrated in clinical trials, albeit with some variations (see Table 1.1).

The most notable and often cited difference between pravastatin and atorvastatin is lipophilicity. Some other important differences between atorvastatin and pravastatin, some of which are relevant clinically and *in vivo* because they affect exposure and therefore efficacy and toxicity, are outlined in Table 7.1

Many reasons for variable effects of individual statins are based in the biology of the recipient. For example, phenomic differences in enzyme activity and carrier proteins affecting intestinal and hepatic uptake, and co-morbidities and/or medications, allergies and diet can all influence efficacy and adverse events (304). Patients with genetic variations in transporters or metabolising enzymes necessary for various statins may suffer adverse events due to greatly increased exposure (761). A recent review describes many examples of this, including polymorphisms in drug metabolism genes of the CYP family, drug transporter genes such as members of the ABC and SLCO transporter families, and other genes that can influence statin efficacy or toxicity, such as APOE, HMGCR and LDLR (175). Pharmacogenomic studies can help to increase awareness of avoidable adverse events within specific genotypes.

Similarly, pharmacological factors such as drug-drug interactions where induction or inhibition of, or competition for a transporter exists can greatly increase plasma concentrations of some statins (761). For these reasons, a one-size-fits-all approach is inadequate for many patients being prescribed statin therapy and the recent interest in personalised medicine may be very helpful in reducing adverse events, including new onset diabetes, in the very large patient cohort who may benefit from these drugs.

**Table 7.1. Pharmacological variations between Pravastatin and Atorvastatin.**

	<b>Pravastatin</b>	<b>Atorvastatin</b>
Type	1 (fungal derived)	2 (synthetic)
Solubility in water	hydrophilic	lipophilic
Form of administration	Acid form	Acid form
Hepatic extraction	Low	Medium (~0.42) Extensive first-pass metabolism in intestine and liver.
Enzymes	None	CYP3A4 (abundant in the intestine)
Transporters	OATP MRP2	Passive diffusion OATP MCT P-glycoprotein (efflux) MRP (efflux) BCRP (efflux)
Potence	Medium (40 mg ≈)	High (≈10 mg)
Bioavailability (%)	18	12
T <sub>max</sub> (hours)	0.9 – 1.6	2 - 3
C <sub>max</sub> ng/mL	45 - 55	27 - 66
Total body clearance (L/h)	371.3 ± 171	37.5
BBB crossing	No	?
T <sub>1/2</sub> (hours)	1.8	9.5 ±3.7 (active form) Up to 60 (total)
Plasma protein binding	Low ~45%	High ~90%
Elimination	Biliary Renal	Direct from blood to intestine Biliary

MRP – multi resistant drug family; OATP – organic anion-transporting polypeptide family; MCT – monocarboxylic acid transporter; BCRP – breast cancer resistance protein. Information extracted from (43, 169, 172, 177, 761-764).

An early step supporting a shift towards a personalised approach to reduce the diabetogenic effects of statins is to identify markers that can accurately predict patients at increased risk of statin-related T2D onset. Recent evidence that even readily available information could be used to make informed decisions about the appropriateness of statin therapy is available from a retrospective analysis of data from two clinical trials (Treating to New Targets, TNT and Stroke Prevention by Aggressive Reduction in Cholesterol Levels, SPARCL). The authors aimed to evaluate the predictive power of insulin resistance plus either elevated triglycerides or BMI on future diagnosis of T2D associated with statin use (765). They found a greatly increased association between statins and T2D in two groups: those with elevated insulin resistance and triglycerides >1.7 mmol/L (27% increase over those receiving placebo) and those with elevated insulin resistance and BMI ≥ 27 kg/m<sup>2</sup> (22% increased risk than the placebo group with a similar profile). This finding is consistent with the mouse study reported in this work to the



extent that statin treatment reduced the capacity to respond to a glucose load in insulin resistant animals as judged by the shape of the OGTT curve, though this was not reflected to the same extent in the AUC. On the other hand,  $\beta$ -cell function (HOMA-%B), representing insulin secretion, was increased by atorvastatin in healthy animals ( $P < 0.01$ ), resulting in a trend, albeit weak ( $P = 0.2$ ), towards reduced fasting glucose, but in diet-induced insulin resistant animals, atorvastatin did not affect  $\beta$ -cell function (HOMA-%B) or fasting glucose. Sizeable individual variation in the statin-treated animals was also observed, which could be due to factors described above.

The problem then remains: by what mechanism is the risk of T2D increased by statins in this cohort? Does this drug simply escalate an inevitable result? Perhaps there is an interaction between statins and an unknown feature of the pre-diabetic metabolic profile? Or do statins exert a diabetogenic pressure that exacerbates a pre-existing tendency to diabetes?

A phenomics approach in a prospective cohort study of prediabetic patients on statins or placebo would be helpful to answer these questions. However, evidence from the current project and other studies (discussed in Chapter 3) suggest that mitochondrial impairment may hold a clue to the diabetogenic effect of statins.

### 7.3 Mitochondrial impairment associated with statins

Mitochondria play a central role in cell fate and, in response to various stimuli, can influence the cell towards apoptosis, necrosis or survival, each of which require mitochondrial participation (766, 767). In  $\beta$ -cells mitochondria are involved in processes that affect survival vs apoptosis, replication (768) and uncoupling (769). These organelles are also fundamental to respiration, fuel sensing, lipogenesis and both triggering and amplifying insulin secretion, the former by mitochondrial glucose oxidation and the latter by mitochondrial coupling factors derived from glucose, amino acids and fatty acids (346, 770). These stimulus-secretion coupling factors include, but are not limited to, ATP, NADPH, glutamate, citrate, cAMP and malonyl-CoA (see Figure 1.3). Loss of mitochondrial flexibility, the ability to utilise a variety of substrates including glucose, amino acids and fatty acids, plays a key role in  $\beta$ -cell dedifferentiation, a vital pathophysiological mechanism in T2D (771). Mitochondria are also of significant interest in understanding the diabetogenic effect of statins. Before statins were found to have a diabetogenic influence, a link was made between patients with genetic mutations causing mitochondrial impairment and statin adverse events, primarily myopathy (167). These include common mutations that impair CoQ10 production (772).

In the current project, mitochondrial impairment characterised by reduced ATP production and maximal respiration was linked to statin exposure in a dose-dependent manner. Interestingly, statins that more potently reduced stimulated insulin secretion also impaired mitochondrial

function to a greater degree. A similar effect of statins on mitochondrial function has been found in muscle (508, 509), and a human endothelial cell line (EA.hy926) (773). This provides a possible explanation for the reduction of insulin secretion, which is directly linked to ATP production. However, how statins cause this effect remains unexplained.

Three possible ways statins may affect mitochondrial function include a) mevalonate pathway-related inhibition of the production of the electron transport chain components CoQ10 and Heme A, b) mitochondrial uncoupling due to ROS production or other mitochondrial stress, and c) the impact of reduced membrane cholesterol on mitochondrial membrane transporters crucial to insulin secretion. The first two processes may also work jointly, as CoQ10 is an efficient antioxidant. The influence of CoQ10 has been discussed in Chapter 3, and the discussion here will be limited to statin-associated ROS production, with a short comment on mitochondrial membrane transporters, whose role in mitochondrial function and insulin secretion has only recently come to the attention of researchers (770).

Mitochondria are obligatory ROS generators, and some ROS is required for normal GSIS (774). However, overproduction of ROS, as occurs in glucolipotoxicity, combined with the well-described limited redox potential in  $\beta$ -cells, is toxic, diminishing insulin secretion and causing apoptosis (18) or dedifferentiation (373, 775). Some statins have been shown to increase mitochondrial ROS production. For example, Chen *et al* (357) demonstrated increased ROS associated with atorvastatin but not pravastatin in NIT-1  $\beta$ -cells. Similarly, mitochondria isolated from rat islets and exposed to atorvastatin showed a dose-dependent increase in ROS, mitochondrial swelling and cytochrome C release, while ATP production was reduced (512). Elsewhere, a decrease in CoQ10 was linked to increased ROS associated with atorvastatin but not pravastatin, due to suppression of  $\beta$ -cell antioxidant defence systems (356).

While these studies clearly demonstrate a connection between statin and increased mitochondrial ROS, other studies, in contrast, suggest antioxidant properties of statins (see Section 1.3.4.3) (213, 440, 638). This apparent discrepancy may be rationalised by the possibility of differential effects in the intra- and extracellular compartments, as studies showing antioxidant effects are primarily measuring ROS in the circulatory system. The mechanisms of this effect are described elsewhere and are related to prenylation of small signalling G-proteins, prenylation moieties being the product of mevalonate pathway intermediates and thus inhibited by statins (210, 304).

ROS are capable of interrupting enzyme activity, ion channel transport, signalling from receptors and gene expression regulation, thereby impairing the function of  $\beta$ -cells and triggering apoptosis (520). More specifically, accumulation of ROS inactivates  $\beta$ -cell specific transcription factors such as duodenal homeobox factor 1 (PDX1) and MAFA, reducing insulin synthesis (545). These transcription factors are also important in the maintenance of normal

$\beta$ -cell function, and their dysregulation may be involved in dedifferentiation (520, 545). A similar mechanism may contribute to the development of T2D (490), directly linking statins and diabetes.

A ROS-related mechanism has also been proposed for myopathy, a widely-experienced adverse effect of statins. Activation of the mitochondrial apoptosis signalling pathway by increased ROS has been documented in the deltoid muscles of patients being treated with statins who also experienced myopathy, and in the glycolytic muscle of atorvastatin-treated rats (227). These effects were rescued in rats by the administration of quercetin, a natural flavonoid and antioxidant. CoQ10 supplementation was also found to recover succinate dehydrogenase activity, mitochondrial membrane pore potential and ATP production in mitochondria from rat liver after these parameters were reduced by atorvastatin or simvastatin treatment (510). This demonstrates a possible role of reduced CoQ10 in ROS accumulation.

Mitochondria in  $\beta$ -cells are also central in the production of mitochondrial coupling factors (MCF) involved in amplifying stimulated insulin secretion. These include citrate, glutamate and pyruvate and/or their products and involve metabolic cycling and anaplerotic and cataplerotic processes. For this reason, demand for mitochondrial membrane transporters pertinent to MCF is high in  $\beta$ -cells (770). In a manner similar to the rationale for examining membrane protein function in Chapter 4, there could be a cholesterol-dependent influence on membrane protein organisation in the mitochondria, which could be susceptible to interruption by statins. This, in turn, would influence insulin amplification.

No studies could be found that have examined this possibility, but it has been shown that cholesterol accumulation in response to chronically elevated insulin exposure decreased mitochondrial membrane fluidity in mouse liver and cultured hepatocytes (776), suggesting that mitochondrial and plasma membranes would respond similarly to cholesterol changes. Interestingly, and in support of the earlier discussion concerning cholesterol flux, liver X receptor (LXR)-mediated upregulation of cholesterol efflux proteins ABCA1 and ABCG1 in primary human islets treated with either of two LXR agonists coincided with increased anaplerosis and enhanced insulin secretion (777).

A concomitant increase in glycolysis akin to the Warburg effect was also observed with statin exposure (Chapter 3). However, there was no accompanying increase in glucose uptake. This may be either compensatory or causal to reduced ATP generation. Further investigation into potential changes in transcription factors important to  $\beta$ -cell maturation and function and to possible mitochondrial uncoupling may shed further light on this.

## 7.4 Environmental factors in statin-associated $\beta$ -cell dysfunction

In the animal study (Chapter 5), statins affected metabolic characteristics of mice differently based on diet. This was anticipated to a degree, as a high fat diet was expected to cause obesity-related insulin resistance and several studies have reported a more diabetogenic effect of statins in the presence of higher T2D risk (219). The findings on glucose tolerance tests and glucagon confirmed that statins exacerbated the effect of the HFD on glucose sensitivity and fasting glucagon concentrations, respectively. However, some other effects of HFD, for example insulin resistance, appeared to be somewhat ameliorated by statins, though not to statistical significance, and not in the ND group, where statins had the opposite effect, also not to statistical significance.

Regardless of the direction of statin influence, it is clear that dietary factors and statin effects interact, and this has been demonstrated in other studies. For example, specific macro and micro nutrients, alcohol and dietary fibre have all been associated with the efficacy and tolerability of statins (reviewed in 175).

Similarly to drug-drug interactions, environmental influences may increase statin exposure as a result of competition for transporters or enzymes, or there may be other unknown mechanisms. A well-known example is grapefruit, which produced a 2.5-fold increase in the AUC for serum atorvastatin, but not pravastatin co-administration (174) due to inhibition of the CYP3A4 isoenzyme, which is required for atorvastatin but not for pravastatin metabolism. Also, a study of the combined effect of atorvastatin and an aqueous extract of *Fructus Schisandrae*, a Chinese herb, demonstrated increased plasma concentrations of atorvastatin and its metabolites, but also protection against liver damage associated with statin therapy (778). Although the mechanism of these effects was not known, it seems clear that competitive enzyme inhibition may have resulted in higher statin plasma concentrations, while additional mechanisms protected liver function.

Cholesterol turnover may be affected by the gut microbiome through bile acid metabolism via the farnesoid X receptor (FXR) (779, 780). Consequently, antibiotics may modulate the efficacy of statins, an effect related to the elimination of gut bacteria (781). A study with exciting prospective clinical consequences disclosed a correlation between secondary bile acids produced by certain bacterial species in the gut microbiome and the effectiveness of simvastatin therapy to lower LDL cholesterol (782). Using a metabolomics approach, the authors identified metabolites that may be predictive of ‘good’ and ‘bad’ responders to statin therapy. This paper also forecasts the possibility of developing probiotics that could potentially improve the response to specific statin regimes. On the flip side, statins have also recently been shown to affect the diversity of the gut microbiome (670, 783), leading to altered bile acid profiles and a

bacterial population similar to that linked to obesity. Links have also been made between alterations in bile acid synthesis and diabetes (784), providing another mechanism by which statins may ultimately have a diabetogenic influence, though much remains to be understood.

To suggest just a few other possible, but unstudied potential mechanisms between environmental factors and statins: the source of fuel being used to generate ATP and mitochondrial coupling factors could influence statin effects if they were dependent on specific transporters sensitive to membrane cholesterol concentrations; the rate of glucose oxidation may have an influence on the statin effect, so far as it relates to antioxidant potential and the ability of antioxidants to neutralise it; adaptation to workload requires several changes (346) that may be influenced by statins, for example they may inhibit the generation of coupling factors; the availability of specific nutrients capable of relieving statin effects (eg vitamin E or other dietary antioxidants) could have an influence, either directly or via the gut microbiome (670, 783).

## 7.5 Phenotypic $\beta$ -cell adaptations associated with cellular cholesterol modification

Metabolic and phenotypic changes accompanied cellular cholesterol modification in this project. These included reduced stimulated insulin secretion, ATP production rate and maximal respiration; increased glycolysis; increased ABCA1, hexokinase I, and mTOR expression; increased insulin receptor and GSK3 $\beta$  (serine 9) phosphorylation; increased cell size and complexity, and increased autofluorescence with cholesterol depletion by either statins or M $\beta$ CD but reduced autofluorescence with cholesterol loading. In addition, acute depletion or loading with M $\beta$ CD or c-M $\beta$ CD, respectively, resulted in changes in the abundance of several proteins, mainly associated with metabolism, transport and protein synthesis in a specific  $\beta$ -cell fraction. Some caveats apply to the latter as discussed previously, and further work needs to be done to assess its reproducibility. Alanyl-glutamine did not rescue insulin secretion or ATP production impaired by atorvastatin, but rather, it tended to exacerbate these effects.

The changes in insulin secretion confirm the diabetogenic influence of a modified cellular cholesterol content that is higher or lower than native levels. This also appears to be dose-dependent, with greater variation from native levels causing greater insulin secretion failure. ATP production decrease confirms a loss of mitochondrial efficiency with statin exposure and the associated increase in non-mitochondrial glycolysis may be compensatory.

Other potentially compensatory mechanisms are the increases in various proteins found to be upregulated with statin treatment. The discussion in Chapters 3 and 4 point out some similarities with the process of dedifferentiation in  $\beta$ -cells, which can occur during glucotoxicity (493, 674), hypoxia (497) and increased oxidative stress (373). This is reversible in favourable

conditions (499) and is likely to be mediated by certain transcription factors including PDX1, MAFA, MAFB, NKX6.1, c-Myc and FOXO (491, 494, 495, 553).

Based on the phenotypic and metabolic changes in response to statins found in this study and in the literature, it is tempting to suggest that statins exert dedifferentiation pressure on  $\beta$ -cells. This may be due to loss of cellular cholesterol exerting an influence on cellular mechanisms, loss of other products of the mevalonate pathway such as isoprenoids and CoQ10, increased ROS, or combinations of these factors. Mitochondrial function is impaired by statin exposure, and other changes observed may be compensatory to reduced respiration capacity. Pro-survival adaptations are likely to compromise native  $\beta$ -cell characteristics and loss of function due to the specialised metabolic requirements of these glucose sensing custodians charged with maintaining glucose homeostasis in a changing milieu of nutrients and other stressors, both favourable and unfavourable.

Many suggestions of further study have been made throughout this work, but possibly the most pressing in response to the suggestion above is the need for further study of the transcription factors defining and maintaining  $\beta$ -cell identity, and further characterisation of statin-mediated phenotypic changes. It is important to keep in mind that the diabetogenic effect of statins is of particular relevance to a small subgroup of patients. It is possible that the potential dedifferentiation pressure of statins alone is not sufficient to produce  $\beta$ -cell failure in healthy cells, but combined with other pressures, for example those associated with glucolipotoxicity or genetic disadvantage, may work in conjunction to hasten dysfunction. To identify the cohort with increased susceptibility would be of great clinical benefit, and this should also be a focus of further study.

In summary, in vitro studies in this project demonstrated that both sub- and supra-optimal cellular cholesterol content reduced robustly stimulated insulin secretion. Statins were associated with mitochondrial impairment, with the effect size dependent on statin type and dose, and this may have influenced insulin secretion in BRIN-BD11  $\beta$ -cells. Statin-associated mitochondrial impairment was characterised by a decrease in maximal respiration and simultaneous increase in glycolysis without changes in glucose uptake. Statins were also associated with increases in hexokinase I, mTOR and ABCA1 expression, insulin receptor phosphorylation and inhibitory GSK3 $\beta$  phosphorylation. These changes reflect certain characteristics of  $\beta$ -cell dedifferentiation but further studies would be necessary to confirm whether statins exert dedifferentiation pressure on  $\beta$ -cells. No beneficial effect on mitochondrial function or insulin secretion was observed when alanyl-glutamine was added to statin-treated cells. In mice, statins were associated with some diabetogenic influences and these were conditional on diet, potentially relating to defects in both glucagon and insulin secretion.

# Bibliography

1. Carlessi R, Rowlands J, Ellison G, Helena de Oliveira Alves H, Newsholme P, Mamotte C. Glutamine deprivation induces metabolic adaptations associated with beta cell dysfunction and exacerbate lipotoxicity. *Mol Cell Endocrinol*. 2019;491:110433.
2. Bridgeman S, Northrop W, Ellison G, Sabapathy T, Melton PE, Newsholme P, et al. Statins Do Not Directly Inhibit the Activity of Major Epigenetic Modifying Enzymes. *Cancers*. 2019;11(4):516.
3. Ellison G, Mamotte C, Cruzat VF, Newsholme P. Importance of glutamine to insulin secretion, insulin action and glycemic control. . In: Meynial-Denis D, editor. *Glutamine: Biochemistry, Physiology, and Clinical Applications* CRC Press, Taylor & Francis Group; 2017.
4. Padwal RS. Obesity, diabetes, and the metabolic syndrome: the global scourge. *The Canadian journal of cardiology*. 2014;30(5):467-72.
5. Lipscombe LL. The US diabetes epidemic: tip of the iceberg: The Lancet – comment; 2014 [Available from: [http://dx.doi.org/10.1016/S2213-8587\(14\)70172-X](http://dx.doi.org/10.1016/S2213-8587(14)70172-X)].
6. Lam DW, LeRoith D. The worldwide diabetes epidemic. *Curr Opin Endocrinol Diabetes Obes*. 2012;19(2):93-6.
7. WHO. World Health Day 2016: Beat diabetes: World Health Organisation; 2016 [Available from: <http://www.who.int/campaigns/world-health-day/2016/en/>].
8. WHO. Health statistics and information systems: World Health Organisation; 2016 [Available from: [http://www.who.int/healthinfo/global\\_burden\\_disease/estimates/en/index2.html](http://www.who.int/healthinfo/global_burden_disease/estimates/en/index2.html)].
9. Wang Y, Lim H. The global childhood obesity epidemic and the association between socio-economic status and childhood obesity. *Int Rev Psychiatry*. 2012;24(3):176-88.
10. Lobstein T, Jackson-Leach R. Planning for the worst: estimates of obesity and comorbidities in school-age children in 2025. *Pediatr Obes*. 2016;11(5):321-5.
11. Osei K, Rhinesmith S, Gaillard T, Schuster D. Impaired insulin sensitivity, insulin secretion, and glucose effectiveness predict future development of impaired glucose tolerance and Type 2 diabetes in pre-diabetic African Americans. *Diabetes Care*. 2004;27(6):1439-46.
12. Regazzi R, Rodriguez-Trejo A, Jacovetti C. Insulin secretion in health and disease: nutrients dictate the pace. *Proc Nutr Soc*. 2016;75(1):19-29.
13. Gallwitz B, Kazda C, Kraus P, Nicolay C, Schernthaner G. Contribution of insulin deficiency and insulin resistance to the development of type 2 diabetes: nature of early stage diabetes. *Acta Diabetol*. 2013;50(1):39-45.
14. Shimabukuro M, Zhou YT, Levi M, Unger RH. Fatty acid-induced beta cell apoptosis: a link between obesity and diabetes. *Proc Natl Acad Sci USA*. 1998;95(5):2498-502.
15. Klop B, Elte JW, Cabezas MC. Dyslipidemia in obesity: mechanisms and potential targets. *Nutrients*. 2013;5(4):1218-40.
16. Hirose H, Lee YH, Inman LR, Nagasawa Y, Johnson JH, Unger RH. Defective fatty acid-mediated beta-cell compensation in Zucker diabetic fatty rats. Pathogenic implications for obesity-dependent diabetes. *J Biol Chem*. 1996;271(10):5633-7.
17. Milburn JL, Jr., Hirose H, Lee YH, Nagasawa Y, Ogawa A, Ohneda M, et al. Pancreatic beta-cells in obesity. Evidence for induction of functional, morphologic, and metabolic abnormalities by increased long chain fatty acids. *J Biol Chem*. 1995;270(3):1295-9.
18. Keane KN, Cruzat VF, Carlessi R, de Bittencourt PI, Jr., Newsholme P. Molecular Events Linking Oxidative Stress and Inflammation to Insulin Resistance and beta-Cell Dysfunction. *Oxidative Medicine and Cellular Longevity*. 2015(Article ID 181643):15 pages.

19. Alempijevic T, Dragasevic S, Zec S, Popovic D, Milosavljevic T. Non-alcoholic fatty pancreas disease. *Postgrad Med J*. 2017;93(1098):226-30.
20. Tushuizen ME, Bunck MC, Pouwels PJ, Bontemps S, van Waesberghe JH, Schindhelm RK, et al. Pancreatic fat content and beta-cell function in men with and without type 2 diabetes. *Diabetes Care*. 2007;30(11):2916-21.
21. Forbes JM, Cooper ME. Mechanisms of diabetic complications. *Physiol Rev*. 2013;93(1):137-88.
22. Moheet A, Mangia S, Seaquist ER. Impact of diabetes on cognitive function and brain structure. *Ann N Y Acad Sci*. 2015;1353:60-71.
23. Chegade JM, Gladysz M, Mooradian AD. Dyslipidemia in type 2 diabetes: prevalence, pathophysiology, and management. *Drugs*. 2013;73(4):327-39.
24. Jaiswal M, Schinske A, Pop-Busui R. Lipids and lipid management in diabetes. *Best Practice & Research Clinical Endocrinology & Metabolism*. 2014;28(3):325-38.
25. Quinones A, Lobach I, Maduro GA, Jr., Smilowitz NR, Reynolds HR. Diabetes and ischemic heart disease death in people age 25-54: a multiple-cause-of-death analysis based on over 400 000 deaths from 1990 to 2008 in New York City. *Clin Cardiol*. 2015;38(2):114-20.
26. The Emerging Risk Factors Collaboration. Diabetes mellitus, fasting blood glucose concentration, and risk of vascular disease: a collaborative meta-analysis of 102 prospective studies. *The Lancet*. 2010;375(9733):2215-22.
27. Zhang PY. Cardiovascular disease in diabetes. *Eur Rev Med Pharmacol Sci*. 2014;18:2205-14.
28. Snow V, Aronson MD, Hornbake R, Mottur-Pilson C, Weiss KB. Lipid control in the management of Type 2 Diabetes Mellitus: A clinical practice guideline from the American College of Physicians. *Annals of Internal Medicine*. 2004;140(8):644-9.
29. Scheen AJ. Drug interactions of clinical importance with antihyperglycaemic agents: an update. *Drug Saf*. 2005;28(7):601-31.
30. Sattar NA, Ginsberg H, Ray K, Chapman MJ, Arca M, Averna M, et al. The use of statins in people at risk of developing diabetes mellitus: Evidence and guidance for clinical practice. *Atherosclerosis Supplements*. 2014;15(1):1-15.
31. RACGP, Australia D. General practice management of Type 2 Diabetes – 2014-2015. In: RACGP, Australia D, editors. Melbourne: The Royal Australian College of General Practitioners; 2014.
32. Gregg EW, Sattar N, Ali MK. The changing face of diabetes complications. *Lancet Diabetes Endocrinol*. 2016;4(6):537-47.
33. Beckett RD, Schepers SM, Gordon SK. Risk of new-onset diabetes associated with statin use. *SAGE Open Medicine*. 2015;3:2050312115605518.
34. Barylski M, Nikolic D, Banach M, Toth PP, Montalto G, Rizzo M. Statins and new-onset diabetes. *Curr Pharm Des*. 2014;20(22):3657-64.
35. Shepherd J, Cobbe SM, Ford I, Isles CG, Lorimer AR, MacFarlane PW, et al. Prevention of coronary heart disease with pravastatin in men with hypercholesterolemia. West of Scotland Coronary Prevention Study Group. *N Engl J Med*. 1995;333(20):1301-7.
36. Ridker PM, Danielson E, Fonseca FA, Genest J, Gotto AM, Jr., Kastelein JJ, et al. Rosuvastatin to prevent vascular events in men and women with elevated C-reactive protein. *N Engl J Med*. 2008;359(21):2195-207.
37. Horvat S, McWhir J, Rozman D. Defects in cholesterol synthesis genes in mouse and in humans: lessons for drug development and safer treatments. *Drug Metabolism Reviews*. 2011;43(1):69-90.



38. Millar JS, Cuchel M. Cholesterol metabolism in humans. *Current Opinion in Lipidology*. 2018;29(1):1-9.
39. Miettinen TA. Diurnal variation of cholesterol precursors squalene and methyl sterols in human plasma lipoproteins. *J Lipid Res*. 1982;23:466-73.
40. Okuyama H, Langsjoen PH, Hamazaki T, Ogushi Y, Hama R, Kobayashi T, et al. Statins stimulate atherosclerosis and heart failure: pharmacological mechanisms. *Expert Rev Clin Pharmacol*. 2015;8(2):189-99.
41. Dietschy JM, Turley SD. Control of cholesterol turnover in the mouse. *J Biol Chem*. 2002;277(6):3801-4.
42. Stellaard F, Lutjohann D. The Interpretation of Cholesterol Balance Derived Synthesis Data and Surrogate Noncholesterol Plasma Markers for Cholesterol Synthesis under Lipid Lowering Therapies. *Cholesterol*. 2017;2017:5046294.
43. Desager JP, Horsmans Y. Clinical pharmacokinetics of 3-hydroxy-3-methylglutaryl-coenzyme A reductase inhibitors. *Clin Pharmacokinet*. 1996;31(5):348-71.
44. Gill S, Stevenson J, Kristiana I, Brown AJ. Cholesterol-dependent degradation of squalene monooxygenase, a control point in cholesterol synthesis beyond HMG-CoA reductase. *Cell Metab*. 2011;13(3):260-73.
45. Sharpe LJ, Howe V, Prabhu AV, Luu W, Brown AJ. Navigating the shallows and rapids of cholesterol synthesis downstream of HMGCR. *Journal of Nutritional Science and Vitaminology*. 2015;61:S154-S6.
46. Nobelprize.org. Konrad Bloch - Facts: Nobel Media AB; 2014 [Available from: [http://www.nobelprize.org/nobel\\_prizes/medicine/laureates/1964/bloch-facts.html](http://www.nobelprize.org/nobel_prizes/medicine/laureates/1964/bloch-facts.html)].
47. Bloch K. The biological synthesis of cholesterol. Nobel Lecture; December 11, 1964/1964.
48. Kandutsch AA, Russell AE. Preputial gland tumor sterols: III. A metabolic pathway from lanosterol to cholesterol. *J Biol Chem*. 1960;235(8):2256-61.
49. Sharpe LJ, Brown AJ. Controlling cholesterol synthesis beyond 3-hydroxy-3-methylglutaryl-CoA reductase (HMGCR). *J Biol Chem*. 2013;288(26):18707-15.
50. Mitsche MA, McDonald JG, Hobbs HH, Cohen JC. Flux analysis of cholesterol biosynthesis in vivo reveals multiple tissue and cell-type specific pathways. *Elife*. 2015;4:e07999.
51. Prabhu AV, Luu W, Sharpe LJ, Brown AJ. Cholesterol-mediated Degradation of 7-Dehydrocholesterol Reductase Switches the Balance from Cholesterol to Vitamin D Synthesis. *Journal of Biological Chemistry*. 2016;291(16):8363-73.
52. Acimovic J, Goyal S, Kosir R, Golicnik M, Perse M, Belic A, et al. Cytochrome P450 metabolism of the post-lanosterol intermediates explains enigmas of cholesterol synthesis. *Sci Rep*. 2016;6:28462.
53. Belic A, Pompon D, Monostory K, Kelly D, Kelly S, Rozman D. An algorithm for rapid computational construction of metabolic networks: a cholesterol biosynthesis example. *Comput Biol Med*. 2013;43(5):471-80.
54. Rondini EA, Pant A, Kocarek TA. Transcriptional Regulation of Cytosolic Sulfotransferase 1C2 by Intermediates of the Cholesterol Biosynthetic Pathway in Primary Cultured Rat Hepatocytes. *The Journal of pharmacology and experimental therapeutics*. 2015;355(3):429-41.
55. Zhang JX, Sun L, Zhang JH, Feng ZY. Sex- and gonad-affecting scent compounds and 3 male pheromones in the rat. *Chem Senses*. 2008;33(7):611-21.
56. Orth M, Bellosta S. Cholesterol: its regulation and role in central nervous system disorders. *Cholesterol*. 2012;2012:292598.

57. Brown MS, Goldstein JL. Cholesterol feedback: from Schoenheimer's bottle to Scap's MELADL. *J Lipid Res.* 2009;50 Suppl:S15-27.
58. Neumann J, Rose-Sperling D, Hellmich UA. Diverse relations between ABC transporters and lipids: An overview. *Biochim Biophys Acta.* 2017;1859(4):605-18.
59. Liu SL, Sheng R, Jung JH, Wang L, Stec E, O'Connor MJ, et al. Orthogonal lipid sensors identify transbilayer asymmetry of plasma membrane cholesterol. *Nat Chem Biol.* 2017;13(3):268-74.
60. Mondal M, Mesmin B, Mukherjee S, Maxfield FR. Sterols are mainly in the cytoplasmic leaflet of the plasma membrane and the endocytic recycling compartment in CHO cells. *Mol Biol Cell.* 2009;20:581-8.
61. Aye MA, Levitan I. Paradoxical impact of cholesterol on lipid packing and cell stiffness. *Frontiers in Bioscience (Landmark Ed).* 2016;21:1245-59.
62. Simons K, Ikonen E. Functional rafts in cell membranes. *Nature.* 1997;387: 569-72.
63. Nyholm TK. Lipid-protein interplay and lateral organization in biomembranes. *Chem Phys Lipids.* 2015;189:48-55.
64. Rituper B, Davletov B, Zorec R. Lipid-protein interactions in exocytotic release of hormones and neurotransmitters. *Clinical Lipidology.* 2010;5(5):747-61.
65. Jacobo SMP, Guerra ML, Jarrard RE, Przybyla JA, Liu G, Watts VJ, et al. The Intracellular II-III Loops of Cav1.2 and Cav1.3 Uncouple L-Type Voltage-Gated Ca<sup>2+</sup> Channels from Glucagon-Like Peptide-1 Potentiation of Insulin Secretion in INS-1 Cells via Displacement from Lipid Rafts. *Journal of Pharmacology and Experimental Therapeutics.* 2009;330(1):283-93.
66. Xia F, Leung YM, Gaisano G, Gao X, Chen Y, Fox JE, et al. Targeting of voltage-gated K<sup>+</sup> and Ca<sup>2+</sup> channels and soluble N-ethylmaleimide-sensitive factor attachment protein receptor proteins to cholesterol-rich lipid rafts in pancreatic alpha-cells: effects on glucagon stimulus-secretion coupling. *Endocrinology.* 2007;148(5):2157-67.
67. Ohtsubo K, Takamatsu S, Gao C, Korekane H, Kurosawa TM, Taniguchi N. N-Glycosylation modulates the membrane sub-domain distribution and activity of glucose transporter 2 in pancreatic beta cells. *Biochem Biophys Res Commun.* 2013;434(2):346-51.
68. Zhou J, Li W, Xie Q, Hou Y, Zhan S, Yang X, et al. Effects of simvastatin on glucose metabolism in mouse MIN6 cells. *J Diabetes Res.* 2014;2014:376570.
69. Xia F, Gao X, Kwan E, Lam PP, Chan L, Sy K, et al. Disruption of pancreatic beta-cell lipid rafts modifies Kv2.1 channel gating and insulin exocytosis. *J Biol Chem.* 2004;279(23):24685-91.
70. Phan BA, Dayspring TD, Toth PP. Ezetimibe therapy: mechanism of action and clinical update. *Vasc Health Risk Manag.* 2012;8:415-27.
71. Tsuchiya M, Hosaka M, Moriguchi T, Zhang S, Suda M, Yokota-Hashimoto H, et al. Cholesterol biosynthesis pathway intermediates and inhibitors regulate glucose-stimulated insulin secretion and secretory granule formation in pancreatic beta-cells. *Endocrinology.* 2010;151(10):4705-16.
72. Hussain SS, Harris MT, Kreutzberger AJB, Inouye CM, Doyle CA, Castle AM, et al. Control of insulin granule formation and function by the ABC transporters ABCG1 and ABCA1 and by Oxysterol Binding Protein OSBP. *Mol Biol Cell.* 2018;29(10):1238-57.
73. Churchward MA, Rogasevskaia T, Hofgen J, Bau J, Coorssen JR. Cholesterol facilitates the native mechanism of Ca<sup>2+</sup>-triggered membrane fusion. *J Cell Sci.* 2005;118(Pt 20):4833-48.
74. Churchward MA, Rogasevskaia T, Brandman DM, Khosravani H, Nava P, Atkinson JK, et al. Specific lipids supply critical negative spontaneous curvature - an essential component of native Ca<sup>2+</sup>-triggered membrane fusion. *Biophys J.* 2008;94:3976-86.

75. Bhagavan HN, Chopra RK. Coenzyme Q10: Absorption, tissue uptake, metabolism and pharmacokinetics. *Free Radical Research*. 2006;40(5):445-53.
76. Molyneux SL, Young JM, Florkowski CM, Lever M, George PM. Coenzyme Q10: Is There a Clinical Role and a Case for Measurement? *Clinical Biochemistry Review*. 2008;29(May):71-82.
77. Newsholme P, Krause M. Nutritional regulation of insulin secretion: implications for diabetes. *Clin Biochem Rev*. 2012;33(2):35-47.
78. Arora DK, Syed I, Machhadieh B, McKenna CE, Kowluru A. Rab-geranylgeranyl transferase regulates glucose-stimulated insulin secretion from pancreatic  $\beta$  cells. *Islets*. 2012;4(5):354-8.
79. Stancu C, Sima A. Statins: mechanism of action and effects. *Journal of cellular and Molecular Medicine*. 2001;5(4):378-87.
80. Chang TY, Yamauchi Y, Hasan MT, Chang C. Cellular cholesterol homeostasis and Alzheimer's disease. *J Lipid Res*. 2017;58(12):2239-54.
81. Goldstein JL, Brown MS. Regulation of the mevalonate pathway. *Nature*. 1990;343(6257):425-30.
82. Hederstedt L. Heme A biosynthesis. *Biochim Biophys Acta*. 2012;1817(6):920-7.
83. Kim HJ, Khalimonchuk O, Smith PM, Winge DR. Structure, function, and assembly of heme centers in mitochondrial respiratory complexes. *Biochim Biophys Acta*. 2012;1823(9):1604-16.
84. Griffiths WJ, Abdel-Khalik J, Yutuc E, Morgan AH, Gilmore I, Hearn T, et al. Cholesterolomics: An update. *Anal Biochem*. 2017;524:56-67.
85. Fakheri RJ, Javitt NB. Autoregulation of cholesterol synthesis: physiologic and pathophysiologic consequences. *Steroids*. 2011;76(3):211-5.
86. Ramasamy I. Recent advances in physiological lipoprotein metabolism. *Clin Chem Lab Med*. 2014;52(12):1695-727.
87. Murray RK, Granner DK, Mayes PA, Rodwell VW. *Harper's Illustrated Biochemistry*. 26 ed. Sydney: Lange Medical Books/McGraw-Hill; 2003.
88. Seidah NG, Awan Z, Chretien M, Mbikay M. PCSK9: a key modulator of cardiovascular health. *Circ Res*. 2014;114(6):1022-36.
89. Silverman MG, Ference BA, Im K, Wiviott SD, Giugliano RP, Grundy SM, et al. Association Between Lowering LDL-C and Cardiovascular Risk Reduction Among Different Therapeutic Interventions: A Systematic Review and Meta-analysis. *Jama*. 2016;316(12):1289-97.
90. Hovingh GK, Rader DJ, Hegele RA. HDL re-examined. *Curr Opin Lipidol*. 2015;26(2):127-32.
91. von Eckardstein A, Widmann C. High-density lipoprotein, beta cells, and diabetes. *Cardiovasc Res*. 2014;103(3):384-94.
92. Rhainds D, Brissette L. The role of scavenger receptor class B type I (SR-BI) in lipid trafficking. *Int J Biochem Cell Biol*. 2004;36(1):39-77.
93. Shah AS, Tan L, Long JL, Davidson WS. Proteomic diversity of high density lipoproteins: our emerging understanding of its importance in lipid transport and beyond. *J Lipid Res*. 2013;54(10):2575-85.
94. Davidson S. LDL Proteome Watch University of Cincinnati website: The Davidson/Shah Lab; 2015 [Available from: <http://homepages.uc.edu/~davidswm/LDLproteome.html>].

95. Emmens JE, Jones DJL, Cao TH, Chan DCS, Romaine SPR, Quinn PA, et al. Proteomic diversity of high-density lipoprotein explains its association with clinical outcome in patients with heart failure. *Eur J Heart Fail.* 2018;20(2):260-7.
96. Vance JE. Dysregulation of cholesterol balance in the brain: contribution to neurodegenerative diseases. *Disease Models & Mechanisms.* 2012;5(6):746-55.
97. Hardy LM, Frisdal E, Le Goff W. Critical Role of the Human ATP-Binding Cassette G1 Transporter in Cardiometabolic Diseases. *Int J Mol Sci.* 2017;18(9).
98. Sturley SL. Conservation of eukaryotic sterol homeostasis: new insights from studies in budding yeast. *Biochim Biophys Acta.* 2000;1529(1-3):155-63.
99. Reeskamp LF, Meessen ECE, Groen AK. Transintestinal cholesterol excretion in humans. *Curr Opin Lipidol.* 2018;29(1):10-7.
100. Lagace TA. Phosphatidylcholine: Greasing the Cholesterol Transport Machinery. *Lipid Insights.* 2015;8(Suppl 1):65-73.
101. Nyren R, Chang CL, Lindstrom P, Barmina A, Vorrsgo E, Ali Y, et al. Localization of lipoprotein lipase and GPIHBP1 in mouse pancreas: effects of diet and leptin deficiency. *BMC Physiol.* 2012;12:14.
102. Goldstein JL, Brown MS. The LDL receptor. *Arterioscler Thromb Vasc Biol.* 2009;29(4):431-8.
103. Goldstein JL, Brown MS. A century of cholesterol and coronaries: from plaques to genes to statins. *Cell.* 2015;161(1):161-72.
104. Abifadel M, Varret M, Rabes JP, Allard D, Ouguerram K, Devillers M, et al. Mutations in PCSK9 cause autosomal dominant hypercholesterolemia. *Nat Genet.* 2003;34(2):154-6.
105. Cohen JC, Boerwinkle E, Mosley TH, Jr., Hobbs HH. Sequence variations in PCSK9, low LDL, and protection against coronary heart disease. *N Engl J Med.* 2006;354(12):1264-72.
106. Fitzpatrick DR, Keeling JW, Evans MJ, Kan AE, Bell JE, Porteous MEM, et al. Clinical Phenotype of Desmosterolosis. *American Journal of Medical Genetics.* 1998;75:145-52.
107. Byskov AG, Baltsen M, Andersen CY. Meiosis-activating sterols: background, discovery, and possible use. *J Mol Med (Berl).* 1998;76(12):818-23.
108. Grondahl C. Oocyte maturation. Basic and clinical aspects of in vitro maturation (IVM) with special emphasis of the role of FF-MAS. *Dan Med Bull.* 2008;55(1):1-16.
109. Lee MH, Lu K, Patel SB. Genetic basis of sitosterolemia. *Curr Opin Lipidol.* 2001;12(2):141-9.
110. Davies JP, Levy B, Ioannou YA. Evidence for a Niemann-pick C (NPC) gene family: identification and characterization of NPC1L1. *Genomics.* 2000;65(2):137-45.
111. Altmann SW, Davis HR, Jr., Zhu LJ, Yao X, Hoos LM, Tetzloff G, et al. Niemann-Pick C1 Like1 protein is critical for intestinal cholesterol absorption. *Science.* 2004;303(5661):1201-4.
112. Myocardial Infarction Genetics Consortium I, Stitzel NO, Won HH, Morrison AC, Peloso GM, Do R, et al. Inactivating mutations in NPC1L1 and protection from coronary heart disease. *N Engl J Med.* 2014;371(22):2072-82.
113. Bernstein DL, Hülkova H, Bialer MG, Desnick RJ. Cholesteryl ester storage disease: Review of the findings in 135 reported patients with an underdiagnosed disease. *Journal of Hepatology.* 2013;58(6):1230-43.
114. Puntoni M, Sbrana F, Bigazzi F, Sampietro T. Tangier disease: epidemiology, pathophysiology, and management. *Am J Cardiovasc Drugs.* 2012;12(5):303-11.
115. Min H-K, Kapoor A, Fuchs M, Mirshahi F, Zhou H, Maher J, et al. Increased Hepatic Synthesis and Dysregulation of Cholesterol Metabolism Is Associated with the Severity of Nonalcoholic Fatty Liver Disease. *Cell Metab.* 2012;15(5):665-74.

116. Yu TY, Wang CY. Impact of non-alcoholic fatty pancreas disease on glucose metabolism. *J Diabetes Investig.* 2017;8(6):735-47.
117. Singh RG, Yoon HD, Wu LM, Lu J, Plank LD, Petrov MS. Ectopic fat accumulation in the pancreas and its clinical relevance: A systematic review, meta-analysis, and meta-regression. *Metabolism.* 2017;69:1-13.
118. Santosa S, Varady KA, AbuMweis S, Jones PJ. Physiological and therapeutic factors affecting cholesterol metabolism: does a reciprocal relationship between cholesterol absorption and synthesis really exist? *Life Sci.* 2007;80(6):505-14.
119. Edwards PA, Muroya H, Gould G. In vivo demonstration of the circadian rhythm of cholesterol biosynthesis in the liver and intestine of the rat. *J Lipid Res.* 1972;13:396-401.
120. Linn TC. The effect of cholesterol feeding and fasting upon beta-hydroxy-beta-methylglutaryl coenzyme A reductase. *J Biol Chem.* 1967;242(5):990-3.
121. Siperstein MD, Guest MJ. Studies on the site of the feedback control of cholesterol synthesis. *J Clin Invest.* 1960;39:642-52.
122. Howe V, Sharpe LJ, Prabhu AV, Brown AJ. New insights into cellular cholesterol acquisition: promoter analysis of human HMGCR and SQLE, two key control enzymes in cholesterol synthesis. *Biochim Biophys Acta.* 2017;1862(7):647-57.
123. Amemiya-Kudo M, Shimano H, Hasty AH, Yahagi N, Yoshikawa T, Matsuzaka T, et al. Transcriptional activities of nuclear SREBP-1a, -1c, and -2 to different target promoters of lipogenic and cholesterologenic genes. *J Lipid Res.* 2002;43(8):1220-35.
124. Horton JD, Goldstein JL, Brown MS. SREBPs: activators of the complete program of cholesterol and fatty acid synthesis in the liver. *J Clin Invest.* 2002;109(9):1125-31.
125. Brown MS, Goldstein JL. A receptor-mediated pathway for cholesterol homeostasis. *Science.* 1986;232(4746):34-47.
126. Brown MS, Goldstein JL. The SREBP pathway: regulation of cholesterol metabolism by proteolysis of a membrane-bound transcription factor. *Cell.* 1997;89(3):331-40.
127. Radhakrishnan A, Ikeda Y, Kwon HJ, Brown MS, Goldstein JL. Sterol-regulated transport of SREBPs from endoplasmic reticulum to Golgi: oxysterols block transport by binding to Insig. *Proc Natl Acad Sci USA.* 2007;104(16):6511-8.
128. Goldstein JL, DeBose-Boyd RA, Brown MS. Protein sensors for membrane sterols. *Cell.* 2006;124(1):35-46.
129. Sun LP, Li L, Goldstein JL, Brown MS. Insig required for sterol-mediated inhibition of Scap/SREBP binding to COPII proteins in vitro. *J Biol Chem.* 2005;280(28):26483-90.
130. Sun LP, Seemann J, Goldstein JL, Brown MS. Sterol-regulated transport of SREBPs from endoplasmic reticulum to Golgi: Insig renders sorting signal in Scap inaccessible to COPII proteins. *Proc Natl Acad Sci USA.* 2007;104(16):6519-26.
131. Hwang S, Hartman IZ, Calhoun LN, Garland K, Young GA, Mitsche MA, et al. Contribution of Accelerated Degradation to Feedback Regulation of 3-Hydroxy-3-methylglutaryl Coenzyme A Reductase and Cholesterol Metabolism in the Liver. *J Biol Chem.* 2016;291(26):13479-94.
132. Zerenturk EJ, Sharpe LJ, Ikonen E, Brown AJ. Desmosterol and DHCR24: Unexpected new directions for a terminal step in cholesterol synthesis. *Progress in Lipid Research.* 2013;52(4):666-80.
133. Wong J, Quinn CM, Gelissen IC, Jessup W, Brown AJ. The effect of statins on ABCA1 and ABCG1 expression in human macrophages is influenced by cellular cholesterol levels and extent of differentiation. *Atherosclerosis.* 2008;196(1):180-9.
134. Mutemberezi V, Guillemot-Legris O, Muccioli GG. Oxysterols: From cholesterol metabolites to key mediators. *Prog Lipid Res.* 2016;64:152-69.

135. Wang L, Xu F, Zhang XJ, Jin RM, Li X. Effect of high-fat diet on cholesterol metabolism in rats and its association with Na(+)/K(+)-ATPase/Src/pERK signaling pathway. *J Huazhong Univ Sci Technolog Med Sci.* 2015;35(4):490-4.
136. Sharpe LJ, Cook EC, Zelcer N, Brown AJ. The UPS and downs of cholesterol homeostasis. *Trends Biochem Sci.* 2014;39(11):527-35.
137. Descamps OS, De Sutter J, Guillaume M, Missault L. Where does the interplay between cholesterol absorption and synthesis in the context of statin and/or ezetimibe treatment stand today? *Atherosclerosis.* 2011;217(2):308-21.
138. Buhman KK, Accad M, Novak S, Choi RS, Wong JS, Hamilton RL, et al. Resistance to diet-induced hypercholesterolemia and gallstone formation in ACAT2-deficient mice. *Nat Med.* 2000;6(12):1341-7.
139. Lambert G, Amar MJ, Guo G, Brewer HB, Jr., Gonzalez FJ, Sinal CJ. The farnesoid X-receptor is an essential regulator of cholesterol homeostasis. *J Biol Chem.* 2003;278(4):2563-70.
140. Wang HH, Afdhal NH, Gendler SJ, Wang DQ. Lack of the intestinal Muc1 mucin impairs cholesterol uptake and absorption but not fatty acid uptake in Muc1<sup>-/-</sup> mice. *Am J Physiol Gastrointest Liver Physiol.* 2004;287(3):G547-54.
141. Otis JP, Shen MC, Quinlivan V, Anderson JL, Farber SA. Intestinal epithelial cell caveolin 1 regulates fatty acid and lipoprotein cholesterol plasma levels. *Dis Model Mech.* 2017;10(3):283-95.
142. Kulig W, Cwiklik L, Jurkiewicz P, Rog T, Vattulainen I. Cholesterol oxidation products and their biological importance. *Chem Phys Lipids.* 2016;199:144-60.
143. Ferderbar S, Pereira EC, Apolinario E, Bertolami MC, Faludi A, Monte O, et al. Cholesterol oxides as biomarkers of oxidative stress in type 1 and type 2 diabetes mellitus. *Diabetes Metab Res Rev.* 2007;23(1):35-42.
144. Bjorkhem I. Five decades with oxysterols. *Biochimie.* 2013;95(3):448-54.
145. Lund EG, Xie C, Kotti T, Turley SD, Dietschy JM, Russell DW. Knockout of the cholesterol 24-hydroxylase gene in mice reveals a brain-specific mechanism of cholesterol turnover. *J Biol Chem.* 2003;278(25):22980-8.
146. Temel RE, Brown JM. Biliary and nonbiliary contributions to reverse cholesterol transport. *Current Opinion in Lipidology.* 2012;23(2):85-90.
147. Stanley MM, Pineda EP, Cheng SH. Serum cholesterol esters and intestinal cholesterol secretion and absorption in obstructive jaundice due to cancer. *The New England Journal of Medicine.* 1959;261(8):368-73.
148. Jakulj L, van Dijk TH, de Boer JF, Kootte RS, Schonewille M, Paalvast Y, et al. Transintestinal Cholesterol Transport Is Active in Mice and Humans and Controls Ezetimibe-Induced Fecal Neutral Sterol Excretion. *Cell Metab.* 2016;24(6):783-94.
149. Degirolamo C, Sabba C, Moschetta A. Intestinal nuclear receptors in HDL cholesterol metabolism. *J Lipid Res.* 2015;56(7):1262-70.
150. Sise ME. Kidney transplant recipients with hepatitis C virus experienced 100% sustained virologic response at 12 weeks when treated with sofosbuvir-ledipasvir. *Hepatology.* 2017;66(4):1335-7.
151. Paalvast Y, de Boer JF, Groen AK. Developments in intestinal cholesterol transport and triglyceride absorption. *Curr Opin Lipidol.* 2017;28(3):248-54.
152. Le May C, Berger JM, Lespine A, Pillot B, Prieur X, Letessier E, et al. Transintestinal cholesterol excretion is an active metabolic process modulated by PCSK9 and statin involving ABCB1. *Arterioscler Thromb Vasc Biol.* 2013;33(7):1484-93.
153. Services USDoHaH. ATPIII guidelines for CVD therapy: National Cholesterol education Program. In: Health NIO, National Heart L, and Blood Institute, editors. 2001.

154. Suchy D, Łabuzek K, Stadnicki A, Okopień B. Ezetimibe – a new approach in hypercholesterolemia management. *Pharmacological Reports*. 2011;63(6):1335-48.
155. Temel RE, Tang W, Ma Y, Rudel LL, Willingham MC, Ioannou YA, et al. Hepatic Niemann-Pick C1-like 1 regulates biliary cholesterol concentration and is a target of ezetimibe. *J Clin Invest*. 2007;117(7):1968-78.
156. Kasza I, Hegyi Z, Szabo K, Andrikovics H, Nemet K, Varadi A, et al. Model system for the analysis of cell surface expression of human ABCA1. *BMC Cell Biol*. 2009;10:93.
157. Farnier M. PCSK9: From discovery to therapeutic applications. *Arch Cardiovasc Dis*. 2014;107(1):58-66.
158. Lagace TA. PCSK9 and LDLR degradation: regulatory mechanisms in circulation and in cells. *Curr Opin Lipidol*. 2014;25(5):387-93.
159. Schmidt AF, Pearce LS, Wilkins JT, Overington JP, Hingorani AD, Casas JP. PCSK9 monoclonal antibodies for the primary and secondary prevention of cardiovascular disease. *Cochrane Database Syst Rev*. 2017;4:CD011748.
160. Baker IDI Heart and Diabetes Institute. National Evidence-Based Guideline on Secondary Prevention of Cardiovascular Disease in Type 2 Diabetes (Part of the Guidelines on Management of Type 2 Diabetes). Melbourne Australia 2015.
161. Scaldaferrri F, Pizzoferrato M, Ponziani FR, Gasbarrini G, Gasbarrini A. Use and indications of cholestyramine and bile acid sequestrants. *Intern Emerg Med*. 2013;8(3):205-10.
162. Feingold K, Grunfeld C. Triglyceride Lowering Drugs. In: De Groot LJ, Chrousos G, Dungan K, Feingold KR, Grossman A, Hershman JM, et al., editors. *Endotext*. South Dartmouth (MA) 2000.
163. van Raalte DH, Li M, Pritchard PH, Wasan KM. Peroxisome Proliferator-Activated Receptor (PPAR)- : A Pharmacological Target with a Promising Future. *Pharmaceutical Research*. 2004;21(9):1531-8.
164. Wolfe BM, Kvach E, Eckel RH. Treatment of Obesity. *Circ Res*. 2016;118(11):1844-55.
165. Ito MK, Maki KC, Brinton EA, Cohen JD, Jacobson TA. Muscle symptoms in statin users, associations with cytochrome P450, and membrane transporter inhibitor use: A subanalysis of the USAGE study. *Journal of Clinical Lipidology*. 2014;8(1):69-76.
166. Endo A. A historical perspective on the discovery of statins. *Proc Jpn Acad Ser B Phys Biol Sci*. 2010;86(5):484-93.
167. Golomb BA, Evans MA. Statin Adverse Effects: A Review of the Literature and Evidence for a Mitochondrial Mechanism. *Am J Cardiovasc Drugs*. 2008;8(6):373-418.
168. Istvan E. Statin inhibition of HMG-CoA reductase: a 3-dimensional view. *Atherosclerosis Supplements*. 2003;4(1):3-8.
169. Egom EE, Hafeez H. Biochemistry of Statins. *Adv Clin Chem*. 2016;73:127-68.
170. Serajuddin ATM, Ranadive S, Mahoney EM. Relative Lipophilicities, Solubilities, and Structure-Pharmacological Considerations of 3-Hydroxy-3-Methylglutaryl-Coenzyme A (HMG-CoA) Reductase Inhibitors Pravastatin, Lovastatin, Mevastatin, and Simvastatin. *Journal of Pharmaceutical Sciences*. 1990;80(9):830-4.
171. Chandra P, Brouwer KLR. The Complexities of Hepatic Drug Transport: Current Knowledge and Emerging Concepts. *Pharmaceutical Research*. 2004;21(5):719-35.
172. Bogman K, Peyer A-K, Török M, Küsters E, Drewe J. HMG-CoA reductase inhibitors and P-glycoprotein modulation. *Br J Pharmacol*. 2001;132:1183-92.
173. Lilja JJ, Neuvonen M, Neuvonen PJ. Effects of regular consumption of grapefruit juice on the pharmacokinetics of simvastatin. *British journal of clinical pharmacology*. 2004;58(1):56-60.

174. Lilja JJ, Kivisto KT, Neuvonen PJ. Grapefruit juice increases serum concentrations of atorvastatin and has no effect on pravastatin. *Clinical pharmacology and therapeutics*. 1999;66(2):118-27.
175. Arrigoni E, Del Re M, Fidilio L, Fogli S, Danesi R, Di Paolo A. Pharmacogenetic Foundations of Therapeutic Efficacy and Adverse Events of Statins. *Int J Mol Sci*. 2017;18(1):104.
176. Dulak J, Jozkowicz A. Anti-angiogenic and anti-inflammatory effects of statins: relevance to anti-cancer therapy. *Current cancer drug targets*. 2005;5(8):579-94.
177. Cilla DD, Jr., Whitfield LR, Gibson DM, Sedman AJ, Posvar EL. Multiple-dose pharmacokinetics, pharmacodynamics, and safety of atorvastatin, an inhibitor of HMG-CoA reductase, in healthy subjects. *Clinical pharmacology and therapeutics*. 1996;60(6):687-95.
178. Corsini A, Bellosta S, Baetta R, Fumagalli R, Paoletti R, Bernini F. New insights into the pharmacodynamic and pharmacokinetic properties of statins. *Pharmacol Ther*. 1999;84(3):413-28.
179. Moghadasian MH. Clinical pharmacology of 3-hydroxy-3-methylglutaryl coenzyme A reductase inhibitors. *Life Sci*. 1999;65(13):1329-37.
180. Schonewille M, de Boer JF, Mele L, Wolters H, Bloks VW, Wolters JC, et al. Statins increase hepatic cholesterol synthesis and stimulate fecal cholesterol elimination in mice. *J Lipid Res*. 2016;57(8):1455-64.
181. Reihner E, Rudling M, Stahlberg D, Berglund L, Ewerth S, Bjorkhem I, et al. Influence of pravastatin, a specific inhibitor of HMG-CoA reductase, on hepatic metabolism of cholesterol. *N Engl J Med*. 1990;323(4):224-8.
182. Brown AJ, Goldstein JL. Familial Hypercholesterolemia: Defective Binding of Lipoproteins to Cultured Fibroblasts Associated with Impaired Regulation of 3-Hydroxy-3-Methylglutaryl Coenzyme A Reductase Activity. *Proceedures of the National Academy of Science USA*. 1974;71(3):788-92.
183. Uauy R, Vega GL, Grundy SM, Bilheimer DM. Lovastatin therapy in receptor-negative homozygous familial hypercholesterolemia: Lack of effect on low-density lipoprotein concentrations or turnover. *J Pediatr*. 1988;113(2):387-92.
184. Kovanen PT, Belheimer DW, Goldstein JL, Haramillo JJ, Brown MS. Regulatory role for hepatic low density lipoprotein receptors in vivo in the dog. *Proceedings of the National Academy of Science*. 1981;78(2):1194-8.
185. Ishida F, Watanabe K, Sato A, Taguchi K, Kakubari K, Kitani K, et al. Comparative effects of simvastatin (MK-733) and pravastatin (CS-514) on hypercholesterolemia induced by cholesterol feeding in rabbits. *Biochim Biophys Acta*. 1990;1042(3):365-73.
186. Kerr AG, Tam LCS, Hale AB, Cioroch M, Douglas G, Agkatsev S, et al. A Genomic DNA Reporter Screen Identifies Squalene Synthase Inhibitors That Act Cooperatively with Statins to Upregulate the Low-Density Lipoprotein Receptor. *The Journal of pharmacology and experimental therapeutics*. 2017;361(3):417-28.
187. Dong B, Wu M, Cao A, Li H, Liu J. Suppression of Idol expression is an additional mechanism underlying statin-induced up-regulation of hepatic LDL receptor expression. *International Journal of Molecular Medicine*. 2011;27:103-10.
188. Vega GL, Grundy SM. Influence of lovastatin therapy on metabolism of low density lipoproteins in mixed hyperlipidaemia. *J Intern Med*. 1991;230:341-9.
189. Pocathikorn A, Taylor RR, Mamotte CD. Atorvastatin increases expression of low-density lipoprotein receptor mRNA in human circulating mononuclear cells. *Clin Exp Pharmacol Physiol*. 2010;37(4):471-6.
190. Powell EE, Kroon PA. Low density lipoprotein receptor and 3-hydroxy-3-methylglutaryl coenzyme A reductase gene expression in human mononuclear leukocytes is



- regulated coordinately and parallels gene expression in human liver. *J Clin Invest*. 1994;93(5):2168-74.
191. Guo H, Shi Y, Liu L, Sun A, Xu F, Chi J. Rosuvastatin inhibits MMP-2 expression and limits the progression of atherosclerosis in LDLR-deficient mice. *Arch Med Res*. 2009;40(5):345-51.
192. Lorza-Gil E, Salerno AG, Wanschel AC, Vettorazzi JF, Ferreira MS, Rentz T, et al. Chronic use of pravastatin reduces insulin exocytosis and increases beta-cell death in hypercholesterolemic mice. *Toxicology*. 2016;344-346:42-52.
193. Bjorkhem-Bergman L, Lindh JD, Bergman P. What is a relevant statin concentration in cell experiments claiming pleiotropic effects? *British journal of clinical pharmacology*. 2011;72(1):164-5.
194. Camus MC, Chapman MJ, Forgez P, Laplaud PM. Distribution and characterization of the serum lipoproteins and apoproteins in the mouse, *Mus musculus*. *J Lipid Res*. 1983;24(9):1210-28.
195. Pitman WA, Osgood DP, Smith D, Schaefer EJ, Ordovas JM. The effects of diet and lovastatin on regression of fatty streak lesions and on hepatic and intestinal mRNA levels for the LDL receptor and HMG CoA reductase in F1B hamsters. *Atherosclerosis*. 1998;138(1):43-52.
196. Ray KK, Seshasai SR, Erqou S, Sever P, Jukema JW, Ford I, et al. Statins and all-cause mortality in high-risk primary prevention: a meta-analysis of 11 randomized controlled trials involving 65,229 participants. *Arch Intern Med*. 2010;170(12):1024-31.
197. Chou R, Dana T, Blazina I, Daeges M, Jeanne TL. Statins for Prevention of Cardiovascular Disease in Adults: Evidence Report and Systematic Review for the US Preventive Services Task Force. *Jama*. 2016;316(19):2008-24.
198. Collins R, Reith C, Emberson J, Armitage J, Baigent C, Blackwell L, et al. Interpretation of the evidence for the efficacy and safety of statin therapy. *The Lancet*. 2016;388(10059):2532-61.
199. Rosenbaum D, Dallongeville J, Sabouret P, Bruckert E. Discontinuation of statin therapy due to muscular side effects: a survey in real life. *Nutr Metab Cardiovasc Dis*. 2013;23(9):871-5.
200. de Lorgeril M, Salen P, Abramson J, Dodin S, Hamazaki T, Kostucki W, et al. Cholesterol lowering, cardiovascular diseases, and the rosuvastatin-JUPITER controversy: a critical reappraisal. *Arch Intern Med*. 2010;170(12):1032-6.
201. DuBroff R. Cholesterol paradox: a correlate does not a surrogate make. *Evid Based Med*. 2017;22(1):15-9.
202. Hamazaki T, Okuyama H, Ogushi Y, Hama R. Towards a Paradigm Shift in Cholesterol Treatment. A Re-examination of the Cholesterol Issue in Japan. *Ann Nutr Metab*. 2015;66 Suppl 4:1-116.
203. Davis TM, Badshah I, Chubb SA, Davis WA. Dose-response relationship between statin therapy and glycaemia in community-based patients with type 2 diabetes: the Fremantle Diabetes Study. *Diabetes Obes Metab*. 2016;18(11):1143-6.
204. Millán Núñez-Cortés J, Cases Amenós A, Ascaso Gimilio JF, Barrios Alonso V, Pascual Fuster V, Pedro-Botet Montoya JC, et al. Consensus on the Statin of Choice in Patients with Impaired Glucose Metabolism: Results of the DIANA Study. *American Journal of Cardiovascular Drugs*. 2016;17(2):135-42.
205. Frayling TM. Statins and type 2 diabetes: genetic studies on target. *The Lancet*. 2015;385(9965):310-2.
206. Jukema JW, Cannon CP, de Craen AJ, Westendorp RG, Trompet S. The controversies of statin therapy: weighing the evidence. *J Am Coll Cardiol*. 2012;60(10):875-81.

207. Park J-B, Jung J-H, Yoon YE, Kim H-L, Lee S-P, Kim H-K, et al. Long-term Effects of high-dose pitavaStatin on Diabetogenicity in comparison with atorvastatin in patients with Metabolic syndrome (LESS-DM): study protocol for a randomized controlled trial. *Trials*. 2017;18(1).
208. Brault M, Ray J, Gomez YH, Mantzoros CS, Daskalopoulou SS. Statin treatment and new-onset diabetes: a review of proposed mechanisms. *Metabolism*. 2014;63(6):735-45.
209. Mosshammer D, Schaeffeler E, Schwab M, Morike K. Mechanisms and assessment of statin-related muscular adverse effects. *British journal of clinical pharmacology*. 2014;78(3):454-66.
210. Costa S, Reina-Couto M, Albino-Teixeira A, Souse T. Statins and oxidative stress in chronic heart failure. *Revista Portuguesa de Cardiologia* 2016;35(1):41-57.
211. Bedi O, Dhawan V, Sharma PL, Kumar P. Pleiotropic effects of statins: new therapeutic targets in drug design. *Naunyn Schmiedebergs Arch Pharmacol*. 2016;389(7):695-712.
212. Lim S, Sakuma I, Quon MJ, Koh KK. Differential Metabolic Actions of Specific Statins: Clinical and Therapeutic Considerations. *Antioxid Redox Signal*. 2014;20(8):1286-99.
213. Lim S, Barter P. Antioxidant effects of statins in the management of cardiometabolic disorders. *J Atheroscler Thromb*. 2014;21(10):997-1010.
214. Palazhy S, Kamath P, Vasudevan DM. Elevated oxidative stress among coronary artery disease patients on statin therapy: A cross sectional study. *Indian Heart J*. 2015;67(3):227-32.
215. Okuyama H, Langsjoen PH, Ohara N, Hashimoto Y, Hamazaki T, Yoshida S, et al. Medicines and Vegetable Oils as Hidden Causes of Cardiovascular Disease and Diabetes. *Pharmacology*. 2016;98(3-4):134-70.
216. Preiss D, Seshasai SR, Welsh P, Murphy SA, Ho JE, Waters DD, et al. Risk of incident diabetes with intensive-dose compared with moderate-dose statin therapy: a meta-analysis. *Jama*. 2011;305(24):2556-64.
217. Wang KL, Liu CJ, Chao TF, Huang CM, Wu CH, Chen SJ, et al. Statins, risk of diabetes, and implications on outcomes in the general population. *J Am Coll Cardiol*. 2012;60(14):1231-8.
218. Betteridge DJ, Carmena R. The diabetogenic action of statins - mechanisms and clinical implications. *Nat Rev Endocrinol*. 2016;12(2):99-110.
219. Waters DD, Ho JE, Boekholdt SM, DeMicco DA, Kastelein JJ, Messig M, et al. Cardiovascular event reduction versus new-onset diabetes during atorvastatin therapy: effect of baseline risk factors for diabetes. *J Am Coll Cardiol*. 2013;61(2):148-52.
220. Anyanwagu U, Idris I, Donnelly R. Drug-Induced Diabetes Mellitus: Evidence for Statins and Other Drugs Affecting Glucose Metabolism. *Clinical Pharmacology & Therapeutics*. 2016;99(4):390-400.
221. Livingstone SJ, Looker HC, Akbar T, Betteridge DJ, Durrington PN, Hitman GA, et al. Effect of atorvastatin on glycaemia progression in patients with diabetes: an analysis from the Collaborative Atorvastatin in Diabetes Trial (CARDS). *Diabetologia*. 2016;59(2):299-306.
222. Sattar N, Preiss D, Murray HM, Welsh P, Buckley BM, de Craen AJ, et al. Statins and risk of incident diabetes: a collaborative meta-analysis of randomised statin trials. *Lancet*. 2010;375(9716):735-42.
223. Colbert JD, Stone JA. Statin use and the risk of incident diabetes mellitus: a review of the literature. *The Canadian journal of cardiology*. 2012;28(5):581-9.
224. Culver AL, Ockene IS, Balasubramanian R, Olendzki BC, Sepavich DM, Wactawski-Wende J, et al. Statin use and risk of diabetes mellitus in postmenopausal women in the Women's Health Initiative. *Arch Intern Med*. 2012;172(2):144-52.

225. Danaei G, Garcia Rodriguez LA, Fernandez Cantero O, Hernan MA. Statins and Risk of Diabetes: An analysis of electronic medical records to evaluate possible bias due to differential survival. *Diabetes Care*. 2012;36(5):1236-40.
226. Bouitbir J, Charles AL, Echaniz-Laguna A, Kindo M, Daussin F, Auwerx J, et al. Opposite effects of statins on mitochondria of cardiac and skeletal muscles: a 'mitohormesis' mechanism involving reactive oxygen species and PGC-1. *Eur Heart J*. 2012;33(11):1397-407.
227. Bouitbir J, Singh F, Charles AL, Schlagowski AI, Bonifacio A, Echaniz-Laguna A, et al. Statins Trigger Mitochondrial Reactive Oxygen Species-Induced Apoptosis in Glycolytic Skeletal Muscle. *Antioxid Redox Signal*. 2016;24(2):84-98.
228. Pal S, Ghosh M, Ghosh S, Bhattacharyya S, Sil PC. Atorvastatin induced hepatic oxidative stress and apoptotic damage via MAPKs, mitochondria, calpain and caspase12 dependent pathways. *Food Chem Toxicol*. 2015;83:36-47.
229. Parihar A, Parihar MS, Zenebe WJ, Ghafourifar P. Statins lower calcium-induced oxidative stress in isolated mitochondria. *Hum Exp Toxicol*. 2012;31(4):355-63.
230. Maechler P. Mitochondrial function and insulin secretion. *Mol Cell Endocrinol*. 2013;379(1-2):12-8.
231. Dean PM. Ultrastructural morphometry of the pancreatic  $\beta$ -cell. *Diabetologia*. 1973;9(2):115-9.
232. Steiner DJ, Kim A, Miller K, Hara M. Pancreatic islet plasticity: interspecies comparison of islet architecture and composition. *Islets*. 2010;2(3):135-45.
233. Katsuta H, Aguayo-Mazzucato C, Katsuta R, Akashi T, Hollister-Lock J, Sharma AJ, et al. Subpopulations of GFP-Marked Mouse Pancreatic  $\beta$ -Cells Differ in Size, Granularity, and Insulin Secretion. *Endocrinology*. 2012;153(11):5180-7.
234. Fu Z, Gilbert ER, Liu D. Regulation of insulin synthesis and secretion and pancreatic Beta-cell dysfunction in diabetes. *Curr Diabetes Rev*. 2013;9(1):25-53.
235. Bush NC, Chandler-Laney PC, Rouse DJ, Granger WM, Oster RA, Gower BA. Higher Maternal Gestational Glucose Concentration Is Associated with Lower Offspring Insulin Sensitivity and Altered  $\beta$ -Cell Function. *The Journal of Clinical Endocrinology & Metabolism*. 2011;96(5):E803-E9.
236. Kiekens R, In 't Veld P, Mahler T, Schuit F, Van De Winkel M, Pipeleers D. Differences in glucose recognition by individual rat pancreatic B cells are associated with intercellular differences in glucose-induced biosynthetic activity. *J Clin Invest*. 1992;89(1):117-25.
237. Martens GA, Jiang L, Verhaeghen K, Connolly JB, Geromanos SG, Stange G, et al. Protein markers for insulin-producing beta cells with higher glucose sensitivity. *PLoS One*. 2010;5(12):e14214.
238. Bader E, Migliorini A, Gegg M, Moruzzi N, Gerdes J, Roscioni SS, et al. Identification of proliferative and mature beta-cells in the islets of Langerhans. *Nature*. 2016;535(7612):430-4.
239. Johnston NR, Mitchell RK, Haythorne E, Pessoa MP, Semplici F, Ferrer J, et al. Beta Cell Hubs Dictate Pancreatic Islet Responses to Glucose. *Cell Metab*. 2016;24(3):389-401.
240. Reinert RB, Cai Q, Hong JY, Plank JL, Aamodt K, Prasad N, et al. Vascular endothelial growth factor coordinates islet innervation via vascular scaffolding. *Development*. 2014;141(7):1480-91.
241. Rodriguez-Diaz R, Menegaz D, Caicedo A. Neurotransmitters act as paracrine signals to regulate insulin secretion from the human pancreatic islet. *J Physiol*. 2014;592(16):3413-7.
242. Tang SC, Peng SJ, Chien HJ. Imaging of the islet neural network. *Diabetes Obes Metab*. 2014;16 Suppl 1:77-86.

243. Mugabo Y, Zhao S, Lamontagne J, Al-Mass A, Peyot ML, Corkey BE, et al. Metabolic fate of glucose and candidate signaling and excess-fuel detoxification pathways in pancreatic beta-cells. *J Biol Chem*. 2017;292(18):7407-22.
244. Newsholme P, Bender K, Kiely A, Brennan L. Amino acid metabolism, insulin secretion and diabetes. *Biochemical Society transactions*. 2007;35(Pt 5):1180-6.
245. Pullen TJ, Rutter GA. When less is more: the forbidden fruits of gene repression in the adult beta-cell. *Diabetes Obes Metab*. 2013;15(6):503-12.
246. Nicholls DG. The Pancreatic  $\beta$ -Cell: A Bioenergetic Perspective. *Physiol Rev*. 2016;96(4):1385-447.
247. Sekine N, Cirulli V, Regazzi R, Brown LJ, Gine E, Tamarit-Rodriguez J, et al. Low lactate dehydrogenase and high mitochondrial glycerol phosphate dehydrogenase in pancreatic beta-cells. Potential role in nutrient sensing. *J Biol Chem*. 1994;269(7):4895-902.
248. Rutter Guy A, Pullen Timothy J, Hodson David J, Martinez-Sanchez A. Pancreatic  $\beta$ -cell identity, glucose sensing and the control of insulin secretion. *Biochemical Journal*. 2015;466(2):203-18.
249. Thorrez L, Laudadio I, Van Deun K, Quintens R, Hendrickx N, Granvik M, et al. Tissue-specific disallowance of housekeeping genes: the other face of cell differentiation. *Genome Res*. 2011;21(1):95-105.
250. Marquard J, Welters A, Buschmann T, Barthlen W, Vogelgesang S, Klee D, et al. Association of exercise-induced hyperinsulinaemic hypoglycaemia with MCT1-expressing insulinoma. *Diabetologia*. 2013;56(1):31-5.
251. Otonkoski T, Jiao H, Kaminen-Ahola N, Tapia-Paez I, Ullah MS, Parton LE, et al. Physical exercise-induced hypoglycemia caused by failed silencing of monocarboxylate transporter 1 in pancreatic beta cells. *Am J Hum Genet*. 2007;81(3):467-74.
252. Schuit F, De Vos A, Farfari S, Moens K, Pipeleers D, Brun T, et al. Metabolic fate of glucose in purified islet cells. Glucose-regulated anaplerosis in beta cells. *J Biol Chem*. 1997;272(30):18572-9.
253. Pullen TJ, Khan AM, Barton G, Butcher SA, Sun G, Rutter GA. Identification of genes selectively disallowed in the pancreatic islet. *Islets*. 2010;2(2):89-95.
254. De Vos A, Haimberg H, Quartier E, Huypens P, Bouwens L, Pipeleers D, et al. Human and rat beta cells differ in glucose transporter but not in glucokinase gene expression. *Journal of Clinical Investigation*. 1995;96:2489-95.
255. McCulloch LJ, van de Bunt M, Braun M, Frayn KN, Clark A, Gloyn AL. GLUT2 (SLC2A2) is not the principal glucose transporter in human pancreatic beta cells: implications for understanding genetic association signals at this locus. *Mol Genet Metab*. 2011;104(4):648-53.
256. Uldry M, Thorens B. The SLC2 family of facilitated hexose and polyol transporters. *Pflugers Archive European Journal of Physiology*. 2004;447(5):480-9.
257. Gould GW, Holman GD. The glucose transporter family: structure, function and tissue-specific expression. *Biochem J*. 1993;295 ( Pt 2):329-41.
258. Lenzen S, Drinkgern J, Tiedge M. Low antioxidant enzyme gene expression in pancreatic islets compared with various other mouse tissues. *Free Radic Biol Med*. 1996;20(3):463-6.
259. Boslem E, Weir JM, MacIntosh G, Sue N, Cantley J, Meikle PJ, et al. Alteration of endoplasmic reticulum lipid rafts contributes to lipotoxicity in pancreatic beta-cells. *J Biol Chem*. 2013;288(37):26569-82.
260. Koren-Gluzer M, Aviram M, Meilin E, Hayek T. The antioxidant HDL-associated paraoxonase-1 (PON1) attenuates diabetes development and stimulates  $\beta$ -cell insulin release. *Atherosclerosis*. 2011;219(2):510-8.

261. Weaver JR, Holman TR, Imai Y, Jadhav A, Kenyon V, Maloney DJ, et al. Integration of pro-inflammatory cytokines, 12-lipoxygenase and NOX-1 in pancreatic islet beta cell dysfunction. *Mol Cell Endocrinol.* 2012;358(1):88-95.
262. Mráček T, Drahota Z, Houštěk J. The function and the role of the mitochondrial glycerol-3-phosphate dehydrogenase in mammalian tissues. *Biochimica et Biophysica Acta (BBA) - Bioenergetics.* 2013;1827(3):401-10.
263. Keane K, Newsholme P. Metabolic regulation of insulin secretion. *Vitam Horm.* 2014;95:1-33.
264. Owen OE, Kalhan SC, Hanson RW. The key role of anaplerosis and cataplerosis for citric acid cycle function. *J Biol Chem.* 2002;277(34):30409-12.
265. Farfari S, Schulz V, Corkey B, Prentki M. Glucose-regulated anaplerosis and cataplerosis in pancreatic beta-cells: possible implication of a pyruvate/citrate shuttle in insulin secretion. *Diabetes.* 2000;49(5):718-26.
266. MacDonald MJ, Fahien LA, Buss JD, Hasan NM, Fallon MJ, Kendrick MA. Citrate oscillates in liver and pancreatic beta cell mitochondria and in INS-1 insulinoma cells. *J Biol Chem.* 2003;278(51):51894-900.
267. Newsholme P, Gaudel C, Krause M. Mitochondria and diabetes. An intriguing pathogenetic role. *Adv Exp Med Biol.* 2012;942:235-47.
268. Matschinsky FM, Ellerman JE. Metabolism of glucose in the islets of Langerhans. *J Biol Chem.* 1968;243(10):2730-6.
269. Vallar L, Biden TJ, Wollheim CB. Guanine nucleotides induce Ca<sup>2+</sup>-independent insulin secretion from permeabilized RINm5F cells. *J Biol Chem.* 1987;262(11):5049-56.
270. Bacova Z, Benicky J, Lukyanetz EE, Lukyanetz IA, Strbak V. Different signaling pathways involved in glucose- and cell swelling-induced insulin secretion by rat pancreatic islets in vitro. *Cell Physiol Biochem.* 2005;16(1-3):59-68.
271. Panten U, Fruh E, Reckers K, Rustenbeck I. Acute metabolic amplification of insulin secretion in mouse islets: Role of cytosolic acetyl-CoA. *Metabolism.* 2016;65(9):1225-9.
272. Panten U, Willenborg M, Schumacher K, Hamada A, Ghaly H, Rustenbeck I. Acute metabolic amplification of insulin secretion in mouse islets is mediated by mitochondrial export of metabolites, but not by mitochondrial energy generation. *Metabolism.* 2013;62(10):1375-86.
273. Henquin JC. Triggering and amplifying pathways of regulation of insulin secretion by glucose. *Diabetes.* 2000;49(11):1751-60.
274. Henquin JC. Regulation of insulin secretion: a matter of phase control and amplitude modulation. *Diabetologia.* 2009;52(5):739-51.
275. El-Azzouny M, Evans CR, Treutelaar MK, Kennedy RT, Burant CF. Increased glucose metabolism and glycerolipid formation by fatty acids and GPR40 receptor signaling underlies the fatty acid potentiation of insulin secretion. *J Biol Chem.* 2014;289(19):13575-88.
276. Dixon G, Nolan J, McClenaghan N, Flatt PR, Newsholme P. A comparative study of amino acid consumption by rat islet cells and the clonal beta-cell line BRIN-BD11 - the functional significance of L-alanine. *J Endocrinol.* 2003;179(3):447-54.
277. Altman BJ, Stine ZE, Dang CV. From Krebs to clinic: glutamine metabolism to cancer therapy. *Nat Rev Cancer.* 2016;16(10):619-34.
278. Sener A, Malaisse WJ. L-leucine and a nonmetabolized analogue activate pancreatic islet glutamate dehydrogenase. *Nature.* 1980;288(5787):187-9.
279. Yang J, Chi Y, Burkhardt BR, Guan Y, Wolf BA. Leucine metabolism in regulation of insulin secretion from pancreatic beta cells. *Nutr Rev.* 2010;68(5):270-9.
280. Zhang T, Li C. Mechanisms of amino acid-stimulated insulin secretion in congenital hyperinsulinism. *Acta Biochim Biophys Sin (Shanghai).* 2013;45(1):36-43.

281. Brennan L, Shine A, Hewage C, Malthouse JP, Brindle KM, McClenaghan N, et al. A nuclear magnetic resonance-based demonstration of substantial oxidative L-alanine metabolism and L-alanine-enhanced glucose metabolism in a clonal pancreatic beta-cell line: metabolism of L-alanine is important to the regulation of insulin secretion. *Diabetes*. 2002;51(6):1714-21.
282. Maechler P, Wollheim CB. Mitochondrial glutamate acts as a messenger in glucose-induced insulin exocytosis. *Nature*. 1999;402(6762):685-9.
283. Charles S, Henquin JC. Distinct effects of various amino acids on  $45\text{Ca}^{2+}$  fluxes in rat pancreatic islets. *Biochem J*. 1983;214(3):899-907.
284. Kristinsson H, Bergsten P, Sargsyan E. Free fatty acid receptor 1 (FFAR1/GPR40) signaling affects insulin secretion by enhancing mitochondrial respiration during palmitate exposure. *Biochim Biophys Acta*. 2015;1853(12):3248-57.
285. Newsholme P, Keane D, Welters Hannah J, Morgan Noel G. Life and death decisions of the pancreatic  $\beta$ -cell: the role of fatty acids. *Clin Sci (Lond)*. 2007;112(1):27-42.
286. Kolic J, MacDonald PE. cAMP-independent effects of GLP-1 on  $\beta$  cells. *Journal of Clinical Investigation*. 2015;125(12):4327-30.
287. Jendle J, Martin SA, Milicevic Z. Insulin and GLP-1 analog combinations in type 2 diabetes mellitus: a critical review. *Expert Opinion on Investigational Drugs*. 2012;21(10):1463-74.
288. Wu B, Wei S, Petersen N, Ali Y, Wang X, Bacaj T, et al. Synaptotagmin-7 phosphorylation mediates GLP-1-dependent potentiation of insulin secretion from beta-cells. *Proc Natl Acad Sci U S A*. 2015;112(32):9996-10001.
289. Ma X, Guan Y, Hua X. Glucagon-like peptide 1-potentiated insulin secretion and proliferation of pancreatic  $\beta$ -cells GLP-1. *Journal of Diabetes*. 2014;6(5):394-402.
290. Shigeto M, Ramracheya R, Tarasov AI, Cha CY, Chibalina MV, Hastoy B, et al. GLP-1 stimulates insulin secretion by PKC-dependent TRPM4 and TRPM5 activation. *J Clin Invest*. 2015;125(12):4714-28.
291. Nishizawa M, Nakabayashi H, Uehara K, Nakagawa A, Uchida K, Koya D. Intraportal GLP-1 stimulates insulin secretion predominantly through the hepatoportal-pancreatic vagal reflex pathways. *American Journal of Physiology-Endocrinology and Metabolism*. 2013;305(3):E376-E87.
292. D'Alessio D. Is GLP-1 a hormone: Whether and When? *J Diabetes Investig*. 2016;7 Suppl 1:50-5.
293. Seino S. Cell signalling in insulin secretion: the molecular targets of ATP, cAMP and sulfonylurea. *Diabetologia*. 2012;55(8):2096-108.
294. de Wet H, Proks P. Molecular action of sulphonylureas on KATP channels: a real partnership between drugs and nucleotides. *Biochemical Society transactions*. 2015;43(5):901-7.
295. Thulé PM, Umpierrez G. Sulfonylureas: A New Look at Old Therapy. *Curr Diab Rep*. 2014;14(4).
296. Arredouani A, Henquin JC, Gilon P. Contribution of the endoplasmic reticulum to the glucose-induced  $[\text{Ca}^{2+}]_i$  response in mouse pancreatic islets. *Am J Physiol Endocrinol Metab*. 2002;282(5):E982-91.
297. Belz M, Willenborg M, Gorgler N, Hamada A, Schumacher K, Rustenbeck I. Insulinotropic effect of high potassium concentration beyond plasma membrane depolarization. *Am J Physiol Endocrinol Metab*. 2014;306(6):E697-706.
298. Goldstein MR, Mascitelli L. Do statins cause diabetes? *Curr Diab Rep*. 2013;13(3):381-90.

299. Swerdlow DI, Preiss D, Kuchenbaecker KB, Holmes MV, Engmann JEL, Shah T, et al. HMG-coenzyme A reductase inhibition, type 2 diabetes, and bodyweight: evidence from genetic analysis and randomised trials. *The Lancet*. 2015;385(9965):351-61.
300. Swerdlow DI, Preiss D. Genetic insights into statin-associated diabetes risk. *Current Opinion in Lipidology*. 2016;27(2):125-30.
301. Chan DC, Pang J, Watts GF. Pathogenesis and Management of the Diabetogenic Effect of Statins: a Role for Adiponectin and Coenzyme Q10? *Current Atherosclerosis Reports*. 2014;17(1).
302. Yaluri N, Modi S, Lopez Rodriguez M, Stancakova A, Kuusisto J, Kokkola T, et al. Simvastatin Impairs Insulin Secretion by Multiple Mechanisms in MIN6 Cells. *PLoS One*. 2015;10(11):e0142902.
303. Matti A, Kyathanahalli C, Kowluru A. Protein farnesylation is requisite for mitochondrial fuel-induced insulin release. *Islets*. 2014;4(1):74-7.
304. Gazzo P, Proto MC, Gangemi G, Malfitano AM, Ciaglia E, Pisanti S, et al. Pharmacological actions of statins: a critical appraisal in the management of cancer. *Pharmacol Rev*. 2012;64(1):102-46.
305. Besseling J, Kastelein JJ, Defesche JC, Hutten BA, Hovingh GK. Association between familial hypercholesterolemia and prevalence of type 2 diabetes mellitus. *Jama*. 2015;313(10):1029-36.
306. Sezgin E, Levental I, Mayor S, Eggeling C. The mystery of membrane organization: composition, regulation and roles of lipid rafts. *Nature Reviews Molecular Cell Biology*. 2017;18(6):361-74.
307. Ohtsubo K, Takamatsu S, Minowa MT, Yoshida A, Takeuchi M, Marth JD. Dietary and genetic control of glucose transporter 2 glycosylation promotes insulin secretion in suppressing diabetes. *Cell*. 2005;123(7):1307-21.
308. Wang X, Chan CB. n-3 polyunsaturated fatty acids and insulin secretion. *J Endocrinol*. 2015;224(3):R97-106.
309. Ohtsubo K, Chen MZ, Olefsky JM, Marth JD. Pathway to diabetes through attenuation of pancreatic beta cell glycosylation and glucose transport.(Report). *Nature Medicine*. 2011;17(9):1067.
310. Reimer MK, Ahren B. Altered beta-cell distribution of pdx-1 and GLUT-2 after a short-term challenge with a high-fat diet in C57BL/6J mice. *Diabetes*. 2002;51 Suppl 1:S138-43.
311. Flanagan SE, Patch AM, Mackay DJG, Edghill EL, Gloyn AL, Robinson D, et al. Mutations in ATP-Sensitive K<sup>+</sup> Channel Genes Cause Transient Neonatal Diabetes and Permanent Diabetes in Childhood or Adulthood. *Diabetes*. 2007;56(7):1930-7.
312. Koster JC, Permutt MA, Nichols CG. Diabetes and insulin secretion: the ATP-sensitive K<sup>+</sup> channel (K ATP) connection. *Diabetes*. 2005;54(11):3065-72.
313. Branstrom R, Aspinwall CA, Valimaki S, Ostensson CG, Tibell A, Eckhard M, et al. Long-chain CoA esters activate human pancreatic beta-cell KATP channels: potential role in Type 2 diabetes. *Diabetologia*. 2004;47(2):277-83.
314. Yang SN, Shi Y, Yang G, Li Y, Yu J, Berggren PO. Ionic mechanisms in pancreatic beta cell signaling. *Cell Mol Life Sci*. 2014;71(21):4149-77.
315. Rorsman P, Eliasson L, Kanno T, Zhang Q, Gopel S. Electrophysiology of pancreatic beta-cells in intact mouse islets of Langerhans. *Prog Biophys Mol Biol*. 2011;107(2):224-35.
316. Rorsman P, Braun M. Regulation of Insulin Secretion in Human Pancreatic Islets. *Annu Rev Physiol*. 2013;75(1):155-79.
317. Tarasov A, Dusonchet J, Ashcroft F. Metabolic regulation of the pancreatic beta-cell ATP-sensitive K<sup>+</sup> channel: a pas de deux. *Diabetes*. 2004;53 Suppl 3:S113-22.

318. Roh E, Song DK, Kim MS. Emerging role of the brain in the homeostatic regulation of energy and glucose metabolism. *Exp Mol Med*. 2016;48:e216.
319. Geng X, Li L, Watkins S, Robbins PD, Drain P. The insulin secretory granule is the major site of K(ATP) channels of the endocrine pancreas. *Diabetes*. 2003;52(3):767-76.
320. Rocheleau JV, Remedi MS, Granada B, Head WS, Koster JC, Nichols CG, et al. Critical role of gap junction coupled KATP channel activity for regulated insulin secretion. *PLoS Biol*. 2006;4(2):e26.
321. Carroll PB, Li MX, Rojas E, Atwater I. The ATP-sensitive potassium channel in pancreatic B-cells is inhibited in physiological bicarbonate buffer. *FEBS Lett*. 1988;234(1):208-12.
322. Sehra D, Sehra S, Sehra ST. Cardiovascular pleiotropic effects of statins and new onset diabetes: is there a common link: do we need to evaluate the role of KATP channels? *Expert Opin Drug Saf*. 2017;16(7):823-31.
323. Yada T, Nakata M, Shiraishi T, Kakei M. Inhibition by simvastatin, but not pravastatin, of glucose-induced cytosolic Ca<sup>2+</sup> signalling and insulin secretion due to blockade of L-type Ca<sup>2+</sup> channels in rat islet beta-cells. *Br J Pharmacol*. 1999;126(5):1205-13.
324. Salunkhe VA, Mollet IG, Ofori JK, Malm HA, Esguerra JL, Reinbothe TM, et al. Dual Effect of Rosuvastatin on Glucose Homeostasis Through Improved Insulin Sensitivity and Reduced Insulin Secretion. *EBioMedicine*. 2016;10:185-94.
325. Rituper B, Flasker A, Gucek A, Chowdhury HH, Zorec R. Cholesterol and regulated exocytosis: a requirement for unitary exocytotic events. *Cell Calcium*. 2012;52(3-4):250-8.
326. Nevins AK, Thurmond DC. Caveolin-1 Functions as a Novel Cdc42 Guanine Nucleotide Dissociation Inhibitor in Pancreatic  $\beta$ -Cells. *Journal of Biological Chemistry*. 2006;281(28):18961-72.
327. Larsson S, Wierup N, Sundler F, Eliasson L, Holm C. Lack of cholesterol mobilization in islets of hormone-sensitive lipase deficient mice impairs insulin secretion. *Biochem Biophys Res Commun*. 2008;376(3):558-62.
328. Sengupta D. Cholesterol Modulates the Structure, Binding Modes, and Energetics of Caveolin-Membrane Interactions. *The Journal of Physical Chemistry B*. 2012;116(50):14556-64.
329. Frank PG, Cheung MWC, Pavlides S, Llaverias G, Park DS, Lisanti MP. Caveolin-1 and regulation of cellular cholesterol homeostasis. *American Journal of Physiology-Heart and Circulatory Physiology*. 2006;291(2):H677-H86.
330. Gleizes C, Kreutter G, Abbas M, Kassem M, Constantinescu AA, Boisrame-Helms J, et al. beta cell membrane remodelling and procoagulant events occur in inflammation-driven insulin impairment: a GLP-1 receptor dependent and independent control. *J Cell Mol Med*. 2016;20(2):231-42.
331. Vikman J, Jimenez-Feltstrom J, Nyman P, Thelin J, Eliasson L. Insulin secretion is highly sensitive to desorption of plasma membrane cholesterol. *Faseb J*. 2009;23(1):58-67.
332. Bacova Z, Hafko R, Orecna M, Kohut P, Hapala I, Strbak V. Effect of cellular cholesterol changes on insulin secretion by tumor cell lines. *Medicinal chemistry*. 2012;8(1):65-71.
333. Ge S, White JG, Haynes CL. Critical role of membrane cholesterol in exocytosis revealed by single platelet study. *ACS Chem Biol*. 2010;5(9):819-28.
334. Linetti A, Fratangeli A, Taverna E, Valnegri P, Francolini M, Cappello V, et al. Cholesterol reduction impairs exocytosis of synaptic vesicles. *Journal of Cell Science*. 2010;123(4):595-605.



335. Tanaka T, Porter CM, Horvath-Arcidiacono JA, Bloom ET. Lipophilic statins suppress cytotoxicity by freshly isolated natural killer cells through modulation of granule exocytosis. *Int Immunol.* 2007;19(2):163-73.
336. Bogan JS, Xu Y, Hao M. Cholesterol accumulation increases insulin granule size and impairs membrane trafficking. *Traffic.* 2012;13(11):1466-80.
337. Wijesekara N, Zhang LH, Kang MH, Abraham T, Bhattacharjee A, Warnock GL, et al. miR-33a modulates ABCA1 expression, cholesterol accumulation, and insulin secretion in pancreatic islets. *Diabetes.* 2012;61(3):653-8.
338. Xia F, Xie L, Mihic A, Gao X, Chen Y, Gaisano HY, et al. Inhibition of cholesterol biosynthesis impairs insulin secretion and voltage-gated calcium channel function in pancreatic beta-cells. *Endocrinology.* 2008;149(10):5136-45.
339. Takahashi N, Hatakeyama H, Okado H, Miwa A, Kishimoto T, Kojima T, et al. Sequential exocytosis of insulin granules is associated with redistribution of SNAP25. *J Cell Biol.* 2004;165(2):255-62.
340. Wang N, Lan D, Chen W, Matsuura F, Tall AR. ATP-binding cassette transporters G1 and G4 mediate cellular cholesterol efflux to high-density lipoproteins. *Proc Natl Acad Sci U S A.* 2004;101(26):9774-9.
341. Kruit JK, Wijesekara N, Fox JE, Dai XQ, Brunham LR, Searle GJ, et al. Islet cholesterol accumulation due to loss of ABCA1 leads to impaired exocytosis of insulin granules. *Diabetes.* 2011;60(12):3186-96.
342. Sturek JM, Castle JD, Trace AP, Page LC, Castle AM, Evans-Molina C, et al. An intracellular role for ABCG1-mediated cholesterol transport in the regulated secretory pathway of mouse pancreatic beta cells. *J Clin Invest.* 2010;120(7):2575-89.
343. Brunham LR, Kruit JK, Pape TD, Timmins JM, Reuwer AQ, VasANJI Z, et al. Beta-cell ABCA1 influences insulin secretion, glucose homeostasis and response to thiazolidinedione treatment. *Nat Med.* 2007;13(3):340-7.
344. Sato T, Herman L. Stereological analysis of normal rabbit pancreatic islets. *Am J Anat.* 1981;161(1):71-84.
345. Prentki M, Matschinsky FM, Madiraju SR. Metabolic signaling in fuel-induced insulin secretion. *Cell Metab.* 2013;18(2):162-85.
346. Wortham M, Sander M. Mechanisms of beta-cell functional adaptation to changes in workload. *Diabetes Obes Metab.* 2016;18 Suppl 1:78-86.
347. Horvath SE, Daum G. Lipids of mitochondria. *Prog Lipid Res.* 2013;52(4):590-614.
348. Martin LA, Kennedy BE, Karten B. Mitochondrial cholesterol: mechanisms of import and effects on mitochondrial function. *J Bioenerg Biomembr.* 2014;48(2):137-51.
349. Stiles L, Shirihai OS. Mitochondrial dynamics and morphology in beta-cells. *Best Practice & Research Clinical Endocrinology & Metabolism.* 2012;26(6):725-38.
350. Kaufman BA, Li C, Soleimanpour SA. Mitochondrial regulation of beta-cell function: maintaining the momentum for insulin release. *Mol Aspects Med.* 2015;42:91-104.
351. Basciano H, Miller AE, Naples M, Baker C, Kohen R, Xu E, et al. Metabolic effects of dietary cholesterol in an animal model of insulin resistance and hepatic steatosis. *Am J Physiol Endocrinol Metab.* 2009;297(2):E462-73.
352. Carrasco-Pozo C, Tan KN, Reyes-Farias M, De La Jara N, Ngo ST, Garcia-Diaz DF, et al. The deleterious effect of cholesterol and protection by quercetin on mitochondrial bioenergetics of pancreatic beta-cells, glycemic control and inflammation: In vitro and in vivo studies. *Redox Biol.* 2016;9:229-43.
353. Brand MD, Nicholls DG. Assessing mitochondrial dysfunction in cells. *Biochem J.* 2011;435(2):297-312.

354. Asalla S, Girada SB, Kuna RS, Chowdhury D, Kandagatla B, Oruganti S, et al. Restoring Mitochondrial Function: A Small Molecule-mediated Approach to Enhance Glucose Stimulated Insulin Secretion in Cholesterol Accumulated Pancreatic beta cells. *Sci Rep*. 2016;6:27513.
355. DuBroff R, de Lorgeril M. Cholesterol confusion and statin controversy. *World J Cardiol*. 2015;7(7):404-9.
356. Urbano F, Bugliani M, Filippello A, Scamporrino A, Di Mauro S, Di Pino A, et al. Atorvastatin but Not Pravastatin Impairs Mitochondrial Function in Human Pancreatic Islets and Rat  $\beta$ -Cells. Direct Effect of Oxidative Stress. *Scientific Reports*. 2017;7(1).
357. Chen YH, Chen YC, Liu CS, Hsieh MC. The Different Effects of Atorvastatin and Pravastatin on Cell Death and PARP Activity in Pancreatic NIT-1 Cells. *J Diabetes Res*. 2016;2016:1828071.
358. Mailloux RJ, Fu A, Robson-Doucette C, Allister EM, Wheeler MB, Sreaton R, et al. Glutathionylation state of uncoupling protein-2 and the control of glucose-stimulated insulin secretion. *J Biol Chem*. 2012;287(47):39673-85.
359. Deichmann R, Lavie C, Andrews S. Coenzyme q10 and statin-induced mitochondrial dysfunction. *Ochsner J*. 2010;10(1):16-21.
360. Jula A, Marniemi J, Huupponen R, Virtanen A, Rastas M, Ronnema T. Effects of diet and simvastatin on serum lipids, insulin, and antioxidants in hypercholesterolemic men: a randomized controlled trial. *Jama*. 2002;287(5):598-605.
361. Galtier F, Mura T, Raynaud de Mauverger E, Chevassus H, Farret A, Gagnol JP, et al. Effect of a high dose of simvastatin on muscle mitochondrial metabolism and calcium signaling in healthy volunteers. *Toxicol Appl Pharmacol*. 2012;263(3):281-6.
362. Brunham LR, Kruit JK, Verchere CB, Hayden MR. Cholesterol in islet dysfunction and type 2 diabetes. *The Journal of Clinical Investigation*. 2008;118(2):403-8.
363. von Eckardstein A, Sibling RA. Possible contributions of lipoproteins and cholesterol to the pathogenesis of diabetes mellitus type 2. *Curr Opin Lipidol*. 2011;22(1):26-32.
364. Fryirs M, Barter PJ, Rye KA. Cholesterol metabolism and pancreatic beta-cell function. *Current opinion in lipidology*. 2009;20(3):159-64.
365. Bagdade JD, Bierman EL, Porte D, Jr. The significance of basal insulin levels in the evaluation of the insulin response to glucose in diabetic and nondiabetic subjects. *J Clin Invest*. 1967;46(10):1549-57.
366. Bruning JC, Gautam D, Burks DJ, Gillette J, Schubert M, Orban PC, et al. Role of brain insulin receptor in control of body weight and reproduction. *Science*. 2000;289(5487):2122-5.
367. Du XL, Edelstein D, Rossetti L, Fantus IG, Goldberg H, Ziyadeh F, et al. Hyperglycemia-induced mitochondrial superoxide overproduction activates the hexosamine pathway and induces plasminogen activator inhibitor-1 expression by increasing Sp1 glycosylation. *Proc Natl Acad Sci USA*. 2000;97(22):12222-6.
368. Buse MG. Hexosamines, insulin resistance, and the complications of diabetes: current status. *Am J Physiol Endocrinol Metab*. 2006;290(1):E1-E8.
369. Soesanto Y, Luo B, Parker G, Jones D, Cooksey RC, McClain DA. Pleiotropic and age-dependent effects of decreased protein modification by O-linked N-acetylglucosamine on pancreatic beta-cell function and vascularization. *J Biol Chem*. 2011;286(29):26118-26.
370. Marshall S, Bacote V, Traxinger RR. Discovery of a metabolic pathway mediating glucose-induced desensitization of the glucose transport system. Role of hexosamine biosynthesis in the induction of insulin resistance. *J Biol Chem*. 1991;266(8):4706-12.
371. Akimoto Y, Hart GW, Wells L, Vosseller K, Yamamoto K, Munetomo E, et al. Elevation of the post-translational modification of proteins by O-linked N-acetylglucosamine

- leads to deterioration of the glucose-stimulated insulin secretion in the pancreas of diabetic Goto-Kakizaki rats. *Glycobiology*. 2007;17(2):127-40.
372. Kaneto H, Xu G, Song KH, Suzuma K, Bonner-Weir S, Sharma A, et al. Activation of the hexosamine pathway leads to deterioration of pancreatic beta-cell function through the induction of oxidative stress. *J Biol Chem*. 2001;276(33):31099-104.
373. Lombardi A, Ulianich L, Treglia AS, Nigro C, Parrillo L, Lofrumento DD, et al. Increased hexosamine biosynthetic pathway flux dedifferentiates INS-1E cells and murine islets by an extracellular signal-regulated kinase (ERK)1/2-mediated signal transmission pathway. *Diabetologia*. 2012;55(1):141-53.
374. Bhonagiri P, Pattar GR, Habegger KM, McCarthy AM, Tackett L, Elmendorf JS. Evidence coupling increased hexosamine biosynthesis pathway activity to membrane cholesterol toxicity and cortical filamentous actin derangement contributing to cellular insulin resistance. *Endocrinology*. 2011;152(9):3373-84.
375. Lange Y, Ory DS, Ye J, Lanier MH, Hsu FF, Steck TL. Effectors of rapid homeostatic responses of endoplasmic reticulum cholesterol and 3-hydroxy-3-methylglutaryl-CoA reductase. *J Biol Chem*. 2008;283(3):1445-55.
376. Shi L, Tu BP. Acetyl-CoA and the regulation of metabolism: mechanisms and consequences. *Current Opinion in Cell Biology*. 2015;33:125-31.
377. Webster NJ, Searle GJ, Lam PPL, Huang Y-C, Riedel MJ, Harb G, et al. Elevation in Intracellular Long-Chain Acyl-Coenzyme A Esters Lead to Reduced  $\beta$ -Cell Excitability via Activation of Adenosine 5'-Triphosphate-Sensitive Potassium Channels. *Endocrinology*. 2008;149(7):3679-87.
378. Branstrom R, Corkey BE, Berggren PO, Larsson O. Evidence for a unique long chain acyl-CoA ester binding site on the ATP-regulated potassium channel in mouse pancreatic beta cells. *J Biol Chem*. 1997;272(28):17390-4.
379. Larsson O, Deeney JT, Branstrom R, Berggren PO, Corkey BE. Activation of the ATP-sensitive K<sup>+</sup> channel by long chain acyl-CoA. A role in modulation of pancreatic beta-cell glucose sensitivity. *J Biol Chem*. 1996;271(18):10623-6.
380. Riedel MJ, Boora P, Steckley D, de Vries G, Light PE. Kir6.2 polymorphisms sensitize beta-cell ATP-sensitive potassium channels to activation by acyl CoAs: a possible cellular mechanism for increased susceptibility to type 2 diabetes? *Diabetes*. 2003;52(10):2630-5.
381. Cibičková Lu. Statins and their influence on brain cholesterol. *Journal of Clinical Lipidology*. 2011;5(5):373-9.
382. Bellosta S, Paoletti R, Corsini A. Safety of Statins: Focus on Clinical Pharmacokinetics and Drug Interactions. *Circulation*. 2004;109(23\_suppl\_1):III-50-III-7.
383. Miao X-S, Metcalfe CD. Determination of cholesterol-lowering statin drugs in aqueous samples using liquid chromatography–electrospray ionization tandem mass spectrometry. *Journal of Chromatography A*. 2003;998(1-2):133-41.
384. Thelen KM, Rentsch KM, Gutteck U, Heverin M, Olin M, Andersson U, et al. Brain cholesterol synthesis in mice is affected by high dose of simvastatin but not of pravastatin. *The Journal of pharmacology and experimental therapeutics*. 2006;316(3):1146-52.
385. Sidaway J, Wang Y, Marsden AM, Orton TC, Westwood FR, Azuma CT, et al. Statin-induced myopathy in the rat: relationship between systemic exposure, muscle exposure and myopathy. *Xenobiotica*. 2009;39(1):90-8.
386. Hu MH, Hung LW, Yang SH, Sun YH, Shih TT, Lin FH. Lovastatin promotes redifferentiation of human nucleus pulposus cells during expansion in monolayer culture. *Artif Organs*. 2011;35(4):411-6.

387. Wagner RJ, Martin KA, Powell RJ, Rzucidlo EM. Lovastatin induces VSMC differentiation through inhibition of Rheb and mTOR. *Am J Physiol Cell Physiol*. 2010;299(1):C119-27.
388. Mailman T, Hariharan M, Karten B. Inhibition of neuronal cholesterol biosynthesis with lovastatin leads to impaired synaptic vesicle release even in the presence of lipoproteins or geranylgeraniol. *J Neurochem*. 2011;119(5):1002-15.
389. Marin L, Traini D, Bebawy M, Colombo P, Buttini F, Haghi M, et al. Multiple dosing of simvastatin inhibits airway mucus production of epithelial cells: Implications in the treatment of chronic obstructive airway pathologies. *Eur J Pharm Biopharm*. 2013.
390. Nordstrand A, Lundholm M, Larsson A, Lerner UH, Widmark A, Wikstrom P. Inhibition of the Insulin-Like Growth Factor-1 Receptor Enhances Effects of Simvastatin on Prostate Cancer Cells in Co-Culture with Bone. *Cancer Microenviron*. 2013.
391. Liu PY, Xu DM. [Effects of simvastatin on lipopolysaccharide induced alpha-subunit epithelial sodium channel mRNA in rat lung alveolar type II epithelial cells]. *Zhongguo Wei Zhong Bing Ji Jiu Yi Xue*. 2012;24(10):604-7.
392. Jemnitz K, Veres Z, Tugyi R, Vereczkey L. Biliary efflux transporters involved in the clearance of rosuvastatin in sandwich culture of primary rat hepatocytes. *Toxicol In Vitro*. 2010;24(2):605-10.
393. Kang BY, Mehta JL. Rosuvastatin attenuates Ang II--mediated cardiomyocyte hypertrophy via inhibition of LOX-1. *J Cardiovasc Pharmacol Ther*. 2009;14(4):283-91.
394. Laumen H, Skurk T, Hauner H. The HMG-CoA reductase inhibitor rosuvastatin inhibits plasminogen activator inhibitor-1 expression and secretion in human adipocytes. *Atherosclerosis*. 2008;196(2):565-73.
395. Kiyari J, Kusch A, Tkachuk S, Kramer J, Haller H, Dietz R, et al. Rosuvastatin regulates vascular smooth muscle cell phenotypic modulation in vascular remodeling: role for the urokinase receptor. *Atherosclerosis*. 2007;195(2):254-61.
396. Sierra S, Ramos MC, Molina P, Esteo C, Vazquez JA, Burgos JS. Statins as neuroprotectants: a comparative in vitro study of lipophilicity, blood-brain-barrier penetration, lowering of brain cholesterol, and decrease of neuron cell death. *J Alzheimers Dis*. 2011;23(2):307-18.
397. Murinson BB, Haughey NJ, Maragakis NJ. Selected statins produce rapid spinal motor neuron loss in vitro. *BMC Musculoskelet Disord*. 2012;13:100.
398. Zhou C, King N, Chen KY, Breslow JL. Activation of PXR induces hypercholesterolemia in wild-type and accelerates atherosclerosis in apoE deficient mice. *J Lipid Res*. 2009;50(10):2004-13.
399. Bergen WG, Mersmann HJ. Comparative aspects of lipid metabolism: impact on contemporary research and use of animal models. *J Nutr*. 2005;135(11):2499-502.
400. Morton RE, Izem L. Cholesteryl ester transfer proteins from different species do not have equivalent activities. *J Lipid Res*. 2014;55(2):258-65.
401. Drayna D, Jarnagin AS, McLean J, Henzel W, Kohr W, Fielding C, et al. Cloning and sequencing of human cholesteryl ester transfer protein cDNA. *Nature*. 1987;327(6123):632-4.
402. Qiu X, Mistry A, Ammirati MJ, Chrnyk BA, Clark RW, Cong Y, et al. Crystal structure of cholesteryl ester transfer protein reveals a long tunnel and four bound lipid molecules. *Nat Struct Mol Biol*. 2007;14(2):106-13.
403. Fernandez ML, Wood RJ. Guinea pigs as models for human cholesterol and lipoprotein metabolism. In: Conn PM, editor. *Sourcebook of Models for Biomedical Research*. London: Humana Press Inc., Totowa, NJ; 2008. p. 201-12.
404. Rubin EM. Studies of Apolipoprotein B And Lipoprotein(a) in Transgenic Mice. In: L.L. G, editor. *Cardiovascular Disease: Cellular and molecular mechanisms, prevention, and*

treatment. Springer, Boston, MA: GWUMC Department of Biochemistry Annual Spring Symposia; 1995.

405. Gordon SM, Li H, Zhu X, Shah AS, Lu LJ, Davidson WS. A comparison of the mouse and human lipoproteome: suitability of the mouse model for studies of human lipoproteins. *J Proteome Res.* 2015;14(6):2686-95.
406. Dolensšek J, Rupnik MS, Stožer A. Structural similarities and differences between the human and the mouse pancreas. *Islets.* 2015;7(1):e1024405.
407. di Cagno MP. The Potential of Cyclodextrins as Novel Active Pharmaceutical Ingredients: A Short Overview. *Molecules.* 2016;22(1).
408. Tsamaloukas A, Szadkowska H, Slotte PJ, Heerklotz H. Interactions of cholesterol with lipid membranes and cyclodextrin characterized by calorimetry. *Biophys J.* 2005;89(2):1109-19.
409. Le Bourg A. Sterol regulation of hepatic lipase: A novel role for sterol regulatory element binding protein in cholesterol homeostasis: Cornell University; 2006.
410. Zidovetzki R, Levitan I. Use of cyclodextrins to manipulate plasma membrane cholesterol content: evidence, misconceptions and control strategies. *Biochim Biophys Acta.* 2007;1768(6):1311-24.
411. Jambhekar SS, Breen P. Cyclodextrins in pharmaceutical formulations II: solubilization, binding constant, and complexation efficiency. *Drug Discov Today.* 2016;21(2):363-8.
412. Vance JE, Karten B. Niemann-Pick C disease and mobilization of lysosomal cholesterol by cyclodextrin. *J Lipid Res.* 2014;55(8):1609-21.
413. Coisne C, Tilloy S, Monflier E, Wils D, Fenart L, Gosselet F. Cyclodextrins as Emerging Therapeutic Tools in the Treatment of Cholesterol-Associated Vascular and Neurodegenerative Diseases. *Molecules.* 2016;21(12).
414. Stelzl D, Nielsen TT, Hansen T, di Cagno M. beta-CD-dextran polymer for efficient sequestration of cholesterol from phospholipid bilayers: Mechanistic and safe-toxicity investigations. *Int J Pharm.* 2015;496(2):896-902.
415. Dotsikas Y, Loukas YL. Kinetic degradation study of insulin complexed with methyl-beta cyclodextrin. Confirmation of complexation with electrospray mass spectrometry and (1)H NMR. *J Pharm Biomed Anal.* 2002;29(3):487-94.
416. Ao M, Gan C, Shao W, Zhou X, Chen Y. Effects of cyclodextrins on the structure of LDL and its susceptibility to copper-induced oxidation. *European Journal of Pharmaceutical Sciences.* 2016;91:183-9.
417. Yancey PG, Rodriguez WV, Kilsdonk EP, Stoudt GW, Johnson WJ, Phillips MC, et al. Cellular cholesterol efflux mediated by cyclodextrins. Demonstration Of kinetic pools and mechanism of efflux. *J Biol Chem.* 1996;271(27):16026-34.
418. van Meer G, Voelker DR, Feigenson GW. Membrane lipids: where they are and how they behave. *Nature Reviews Molecular Cell Biology.* 2008;9(2):112-24.
419. Yamaguchi R, Perkins G, Hirota K. Targeting cholesterol with beta-cyclodextrin sensitizes cancer cells for apoptosis. *FEBS Lett.* 2015;589(24 Pt B):4097-105.
420. Sano O, Ito S, Kato R, Shimizu Y, Kobayashi A, Kimura Y, et al. ABCA1, ABCG1, and ABCG4 Are Distributed to Distinct Membrane Meso-Domains and Disturb Detergent-Resistant Domains on the Plasma Membrane. *PLoS ONE.* 2014;9(10):e109886.
421. Vedhachalam C, Duong PT, Nickel M, Nguyen D, Dhanasekaran P, Saito H, et al. Mechanism of ATP-binding cassette transporter A1-mediated cellular lipid efflux to apolipoprotein A-I and formation of high density lipoprotein particles. *J Biol Chem.* 2007;282(34):25123-30.

422. Chubinskiy-Nadezhdin VI, Efremova TN, Khaitlina SY, Morachevskaya EA. Functional impact of cholesterol sequestration on actin cytoskeleton in normal and transformed fibroblasts. *Cell Biol Int*. 2013;37(6):617-23.
423. Matthews LC, Taggart MJ, Westwood M. Effect of cholesterol depletion on mitogenesis and survival: the role of caveolar and noncaveolar domains in insulin-like growth factor-mediated cellular function. *Endocrinology*. 2005;146(12):5463-73.
424. Hao M, Bogan JS. Cholesterol regulates glucose-stimulated insulin secretion through phosphatidylinositol 4,5-bisphosphate. *J Biol Chem*. 2009;284(43):29489-98.
425. Hissa B, Pontes B, Roma PMS, Alves AP, Rocha CD, Valverde TM, et al. Membrane Cholesterol Removal Changes Mechanical Properties of Cells and Induces Secretion of a Specific Pool of Lysosomes. *PLoS ONE*. 2013;8(12):e82988.
426. Gaus K, Gratton E, Kable EP, Jones AS, Gelissen I, Kritharides L, et al. Visualizing lipid structure and raft domains in living cells with two-photon microscopy. *Proc Natl Acad Sci USA*. 2003;100(26):15554-9.
427. Kiss T, Fenyvesi F, Bacskay I, Varadi J, Fenyvesi E, Ivanyi R, et al. Evaluation of the cytotoxicity of beta-cyclodextrin derivatives: evidence for the role of cholesterol extraction. *Eur J Pharm Sci*. 2010;40(4):376-80.
428. Irie T, Otagiri M, Sunada M, Uekama K, Ohtani Y, Yamada Y, et al. Cyclodextrin-induced hemolysis and shape changes of human erythrocytes in vitro. *J Pharmacobiodyn*. 1982;5(9):741-4.
429. Skelin M, Rupnik M, Cencic A. Pancreatic beta cell lines and their applications in diabetes mellitus research. *Altex*. 2010;27(2):105-13.
430. McClenaghan NH, Barnett CR, Ah-Sing E, Abdel-Wahab YH, O'Harte FP, Yoon TW, et al. Characterization of a novel glucose-responsive insulin-secreting cell line, BRIN-BD11, produced by electrofusion. *Diabetes*. 1996;45(8):1132-40.
431. Kiely A, McClenaghan NH, Flatt PR, Newsholme P. Pro-inflammatory cytokines increase glucose, alanine and triacylglycerol utilization but inhibit insulin secretion in a clonal pancreatic beta-cell line. *J Endocrinol*. 2007;195(1):113-23.
432. McCluskey JT, Hamid M, Guo-Parke H, McClenaghan NH, Gomis R, Flatt PR. Development and functional characterization of insulin-releasing human pancreatic beta cell lines produced by electrofusion. *J Biol Chem*. 2011;286(25):21982-92.
433. Cunningham GA, McClenaghan NH, Flatt PR, Newsholme P. L-Alanine induces changes in metabolic and signal transduction gene expression in a clonal rat pancreatic beta-cell line and protects from pro-inflammatory cytokine-induced apoptosis. *Clin Sci (Lond)*. 2005;109(5):447-55.
434. Chapman JC, McClenaghan NH, Cosgrove KE, Hashmi MN, Shepherd RM, Giesberts AN, et al. ATP-sensitive potassium channels and efaroxan-induced insulin release in the electrofusion-derived BRIN-BD11 beta-cell line. *Diabetes*. 1999;48(12):2349-57.
435. Zhao C, Wilson MC, Schuit F, Halestrap AP, Rutter GA. Expression and distribution of lactate/monocarboxylate transporter isoforms in pancreatic islets and the exocrine pancreas. *Diabetes*. 2001;50(2):361-6.
436. Casula M, Mozzanica F, Scotti L, Tragni E, Pirillo A, Corrao G, et al. Statin use and risk of new-onset diabetes: A meta-analysis of observational studies. *Nutr Metab Cardiovasc Dis*. 2017;27(5):396-406.
437. Jackevicius CA, Mamdani M, Tu JV. Adherence with statin therapy in elderly patients with and without acute coronary syndromes. *Jama*. 2002;288(4):462-7.
438. Zhang H, Plutzky J, Skentzos S, Morrison F, Mar P, Shubina M, et al. Discontinuation of statins in routine care settings: a cohort study. *Ann Intern Med*. 2013;158(7):526-34.

439. Ferenczi EA, Asaria P, Hughes AD, Chaturvedi N, Francis DP. Can a statin neutralize the cardiovascular risk of unhealthy dietary choices? *Am J Cardiol.* 2010;106(4):587-92.
440. Guan JZ, Murakami H, Yamato K, Tanabe J, Matsui J, Tamasawa N, et al. Effects of fluvastatin in type 2 diabetic patients with hyperlipidemia: reduction in cholesterol oxidation products and VCAM-1. *J Atheroscler Thromb.* 2004;11(2):56-61.
441. Sattar N, Taskinen MR. Statins are diabetogenic--myth or reality? *Atheroscler Suppl.* 2012;13(1):1-10.
442. Cederberg H, Stancakova A, Yaluri N, Modi S, Kuusisto J, Laakso M. Increased risk of diabetes with statin treatment is associated with impaired insulin sensitivity and insulin secretion: a 6 year follow-up study of the METSIM cohort. *Diabetologia.* 2015;58(5):1109-17.
443. Sampson UK, Linton MF, Fazio S. Are statins diabetogenic? *Curr Opin Cardiol.* 2011;26(4):342-7.
444. Souza JC, Vanzela EC, Ribeiro RA, Rezende LF, de Oliveira CA, Carneiro EM, et al. Cholesterol reduction ameliorates glucose-induced calcium handling and insulin secretion in islets from low-density lipoprotein receptor knockout mice. *Biochim Biophys Acta.* 2013;1831(4):769-75.
445. Tse A, Lee AK, Yan L, Tse FW. Influence of cholesterol on cellular signaling and fusion pore kinetics. *J Mol Neurosci.* 2012;48(2):395-401.
446. Goldstein JL, Basu SK, Brown MS. Receptor-mediated endocytosis of low-density lipoprotein in cultured cells. In: Fleischer S, Fleischer B, editors. *Methods in Enzymology. Biomembranes Part L: Membrane Biogenesis: Processing and Recycling.* 98: ScienceDirect; 1983. p. 241-60.
447. Mamotte CD, Sturm M, Foo JI, van Bockxmeer FM, Taylor RR. Comparison of the LDL-receptor binding of VLDL and LDL from apoE4 and apoE3 homozygotes. *Am J Physiol.* 1999;276(3 Pt 1):E553-7.
448. Robinet P, Wang Z, Hazen SL, Smith JD. A simple and sensitive enzymatic method for cholesterol quantification in macrophages and foam cells. *J Lipid Res.* 2010;51(11):3364-9.
449. Thermo Fischer Scientific. Technical Resources 11875 - RPMI 1640 2014 [Available from: <https://www.thermofisher.com/au/en/home/technical-resources/media-formulation.114.html>].
450. McClenaghan NH, Barnett CR, O'Harte FP, Flatt PR. Mechanisms of amino acid-induced insulin secretion from the glucose-responsive BRIN-BD11 pancreatic B-cell line. *J Endocrinol.* 1996;151(3):349-57.
451. Tang J-s, Li Q-r, Li J-m, Wu J-r, Zeng R. Systematic Synergy of Glucose and GLP-1 to Stimulate Insulin Secretion Revealed by Quantitative Phosphoproteomics. *Scientific Reports.* 2017;7(1).
452. Henquin J-C. Misunderstandings and controversies about the insulin-secreting properties of antidiabetic sulfonylureas. *Biochimie.* 2017;143:3-9.
453. Carlessi R, Lemos NE, Dias AL, Oliveira FS, Brondani LA, Canani LH, et al. Exendin-4 protects rat islets against loss of viability and function induced by brain death. *Mol Cell Endocrinol.* 2015;412:239-50.
454. Szot GL, Koudria P, Bluestone JA. Murine pancreatic islet isolation. *J Vis Exp.* 2007(7):255.
455. Stange G, Van De Castele M, Heimberg H. Purification of rat pancreatic B-cells by fluorescence-activated cell sorting. *Methods Mol Med.* 2003;83:15-22.
456. Jackson Laboratories. Pancreatic Insulin Content by Acid-Ethanol Extraction. In: Leiter E, editor.: *Animal Models of Diabetes Complications Consortium Protocols*; 2009.

457. Sabapathy T. The Interaction of Insulin with the Insulin Receptor in a Membrane Environment. Thesis under examination: Curtin University; 2018.
458. Chintagari NR, Jin N, Wang P, Narasaraju TA, Chen J, Liu L. Effect of cholesterol depletion on exocytosis of alveolar type II cells. *Am J Respir Cell Mol Biol*. 2006;34(6):677-87.
459. Fulop T, Jr., Douziech N, Goulet AC, Desgeorges S, Linteau A, Lacombe G, et al. Cyclodextrin modulation of T lymphocyte signal transduction with aging. *Mech Ageing Dev*. 2001;122(13):1413-30.
460. McClenaghan NH, Gray AM, Barnett CR, Flatt PR. Hexose recognition by insulin-secreting BRIN-BD11 cells. *Biochem Biophys Res Commun*. 1996;223(3):724-8.
461. Hamid M, McCluskey JT, McClenaghan NH, Flatt PR. Comparison of the Secretory Properties of Four Insulin-Secreting Cell Lines. *Endocrine Research*. 2002;28(1-2):35-47.
462. Mel M, Karim MIA, Yusuf SAM, Hashim YZH-Y, Ahmad Nor Y. Comparing BRIN-BD11 culture producing insulin using different type of microcarriers. *Cytotechnology*. 2010;62(5):423-30.
463. Hamid M, McCluskey JT, McClenaghan NH, Flatt PR. Culture and function of electrofusion-derived clonal insulin-secreting cells immobilized on solid and macroporous microcarrier beads. *Biosci Rep*. 2000;20(3):167-76.
464. Stangroom J. Effect size calculator for T-Test 2019 [Available from: <https://www.socscistatistics.com/effectsize/default3.aspx>].
465. Ma L, Bindokas VP, Kuznetsov A, Rhodes C, Hays L, Edwardson JM, et al. Direct imaging shows that insulin granule exocytosis occurs by complete vesicle fusion. *Proc Natl Acad Sci USA*. 2004;101(25):9266-71.
466. Hou JC, Min L, Pessin JE. Chapter 16 Insulin Granule Biogenesis, Trafficking and Exocytosis. 2009;80:473-506.
467. MacDonald MJ, Ade L, Ntambi JM, Ansari IU, Stoker SW. Characterization of phospholipids in insulin secretory granules and mitochondria in pancreatic beta cells and their changes with glucose stimulation. *J Biol Chem*. 2015;290(17):11075-92.
468. Elhamdani A, Palfrey HC, Artalejo CR. Quantal size is dependent on stimulation frequency and calcium entry in calf chromaffin cells. *Neuron*. 2001;31(5):819-30.
469. Min L, Leung YM, Tomas A, Watson RT, Gaisano HY, Halban PA, et al. Dynamin is functionally coupled to insulin granule exocytosis. *J Biol Chem*. 2007;282(46):33530-6.
470. Salunkhe VA, Elvstam O, Eliasson L, Wendt A. Rosuvastatin Treatment Affects Both Basal and Glucose-Induced Insulin Secretion in INS-1 832/13 Cells. *Plos One*. 2016;11(3):e0151592.
471. Zhao W, Zhao SP. Different effects of statins on induction of diabetes mellitus: an experimental study. *Drug Des Devel Ther*. 2015;9:6211-23.
472. Metz SA, Rabaglia ME, Stock JB, Kowluru A. Modulation of insulin secretion from normal rat islets by inhibitors of the post-translational modifications of GTP-binding proteins. *Biochem J*. 1993;295 (Pt 1):31-40.
473. Li G, Regazzi R, Roche E, Wollheim CB. Blockade of mevalonate production by lovastatin attenuates bombesin and vasopressin potentiation of nutrient-induced insulin secretion in HIT-T15 cells. Probable involvement of small GTP-binding proteins. *Biochem J*. 1993;289 (Pt 2):379-85.
474. Xu Y, Toomre DK, Bogan JS, Hao M. Excess cholesterol inhibits glucose-stimulated fusion pore dynamics in insulin exocytosis. *J Cell Mol Med*. 2017;21(11):2950-62.
475. Koh KK, Quon MJ, Han SH, Lee Y, Kim SJ, Park JB, et al. Differential metabolic effects of pravastatin and simvastatin in hypercholesterolemic patients. *Atherosclerosis*. 2009;204(2):483-90.



476. Hatanaka T. Clinical pharmacokinetics of pravastatin: mechanisms of pharmacokinetic events. *Clin Pharmacokinet*. 2000;39(6):397-412.
477. Brayton CF. Dimethyl sulfoxide (DMSO): a review. *Cornell Vet*. 1986;76(1):61-90.
478. Scattolini V, Luni C, Zambon A, Galvanin S, Gagliano O, Ciubotaru CD, et al. Simvastatin Rapidly and Reversibly Inhibits Insulin Secretion in Intact Single-Islet Cultures. *Diabetes Ther*. 2016;7(4):679-93.
479. Rutter GA. Think zinc: New roles for zinc in the control of insulin secretion. *Islets*. 2014;2(1):49-50.
480. Davidson HW, Wenzlau JM, O'Brien RM. Zinc transporter 8 (ZnT8) and beta cell function. *Trends Endocrinol Metab*. 2014;25(8):415-24.
481. Slepchenko KG, Daniels NA, Guo A, Li YV. Autocrine effect of Zn(2)(+) on the glucose-stimulated insulin secretion. *Endocrine*. 2015;50(1):110-22.
482. Guzman H, Almarsson O, Remenar J, inventors; Almburg LLC, assignee. Novel Statin Pharmaceutical Compositions and Related Methods of Treatment. US2008.
483. Zuniga-Hertz JP, Rebelato E, Kassan A, Khalifa AM, Ali SS, Patel HH, et al. Distinct pathways of cholesterol biosynthesis impact on insulin secretion. *J Endocrinol*. 2015;224(1):75-84.
484. Rasschaert J, Flatt PR, Barnett CR, McClenaghan NH, Malaisse WJ. D-glucose metabolism in BRIN-BD11 islet cells. *Biochem Mol Med*. 1996;57(2):97-105.
485. Thorens B, Gerard N, Deriaz N. GLUT2 surface expression and intracellular transport via the constitutive pathway in pancreatic beta cells and insulinoma: evidence for a block in trans-Golgi network exit by brefeldin A. *J Cell Biol*. 1993;123(6 Pt 2):1687-94.
486. MacDonald PE, Rorsman P. Oscillations, Intercellular Coupling, and Insulin Secretion in Pancreatic  $\beta$  Cells. *PLoS Biol*. 2006;4(2):e49.
487. Newgard CB, Lu D, Jensen MV, Schissler J, Boucher A, Burgess S, et al. Stimulus/secretion coupling factors in glucose-stimulated insulin secretion: insights gained from a multidisciplinary approach. *Diabetes*. 2002;51 Suppl 3:S389-93.
488. Esguerra J, Mollet I, Salunkhe V, Wendt A, Eliasson L. Regulation of Pancreatic Beta Cell Stimulus-Secretion Coupling by microRNAs. *Genes*. 2014;5(4):1018-31.
489. LeRoith D. Beta-cell dysfunction and insulin resistance in type 2 diabetes: role of metabolic and genetic abnormalities. *Am J Med*. 2002;113 Suppl 6A:3S-11S.
490. Robertson RP. Chronic oxidative stress as a central mechanism for glucose toxicity in pancreatic islet beta cells in diabetes. *J Biol Chem*. 2004;279(41):42351-4.
491. Talchai C, Xuan S, Lin HV, Sussel L, Accili D. Pancreatic beta cell dedifferentiation as a mechanism of diabetic beta cell failure. *Cell*. 2012;150(6):1223-34.
492. Weir GC, Aguayo-Mazzucato C, Bonner-Weir S. beta-cell dedifferentiation in diabetes is important, but what is it? *Islets*. 2013;5(5):233-7.
493. Jonas JC, Sharma A, Hasenkamp W, Ilkova H, Patane G, Laybutt R, et al. Chronic hyperglycemia triggers loss of pancreatic beta cell differentiation in an animal model of diabetes. *J Biol Chem*. 1999;274(20):14112-21.
494. Laybutt DR, Glandt M, Xu G, Ahn YB, Trivedi N, Bonner-Weir S, et al. Critical reduction in beta-cell mass results in two distinct outcomes over time. Adaptation with impaired glucose tolerance or decompensated diabetes. *J Biol Chem*. 2003;278(5):2997-3005.
495. Nishimura W, Takahashi S, Yasuda K. MafA is critical for maintenance of the mature beta cell phenotype in mice. *Diabetologia*. 2015;58(3):566-74.
496. Pajvani UB, Accili D. The new biology of diabetes. *Diabetologia*. 2015;58(11):2459-68.

497. Cantley J, Grey ST, Maxwell PH, Withers DJ. The hypoxia response pathway and beta-cell function. *Diabetes Obes Metab.* 2010;12 Suppl 2:159-67.
498. Cinti F, Bouchi R, Kim-Muller JY, Ohmura Y, Sandoval PR, Masini M, et al. Evidence of  $\beta$ -Cell Dedifferentiation in Human Type 2 Diabetes. *The Journal of Clinical Endocrinology & Metabolism.* 2016;101(3):1044-54.
499. Wang Z, York NW, Nichols CG, Remedi MS. Pancreatic beta cell dedifferentiation in diabetes and redifferentiation following insulin therapy. *Cell Metab.* 2014;19(5):872-82.
500. Larsen S, Stride N, Hey-Mogensen M, Hansen CN, Bang LE, Bundgaard H, et al. Simvastatin effects on skeletal muscle: relation to decreased mitochondrial function and glucose intolerance. *J Am Coll Cardiol.* 2013;61(1):44-53.
501. Anagnostis P, Selalmatzidou D, Polyzos SA, Panagiotou A, Slavakis A, Panagiotidou A, et al. Comparative effects of rosuvastatin and atorvastatin on glucose metabolism and adipokine levels in non-diabetic patients with dyslipidaemia: a prospective randomised open-label study. *Int J Clin Pract.* 2011;65(6):679-83.
502. Wang M, Casey PJ. Protein prenylation: unique fats make their mark on biology. *Nature Reviews Molecular Cell Biology.* 2016;17(2):110-22.
503. Kowluru A. A lack of 'glue' misplaces Rab27A to cause islet dysfunction in diabetes. *The Journal of pathology.* 2016;238(3):375-7.
504. Romero N, Rogers G, Neilson A, Dranka BP. Quantifying Cellular ATP Production Rate Using Agilent Seahorse XF Technology. White paper. USA: Agilent Technologies, Inc.; 2018.
505. Romero N, Swain P, Neilson A, Dranka BP. Improving quantification of cellular glycolytic rate using Agilent Seahorse WF technology. White paper. USA: Agilent Technologies, Inc.; 2017.
506. Carlessi R, Chen Y, Rowlands J, Cruzat VF, Keane KN, Egan L, et al. GLP-1 receptor signalling promotes  $\beta$ -cell glucose metabolism via mTOR-dependent HIF-1 $\alpha$  activation. *Scientific Reports.* 2017;7(1):Article number 2661.
507. Rampersad SN. Multiple applications of Alamar Blue as an indicator of metabolic function and cellular health in cell viability bioassays. *Sensors (Basel).* 2012;12(9):12347-60.
508. Schirris TJ, Renkema GH, Ritschel T, Voermans NC, Bilos A, van Engelen BG, et al. Statin-Induced Myopathy Is Associated with Mitochondrial Complex III Inhibition. *Cell Metab.* 2015;22(3):399-407.
509. Sirvent P, Fabre O, Bordenave S, Hillaire-Buys D, Raynaud De Mauverger E, Lacampagne A, et al. Muscle mitochondrial metabolism and calcium signaling impairment in patients treated with statins. *Toxicol Appl Pharmacol.* 2012;259(2):263-8.
510. Mohammadi-Bardbori A, Najibi A, Amirzadegan N, Gharibi R, Dashti A, Omidi M, et al. Coenzyme Q10 remarkably improves the bio-energetic function of rat liver mitochondria treated with statins. *Eur J Pharmacol.* 2015;762:270-4.
511. Tolosa L, Carmona A, Castell JV, Gomez-Lechon MJ, Donato MT. High-content screening of drug-induced mitochondrial impairment in hepatic cells: effects of statins. *Arch Toxicol.* 2015;89(10):1847-60.
512. Sadighara M, Amirshardost Z, Minaiyan M, Hajhashemi V, Naserzadeh P, Salimi A, et al. Toxicity of Atorvastatin on Pancreas Mitochondria: A Justification for Increased Risk of Diabetes Mellitus. *Basic Clin Pharmacol Toxicol.* 2017;120(2):131-7.
513. Hill BG, Benavides GA, Lancaster JR, Jr., Ballinger S, Dell'Italia L, Jianhua Z, et al. Integration of cellular bioenergetics with mitochondrial quality control and autophagy. *Biol Chem.* 2012;393(12):1485-512.
514. Mikashinovich ZI, Belousova ES. Analysis of biochemical changes in rat erythrocytes induced by long-term simvastatin treatment. *Bull Exp Biol Med.* 2013;155(5):628-30.

515. Nowis D, Malenda A, Furs K, Oleszczak B, Sadowski R, Chlebowska J, et al. Statins impair glucose uptake in human cells. *BMJ open diabetes research & care*. 2014;2(1):e000017.
516. Takaguri A, Satoh K, Itagaki M, Tokumitsu Y, Ichihara K. Effects of Atorvastatin and Pravastatin on Signal Transduction Related to Glucose Uptake in 3T3L1 Adipocytes. *Journal of Pharmacological Sciences*. 2008;107(1):80-9.
517. Rorsman P, Eliasson L, Renstrom E, Gromada J, Barg S, Gopel S. The Cell Physiology of Biphasic Insulin Secretion. *News Physiol Sci*. 2000;15:72-7.
518. Yang W, Zheng Y, Xia Y, Ji H, Chen X, Guo F, et al. ERK1/2-dependent phosphorylation and nuclear translocation of PKM2 promotes the Warburg effect. *Nat Cell Biol*. 2012;14(12):1295-304.
519. Mathupala SP, Ko YH, Pedersen PL. Hexokinase II: cancer's double-edged sword acting as both facilitator and gatekeeper of malignancy when bound to mitochondria. *Oncogene*. 2006;25(34):4777-86.
520. Gerber PA, Rutter GA. The Role of Oxidative Stress and Hypoxia in Pancreatic Beta-Cell Dysfunction in Diabetes Mellitus. *Antioxid Redox Signal*. 2017;26(10):501-18.
521. Maiztegui B, Borelli MI, Massa ML, Del Zotto H, Gagliardino JJ. Enhanced expression of hexokinase I in pancreatic islets induced by sucrose administration. *J Endocrinol*. 2006;189(2):311-7.
522. Cheng S, Rhee EP, Larson MG, Lewis GD, McCabe EL, Shen D, et al. Metabolite profiling identifies pathways associated with metabolic risk in humans. *Circulation*. 2012;125(18):2222-31.
523. Heddi A, Stepien G, Benke PJ, Wallace DC. Coordinate induction of energy gene expression in tissues of mitochondrial disease patients. *J Biol Chem*. 1999;274(33):22968-76.
524. Linding R, Jensen LJ, Ostheimer GJ, van Vugt MATM, Jørgensen C, Miron IM, et al. Systematic Discovery of In Vivo Phosphorylation Networks. *Cell*. 2007;129(7):1415-26.
525. Beurel E, Grieco SF, Jope RS. Glycogen synthase kinase-3 (GSK3): regulation, actions, and diseases. *Pharmacol Ther*. 2015;148:114-31.
526. Hughes K, Nikolakaki E, Plyte SE, Totty NF, Woodgett JR. Modulation of the glycogen synthase kinase-3 family by tyrosine phosphorylation. *Embo J*. 1993;12(2):803-8.
527. Semache M, Zarrouki B, Fontés G, Fogarty S, Kikani C, Chawki MB, et al. Per-Arnt-Sim Kinase Regulates Pancreatic Duodenal Homeobox-1 Protein Stability via Phosphorylation of Glycogen Synthase Kinase 3 $\beta$  in Pancreatic  $\beta$ -Cells. *Journal of Biological Chemistry*. 2013;288(34):24825-33.
528. Amar S, Belmaker RH, Agam G. The possible involvement of glycogen synthase kinase-3 (GSK-3) in diabetes, cancer and central nervous system diseases. *Curr Pharm Des*. 2011;17(22):2264-77.
529. Gao C, Holscher C, Liu Y, Li L. GSK3: a key target for the development of novel treatments for type 2 diabetes mellitus and Alzheimer disease. *Rev Neurosci*. 2011;23(1):1-11.
530. Takahashi-Yanaga F. Activator or inhibitor? GSK-3 as a new drug target. *Biochemical Pharmacology*. 2013;86(2):191-9.
531. Henriksen E, Dokken B. Role of Glycogen Synthase Kinase-3 in Insulin Resistance and Type 2 Diabetes. *Current Drug Targets*. 2006;7(11):1435-41.
532. Kim KM, Lee K-S, Lee GY, Jin H, Durrance ES, Park HS, et al. Anti-diabetic efficacy of KICG1338, a novel glycogen synthase kinase-3 $\beta$  inhibitor, and its molecular characterization in animal models of type 2 diabetes and insulin resistance. *Mol Cell Endocrinol*. 2015;409:1-10.
533. Chen H, Fajol A, Hoene M, Zhang B, Schleicher ED, Lin Y, et al. PI3K-resistant GSK3 controls adiponectin formation and protects from metabolic syndrome. *Proceedings of the National Academy of Sciences*. 2016;113(20):5754-9.

534. Yaluri N, Modi S, Kokkola T. Simvastatin induces insulin resistance in L6 skeletal muscle myotubes by suppressing insulin signaling, GLUT4 expression and GSK-3 $\beta$  phosphorylation. *Biochem Biophys Res Commun.* 2016;480(2):194-200.
535. Cai G, Wang J, Xin X, Ke Z, Luo J. Phosphorylation of glycogen synthase kinase-3 $\beta$  at serine 9 confers cisplatin resistance in ovarian cancer cells. *Int J Oncol.* 2007;31(3):657-62.
536. Marchand B, Arsenault D, Raymond-Fleury A, Boisvert F-M, Boucher M-J. Glycogen Synthase Kinase-3 (GSK3) Inhibition Induces Prosurvival Autophagic Signals in Human Pancreatic Cancer Cells. *Journal of Biological Chemistry.* 2015;290(9):5592-605.
537. Pastorino JG, Hoek JB. Regulation of hexokinase binding to VDAC. *J Bioenerg Biomembr.* 2008;40(3):171-82.
538. Stocker R, Pollicino C, Gay CA, Nestel P, Colquhoun D, Whiting M, et al. Neither plasma coenzyme Q10 concentration, nor its decline during pravastatin therapy, is linked to recurrent cardiovascular disease events: a prospective case-control study from the LIPID study. *Atherosclerosis.* 2006;187(1):198-204.
539. Mabuchi H, Higashikata T, Kawashiri M, Katsuda S, Mizuno M, Nohara A, et al. Reduction of serum ubiquinol-10 and ubiquinone-10 levels by atorvastatin in hypercholesterolemic patients. *J Atheroscler Thromb.* 2005;12(2):111-9.
540. Hodgson JM, Watts GF, Playford DA, Burke V, Croft KD. Coenzyme Q10 improves blood pressure and glycaemic control: a controlled trial in subjects with type 2 diabetes. *Eur J Clin Nutr.* 2002;56(11):1137-42.
541. De Pinieux G, Chariot P, Ammi-Said M, Louarn F, Lejonc JL, Astier A, et al. Lipid-lowering drugs and mitochondrial function: effects of HMG-CoA reductase inhibitors on serum ubiquinone and blood lactate/pyruvate ratio. *British journal of clinical pharmacology.* 1996;42(3):333-7.
542. Munnich A, Rustin P, Rotig A, Chretien D, Bonnefont JP, Nuttin C, et al. Clinical aspects of mitochondrial disorders. *J Inherit Metab Dis.* 1992;15(4):448-55.
543. Thornton B, Cohen B, Copeland W, Maria BL. Mitochondrial disease: clinical aspects, molecular mechanisms, translational science, and clinical frontiers. *J Child Neurol.* 2014;29(9):1179-207.
544. Zehetner J, Danzer C, Collins S, Eckhardt K, Gerber PA, Ballschmieter P, et al. pVHL is a regulator of glucose metabolism and insulin secretion in pancreatic  $\beta$ -cells. *Genes & Development.* 2008;22(22):3135-46.
545. Efrat S. Mechanisms of adult human  $\beta$ -cell in vitro dedifferentiation and redifferentiation. *Diabetes, Obesity and Metabolism.* 2016;18:97-101.
546. Dunning BE, Gerich JE. The role of alpha-cell dysregulation in fasting and postprandial hyperglycemia in type 2 diabetes and therapeutic implications. *Endocr Rev.* 2007;28(3):253-83.
547. Wollheim CB. Beta-cell mitochondria in the regulation of insulin secretion: a new culprit in type II diabetes. *Diabetologia.* 2000;43(3):265-77.
548. Ishihara H, Wang H, Drewes LR, Wollheim CB. Overexpression of monocarboxylate transporter and lactate dehydrogenase alters insulin secretory responses to pyruvate and lactate in beta cells. *J Clin Invest.* 1999;104(11):1621-9.
549. Hitosugi T, Kang S, Vander Heiden MG, Chung TW, Elf S, Lythgoe K, et al. Tyrosine phosphorylation inhibits PKM2 to promote the Warburg effect and tumor growth. *Sci Signal.* 2009;2(97):ra73.
550. Wiese EK, Hitosugi T. Tyrosine Kinase Signaling in Cancer Metabolism: PKM2 Paradox in the Warburg Effect. *Front Cell Dev Biol.* 2018;6:79.

551. Fan J, Hitosugi T, Chung TW, Xie J, Ge Q, Gu TL, et al. Tyrosine Phosphorylation of Lactate Dehydrogenase A Is Important for NADH/NAD<sup>+</sup> Redox Homeostasis in Cancer Cells. *Mol Cell Biol*. 2011;31(24):4938-50.
552. Jin L, Chun J, Pan C, Alesi GN, Li D, Magliocca KR, et al. Phosphorylation-mediated activation of LDHA promotes cancer cell invasion and tumour metastasis. *Oncogene*. 2017;36(27):3797-806.
553. Guo S, Dai C, Guo M, Taylor B, Harmon JS, Sander M, et al. Inactivation of specific  $\beta$  cell transcription factors in type 2 diabetes. *Journal of Clinical Investigation*. 2013;123(8):3305-16.
554. Krause MR, Regen SL. The structural role of cholesterol in cell membranes: from condensed bilayers to lipid rafts. *Acc Chem Res*. 2014;47(12):3512-21.
555. Warnock DE, Roberts C, Lutz MS, Blackburn WA, Young WW, Jr., Baenziger JU. Determination of plasma membrane lipid mass and composition in cultured Chinese hamster ovary cells using high gradient magnetic affinity chromatography. *J Biol Chem*. 1993;268(14):10145-53.
556. Kraft ML. Plasma membrane organization and function: moving past lipid rafts. *Mol Biol Cell*. 2013;24(18):2765-8.
557. Simons K, Sampaio JL. Membrane organization and lipid rafts. *Cold Spring Harb Perspect Biol*. 2011;3(10):a004697.
558. Cunha DA, Amaral ME, Carvalho CP, Collares-Buzato CB, Carneiro EM, Boschero AC. Increased expression of SNARE proteins and synaptotagmin IV in islets from pregnant rats and in vitro prolactin-treated neonatal islets. *Biol Res*. 2006;39(3):555-66.
559. Kowluru A, Veluthakal R, Rhodes CJ, Kamath V, Syed I, Koch BJ. Protein Farnesylation-Dependent Raf/Extracellular Signal-Related Kinase Signaling Links to Cytoskeletal Remodeling to Facilitate Glucose-Induced Insulin Secretion in Pancreatic  $\beta$ -Cells. *Diabetes*. 2010;59(4):967-77.
560. Asahara S, Shibutani Y, Teruyama K, Inoue HY, Kawada Y, Etoh H, et al. Ras-related C3 botulinum toxin substrate 1 (RAC1) regulates glucose-stimulated insulin secretion via modulation of F-actin. *Diabetologia*. 2013;56(5):1088-97.
561. Suski JM, Lebedzinska M, Wojtala A, Duszynski J, Giorgi C, Pinton P, et al. Isolation of plasma membrane-associated membranes from rat liver. *Nature Protocols*. 2014;9(2):312-22.
562. Seenarain V, Viola HM, Ravenscroft G, Casey TM, Lipscombe RJ, Ingley E, et al. Evidence of altered guinea pig ventricular cardiomyocyte protein expression and growth in response to a 5 min in vitro exposure to H<sub>2</sub>O<sub>2</sub>. *J Proteome Res*. 2010;9(4):1985-94.
563. Casey TM, Khan JM, Bringans SD, Koudelka T, Takle PS, Downs RA, et al. Analysis of Reproducibility of Proteome Coverage and Quantitation Using Isobaric Mass Tags (iTRAQ and TMT). *J Proteome Res*. 2017;16(2):384-92.
564. Boothe T, Lim GE, Cen H, Skovso S, Piske M, Li SN, et al. Inter-domain tagging implicates caveolin-1 in insulin receptor trafficking and Erk signaling bias in pancreatic beta-cells. *Mol Metab*. 2016;5(5):366-78.
565. Ghoshal K, Chakraborty S, Das C, Chattopadhyay S, Chowdhury S, Bhattacharyya M. Dielectric properties of plasma membrane: A signature for dyslipidemia in diabetes mellitus. *Arch Biochem Biophys*. 2017;635:27-36.
566. Veluthakal R, Kaur H, Goalstone M, Kowluru A. Dominant-negative alpha-subunit of farnesyl- and geranyltransferase inhibits glucose-stimulated, but not KCl-stimulated, insulin secretion in INS 832/13 cells. *Diabetes*. 2007;56(1):204-10.
567. Graham J. Preparation of Crude Subcellular Fractions by Differential Centrifugation. *The Scientific World Journal*. 2002;2:1638-42.

568. Broadway NM, Saggerson ED. Solubilization and separation of two distinct carnitine acyltransferases from hepatic microsomes: characterization of the malonyl-CoA-sensitive enzyme. *Biochem J.* 1995;310 ( Pt 3):989-95.
569. Goldfine ID, Maddux BA, Youngren JF, Reaven G, Accili D, Trischitta V, et al. The role of membrane glycoprotein plasma cell antigen 1/ectonucleotide pyrophosphatase phosphodiesterase 1 in the pathogenesis of insulin resistance and related abnormalities. *Endocr Rev.* 2008;29(1):62-75.
570. Blacker TS, Duchon MR. Investigating mitochondrial redox state using NADH and NADPH autofluorescence. *Free Radical Biology and Medicine.* 2016;100:53-65.
571. Van De Winkel M, Pipeleers D. Autofluorescence-activated cell sorting of pancreatic islet cells: purification of insulin-containing  $\beta$ -cells according to glucose-induced changes in cellular redox state. *Biochem Biophys Res Commun.* 1983;114(2):835-42.
572. Hanson MS, Steffen A, Danobeitia JS, Ludwig B, Fernandez LA. Flow cytometric quantification of glucose-stimulated beta-cell metabolic flux can reveal impaired islet functional potency. *Cell Transplant.* 2008;17(12):1337-47.
573. Smelt MJ, Faas MM, de Haan BJ, de Vos P. Pancreatic beta-cell purification by altering FAD and NAD(P)H metabolism. *Exp Diabetes Res.* 2008;2008:165360.
574. Rocheleau JV, Head WS, Piston DW. Quantitative NAD(P)H/flavoprotein autofluorescence imaging reveals metabolic mechanisms of pancreatic islet pyruvate response. *J Biol Chem.* 2004;279(30):31780-7.
575. Sun MY, Yoo E, Green BJ, Altamentova SM, Kilkenny DM, Rocheleau JV. Autofluorescence imaging of living pancreatic islets reveals fibroblast growth factor-21 (FGF21)-induced metabolism. *Biophys J.* 2012;103(11):2379-88.
576. Donner KJ, Becker KM, Hissong BD, Ahmed SA. Comparison of multiple assays for kinetic detection of apoptosis in thymocytes exposed to dexamethasone or diethylstilbesterol. *Cytometry.* 1999;35(1):80-90.
577. Jacob MC, Favre M, Bensa J-C. Membrane Cell Permeabilisation With Saponin and Multiparametric Analysis by Flow Cytometry. *Cytometry.* 1991;12:550-8.
578. Tzur A, Moore JK, Jorgensen P, Shapiro HM, Kirschner MW. Optimizing optical flow cytometry for cell volume-based sorting and analysis. *PLoS One.* 2011;6(1):e16053.
579. Lee E, Choi J, Jo Y, Kim JY, Jang YJ, Lee HM, et al. ACT-PRESTO: Rapid and consistent tissue clearing and labeling method for 3-dimensional (3D) imaging. *Sci Rep.* 2016;6:18631.
580. Kulig W, Olzynska A, Jurkiewicz P, Kantola AM, Komulainen S, Manna M, et al. Cholesterol under oxidative stress-How lipid membranes sense oxidation as cholesterol is being replaced by oxysterols. *Free Radic Biol Med.* 2015;84:30-41.
581. Salaun C, James DJ, Chamberlain LH. Lipid rafts and the regulation of exocytosis. *Traffic.* 2004;5(4):255-64.
582. Rorato R, Borges BC, Uchoa ET, Antunes-Rodrigues J, Elias CF, Elias LLK. LPS-Induced Low-Grade Inflammation Increases Hypothalamic JNK Expression and Causes Central Insulin Resistance Irrespective of Body Weight Changes. *Int J Mol Sci.* 2017;18(7).
583. Veluthakal R, Chvyrkova I, Tannous M, McDonald P, Amin R, Hadden T, et al. Essential role for membrane lipid rafts in interleukin-1 $\beta$ -induced nitric oxide release from insulin-secreting cells: potential regulation by caveolin-1. *Diabetes.* 2005;54(9):2576-85.
584. Kepner EM, Yoder SM, Oh E, Kalwat MA, Wang Z, Quilliam LA, et al. Cool-1/ $\beta$ PIX functions as a guanine nucleotide exchange factor in the cycling of Cdc42 to regulate insulin secretion. *Am J Physiol Endocrinol Metab.* 2011;301(6):E1072-80.

585. Rohrer L, Ohnsorg PM, Lehner M, Landolt F, Rinninger F, von Eckardstein A. High-density lipoprotein transport through aortic endothelial cells involves scavenger receptor BI and ATP-binding cassette transporter G1. *Circ Res*. 2009;104(10):1142-50.
586. Miao L, Okoro EU, Cao Z, Yang H, Motley-Johnson E, Guo Z. High-density lipoprotein-mediated transcellular cholesterol transport in mouse aortic endothelial cells. *Biochem Biophys Res Commun*. 2015;465(2):256-61.
587. Pandzic E, Gelissen IC, Whan R, Barter PJ, Sviridov D, Gaus K, et al. The ATP binding cassette transporter, ABCG1, localizes to cortical actin filaments. *Sci Rep*. 2017;7:42025.
588. Tarling EJ, Edwards PA. ATP binding cassette transporter G1 (ABCG1) is an intracellular sterol transporter. *Proc Natl Acad Sci U S A*. 2011;108(49):19719-24.
589. Volgyi K, Badics K, Sialana FJ, Gulyassy P, Udvari EB, Kis V, et al. Early Presymptomatic Changes in the Proteome of Mitochondria-Associated Membrane in the APP/PS1 Mouse Model of Alzheimer's Disease. *Mol Neurobiol*. 2018;55(10):7839-57.
590. Howell SL, Fink CJ, Lacy PE. Isolation and properties of secretory granules from rat islets of Langerhans. I. Isolation of a secretory granule fraction. *J Cell Biol*. 1969;41(1):154-61.
591. Urquhart KR, Zhao Y, Baker JA, Lu Y, Yan L, Cook MN, et al. A novel heat shock protein alpha 8 (Hspa8) molecular network mediating responses to stress- and ethanol-related behaviors. *neurogenetics*. 2016;17(2):91-105.
592. Pockley AG. Heat shock proteins as regulators of the immune response. *The Lancet*. 2003;362(9382):469-76.
593. Brunham L, Kruit JK, Verchere B, Hayden MR. Cholesterol in islet dysfunction and type 2 diabetes. *The Journal of Clinical Investigation*. 2008;118(2):403.
594. Edwards PA, Tabor D, Kast HR, Venkateswaran A. Regulation of gene expression by SREBP and SCAP. *Biochim Biophys Acta*. 2000;1529(1-3):103-13.
595. Preiss D, Sattar N. Does the LDL receptor play a role in the risk of developing type 2 diabetes? *Jama*. 2015;313(10):1016-7.
596. Wang X, Briggs MR, Hua X, Yokoyama C, Goldstein JL, Brown MS. Nuclear protein that binds sterol regulatory element of low density lipoprotein receptor promoter. II. Purification and characterization. *J Biol Chem*. 1993;268(19):14497-504.
597. Smith JR, Osborne TF, Goldstein JL, Brown MS. Identification of nucleotides responsible for enhancer activity of sterol regulatory element in low density lipoprotein receptor gene. *J Biol Chem*. 1990;265(4):2306-10.
598. Kotzka J, Knebel B, Avci H, Jacob S, Nitzgen U, Jockenhovel F, et al. Phosphorylation of sterol regulatory element-binding protein (SREBP)-1a links growth hormone action to lipid metabolism in hepatocytes. *Atherosclerosis*. 2010;213(1):156-65.
599. Kruit JK, Wijesekara N, Westwell-Roper C, Vanmierlo T, de Haan W, Bhattacharjee A, et al. Loss of Both ABCA1 and ABCG1 Results in Increased Disturbances in Islet Sterol Homeostasis, Inflammation, and Impaired  $\alpha$ -Cell Function. *Diabetes*. 2012;61(3):659-64.
600. Rigotti A, Trigatti BL, Penman M, Rayburn H, Herz J, Krieger M. A targeted mutation in the murine gene encoding the high density lipoprotein (HDL) receptor scavenger receptor class B type I reveals its key role in HDL metabolism. *Proc Natl Acad Sci U S A*. 1997;94(23):12610-5.
601. Zanotti I, Favari E, Sposito AC, Rothblat GH, Bernini F. Pitavastatin increases ABCA1-mediated lipid efflux from Fu5AH rat hepatoma cells. *Biochem Biophys Res Commun*. 2004;321(3):670-4.
602. Chong PH, Kezele R, Franklin C. High-density lipoprotein cholesterol and the role of statins. *Circ J*. 2002;66(11):1037-44.

603. Khera AV, Demler OV, Adelman SJ, Collins HL, Glynn RJ, Ridker PM, et al. Cholesterol Efflux Capacity, High-Density Lipoprotein Particle Number, and Incident Cardiovascular Events. *Circulation*. 2017;135(25):2494-504.
604. Guan JZ, Tamasawa N, Murakami H, Matsui J, Tanabe J, Matsuki K, et al. HMG-CoA reductase inhibitor, simvastatin improves reverse cholesterol transport in type 2 diabetic patients with hyperlipidemia. *J Atheroscler Thromb*. 2008;15(1):20-5.
605. Ando H, Tsuruoka S, Yamamoto H, Takamura T, Kaneko S, Fujimura A. Effects of pravastatin on the expression of ATP-binding cassette transporter A1. *The Journal of pharmacology and experimental therapeutics*. 2004;311(1):420-5.
606. Sone H, Shimano H, Shu M, Nakakuki M, Takahashi A, Sakai M, et al. Statins downregulate ATP-binding-cassette transporter A1 gene expression in macrophages. *Biochem Biophys Res Commun*. 2004;316(3):790-4.
607. Maejima T, Yamazaki H, Aoki T, Tamaki T, Sato F, Kitahara M, et al. Effect of pitavastatin on apolipoprotein A-I production in HepG2 cell. *Biochem Biophys Res Commun*. 2004;324(2):835-9.
608. Kobayashi M, Gouda K, Chisaki I, Ochiai M, Itagaki S, Iseki K. Regulation mechanism of ABCA1 expression by statins in hepatocytes. *Eur J Pharmacol*. 2011;662(1-3):9-14.
609. Argmann CA, Edwards JY, Sawyez CG, O'Neil CH, Hegele RA, Pickering JG, et al. Regulation of macrophage cholesterol efflux through hydroxymethylglutaryl-CoA reductase inhibition: a role for RhoA in ABCA1-mediated cholesterol efflux. *J Biol Chem*. 2005;280(23):22212-21.
610. Genvigir FD, Hirata MH, Hirata RD. ABCA1 expression and statins: inhibitory effect in peripheral blood mononuclear cells. *Pharmacogenomics*. 2009;10(6):997-1005.
611. Niesor EJ, Schwartz GG, Perez A, Stauffer A, Durrwell A, Bucklar-Suchankova G, et al. Statin-Induced Decrease in ATP-Binding Cassette Transporter A1 Expression via microRNA33 Induction may Counteract Cholesterol Efflux to High-Density Lipoprotein. *Cardiovascular Drugs and Therapy*. 2015;29(1):7-14.
612. Cerda A, Issa MH, Genvigir FD, Rohde CB, Cavalli SA, Bertolami MC, et al. Atorvastatin and hormone therapy influence expression of ABCA1, APOA1 and SCARB1 in mononuclear cells from hypercholesterolemic postmenopausal women. *J Steroid Biochem Mol Biol*. 2013;138:403-9.
613. Chen WM, Sheu WH, Tseng PC, Lee TS, Lee WJ, Chang PJ, et al. Modulation of microRNA Expression in Subjects with Metabolic Syndrome and Decrease of Cholesterol Efflux from Macrophages via microRNA-33-Mediated Attenuation of ATP-Binding Cassette Transporter A1 Expression by Statins. *PLoS One*. 2016;11(5):e0154672.
614. Sato R. Sterol metabolism and SREBP activation. *Arch Biochem Biophys*. 2010;501(2):177-81.
615. Sanchez-Muniz FJ, Bastida S. Do not use the Friedewald formula to calculate LDL-cholesterol in hypercholesterolaemic rats. *European Journal of Lipid Science and Technology*. 2008;110(4):295-301.
616. Rhodes CJ, White MF. Molecular insights into insulin action and secretion. *Eur J Clin Invest*. 2002;32 Suppl 3:3-13.
617. Bedinger DH, Adams SH. Metabolic, anabolic, and mitogenic insulin responses: A tissue-specific perspective for insulin receptor activators. *Mol Cell Endocrinol*. 2015;415:143-56.
618. Braun M, Ramracheya R, Rorsman P. Autocrine regulation of insulin secretion. *Diabetes Obes Metab*. 2012;14 Suppl 3:143-51.
619. Rhodes CJ, White MF, Leahy JL, Kahn SE. Direct autocrine action of insulin on beta-cells: does it make physiological sense? *Diabetes*. 2013;62(7):2157-63.



620. Kosacka J, Kern M, Klötting N, Paeschke S, Rudich A, Haim Y, et al. Autophagy in adipose tissue of patients with obesity and type 2 diabetes. *Mol Cell Endocrinol.* 2015;409:21-32.
621. Lavallard VJ, Meijer AJ, Codogno P, Gual P. Autophagy, signaling and obesity. *Pharmacological Research.* 2012;66(6):513-25.
622. Chong ZZ, Shang YC, Wang S, Maiese K. Shedding new light on neurodegenerative diseases through the mammalian target of rapamycin. *Progress in Neurobiology.* 2012;99(2):128-48.
623. Anisimov VN. Metformin: do we finally have an anti-aging drug? *Cell Cycle.* 2013;12(22):3483-9.
624. Saxton RA, Sabatini DM. mTOR Signaling in Growth, Metabolism, and Disease. *Cell.* 2017;168(6):960-76.
625. Verges B, Cariou B. mTOR inhibitors and diabetes. *Diabetes Res Clin Pract.* 2015;110(2):101-8.
626. Xu J, Dang Y, Ren YR, Liu JO. Cholesterol trafficking is required for mTOR activation in endothelial cells. *Proc Natl Acad Sci U S A.* 2010;107(10):4764-9.
627. Ai D, Chen C, Han S, Ganda A, Murphy AJ, Haeusler R, et al. Regulation of hepatic LDL receptors by mTORC1 and PCSK9 in mice. *J Clin Invest.* 2012;122(4):1262-70.
628. Roudier E, Mistafa O, Stenius U. Statins induce mammalian target of rapamycin (mTOR)-mediated inhibition of Akt signaling and sensitize p53-deficient cells to cytostatic drugs. *Mol Cancer Ther.* 2006;5(11):2706-15.
629. Wang HJ, Park JY, Kwon O, Choe EY, Kim CH, Hur KY, et al. Chronic HMGCR/HMG-CoA reductase inhibitor treatment contributes to dysglycemia by upregulating hepatic gluconeogenesis through autophagy induction. *Autophagy.* 2015;11(11):2089-101.
630. Jin Y, Sui HJ, Dong Y, Ding Q, Qu WH, Yu SX, et al. Atorvastatin enhances neurite outgrowth in cortical neurons in vitro via up-regulating the Akt/mTOR and Akt/GSK-3beta signaling pathways. *Acta Pharmacol Sin.* 2012;33(7):861-72.
631. Yoon MS. The Role of Mammalian Target of Rapamycin (mTOR) in Insulin Signaling. *Nutrients.* 2017;9(11).
632. Di Camillo B, Carlon A, Eduati F, Toffolo GM. A rule-based model of insulin signalling pathway. *BMC Syst Biol.* 2016;10(1):38.
633. Bacova Z, Orecna M, Hafko R, Strbak V. Cell swelling-induced signaling for insulin secretion bypasses steps involving G proteins and PLA2 and is N-ethylmaleimide insensitive. *Cell Physiol Biochem.* 2007;20(5):387-96.
634. Orecna M, Hafko R, Toporcerova V, Strbak V, Bacova Z. Cell swelling-induced insulin secretion from INS-1E cells is inhibited by extracellular Ca<sup>2+</sup> and is tetanus toxin resistant. *Cell Physiol Biochem.* 2010;26(2):197-208.
635. Walker L, Peterson CM. Flow cytometric staining of pancreatic endocrine cells. *Ann Clin Lab Sci.* 1994;24(6):501-8.
636. Gombos I, Bacso Z, Detre C, Nagy H, Goda K, Andrasfalvy M, et al. Cholesterol sensitivity of detergent resistance: a rapid flow cytometric test for detecting constitutive or induced raft association of membrane proteins. *Cytometry A.* 2004;61(2):117-26.
637. Fong CW. Statins in therapy: Understanding their hydrophilicity, lipophilicity, binding to 3-hydroxy-3-methylglutaryl-CoA reductase, ability to cross the blood brain barrier and metabolic stability based on electrostatic molecular orbital studies. *European Journal of Medicinal Chemistry.* 2014;85:661-74.

638. Ansari JA, Bhandari U, Pillai KK, Haque SE. Effect of rosuvastatin on obesity-induced cardiac oxidative stress in Wistar rats--a preliminary study. *Indian J Exp Biol.* 2012;50(3):216-22.
639. Hashimoto Y, Okuyama H. Statins Cause Lifestyle-Related Diseases-Biochemical Mechanism. *Endocrinology & Diabetes Research.* 2017;03(02).
640. el-Sayed MY, Guion TA, Fayer MD. Effect of cholesterol on viscoelastic properties of dipalmitoylphosphatidylcholine multibilayers as measured by a laser-induced ultrasonic probe. *Biochemistry.* 1986;25(17):4825-32.
641. Duan X, Chen CF. Does coenzyme Q10 play a role in the risk of new-onset diabetes due to statins? *Int J Cardiol.* 2016;225:260-1.
642. Waters DD, Ho JE, DeMicco DA, Breazna A, Arsenault BJ, Wun C-C, et al. Predictors of New-Onset Diabetes in Patients Treated With Atorvastatin. *J Am Coll Cardiol.* 2011;57(14):1535-45.
643. Briant L, Salehi A, Vergari E, Zhang Q, Rorsman P. Glucagon secretion from pancreatic  $\alpha$ -cells. *Upsala Journal of Medical Sciences.* 2016;121(2):113-9.
644. Lund A, Bagger JI, Christensen M, Knop FK, Vilsbøll T. Glucagon and Type 2 Diabetes: the Return of the Alpha Cell. *Curr Diab Rep.* 2014;14(12).
645. Lai YS, Chen WC, Kuo TC, Ho CT, Kuo CH, Tseng YJ, et al. Mass-Spectrometry-Based Serum Metabolomics of a C57BL/6J Mouse Model of High-Fat-Diet-Induced Non-alcoholic Fatty Liver Disease Development. *J Agric Food Chem.* 2015;63(35):7873-84.
646. Andrikopoulos S, Blair AR, Deluca N, Fam BC, Proietto J. Evaluating the glucose tolerance test in mice. *Am J Physiol Endocrinol Metab.* 2008;295(6):E1323-32.
647. Cersosimo E, Solis-Herrera C, Trautmann ME, Malloy J, Triplitt CL. Assessment of pancreatic beta-cell function: review of methods and clinical applications. *Curr Diabetes Rev.* 2014;10(1):2-42.
648. Burns C, Morris T, Jones B, Koch W, Borer M, Riber U, et al. Proposal to initiate a project to evaluate a candidate International Standard for Human Recombinant Insulin. Geneva: World Health Organization, Expert committee on biological standardization, preparations Ecosfp; 2010. Contract No.: WHO/BS/10.2143.
649. Churchill Hospital O. HOMA Calculator Oxford: Oxford University; 2013 [Available from: <https://www.dtu.ox.ac.uk/homacalculator/index.php>].
650. Van Dijk TH, Laskewitz AJ, Grefhorst A, Boer TS, Bloks VW, Kuipers F, et al. A novel approach to monitor glucose metabolism using stable isotopically labelled glucose in longitudinal studies in mice. *Laboratory Animals.* 2013;47(2):79-88.
651. Wallace TM, Levy JC, Matthews DR. Use and abuse of HOMA modeling. *Diabetes Care.* 2004;27(6):1487-95.
652. Katz A, Nambi SS, Mather K, Baron AD, Follmann DA, Sullivan G, et al. Quantitative insulin sensitivity check index: a simple, accurate method for assessing insulin sensitivity in humans. *J Clin Endocrinol Metab.* 2000;85(7):2402-10.
653. Cacho J, Sevillano J, de Castro J, Herrera E, Ramos MP. Validation of simple indexes to assess insulin sensitivity during pregnancy in Wistar and Sprague-Dawley rats. *Am J Physiol Endocrinol Metab.* 2008;295(5):E1269-76.
654. Singh B, Saxena A. Surrogate markers of insulin resistance: A review. *World Journal of Diabetes.* 2010;1(2):36.
655. Dallal GE. Obtaining Superscripts to Affix to Means That Are Not Significantly Different From Each Other Boston, MA2000 [Jean Mayer USDA Human Nutrition Research Centre on Aging, Tufts University]. Available from: [http://www.jerrydallal.com/LHSP/similar\\_prog.htm](http://www.jerrydallal.com/LHSP/similar_prog.htm).

656. GraphPad. GraphPad Prism7 User Guide: Box and whiskers graphs 1995 - 2017. Available from: <https://www.graphpad.com/guides/prism/7/user-guide/index.htm?box-and-whiskers.htm>.
657. Gargiulo S, Gramanzini M, Megna R, Greco A, Albanese S, Manfredi C, et al. Evaluation of Growth Patterns and Body Composition in C57Bl/6J Mice Using Dual Energy X-Ray Absorptiometry. *BioMed Research International*. 2014;2014:1-11.
658. Kramer CK, Ye C, Hanley AJ, Connelly PW, Sermer M, Zinman B, et al. Delayed timing of post-challenge peak blood glucose predicts declining beta cell function and worsening glucose tolerance over time: insight from the first year postpartum. *Diabetologia*. 2015;58(6):1354-62.
659. Kramer CK, Vuksan V, Choi H, Zinman B, Retnakaran R. Emerging parameters of the insulin and glucose response on the oral glucose tolerance test: reproducibility and implications for glucose homeostasis in individuals with and without diabetes. *Diabetes Res Clin Pract*. 2014;105(1):88-95.
660. Wigmore SJ, Stutchfield BM, Forbes SJ. Liver function and failure. In: Garden OJ, Parks RW, editors. *Hepatobiliary and Pancreatic Surgery. Companion to specialist surgical practice*. Fifth edition ed: Saunders Elsevier; 2014.
661. Ravier MA, Rutter GA. Glucose or insulin, but not zinc ions, inhibit glucagon secretion from mouse pancreatic alpha-cells. *Diabetes*. 2005;54(6):1789-97.
662. Leung YM, Ahmed I, Sheu L, Gao X, Hara M, Tsushima RG, et al. Insulin regulates islet alpha-cell function by reducing KATP channel sensitivity to adenosine 5'-triphosphate inhibition. *Endocrinology*. 2006;147(5):2155-62.
663. Olsen HL, Theander S, Bokvist K, Buschard K, Wollheim CB, Gromada J. Glucose stimulates glucagon release in single rat alpha-cells by mechanisms that mirror the stimulus-secretion coupling in beta-cells. *Endocrinology*. 2005;146(11):4861-70.
664. Gylfe E, Gilon P. Glucose regulation of glucagon secretion. *Diabetes Res Clin Pract*. 2014;103(1):1-10.
665. Walker JN, Ramracheya R, Zhang Q, Johnson PR, Braun M, Rorsman P. Regulation of glucagon secretion by glucose: paracrine, intrinsic or both? *Diabetes Obes Metab*. 2011;13 Suppl 1:95-105.
666. Watts M, Ha J, Kimchi O, Sherman A. Paracrine regulation of glucagon secretion: the beta/alpha/delta model. *Am J Physiol Endocrinol Metab*. 2016;310(8):E597-E611.
667. Lush IE. The genetics of tasting in mice. VI. Saccharin, acesulfame, dulcin and sucrose. *Genet Res*. 1989;53(2):95-9.
668. Cham S, Koslik HJ, Golomb BA. Mood, Personality, and Behavior Changes During Treatment with Statins: A Case Series. *Drug Saf Case Rep*. 2016;3(1):1.
669. Lang UE, Beglinger C, Schweinfurth N, Walter M, Borgwardt S. Nutritional Aspects of Depression. *Cellular Physiology and Biochemistry*. 2015;37(3):1029-43.
670. Caparros-Martin JA, Lareu RR, Ramsay JP, Peplies J, Reen FJ, Headlam HA, et al. Statin therapy causes gut dysbiosis in mice through a PXR-dependent mechanism. *Microbiome*. 2017;5(1):95.
671. Sugiyama T, Tsugawa Y, Tseng CH, Kobayashi Y, Shapiro MF. Different time trends of caloric and fat intake between statin users and nonusers among US adults: gluttony in the time of statins? *JAMA Intern Med*. 2014;174(7):1038-45.
672. Gustavsson N, Seah T, Lao Y, Radda GK, Sudhof TC, Han W. Delayed onset of hyperglycaemia in a mouse model with impaired glucagon secretion demonstrates that dysregulated glucagon secretion promotes hyperglycaemia and type 2 diabetes. *Diabetologia*. 2011;54(2):415-22.

673. Lefebvre PJ, Paquot N, Scheen AJ. Inhibiting or antagonizing glucagon: making progress in diabetes care. *Diabetes, Obesity and Metabolism*. 2015;17(8):720-5.
674. Brereton MF, Iberl M, Shimomura K, Zhang Q, Adriaenssens AE, Proks P, et al. Reversible changes in pancreatic islet structure and function produced by elevated blood glucose. *Nature Communications*. 2014;5(1).
675. Farhy LS, McCall AL. Glucagon – the new ‘insulin’ in the pathophysiology of diabetes. *Curr Opin Clin Nutr Metab Care*. 2015;18(4):407-14.
676. McShane LM, Franklin ZJ, O’Harte FPM, Irwin N. Ablation of glucagon receptor signaling by peptide-based glucagon antagonists improves glucose tolerance in high fat fed mice. *Peptides*. 2014;60:95-101.
677. O’Harte FPM, Franklin ZJ, Irwin N. Two novel glucagon receptor antagonists prove effective therapeutic agents in high-fat-fed and obese diabetic mice. *Diabetes, Obesity and Metabolism*. 2014;16(12):1214-22.
678. Scheen AJ, Paquot N, Lefebvre PJ. Investigational glucagon receptor antagonists in Phase I and II clinical trials for diabetes. *Expert Opin Investig Drugs*. 2017;26(12):1373-89.
679. Steenberg VR, Jensen SM, Pedersen J, Madsen AN, Windeløv JA, Holst B, et al. Acute disruption of glucagon secretion or action does not improve glucose tolerance in an insulin-deficient mouse model of diabetes. *Diabetologia*. 2015;59(2):363-70.
680. Cederholm J, Wibell L. Insulin release and peripheral sensitivity at the oral glucose tolerance test. *Diabetes Res Clin Pract*. 1990;10(2):167-75.
681. Guzzaloni G, Grugni G, Mazzilli G, Moro D, Morabito F. Comparison between beta-cell function and insulin resistance indexes in prepubertal and pubertal obese children. *Metabolism*. 2002;51(8):1011-6.
682. Matthews DR, Hosker JP, Rudenski AS, Naylor BA, Treacher DF, Turner RC. Homeostasis model assessment: insulin resistance and beta-cell function from fasting plasma glucose and insulin concentrations in man. *Diabetologia*. 1985;28(7):412-9.
683. Levy JC, Matthews DR, Hermans MP. Correct homeostasis model assessment (HOMA) evaluation uses the computer program. *Diabetes Care*. 1998;21(12):2191-2.
684. Mouse strain datasheet - 000664 C57BL/6J: The Jackson Laboratory; [Available from: <https://www.jax.org/strain/000664>].
685. Gupta D, Jetton TL, LaRock K, Monga N, Satish B, Lausier J, et al. Temporal characterization of  $\beta$  cell-adaptive and -maladaptive mechanisms during chronic high-fat feeding in C57BL/6NTac mice. *Journal of Biological Chemistry*. 2017;292(30):12449-59.
686. Abramson J. Statins in Persons at Low Risk of Cardiovascular Disease 2017 [Available from: <http://www.thennt.com/nnt/statins-persons-low-risk-cardiovascular-disease/>].
687. Chen ZY, Liu SN, Li CN, Sun SJ, Liu Q, Lei L, et al. Atorvastatin helps preserve pancreatic beta cell function in obese C57BL/6 J mice and the effect is related to increased pancreas proliferation and amelioration of endoplasmic-reticulum stress. *Lipids Health Dis*. 2014;13:98.
688. Koza RA, Nikonova L, Hogan J, Rim JS, Mendoza T, Faulk C, et al. Changes in gene expression foreshadow diet-induced obesity in genetically identical mice. *PLoS Genet*. 2006;2(5):e81.
689. O’Brien RM. Moving on from GWAS: Functional Studies on the G6PC2 Gene Implicated in the Regulation of Fasting Blood Glucose. *Curr Diab Rep*. 2013;13(6):768-77.
690. Peyot ML, Pepin E, Lamontagne J, Latour MG, Zarrouki B, Lussier R, et al. -Cell Failure in Diet-Induced Obese Mice Stratified According to Body Weight Gain: Secretory Dysfunction and Altered Islet Lipid Metabolism Without Steatosis or Reduced -Cell Mass. *Diabetes*. 2010;59(9):2178-87.

691. Pepin E, Al-Mass A, Attane C, Zhang K, Lamontagne J, Lussier R, et al. Pancreatic beta-Cell Dysfunction in Diet-Induced Obese Mice: Roles of AMP-Kinase, Protein Kinase Cepsilon, Mitochondrial and Cholesterol Metabolism, and Alterations in Gene Expression. *PLoS One*. 2016;11(4):e0153017.
692. Kahl CG, Deas C. Exercise-Induced Anaphylaxis in an Air Force Aviator Taking a HMG-CoA Reductase Inhibitor: A Case Report and Review of the Presentation, Diagnoses, and Treatment. *Military Medicine*. 2017;182(5):e1816-e9.
693. Moulis G, Bene J, Sommet A, Sailler L, Lapeyre-Mestre M, Montastruc JL, et al. Statin-induced lupus: a case/non-case study in a nationwide pharmacovigilance database. *Lupus*. 2012;21(8):885-9.
694. Peringat J, Manappallil RG, Karadan U. Rhabdomyolysis: a rare complication of Hashimoto's thyroiditis precipitated by statin therapy. *BMJ Case Rep*. 2018;2018.
695. Nichols L, Pfeifer K, Mammen AL, Shahnoor N, Konersman CG. An Unusual Case of Statin-Induced Myopathy: Anti-HMGCoA Necrotizing Autoimmune Myopathy. *J Gen Intern Med*. 2015;30(12):1879-83.
696. Fischer S, Julius U. Management of patients with statin intolerance. *Atherosclerosis Supplements*. 2017;30:33-7.
697. Palamuthusingam D, Mantha M, Dheda S. HMG CoA reductase inhibitor associated myositis and autoimmune hepatitis. *Internal Medicine Journal*. 2017;47(10):1213-5.
698. Ramachandran S, Saraf S, Shetty C, Capps N, Bailey C. Paradoxical decrease in HDL-cholesterol and apolipoprotein A1 with simvastatin and atorvastatin in a patient with type 2 diabetes. *Annals of Clinical Biochemistry*. 2010;48(1):75-8.
699. Okeahialam BN, Isiguzoro I. Statin related memory dysfunction in a Nigerian woman: a case report. *Curr Drug Saf*. 2012;7(1):33-4.
700. Ohmura C, Watada H, Hirose T, Tanaka Y, Kawamori R. Acute onset and worsening of diabetes concurrent with administration of statins. *Endocr J*. 2005;52(3):369-72.
701. Spence JD, Dresser GK. Overcoming Challenges With Statin Therapy. *Journal of the American Heart Association*. 2016;5(1).
702. Finsterer J, Segall L. Drugs interfering with mitochondrial disorders. *Drug and Chemical Toxicology*. 2009;33(2):138-51.
703. Apostolopoulou M, Corsini A, Roden M. The role of mitochondria in statin-induced myopathy. *European Journal of Clinical Investigation*. 2015;45(7):745-54.
704. Bjorkhem-Bergman L, Acimovic J, Torndal UB, Parini P, Eriksson LC. Lovastatin prevents carcinogenesis in a rat model for liver cancer. Effects of ubiquinone supplementation. *Anticancer Res*. 2010;30(4):1105-12.
705. Pecoraro V, Moja L, Dall'Olmo L, Cappellini G, Garattini S. Most appropriate animal models to study the efficacy of statins: a systematic review. *Eur J Clin Invest*. 2014;44(9):848-71.
706. Russell JC, Proctor SD. Small animal models of cardiovascular disease: tools for the study of the roles of metabolic syndrome, dyslipidemia, and atherosclerosis. *Cardiovascular Pathology*. 2006;15(6):318-30.
707. Yin W, Carballo-Jane E, McLaren DG, Mendoza VH, Gagen K, Geoghagen NS, et al. Plasma lipid profiling across species for the identification of optimal animal models of human dyslipidemia. *J Lipid Res*. 2012;53:51-65.
708. Fernandez ML. Guinea pigs as models for cholesterol and lipoprotein metabolism. *J Nutr*. 2001;131(1):10-20.

709. Schlosser MJ, Kapeghian JC, Verlangieri AJ. Selected physical and biochemical parameters in the streptozotocin-treated guinea pig: insights into the diabetic guinea pig model. *Life Sci.* 1987;41(11):1345-53.
710. Tveden-Nyborg P, Birck MM, Ipsen DH, Thiessen T, Feldmann LB, Lindblad MM, et al. Diet-induced dyslipidemia leads to nonalcoholic fatty liver disease and oxidative stress in guinea pigs. *Transl Res.* 2016;168:146-60.
711. Zimmerman AE, Yip CC. Guinea pig insulin. I. Purification and physical properties. *J Biol Chem.* 1974;249(13):4021-5.
712. Li YV. Zinc and insulin in pancreatic beta-cells. *Endocrine.* 2013;45(2):178-89.
713. Halperin F, Lopez X, Manning R, Kahn CR, Kulkarni RN, Goldfine AB. Insulin Augmentation of Glucose-Stimulated Insulin Secretion Is Impaired in Insulin-Resistant Humans. *Diabetes.* 2012;61(2):301-9.
714. Kanda M, Satoh K, Ichihara K. Effects of atorvastatin and pravastatin on glucose tolerance in diabetic rats mildly induced by streptozotocin. *Biol Pharm Bull.* 2003;26(12):1681-4.
715. Brennan L, Corless M, Hewage C, Malthouse JP, McClenaghan NH, Flatt PR, et al. <sup>13</sup>C NMR analysis reveals a link between L-glutamine metabolism, D-glucose metabolism and gamma-glutamyl cycle activity in a clonal pancreatic beta-cell line. *Diabetologia.* 2003;46(11):1512-21.
716. Newsholme P, Procopio J, Lima MM, Pithon-Curi TC, Curi R. Glutamine and glutamate--their central role in cell metabolism and function. *Cell Biochem Funct.* 2003;21(1):1-9.
717. Newsholme P, Brennan L, Bender K. Amino Acid Metabolism,  $\beta$ -cell Function, and Diabetes. *Diabetes.* 2006;55(Supplement 2):S39-S47.
718. Lacey JM, Wilmore DW. Is glutamine a conditionally essential amino acid? *Nutr Rev.* 1990;48(8):297-309.
719. Smith RJ. Glutamine metabolism and its physiologic importance. *Journal of Parenteral and Enteral Nutrition.* 1990;14(4, Supplement):40S-4S.
720. Grintescu IM, Luca Vasiliu I, Cucereanu Badica I, Mirea L, Pavelescu D, Balanescu A, et al. The influence of parenteral glutamine supplementation on glucose homeostasis in critically ill polytrauma patients—A randomized-controlled clinical study. *Clin Nutr.* 2015;34(3):377-82.
721. Menge BA, Schrader H, Ritter PR, Ellrichmann M, Uhl W, Schmidt WE, et al. Selective amino acid deficiency in patients with impaired glucose tolerance and type 2 diabetes. *Regulatory peptides.* 2010;160(1-3):75-80.
722. Guasch-Ferre M, Hruby A, Toledo E, Clish CB, Martinez-Gonzalez MA, Salas-Salvado J, et al. Metabolomics in Prediabetes and Diabetes: A Systematic Review and Meta-analysis. *Diabetes Care.* 2016;39(5):833-46.
723. Samocha-Bonet D, Wong O, Synnott EL, Piyaratna N, Douglas A, Gribble FM, et al. Glutamine reduces postprandial glycemia and augments the glucagon-like peptide-1 response in type 2 diabetes patients. *J Nutr.* 2011;141(7):1233-8.
724. Wischmeyer PE. Glutamine: mode of action in critical illness. *Crit Care Med.* 2007;35(9 Suppl):S541-4.
725. Chang J, Wu T, Greenfield JR, Samocha-Bonet D, Horowitz M, Rayner CK. Effects of intraduodenal glutamine on incretin hormone and insulin release, the glycemic response to an intraduodenal glucose infusion, and antropyloroduodenal motility in health and type 2 diabetes. *Diabetes care.* 2013;36(8):2262-5.

726. de Souza AZ, Zambom AZ, Abboud KY, Reis SK, Tannihao F, Guadagnini D, et al. Oral supplementation with L-glutamine alters gut microbiota of obese and overweight adults: A pilot study. *Nutrition*. 2015;31(6):884-9.
727. Wurtz P, Wang Q, Soinen P, Kangas AJ, Fatemifar G, Tynkkynen T, et al. Metabolomic Profiling of Statin Use and Genetic Inhibition of HMG-CoA Reductase. *J Am Coll Cardiol*. 2016;67(10):1200-10.
728. Eagle H, Oyama VI, Levy M, Horton CL, Fleischman R. The growth response of mammalian cells in tissue culture to L-glutamine and L-glutamic acid. *J Biol Chem*. 1956;218(2):607-16.
729. Engstrom W. Requirements for competence and commitment of quiescent 3T3-cells to initiate DNA synthesis after growth stimulation in low serum concentration. *Exp Cell Res*. 1981;135(1):115-25.
730. Curi R, Lagranha CJ, Doi SQ, Sellitti DF, Procopio J, Pithon-Curi TC, et al. Molecular mechanisms of glutamine action. *J Cell Physiol*. 2005;204(2):392-401.
731. Li C, Buettger C, Kwagh J, Matter A, Daikhin Y, Nissim IB, et al. A signaling role of glutamine in insulin secretion. *J Biol Chem*. 2004;279(14):13393-401.
732. Torres-Santiago L, Mauras N, Hossain J, Weltman AL, Darmaun D. Does oral glutamine improve insulin sensitivity in adolescents with type 1 diabetes? *Nutrition*. 2017;34:1-6.
733. Hakvoort TB, He Y, Kulik W, Vermeulen JL, Duijst S, Ruijter JM, et al. Pivotal role of glutamine synthetase in ammonia detoxification. *Hepatology*. 2017;65(1):281-93.
734. Krebs HA. Metabolism of amino-acids: The synthesis of glutamine from glutamic acid and ammonia, and the enzymic hydrolysis of glutamine in animal tissues. *Biochem J*. 1935;29(8):1951-69.
735. Ivarsson R, Quintens R, Dejonghe S, Tsukamoto K, in 't Veld P, Renstrom E, et al. Redox control of exocytosis: regulatory role of NADPH, thioredoxin, and glutaredoxin. *Diabetes*. 2005;54(7):2132-42.
736. Tanha T, Amanlou H, Chamani M, Ebrahimnezhad Y, Salamatdost R, Maheri N, et al. Impact of glutamine on glutathione peroxidase activity (GPX) and total antioxidant status (TAS) during transition period in Holstein dairy cows. *Journal of cell and Animal Biology*. 2011;5(10):206-14.
737. Cruzat VF, Newsholme P. An introduction to glutamine metabolism. In: Meynial-Denis D, editor. *Glutamine: Biochemistry, Physiology, and Clinical Applications* CRC Press, Taylor & Francis Group; 2017.
738. Albrecht J, Norenberg MD. Glutamine: a Trojan horse in ammonia neurotoxicity. *Hepatology*. 2006;44(4):788-94.
739. Tjader I, Berg A, Wernerman J. Exogenous glutamine--compensating a shortage? *Crit Care Med*. 2007;35(9 Suppl):S553-6.
740. Mates JM, Segura JA, Campos-Sandoval JA, Lobo C, Alonso L, Alonso FJ, et al. Glutamine homeostasis and mitochondrial dynamics. *Int J Biochem Cell Biol*. 2009;41(10):2051-61.
741. Krajcova A, Ziak J, Jiroutkova K, Patkova J, Elkalaf M, Dzupa V, et al. Normalizing Glutamine Concentration Causes Mitochondrial Uncoupling in an In Vitro Model of Human Skeletal Muscle. *JPEN J Parenter Enteral Nutr*. 2013.
742. Newsholme P, Haber EP, Hirabara SM, Rebelato EL, Procopio J, Morgan D, et al. Diabetes associated cell stress and dysfunction: role of mitochondrial and non-mitochondrial ROS production and activity. *J Physiol*. 2007;583(Pt 1):9-24.

743. Moosmann B, Behl C. Selenoproteins, cholesterol-lowering drugs, and the consequences: revisiting of the mevalonate pathway. *Trends Cardiovasc Med.* 2004;14(7):273-81.
744. Kromer A, Moosmann B. Statin-induced liver injury involves cross-talk between cholesterol and selenoprotein biosynthetic pathways. *Mol Pharmacol.* 2009;75(6):1421-9.
745. Bouillaud F. UCP2, not a physiologically relevant uncoupler but a glucose sparing switch impacting ROS production and glucose sensing. *Biochimica et Biophysica Acta (BBA) - Bioenergetics.* 2009;1787(5):377-83.
746. Mauser W, Perwitz N, Meier B, Fasshauer M, Klein J. Direct adipotropic actions of atorvastatin: differentiation state-dependent induction of apoptosis, modulation of endocrine function, and inhibition of glucose uptake. *Eur J Pharmacol.* 2007;564(1-3):37-46.
747. Balaz M, Becker AS, Balazova L, Straub L, Muller J, Gashi G, et al. Inhibition of Mevalonate Pathway Prevents Adipocyte Browning in Mice and Men by Affecting Protein Prenylation. *Cell Metab.* 2019;29(4):901-16 e8.
748. Vieira LR, Martinez D, Forgiarini LF, Rosa DP, Munoz GA, Fagundes M, et al. Uncoupling protein-2 mRNA expression in mice subjected to intermittent hypoxia. *J Bras Pneumol.* 2015;41(2):167-74.
749. Cruzat VF, Pantaleao LC, Donato JJ, Homem De Bittencourt PI, Tirapegui J. Oral supplementations with free and dipeptide forms of L-glutamine in endotoxemic mice: effects on muscle glutamine-glutathione axis and heat shock proteins. *Journal of Nutritional Biochemistry.* 2014; Accepted manuscript.
750. Real J, Miranda C, Olofsson CS, Smith PA. Lipophilicity predicts the ability of nonsulphonylurea drugs to block pancreatic beta-cell KATP channels and stimulate insulin secretion; statins as a test case. *Endocrinology, Diabetes & Metabolism.* 2018;1(2):e00017.
751. Furst P. New developments in glutamine delivery. *J Nutr.* 2001;131(9 Suppl):2562S-8S.
752. Ahmad S, White CW, Chang LY, Schneider BK, Allen CB. Glutamine protects mitochondrial structure and function in oxygen toxicity. *Am J Physiol Lung Cell Mol Physiol.* 2001;280(4):L779-91.
753. Laakso M, Kuusisto J. Diabetes Secondary to Treatment with Statins. *Curr Diab Rep.* 2017;17(2):10.
754. Navarese EP, Buffon A, Andreotti F, Kozinski M, Welton N, Fabiszak T, et al. Meta-analysis of impact of different types and doses of statins on new-onset diabetes mellitus. *Am J Cardiol.* 2013;111(8):1123-30.
755. Naci H, Brugts J, Ades T. Comparative tolerability and harms of individual statins: a study-level network meta-analysis of 246 955 participants from 135 randomized, controlled trials. *Circ Cardiovasc Qual Outcomes.* 2013;6(4):390-9.
756. Thakker D, Nair S, Pagada A, Jamdade V, Malik A. Statin use and the risk of developing diabetes: a network meta-analysis. *Pharmacoepidemiol Drug Saf.* 2016;25(10):1131-49.
757. Romano S, Mitro N, Diviccaro S, Spezzano R, Audano M, Garcia-Segura LM, et al. Short-term effects of diabetes on neurosteroidogenesis in the rat hippocampus. *J Steroid Biochem Mol Biol.* 2017;167:135-43.
758. Peri A. Neuroprotective effects of estrogens: the role of cholesterol. *J Endocrinol Invest.* 2016;39(1):11-8.
759. Genvigir FD, Rodrigues AC, Cerda A, Hirata MH, Curi R, Hirata RD. ABCA1 and ABCG1 expressions are regulated by statins and ezetimibe in Caco-2 cells. *Drug Metabol Drug Interact.* 2011;26(1):33-6.
760. Jiang YJ, Lu B, Kim P, Elias PM, Feingold KR. Regulation of ABCA1 expression in human keratinocytes and murine epidermis. *J Lipid Res.* 2006;47(10):2248-58.



761. Kellick KA, Bottorff M, Toth PP. A clinician's guide to statin drug-drug interactions. *Journal of Clinical Lipidology*. 2014;8(3):S30-S46.
762. Lennernas H. Clinical pharmacokinetics of atorvastatin. *Clin Pharmacokinet*. 2003;42(13):1141-60.
763. Sirtori CR. The pharmacology of statins. *Pharmacological research : the official journal of the Italian Pharmacological Society*. 2014;88:3-11.
764. Causevic-Ramosevac A, Semiz S. Drug interactions with statins. *Acta Pharmaceutica*. 2013;63(3):277-93.
765. Kohli P, Knowles JW, Sarraju A, Waters DD, Reaven G. Metabolic Markers to Predict Incident Diabetes Mellitus in Statin-Treated Patients (from the Treating to New Targets and the Stroke Prevention by Aggressive Reduction in Cholesterol Levels Trials). *Am J Cardiol*. 2016;118(9):1275-81.
766. Borutaite V. Mitochondria as decision-makers in cell death. *Environmental and Molecular Mutagenesis*. 2010:NA-NA.
767. Bholra PD, Letai A. Mitochondria-Judges and Executioners of Cell Death Sentences. *Mol Cell*. 2016;61(5):695-704.
768. Montemurro C, Vadrevu S, Gurlo T, Butler AE, Vongbunyong KE, Petcherski A, et al. Cell cycle-related metabolism and mitochondrial dynamics in a replication-competent pancreatic beta-cell line. *Cell Cycle*. 2017;16(21):2086-99.
769. Jezek P, Olejar T, Smolkova K, Jezek J, Dlaskova A, Plecita-Hlavata L, et al. Antioxidant and regulatory role of mitochondrial uncoupling protein UCP2 in pancreatic beta-cells. *Physiol Res*. 2014;63 Suppl 1:S73-91.
770. Brun T, Maechler P. Beta-cell mitochondrial carriers and the diabetogenic stress response. *Biochimica et Biophysica Acta (BBA) - Molecular Cell Research*. 2016;1863(10):2540-9.
771. Accili D, Talchai SC, Kim-Muller JY, Cinti F, Ishida E, Ordelheide AM, et al. When beta-cells fail: lessons from dedifferentiation. *Diabetes Obes Metab*. 2016;18 Suppl 1:117-22.
772. Oh J, Ban MR, Miskie BA, Pollex RL, Hegele RA. Genetic determinants of statin intolerance. *Lipids Health Dis*. 2007;6:7.
773. Broniarek I, Jarmuszkiewicz W. Atorvastatin affects negatively respiratory function of isolated endothelial mitochondria. *Arch Biochem Biophys*. 2018;637:64-72.
774. Leloup C, Tourrel-Cuzin C, Magnan C, Karaca M, Castel J, Carneiro L, et al. Mitochondrial reactive oxygen species are obligatory signals for glucose-induced insulin secretion. *Diabetes*. 2009;58(3):673-81.
775. Harmon JS, Stein R, Robertson RP. Oxidative stress-mediated, post-translational loss of MafA protein as a contributing mechanism to loss of insulin gene expression in glucotoxic beta cells. *J Biol Chem*. 2005;280(12):11107-13.
776. Mei S, Gu H, Yang X, Guo H, Liu Z, Cao W. Prolonged Exposure to Insulin Induces Mitochondrion-Derived Oxidative Stress through Increasing Mitochondrial Cholesterol Content in Hepatocytes. *Endocrinology*. 2012;153(5):2120-9.
777. Ogihara T, Chuang JC, Vestermark GL, Garmey JC, Ketchum RJ, Huang X, et al. Liver X receptor agonists augment human islet function through activation of anaplerotic pathways and glycerolipid/free fatty acid cycling. *J Biol Chem*. 2010;285(8):5392-404.
778. Wat E, Ng CF, Liu CL, Zhang C, Koon CM, Lau CP, et al. Effect of combined use of Fructus Schisandrae and statin on high-fat-diet-induced metabolic syndrome in rats. *Hong Kong Med J*. 2016;22 Suppl 6(6):24-7.
779. Mistry RH, Verkade HJ, Tietge UJ. Reverse Cholesterol Transport Is Increased in Germ-Free Mice-Brief Report. *Arterioscler Thromb Vasc Biol*. 2017;37(3):419-22.

780. Degirolamo C, Rainaldi S, Bovenga F, Murzilli S, Moschetta A. Microbiota modification with probiotics induces hepatic bile acid synthesis via downregulation of the Fxr-Fgf15 axis in mice. *Cell Rep.* 2014;7(1):12-8.
781. He X, Zheng N, He J, Liu C, Feng J, Jia W, et al. Gut Microbiota Modulation Attenuated the Hypolipidemic Effect of Simvastatin in High-Fat/Cholesterol-Diet Fed Mice. *J Proteome Res.* 2017;16(5):1900-10.
782. Kaddurah-Daouk R, Baillie RA, Zhu H, Zeng Z-B, Wiest MM, Nguyen UT, et al. Enteric Microbiome Metabolites Correlate with Response to Simvastatin Treatment. *PLoS ONE.* 2011;6(10):e25482.
783. Nolan JA, Skuse P, Govindarajan K, Patterson E, Konstantinidou N, Casey PG, et al. The influence of rosuvastatin on the gastrointestinal microbiota and host gene expression profiles. *Am J Physiol Gastrointest Liver Physiol.* 2017;312(5):G488-G97.
784. Qi Y, Jiang C, Cheng J, Krausz KW, Li T, Ferrell JM, et al. Bile acid signaling in lipid metabolism: metabolomic and lipidomic analysis of lipid and bile acid markers linked to anti-obesity and anti-diabetes in mice. *Biochim Biophys Acta.* 2015;1851(1):19-29.
785. John S, Weiss JN, Ribalet B. Subcellular Localization of Hexokinases I and II Directs the Metabolic Fate of Glucose. *PLoS ONE.* 2011;6(3):e17674.
786. Davis EA, Cuesta-Munoz A, Raoul M, Buettger C, Sweet I, Moates M, et al. Mutants of glucokinase cause hypoglycaemia- and hyperglycaemia syndromes and their analysis illuminates fundamental quantitative concepts of glucose homeostasis. *Diabetologia.* 1999;42(10):1175-86.
787. TeSlaa T, Teitell MA. Techniques to monitor glycolysis. *Methods Enzymol.* 2014;542:91-114.
788. Lenzen S. A Fresh View of Glycolysis and Glucokinase Regulation: History and Current Status. *Journal of Biological Chemistry.* 2014;289(18):12189-94.
789. Satin LS, Butler PC, Ha J, Sherman AS. Pulsatile insulin secretion, impaired glucose tolerance and type 2 diabetes. *Molecular Aspects of Medicine.* 2015;42:61-77.
790. Morgan AR, Thompson JMD, Murphy R, Black PN, Lam W-J, Ferguson LR, et al. Obesity and diabetes genes are associated with being born small for gestational age: Results from the Auckland Birthweight Collaborative study. *BMC Medical Genetics.* 2010;11(1).
791. Roche E, Assimacopoulos-Jeannet F, Witters LA, Perruchoud B, Yaney G, Corkey B, et al. Induction by glucose of genes coding for glycolytic enzymes in a pancreatic beta-cell line (INS-1). *J Biol Chem.* 1997;272(5):3091-8.
792. Anand P, Murali KY, Tandon V, Murthy PS, Chandra R. Insulinotropic effect of cinnamaldehyde on transcriptional regulation of pyruvate kinase, phosphoenolpyruvate carboxykinase, and GLUT4 translocation in experimental diabetic rats. *Chem Biol Interact.* 2010;186(1):72-81.
793. Krus U, Kotova O, Spégel P, Hallgard E, Sharoyko Vladimir V, Vedin A, et al. Pyruvate dehydrogenase kinase 1 controls mitochondrial metabolism and insulin secretion in INS-1 832/13 clonal  $\beta$ -cells. *Biochemical Journal.* 2010;429(1):205-13.
794. Bishop ML, Fody EP, Schoeff LE. *Clinical Chemistry: Principles, Techniques, Correlations.* 7th ed. Philadelphia, USA: Lippincott Williams & Wilkins; 2013.

***Every reasonable effort has been made to acknowledge the owners of copyright material. I would be pleased to hear from any copyright owner who has been omitted or incorrectly acknowledged.***

## Appendix A      Supplementary Material

### A.1      Chapter 2 Supplementary Figure

#### A.1.1      Failure to rescue insulin after cholesterol restoration

To assess whether the blunted insulin secretion observed with statin treatment was due to cholesterol content alone, atorvastatin-treated cells, prepared as described in Section 2.1 were subsequently treated for 30 min with c-M $\beta$ CD to replenish cellular cholesterol via membrane loading before stimulated insulin secretion experiments were undertaken. Cholesterol was reduced by atorvastatin, increased by c-M $\beta$ CD and restored by c-M $\beta$ CD after atorvastatin treatment, with no significant difference between untreated and atorvastatin plus c-M $\beta$ CD groups (Figure App A1). Unfortunately, the characteristic blunting of insulin secretion with atorvastatin treatment was not apparent in these experiments, possibly due to atorvastatin batch discrepancies; hence they are inconclusive and have been added as preliminary results. However, moderation of the insulin-blunting effect of atorvastatin treatment by replenishing cholesterol via c-M $\beta$ CD appears to be an unlikely outcome. On the contrary, from these results, cholesterol replenishment appears to exacerbate blunting when stimulated with alanine or exendin-4.

This failure of c-M $\beta$ CD to rescue the insulin response in atorvastatin-treated cells indicates that factors other than membrane cholesterol abundance alone may influence statin-related insulin blunting. Further experiments would be needed to establish whether longer cholesterol recovery would improve insulin responsiveness, for example after the restoration of cholesterol content in intracellular organelle membranes.

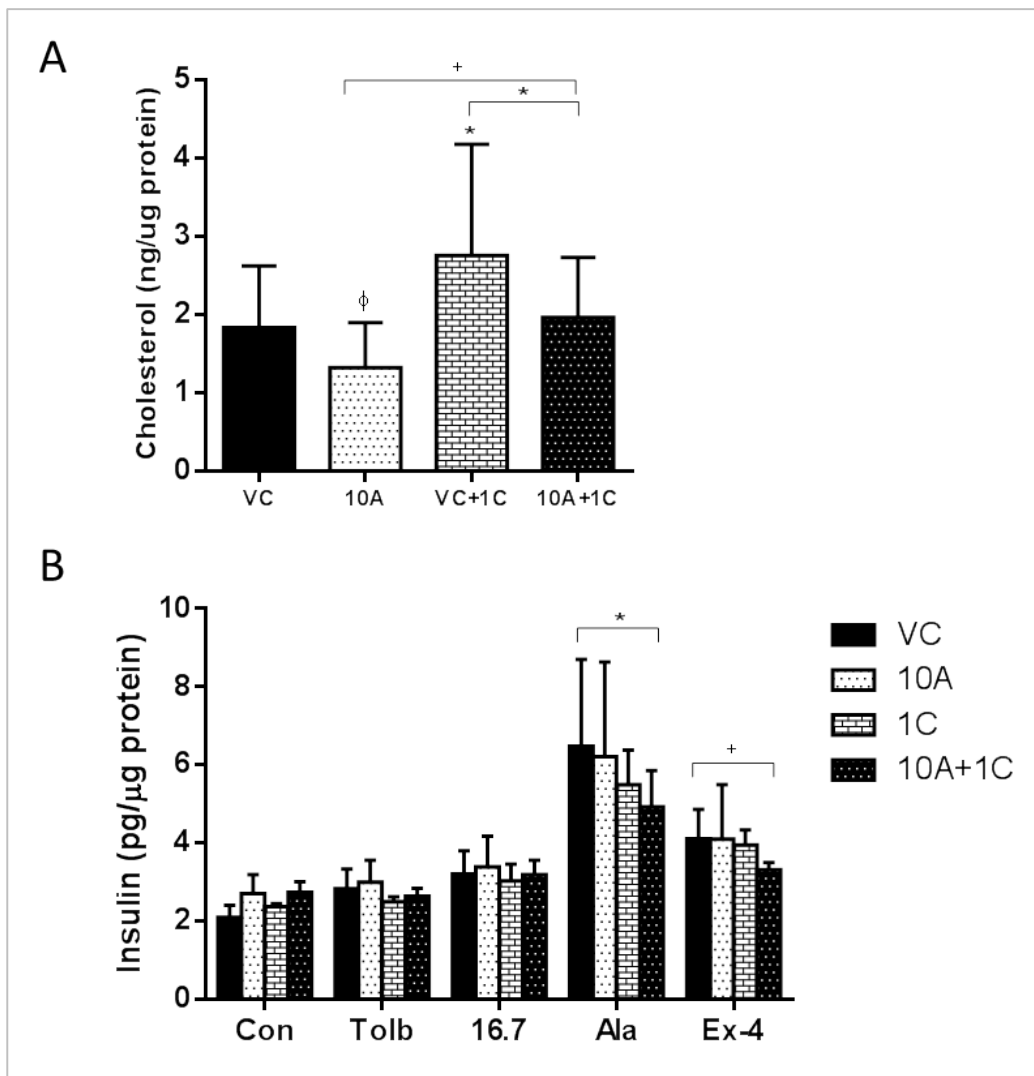


**Figure SA.1 Cholesterol 'rescue'.**

**A.** Cholesterol shows depletion with 10  $\mu$ M Atorvastatin treatment and is replenished by 30 min incubation with 1 mM c-M $\beta$ CD. **B.** Insulin stimulated by various secretagogues is affected by cholesterol reduction then loading. A, atorvastatin; n=3; \*  $P < 0.001$ ; +  $P < 0.01$ ;  $\phi$   $P < 0.05$  compared to control unless otherwise indicated.

## A.2 Chapter 3 Supplementary Table

**Table SA.1. Table of Enzymes Assessed in Chapter 3**

Enzyme	Full Name	Function
Hexokinases I, II & GLK	Hexokinase I Hexokinase II Hexokinase IV (Glucokinase)	Hexokinases are responsible for the first step in glycolysis; phosphorylation of glucose to glucose-6-phosphate. There are four known hexokinases. Hex I and II are thought to mainly facilitate either glycolysis (catabolic) or glycogen formation (anabolic), respectively. Hexokinase I is associated with the mitochondrial cellular compartment. It is also selectively excluded from $\beta$ -cells and liver (245). Hexokinase II is mainly expressed in muscle and is sensitive to signalling factors that can cause its cellular translocation from cytoplasm to mitochondria and subsequent alteration of glucose fate from glycogen synthesis to glycolysis (785). Hexokinase IV (glucokinase, GLK) is more specific to glucose while having a lower affinity for it, and is more abundantly expressed in $\beta$ -cells, including BRIN-BD11 cells, than Hex I or II. It is used as a functional marker for glucose sensing capacity (237, 786) and was found to be upregulated in recently described islet 'hubs' responsible for coordinated insulin secretion (239).
PFKP	Phosphofructokinase (platelet isoform, also expressed in $\beta$ -cells)	PFKP catalyses the first step committing a glucose molecule to glycolysis and is rate-limiting (87, 787). PFK is regulated by a complex feedback system and may be involved in establishing calcium oscillations (246, 788, 789). PFKP is associated with both low birth weight and obesity in humans (790) and is expressed in the rat $\beta$ -cell (791).
PKM2	Pyruvate kinase (muscle isoform type 2, also found in islets)	Pyruvate kinase (PK) transfers phosphate from phosphoenolpyruvate to ADP in the final step of glycolysis, concurrently creating pyruvate and ATP. This is an irreversible reaction and a regulatory step in glycolysis (87). Besides this function, PKM2 (the isoform found mainly in islets) is translocated to the nucleus after being phosphorylated by extracellular signal-regulated kinase (ERK). It then acts as a transcription factor to regulate its own expression and that of several other rate-limiting glycolytic enzymes, initiating the Warburg effect during tumorigenesis (518). Similarly, PK activity was increased in diabetes (792). Pyruvate kinase (PK) transfers phosphate from phosphoenolpyruvate to ADP in the final step of glycolysis, concurrently creating pyruvate and ATP. This is an irreversible reaction and a regulatory step in glycolysis.
GAPDH	Glyceraldehyde-3-phosphate dehydrogenase	GAPDH catalyses the reversible oxidation of glyceraldehyde 3-phosphate. Nicotinamide adenine dinucleotide (NAD <sup>+</sup> ) and inorganic phosphate are required for this process, a reaction which harnesses the first energy from a glucose molecule during glycolysis. It is often used as a housekeeping gene or protein because of its ubiquitous distribution and consistent expression.

Enzyme	Full Name	Function
PDH	Pyruvate dehydrogenase	Pyruvate enters the mitochondria in aerobic conditions and is converted to acetyl-CoA by pyruvate dehydrogenase (PDH) (87), thus determining the transition from glycolysis to oxidative phosphorylation (246). This is an important step in efficient metabolic coupling and requires PDH to remain in an active, dephosphorylated state (793).
GSK3 $\beta$	Glycogen synthase kinase	<p>Glycogen synthase kinase 3 (GSK3) is a complex kinase involved in several signalling pathways, including insulin. It has the unusual characteristic of constitutive activity but can also be phosphorylated at tyrosine 216 for maximal activation or at serine 9 for inhibition of many, but not all, of its phosphorylating activities (525). In addition to inactivating glycogen synthase by phosphorylation (87), GSK3 has more predicted substrates than any other kinase (524, 525), including numerous transcription factors, implicating widespread influence on gene expression (525).</p> <p>Increased activation of GSK3<math>\beta</math> has been associated with several diseases, including T2D (528-531). Inhibitors of GSK3<math>\beta</math> are consequently being investigated for their therapeutic potential (528, 529, 532). The role of GSK3<math>\beta</math> in <math>\beta</math>-cells is complex. Among other actions, it phosphorylates the transcription factor promoting insulin gene transcription, pancreatic duodenal homeobox-1 (PDX-1), triggering its proteasomal degradation in low glucose (527). In high glucose conditions, phosphorylation of GSK3<math>\beta</math> by Per-Arnt-Sim domain-containing kinase (PASK) inactivates it to stabilise PDX-1.</p>
LDHA	Lactate dehydrogenase	Pyruvate is converted to lactate and vice versa by lactate dehydrogenase (LDHA) under anaerobic conditions (87). LDHA is not normally expressed in $\beta$ cells (247), its absence helping to maintain a highly aerobic phenotype (246). However, BRIN-BD11 cells do express this enzyme due to their origin as transformed cells with some tumour-like phenotypic adaptations, and this is verified by iTRAQ (see Chapter 4) and WB results (Figure 3.7) in this project. A heavy band lies in a region with a higher molecular weight (~44 kDa) while a light band lies at the expected 36 kDa. This may be due to complexing with immunoglobulins, a common reason for atypical bands during electrophoresis (794 p. 305). Statin treatment was not associated with changes in LDHA expression in this study, but Chen (357) found increased LDH production in another $\beta$ -cell line (NIT-1) when treated with atorvastatin.

### A.3 Chapter 5 Supplementary Figure

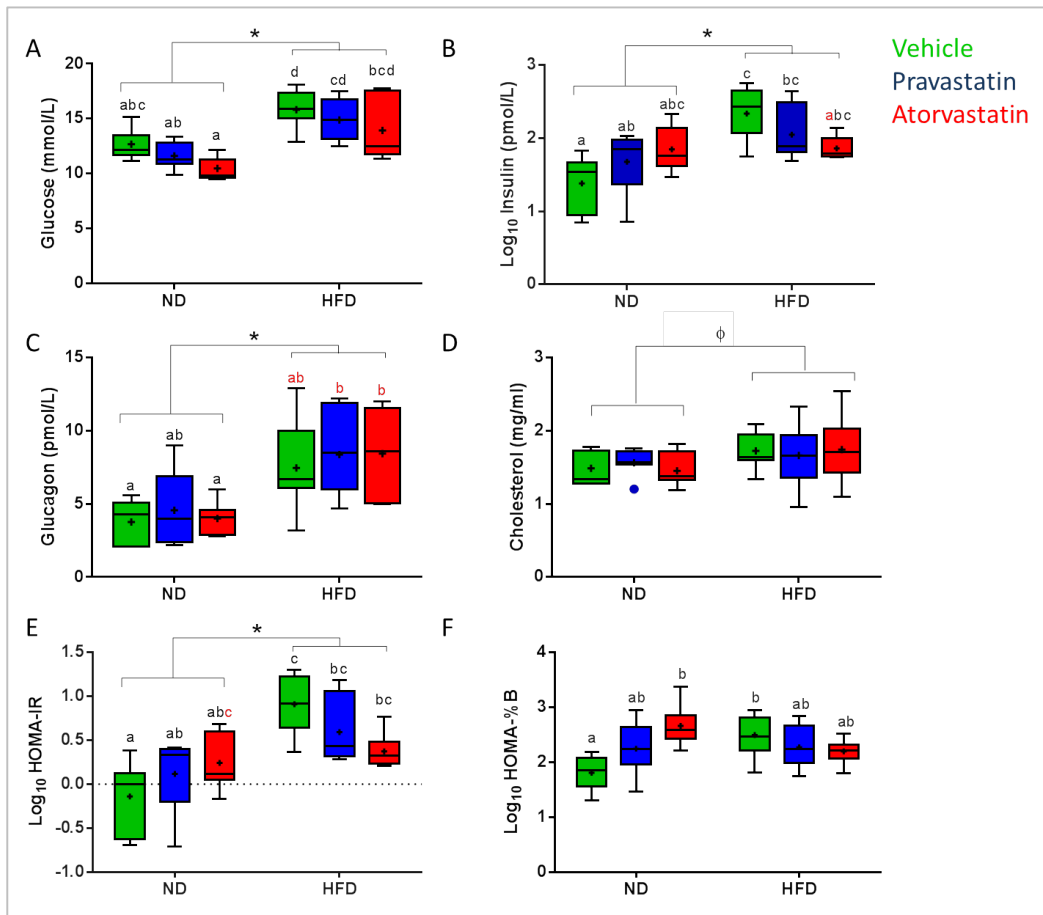


**Figure SA.2 The effect of diet and statins on metabolic parameters minus the outlier.**

Compare with **Figure 5.3**. Leaving out the potential outlier does not change significant effects except where indicated by a red superscript. Changes are as follows: **(A)** Fasting glucose, no change; **(B)** fasting insulin, A-HFD is not significantly different from the ND groups; **(C)** fasting glucagon, the loss of a category of significant difference exclusively in HFD groups; **(D)** plasma cholesterol, no difference; **(E)** HOMA-IR, The addition of a 'c' superscript in the A-ND group; **(F)** HOMA-%B, no change. Data is presented as Tukey box plots and represents data from 6 or 7 mice per group. Means with superscripts in common are not significantly different from each other (2way ANOVA with Tukey's multiple comparisons test,  $P < 0.05$  indicating significance). ND, Normal diet; HFD, High fat diet.  $\Phi$ ,  $P < 0.05$ ; \*,  $P < 0.001$ .

# Appendix B iTRAQ Results in Full

Data analysis and protein identifications were done with ProteinPilot version 4.0		
<b>Database: Swissprot</b>		
Your results were searched against the Swissprot database (taxonomy = <i>Aspergillus fumigatus</i> ), a comprehensive, audited database designed specifically for mass spectrometry applications. It contains nonidentical protein sequence information based on publicly available datasets.		
<b>Unused (ProtScore)</b>		
A measure of the protein confidence for a detected protein, calculated from the peptide confidence for peptides from spectra that have not already been completely "used" by higher scoring winning proteins. A "good" Unused ProtScore is one that corresponds to the level of confidence you require in your results. For 95% confidence, the required Unused ProtScore is 1.3.		
<b>Total (ProtScore)</b>		
A measure of the total amount of evidence for a detected protein. The Total ProtScore is calculated using all of the peptides detected for the protein. The Total ProtScore does not indicate the percent confidence for the identification of a protein.		
<b>% Cov (Coverage)</b>		
The percentage of matching amino acids from identified peptides having confidence greater than 0 divided by the total number of amino acids in the sequence.		
<b>Ratio</b>		
The average ratio for the protein, relative to the 114, 115, 116 or 117.		
<b>The p-value</b>		
For each protein ratio reported the program calculates a p-value to help you assess whether changes in protein expression are real or not. A p-value is a standard statistical metric in hypothesis testing. The p-value reports the probability that the null hypothesis "the observed value is different from unity by chance" is true. P-values range from 0 to 1.		
<b>Colour coding</b>		
The quantitative ratios of identified proteins are colour coded to indicate differential expression. Red indicates up-regulation and blue indicates down-regulation. The intensity of the colouring indicates the certainty of the differential expression, not the magnitude of the change. For example, the more certain the up-regulation, the more red the cells; the more certain the down-regulation, the more blue the cells.		
<b>Note:</b> The coloring is only indicative of altered expression levels, and is determined by the p-value not by the size of the ratio.		
<b>Global False Discovery Rate (FDR)</b>		
The FDR was automatically calculated by the Proteomics System Performance Evaluation Pipeline (PSPEP) feature in the ProteinPilot™ software using the reversed version of the protein sequences contained in the search database. The software calculates both a local and a global FDR. The local FDR estimates the "local" error rate around a given identification, which indicates the likelihood that that the specific identification is incorrect. The global FDR estimates the error rate of the whole "global" set of answers defined by a threshold value. That is, the global FDR estimates the likely error rate of the entire set of identifications with scores as good as or better than the threshold.		
<b>Colour codes</b>	<b>P-value</b>	<b>Ratio</b>
Dark red	< 0.001	> 1
Medium red	0.001 - < 0.01	> 1
Light red	0.01 - < 0.05	> 1
No color	>= 0.05	Any
Light blue	0.01 - < 0.05	< 1
Medium blue	0.001 - < 0.01	< 1
Dark blue	< 0.001	< 1
<b>Local FDR</b>	< 0.1 %	
<b>Global FDR</b>	< 0.1%	
<b>Tag Code</b>		
114 Control A		
115 MβCD (5 mM)		
116 c-MβCD (5 mM)		
117 Control B		



N	% Cov (95)	Accession #	Pep 95%	PVal			PVal		
				115:114	115:114	116:114	116:114	117:114	117:114
1	15.8	sp P38650 DYHC1_RAT	69	0.8166	0.11	0.8318	0.2331	0.9036	0.1046
2	14.6	sp P16086 SPTN1_RAT	32	1	0.8572	0.9727	0.6613	0.9817	0.5516
3	26.5	sp Q5SGE0 LPPRC_RAT	42	1.0186	0.2311	0.9908	0.9362	1.0093	0.2944
4	48.3	sp P06761 GRP78_RAT	60	2.9376	0.0001	2.3768	0.0047	2.3335	0.0018
5	18.9	sp P15205 MAP1B_RAT	42	0.9376	0.3506	1.3677	0.355	1.4588	0.0435
6	22.8	sp P11442 CLH1_RAT	41	1.6904	0.0141	1.3305	0.1058	1.2706	0.0786
7	55.3	sp P11598 PDIA3_RAT	51	2.1281	0.0001	2.0512	0.0024	2.3335	0.0002
8	60	sp P63039 CH60_RAT	43	3.7325	0.0064	2.0324	0.2821	3.281	0.0003
9	49.5	sp P48721 GRP75_RAT	51	2.0701	0.0084	1.0568	0.4455	1.4997	0.2148
10	49.2	sp P15999 ATPA_RAT	65	1.0093	0.3901	0.9908	0.4624	1.0093	0.518
11	56.2	sp P04785 PDIA1_RAT	34	2.0512	0.0278	1.8535	0.0049	1.9953	0.0516
12	14.8	sp Q62812 MYH9_RAT	26	0.9376	0.7046	0.7447	0.3366	0.673	0.0204
13	47.1	sp P63018 HSP7C_RAT	78	1.8535	0.0128	1.3305	0.259	1.1803	0.2431
14	30.7	sp P34058 HS90B_RAT	40	0.929	0.1412	1.4454	0.5637	1.2589	0.9379
15	45.4	sp P50878 RL4_RAT	38	2.2699	0.019	1.803	0.1605	1.5704	0.2026
16	28.9	sp P06685 AT1A1_RAT	40	1.0186	0.4334	0.9462	0.7602	0.7516	0.815
17	66.9	sp A7VJC2 ROA2_RAT	58	1.0186	0.6374	0.5395	0.0441	0.8017	0.5046
18	11.7	sp P12785 FAS_RAT	26	0.955	0.1179	0.9817	0.1577	1	0.3356
19	69.1	sp P63259 ACTG_RAT	111	1.9409	0.6784	0.9376	0.9621	1.1912	0.861
20	50.9	sp P62630 EF1A1_RAT	51	1.3183	0.0757	1.5276	0.1208	0.863	0.1879
21	25.9	sp Q63617 HYOU1_RAT	27	2.1677	0.0572	2.3988	0.0141	1.9953	0.245
22	28.5	sp P13383 NUCL_RAT	24	0.9036	0.9011	0.7112	0.0835	0.929	0.907
23	53.3	sp P10719 ATPB_RAT	68	1	0.0999	0.9817	0.3218	0.9908	0.2101
24	29.4	sp Q66X93 SND1_RAT	24	0.863	0.5798	1.2359	0.6742	0.9462	0.9693
25	31.6	sp Q66HD0 ENPL_RAT	35	1.7378	0.0102	1.2474	0.0792	1.1695	0.1686
26	33.3	sp Q9ER34 ACON_RAT	31	1.2706	0.2647	0.5598	0.014	1.2023	0.3866
27	39.4	sp Q68FR6 EF1G_RAT	28	1.1482	0.4214	1.3677	0.1248	1.5417	0.2608
28	33.7	sp P48679 LMNA_RAT	24	1.5136	0.9607	0.8241	0.0442	0.8954	0.2408
29	34.7	sp Q99PF5 FUBP2_RAT	20	0.9908	0.5707	0.9817	0.9073	1.0186	0.5671
30	32	sp Q64428 ECHA_RAT	26	1.4588	0.2778	0.7047	0.4555	1.2246	0.7123
31	65.7	sp P04636 MDHM_RAT	39	3.0761	0.0076	1.5996	0.1787	2.7797	0.0046
32	25.3	sp P05197 EF2_RAT	24	1.1482	0.6465	1.5996	0.1802	1.1588	0.3842
33	36.3	sp Q3KR86 MIC60_RAT	21	1.0568	0.5986	0.6792	0.9354	0.5861	0.3359
34	4.9	sp D3ZH2 MACF1_RAT	19	1.0471	0.6483	0.9727	0.4718	0.9908	0.7312
35	22.3	sp P46462 TERA_RAT	20	0.8395	0.69	0.871	0.5473	0.787	0.8638
36	37.2	sp P28480 TCPA_RAT	22	0.9727	0.3952	1.2942	0.2136	1.1912	0.1997
37	20.8	sp Q5M7W5 MAP4_RAT	20	0.9462	0.9992	0.9376	0.7442	0.9727	0.5872
38	10.2	sp F1LNJ2 U520_RAT	19	1.2823	0.7752	0.6607	0.0418	1.2023	0.7888
39	23.5	sp P27653 C1TC_RAT	20	0.7311	0.1895	1.1376	0.7286	0.9462	0.768
40	47.3	sp P05426 RL7_RAT	20	1.1272	0.3815	1.4322	0.2062	1.5849	0.0189
41	39.1	sp Q6P502 TCPG_RAT	26	1.1169	0.7897	1.0965	0.6905	0.8241	0.2498
42	42.2	sp Q6URK4 ROA3_RAT	43	0.8017	0.1161	0.6607	0.1154	0.7798	0.1422
43	29.5	sp P70615 LMNB1_RAT	24	1.2134	0.6445	0.863	0.4112	1	0.1146
44	18	sp Q04462 SYVC_RAT	20	1.4588	0.5608	1.5417	0.1583	1.2589	0.2804
45	39.7	sp P21807 PERI_RAT	31	0.8472	0.4137	0.6252	0.0347	0.6792	0.0475
46	29.8	sp P07153 RPN1_RAT	17	0.9908	0.9633	0.9908	0.5574	0.9638	0.6884
47	50.2	sp P62703 RS4X_RAT	20	1	0.8494	1.7701	0.0133	1.5417	0.116
48	29	sp Q68FQ0 TCPE_RAT	20	0.9204	0.7199	1.6444	0.1454	1.2706	0.4757
49	54.4	sp Q05962 ADT1_RAT	22	1.4997	0.3268	0.9204	0.882	0.8954	0.9785
50	14.7	sp P11507 AT2A2_RAT	18	1	0.8394	1.0186	0.2658	0.9817	0.4979
51	20.2	sp P52303 AP1B1_RAT	20	1.3183	0.4359	1.1695	0.5148	0.8551	0.2486
52	31	sp P21531 RL3_RAT	17	1.8535	0.9912	1.5136	0.3864	1.6904	0.2976
53	37.4	sp Q5XIM9 TCPB_RAT	19	1	0.4217	1	0.6455	0.9727	0.8113
54	26.7	sp P35565 CALX_RAT	21	1.0093	0.4883	0.9908	0.9923	0.9727	0.6672
55	22.7	sp P38659 PDIA4_RAT	22	2.0701	0.0226	1.8535	0.1053	1.4723	0.0977
56	41	sp P62425 RL7A_RAT	20	2.208	0.3277	1.8365	0.1424	2.0893	0.5612
57	16	sp P28023 DCTN1_RAT	17	0.9817	0.3724	0.9908	0.9805	1	0.4488

N	% Cov (95)	Accession #	Pep 95%	PVal		PVal		PVal	
				115:114	115:114	116:114	116:114	117:114	117:114
58	64	sp Q9Z2L0 VDAC1_RAT	25	1.1695	0.3718	0.8551	0.7725	0.8872	0.8292
59	12.8	sp O35821 MBB1A_RAT	16	0.9638	0.9727	0.9817	0.9066	1.0375	0.5211
60	68.9	sp P62804 H4_RAT	46	0.9817	0.7058	0.9462	0.4333	0.9727	0.9571
61	27.4	sp Q62826 HNRPM_RAT	31	1.3183	0.1529	0.8872	0.1946	0.9638	0.1412
62	29.7	sp Q9EPH8 PABP1_RAT	19	1.2823	0.4667	1.4997	0.0819	1.4588	0.1098
63	23.5	sp Q641Y8 DDX1_RAT	17	0.9727	0.935	0.955	0.7466	0.9727	0.9816
64	23.3	sp Q62667 MVP_RAT	17	0.7447	0.1268	0.7798	0.4835	0.9204	0.8975
65	41.3	sp P49242 RS3A_RAT	16	1	0.2721	1.1272	0.2951	0.8091	0.8461
66	19.9	sp P43244 MATR3_RAT	25	0.9036	0.9327	0.5248	0.0983	0.6918	0.1975
67	36.6	sp Q7TPB1 TCPD_RAT	21	1.028	0.2795	1.2023	0.2677	0.9204	0.3299
68	27.3	sp P11980 KPYM_RAT	18	0.5445	0.0626	1.406	0.0591	0.871	0.5667
69	31.5	sp P23785 GRN_RAT	21	1.4454	0.2593	1.4997	0.0559	1.5849	0.1576
70	56.8	sp P62909 RS3_RAT	16	0.871	0.4413	1.7061	0.0491	0.9638	0.9274
71	32.7	sp P69897 TBB5_RAT	26	0.9376	0.6681	1.2942	0.3061	0.8395	0.7897
72	15.1	sp Q6P7A9 LYAG_RAT	19	1.0186	0.857	1.0186	0.9877	1.028	0.4442
73	31.5	sp P18418 CALR_RAT	14	3.0761	0.0016	2.8576	0.0494	3.02	0.0007
74	53.3	sp Q63716 PRDX1_RAT	19	1.0375	0.7949	0.8472	0.7223	0.7447	0.9245
75	36.5	sp P27952 RS2_RAT	14	1	0.5789	1.4588	0.4655	1.1588	0.7421
76	3	sp P30427 PLEC_RAT	11	1.0186	0.6034	0.955	0.4713	1.0093	0.6626
77	11.9	sp Q64560 TPP2_RAT	14	1.977	0.3906	2.1281	0.3259	0.7516	0.5211
78	16.7	sp Q9QUL6 NSF_RAT	11	0.955	0.8278	1.0186	0.1226	0.9908	0.3007
79	18.8	sp Q3B8Q1 DDX21_RAT	14	0.9908	0.4637	0.6918	0.1961	0.7112	0.3185
80	37.7	sp P00507 AATM_RAT	20	2.1281	0.0137	1.4859	0.1411	1.9055	0.0132
81	39.5	sp P52925 HMGB2_RAT	14	1.4191	0.2218	1.3062	0.2427	1.4723	0.0121
82	31.2	sp B2GV06 SCOT1_RAT	17	1.7539	0.1689	1.1695	0.1686	1.4859	0.1192
83	32.4	sp Q5BJY9 K1C18_RAT	16	1.3804	0.1699	0.8241	0.3661	1.028	0.9612
84	42.9	sp P05065 ALDOA_RAT	16	1.3183	0.9837	2.6792	0.0048	1.6293	0.0333
85	49.5	sp P19945 RLAO_RAT	26	0.7516	0.9332	0.912	0.876	0.912	0.9495
86	28.3	sp Q8VHF5 CISY_RAT	17	1.5996	0.2147	1.3932	0.4632	1.5704	0.1525
87	7.9	sp P41516 TOP2A_RAT	14	0.9908	0.8028	0.955	0.6323	0.9817	0.9013
88	11.4	sp Q9Z1A6 VIGLN_RAT	11	0.7586	0.2185	0.597	0.0936	0.6368	0.2244
89	48.8	sp P04256 ROA1_RAT	26	0.7178	0.4833	0.5649	0.1852	0.6546	0.3662
90	51.4	sp P24368 PPIB_RAT	15	1.028	0.5941	1.0093	0.8357	1.028	0.2569
91	35.5	sp Q6P9V9 TBA1B_RAT	22						
92	20.8	sp P00388 NCPR_RAT	15	1.0186	0.8756	0.9727	0.3692	0.9817	0.5814
93	22.9	sp P13264 GLSK_RAT	17	2.0137	0.2989	0.7379	0.7238	1.6144	0.1788
94	36.8	sp Q6AYD3 PA2G4_RAT	13	1	0.1795	1.0471	0.8893	1.0093	0.679
95	32.7	sp Q63081 PDIA6_RAT	19	1.8365	0.1417	1.6749	0.2477	1.6596	0.227
96	7.4	sp Q9JLA3 UGGG1_RAT	13	1.3062	0.4377	1.0375	0.7863	0.8241	0.2288
97	34.2	sp Q00438 PTBP1_RAT	25	1.406	0.5031	2.1878	0.345	1.5136	0.4398
98	15	sp O88941 MOGS_RAT	13	2.0137	0.1273	1.028	0.5517	1.2942	0.442
99	32	sp P15865 H14_RAT	23	0.8551	0.7736	0.3162	0.2086	0.3908	0.5471
100	63.1	sp P0CC09 H2A2A_RAT	39	2.0512	0.2251	0.863	0.8402	1.4997	0.1491
101	30.8	sp P32551 QCR2_RAT	14	1	0.696	1	0.3178	0.9727	0.5361
102	26.3	sp P56574 IDHP_RAT	12	2.0324	0.0118	2.208	0.0828	2.8576	0.0112
103	42.1	sp Q6PDV7 RL10_RAT	16	1.2134	0.9444	1.4191	0.8889	1.2359	0.4055
104	46.7	sp P62260 1433E_RAT	17	0.7311	0.1367	1.0186	0.2166	0.6855	0.9736
105	18.2	sp Q99376 TFR1_RAT	16	1.0375	0.2043	1.0093	0.1946	1.0186	0.4547
106	9.4	sp Q1JU68 EIF3A_RAT	12	1.7378	0.1087	1.0864	0.4631	1.2246	0.7755
107	25.4	sp Q5FVM4 NONO_RAT	24	1.4454	0.4205	0.912	0.9007	1.2589	0.658
108	28.5	sp Q5RK11 IF4A2_RAT	15	0.8017	0.2028	0.912	0.6916	1.0375	0.3215
109	15.7	sp Q9QXQ0 ACTN4_RAT	14	1.0093	0.5639	1.0471	0.6588	0.9908	0.4927
110	31.1	sp P68101 IF2A_RAT	13	0.7727	0.0898	0.6668	0.0176	0.7798	0.1052
111	12.6	sp P41777 NOLC1_RAT	9	1.0093	0.6555	0.3373	0.0135	0.7656	0.7778
112	12.3	sp P18484 AP2A2_RAT	9	0.9638	0.6849	0.9817	0.947	0.955	0.9416
113	44.4	sp Q6NYB7 RAB1A_RAT	13	1.1272	0.8996	0.8395	0.9822	0.673	0.4392
114	31.4	sp Q62733 LAP2_RAT	12	1.7865	0.1025	0.7447	0.5532	1.2023	0.6529

N	% Cov (95)	Accession #	Pep		PVal		PVal		PVal
			95%	115:114	115:114	116:114	116:114	117:114	117:114
115	18.4	sp Q4KM49 SYYC_RAT	10	0.871	0.4963	0.929	0.6884	0.4446	0.1121
116	28.3	sp P04642 LDHA_RAT	11	0.5861	0.0957	1.5704	0.0368	0.8395	0.8092
117	44.9	sp P09527 RAB7A_RAT	21	1.028	0.6162	0.7798	0.6771	0.7516	0.6056
118	25.8	sp P62815 VATB2_RAT	12	0.9817	0.5913	0.9817	0.5804	1.0093	0.2483
119	24.1	sp P85834 EFTU_RAT	9	1.6293	0.4859	0.8091	0.3215	1.1376	0.2783
120	25.3	sp Q10758 K2C8_RAT	13	1.0666	0.5144	1.2706	0.6362	1.5996	0.2272
121	27.4	sp P61980 HNRPK_RAT	20	1.4454	0.9921	1.0568	0.8952	1.1272	0.9787
122	13.5	sp Q9JIL3 ILF3_RAT	12	0.879	0.0844	0.3631	0.0868	0.5297	0.0342
123	18.9	sp Q6AXS5 PAIRB_RAT	10	0.9908	0.9616	0.9727	0.4687	0.9817	0.4934
124	11.2	sp P16638 ACLY_RAT	11	1.028	0.9366	0.955	0.7781	0.9817	0.4919
125	24.2	sp P23565 AINX_RAT	12	0.7178	0.3134	0.7047	0.1479	0.4699	0.1765
126	9.9	sp Q924C3 ENPP1_RAT	10	1.6293	0.5885	1.8535	0.0472	1.8535	0.0822
127	38.2	sp P67779 PHB_RAT	14	1.0765	0.9484	0.4831	0.1691	0.8551	0.7942
128	18.2	sp P97852 DHB4_RAT	14	1.0093	0.464	1	0.7878	0.9638	0.7521
129	56	sp Q00715 H2B1_RAT	44	0.7311	0.4917	0.1294	0.0803	0.8318	0.4512
130	30	sp Q3MIE4 VAT1_RAT	13	0.9727	0.5176	1.3428	0.3701	0.955	0.9654
131	12.1	sp Q5XI78 ODO1_RAT	13	1.0093	0.8713	0.9376	0.223	0.9462	0.3651
132	25.3	sp P84092 AP2M1_RAT	14	1.1695	0.8122	0.7112	0.107	1.4191	0.332
133	26.4	sp Q6AYH5 DCTN2_RAT	10	1	0.3534	1	0.1716	0.6427	0.1619
134	11.6	sp Q9WUL0 TOP1_RAT	9	1.0093	0.4733	0.9727	0.1862	1.0186	0.1681
135	27.3	sp P09895 RL5_RAT	18	1.5136	0.1896	0.929	0.3486	1.0765	0.2
136	37.6	sp P29314 RS9_RAT	13	1.0093	0.5892	1.5136	0.3212	1.3062	0.9096
137	26.1	sp Q6P6R2 DLDH_RAT	11	1.9055	0.0806	1.2823	0.3697	1.7061	0.2769
138	24.9	sp P25235 RPN2_RAT	11	1.0375	0.3672	0.955	0.0205	0.9908	0.6385
139	18.3	sp P62944 AP2B1_RAT	28	1.0186	0.3567	1.5704	0.5067	1.2942	0.4878
140	23.3	sp Q63347 PRS7_RAT	8	1.0375	0.9828	1.0375	0.6274	1.028	0.4006
141	12.5	sp P25286 VPP1_RAT	12	1.028	0.7977	0.9817	0.7416	1.0186	0.8486
142	38.1	sp Q68FR9 EF1D_RAT	15	1.7219	0.5743	1.2023	0.9479	1.4723	0.4108
143	37.6	sp P81155 VDAC2_RAT	10	1.0864	0.6767	1.4454	0.1914	1.803	0.215
144	30.2	sp G3V9R8 HNRPC_RAT	9	1.028	0.6751	0.5058	0.6677	0.6486	0.7296
145	12.4	sp Q66HF1 NDUS1_RAT	7	0.8872	0.3699	0.6607	0.5551	1.3932	0.3303
146	11.7	sp P52296 IMB1_RAT	10	0.8872	0.7414	0.6546	0.1127	0.631	0.1082
147	8.1	sp P97690 SMC3_RAT	7	1.1376	0.2987	1.1376	0.3438	1.0568	0.8018
148	19.8	sp Q6AYT3 RTCB_RAT	12	1	0.9496	1.0375	0.4463	1.0093	0.8962
149	34.1	sp Q63507 RL14_RAT	16	0.9036	0.664	0.9727	0.2816	1.1695	0.0391
150	21.4	sp P16036 MPCP_RAT	12	1.8707	0.1878	0.912	0.4033	1.9409	0.4297
151	48.7	sp P62282 RS11_RAT	10	1.6293	0.374	2.0324	0.0782	1.6596	0.2388
152	26.5	sp P21533 RL6_RAT	19	0.8551	0.1612	0.8872	0.9095	0.7943	0.6364
153	29.8	sp Q8VHV7 HNRH1_RAT	12	1	0.7487	0.9376	0.6219	0.9908	0.878
154	17.9	sp O35814 STIP1_RAT	8	0.8318	0.6869	1.2359	0.1626	1.1695	0.3732
155	44.2	sp P62243 RS8_RAT	12	1.3428	0.4798	1.7061	0.1974	1.4454	0.235
156	31.6	sp Q5RJR8 LRC59_RAT	14	1.3062	0.6664	0.9817	0.8626	0.871	0.736
157	43.7	sp P62278 RS13_RAT	9	0.7244	0.9507	1.1695	0.9986	1.2246	0.1977
158	8.8	sp Q3ZAV8 EDC4_RAT	10	0.9817	0.7309	0.9908	0.645	0.929	0.4265
159	20	sp Q32PX7 FUBP1_RAT	12	0.9462	0.8902	0.929	0.8645	0.9462	0.5841
160	34.5	sp P35427 RL13A_RAT	11	1.0471	0.6671	1.2942	0.7865	1.556	0.4589
161	28.6	sp Q02874 H2AY_RAT	9	0.8166	0.7434	0.7047	0.6776	1.1169	0.858
162	35	sp P62907 RL10A_RAT	14	1.4191	0.7656	1.2942	0.8582	1.5136	0.6865
163	34.5	sp P04797 G3P_RAT	17	1.4723	0.5161	2.8054	0.0923	1.4322	0.5207
164	33	sp P63159 HMGB1_RAT	10	1.6144	0.63	0.7047	0.156	1.3552	0.7278
165	14.6	sp Q920L2 SDHA_RAT	8	1.0965	0.7072	0.6252	0.5047	1.6144	0.1708
166	16.9	sp P10860 DHE3_RAT	10	1.0186	0.9386	1.0186	0.8711	1.028	0.9144
167	11.2	sp Q562A2 ZFR_RAT	10	0.863	0.9996	0.6194	0.2757	0.5702	0.204
168	30.1	sp B5DEH2 ERLN2_RAT	11	1.1588	0.436	1.4191	0.1448	1.4588	0.2524
169	47	sp Q4KM74 SC22B_RAT	12	0.6368	0.6174	0.4966	0.2263	0.4742	0.3716
170	10.8	sp P23514 COPB_RAT	10	1.0375	0.2928	1.0666	0.4279	1.0864	0.2281
171	19.8	sp Q60587 ECHB_RAT	10	1.0765	0.6388	0.6427	0.3014	0.7943	0.9616

N	% Cov (95)	Accession #	Pep 95%	PVal			PVal		
				115:114	115:114	116:114	116:114	117:114	117:114
172	42.1	sp P62718 RL18A_RAT	12	1.1272	0.6739	1.6444	0.1107	1.0093	0.4388
173	25.9	sp P60123 RUVB1_RAT	8	0.9462	0.7782	0.787	0.9834	0.5916	0.8185
174	40.4	sp Q6LED0 H31_RAT	11	0.4055	0.1854	0.4325	0.1156	0.7586	0.7085
175	32.9	sp P38983 RSSA_RAT	10	0.7311	0.9907	1.2589	0.2719	0.863	0.9446
176	15	sp P10960 SAP_RAT	8	0.3076	0.0361	0.9036	0.543	0.7943	0.17
177	28.2	sp Q63610 TPM3_RAT	9	2.3121	0.1155	2.7542	0.0103	1.3552	0.8386
178	24.4	sp P04764 ENOA_RAT	8	1.2134	0.2896	2.704	0.0797	1.4723	0.701
179	15.7	sp P08461 ODP2_RAT	10	0.9376	0.2481	0.9376	0.2177	0.955	0.3834
180	27.3	sp P19511 AT5F1_RAT	9	2.355	0.1831	1.0965	0.586	1.2359	0.3048
181	20.5	sp Q63083 NUCB1_RAT	8	0.8318	0.651	1.3677	0.0333	0.9908	0.8127
182	12.6	sp O08629 TIF1B_RAT	11	1.0186	0.4512	0.9638	0.9971	1.028	0.8328
183	32.6	sp P21775 THIKA_RAT	8	1.0471	0.9278	0.2655	0.0133	0.6368	0.1318
184	37.4	sp P41123 RL13_RAT	13	1.3804	0.6017	1.6444	0.2199	1.1695	0.5507
185	25.7	sp P13086 SUCA_RAT	9	1.2474	0.7682	0.6918	0.6266	1.9055	0.0484
186	16.2	sp Q5XI81 FXR1_RAT	10	1.0471	0.4489	1.0093	0.4813	1.0093	0.8446
187	26.8	sp Q5XIH7 PHB2_RAT	9	0.9908	0.6336	0.9908	0.5093	1	0.4102
188	17	sp O55012 PICAL_RAT	9	1.4322	0.2315	0.8091	0.5807	0.6792	0.3645
189	19	sp Q9EPB1 DPP2_RAT	11	1.028	0.8438	0.9908	0.9922	1.0093	0.8677
190	42.8	sp P62271 RS18_RAT	11	1.4997	0.6807	1.5136	0.2874	1.3062	0.8291
191	17.1	sp F1LMZ8 PSD11_RAT	8	0.9817	0.8521	1.028	0.5347	0.9727	0.7316
192	22.6	sp Q91V33 KHDR1_RAT	9	1.8197	0.1558	1.0965	0.6706	1.3677	0.8148
193	15.3	sp Q6UPE1 ETFD_RAT	9	1.3677	0.1233	0.8318	0.8808	1.3062	0.2993
194	37.3	sp P10888 COX41_RAT	11	1.028	0.9813	0.6368	0.3648	1.0471	0.9062
195	23.6	sp P62193 PRS4_RAT	11	1.3305	0.957	1.6293	0.3739	1.4997	0.8018
196	21.8	sp P81795 IF2G_RAT	8	0.6668	0.142	1.2474	0.6707	0.4365	0.0849
197	15.3	sp Q66HL2 SRC8_RAT	10	1.6596	0.0614	1.0666	0.5538	1.3677	0.4357
198	18.7	sp P24268 CATD_RAT	12	1.9588	0.8437	1.7219	0.9866	1.556	0.4686
199	28.4	sp P22509 FBRL_RAT	7	1.1376	0.8852	0.7798	0.3304	1.3428	0.2849
200	40.4	sp P62752 RL23A_RAT	12	0.8954	0.5416	1.0568	0.5925	0.9376	0.5212
201	38	sp Q06647 ATPO_RAT	13	2.8576	0.1858	1.4859	0.2975	2.355	0.386
202	11.4	sp Q6P0K8 PLAK_RAT	8	1.1169	0.7799	1.0186	0.9557	0.7047	0.3844
203	14.1	sp Q62902 LMAN1_RAT	8	1.1066	0.8008	0.9204	0.8979	1.2023	0.6806
204	10.6	sp Q4FZT9 PSMD2_RAT	7	0.4055	0.0166	1.4723	0.6616	0.9376	0.9183
205	23.8	sp Q3B8Q2 IF4A3_RAT	9	0.4742	0.1238	0.9727	0.6129	0.5248	0.3193
206	15.9	sp Q66H80 COPD_RAT	8	0.955	0.3701	0.929	0.3506	0.9817	0.8218
207	7.8	sp Q924S5 LONM_RAT	8	0.7656	0.8094	0.7727	0.9545	0.929	0.8724
208	20.7	sp P82995 HS90A_RAT	22	0.7047	0.2818	0.879	0.9799	0.9036	0.9089
209	32.4	sp P17074 RS19_RAT	7	0.9908	0.9692	1.1272	0.2485	0.9462	0.9082
210	13.7	sp Q7TP47 HNRPQ_RAT	8	0.871	0.4686	1.1169	0.4307	0.8318	0.5843
211	44.7	sp P62632 EF1A2_RAT	34	1.4997	0.3443	1.7865	0.2403	1.3552	0.4091
212	47.2	sp P31399 ATP5H_RAT	8	1.4454	0.7872	1.028	0.4704	0.8954	0.0792
213	42	sp P20788 UCRI_RAT	8	0.6918	0.0714	0.4786	0.2977	0.2228	0.0893
214	16.3	sp P47942 DPYL2_RAT	9	0.8318	0.7992	1.0093	0.6517	0.9204	0.7955
215	24.3	sp Q562B5 PGAM5_RAT	7	1.556	0.2005	1.2589	0.9293	1.3552	0.3317
216	44.5	sp P62250 RS16_RAT	9	0.52	0.8526	1.1066	0.8043	1.0186	0.531
217	17.8	sp Q794F9 4F2_RAT	7	0.9817	0.4686	0.9727	0.2983	0.9817	0.182
218	34	sp Q4FZT0 STML2_RAT	8	1.0093	0.8914	1.0186	0.7593	1.0093	0.7307
219	14	sp Q6AXR4 HEXB_RAT	9	1.0471	0.3304	1.0375	0.5138	0.7727	0.9674
220	22.2	sp Q6AY23 P5CR2_RAT	6	1.0471	0.6297	1.028	0.5772	1.0186	0.6555
221	14.5	sp Q641Y0 OST48_RAT	8	0.7244	0.8234	0.413	0.5711	0.7943	0.9838
222	24	sp P13084 NPM_RAT	10	1.2823	0.2232	0.7943	0.9428	1.2359	0.6457
223	17.5	sp Q641Y2 NDUS2_RAT	6	0.9462	0.1932	0.912	0.0587	0.9908	0.7871
224	30.3	sp P12001 RL18_RAT	12	1.8197	0.2037	1.6444	0.1656	1.9953	0.1354
225	39.7	sp P13471 RS14_RAT	7	0.9638	0.6884	0.9462	0.6998	1	0.8041
226	14.3	sp Q9Z1W6 LYRIC_RAT	6	2.9648	0.1151	2.3768	0.6126	2.466	0.0528
227	10.6	sp Q9QZR6 SEPT9_RAT	7	0.879	0.3948	0.8551	0.3797	1.0375	0.9503
228	15.6	sp P25809 KCRU_RAT	6	1.2942	0.4904	0.7311	0.4274	0.8472	0.886

N	% Cov (95)	Accession #	Pep 95%	PVal		PVal		PVal	
				115:114	115:114	116:114	116:114	117:114	117:114
229	31.9	sp P61314 RL15_RAT	7	0.9727	0.9641	1.0471	0.1545	1.0568	0.2681
230	54.6	sp P23358 RL12_RAT	13	1.8707	0.9592	1.5996	0.9787	1.6904	0.502
231	26.4	sp P13803 ETFA_RAT	9	0.9817	0.8979	0.9817	0.9069	1	0.9875
232	22.3	sp Q4KLL0 TCEA1_RAT	8	1.0186	0.8795	1	0.4131	1.0864	0.3268
233	34.1	sp P48500 TPIS_RAT	7	1.028	0.6751	0.9908	0.7387	1.0375	0.9439
234	49	sp P26772 CH10_RAT	9	2.1677	0.5624	1.3062	0.9222	1.5276	0.4758
235	36.4	sp P12075 COX5B_RAT	9	0.7311	0.4464	0.6668	0.1496	0.879	0.805
236	74.8	sp P02401 RLA2_RAT	14	1.4191	0.66	1.8365	0.4424	1.3804	0.6446
237	26.4	sp P62961 YBOX1_RAT	11	0.8872	0.613	0.9908	0.2592	0.912	0.3488
238	6.8	sp Q9JHW1 CBPD_RAT	6	0.9462	0.9433	0.879	0.4248	0.9908	0.835
239	8	sp Q63355 MYO1C_RAT	6	1.1912	0.7034	1.6904	0.1832	0.871	0.8144
240	15.2	sp P15178 SYDC_RAT	6	0.7047	0.1496	1.4588	0.0937	0.955	0.6755
241	26	sp P84100 RL19_RAT	10	1.0765	0.337	0.8872	0.6051	0.787	0.763
242	19.4	sp P14562 LAMP1_RAT	13	0.7656	0.7211	0.8954	0.9568	0.7516	0.814
243	14.6	sp Q62991 SCFD1_RAT	6	0.597	0.0733	0.413	0.0208	0.7727	0.5733
244	32.4	sp P18445 RL27A_RAT	10	0.871	0.5844	1.3428	0.4472	1.1482	0.8643
245	35	sp P18421 PSB1_RAT	10	0.8872	0.5286	0.879	0.3262	0.8872	0.3707
246	25.7	sp P62755 RS6_RAT	9	1.1588	0.6746	1.4859	0.1851	1.3677	0.2809
247	46.4	sp P62832 RL23_RAT	16	0.6368	0.7194	1.1066	0.1004	0.8954	0.2503
248	23.4	sp Q794E4 HNRPF_RAT	7	0.9908	0.174	0.6855	0.0984	0.4406	0.0413
249	53.1	sp P10111 PPIA_RAT	10	0.3908	0.0527	1.3183	0.3886	1.1803	0.798
250	11.3	sp P61765 STXB1_RAT	6	1.5136	0.4784	1.3552	0.6932	1.3552	0.7725
251	26	sp P35435 ATPG_RAT	12	2.3768	0.9159	1.1066	0.2901	2.0512	0.3707
252	14.9	sp P38062 MAP2_RAT	6	1.0471	0.5449	1.0471	0.6085	1.0765	0.0702
253	16.4	sp Q5M9G3 CAPR1_RAT	18	1.0186	0.7843	1.0093	0.347	1.0093	0.6211
254	15	sp Q63413 DX39B_RAT	8	0.9462	0.8924	0.9376	0.4448	0.9376	0.8152
255	33.9	sp Q63965 SFXN1_RAT	7	1.3677	0.27	0.955	0.9838	1.1803	0.7616
256	34.1	sp P24473 GSTK1_RAT	9	1.0375	0.4135	1.0375	0.8681	1.0471	0.4439
257	11.8	sp Q5XHZ0 TRAP1_RAT	8	1.3305	0.7909	0.879	0.4749	0.8017	0.3776
258	17.5	sp Q68FY0 QCR1_RAT	8	1.0568	0.8327	0.9817	0.8304	1.0186	0.5802
259	7.9	sp B5DFC8 EIF3C_RAT	7	1.3677	0.6729	1.3932	0.615	1.2474	0.0831
260	34.9	sp Q6RUV5 RAC1_RAT	8	1.5276	0.9035	0.879	0.2714	0.6918	0.3419
261	26.2	sp P52555 ERP29_RAT	10	1.5276	0.58	1.406	0.462	1.028	0.8117
262	35.9	sp P62982 RS27A_RAT	11	0.955	0.6389	0.9462	0.8721	0.6194	0.3628
263	12.7	sp Q9JMJ4 PRP19_RAT	6	0.9204	0.3696	0.7112	0.0877	0.6918	0.1347
264	7.7	sp P11915 NLTP_RAT	9	1.5849	0.1463	1.1803	0.9155	1.1169	0.4699
265	4.9	sp Q9Z1M9 SMC1A_RAT	6	0.9036	0.2285	0.9204	0.3768	0.9036	0.3436
266	36	sp D4A3K5 H11_RAT	25	1.1912	0.4473	0.673	0.0339	0.879	0.4648
267	16.2	sp P54313 GBB2_RAT	7	0.929	0.4964	0.9638	0.6681	0.9638	0.5622
268	32.2	sp P37805 TAGL3_RAT	10	1.4997	0.4647	1.5136	0.6254	1.977	0.6
269	9.4	sp P13596 NCAM1_RAT	6	1.0186	0.1452	1	0.5353	0.955	0.9306
270	35.4	sp P05712 RAB2A_RAT	14	1.0375	0.7821	1.0568	0.1318	1.0186	0.9419
271	28	sp P62919 RL8_RAT	11	0.871	0.2437	1.3804	0.5331	1.0965	0.7051
272	16.3	sp P15650 ACADL_RAT	8	0.6607	0.5383	0.8472	0.7116	1.1272	0.5856
273	26.5	sp Q62785 HAP28_RAT	5	1.0965	0.8408	1.0093	0.9375	0.9908	0.8443
274	9.8	sp O35314 SCG1_RAT	7	2.1281	0.6078	1.7865	0.9221	1.8707	0.8337
275	9.1	sp Q1LZ53 DNM3A_RAT	6	1.0666	0.6461	0.8551	0.7682	1.3552	0.381
276	9	sp Q9Z1X1 ESYT1_RAT	6	0.6368	0.0921	0.6918	0.2786	0.492	0.0754
277	29.6	sp P62912 RL32_RAT	8	0.9727	0.7627	0.9817	0.8474	0.9462	0.462
278	3.6	sp Q6MG48 PRC2A_RAT	7	0.6081	0.0494	0.5598	0.071	0.5861	0.1825
279	23.1	sp Q5XIG8 STRAP_RAT	7	0.929	0.7956	1.0375	0.2945	0.9727	0.7375
280	9.9	sp Q63028 ADDA_RAT	5	1.9231	0.3081	2.1677	0.0536	1	0.8497
281	6.1	sp Q5M7V8 TR150_RAT	6	0.8091	0.4278	0.5546	0.5169	0.3733	0.1009
282	12.5	sp P38656 LA_RAT	8	0.9908	0.6667	0.9376	0.7705	0.9376	0.6284
283	20.6	sp Q63570 PRS6B_RAT	5	0.9817	0.904	1.0093	0.7939	1.0093	0.5902
284	7.3	sp P27881 HXK2_RAT	6	0.3981	0.0067	0.5808	0.1754	0.5916	0.0686
285	9.2	sp Q04931 SSRP1_RAT	5	1	0.4642	1.028	0.6776	0.8954	0.3231

N	% Cov (95)	Accession #	Pep 95%	PVal		PVal		PVal	
				115:114	115:114	116:114	116:114	117:114	117:114
286	6.8	sp P27008 PARP1_RAT	6	1.5417	0.2121	1.2134	0.1761	1.5136	0.0842
287	3.6	sp F1MA98 TPR_RAT	6	2.5119	0.0459	0.879	0.9071	2.0137	0.4552
288	33.1	sp P61354 RL27_RAT	10	0.9817	0.9617	1.0093	0.203	1	0.799
289	16.7	sp Q6IFW6 K1C10_RAT	10	1.1272	0.6788	0.8472	0.5136	2.9107	0.1186
290	14.5	sp Q9Z1E1 FLOT1_RAT	6	1.0568	0.6864	0.9036	0.4204	0.955	0.845
291	8.4	sp O08837 CDC5L_RAT	5	0.5105	0.5085	0.3597	0.0956	0.9908	0.9638
292	21	sp P29147 BDH_RAT	7	1.2246	0.6896	0.5598	0.1604	0.8241	0.671
293	21.9	sp B1WBW4 ARM10_RAT	8	0.9376	0.4727	0.9817	0.5611	0.929	0.4386
294	7.2	sp Q6IMF3 K2C1_RAT	9	0.7178	0.2724	0.4093	0.308	1.3677	0.3102
295	5.6	sp P11505 AT2B1_RAT	5	1.0186	0.9835	0.9727	0.7185	1.1272	0.2066
296	6.7	sp Q62839 GOGA2_RAT	6	1.3552	0.399	0.7447	0.5847	1.1066	0.3068
297	16.1	sp Q68FX0 IDH3B_RAT	6	1.028	0.9647	1.028	0.9312	1.0186	0.6478
298	23	sp Q4V8C7 PRKRA_RAT	6	0.8872	0.2069	0.9204	0.3776	0.929	0.4264
299	34.8	sp Q62636 RAP1B_RAT	8	1.0093	0.9449	0.912	0.5526	1	0.9844
300	8.4	sp Q75Q39 TOM70_RAT	6	0.9376	0.4232	0.5916	0.0094	0.8395	0.2067
301	6.9	sp A1A5S1 PRP6_RAT	6	0.8954	0.3366	0.9638	0.5751	0.8872	0.3436
302	18.3	sp O88989 MDHC_RAT	5	0.7516	0.3127	1.3062	0.7488	1.1376	0.985
303	20.6	sp B0BNA7 EIF3I_RAT	6	1.0471	0.3422	0.9908	0.8466	1.0375	0.6785
304	31.2	sp P62902 RL31_RAT	6	0.6668	0.612	0.8954	0.2369	1.0864	0.2058
305	15.3	sp B2RZ37 REEP5_RAT	6	1.3428	0.2487	0.8241	0.6491	0.6546	0.3708
306	14.4	sp Q5XIT9 MCCB_RAT	5	1.977	0.2411	0.5248	0.342	1.3428	0.9616
307	45.2	sp P62890 RL30_RAT	8	1.0471	0.9118	1.6144	0.3781	1.1376	0.4105
308	30	sp P62246 RS15A_RAT	7	1.1695	0.7536	1.8365	0.1121	1.1912	0.6718
309	13.3	sp Q9JJ54 HNRPD_RAT	7	0.8954	0.7964	0.8551	0.6876	0.7656	0.5298
310	7.5	sp Q9JK11 RTN4_RAT	5	1.4997	0.899	0.6792	0.2675	0.7178	0.0831
311	30.6	sp P63102 1433Z_RAT	13	0.7798	0.2055	1.0965	0.8826	0.912	0.5411
312	6.2	sp P97536 CAND1_RAT	6	1.1066	0.2538	1.1272	0.0498	1.028	0.6731
313	18.4	sp O35509 RB11B_RAT	4	0.5058	0.0193	0.7112	0.1083	0.6081	0.0771
314	11.6	sp P11730 KCC2G_RAT	5	0.955	0.7857	1.0666	0.8669	0.955	0.2429
315	27.9	sp P61983 1433G_RAT	13	0.9204	0.3153	1.0568	0.5269	1.0568	0.931
316	25.1	sp P29410 KAD2_RAT	6	1.0864	0.779	0.7656	0.8894	0.955	0.2695
317	16.2	sp P49432 ODPB_RAT	6	1.2134	0.8094	0.7112	0.2767	1.4997	0.2156
318	22.4	sp P54921 SNAA_RAT	6	1.028	0.9638	0.787	0.7108	0.929	0.7625
319	12.3	sp B3GNI6 SEP11_RAT	4	0.9908	0.9748	1.1482	0.9641	1.0471	0.7823
320	4.1	sp O35889 AFAD_RAT	7	0.7447	0.0467	0.5105	0.0094	0.4093	0.0025
321	6.8	sp Q4AEF8 COPG1_RAT	4	1.1169	0.6121	0.9727	0.9701	1.1482	0.4691
322	3.2	sp Q62638 GSLG1_RAT	5	1.4322	0.0992	0.8472	0.9105	0.9638	0.7648
323	25	sp P24049 RL17_RAT	6	1	0.7219	1.0568	0.3542	0.9908	0.8732
324	31.3	sp P17077 RL9_RAT	5	0.929	0.7589	1.0093	0.6694	1.3677	0.3507
325	15.3	sp Q6AXS3 DEK_RAT	5	1	0.6445	0.9727	0.9466	1.0186	0.6164
326	12.6	sp Q99NA5 IDH3A_RAT	6	1.0568	0.4098	1.0666	0.6212	1.0765	0.991
327	8.1	sp O35303 DNM1L_RAT	5	0.9462	0.8532	0.929	0.1886	1.028	0.7704
328	30.3	sp P19804 NDKB_RAT	5	0.9908	0.7005	1.0093	0.9817	0.9638	0.767
329	3.1	sp P15146 MTAP2_RAT	6	0.787	0.9786	1.5996	0.2684	1.4454	0.3861
330	32.5	sp P20280 RL21_RAT	6	0.9204	0.7228	1.0471	0.7214	1.0666	0.5672
331	6.7	sp Q07803 EFGM_RAT	4	1.4997	0.2146	2.0324	0.0806	1.6293	0.5086
332	8.7	sp Q641X3 HEXA_RAT	6	0.7447	0.2946	0.4613	0.1245	0.3404	0.1446
333	9.9	sp Q925S8 YMEL1_RAT	6	1	0.8525	0.9376	0.4566	1.0568	0.554
334	3.2	sp Q8K1P7 SMCA4_RAT	5	1.1272	0.4382	0.9817	0.5739	1.0666	0.7551
335	15.6	sp G3V6S8 SRSF6_RAT	7	0.8017	0.1734	0.6138	0.1377	0.7244	0.162
336	36.1	sp P60868 RS20_RAT	9	0.955	0.8384	0.9908	0.7016	0.9727	0.6325
337	14.5	sp Q5XIP6 FEN1_RAT	4	0.8872	0.6095	1.0471	0.5752	1.3183	0.2475
338	9	sp Q498R3 DJC10_RAT	7	0.929	0.3443	0.9204	0.2864	0.9638	0.5786
339	58.3	sp Q6PDU7 ATP5L_RAT	6	0.9036	0.8244	0.6855	0.5812	1.028	0.899
340	5.2	sp O35142 COPB2_RAT	5	0.9204	0.7006	0.631	0.4448	0.8472	0.9012
341	13.7	sp P61621 S61A1_RAT	5	1.1695	0.3411	1.028	0.5175	1.0471	0.5473
342	27.6	sp Q498U4 SARNP_RAT	5	1.0375	0.413	1.0093	0.4774	1.0471	0.6784

N	% Cov (95)	Accession #	Pep 95%	PVal			PVal		
				115:114	115:114	116:114	116:114	117:114	117:114
343	19.1	sp P60901 PSA6_RAT	4	0.7379	0.522	0.9727	0.8493	0.6486	0.4857
344	3	sp Q9Z330 DNMT1_RAT	5	0.9727	0.3897	0.9462	0.1834	0.955	0.5495
345	21.3	sp Q9Z270 VAPA_RAT	5	1.1169	0.8053	0.4966	0.2392	1.0568	0.4062
346	32.4	sp B0K020 CISD1_RAT	7	0.9908	0.5247	0.9817	0.9306	0.9817	0.2254
347	23.7	sp Q66H20 PTBP2_RAT	8	0.7656	0.9166	0.2188	0.2604	0.7586	0.9421
348	10.9	sp P04182 OAT_RAT	5	1.8535	0.0125	1.3305	0.034	1.7061	0.0469
349	10.9	sp P63095 GNAS2_RAT	4	1.1066	0.9903	1.028	0.5739	1.0093	0.6386
350	21.7	sp Q6PDU1 SRSF2_RAT	6	1.1803	0.5059	1.9588	0.5193	1.5849	0.3641
351	5.4	sp Q7TP54 FA65B_RAT	5	0.7943	0.141	0.955	0.4425	1.1272	0.7684
352	53.9	sp P0C0S7 H2AZ_RAT	10	1.0965	0.8214	0.3076	0.3639	0.6138	0.5076
353	18.6	sp P56603 SCAM1_RAT	8	1.5276	0.0723	1.0765	0.5982	1.0471	0.9135
354	45.6	sp Q09073 ADT2_RAT	21	2.0701	0.0847	1.1482	0.1573	1.1169	0.578
355	17	sp P85515 ACTZ_RAT	6	1.0471	0.806	0.9908	0.8277	0.9638	0.7613
356	29.6	sp Q9R063 PRDX5_RAT	4	1.1376	0.965	1.2359	0.3744	1.1169	0.9101
357	26.7	sp P39032 RL36_RAT	6	1	0.5702	0.9908	0.2198	1.028	0.393
358	24.8	sp P17136 RSMB_RAT	6	0.5702	0.484	0.5495	0.6806	0.4093	0.2941
359	39.3	sp Q71TY3 RS27_RAT	5	1.028	0.6893	0.9908	0.4623	0.9908	0.7163
360	25.3	sp P45592 COF1_RAT	4	0.7447	0.4893	1.4723	0.5499	0.9462	0.7863
361	13.2	sp Q01205 ODO2_RAT	5	1.0186	0.7876	0.9727	0.5415	1	0.7631
362	10.3	sp O35112 CD166_RAT	6	0.912	0.8033	0.863	0.8001	0.8091	0.5523
363	4.5	sp Q9JLT0 MYH10_RAT	9	0.9908	0.3335	0.9727	0.8643	0.9462	0.7458
364	6.9	sp Q80Z70 SE1L1_RAT	4	1.1272	0.4588	1.0765	0.6145	1.0965	0.3786
365	9.5	sp Q9JLH7 CK5P3_RAT	4	1.0186	0.8012	0.9908	0.994	1.0186	0.663
366	31.4	sp P62898 CYC_RAT	4	1.7219	0.0739	1.4191	0.3027	1.4322	0.526
367	13.4	sp Q5HZY0 UBXN4_RAT	6	0.912	0.3259	0.9817	0.5739	0.9727	0.6993
368	15.8	sp P17764 THIL_RAT	4	1.1272	0.6531	1.1066	0.9509	1.1588	0.5757
369	18.6	sp P12749 RL26_RAT	5	1.8535	0.1046	1.0375	0.6927	1.3932	0.1774
370	6.4	sp Q6MG08 ABCF1_RAT	5	1.0093	0.9913	1.0186	0.783	1.0568	0.8158
371	12.2	sp Q5M7U6 ARP2_RAT	4	0.879	0.7428	0.9462	0.4793	0.7727	0.0629
372	9.4	sp Q35763 MOES_RAT	4	0.413	0.2567	1.0471	0.6809	0.7244	0.9959
373	12.4	sp Q9QUR2 DCTN4_RAT	4	0.5297	0.0699	0.955	0.8213	0.955	0.9323
374	5.6	sp P35952 LDLR_RAT	4	1.0965	0.4139	1.3305	0.0583	0.9462	0.8364
375	8.9	sp Q8CGU6 NICA_RAT	4	1.0666	0.8511	1.0375	0.9102	1.0093	0.504
376	14.5	sp P63245 RACK1_RAT	4	0.9462	0.8583	0.955	0.7525	0.9376	0.5869
377	23.3	sp Q91Y81 SEPT2_RAT	5	0.9204	0.9128	0.9817	0.9144	1.1066	0.5491
378	32.9	sp P11240 COX5A_RAT	6	0.6252	0.3166	0.8166	0.8785	0.929	0.5293
379	7.1	sp O88453 SAFB1_RAT	6	0.9376	0.9688	0.9817	0.9102	0.9638	0.7102
380	12	sp P14408 FUMH_RAT	6	1.3804	0.3997	1.0765	0.7291	0.879	0.8497
381	4.5	sp P49791 NU153_RAT	4	2.4434	0.2044	2.9376	0.0166	2.5351	0.3474
382	12.9	sp Q6IN36 WIPF1_RAT	4	0.597	0.1887	0.492	0.1633	0.929	0.5046
383	8.7	sp P50430 ARSB_RAT	5	1.3183	0.858	0.8166	0.4651	0.912	0.8198
384	16.9	sp P48004 PSA7_RAT	4	1.0186	0.7244	1.0471	0.4946	0.9817	0.4131
385	27.9	sp P0C5H9 MANF_RAT	4	1.1169	0.1998	1.1066	0.4131	1.0471	0.6319
386	11	sp Q4V7C7 ARP3_RAT	4	0.9908	0.5947	0.8954	0.7511	0.9817	0.6342
387	29.5	sp P13668 STMN1_RAT	4	0.6982	0.4719	1.2246	0.3363	0.863	0.8521
388	29.3	sp Q8CFN2 CDC42_RAT	6	1.3062	0.5733	1.1376	0.5919	0.8472	0.9221
389	15.3	sp P08082 CLCB_RAT	4	0.9727	0.9426	1.0375	0.8074	0.9817	0.6846
390	15.1	sp P07340 AT1B1_RAT	9	0.9727	0.9575	0.9638	0.7995	0.9638	0.8822
391	17.5	sp Q4FZX7 SRPRB_RAT	4	0.8166	0.3508	0.871	0.5361	0.879	0.8214
392	6.3	sp Q9Z1Y3 CADH2_RAT	5	0.9638	0.9308	0.8551	0.5382	0.5395	0.2451
393	7.3	sp B2GV24 UFL1_RAT	6	0.7943	0.4843	0.5649	0.3008	0.4966	0.2075
394	8.2	sp F1LRS8 CD2AP_RAT	4	1.1169	0.9933	0.5012	0.3224	0.4742	0.2811
395	9.5	sp Q7TP98 ILF2_RAT	5	1.0666	0.7907	0.9727	0.4286	1.0568	0.7441
396	7.8	sp Q9Z272 GIT1_RAT	5	0.955	0.7548	0.9204	0.6732	0.9727	0.9348
397	16.2	sp A0JPM9 EIF3J_RAT	4	0.7586	0.584	0.8395	0.821	0.7798	0.686
398	12.5	sp Q812D1 PSIP1_RAT	4	0.9817	0.874	0.955	0.9893	0.955	0.5241
399	28.8	sp Q63584 TMEDA_RAT	5	1.0471	0.1328	1.0186	0.1184	1.0471	0.2248

N	% Cov (95)	Accession #	Pep	PVal			PVal		
			95%	115:114	115:114	116:114	116:114	117:114	117:114
400	6.2	sp Q9EQR2 ADAS_RAT	4	0.929	0.975	0.955	0.6887	1.028	0.4797
401	9.8	sp Q5XI28 RAVR1_RAT	6	0.863	0.1064	0.9817	0.8633	0.912	0.1315
402	10	sp Q6AYK8 EIF3D_RAT	9	2.1478	0.315	1.4859	0.3936	1.2589	0.9506
403	7	sp Q9QZA2 PDC6I_RAT	5	1.977	0.1022	1.4588	0.6552	1.7865	0.1923
404	8.6	sp Q3KRE0 ATAD3_RAT	4	1.1695	0.4482	1.0186	0.6571	1.0186	0.8518
405	11.4	sp O08587 NUP50_RAT	5	1.5996	0.3058	0.6026	0.8929	1	0.8967
406	7.2	sp Q5RKG2 HCFC2_RAT	5	1.0666	0.8676	1	0.9142	1	0.9013
407	6.1	sp Q5XIW8 SNUT1_RAT	7	0.5058	0.2078	0.4656	0.2011	0.787	0.7499
408	7	sp P18395 CSDE1_RAT	4	1	0.5829	1.0471	0.6098	1.0568	0.3674
409	19.9	sp P04961 PCNA_RAT	6	1.0093	0.3133	1.9231	0.5016	2.704	0.7334
410	12.2	sp Q9JIM9 SEPT5_RAT	4	1.0965	0.3803	0.8551	0.7234	0.879	0.7117
411	6	sp Q9ESW0 DDB1_RAT	4	0.9817	0.8771	1.0186	0.9216	0.9204	0.1962
412	11.3	sp Q9QXU8 DC1L1_RAT	5	0.5754	0.8852	0.8091	0.513	0.7311	0.7344
413	14.2	sp G3V7P1 STX12_RAT	3	1.0965	0.3202	1.0568	0.289	1.0375	0.6837
414	14.6	sp P63326 RS10_RAT	6	0.9908	0.966	1.0186	0.9312	1.0093	0.9849
415	13	sp Q3SWU3 HNRDL_RAT	4	0.9908	0.983	0.9727	0.6798	0.9036	0.4599
416	5	sp Q4KLL4 TM9S4_RAT	3	0.9376	0.6171	1.0186	0.7639	0.9462	0.9558
417	3.9	sp O35867 NEB1_RAT	3	0.9462	0.9982	0.8091	0.511	0.871	0.4111
418	21.2	sp P17702 RL28_RAT	7	1.2706	0.5949	1.4997	0.1559	0.871	0.6339
419	4.5	sp Q5U2M8 MDC1_RAT	3	0.8091	0.2237	0.9727	0.8022	0.871	0.4421
420	5.2	sp Q9JKL8 ADNP_RAT	4	1	0.8362	0.929	0.4781	1	0.6842
421	3.9	sp B2GUV7 IF2P_RAT	4	1.0471	0.489	0.9462	0.6832	1.1066	0.632
422	7.7	sp Q9ES21 SAC1_RAT	4	0.9376	0.6686	0.871	0.3392	1	0.6346
423	5.5	sp Q2KN99 CYTSA_RAT	4	1.1272	0.1392	1.0093	0.7194	0.9204	0.9225
424	8.8	sp P24050 RS5_RAT	3	1.0864	0.9214	1.0093	0.9926	0.955	0.9644
425	6.8	sp Q9WU82 CTNB1_RAT	6	0.9204	0.4714	1.028	0.8185	0.9908	0.9944
426	7.1	sp P20611 PPAL_RAT	3	1.3804	0.3943	1.1482	0.9768	1.028	0.6336
427	9.8	sp Q9WTV0 PREB_RAT	4	0.955	0.643	0.871	0.5273	0.863	0.42
428	19.6	sp P62268 RS23_RAT	4	0.7727	0.6161	0.9204	0.8671	1.2359	0.7196
429	4	sp P52873 PYC_RAT	3	0.9204	0.7553	0.9817	0.9351	0.9908	0.754
430	6.6	sp Q5XIN6 LETM1_RAT	5	1.0666	0.5968	0.9908	0.7899	1.0471	0.9363
431	10.3	sp Q99ML5 PCYOX_RAT	5	2.2699	0.176	0.631	0.9137	2.7797	0.0524
432	10.7	sp P51650 SSDH_RAT	4	1.5996	0.2344	1.4588	0.3425	2.2909	0.0712
433	6.4	sp Q66HA8 HS105_RAT	4	1.2134	0.2921	1.0864	0.7682	1.1803	0.1058
434	5.7	sp P04762 CATA_RAT	3	1.0864	0.5229	0.9908	0.601	1.0965	0.7407
435	3.1	sp A4L9P7 PDS5A_RAT	3	0.9462	0.2551	1.1272	0.9983	1	0.7509
436	2.3	sp P34926 MAP1A_RAT	5	1.0375	0.9195	1.0666	0.7415	1.1695	0.5681
437	3.5	sp Q10728 MYPT1_RAT	3	0.9908	0.932	1.1803	0.2822	1.1272	0.5298
438	10.1	sp Q64654 CP51A_RAT	3	1.1376	0.6988	1.0471	0.7462	1.0568	0.7505
439	13.7	sp Q68FU3 ETFB_RAT	3	0.9376	0.1844	0.9727	0.2884	1.0765	0.9653
440	13	sp P62916 TF2B_RAT	3	1.0375	0.4059	1.0186	0.5279	0.9204	0.9687
441	11.6	sp P62198 PRS8_RAT	5	0.3873	0.9751	1.2134	0.5229	1.2706	0.1917
442	17.9	sp P18420 PSA1_RAT	4	0.9908	0.9238	1.0965	0.6086	1.0965	0.582
443	33.9	sp P35434 ATPD_RAT	6	1.8707	0.5486	1.7061	0.8312	1.7865	0.4281
444	13.3	sp P85970 ARPC2_RAT	4	0.871	0.3412	1.028	0.8122	0.8551	0.291
445	1.5	sp D3ZD32 CHD5_RAT	3	1.0471	0.7354	0.9817	0.65	1.0568	0.4361
446	14.2	sp P82471 GNAQ_RAT	4	0.7379	0.6083	0.8472	0.5038	0.631	0.2993
447	20.8	sp Q3T1J1 IF5A1_RAT	3	0.673	0.5926	1.5704	0.9639	1.4454	0.9152
448	11.2	sp Q5XIK2 TMX2_RAT	4	1.556	0.2888	1	0.5707	1.4588	0.2052
449	2.4	sp Q6MG49 BAG6_RAT	3	0.9908	0.7355	1.028	0.4141	0.8872	0.6808
450	26.9	sp P62845 RS15_RAT	10	0.6982	0.7331	1.1169	0.9498	1.1066	0.9466
451	11.8	sp P62997 TRA2B_RAT	4	1.0093	0.9376	1.0186	0.715	0.9908	0.9802
452	14.7	sp P59215 GNAO_RAT	4	0.4742	0.5551	0.673	0.8748	0.3251	0.4376
453	22.2	sp Q9Z269 VAPB_RAT	5	1.1803	0.9737	0.929	0.9882	1.7219	0.9042
454	11.7	sp Q9WVC0 SEPT7_RAT	4	1.0093	0.3982	0.9462	0.2103	1.0186	0.9531
455	10.1	sp Q9WV25 PUF60_RAT	5	0.8954	0.5017	0.9036	0.6774	0.8472	0.5887
456	14.6	sp Q6PCT3 TPD54_RAT	4	0.8318	0.6038	1.0666	0.7333	1.0666	0.5472



N	% Cov (95)	Accession #	Pep 95%	PVal		PVal		PVal	
				115:114	115:114	116:114	116:114	117:114	117:114
457	6.4	sp Q5XIA1 NCLN_RAT	3	1.0471	0.4141	1.0864	0.4798	1.028	0.7884
458	8.9	sp P16391 HA12_RAT	3	0.631	0.7987	0.5598	0.4299	0.871	0.9214
459	14.4	sp Q9WUS0 KAD4_RAT	3	1.7701	0.3777	0.9727	0.0161	1.1272	0.7085
460	14.8	sp Q8K586 RANT_RAT	3	0.9727	0.7569	0.9638	0.8263	0.9462	0.9195
461	18.8	sp Q66HA6 ARL8B_RAT	3	0.9908	0.9906	1.0093	0.9871	1.0471	0.6021
462	24	sp P62853 RS25_RAT	4	0.863	0.9445	1.028	0.5963	0.4487	0.4204
463	18.9	sp P40307 PSB2_RAT	4	0.6607	0.3659	1.2246	0.5034	0.8954	0.9948
464	15.8	sp P25113 PGAM1_RAT	3	1.0186	0.7401	0.9727	0.991	1.0093	0.9807
465	10.1	sp Q5BK63 NDUA9_RAT	3	0.7516	0.526	0.3597	0.2684	0.7178	0.7021
466	21.2	sp P63324 RS12_RAT	3	0.6546	0.4159	0.787	0.642	1	0.8096
467	33.9	sp P62856 RS26_RAT	4	1.028	0.5879	1.0765	0.2434	1.0568	0.2621
468	20.3	sp P62850 RS24_RAT	6	2.6062	0.4341	2.9648	0.1692	1.2823	0.7422
469	27.3	sp P55770 NH2L1_RAT	4	0.7244	0.6536	0.4487	0.4024	1	0.5076
470	17.4	sp P34064 PSA5_RAT	5	0.8395	0.8404	1.4859	0.5071	0.5861	0.5256
471	28.3	sp P61805 DAD1_RAT	3	1.0093	0.7686	0.9462	0.9346	0.9204	0.6708
472	2	sp P11654 PO210_RAT	3	0.955	0.9824	0.9638	0.9475	0.9817	0.868
473	20.2	sp Q5XI72 IF4H_RAT	4	1.556	0.6258	0.3767	0.7726	1.1272	0.6728
474	10.5	sp P08081 CLCA_RAT	4	0.6026	0.4009	0.7943	0.5771	0.7447	0.5513
475	5.2	sp Q2PQA9 KINH_RAT	4	0.7727	0.4031	0.863	0.9048	0.8872	0.575
476	26.2	sp Q9R1Z0 VDAC3_RAT	6	1.1695	0.4142	1.0568	0.997	1.2134	0.2916
477	9.6	sp Q6P747 HP1B3_RAT	5	1.028	0.5338	1.0186	0.6546	1.028	0.3487
478	8.8	sp Q6P7P5 BZW1_RAT	4	0.4169	0.1403	1.1272	0.9761	1.2359	0.475
479	21.1	sp P17078 RL35_RAT	6	1.2589	0.7765	1.4454	0.3259	1.0093	0.936
480	9.9	sp Q5U2X6 CCD47_RAT	5	1	0.6505	0.9638	0.8848	1.0093	0.8819
481	5.4	sp Q4G061 EIF3B_RAT	6	0.9817	0.6937	1.0093	0.4829	0.9908	0.7728
482	13.9	sp Q68FY1 NUP53_RAT	3	1.1066	0.6299	1.1482	0.9382	0.5346	0.2908
483	8.2	sp Q5U317 FIP1_RAT	3	0.8872	0.6288	0.9376	0.8969	0.9204	0.8803
484	9.3	sp A1L134 AUP1_RAT	3	1.0093	0.7264	0.8872	0.8845	0.879	0.6565
485	8.3	sp Q9JI85 NUCB2_RAT	3	1.1912	0.9584	3.3113	0.1033	1.5276	0.7233
486	18.7	sp Q68A21 PURB_RAT	4	1.0568	0.7173	1.028	0.4748	0.9727	0.9983
487	19.7	sp P62914 RL11_RAT	6	1.7061	0.5342	2.1677	0.2238	2.5586	0.1935
488	12.8	sp P08503 ACADM_RAT	4	1.6293	0.6169	0.7943	0.3898	1	0.6579
489	12.5	sp Q6P7R8 DHB12_RAT	3	0.9908	0.989	0.9908	0.9549	0.9817	0.637
490	8.7	sp Q4V898 RBMX_RAT	4	0.8017	0.2864	0.8241	0.1921	0.863	0.6711
491	20	sp P04646 RL35A_RAT	4	1	0.8619	0.9638	0.3583	1.0186	0.7663
492	9.7	sp Q505J9 ATAD1_RAT	3	1.028	0.5617	1	0.8811	1.0864	0.7082
493	3.1	sp Q6QI44 NAA25_RAT	3	1.0375	0.9774	1	0.6512	1.1482	0.2563
494	19.7	sp Q9JI92 SDCB1_RAT	7	1.2589	0.5483	1.7378	0.5151	1.1803	0.9538
495	17.1	sp Q9Z0V6 PRDX3_RAT	5	0.9462	0.5737	0.9638	0.8458	1.028	0.4589
496	6.8	sp Q5FV16 VATC1_RAT	3	1.1376	0.4567	1.1272	0.3772	1.0568	0.4085
497	4.8	sp Q5RJT2 SPB1_RAT	3	1.1695	0.3764	1.0186	0.8842	1.0471	0.3539
498	15.3	sp Q6AXX6 F213A_RAT	3	0.9908	0.5348	0.8954	0.213	0.879	0.1336
499	15.6	sp P00787 CATB_RAT	4	1.2359	0.9994	1.2134	0.9802	0.4325	0.6031
500	8.7	sp P26284 ODPA_RAT	3	1.1066	0.8177	1.0375	0.7373	1.0375	0.6655
501	7.1	sp Q5U2Q7 ERF1_RAT	3	0.7447	0.4373	1.0471	0.72	0.5445	0.2423
502	15.7	sp Q5I0E7 TMED9_RAT	5	1.2942	0.2759	0.8241	0.8132	0.3631	0.1809
503	12.3	sp Q6IG12 K2C7_RAT	4	2.9376	0.1489	1.7378	0.5195	2.884	0.1841
504	3.8	sp P70501 RBM10_RAT	3	0.912	0.3886	0.8318	0.3294	1.0186	0.6301
505	5.9	sp P07872 ACOX1_RAT	6	1.3677	0.6258	1.5276	0.2628	1.0765	0.5629
506	74.6	sp P19944 RLA1_RAT	3	0.7447	0.6116	1.5849	0.8572	0.7656	0.6244
507	10.3	sp Q8CH84 ELAV2_RAT	3	0.9908	0.3593	1.0568	0.2618	0.9817	0.5755
508	13.9	sp P28073 PSB6_RAT	3	1.0093	0.9925	1.0765	0.7037	1.1803	0.5893
509	4.7	sp Q6IG02 K22E_RAT	3	0.5105	0.3087	0.7112	0.5385	0.7516	0.7946
510	6	sp E9PU28 IMDH2_RAT	2	1.3677	0.8871	0.9204	0.5858	1.6904	0.5844
511	9.8	sp B0BN93 PSD13_RAT	4	0.5754	0.3206	1.3552	0.9505	0.955	0.2922
512	7.8	sp Q6P7D4 CP20A_RAT	3	1.6444	0.4092	1.0375	0.5404	1.1588	0.5458
513	4	sp Q05764 ADDB_RAT	3	0.8551	0.4501	1	0.8792	0.8872	0.6814

N	% Cov (95)	Accession #	Pep 95%	PVal			PVal		
				115:114	115:114	116:114	116:114	117:114	117:114
514	18.5	sp P83732 RL24_RAT	4	0.9727	0.9127	0.9908	0.7577	1.0093	0.7247
515	5.2	sp Q7TMD5 ZC3HE_RAT	4	1.1482	0.7798	0.5916	0.1268	0.8954	0.3687
516	54.9	sp P29418 ATP5E_RAT	5	1.7701	0.4908	0.8318	0.4619	1.7061	0.6811
517	9.3	sp Q99P39 NFS1_RAT	4	0.9727	0.9524	0.863	0.9092	0.955	0.9638
518	11.8	sp Q5XI32 CAPZB_RAT	3	1.8365	0.1344	1.3552	0.5031	0.8166	0.1411
519	3.9	sp Q6UPR8 ERMP1_RAT	4	1.0568	0.8333	1.0093	0.7826	1.028	0.7793
520	4.6	sp Q8CHN6 SGPL1_RAT	2	0.955	0.7192	1.0093	0.651	1.028	0.6227
521	3.8	sp Q2TA68 OPA1_RAT	4	1.0765	0.7389	1.1482	0.3006	0.9727	0.9419
522	17.3	sp P20070 NB5R3_RAT	4	1.0864	0.8708	0.7112	0.4456	1.0471	0.9259
523	14.4	sp P22734 COMT_RAT	3	0.9638	0.9103	1.028	0.8998	1.0186	0.7604
524	5.9	sp Q6AYB4 HSP7E_RAT	3	0.9727	0.7808	1.0666	0.3017	1.0568	0.5794
525	6.4	sp P50137 TKT_RAT	3	0.9727	0.7038	1.1695	0.74	1.0666	0.9683
526	5.8	sp Q4FZU2 K2C6A_RAT	4	0.4406	0.7382	0.5598	0.6267	2.2909	0.283
527	43.1	sp Q00728 H2A4_RAT	35	1.7701	0.4504	1.5136	0.5737	1.3552	0.9051
528	3.9	sp Q05096 MYO1B_RAT	4	1.028	0.5462	1.028	0.4527	0.9376	0.8455
529	6.1	sp P21396 AOFA_RAT	3	1.0093	0.8312	1	0.6221	0.9908	0.7675
530	2.2	sp O08662 PI4KA_RAT	3	1.1169	0.5891	1.028	0.9894	0.9462	0.7499
531	16.7	sp P25886 RL29_RAT	4	1.0765	0.3337	1	0.8639	1.0186	0.8249
532	10.8	sp Q64057 AL7A1_RAT	3	0.879	0.3542	0.6194	0.2264	1.1482	0.6225
533	12	sp Q5FVQ4 MLEC_RAT	3	0.955	0.3817	0.955	0.8148	0.912	0.3923
534	17.3	sp Q6PCU2 VATE1_RAT	6	1.1482	0.1857	1.0765	0.1809	1.2023	0.1059
535	18.7	sp Q5XIE3 RM11_RAT	3	0.929	0.3773	0.9727	0.9559	0.929	0.8131
536	7.5	sp Q63569 PRS6A_RAT	3	0.9462	0.9289	1.0186	0.7798	1	0.7093
537	9.1	sp Q5RK09 EIF3G_RAT	3	1.0093	0.7668	0.929	0.365	1	0.9445
538	5.6	sp Q5XI31 PIGS_RAT	2	1.0375	0.9445	0.8395	0.8175	0.9817	0.9984
539	15.3	sp P62634 CNBP_RAT	3	1.0965	0.7558	0.2291	0.0918	1.1272	0.7867
540	9.3	sp Q561S0 NDUAA_RAT	3	0.5495	0.4381	1.1066	0.5354	1.2589	0.5319
541	5.1	sp Q9QZ86 NOP58_RAT	2	1.4723	0.3223	0.5012	0.3005	0.879	0.6665
542	2	sp Q6RJR6 RTN3_RAT	2	1.3804	0.4616	0.9638	0.5551	0.3631	0.389
543	3.6	sp Q62599 MTA1_RAT	2	0.8318	0.4892	0.8954	0.7389	0.6855	0.2933
544	4.3	sp Q9WV63 KIF2A_RAT	3	0.9036	0.9324	0.7727	0.4452	0.8954	0.9383
545	5.2	sp Q811S9 GNL3_RAT	2	1.0375	0.8153	0.9462	0.595	0.955	0.9097
546	13	sp D4A7N1 MIC25_RAT	3	0.7311	0.6582	0.6081	0.6381	0.5395	0.7532
547	30.2	sp P83883 RL36A_RAT	3	0.2559	0.4705	1.4588	0.2876	1.1066	0.9556
548	2.6	sp POC5W1 MAP1S_RAT	2	0.9727	0.7396	0.9638	0.8414	0.9462	0.7315
549	6.7	sp Q66H12 NAGAB_RAT	3	0.9376	0.7622	0.9204	0.8346	0.4571	0.2112
550	33.9	sp P62275 RS29_RAT	2	0.8551	0.7456	1.0965	0.3832	0.673	0.9213
551	5.8	sp P62138 PP1A_RAT	2	1.0186	0.9646	1.0375	0.471	1.0765	0.2793
552	5.2	sp Q9WUD9 SRC_RAT	2	0.8954	0.618	1.1066	0.4958	0.9727	0.8818
553	11.8	sp Q5FVL6 TSN13_RAT	2	1.0186	0.1037	0.5012	0.1688	6.5464	0.0407
554	7	sp Q641X8 EIF3E_RAT	3	1.0864	0.6107	1.1066	0.5796	1.0568	0.975
555	37.1	sp P63174 RL38_RAT	5	0.9638	0.944	0.9908	0.8811	0.9727	0.8112
556	3.3	sp P85972 VINC_RAT	2	1.9409	0.1311	1.3428	0.7773	1.5276	0.7018
557	3.8	sp Q71UF4 RBBP7_RAT	2	1.1482	0.57	1.0093	0.9261	1.0666	0.7891
558	6.4	sp Q9JHL4 DBNL_RAT	2	0.8091	0.6822	0.879	0.8012	0.2606	0.1606
559	32.4	sp P29419 ATP5I_RAT	3	0.492	0.3931	0.5861	0.3827	0.6427	0.7893
560	15.6	sp P04644 RS17_RAT	3	0.7943	0.4276	1.5276	0.3758	0.6486	0.3266
561	6.6	sp Q62698 DC1L2_RAT	2	1.1272	0.7183	1.1169	0.8545	1.0765	0.769
562	8	sp Q62651 ECH1_RAT	2	0.955	0.7073	1.0375	0.7856	1	0.7672
563	7.1	sp Q3SWS8 RAE1L_RAT	2	1.2023	0.6696	0.7798	0.6363	0.2014	0.0551
564	4	sp Q5U367 PLOD3_RAT	2	0.8017	0.0299	0.9036	0.0798	0.9638	0.0565
565	1	sp P42346 MTOR_RAT	3	0.8395	0.3453	1.0186	0.9567	0.955	0.5255
566	2.8	sp Q5BJS0 DHX30_RAT	3	0.6918	0.6028	0.3076	0.2085	0.6486	0.75
567	1.8	sp P37199 NU155_RAT	2	0.9908	0.959	0.9638	0.839	1.028	0.4555
568	5.9	sp Q9ER24 ATX10_RAT	3	1.1169	0.5812	1.0186	0.9923	1.1066	0.5845
569	23.9	sp D3ZAF6 ATPK_RAT	2	1.0471	0.8479	0.6855	0.4438	0.955	0.7658
570	3	sp Q5U2W5 TBL3_RAT	2	0.912	0.8855	0.8954	0.447	0.8954	0.6127

N	% Cov (95)	Accession #	Pep 95%	PVal			PVal		
				115:114	115:114	116:114	116:114	117:114	117:114
571	18.5	sp Q07984 SSRD_RAT	4	0.9638	0.8163	0.9817	0.9125	0.9462	0.7819
572	35.8	sp P68035 ACTC_RAT	49	1.0864	0.7956	1.0471	0.8174	1.0965	0.7785
573	12.2	sp D4ACN8 PLRKT_RAT	2	1.0666	0.4167	1.0965	0.5913	1.2023	0.2951
574	5.7	sp Q6AXT8 SF3A2_RAT	3	1.0666	0.4218	1.0093	0.9557	0.9908	0.8454
575	19.4	sp Q4KM65 CPSF5_RAT	3	1.4723	0.4982	1.3677	0.5592	1.4454	0.5086
576	19.1	sp Q05175 BASP1_RAT	3	1.0375	0.8117	1.0093	0.8492	0.9204	0.8876
577	9.6	sp P21670 PSA4_RAT	4	0.871	0.8632	0.9376	0.9193	0.9727	0.5453
578	4.4	sp P17046 LAMP2_RAT	2	1.0186	0.8007	1.5849	0.1607	1.2134	0.1373
579	3.7	sp P41542 USO1_RAT	3	0.863	0.4588	0.8091	0.5673	1	0.8655
580	12.8	sp Q5I0K8 RT07_RAT	2	1.0765	0.8422	0.9204	0.7916	0.9376	0.9516
581	7.4	sp Q3B7U9 FKBP8_RAT	2	1.0965	0.7876	2.5119	0.3255	1.9953	0.4694
582	3.8	sp P84903 STIM1_RAT	2	0.6486	0.2755	0.5916	0.1383	0.6368	0.3649
583	5.4	sp B5DFN2 SAHH2_RAT	2	0.9908	0.8627	0.9817	0.8302	1.0765	0.8217
584	21	sp P11232 THIO_RAT	2	0.9462	0.9003	1.4454	0.2986	1.3804	0.4152
585	4.1	sp O54924 EXOC8_RAT	2	0.8872	0.8434	0.871	0.8612	0.929	0.8597
586	2.7	sp Q56B11 PELP1_RAT	2	0.871	0.8006	0.6138	0.4382	0.7311	0.5812
587	32.6	sp P61515 RL37P_RAT	3	1.0965	0.6854	0.7656	0.7245	1.888	0.4529
588	32.8	sp P10536 RAB1B_RAT	8	1	0.995	0.9376	0.8154	0.9638	0.9745
589	24.6	sp P35280 RAB8A_RAT	5	1.1066	0.1975	1.6596	0.4976	0.5012	0.0734
590	18	sp P35281 RAB10_RAT	4	1.0471	0.8492	1.0093	0.6396	0.9638	0.543
591	8.8	sp P54311 GBB1_RAT	5	0.5598	0.3674	0.6546	0.4913	0.631	0.4172
592	17.7	sp P61107 RAB14_RAT	3	0.863	0.5182	0.9908	0.8408	0.8954	0.5395
593	6	sp P63036 DNJA1_RAT	3	1.0186	0.7617	0.929	0.6872	0.9817	0.8031
594	8.3	sp O88656 ARC1B_RAT	2	1.7865	0.3471	1.2942	0.7385	1.3428	0.4859
595	1.8	sp Q80X08 FAM21_RAT	2	3.1623	0.2394	3.1333	0.189	0.3945	0.2532
596	5.9	sp P26453 BASI_RAT	2	1.0186	0.8758	0.9462	0.9415	0.9376	0.7632
597	11.9	sp Q75Q40 TOM40_RAT	3	0.4365	0.7536	0.879	0.9984	0.6792	0.7047
598	11.1	sp Q9EPH2 MRP_RAT	2	0.912	0.9257	1.5417	0.9982	1.3062	0.8482
599	4.6	sp Q8K1Q0 NMT1_RAT	3	0.9727	0.7557	0.9908	0.9238	1.1066	0.6568
600	9.7	sp Q641W4 RFC2_RAT	2	1.0864	0.3187	0.9376	0.5687	0.879	0.5898
601	7.3	sp Q5XII9 MFR1L_RAT	2	1.1169	0.7294	0.9727	0.9173	1.2706	0.6067
602	9	sp Q5XIC0 ECI2_RAT	3	0.9727	0.7908	0.8318	0.6738	0.8954	0.9353
603	4.5	sp Q5FVH2 PLD3_RAT	2	0.8472	0.6685	0.879	0.8023	0.7379	0.7268
604	11.3	sp P52947 PDX1_RAT	3	1.0965	0.8304	0.8017	0.6736	0.6194	0.4305
605	6	sp Q920R3 FADS1_RAT	2	0.227	0.1655	0.9908	0.9994	0.4055	0.2632
606	8.1	sp Q5M7T4 YIPF4_RAT	2	1.0864	0.9836	0.6427	0.6347	1.4588	0.7558
607	6.3	sp Q06486 KC1D_RAT	2	0.7047	0.3974	0.879	0.5552	0.7047	0.4612
608	30.4	sp P62859 RS28_RAT	3	0.4285	0.4267	1.028	0.7386	1.1588	0.9544
609	8.8	sp P62083 RS7_RAT	3	0.8017	0.8739	1.7219	0.7205	1.0471	0.9393
610	7	sp P13221 AATC_RAT	2	1.1169	0.7697	1.2134	0.6012	1.028	0.8717
611	31.3	sp P11608 ATP8_RAT	2	0.9908	0.9455	1.2589	0.7985	1.6293	0.5322
612	13.6	sp Q5EB77 RAB18_RAT	2	1.1169	0.7554	2.0137	0.2712	1.2023	0.3074
613	6.5	sp P97633 KC1A_RAT	3	1.1066	0.8884	1.1272	0.6987	1	0.8487
614	20.5	sp P83941 ELOC_RAT	2	1.5417	0.5234	0.9204	0.9349	0.912	0.9041
615	12.1	sp P63322 RALA_RAT	2	0.9462	0.995	1.2134	0.4907	1.0666	0.6327
616	28.5	sp P63045 VAMP2_RAT	4	0.9727	0.8384	0.9908	0.9525	1.0471	0.9166
617	26.3	sp P62076 TIM13_RAT	3	1.0375	0.8054	1	0.9787	0.9462	0.9063
618	9.1	sp P34067 PSB4_RAT	3	0.4742	0.5616	0.871	0.8303	0.7516	0.691
619	17.7	sp P31044 PEBP1_RAT	2	0.5495	0.5876	1.1695	0.5814	0.7447	0.9583
620	3.8	sp P28841 NEC2_RAT	2	0.9462	0.9894	0.8872	0.8232	0.9204	0.8643
621	11.8	sp O35796 C1QBP_RAT	3	0.9462	0.5857	1.028	0.9913	0.9638	0.8468
622	16.5	sp P84817 FIS1_RAT	4	1.0186	0.8238	0.9817	0.7407	0.8017	0.8002
623	4.5	sp Q7TSA0 MIRO2_RAT	2	0.7244	0.569	0.7943	0.6749	0.9036	0.8493
624	5.2	sp Q6AYB5 SRP54_RAT	2	0.673	0.8119	0.1905	0.1282	0.2992	0.1251
625	25.2	sp P28042 SSBP_RAT	3	0.8091	0.6984	0.2466	0.1742	1.0186	0.9521
626	2.9	sp Q64060 DDX4_RAT	3	0.9727	0.882	1	0.8468	1.0375	0.876
627	3.5	sp P97686 NRCAM_RAT	3	0.6546	0.3107	0.6982	0.3897	0.8551	0.8326

N	% Cov (95)	Accession #	Pep 95%	PVal			PVal		
				115:114	115:114	116:114	116:114	117:114	117:114
628	9.7	sp P19234 NDUV2_RAT	2	0.8166	0.7514	0.7586	0.6992	0.7943	0.8325
629	4.3	sp Q99M63 SMU1_RAT	2	0.6026	0.1883	0.7447	0.6019	0.7943	0.9598
630	9.5	sp Q641X9 RM09_RAT	2	1.6596	0.432	0.5649	0.1405	1.0375	0.7321
631	3.1	sp Q8K3Y6 ZCCHV_RAT	2	1.0765	0.9614	0.9817	0.8896	0.9908	0.9933
632	22.4	sp Q4QRB4 TBB3_RAT	18	0.9638	0.9915	1.0568	0.7258	1.0471	0.9178
633	4.9	sp P0CE46 ZNT8_RAT	2	1.0471	0.7736	0.9727	0.9702	0.9727	0.849
634	47	sp P05765 RS21_RAT	4	1.0186	0.298	1.1482	0.2556	1.0093	0.6281
635	1.2	sp P97526 NF1_RAT	4	0.9462	0.7876	0.787	0.4772	1.0568	0.9924
636	6.2	sp Q9WUC8 PLRG1_RAT	3	0.9727	0.9996	1.2134	0.548	1.406	0.3951
637	8.5	sp Q4QQW4 HDAC1_RAT	3	1.0093	0.7977	1.1588	0.5189	1.2359	0.3474
638	4.3	sp P18886 CPT2_RAT	2	1	0.7163	0.9638	0.6547	1.0375	0.9013
639	12.9	sp Q62950 DPYL1_RAT	7	0.9376	0.9283	1.8197	0.5859	1.0864	0.9016
640	15.4	sp P11250 RL34_RAT	4	0.9817	0.6523	1.0186	0.8806	0.863	0.2801
641	11.5	sp P19132 FRIH_RAT	2	0.6982	0.6997	0.9817	0.8343	0.863	0.8339
642	15.2	sp Q5XI73 GDIR1_RAT	2	1.1912	0.5955	1.2706	0.6399	1.1169	0.7151
643	15.2	sp Q5XIU9 PGRC2_RAT	3	0.8954	0.988	0.912	0.9007	0.8091	0.7116
644	19	sp Q9WUF4 VAMP8_RAT	2	0.955	0.9563	0.9727	0.7403	0.8872	0.4639
645	16.9	sp P07632 SODC_RAT	3	0.9638	0.5235	1.0568	0.6679	0.9908	0.9691
646	19.4	sp P52164 MAX_RAT	2	0.6194	0.4203	0.9036	0.8466	1.0093	0.9714
647	7	sp Q5XIB5 CCD86_RAT	2	0.9036	0.3939	0.8954	0.2964	0.9727	0.9189
648	2.2	sp O88761 PSMD1_RAT	2	0.4656	0.3898	1.406	0.3074	0.7656	0.6078
649	2.9	sp O55035 PPIG_RAT	2	0.5152	0.3437	1.2706	0.6409	0.5495	0.3744
650	3.2	sp Q5XIK8 CTSL2_RAT	2	1.2474	0.6633	1.0666	0.8799	0.8166	0.7039
651	3.4	sp Q4QQW8 PLBL2_RAT	2	1.028	0.8609	0.9376	0.8309	0.9376	0.8543
652	9.5	sp P28075 PSB5_RAT	2	1.0375	0.8031	1.0568	0.9856	1.0765	0.6064
653	12.5	sp P32089 TXTP_RAT	4	0.5248	0.0973	0.5916	0.2366	0.5395	0.3394
654	0.6	sp Q2TL32 UBR4_RAT	3	1.0471	0.6507	1.1272	0.4781	0.871	0.4027
655	3.3	sp Q8VHE9 RETST_RAT	2	0.6668	0.2422	0.955	0.9453	0.8241	0.7668
656	3.8	sp P05708 HXX1_RAT	4	0.5105	0.0413	0.4207	0.1389	0.3597	0.0485
657	5.9	sp P16970 ABCD3_RAT	2	1.1066	0.5362	1.0093	0.8457	0.9462	0.6784
658	3.6	sp P16617 PGK1_RAT	2	0.7379	0.7481	1.5849	0.2699	0.871	0.953
659	3.1	sp Q6P799 SYSC_RAT	2	0.8551	0.7123	0.8954	0.8831	0.6668	0.6671
660	9.1	sp Q9Z311 MECR_RAT	2	0.8954	0.8289	0.8395	0.5737	0.9036	0.8828
661	20.6	sp Q63750 RM23_RAT	2	1.4588	0.5169	1	0.9577	1.0965	0.7263
662	10.4	sp Q6AXW0 BOREA_RAT	2	0.8872	0.8226	1.3804	0.5578	1.2023	0.6768
663	20.7	sp P68511 1433F_RAT	10	0.863	0.5834	0.9908	0.9332	0.871	0.8827
664	14.3	sp Q3T1K5 CAZA2_RAT	3	0.5495	0.0934	0.6427	0.1453	0.8166	0.4599
665	5.4	sp Q02253 MMSA_RAT	2	1.0864	0.2632	0.9908	0.4903	1.3062	0.061
666	6.7	sp P50399 GDIB_RAT	3	1.0375	0.8592	1.1588	0.5668	1.1376	0.525
667	27.6	sp Q9JJW3 USMG5_RAT	3	0.7798	0.7393	1.4191	0.9467	0.7047	0.8018
668	8.2	sp Q7TPJ0 SSRA_RAT	2	1.3062	0.9377	1.3062	0.8405	0.879	0.7878
669	13.6	sp P30009 MARCS_RAT	4	0.8551	0.6859	1.4322	0.7838	0.6982	0.8971
670	9.1	sp Q9Z2S9 FLOT2_RAT	3	0.912	0.7002	0.9036	0.2303	1.0186	0.3949
671	2.7	sp Q5U300 UBA1_RAT	2	0.5058	0.2621	1.2359	0.6283	1.0666	0.8613
672	7.4	sp Q6P7S1 ASAH1_RAT	3	1.2023	0.8865	1.1066	0.7401	1.2942	0.5431
673	11.1	sp Q8K3E7 DPY30_RAT	3	0.8241	0.5134	0.8318	0.6433	0.8091	0.6757
674	5.6	sp O35824 DNJA2_RAT	3	0.8954	0.6452	0.912	0.8408	0.879	0.7964
675	2.5	sp P49134 ITB1_RAT	2	1.028	0.5623	0.9638	0.8399	0.9638	0.7386
676	3.4	sp Q05140 AP180_RAT	2	1.1376	0.7043	0.929	0.2637	0.9727	0.3392
677	8	sp Q68FW9 CSN3_RAT	3	1.0568	0.712	0.9727	0.8818	1.0864	0.648
678	15.8	sp P55063 HS71L_RAT	17	1.0375	0.7919	1.0375	0.6924	0.955	0.8946
679	18.5	sp P58200 VTI1B_RAT	4	1.3062	0.1885	1.1272	0.4627	1.4191	0.1347
680	4.2	sp O88984 NXF1_RAT	2	1.3062	0.1737	1.1695	0.4522	0.5702	0.1259
681	10.8	sp Q5M818 RM16_RAT	2	1.028	0.9428	1.1169	0.6717	1.0765	0.6125
682	7.1	sp P15087 CBPE_RAT	2	1.0965	0.2519	1.1912	0.1444	1.0186	0.665
683	1.4	sp P49793 NUP98_RAT	2	1.2023	0.5058	1.1482	0.3498	1.1169	0.3028
684	3	sp Q9JJ22 ERAP1_RAT	3	0.912	0.8713	1.0093	0.968	0.9638	0.9514

N	% Cov (95)	Accession #	Pep 95%	PVal		PVal		PVal	
				115:114	115:114	116:114	116:114	117:114	117:114
685	4.8	sp P40329 SYRC_RAT	3	1.0765	0.6207	1.1066	0.4432	1.0375	0.7175
686	8.9	sp Q0VGK4 GDPD1_RAT	2	1.0666	0.9262	0.7379	0.3218	0.8017	0.4803
687	5.2	sp P12007 IVD_RAT	2	1.1169	0.3309	1.1169	0.4945	1.0568	0.4385
688	32.6	sp Q78P75 DYL2_RAT	2	0.9036	0.4242	0.9817	0.6551	0.929	0.4325
689	5	sp Q9R0T3 DNJC3_RAT	3	0.3373	0.2343	0.6081	0.3823	0.9376	0.7602
690	11.7	sp P14604 ECHM_RAT	2	0.8472	0.6141	0.2228	0.0322	0.4966	0.7747
691	4.3	sp Q5RKHO GLYR1_RAT	2	0.8395	0.5804	0.9908	0.6869	1.0186	0.69
692	11.2	sp P11348 DHPR_RAT	2	0.8954	0.6451	1.1169	0.6869	0.863	0.5739
693	2.2	sp Q765A7 PGAP1_RAT	2	1.2134	0.6983	1.0965	0.8373	1.3183	0.6003
694	18.3	sp Q9WVB1 RAB6A_RAT	5	0.879	0.8093	0.7516	0.6069	0.6081	0.4303
695	7.4	sp Q63528 RFA2_RAT	2	12.3595	0.0983	10.666	0.1041	17.378	0.0867
696	34.2	sp P11951 CX6C2_RAT	4	0.9376	0.9997	0.9462	0.9107	0.9036	0.8018
697	16.1	sp Q5XIM5 CDV3_RAT	2	0.6855	0.5154	0.52	0.3492	0.7727	0.6383
698	4.1	sp P70582 NUP54_RAT	2	2.0137	0.5907	0.8017	0.665	2.0512	0.5631
699	5.2	sp Q5FWT1 FA98A_RAT	2	0.413	0.8881	2.0893	0.3507	0.3192	0.3946
700	7.1	sp P50503 F10A1_RAT	2	0.863	0.1509	1.0186	0.727	0.9462	0.4497
701	8.1	sp P30839 AL3A2_RAT	4	2.0701	0.5445	0.7727	0.7714	1.6749	0.542
702	4.9	sp P86173 ACL6B_RAT	2	1.2246	0.5037	1.2474	0.6769	1.2134	0.7605
703	13.8	sp P04897 GNAI2_RAT	4	0.9817	0.9247	1	0.9812	0.955	0.8905
704	11.3	sp Q4FZY0 EFHD2_RAT	2	1.2359	0.1015	1.0765	0.3008	0.9817	0.5845
705	5.2	sp Q99PM1 TOX4_RAT	2	1.1066	0.9728	0.9727	0.9475	0.9204	0.6126
706	10.4	sp P70470 LYPA1_RAT	2	0.9727	0.7435	1.0186	0.9651	0.8395	0.5017
707	14.4	sp P70580 PGRC1_RAT	3	0.9462	0.3558	1.0093	0.9399	1.0093	0.4042
708	26.1	sp Q75Q41 TOM22_RAT	3	1.2823	0.6548	0.9908	0.9096	1.3062	0.6797
709	7.8	sp P97576 GRPE1_RAT	2	1.0093	0.4567	0.9204	0.472	0.929	0.6073
710	5.7	sp P53676 AP3M1_RAT	2	0.6792	0.6323	0.5808	0.1426	0.4169	0.2879
711	12.8	sp Q920J4 TXNL1_RAT	2	0.7586	0.6071	0.7656	0.5408	0.7311	0.6652
712	5.4	sp Q923K9 A1CF_RAT	2	1.028	0.8868	0.863	0.8929	0.8954	0.7982
713	0.7	sp D3ZHA0 FLNC_RAT	3	0.8395	0.0355	0.9376	0.8187	0.9462	0.5734
714	5.1	sp P15651 ACADS_RAT	2	0.9462	0.9648	0.8318	0.5589	0.9036	0.8224
715	2.4	sp Q07266 DREB_RAT	1	1.1803	0.2563	1.028	0.6701	0.7656	0.2691
716	6.2	sp Q920A6 RISC_RAT	2	1.0375	0.8531	0.4613	0.5118	0.6855	0.6683
717	2.3	sp P55266 DSRAD_RAT	2	1	0.766	0.955	0.9755	0.9817	0.8203
718	17.3	sp Q63396 TCP4_RAT	4	0.9908	0.4888	1.1588	0.5897	1.1482	0.5832
719	9.9	sp Q08851 STX5_RAT	2	1.1066	0.7491	0.5445	0.4363	0.7943	0.655
720	13.4	sp P61928 RL37_RAT	2	1.8365	0.5474	1.7061	0.8045	1.9055	0.6641
721	4.1	sp Q5U2Y6 TFP11_RAT	2	0.9817	0.9262	0.7379	0.1271	0.9462	0.6405
722	10.5	sp Q66HR2 MARE1_RAT	3	0.4966	0.1729	1.4191	0.4359	0.6486	0.5774
723	9.4	sp P69682 NECP1_RAT	2	2.0893	0.2184	1.2474	0.4638	0.9727	0.7948
724	6.6	sp P29315 RINI_RAT	2	0.7244	0.365	1.8707	0.2557	2.2491	0.2104
725	7.7	sp O70351 HCD2_RAT	2	0.6546	0.7725	0.597	0.6898	0.7943	0.7614
726	4.9	sp O35094 TIM44_RAT	2	0.879	0.1951	0.9817	0.7159	1.0093	0.3543
727	11.7	sp Q792I0 LIN7C_RAT	2	0.5702	0.1935	0.6427	0.8076	1.2134	0.973
728	7.6	sp P62870 ELOB_RAT	1	0.9727	0.6774	0.8872	0.8607	0.8872	0.5318
729	9.4	sp Q5U2R7 MESD_RAT	3	1.0568	0.5726	1.0093	0.4968	0.9638	0.9927
730	14.9	sp Q498T2 CHTOP_RAT	3	1.028	0.607	0.8872	0.904	1	0.6457
731	6.6	sp Q505J6 GHC2_RAT	2	0.9638	0.9462	0.8954	0.6954	0.8091	0.493
732	5.4	sp B0BN56 RT31_RAT	2	1.3932	0.4285	1	0.7307	1.3804	0.3609
733	3.7	sp Q8VH46 AFAP1_RAT	2	0.955	0.7493	0.8395	0.5575	1.1588	0.2887
734	17.6	sp P21571 ATP5J_RAT	1	0.2805	0.319	0.8091	0.78	0.4169	0.3996
735	9	sp Q498M4 WDR5_RAT	2	0.9036	0.5435	1.0375	0.8646	0.9376	0.502
736	1.8	sp Q9QYF3 MYO5A_RAT	3	1.0375	0.7782	0.7798	0.2753	1.1272	0.5137
737	6.9	sp Q7TQ84 UIF_RAT	2	0.9204	0.7559	0.8472	0.463	0.8551	0.487
738	2.4	sp Q99P77 NOG1_RAT	2	0.5808	0.3626	1.1588	0.8314	0.9376	0.9773
739	2.6	sp Q9JHZ4 GRAP1_RAT	2	1.2589	0.3052	1.0186	0.6892	1.0765	0.501
740	0.8	sp P53565 CUX1_RAT	1	0.9376	0.3725	0.9204	0.2411	0.9376	0.4043
741	15.1	sp P60881 SNP25_RAT	2	1.0471	0.8826	0.8318	0.7554	0.912	0.8668

N	% Cov (95)	Accession #	Pep 95%	PVal		PVal		PVal	
				115:114	115:114	116:114	116:114	117:114	117:114
742	7.1	sp O08623 SQSTM_RAT	2	0.6918	0.6821	0.2399	0.4839	0.2992	0.5767
743	18.3	sp Q7TQ16 QCR8_RAT	2	2.8314	0.416	2.2909	0.5061	2.5823	0.4255
744	6.7	sp Q6TUG0 DJB11_RAT	2	0.871	0.2787	1.1169	0.883	0.9817	0.5807
745	7.1	sp P22288 GCH1_RAT	2	0.7943	0.6126	0.7447	0.7507	0.7447	0.5951
746	3.4	sp D4AD37 IMPA3_RAT	2	1.2246	0.2592	1.2474	0.2475	1.2474	0.3658
747	1.6	sp P32198 CPT1A_RAT	1	0.8091	0.668	0.8551	0.7873	0.6982	0.5039
748	3.1	sp P42676 NEUL_RAT	2	1.0186	0.9371	1.1695	0.3082	1.0093	0.8857
749	4.9	sp Q3KRD5 TOM34_RAT	1	1.0864	0.8537	0.4325	0.282	1.1066	0.8189
750	6	sp Q62725 NFYC_RAT	2	2.8054	0.4027	0.6607	0.9258	2.729	0.4295
751	9.1	sp Q5U216 DX39A_RAT	6	1.4191	0.85	1.0093	0.7877	0.7178	0.9321
752	3.6	sp P54001 P4HA1_RAT	2	1.1803	0.4735	1.3932	0.4086	1.1169	0.4925
753	4.6	sp Q63190 EMD_RAT	2	1.1912	0.5637	0.9204	0.8636	0.8091	0.4319
754	9	sp P15791 KCC2D_RAT	4	1.4191	0.181	1.1803	0.3419	0.9462	0.918
755	2.3	sp Q5U2Y1 GTF2I_RAT	3	0.9036	0.1564	0.9204	0.7071	0.9727	0.6297
756	9.1	sp Q6R556 SEGN_RAT	2	1.1272	0.8932	0.955	0.9226	1.2589	0.7297
757	6.5	sp Q03344 ATIF1_RAT	1	1.3305	0.2165	0.8551	0.7586	0.7244	0.1972
758	7.5	sp P18422 PSA3_RAT	2	0.9036	0.5446	0.9462	0.9566	1.0093	0.6002
759	3.5	sp P40615 DKC1_RAT	2	1.0568	0.8051	0.6486	0.2055	0.7379	0.3305
760	3.7	sp P63004 LIS1_RAT	1	1.7219	0.1225	2.1677	0.1144	2.1478	0.1321
761	2.2	sp Q5PPF5 ZGPAT_RAT	1	1.0765	0.39	1.0186	0.1186	1.0568	0.2381
762	4	sp P47727 CBR1_RAT	1	0.7379	0.5476	0.929	0.89	0.6918	0.4974
763	7.1	sp P60905 DNJC5_RAT	1	1.0093	0.8639	0.8472	0.5326	0.9376	0.7761
764	1.9	sp O54921 EXOC2_RAT	1	0.8954	0.3702	0.929	0.8564	1.028	0.5626
765	12.1	sp P35171 CX7A2_RAT	1	0.5861	0.1077	0.863	0.3961	0.8318	0.2436
766	7.4	sp Q6XVN8 MLP3A_RAT	1	1.4723	0.7463	1.3677	0.5893	1.4723	0.4731
767	4.9	sp Q6AYK1 RNPS1_RAT	1	1.0864	0.292	1	0.8239	1.1482	0.2209
768	6.7	sp P28648 CD63_RAT	3	2.421	0.2312	2.2699	0.2081	1.5417	0.2813
769	1.6	sp Q8CJB9 BRE1B_RAT	1	0.8091	0.0832	0.863	0.2015	0.912	0.2306
770	6.4	sp B0BNM1 NNRE_RAT	1	1.0471	0.5086	1.1272	0.462	1	0.5359
771	16.4	sp Q6IUR5 NENF_RAT	2	0.9462	0.3168	1.0666	0.3069	1.0568	0.7092
772	1.2	sp Q62780 DDX46_RAT	1	1.1588	0.5476	1.1066	0.7338	1.0666	0.6791
773	2.8	sp A0JPJ7 OLA1_RAT	1	0.7516	0.9128	1.1803	0.7132	0.9376	0.8819
774	17	sp P62864 RS30_RAT	3	1.5276	0.8794	1.3183	0.7679	0.5916	0.4981
775	6.6	sp Q91ZW1 TFAM_RAT	2	1	0.416	0.955	0.4769	1.0093	0.8888
776	1.8	sp Q66HC5 NUP93_RAT	1	0.9908	0.6062	0.9727	0.945	1.028	0.3336
777	4.8	sp P17164 FUCO_RAT	2	0.929	0.7626	0.9817	0.7914	0.9036	0.7186
778	4.6	sp Q4G063 CREL2_RAT	1	0.929	0.6703	0.8241	0.6086	1.028	0.9129
779	6.5	sp P63074 IF4E_RAT	1	0.955	0.9887	0.9727	0.975	0.6918	0.2995
780	12.4	sp D3ZTX0 TMED7_RAT	3	0.6546	0.4679	0.5445	0.371	0.7379	0.5685
781	3.8	sp P56571 ES1_RAT	1	1.6144	0.6718	1.1912	0.9635	1.9953	0.4258
782	1.4	sp Q8K3M6 ERC2_RAT	1	0.9462	0.594	0.9036	0.6006	0.7379	0.1154
783	8.6	sp Q09167 SRSF5_RAT	3	0.9462	0.435	0.871	0.3603	1.0093	0.9581
784	8.2	sp Q9R064 GORS2_RAT	3	0.955	0.8111	0.8954	0.6175	0.8551	0.5064
785	2.9	sp O55166 VPS52_RAT	1						
786	2.2	sp Q64548 RTN1_RAT	2	1.3804	0.8948	1.0375	0.5763	0.5754	0.3881
787	2.5	sp Q62909 KIF2C_RAT	2	0.8954	0.4277	0.8551	0.2341	0.871	0.5436
788	2.3	sp Q9ES54 NPL4_RAT	1	0.879	0.6943	0.955	0.9774	1.0568	0.7397
789	1.6	sp P0C1X8 AAK1_RAT	1	0.8872	0.6625	0.9204	0.3074	1.0375	0.8656
790	8.8	sp P40112 PSB3_RAT	2	1.1588	0.4988	1.1272	0.5735	0.9638	0.9773
791	1.5	sp Q3KR59 UBP10_RAT	1	0.8241	0.6957	1.0093	0.9657	1	0.8604
792	7.8	sp P61589 RHOA_RAT	1	0.6792	0.6603	0.5058	0.5239	0.5861	0.5163
793	2.9	sp Q4QQS8 NUP85_RAT	1	1.0375	0.9039	0.7727	0.5617	0.8395	0.6805
794	1.7	sp Q9R0L4 CAND2_RAT	1	0.0111	0.0055	0.912	0.8345	0.2992	0.0793
795	2.4	sp O08984 LBR_RAT	1	1.6596	0.2039	1.6144	0.1685	1.7219	0.118
796	1.7	sp Q62824 EXOC4_RAT	1	0.6855	0.2009	0.8091	0.4748	0.9908	0.7972
797	1.6	sp Q80WF4 T132A_RAT	1	1.2942	0.619	1.0765	0.8601	1.3183	0.5999
798	9.1	sp Q9JHW5 VAMP7_RAT	2	1.1066	0.8056	1.0471	0.8444	1.0965	0.8175

N	% Cov (95)	Accession #	Pep 95%	PVal		PVal		PVal	
				115:114	115:114	116:114	116:114	117:114	117:114
799	3	sp O35987 NSF1C_RAT	1	0.9376	0.8408	0.9727	0.945	0.9376	0.7921
800	2.7	sp Q4QQT3 CELF1_RAT	2	0.8472	0.6116	1.0568	0.8269	0.6546	0.2785
801	8.6	sp P62963 PROF1_RAT	1	1.028	0.8265	1.0186	0.8288	0.9376	0.891
802	5.1	sp M0RC99 RAB5A_RAT	1	1.3804	0.457	1.9953	0.4198	1.5849	0.5296
803	1.5	sp Q80U96 XPO1_RAT	1	0.7112	0.3645	1.5136	0.6286	1.3305	0.8593
804	8.6	sp Q64119 MYL6_RAT	1	1.5276	0.0197	1.406	0.058	1.3183	0.035
805	16.7	sp P86252 PURA_RAT	1	1.0186	0.7691	0.8472	0.7976	0.929	0.9713
806	0.3	sp Q7TMA5 APOB_RAT	2	0.9204	0.2564	0.8872	0.5322	1.028	0.5973
807	1	sp Q63120 MRP2_RAT	2	0.929	0.5091	0.8472	0.5515	0.9727	0.688
808	2	sp O55156 CLIP2_RAT	1	0.9462	0.8834	0.9817	0.9992	1.1066	0.5808
809	3	sp Q6TQE1 ZCH18_RAT	2	1.0965	0.8089	0.7798	0.0291	0.9638	0.3603
810	1.8	sp O88884 AKAP1_RAT	1	1.0864	0.7666	0.912	0.7695	0.9376	0.8454
811	2.3	sp Q5I0L3 SYYM_RAT	1	1.0568	0.7625	0.8395	0.6035	0.9462	0.799
812	2.6	sp Q6AXV4 SAM50_RAT	1	0.912	0.8852	1.0093	0.9774	0.955	0.9413
813	4.9	sp Q9ES53 UFD1_RAT	1	0.6855	0.1451	0.8954	0.4614	0.8551	0.5888
814	17.7	sp Q5BJP3 UFM1_RAT	1	0.5058	0.2197	1.0568	0.8681	0.4365	0.1615
815	1.7	sp P18163 ACSL1_RAT	1	1.3804	0.4425	1.3552	0.4746	1.1695	0.8164
816	6.8	sp Q6PDW6 RM17_RAT	1	0.5445	0.3592	1.0864	0.8315	1.3062	0.6179
817	6.8	sp P69736 EDF1_RAT	1	1.0471	0.1569	1.1169	0.1364	0.955	0.2328
818	5.2	sp P70500 CDIPT_RAT	1	1.1066	0.7144	1.1169	0.7998	1.1376	0.4583
819	4.9	sp Q9Z142 TMM33_RAT	1	0.9908	0.7136	0.9727	0.8072	0.879	0.7702
820	2.1	sp Q5XIL3 RPC3_RAT	1	1.2942	0.6189	1.3183	0.602	0.6252	0.4458
821	4.3	sp P70566 TMOD2_RAT	1	0.6855	0.4666	1.1588	0.6347	0.879	0.7109
822	3.3	sp Q6AY30 SCPD_L_RAT	1	1.1482	0.4766	1.028	0.4745	1.0666	0.8291
823	3	sp Q66HG9 MAVS_RAT	1	0.5649	0.3106	0.8166	0.6466	0.6918	0.4553
824	2.9	sp P45479 PPT1_RAT	1	0.7656	0.3268	0.9727	0.8336	0.8472	0.487
825	2.6	sp P82450 SIAE_RAT	1	0.6607	0.4896	1.4454	0.5105	0.3837	0.25
826	1.8	sp Q66H34 CFA97_RAT	1	0.8472	0.5825	1.0093	0.7752	0.8091	0.5395
827	4.8	sp Q6NX65 PDC10_RAT	1	1.0568	0.5664	1.3305	0.3941	1.0093	0.3773
828	0.8	sp Q63679 KDM3A_RAT	1	0.8318	0.6783	1.2474	0.6618	1.028	0.9237
829	5.6	sp Q5U211 SNX3_RAT	1	0.9462	0.7148	0.863	0.2554	0.929	0.5867
830	5.2	sp Q568Z6 IST1_RAT	1	1.2359	0.2182	1.1912	0.1885	1.3428	0.1053
831	3.4	sp Q08163 CAP1_RAT	3	1.0471	0.8876	1.0568	0.861	1	0.9911
832	3.1	sp Q09137 AAPK2_RAT	1	0.929	0.8966	0.787	0.6576	0.912	0.8662
833	2	sp O70277 TRIM3_RAT	1	1.1482	0.7716	0.8091	0.6934	1.2359	0.6449
834	3	sp Q6MGB6 RING1_RAT	1	0.863	0.957	0.871	0.5942	0.8091	0.5305
835	4.4	sp Q80WE1 FMR1_RAT	3	1.3183	0.5923	1.4723	0.4774	0.5495	0.3771
836	4.6	sp P97829 CD47_RAT	2	1.1272	0.8682	1.0864	0.9576	1.1695	0.7467
837	11.5	sp P05714 RAB4A_RAT	2	0.278	0.1909	0.4325	0.3061	0.7727	0.6129
838	7.1	sp P07323 ENOG_RAT	2	0.9817	0.9478	0.9376	0.8858	1.4859	0.4134
839	12.3	sp P63012 RAB3A_RAT	3	0.863	0.7897	1.2589	0.6178	1.0666	0.8444
840	2.1	sp Q5M9H1 LRC41_RAT	2						
841	4	sp P11884 ALDH2_RAT	2	0.6194	0.4447	0.413	0.2683	0.6546	0.4826
842	11.6	sp P20171 RASH_RAT	2	1.0471	0.9215	1.0471	0.9407	0.9727	0.9587
843	7.7	sp Q52KK3 S2551_RAT	2	1.9409	0.2674	0.5346	0.7452	0.5702	0.6723
844	2	sp D3ZU57 NO66_RAT	1	0.8872	0.8297	1.0666	0.879	0.9638	0.956
845	1.5	sp Q5RK27 S12A7_RAT	1	1.3428	0.5826	1.1169	0.8048	1.8707	0.3496
846	3.3	sp Q5PQX1 TOIP1_RAT	1	1.2589	0.6712	1.1912	0.443	1.0471	0.924
847	2.1	sp P97612 FAAH1_RAT	1	1.2023	0.7042	1.888	0.3481	0.7047	0.5417
848	7.8	sp P83565 RM40_RAT	1	0.9908	0.8805	1.1169	0.7495	0.9204	0.8198
849	1.1	sp Q66HG5 TM9S2_RAT	1	1.0666	0.878	0.929	0.8893	0.8241	0.7203
850	1.5	sp Q562C2 BOP1_RAT	1	0.9204	0.5874	0.597	0.3019	0.6252	0.3215
851	4.1	sp Q8VIL3 ZWINT_RAT	1	1.028	0.7276	0.9204	0.9498	1	0.9664
852	5.2	sp Q5XIE9 MED20_RAT	1	0.7943	0.6454	0.7516	0.5945	0.787	0.4911
853	2	sp Q5XHY5 SYTC_RAT	1	0.9908	0.6576	1.0186	0.5283	0.8954	0.306
854	0.5	sp Q63505 TF3C1_RAT	1						
855	5.1	sp Q9EST6 AN32B_RAT	1	1.0471	0.59	1.0666	0.8446	0.8091	0.3065

N	% Cov (95)	Accession #	Pep 95%	PVal		PVal		PVal	
				115:114	115:114	116:114	116:114	117:114	117:114
856	2.8	sp Q4QQT4 2AAB_RAT	1	0.9817	0.9606	0.9462	0.5748	0.871	0.5451
857	1	sp Q9WTQ1 KPCD1_RAT	1	1.6444	0.3781	0.9908	0.9909	1.2023	0.669
858	4.5	sp Q63525 NUDC_RAT	1	1.2359	0.2307	0.8091	0.1704	0.871	0.2368
859	1.3	sp P15943 APLP2_RAT	1	1.7219	0.5759	0.6368	0.2842	2.1086	0.7467
860	2	sp B2RYI0 WDR91_RAT	1	1.1169	0.7053	0.912	0.3567	1.0965	0.9343
861	4.7	sp Q6IUP3 ELP5_RAT	1	1.028	0.8698	0.9204	0.5695	1.0965	0.8224
862	6.3	sp Q6AYQ8 FAHD1_RAT	1	0.6668	0.5586	0.2805	0.1373	0.4831	0.2153
863	5	sp Q68FR3 INT12_RAT	1						
864	1.7	sp Q64350 EI2BE_RAT	1	2.0324	0.18	1.5276	0.2515	1.0666	0.516
865	3.6	sp Q5XI13 GRWD1_RAT	1	0.3597	0.2352	0.6982	0.5339	0.6252	0.4508
866	5	sp Q4V8J7 SPIN1_RAT	1	1.2823	0.0823	1.2474	0.0879	1.3804	0.0589
867	3.8	sp Q4V8C8 CDC73_RAT	1	2.0324	0.3165	3.3113	0.1992	2.7797	0.2304
868	24.7	sp P63170 DYL1_RAT	3	0.9908	0.2198	0.8954	0.2541	2.1281	0.1165
869	4.5	sp P32851 STX1A_RAT	1	1.0093	0.9144	0.871	0.6575	1.028	0.8452
870	6.1	sp B2GV54 NCEH1_RAT	1	1.0375	0.2514	1.0375	0.3795	1.0186	0.5129
871	4.9	sp Q6AYQ4 TM109_RAT	1	1	0.8883	0.9462	0.8699	0.413	0.6123
872	2.9	sp Q5XI41 TRAM1_RAT	1	1.6749	0.2786	1.1912	0.556	1.2359	0.4744
873	4.5	sp Q5HZF2 WBP4_RAT	1	0.7727	0.5689	0.0331	0.0727	0.6138	0.3379
874	2.6	sp Q56R16 IMA6_RAT	1	1.1912	0.7198	0.6792	0.5128	1.0864	0.8503
875	4.2	sp P05369 FPPS_RAT	1	0.7798	0.6629	0.8954	0.9104	1.0864	0.6994
876	5.3	sp B3DMA0 P5I11_RAT	1	1.0375	0.907	1.0765	0.8496	0.9727	0.9297
877	5.2	sp P09626 ATP4A_RAT	5	1.3552	0.5077	1.0093	0.7998	1.2023	0.7151
878	13.6	sp Q62764 YBOX3_RAT	6	0.9817	0.8055	1.1272	0.5944	0.9908	0.7815
879	9.7	sp Q08013 SSRG_RAT	2	1.6444	0.9321	2.2699	0.7919	0.4875	0.6556
880	8.7	sp B2GUZ5 CAZA1_RAT	2	0.492	0.5802	0.2606	0.46	0.4529	0.5328
881	6.4	sp P85969 SNAB_RAT	2	1.7219	0.39	2.1281	0.3006	2.0893	0.3091
882	11.6	sp Q04970 RASN_RAT	2	0.9638	0.6907	0.8872	0.5552	0.7379	0.528
883	6.4	sp Q9JID2 GNA11_RAT	2						
884	2.5	sp P11661 NU5M_RAT	2	1.2823	0.6284	0.9036	0.8672	1.0568	0.8717
885	6.4	sp P97700 M2OM_RAT	3	0.9817	0.9422	1.0186	0.8836	1.028	0.8644
886	4.3	sp Q8CFC1 MINA_RAT	3	1.0375	0.72	0.8551	0.8745	0.8091	0.6763
887	5.1	sp Q5PPN7 CCD51_RAT	1	0.8954	0.8438	0.5152	0.342	0.7311	0.5823
888	8.3	sp P61206 ARF3_RAT	2	0.9036	0.8449	0.9204	0.7797	0.787	0.5496
889	1.4	sp Q56A27 NCBP1_RAT	1	1.1376	0.7464	1.2823	0.6939	0.7798	0.4077
890	1.5	sp P54275 MSH2_RAT	1	1.977	0.3278	3.1046	0.2112	2.3768	0.2667
891	3.4	sp P19814 TGON3_RAT	1	0.4169	0.3004	0.4018	0.306	0.3192	0.2144
892	1.1	sp Q6UE39 GLT13_RAT	1	0.3076	0.5136	0.8091	0.9365	0.207	0.4645
893	7.2	sp P0C2C4 RM10_RAT	1						
894	1.1	sp Q9Z2Q1 SC31A_RAT	1	0.2858	0.4404	0.413	0.7592	0.879	0.4811
895	1.6	sp P52631 STAT3_RAT	1	1	0.607	1.1376	0.6915	1.2474	0.5819
896	1.6	sp Q66HR0 S12A9_RAT	1	0.8318	0.739	0.5702	0.3783	0.955	0.9416
897	2.6	sp Q9JM53 AIFM1_RAT	2	1.0666	0.7985	1.028	0.6973	1.1066	0.716
898	3.9	sp Q68FS2 CSN4_RAT	1	1.2134	0.7186	1.1588	0.633	1.0965	0.8545
899	3	sp Q64591 DECR_RAT	2	0.6918	0.9366	0.2291	0.8117	0.6546	0.957
900	5.6	sp Q63797 PSME1_RAT	1	0.8472	0.7044	1	0.9853	0.8395	0.6663
901	2.9	sp Q63692 CDC37_RAT	1	0.9817	0.8911	1.2474	0.576	1.0765	0.8859
902	6.8	sp Q63690 BAX_RAT	2	1.7378	0.386	1.4454	0.5106	1.977	0.3272
903	5.1	sp Q5I0L7 KTI12_RAT	1						
904	7.4	sp Q5I0H4 TMCO1_RAT	1	1.2823	0.7446	0.6982	0.615	0.8241	0.9549
905	3.2	sp Q5HZE2 T120A_RAT	1	1.1695	0.5074	1.1272	0.5172	1.1803	0.5904
906	5.1	sp Q4KM73 KCY_RAT	1						
907	0.8	sp G3V735 AMOL2_RAT	1	1.8535	0.7088	0.1871	0.6333	0.7447	0.8602
908	3.9	sp Q8CHJ1 PIGU_RAT	1	0.871	0.9999	0.4093	0.2392	1.0186	0.909
909	9.5	sp Q6PCT5 PQBP1_RAT	1						
910	3.6	sp Q6AYU3 DNJB6_RAT	1	0.787	0.7057	0.6607	0.5318	0.4446	0.6348
911	4.7	sp P43138 APEX1_RAT	1	1.3552	0.5681	1.977	0.3272	2.208	0.2899
912	2.2	sp Q68FX7 THOC5_RAT	1	1.0375	0.921	0.9908	0.9985	0.6252	0.4484



N	% Cov (95)	Accession #	Pep 95%	PVal			PVal		
				115:114	115:114	116:114	116:114	117:114	117:114
913	2.5	sp Q5PPG7 EIF2D_RAT	1	1.0965	0.3292	0.9817	0.8643	1.1169	0.3925
914	1.4	sp P23347 B3A2_RAT	1						
915	2.5	sp Q5QJC9 BAG5_RAT	1						
916	3.4	sp Q3B7D0 HEM6_RAT	1	0.8872	0.7987	0.8395	0.8851	0.8091	0.9666
917	3.6	sp Q6AYK5 LYAR_RAT	1	1.7701	0.3781	0.6138	0.4376	0.9462	0.9271
918	2.3	sp Q68FS4 AMPL_RAT	1	1.0186	0.9139	0.6982	0.5284	0.6918	0.7573
919	1.2	sp Q62640 GRID1_RAT	2						
920	1.5	sp Q4FZV0 MANBA_RAT	1	1.1272	0.8019	1.1695	0.7465	1.1912	0.7213
921	2.7	sp P38652 PGM1_RAT	1	0.9727	0.745	0.8241	0.6017	0.955	0.922
922	2.4	sp P10354 CMGA_RAT	1	0.9376	0.7848	1.0471	0.8126	1.0765	0.8312
923	27	sp Q9R1T1 BAF_RAT	2	1.0765	0.8713	1	0.9894	0.9462	0.9289
924	5	sp Q9ERE4 GOLP3_RAT	1	1.7061	0.4264	1.2359	0.6149	1.8707	0.3735
925	6.6	sp Q9EQX9 UBE2N_RAT	1	0.9727	0.8549	0.8241	0.6061	1.0093	0.8766
926	0.7	sp Q75WE7 VWA5A_RAT	1	3.0761	0.609	3.4995	0.4937	2.8054	0.4788
927	2.5	sp Q6AYU1 MO4L1_RAT	1	0.7586	0.6062	0.8241	0.708	0.8954	0.8487
928	3.7	sp Q6AY86 VP26A_RAT	1						
929	2.2	sp Q63598 PLST_RAT	1	1.1169	0.602	0.8954	0.9287	1.0093	0.7697
930	4.6	sp Q63159 COQ3_RAT	1	1.1695	0.7765	0.4966	0.3227	1.0471	0.9359
931	1.9	sp Q5XI63 KIFC1_RAT	1	0.955	0.6682	0.955	0.8197	1.0375	0.8653
932	2.6	sp Q5RJR2 TWF1_RAT	1	1.1695	0.8624	1.3183	0.5263	1.5996	0.4627
933	7.4	sp Q5FVR7 CPSF4_RAT	1						
934	4.3	sp Q5BK32 FAF2_RAT	1	0.955	0.9418	1.7378	0.439	1.2942	0.5853
935	6.9	sp Q499V6 ZCRB1_RAT	1						
936	2.6	sp Q0ZHH6 ATLA3_RAT	1	1.2589	0.5422	1.2246	0.593	1.3932	0.434
937	2.6	sp P53987 MOT1_RAT	1	1.6596	0.4135	1.3305	0.5917	1.4859	0.4912
938	18.8	sp P47198 RL22_RAT	2	0.5105	0.6862	0.9817	0.7678	0.9817	0.8526
939	0.9	sp P28840 NEC1_RAT	1	0.8091	0.6937	0.8091	0.699	1.0965	0.8424
940	3.5	sp P18665 RM03_RAT	1	1.1066	0.8514	1.0186	0.9455	1.0765	0.9271
941	16.7	sp P18437 HMG2_RAT	1	1.7219	0.3946	0.9376	0.9302	1.5417	0.4499
942	6.9	sp P00763 TRY2_RAT	4	0.7178	0.7838	0.7656	0.8252	0.631	0.7823
943	3.1	sp Q35217 MINP1_RAT	1	1.1272	0.796	0.9638	0.9544	0.7112	0.5531
944	2.4	sp O08839 BIN1_RAT	1						
945	5.1	sp A6YP92 ARX_RAT	1						
946	4.5	sp Q9QZP1 GEMI2_RAT	1						
947	5.5	sp Q9EPJ3 RT26_RAT	1						
948	2.6	sp Q6P9U8 EIF3H_RAT	1	0.5495	0.3753	0.6855	0.517	0.7311	0.5835
949	2.1	sp Q6P752 TOIP2_RAT	1						
950	4.1	sp Q6EV70 OFUT1_RAT	1	2.421	0.2622	1.888	0.3491	2.2491	0.2848
951	2.7	sp Q6AYR2 NDRG3_RAT	1	1.0186	0.914	0.9727	0.6719	1.0568	0.9248
952	7.3	sp Q6AY87 THOC6_RAT	1	0.7244	0.5697	0.8472	0.7537	0.5808	0.4045
953	2.5	sp Q66HG8 RED_RAT	1	0.9376	0.7814	0.879	0.7786	0.8954	0.9059
954	3.7	sp Q5XI79 NDUF7_RAT	1	0.8954	0.804	1.4322	0.5428	1.4588	0.5149
955	2.9	sp Q5M9G9 TBRG4_RAT	1	0.9376	0.9529	0.6855	0.36	0.6252	0.4108
956	4.8	sp Q5FVN2 TM41B_RAT	1						
957	2.2	sp Q5BJP6 RRF2M_RAT	1						
958	10.3	sp Q50514 CO040_RAT	1	2.421	0.263	1.0765	0.872	0.7379	0.5905
959	3.6	sp Q01714 SP1_RAT	1	0.52	0.3481	1.0471	0.9057	0.879	0.811
960	2.5	sp P97546 NPTN_RAT	1	0.6026	0.4231	1	0.9899	0.3192	0.2118
961	13.3	sp P55053 FABP5_RAT	1	0.8318	0.7295	1.3428	0.5789	0.879	0.8053
962	6.3	sp P07895 SODM_RAT	2	1.0965	0.9081	1.0765	0.8512	1.1066	0.8025
963	2	sp Q35567 PUR9_RAT	1	1.0375	0.8508	1.1272	0.7314	1.0666	0.7398
964	1.8	sp D4ABY2 COPG2_RAT	1	1.0965	0.6045	0.9204	0.7844	0.929	0.7746
965	14.2	sp Q9Z336 DYL1_RAT	2	0.8954	0.8397	0.863	0.7805	0.6918	0.5301
966	7.8	sp Q9JKW1 TIM22_RAT	1	0.8241	0.7064	0.2208	0.3858	0.8872	0.7538
967	2.6	sp Q8CHM7 HACL1_RAT	1	0.7244	0.5092	1.1482	0.8388	0.9462	0.8843
968	6.2	sp Q7M767 UB2V2_RAT	1	0.8017	0.3479	1.4997	0.747	1.1482	0.6659
969	8.1	sp Q6P791 LTOR1_RAT	1	2.6792	0.4605	1.6749	0.7167	3.4356	0.4892

N	% Cov (95)	Accession #	Pep 95%	PVal		PVal		PVal	
				115:114	115:114	116:114	116:114	117:114	117:114
970	4.3	sp Q6JE36 NDRG1_RAT	3	1.2359	0.678	0.8318	0.7295	1.2134	0.6962
971	7.3	sp Q6IMX7 HPBP1_RAT	1	1.7378	0.388	1.7378	0.3894	2.8576	0.2258
972	5.9	sp Q6AXT7 RBM42_RAT	1	0.9817	0.9627	1.0375	0.9396	0.7047	0.531
973	6.5	sp Q66H47 RM24_RAT	1	0.8017	0.5093	0.7943	0.604	0.5916	0.2949
974	5.5	sp Q642A4 CH082_RAT	1	3.0761	0.2113	1.977	0.3279	4.4463	0.1627
975	5.1	sp Q63486 RRAGA_RAT	1	2.0137	0.3205	0.0929	0.1051	0.3221	0.2138
976	5.1	sp Q62876 SNG1_RAT	1						
977	1.3	sp Q62786 FPRP_RAT	1	1.4322	0.516	1.888	0.3461	1.8197	0.3622
978	10.9	sp Q5XIF4 SUMO3_RAT	1	1.8535	0.7672	1.4191	0.8548	1.1912	0.9207
979	7.1	sp Q5XFW8 SEC13_RAT	1	3.3113	0.1991	2.704	0.2364	2.2699	0.282
980	5.2	sp Q4V7A0 WDR61_RAT	1						
981	5.3	sp Q498E0 TXD12_RAT	1	2.0137	0.3224	0.0603	0.0887	1.3183	0.5965
982	10.4	sp Q3SWT1 SOSB1_RAT	1						
983	2.5	sp Q3KRF1 SP110_RAT	1	1.9231	0.3276	0.9204	0.7632	1.888	0.3313
984	6.3	sp P63140 NFYB_RAT	1	0.2228	0.1629	1.2023	0.7071	0.5495	0.3723
985	5.6	sp P61751 ARF4_RAT	1	0.7656	0.7222	0.9727	0.9733	0.9036	0.785
986	9.2	sp P50408 VATF_RAT	1	0.912	0.7678	1.0568	0.7716	1.0666	0.8944
987	8.4	sp P08011 MGST1_RAT	1						
988	13	sp P05506 NU3M_RAT	1	0.8166	0.7663	0.8551	0.644	0.8551	0.6763
989	4.4	sp P00406 COX2_RAT	2	1.1912	0.9594	0.7178	0.7022	1.1272	0.9264
990	3.5	sp B4F777 HMG5_RAT	1						
991	0.5	sp P04937 FINC_RAT	1	0.8872	0.4976	0.9462	0.785	1	0.9444
992	3.2	sp Q9EQV6 TPP1_RAT	2	1.0093	0.8335	0.9638	0.6929	1	0.545
993	3.7	sp B0LT89 STK24_RAT	1						
994	3.2	sp Q62825 EXOC3_RAT	2	1.2359	0.587	0.929	0.9447	1.6904	0.2919
995	1.6	sp Q10473 GALT1_RAT	1	0.7379	0.5852	0.1722	0.1404	1.0666	0.8779
996	4.2	sp Q8VHK7 HDGF_RAT	1	0.9727	0.9816	0.9817	0.9643	1.0093	0.963
997	1.3	sp Q9JHY8 DNLI1_RAT	1	0.7379	0.3653	0.9036	0.7449	0.8318	0.5532
998	3.8	sp Q5XIP9 TMM43_RAT	1						
999	0.9	sp Q91Z79 LIPA3_RAT	1	1.4454	0.2264	1.1066	0.6594	1.1588	0.6785
1000	4.5	sp P56700 RGS16_RAT	1	3.0761	0.2321	1.7061	0.4789	1.4322	0.6431
1001	21.7	sp P35704 PRDX2_RAT	4	0.6918	0.7382	0.4966	0.5452	0.955	0.9468
1002	7.4	sp Q76MX4 MAFG_RAT	1	0.8091	0.7251	0.7798	0.6672	0.871	0.8573
1003	2.1	sp P07154 CATL1_RAT	1	0.9727	0.861	1.2823	0.6151	0.9727	0.9981
1004	4.5	sp B2RZ55 SIR7_RAT	1	0.597	0.419	0.3499	0.2282	0.4018	0.2602
1005	1.5	sp Q8R4E1 TIP_RAT	1	1.0375	0.9535	1.2134	0.6782	0.9908	0.9815
1006	9.5	sp Q5RK03 C2AIL_RAT	1						
1007	32.7	sp Q6AYZ1 TBA1C_RAT	17	0.9462	0.7464	1.028	0.8795	0.879	0.6981
1008	27.9	sp Q5XIF6 TBA4A_RAT	17	0.6607	0.491	0.2333	0.1684	0.4571	0.2997
1009	14.4	sp P62775 MTPN_RAT	1	1.2134	0.6985	1.0471	0.9061	0.5445	0.367
1010	2.2	sp Q68H95 REPI1_RAT	1	1.0186	0.9499	0.492	0.3256	1.1272	0.8039
1011	3.2	sp Q642G4 PEX14_RAT	1						
1012	10	sp P37397 CNN3_RAT	2	0.9817	0.9329	1	0.9427	0.9817	0.9236
1013	0.9	sp P97874 GAK_RAT	1	0.5346	0.3619	0.4365	0.2846	0.6026	0.4241
1014	2	sp Q99MZ4 GGT7_RAT	1	1.1588	0.3181	1.2134	0.2644	1.0186	0.898
1015	2.7	sp Q6P6V0 G6PI_RAT	1	0.038	0.2946	0.673	0.5894	0.5546	0.4213
1016	1.9	sp O55165 KIF3C_RAT	1	0.871	0.582	0.871	0.5297	0.9204	0.6057
1017	8.1	sp O35394 PRAF1_RAT	1	0.6546	0.4004	0.7379	0.4776	0.8241	0.6783
1018	4.9	sp Q5XII0 EPDR1_RAT	1	1.1482	0.2387	1.1272	0.5495	0.9638	0.276
1019	7.3	sp Q6AYT7 ABD12_RAT	2	1.6444	0.4086	0.8395	0.8966	1.0965	0.797
1020	9.6	sp B5DFN3 UQCC2_RAT	1	1	0.9659	1.3804	0.5311	1.3677	0.5585
1021	6.9	sp Q7TP40 PCNP_RAT	1	1.4859	0.512	0.8954	0.8233	1.0864	0.856
1022	2.7	sp Q99M64 P4K2A_RAT	1	1.4723	0.9234	0.6194	0.292	3.1623	0.1213
1023	7.7	sp P24528 MGMT_RAT	1	0.6855	0.5162	1.1803	0.7271	1.1066	0.8268
1024	27.7	sp P62836 RAP1A_RAT	5	0.7798	0.6504	0.3873	0.2516	0.166	0.1373
1025	4.1	sp Q3KRD8 IF6_RAT	1	1.3428	0.5453	1.2823	0.6566	1.1482	0.7986
1026	18.4	sp P68255 1433T_RAT	7						

N	% Cov (95)	Accession #	Pep 95%	PVal			PVal		
				115:114	115:114	116:114	116:114	117:114	117:114
1027	2.2	sp Q9WU61 CLCC1_RAT	1	1.2942	0.5996	1.0765	0.8454	1.0471	0.9245
1028	3.8	sp Q9HB97 PARVA_RAT	1	1.4454	0.3249	1.0568	0.7824	1.406	0.3383
1029	0.9	sp Q63623 SCAF8_RAT	1	1.1695	0.1321	1.1588	0.0903	1.1588	0.1271
1030	3.3	sp Q32Q06 AP1M1_RAT	1	0.8017	0.9085	1.6293	0.1014	0.8017	0.9724
1031	5.1	sp Q5M9G1 HEX11_RAT	1	0.863	0.3979	0.7178	0.1403	0.8395	0.3426
1032	5.3	sp B5DEQ3 XPP3_RAT	2	0.955	0.6328	1.1272	0.9612	1.2942	0.3685
1033	4.8	sp Q5FVL2 EMC8_RAT	1	1.1482	0.7932	1.2023	0.7681	0.8395	0.6833
1034	6	sp P57113 MAAI_RAT	1	0.6668	0.498	1.0471	0.9113	0.879	0.8136
1035	2.3	sp Q3MJK5 CDK12_RAT	2	1.2359	0.6266	1.1376	0.5232	0.9638	0.9304
1036	2.6	sp Q5BJM8 ZNT7_RAT	1	0.9376	0.8404	1.2023	0.4186	1.2589	0.3739
1037	4.5	sp Q9JJP9 UBQL1_RAT	2	1.3932	0.5468	0.6546	0.4822	0.3467	0.2276
1038	2.7	sp Q9JJK4 PEX3_RAT	1	1.028	0.829	0.6855	0.0872	1.1272	0.5926
1039	10.6	sp Q5EGY4 YKT6_RAT	2	1.3804	0.4079	1.1272	0.6626	0.8395	0.5538
1040	13.8	sp Q9WVJ4 SYJ2B_RAT	2	1.3183	0.2872	1.0965	0.5271	1.4322	0.2198
1041	2.2	sp Q9R066 CXAR_RAT	1	0.7047	0.2429	1	0.9685	0.8017	0.4201
1042	1.8	sp Q63801 TAF6_RAT	1	1.1588	0.3154	1.2134	0.2354	1.0864	0.682
1043	2.8	sp Q9R050 SSBP3_RAT	1						
1044	7.9	sp Q4KLF8 ARPC5_RAT	1	0.871	0.8079	0.8241	0.6412	0.8017	0.5749
1045	2.8	sp B1WBU8 PLHD1_RAT	2	1.0375	0.9747	0.8954	0.9434	0.8954	0.985
1046	5.3	sp Q810F4 FAM3C_RAT	1	1.2823	0.6088	1	0.689	1.0375	0.9992
1047	0.9	sp P97603 NEO1_RAT	1	1.1066	0.8294	0.7447	0.6005	0.7516	0.6044
1048	2.3	sp Q5XI01 LARP7_RAT	1	0.8395	0.7435	0.863	0.7519	0.6427	0.4404
1049	7.7	sp Q5PPM8 TM55B_RAT	2	1.1482	0.7805	1.028	0.961	1.0965	0.9108

# Appendix C Diet Description

Information supplied by Specialty Feeds



**Specialty Feeds**

3150 Great Eastern Hwy  
Glen Forrest  
Western Australia 6071  
p: +61 8 9298 8111  
F: +61 8 9298 8700  
Email: [info@specialtyfeeds.com](mailto:info@specialtyfeeds.com)

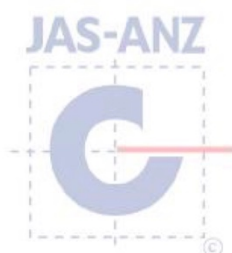
## Diet **Meat Free Rat and Mouse Maintenance Diet**

A fixed formulation diet for Laboratory Rats and Mice fortified with vitamins and minerals to meet the requirements of breeding animals after the diet is autoclaved or irradiated.

- All nutritional parameters of this diet meet or exceed the NRC maintenance guidelines for Rats and Mice.
- The diet has been designed as a maintenance ration for non breeding mature rodents.
- Protein content has been reduced from 19% in the standard ration to 15%.
- Crude Fibre content has been increased from 4.5% to 6.5%.
- Calculated energy has been reduced from 14.3 MJ/Kg to 13 MJ/Kg.
- Mineral content has been changed from the standard ration, reducing Ca and P but maintaining the Ca:P ratio.
- Mammalian meals have been excluded from the diet, however the diet does contain fish meal. We have formulated totally vegetarian diets, and maintained colonies for some time on these diets. Please contact us if you require such a diet.
- The feed is manufactured in a cylindrical form with a diameter of around 12 mm, length is variable from 10 mm to 30 mm. We have found that this form is ideal for overhead hopper feeding, maximising the ease of handling whilst minimising fines formation and the risk of bridging in the feed hopper. Pellet strength has been kept lower than conventional pelletised diets. While this leads to a slight increase in transit and storage damage to the diet (fines generation), we have found that juvenile mice often have a lower feed intake on harder pellets.
- The diet is packed in permeable bags suitable for direct loading into an autoclave. It is recommended that the diet be autoclaved at 120° C for 20 minutes with a post autoclaving vacuum drying cycle. Some clumping of the diet can be expected, but the diet clumps can usually be easily broken. Modifying the drying time to leave some residual moisture in the diet can minimise the clumping. Do not autoclave at 135° C as this will result in significant clumping that will be difficult to break.



VS Rat and Mouse Maintenance



Page 1 of 3



09/08/12

Calculated Nutritional Parameters	
Protein	14.50%
Total Fat	4.80%
Crude Fibre	7.00%
Acid Detergent Fibre	7.63%
Neutral Detergent Fibre	16.35%
Total Carbohydrate	59.40%
Digestible Energy	12.8 MJ / Kg
% Total Calculated Energy from Protein	19.00%
% Total Calculated Energy From Lipids	14.00%

Diet Form and Features	
<ul style="list-style-type: none"> <li>• Cereal grain base diet. 12 mm diameter pellets.</li> <li>• Pack size 5 Kg, vacuum packed under nitrogen in oxygen impermeable plastic bags. Packs are double bagged and packed into cardboard cartons to protect them during transit and to ensure sterility is maintained.</li> <li>• Also available in 10 and 15Kg woven polyethylene bags, suitable for direct loading into an autoclave.</li> <li>• Diet suitable for irradiation, also suitable for autoclave.</li> <li>• Lead time 2 weeks or 4 weeks for irradiation.</li> </ul>	

Ingredients	
A Fixed formula ration using the following ingredients:	
Wheat, Bran, Oats, Soya meal, Fish meal, Mixed vegetable oils, Canola oil, Salt, Calcium Carbonate, Dicalcium phosphate, Magnesium oxide, and a Vitamin and trace mineral premix.	

Added Trace Minerals	
Magnesium	100 mg/Kg
Iron	70 mg/Kg
Copper	16 mg/Kg
Iodine	0.5 mg/Kg
Manganese	70 mg/Kg
Zinc	60 mg/Kg
Molybdenum	0.5 mg/Kg
Selenium	0.1 mg/Kg

Calculated Total Minerals	
Calcium	0.80%
Phosphorous	0.70%
Available Phosphorous	0.40%
Magnesium	0.20%
Sodium	0.20%
Potassium	0.80%
Sulphur	0.20%
Iron	219 mg/Kg
Copper	25 mg/Kg
Iodine	0.5 mg/Kg
Manganese	120 mg/Kg
Cobalt	0.7 mg/Kg
Zinc	95 mg/Kg
Molybdenum	1.2 mg/Kg
Selenium	0.4 mg/Kg
Cadmium	0.12 mg/Kg
Chromium	No data
Boron	2.4 mg/Kg

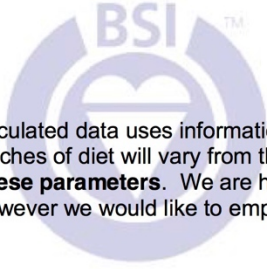
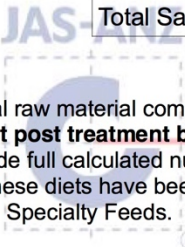
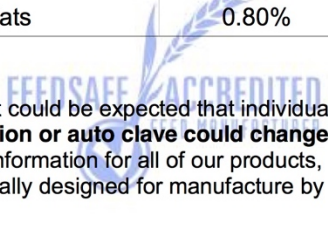
Calculated Amino Acids	
Valine	0.90%
Leucine	1.50%
Isoleucine	0.80%
Threonine	0.70%
Methionine	0.30%
Cystine	0.30%
Lysine	0.90%
Phenylalanine	0.90%
Tyrosine	0.70%
Tryptophan	0.20%
Histidine	0.37%

Added Vitamins	
Vitamin A (Retinol)	10 000 IU/Kg
Vitamin D3 (Cholecalciferol)	2 000 IU/Kg
Vitamin E (a Tocopherol acetate)	100 mg/Kg
Vitamin K (Menadione)	20 mg/Kg
Vitamin B1 (Thiamine)	80 mg/Kg
Vitamin B2 (Riboflavin)	30 mg/Kg
Niacin (Nicotinic acid)	100 mg/Kg
Vitamin B6 (Pryridoxine)	25 mg/Kg
Calcium Pantothenate	50 mg/Kg
Biotin	300 ug/Kg
Folic Acid	5.0 mg/Kg
Vitamin B12 (Cyancobalamin)	150 ug/Kg

Calculated Total Minerals	
Calcium	0.39%
Phosphorous	0.60%
Available Phosphorous	0.30%
Magnesium	0.20%
Sodium	0.20%
Potassium	0.70%
Sulphur	0.20%
Iron	154 mg/Kg
Copper	25 mg/Kg
Iodine	0.5 mg/Kg
Manganese	122 mg/Kg
Cobalt	0.5 mg/Kg
Zinc	97 mg/Kg
Molybdenum	0.5 mg/Kg
Selenium	0.3 mg/Kg
Cadmium	0.3 mg/Kg
Chromium	No data

Calculated Total Vitamins	
Vitamin A (Retinol)	17 000 IU/Kg
Vitamin D (Cholecalciferol)	2 000 IU/Kg
Vitamin E (a Tocopherol acetate)	112 mg/Kg
Vitamin K (Menadione)	20 mg/Kg
Vitamin C (Ascorbic acid)	No data
Vitamin B1 (Thiamine)	84 mg/Kg
Vitamin B2 (Riboflavin)	31 mg/Kg
Niacin (Nicotinic acid)	147 mg/Kg
Vitamin B6 (Pryridoxine)	28 mg/Kg
Pantothenic Acid	61 mg/Kg
Biotin	430 ug/Kg
Folic Acid	5.5 mg/Kg
Inositol	No data
Vitamin B12 (Cyancobalamin)	150 ug/Kg
Choline	1 670 mg/Kg

Calculated Fatty Acid Composition	
Myristic Acid 14:0	0.02%
Palmitic Acid 16:0	0.60%
Stearic Acid 18:0	0.15%
Palmitoleic Acid 16:1	Trace
Oleic Acid 18:1	2.20%
Gadoleic Acid 20:1	0.04%
Linoleic Acid 18:2 n6	1.60%
a Linolenic Acid 18:3 n3	0.30%
Arachadonic Acid 20:4 n6	Trace
EPA 20:5 n3	0.02%
DHA 22:6 n3	0.05%
Total n3	0.37%
Total n6	1.61%
Total Mono Unsaturated Fats	1.67%
Total Polyunsaturated Fats	2.10%
Total Saturated Fats	0.80%




  
 Calculated data uses information from typical raw material composition. It could be expected that individual batches of diet will vary from this figure. **Diet post treatment by irradiation or autoclave could change these parameters.** We are happy to provide full calculated nutritional information for all of our products, however we would like to emphasise that these diets have been specifically designed for manufacture by Specialty Feeds.



**Diet  
SF03-002**

**36% Fat Modification of AIN93G  
(59% of Total Energy From Fats)**

A very high fat semi-pure diet formulation for laboratory rats and mice based on AIN-93G.

- Total fat content has been increased to 36% fat. Using generally recognised energy data this would equate to a diet where 59% of total energy is from lipids.
- The fats included to make up the total fat content have been chosen to maximise diet palatability whilst retaining a good spread of fatty acids. All known fatty acid requirements have been met or exceeded.
- We would recommend that this diet be transported and stored at less than 15°C. At higher temperatures the diet softens considerably.
- Calculated digestible energy has increased as a result of the increased fat inclusion.
- Dietary carbohydrate content is from sucrose only. All starch has been removed from the diet. This has been done primarily to improve pellet strength but may also have some physiological implications.

Calculated Nutritional Parameters	
Protein	19.40%
Total Fat	36.00%
Crude Fibre	4.70%
AD Fibre	4.70%
Digestible Energy	22.8 MJ / Kg
% Total calculated digestible energy from lipids	59.00%
% Total calculated digestible energy from protein	15.00%

#### Diet Form and Features

- Semi pure diet. 15mm x 20mm block to mimic similar size of pellet.
- Packed in plastic trays. Trays packed in groups of five (5). with layer of glad wrap between each to protect diet.
- Vacuum packed under nitrogen in oxygen impermeable bags. Packed in cardboard cartons for protection during transit.
- Diet must be stored at or below 15°C
- Diet not suitable for irradiation or autoclave
- Lead time 2 weeks

Ingredients	
Casein (Acid)	200 g/Kg
Sucrose	346 g/Kg
Canola Oil	60 g/Kg
Cocoa Butter	240 g/Kg
Hydrogenated Vegetable Oil (Cofa)	60 g/Kg
Cellulose	50 g/Kg
DL Methionine	3.0 g/Kg
Calcium Carbonate	13.1 g/Kg
Sodium Chloride	2.6 g/Kg
AIN93 Trace Minerals	1.4 g/Kg
Potassium Citrate	2.5 g/Kg
Potassium Dihydrogen Phosphate	6.9 g/Kg
Potassium Sulphate	1.6 g/Kg
Choline Chloride (75%)	2.5 g/Kg
AIN93 Vitamins	10 g/Kg
Antioxidant (Oxicap E2)	0.04 g/Kg

Calculated Amino Acids	
Valine	1.30%
Leucine	1.80%
Isoleucine	0.90%
Threonine	0.80%
Methionine	0.80%
Cystine	0.06%
Lysine	1.50%
Phenylalanine	1.00%
Tyrosine	1.00%
Tryptophan	0.30%
Histidine	0.60%

Calculated Total Minerals	
Calcium	0.46%
Phosphorous	0.32%
Magnesium	0.09%
Sodium Chloride	0.12%
Potassium	0.16%
Sulphur	0.40%
Iron	0.20%
Copper	72 mg/Kg
Iodine	7.0 mg/Kg
Manganese	0.2 mg/Kg
Cobalt	18 mg/Kg
Zinc	No data
Molybdenum	51 mg/Kg
Selenium	0.15 mg/Kg
Cadmium	0.3 mg/Kg
Chromium	No data
Fluoride	1.0 mg/Kg
Lithium	1.0 mg/Kg
Boron	0.1 mg/Kg
Nickel	2.1 mg/Kg
Vanadium	0.5 mg/Kg
	0.1 mg/Kg



Calculated Total Vitamins		Calculated Fatty Acid Composition	
Vitamin A (Retinol)	4 000 IU/Kg	Saturated Fats C12:0 or less	3.20%
Vitamin D (Cholecalciferol)	1 000 IU/Kg	Myristic Acid 14:0	0.90%
Vitamin E (a Tocopherol acetate)	86 mg/Kg	Palmitic Acid 16:0	7.10%
Vitamin K (Menadione)	1 mg/Kg	Stearic Acid 18:0	9.30%
Vitamin C (Ascorbic acid)	None added	Arachidic Acid 20:0	0.30%
Vitamin B1 (Thiamine)	6.1 mg/Kg	Palmitoleic Acid 16:1	0.10%
Vitamin B2 (Riboflavin)	6.3 mg/Kg	Oleic Acid 18:1	12.00%
Niacin (Nicotinic acid)	30 mg/Kg	Gadoleic Acid 20:1	0.10%
Vitamin B6 (Pryridoxine)	7 mg/Kg	Linoleic Acid 18:2 n6	2.00%
Pantothenic Acid	16.5 mg/Kg	a Linolenic Acid 18:3 n3	0.70%
Biotin	200 ug/Kg	Arachadonic Acid 20:4 n6	No data
Folic Acid	2 mg/Kg	EPA 20:5 n3	Trace
Inositol	None added	DHA 22:6 n3	No data
Vitamin B12 (Cyancobalamin)	103 ug/Kg	Total n3	0.74%
Choline	1670 mg/Kg	Total n6	2.05%
		Total Mono Unsaturated Fats	12.20%
		Total Polyunsaturated Fats	2.79%
		Total Saturated Fats	20.92%

Calculated data uses information from typical raw material composition. It could be expected that individual batches of diet will vary from this figure. **Diet post treatment by irradiation or auto clave could change these parameters.**

We are happy to provide full calculated nutritional information for all of our products, however we would like to emphasise that these diets have been specifically designed for manufacture by Specialty Feeds.